

Anders Nilsson · Bilong Liu

Vibro- Acoustics, Volume 1



Science Press
Beijing



Springer

Vibro-Acoustics, Volume 1

Anders Nilsson · Bilong Liu

Vibro-Acoustics, Volume 1

 Science Press
Beijing

 Springer

Anders Nilsson
MWL-Marcus Wallenberg Laboratory
for Sound and Vibration Research
KTH, The Royal Institute of Technology
Stockholm
Sweden

Bilong Liu
Key Laboratory of Noise and Vibration
Research
Institute of Acoustics, Chinese Academy
of Sciences
Beijing
China

ISBN 978-3-662-47806-6 ISBN 978-3-662-47807-3 (eBook)
DOI 10.1007/978-3-662-47807-3

Jointly published with Science Press, Beijing
ISBN: 978-7-03-033624-8 Science Press, Beijing

Library of Congress Control Number: 2015946068

Springer Heidelberg New York Dordrecht London
© Science Press, Beijing and Springer-Verlag Berlin Heidelberg 2015

This work is subject to copyright. All rights are reserved by the Publishers, whether the whole or part of the material is concerned, specifically the rights of translation, reprinting, reuse of illustrations, recitation, broadcasting, reproduction on microfilms or in any other physical way, and transmission or information storage and retrieval, electronic adaptation, computer software, or by similar or dissimilar methodology now known or hereafter developed.

The use of general descriptive names, registered names, trademarks, service marks, etc. in this publication does not imply, even in the absence of a specific statement, that such names are exempt from the relevant protective laws and regulations and therefore free for general use.

The publishers, the authors and the editors are safe to assume that the advice and information in this book are believed to be true and accurate at the date of publication. Neither the publishers nor the authors or the editors give a warranty, express or implied, with respect to the material contained herein or for any errors or omissions that may have been made.

Printed on acid-free paper

Springer-Verlag GmbH Berlin Heidelberg is part of Springer Science+Business Media
(www.springer.com)

Preface

Noise pollution is an environmental problem. Structures excited by dynamic forces radiate noise. The art of noise reduction requires an understanding of vibro-acoustics. This topic describes how structures are excited, energy flows from an excitation point to a sound radiating surface, and finally how a structure radiates noise to a surrounding fluid. The aim of this text is to give a fundamental analysis and a mathematical presentation of these phenomena. The text is intended for graduate students, researchers and engineers working in the field of sound and vibration.

Part of the text has evolved from an advanced course on acoustics initially given at Chalmers University, Sweden, in the early nineteen seventies. Over the years, these lectures were transformed to MSc and Ph.D. courses on vibro-acoustics. These courses were given at MWL, KTH, Sweden. During the years, much material has been added as inspired by research work, colleagues and Ph.D. students at many of the universities and research institutes I have been fortunate enough to be associated with.

The main text is published as two volumes. There are eight chapters in each volume. A number of problems is given at the end of each chapter. The solutions to the problems plus a summary of the main formulae are presented in a third volume. In the text, frequent references are made to the behaviour of simple vibratory systems and their response in the frequency domain. Therefore and for the sake of completeness, though well-known to the reader, the first chapter includes discussions of simple one degree of freedom systems. In this way, energy and power of simple vibratory systems are introduced. Various types of losses are discussed. In the second chapter the vibration of linear mechanical systems is studied in the frequency domain. In particular, the response of systems excited by harmonic and random forces is analysed. In Chap. 3, the basic differential equations governing longitudinal, transverse and bending waves are discussed. The equations are derived based on the concept of stresses and strains in solids. Energy stored and energy flow in structures caused by the various wave types are analysed. The general wave equation is introduced in Chap. 4. This equation is shown to govern all elastic motion of a solid. The generalised wave equation is utilized to describe

the bending of thick plates, sandwich beams and I-beams. It is demonstrated that in-plane waves like longitudinal and transverse waves are strongly coupled. In Chap. 5, it is shown that in-plane and bending waves also are well coupled. As presented, waves are attenuated by internal losses and added damping. More importantly, any discontinuity or junction will influence the energy flow in a structure. A number of examples are given. Measurement techniques to determine losses across junctions are introduced. Chapter 6 deals with longitudinal waves in finite beams. Eigenfunctions and eigenvalues are discussed for various boundary conditions. The results are used to model free and forced vibrations of beams. Green's function is derived for some cases and used for the calculation of the forced response of beams. The mobility concept is used to determine the response of coupled systems. In addition, the transfer matrix system is introduced. Flexural vibrations of finite beams are discussed in Chap. 7. Again, eigenfunctions and eigenvalues are derived for a number of boundary conditions. Free and forced vibrations are considered. The free and forced vibration of isotropic rectangular and circular plates is investigated in Chap. 8. The responses of structures excited by random and harmonic forces are compared. The mobility concepts of finite and infinite plates are investigated, and simplified models for the calculation of the energy of plates are introduced.

Chapter 9 in Volume II is on variational methods. The variational technique is used for the derivation of equations governing the vibration of sandwich and other composite elements and some simple shell elements. In the following Chap. 10, the coupling between mechanical systems is explored. This includes an introduction to the vibration of rubber mounts, resilient mountings and the design of foundations. The topics of Chap. 11 are waves in fluids including discussions on various types of monopole, dipole and multipole sources. Also included are out-door and room acoustics. Chapter 12 is on fluid structure interaction and radiation of sound. Sound radiation from infinite and finite plates as well as the fluid loading on structures are investigated. Chapter 13 is on sound transmission loss of panels. The sound transmission through infinite and finite panels is discussed. The influence of boundary conditions and geometry of transmission rooms on the measured and predicted sound transmission loss is illustrated. The title of Chap. 14 is Waveguides. In this chapter the prediction and reduction of energy flow in structural waveguides typical for ship, aircraft and train constructions are investigated. Also included are discussions on energy flow and sound transmission through composite structures and shells. In particular, the prediction of sound transmission loss of aircraft structures is highlighted. The contents of Chap. 15 include random excitation of structures and flow induced vibrations. Both phenomena are of importance for interior noise in aircraft, ships and fast trains. Finally, Chap. 16 is on the prediction of velocity and noise levels in large structures like vehicles. The basic concept of the Statistical Energy Analysis is presented. Predictions based on the waveguide technique are also illustrated in the same chapter.

The completion of this work would not have been possible without the determined support of Professor Jing Tian and the Key Laboratory of Noise and Vibration Research, Institute of Acoustics, Chinese Academy of Sciences in Beijing

and the assistance and support of my coauthor Professor Bilong Liu. I would also like to express my gratitude to many former colleagues in many countries and in particular to Professor Leping Feng, MWL, KTH, for always being an inspiring discussion partner.

A number of measurement results are presented in Volume II. Most of these measurements could not have been performed without the expert help of Fritiof Torstensson and Arne Jagenäs at Chalmers, Knut Ulvund at DNV and Kent Lindgren and Danilo Prilovic at KTH.

I would like to express my gratitude to Hector Valenzuela who helped me with most of the figures. Without the very efficient expert help of Edoardo Piana and in particular Benedetta Grassi these volumes could never have been completed.

Any comments or questions on the text are most welcome. Contact by email, address andersc.nilsson@gmail.com and liubl@mail.ioa.ac.cn.

Genova, Italy
April 2015

Anders Nilsson

Contents

1	Mechanical Systems with One Degree of Freedom	1
1.1	A Simple Mass–Spring System	1
1.2	Free Vibrations	5
1.3	Transient Vibrations	11
1.4	Forced Harmonic Vibrations	19
1.5	Fourier Series	23
1.6	Complex Notation	25
	Problems	29
2	Frequency Domain	31
2.1	Introduction	31
2.2	Frequency Response	33
2.3	Correlation Functions	36
2.4	Spectral Density	38
2.5	Examples of Spectral Density	40
2.6	Coherence	44
2.7	Time Averages of Power and Energy	45
2.8	Frequency Response and Point Mobility Functions	51
2.9	Loss Factor	57
2.10	Response of a 1-DOF System, A Summary	61
	Problems	64
3	Waves in Solids	67
3.1	Stresses and Strains	67
3.2	Losses in Solids	75
3.3	Transverse Waves	79
3.4	Longitudinal Waves	82
3.5	Torsional Waves	85
3.6	Waves on a String	87
3.7	Bending or Flexural Waves—Beams	89
3.8	Waves on Strings and Beams—A Comparison	96

3.9	Flexural Waves-Plates	99
3.10	Orthotropic Plates	105
3.11	Energy Flow	107
	Problems	109
4	Interaction Between Longitudinal and Transverse Waves	111
4.1	Generalized Wave Equation	111
4.2	Intensity	115
4.3	Coupling Between Longitudinal and Transverse Waves	116
4.4	Bending of Thick Beams/Plates	121
4.5	Quasi-Longitudinal Waves in Thick Plates	134
4.6	Rayleigh Waves	137
4.7	Sandwich Plates-General	138
4.8	Bending of Sandwich Plates	140
4.9	Equations Governing Bending of Sandwich Plates	141
4.10	Wavenumbers of Sandwich Plates	144
4.11	Bending Stiffness of Sandwich Plates	145
4.12	Bending of I-Beams	146
	Problems	150
5	Wave Attenuation Due to Losses and Transmission	
	Across Junctions	153
5.1	Excitation and Propagation of L-waves	153
5.2	Excitation and Propagation of F-Waves	158
5.3	Point Excited Infinite Plate	162
5.4	Spatial Fourier Transforms	166
5.5	Added Damping	173
5.6	Losses in Sandwich Plates	179
5.7	Coupling Between Flexural and Inplane Waves	182
5.8	Transmission of F-Waves Across Junctions, Diffuse Incidence	186
5.9	Transmission of F-Waves Across Junctions, Normal Incidence	193
5.10	Attenuation Due to Change of Cross Section	195
5.11	Some Other Methods to Increase Attenuation	198
5.12	Velocity Level Differences and Transmission Losses	199
5.13	Measurements on Junctions Between Beams	203
	Problems	209
6	Longitudinal Vibrations of Finite Beams	213
6.1	Free Longitudinal Vibrations in Finite Beams	213
6.2	Forced Longitudinal Vibrations in Finite Beams	223
6.3	The Mode Summation Technique	228
6.4	Kinetic Energy of Vibrating Beam	232

6.5	Mobilities	237
6.6	Mass Mounted on a Rod	240
6.7	Transfer Matrices	244
	Problems	248
7	Flexural Vibrations of Finite Beams	251
7.1	Free Flexural Vibrations of Beams	251
7.2	Orthogonality and Norm of Eigenfunctions	260
7.3	Forced Excitation of F-Waves	264
7.4	Mode Summation and Modal Parameters	268
7.5	Point Mobility and Power	274
7.6	Transfer Matrices for Bending of Beams	278
7.7	Infinite Periodic Structures	282
7.8	Forced Vibration of Periodic Structures	287
7.9	Finite Composite Beam	292
	Problems	297
8	Flexural Vibrations of Finite Plates	301
8.1	Free Vibrations of Simply Supported Plates	301
8.2	Forced Response of a Simply Supported Plate	308
8.3	Forced Excitation of a Rectangular Plate with Two Opposite Sides Simply Supported	313
8.4	Power and Energy	318
8.5	Mobility of Plates	322
8.6	The Rayleigh–Ritz Method	326
8.7	Application of the Rayleigh–Ritz Method	331
8.8	Non-Flat Plates	338
8.9	The Effect of an Added Mass or Mass-Spring System on Plate Vibrations	340
8.10	Small Disturbances	344
8.11	Plates Mounted on Resilient Layers	347
8.12	Vibration of Orthotropic Plates	353
8.13	Circular and Homogeneous Plates	354
8.14	Bending of Plates in Tension	360
	Problems	362
	References	365
	Index	369

Notations

b	Width
c	Damping factor, viscous losses
c_b	Phase velocity, bending/flexural waves
c_g	Group velocity
c_l	Phase velocity, longitudinal waves
c_r	Phase velocity, Rayleigh waves
c_t	Phase velocity, transverse waves
f	Frequency
f_n	Natural frequency corresponding to mode n
f_c	Critical frequency
f_r	Dilatation frequency
g	Acceleration due to gravity
$g_n(t)$	Time dependent solution corresponding to eigenfunction $\varphi_n(x)$
$h(t)$	Response function due to unit pulse, Eq. (1–36)
i	$\sqrt{-1}$
k	$k_0(1 + i\delta)$, complex spring constant
k_0	Real part of spring constant
k_l	Wavenumber longitudinal waves
k_t	Wavenumber transverse waves
k_r	Wavenumber Rayleigh waves
m	Mass
m'	Mass per unit length
r	Radial distance
s	Spring constant per unit length or unit area
t	Time
v	Velocity
w	Transverse displacement
B	Torsional rigidity
$C(\tau)$	Memory function
D'	Bending stiffness beam

D	Bending stiffness plate
D_x, D_y	Bending stiffness, orthotropic plate
E	Young's modulus of elasticity
E_0	Real part of Young's modulus of elasticity
E_x	σ_x/ε_x
F_d	Damping force
F_n, F_{mn}	Modal force
$F(t)$	Force as function of time
F'	Force per unit length
G	Shear modulus
$G(x x_1)$	Green's function, 1-dimension
$G_{xx}(\omega)$	Power spectral density, one sided
$G_{xy}(\omega)$	Cross power spectral density, one sided
$H(\omega)$	Frequency response function
$I(t)$	Impulse
I	Moment of inertia
\mathbf{I}	(I_x, I_y, I_z) intensity vector
K	Bulk modulus
K_n, K_{mn}	Modal stiffness
L, L_x, L_y	Length
M_n, M_{mn}	Modal mass
M'_x	Bending moment per unit width around x -axis
M'_{xy}	Bending moment per unit width due to torsional stress
$R_{xx}(\tau)$	Autocorrelation function
$R_{xy}(\tau)$	Cross-correlation function
R	$10 \log(1/\tau)$
S	Cross section area
$S_{xx}(\omega)$	Power spectral density, two sided
$S_{xy}(\omega)$	Cross power spectral density, two sided
T	Time period, harmonic oscillations
T_b	Timoshenko constant
T_x	Shear force per unit width
$Y(\omega)$	Point mobility
$Y(x, y x_0, y_0)$	Transfer mobility, plates
Y_∞	Point mobility, infinite structure
\mathcal{E}	Total energy
\mathcal{T}	Kinetic energy
\mathcal{U}	Potential energy
χ	Shear parameter
γ	Stiffness parameter
β	$c/(2m)$
γ	Euler constant
γ_{xy}	Shear angle
$\gamma_{xy}^2(f)$	Coherence function

δ	Loss factor
$\delta(t)$	Dirac function
δ_{ij}	Kronecker delta
ε	Strain
ε_x	Strain in x -direction
ζ	Displacement in z -direction
η	Displacement in y -direction
η_0	Loss factor
η_{tot}	Total loss factor
κ	Wavenumber, flexural waves
κ_0	Real part of wavenumber, flexural waves
λ	Wavelength but also Lamé constant
μ	Mass per unit area
ν	Poisson's ratio
ξ	Displacement, x -direction
ρ	Density
ρ_a	Apparent density
σ	Stress
σ_x	Stress in x -direction
τ	Transmission coefficient
$\tau(\alpha)$	Transmission coefficient as function of angle of incidence, α
τ_{ij}	Transmission coefficient between the structures i and j
τ_{xy}	Shear stress component
φ	Phase angle
$\varphi_n(x)$	One dimensional eigenfunction
$\varphi_{mn}(x, y)$	Two dimensional eigenfunction
ω	Angular frequency
ω_0	$\sqrt{k_0/m}$
ω_r	$\sqrt{\omega_0^2 - \beta^2}$
ω_{n_0}	Real part of angular frequency corresponding to f_n
Θ	(torsional) angle
Π	Power
Π_d	Dissipated power
Π_x	$I_x \cdot S$, energy flow in x -direction
Π_{ij}	Energy flow from structure i to j
ϕ	Scalar potential
ψ	Vector potential
ΔL_v	Velocity level difference
\dot{x}	dx/dt
\ddot{x}	d^2x/dt^2
x^*	Complex conjugate of x
$\langle x^2 \rangle$	Space average of x^2
$\langle f g \rangle$	$\int f(x)g(x)dx$

(m, n)	Mode m, n of vibrating plate
$\text{Re}z$	Real part of z
$\text{Im}z$	Imaginary part of z
$E[x]$	Expected value of x
$\text{FT}(x)$	Fourier transform of x

Operators

Cartesian Coordinates

$$\begin{aligned}
 \mathbf{grad} \, u & \quad \frac{\partial u}{\partial x} \cdot \mathbf{e}_x + \frac{\partial u}{\partial y} \cdot \mathbf{e}_y + \frac{\partial u}{\partial z} \cdot \mathbf{e}_z = \left(\frac{\partial u}{\partial x}, \frac{\partial u}{\partial y}, \frac{\partial u}{\partial z} \right) \\
 \text{div} \, (\mathbf{u}) = \nabla \cdot \mathbf{u} & \quad \frac{\partial u_x}{\partial x} + \frac{\partial u_y}{\partial y} + \frac{\partial u_z}{\partial z} \\
 \mathbf{curl} \, \mathbf{u} = \nabla \times \mathbf{u} & \quad \left(\frac{\partial u_z}{\partial y} - \frac{\partial u_y}{\partial z} \right) \cdot \mathbf{e}_x + \left(\frac{\partial u_x}{\partial z} - \frac{\partial u_z}{\partial x} \right) \cdot \mathbf{e}_y + \left(\frac{\partial u_y}{\partial x} - \frac{\partial u_x}{\partial y} \right) \cdot \mathbf{e}_z \\
 \nabla^2 u & \quad \frac{\partial^2 u}{\partial x^2} + \frac{\partial^2 u}{\partial y^2} + \frac{\partial^2 u}{\partial z^2}
 \end{aligned}$$

Cylindrical Coordinates

$$x = r \cdot \cos \varphi, y = r \cdot \sin \varphi$$

$$\begin{aligned}
 \mathbf{grad} \, u & \quad \frac{\partial u}{\partial r} \cdot \mathbf{e}_r + \frac{1}{r} \frac{\partial u}{\partial \varphi} \cdot \mathbf{e}_\varphi + \frac{\partial u}{\partial z} \cdot \mathbf{e}_z \\
 \text{div} \, \mathbf{u} & \quad \frac{1}{r} \frac{\partial}{\partial r} (ru_r) + \frac{1}{r} \frac{\partial u_\varphi}{\partial \varphi} + \frac{\partial u_z}{\partial z} \\
 \mathbf{curl} \, \mathbf{u} & \quad \left(\frac{1}{r} \frac{\partial u_z}{\partial \varphi} - \frac{\partial u_\varphi}{\partial z} \right) \cdot \mathbf{e}_r + \left(\frac{\partial u_r}{\partial z} - \frac{\partial u_z}{\partial r} \right) \cdot \mathbf{e}_\varphi + \left(\frac{1}{r} \frac{\partial (ru_\varphi)}{\partial r} - \frac{1}{r} \frac{\partial u_r}{\partial \varphi} \right) \cdot \mathbf{e}_z \\
 \nabla^2 u & \quad \frac{1}{r} \frac{\partial}{\partial r} \left[r \frac{\partial u}{\partial r} \right] + \frac{1}{r^2} \frac{\partial^2 u}{\partial \varphi^2} + \frac{\partial^2 u}{\partial z^2}
 \end{aligned}$$

Spherical Coordinates

$$x = r \cdot \cos \varphi \sin \theta, y = r \cdot \sin \varphi \cdot \sin \theta, z = r \cdot \cos \theta$$

$$\mathbf{grad} \, u \quad \frac{\partial u}{\partial r} \cdot \mathbf{e}_r + \frac{1}{r} \frac{\partial u}{\partial \theta} \cdot \mathbf{e}_\theta + \frac{1}{r \sin \theta} \frac{\partial u}{\partial \varphi} \cdot \mathbf{e}_\varphi$$

$$\operatorname{div} \mathbf{u} \quad \frac{1}{r^2} \frac{\partial}{\partial r} (r^2 u_r) + \frac{1}{r \cdot \sin \theta} \frac{\partial}{\partial \theta} (u_\theta \sin \theta) + \frac{1}{r \cdot \sin \theta} \frac{\partial u_\varphi}{\partial \varphi}$$

$$\begin{aligned} \mathbf{curl} \, \mathbf{u} \quad & \left(\frac{1}{r \sin \theta} \frac{\partial (u_\varphi \sin \theta)}{\partial \theta} - \frac{1}{r \sin \theta} \frac{\partial u_\theta}{\partial \varphi} \right) \cdot \mathbf{e}_r + \left(\frac{1}{r \sin \theta} \frac{\partial u_r}{\partial \varphi} - \frac{1}{r} \frac{\partial (r u_\varphi)}{\partial r} \right) \cdot \mathbf{e}_\theta \\ & + \left(\frac{1}{r} \frac{\partial (r u_\theta)}{\partial r} - \frac{1}{r} \frac{\partial u_r}{\partial \theta} \right) \cdot \mathbf{e}_\varphi \end{aligned}$$

$$\nabla^2 u \quad \frac{1}{r^2} \frac{\partial}{\partial r} \left(r^2 \frac{\partial u}{\partial r} \right) + \frac{1}{r^2 \sin \theta} \frac{\partial}{\partial \theta} \left(\sin \theta \frac{\partial u}{\partial \theta} \right) + \frac{1}{(r \sin \theta)^2} \frac{\partial^2 u}{\partial \varphi^2}$$

Chapter 1

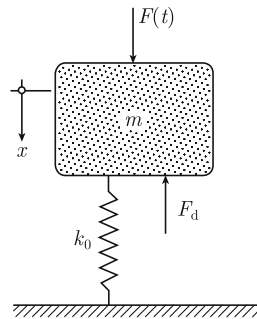
Mechanical Systems with One Degree of Freedom

In noise reducing engineering, the consequences of changes made to a system must be understood. Questions posed could be on the effects of changes to the mass, stiffness, or losses of the system and how these changes can influence the vibration of or noise radiation from some structures. Real constructions certainly have many or in fact infinite modes of vibration. However, to a certain extent, each mode can often be modeled as a simple vibratory system. The most simple vibratory system can be described by means of a rigid mass, mounted on a vertical mass less spring, which in turn is fastened to an infinitely stiff foundation. If the mass can only move in the vertical direction along the axis of the spring, the system has one degree of freedom (1-DOF). This is a vibratory system never actually encountered in practice. However, certain characteristics of systems with many degrees of freedom, or rather, continuous systems with an infinite degree of freedom, can be demonstrated by means of the very simple 1-DOF model. For this reason, the basic mass–spring system is used in this chapter to illustrate some of the basic concepts concerning free vibrations, transient, harmonic and other types of forced excitation. Kinetic and potential energies are discussed as well their dependence on the input power to the system and its losses.

1.1 A Simple Mass–Spring System

A simple mass–spring system is shown in Fig. 1.1. The mass is m and the spring constant k_0 . The foundation to which the spring is coupled is completely stiff and unyielding. It is assumed that the spring is mass less and that the spring force follows the simple Hooke's law. Thus, when the spring is compressed the distance x , the reacting force from the spring on the mass is equal to k_0x . The damping force due to losses in the system is denoted F_d . When the system is at rest, the damping force F_d is equal to zero. The static load on the spring is mg where g is the acceleration due to gravity. Due to the static load, the spring is compressed the distance Δx . The reacting force on the mass is $k_0 \cdot \Delta x$. Thus

Fig. 1.1 Simple mass–spring system



$$\Delta x \cdot k_0 = mg \quad (1.1)$$

Therefore, in principle if the static deflection is known, then the spring constant can be determined. However, for real systems, the static and dynamic stiffness are not necessarily equal. In particular, this is quite evident for various types of rubber springs. In addition, a real mount has a certain mass.

Figure 1.1 shows a simple mass–spring system excited by an external force $F(t)$ and a damping force F_d . The equation of motion for this simple system is

$$m\ddot{x} + k_0x + F_d = F(t) \quad (1.2)$$

The deviation of the mass from its equilibrium position is $x = x(t)$. When the mass is at rest, then $x = 0$. The damping force F_d is determined by the losses in the system. Various processes can cause these losses. Some examples of often used simple theoretical models are:

- (i) Viscous damping;
- (ii) Structural or hysteretic damping;
- (iii) Frictional losses or Coulomb damping;
- (iv) Velocity squared damping.

The damping forces can be illustrated by assuming a simple harmonic displacement of the mass. The motion is given by $x = x_0 \cdot \sin(\omega t)$. Here time is t and $\omega = 2\pi f$ where ω is the angular frequency and f the corresponding frequency. The damping forces for the four cases are:

- (i) Viscous damping

$$F_d = c\dot{x} = cx_0\omega \cdot \cos(\omega t) \quad (1.3)$$

The damping force is proportional to the velocity \dot{x} of the mass, c is a constant. The energy dissipated per cycle, i.e., in a time interval $t_0 \leq t \leq t_0 + T$, where $\omega T = 2\pi$, depends linearly on ω , the angular frequency of oscillation. This type of damping occurs for small velocities for a surface sliding on a fluid film and for dashpots and hydraulic dampers.

(ii) Structural damping

$$F_d = \frac{\alpha}{\pi\omega} \cdot \dot{x} = \frac{\alpha}{\pi} \cdot x_0 \cdot \cos(\omega t) \quad (1.4)$$

The amplitude of the damping force is proportional to the amplitude of the displacement but independent of the frequency for harmonic oscillations. The energy dissipated per cycle of motion is frequency independent over a wide frequency range and proportional to the square of the amplitude of vibration. The losses in solids can often be described in this way. In Eq. (1.4) α is a constant.

(iii) Frictional damping

$$F_d = \pm F \quad (1.5)$$

The frictional force has a constant magnitude. The plus or minus sign should be determined so that the frictional force is counteracting the motion of the mass. The frictional force can be due to sliding between dry surfaces.

(iv) Velocity squared damping

$$F_d = \pm q \cdot \dot{x}^2 = \pm q \cdot (x_0\omega \cdot \cos(\omega t))^2 \quad (1.6)$$

The damping force is proportional to the velocity squared and the sign should be chosen so that the force again is counteracting the motion of the mass. In Eq. (1.6) q is a constant. A body moving fairly rapidly in a fluid could cause this damping force.

The structural damping of Eq. (1.4) only applies for a harmonic displacement of the mass. A more general description of structural damping is presented in Chap. 3. Examples of energy dissipation due to viscous, structural, and frictional losses are given in Problems 1.1–1.3.

The force required for moving the mass of a simple 1-DOF system depends on the type damping in the spring. For maintaining a motion $x = x_0 \cdot \sin(\omega t)$ of the mass, the force which must be applied to the mass is obtained from Eq. (1.2) as $F = m\ddot{x} + k_0x + F_d$. Two cases are illustrated in Figs. 1.2 and 1.3. In the first example, Fig. 1.2, the damping force is viscous. An ellipse represents the force-displacement relationship for this case. The minor axis of the ellipse is proportional

Fig. 1.2 Force-displacement curve for sinusoidal motion of a 1-DOF system with viscous damping

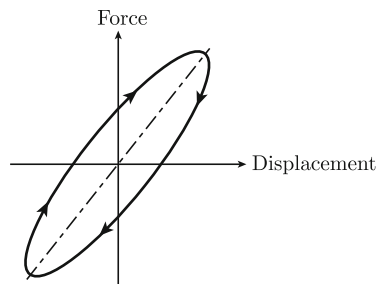


Fig. 1.3 Force-displacement curve for sinusoidal motion of a 1-DOF system with frictional damping

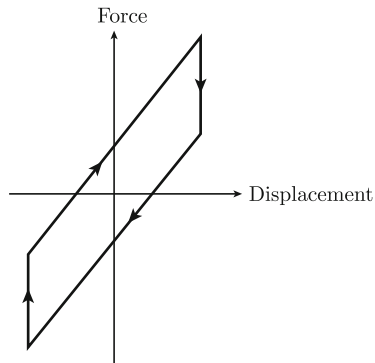
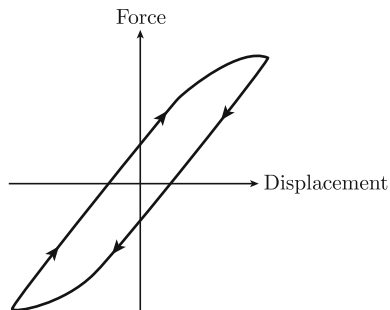


Fig. 1.4 Force-displacement curve for sinusoidal motion of a 1-DOF system with distorted structural or hysteretic damping



to the angular frequency ω and the parameter c of Eq. (1.3). Structural damping gives the same type of force-displacement curve. However, for this case the minor axis of the ellipse is just proportional to the coefficient α , Eq. (1.4), and not to the angular frequency. In the second example, Fig. 1.3, the mass is exposed to frictional damping. The arrow in the diagram indicates how force and displacement vary as time increases. The area enclosed by one loop is equivalent to the energy required to perform one cycle of motion of the mass. For a system with structural damping, the energy dissipated per cycle is independent of the angular frequency. This is not the case when the losses are viscous as discussed in Problems 1.1 and 1.2.

Real structures subjected to vibrations tend to show a force-displacement behaviour shown in Fig. 1.4. The force-displacement curve follows a distorted hysteresis loop, which is not readily described mathematically or physically. However, in general, the energy dissipated per cycle rather than the exact force-displacement relationship is of primary importance for real vibratory systems. Therefore, for most practical purposes viscous or material or for that matter a frequency dependent damping can be assumed for the simple harmonic motion of a structure.

Frictional losses and velocity squared damping result in nonlinear equations when introduced in Eq. (1.2). Examples of nonlinear equations and their solutions are presented for example Refs. [1–3]. The Runge–Kutta method, used for numerical solutions in the time domain, is discussed in Refs. [1, 4, 5].

For linear problems, damping is often described as viscous or structural. In practice, this is not necessarily the case. However, if, for example the losses are small and almost structural, the parameter α in Eq. (1.4) can be allowed to depend on frequency for harmonic or approximately harmonic motion. This type of damping model is discussed in subsequent chapters. Further and most importantly, if viscous or structural damping is introduced in Eq. (1.2), the resulting equation of motion is linear.

For some applications, like experimental modal analysis and finite element calculations, a certain form of damping is often assumed, see Chap. 10. A specific damping model might be necessary for mathematical or numerical reasons. However, the model could violate the physical characteristics of the damping mechanism.

1.2 Free Vibrations

Free vibrations of a system occur if for example the system at a certain instant is given a displacement from its equilibrium position or an initial velocity at that particular time. After this initial excitation, no external forces are applied to the system. The resulting motion of the system is due to free vibrations. For all natural systems, there is always some type of damping present. For such systems, the free vibrations die out after a certain length of time. The initial energy of the system is absorbed by losses.

For a simple mass–spring system (1-DOF) with viscous losses, the equation of motion for free vibrations, $F(t) = 0$, given by Eqs. (1.2) and (1.3) as

$$m\ddot{x} + c\dot{x} + k_0x = 0 \quad (1.7)$$

The general boundary conditions or initial values are

$$x(0) = x_0, \quad \dot{x}(0) = v_0 \quad (1.8)$$

The traditional approach to solving this equation is to assume a solution of the form

$$x(t) = A \cdot e^{\lambda t} \quad (1.9)$$

The eigenvalue λ is obtained by inserting this expression in Eq. (1.7). Consequently,

$$\lambda^2 m + \lambda c + k_0 = 0 \quad (1.10)$$

It is convenient to define the following parameters:

$$\omega_0^2 = k_0/m, \quad \beta = c/(2m) \quad (1.11)$$

Using these parameters, the solution to Eq. (1.10) is

$$\lambda_{1,2} = -\beta \pm \sqrt{\beta^2 - \omega_0^2} \quad \text{or} \quad \lambda_{1,2} = -\beta \pm i\sqrt{\omega_0^2 - \beta^2} \quad (1.12)$$

with $i = \sqrt{-1}$. In general, there are two solutions to Eq. (1.7). The expression for the displacement x is therefore of the form

$$x(t) = A_1 \cdot e^{\lambda_1 t} + A_2 \cdot e^{\lambda_2 t} \quad (1.13)$$

The parameters A_1 and A_2 are determined from the initial condition (1.8).

The general result (1.13) can be written in a more tractable way depending on the magnitude of ω_0 as compared to β .

For $\omega_0 > \beta$ the eigenvalues $\lambda_{1,2}$ are complex. Introducing the real parameter ω_r as

$$\omega_r = \sqrt{\omega_0^2 - \beta^2} \quad (1.14)$$

the general solution (1.13) is written

$$x(t) = A_1 \cdot e^{-\beta t - i\omega_r t} + A_2 \cdot e^{-\beta t + i\omega_r t}$$

or

$$x(t) = e^{-\beta t} (B_1 \cdot \sin \omega_r t + B_2 \cdot \cos \omega_r t) \quad (1.15)$$

where B_1 and B_2 are some new parameters to be determined from the initial conditions. The equalities

$$\sin \alpha = (e^{i\alpha} - e^{-i\alpha}) / 2i \quad \text{and} \quad \cos \alpha = (e^{i\alpha} + e^{-i\alpha}) / 2$$

have been used to obtain Eq. (1.15). The initial conditions (1.8) in combination with Eq. (1.15) yield for $t \geq 0$

$$x(t) = e^{-\beta t} \left(x_0 \cos \omega_r t + \frac{v_0 + \beta x_0}{\omega_r} \sin \omega_r t \right) \quad (1.16)$$

The motion $x(t)$ of the mass is described by a damped oscillatory motion as shown in Fig. 1.5 for $\omega_0 > \beta$. The angular frequency of the oscillations is given by the system parameters: stiffness, mass, and losses. The decay rate of the oscillations depends on the damping of the system.

When the damping or β is increased, the angular frequency ω_r decreases and approaches zero as β approaches ω_0 . For the limiting case

$$\lim_{\beta \rightarrow \omega_0} \cos \omega_r t = 1 \quad \text{and} \quad \lim_{\beta \rightarrow \omega_0} \frac{\sin \omega_r t}{\omega_r} = t$$

Fig. 1.5 Damped oscillatory motion of a 1-DOF system

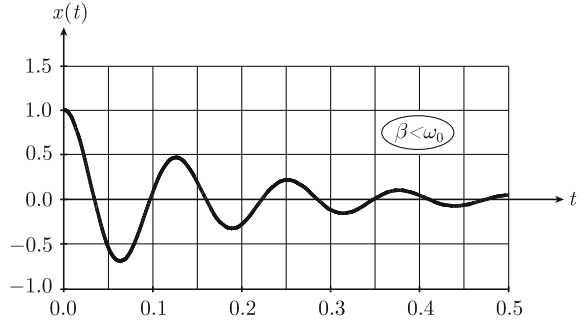
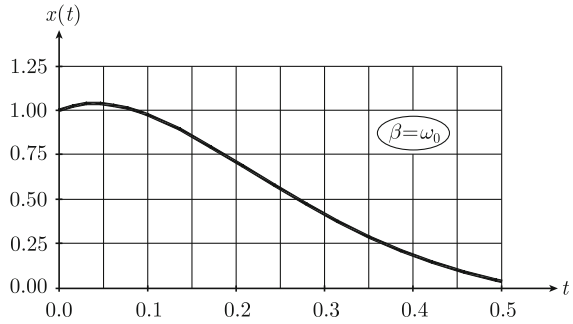


Fig. 1.6 Motion of a critically damped 1-DOF system



Thus, for the case $\beta = \omega_0$ the solution (1.16) is

$$x(t) = e^{-\beta t} [x_0 + t(v_0 + \beta x_0)] \quad (1.17)$$

The result is a critically damped motion for $t \geq 0$ shown in Fig. 1.6.

For a heavily damped system $\beta > \omega_0$. For this case, the eigenvalues (1.12) are written:

$$\lambda_{1,2} = -\beta \pm \gamma, \quad \gamma = \sqrt{\beta^2 - \omega_0^2} \quad (1.18)$$

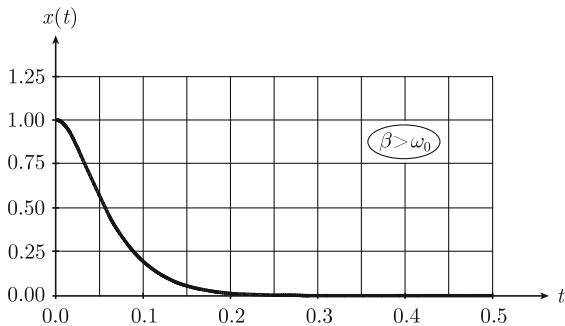
The parameter γ is real for $\beta > \omega_0$. The solution for this case is obtained from (1.16) by replacing ω_r by $i\gamma$ since $\omega_r = \sqrt{\omega_0^2 - \beta^2} = i\sqrt{\beta^2 - \omega_0^2} = i\gamma$. Thus according to definition

$$\begin{aligned} \cos \omega_r t &= (e^{i\omega_r t} + e^{-i\omega_r t}) / 2 = (e^{-\gamma t} + e^{\gamma t}) / 2, \\ \sin \omega_r t &= (e^{i\omega_r t} - e^{-i\omega_r t}) / 2i = (e^{-\gamma t} - e^{\gamma t}) / 2i \end{aligned}$$

Thus for $\beta > \omega_0$ and $t \geq 0$ the displacement $x(t)$ is given by

$$x(t) = \frac{e^{-\beta t}}{2\gamma} \{e^{\gamma t} [x_0(\gamma + \beta) + v_0] + e^{-\gamma t} [x_0(\gamma - \beta) - v_0]\} \quad (1.19)$$

Fig. 1.7 Motion of a heavily damped 1-DOF system



The result is a nonoscillatory motion of the mass as shown in Fig. 1.7.

Mathematically, the solutions to the three cases $\beta < \omega_0$, $\beta = \omega_0$ and $\beta > \omega_0$ are basically the same. However, the physical interpretations of the results are most apparent from the expressions (1.16), (1.17) and (1.19).

In most practical cases in vibro-acoustics, losses are small, i.e., $\beta < \omega_0$. In fact, as discussed later, typical losses for vibrating structures, which radiates sound in the audible frequency range, satisfy the inequality $\beta \ll \omega_0$. These structures are consequently lightly damped. For a lightly damped 1-DOF system performing an oscillatory motion, the displacement is given by (1.16) as

$$x(t) = e^{-\beta t} \left(x_0 \cos \omega_r t + \frac{v_0 + \beta x_0}{\omega_r} \sin \omega_r t \right)$$

The system oscillates with the frequency $f_r = \omega_r/(2\pi) = \sqrt{\omega_0^2 - \beta^2}/(2\pi)$. Whatever the initial conditions are, a freely lightly damped vibrating 1-DOF system oscillates with a natural, eigen or characteristic frequency f_r , which is a function of mass, stiffness and damping of the system.

The displacement, Eq. (1.16), can also be written as

$$x(t) = C \cdot e^{-\beta t} \cdot \sin(\omega_r t + \varphi) = C \cdot e^{-\beta t} \cdot (\sin \omega_r t \cdot \cos \varphi + \cos \omega_r t \cdot \sin \varphi) \quad (1.20)$$

The amplitude C and the phase angle φ are obtained by comparing the two expressions defining $x(t)$. Consequently, for equality at any time t , it follows that

$$C \cos \varphi = (v_0 + \beta x_0)/\omega_r, \quad C \sin \varphi = x_0$$

and thus

$$\tan \varphi = x_0 \omega_r / (v_0 + \beta x_0), \quad C = \sqrt{v_0^2 + \omega_0^2 x_0^2 + 2\beta x_0 v_0 / \omega_r} \quad (1.21)$$

Based on the expressions (1.20) and (1.21) the kinetic and potential energies can be derived. The potential energy \mathcal{U} stored in a mass less spring with the spring constant k_0 is

$$\mathcal{U} = \int dx \cdot k_0 x = k_0 x^2 / 2$$

The time average of the potential energy over a period T where $T\omega_r = 2\pi$ is

$$\bar{\mathcal{U}}_T = \frac{1}{2T} \int_t^{t+T} dt \cdot k_0 \cdot e^{-2\beta t} \cdot C^2 \sin^2(\omega_r t + \varphi) \quad (1.22)$$

The subscript T denotes that the potential energy is averaged over one period. In general, for a lightly damped system radiating sound in the audible frequency range $\beta T \ll 1$. This means that the exponential function in the integral (1.22) is approximately constant and equal to $\exp(-2\beta t)$ in the time interval of integration. Considering this the integral (1.22) defining $\bar{\mathcal{U}}$ can be approximated by the expression

$$\bar{\mathcal{U}}_T \approx \frac{e^{-2\beta t}}{2T} \int_t^{t+T} dt \cdot k_0 \cdot C^2 \sin^2(\omega_r t + \varphi) = e^{-2\beta t} \cdot k_0 C^2 / 4 \quad (1.23)$$

Thus, the time average over a period t to $t + T$ of the potential energy is for small losses approximately decaying as $\exp(-2\beta t)$.

The velocity $\dot{x}(t)$ of the freely vibrating mass is from (1.20) obtained as

$$\dot{x}(t) = C e^{-\beta t} [\omega_r \cos(\omega_r t + \varphi) - \beta \sin(\omega_r t + \varphi)] \quad (1.24)$$

The time average of the kinetic energy over one period is

$$\bar{\mathcal{T}}_T = \frac{m}{2T} \int_t^{t+T} dt \cdot \dot{x}^2 \quad (1.25)$$

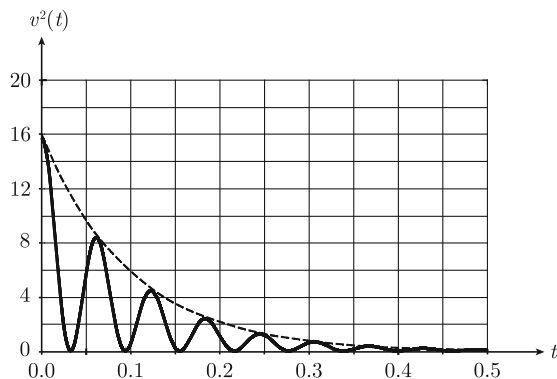
Following the same procedure as above, the average kinetic energy $\bar{\mathcal{T}}_T$ is for $\beta T \ll 1$ and when averaged over a time period t to $t + T$ given as

$$\begin{aligned} \bar{\mathcal{T}}_T &\approx \frac{m C^2 e^{-2\beta t}}{2T} \int_t^{t+T} dt \cdot \{ \omega_r^2 \cos^2(\omega_r t + \varphi) \\ &\quad + \beta^2 \sin^2(\omega_r t + \varphi) - \omega_r \beta \sin[2(\omega_r t + \varphi)] \} \\ &= \frac{m \omega_0^2 C^2 e^{-2\beta t}}{4} \end{aligned} \quad (1.26)$$

The parameter ω_0^2 is equal to k_0/m . Thus, it follows from the Eqs. (1.23) and (1.26) that

$$\bar{\mathcal{T}}_T \approx \bar{\mathcal{U}}_T \quad (1.27)$$

Fig. 1.8 Decay of the temporal average of the velocity squared of a lightly damped 1-DOF system

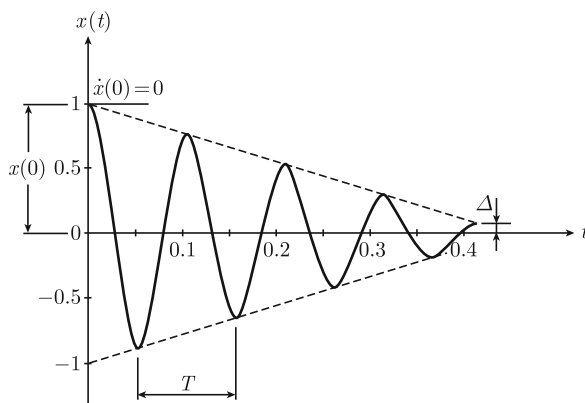


The time averages of kinetic and potential energies for a freely vibrating and lightly damped 1-DOF system are approximately equal. Equality holds for nondamped systems, i.e., for $\beta = 0$.

The velocity squared is as function of time shown in Fig. 1.8. For small losses the time average of the velocity squared decays as $\exp(-2\beta t)$. This result can be used to estimate through measurements the losses in the system. For viscous or structural damping, the time average of the kinetic energy or for that matter the total energy is decaying exponentially with time as $\exp(-2\beta t)$ if $\beta \ll \omega_0$.

For Coulomb or frictional damping it can be shown (see Problem 1.3) that the decay in amplitude per cycle is constant. Two straight lines can envelop the amplitude of the oscillating motion. The decay rate of the amplitude as a function of time is shown in Fig. 1.9. The mass is at rest at $x = \Delta$. At this position, the frictional force exceeds the spring force.

Fig. 1.9 Decay of the amplitude of a 1-DOF system with frictional damping



1.3 Transient Vibrations

When an external force is suddenly applied to a mechanical system at rest, transient vibrations are excited. Examples of transient excitation are a ship hit by a large wave, a car running on a bumpy road, an engine started up, and even the extreme case of an earthquake. For this type of excitation, it is important to estimate for the resulting motion the maximum deflection, velocity, or acceleration of the system. A severe transient excitation can cause great damage to a system. In its milder form it could, for example, be a resiliently mounted engine in a car or a ship vibrating so violently that damage is caused to the adjoining structures.

A simple case of transient excitation can be demonstrated by means of the simple mass–spring system. The mass is initially at rest when at time $t = 0$ the system or mass is given an impulse I . The equation of motion for the mass can be written as:

$$m\ddot{x} + c\dot{x} + k_0x = I \cdot \delta(t) \quad (1.28)$$

The displacement and the impulse are positive in the same direction. Since the mass initially is at rest, it follows that

$$x(t) = 0 \text{ for } t \leq 0 \quad (1.29)$$

In Eq. (1.28) I is the magnitude of the impulse and $\delta(t)$ the Dirac pulse defined so that

$$\delta(t) = 0 \text{ for } t \neq 0, \quad \lim_{\varepsilon \rightarrow 0} \int_{-\varepsilon}^{\varepsilon} dt \cdot \delta(t) = 1 \quad (1.30)$$

The expression $I \cdot \delta(t)$ is defined as the force $F(t)$ acting on the system since

$$\int F(t)dt = \int I\delta(t)dt = I$$

For $t > 0$ no external force is applied to the system resulting in free vibrations. If, according to the discussion in Sect. 1.2, $\beta < \omega_0$ the result for $t > 0$ is given by

$$x(t) = e^{-\beta t} \frac{v_0}{\omega_r} \sin \omega_r t \quad (1.31)$$

This is obtained from Eq. (1.16) for $x_0 = 0$. The unknown parameter in Eq. (1.31) is the initial velocity v_0 of the mass. However, this velocity is obtained from Eq. (1.28). This expression is integrated with respect time as

$$\int_{-\varepsilon}^{\varepsilon} dt (m\ddot{x} + c\dot{x} + k_0x) = \int_{-\varepsilon}^{\varepsilon} dt I \cdot \delta(t) = I \quad (1.32)$$

The result is

$$m\dot{x}(\varepsilon) - m\dot{x}(-\varepsilon) + cx(\varepsilon) - cx(-\varepsilon) + \int_{-\varepsilon}^{\varepsilon} dt k_0 x = I \quad (1.33)$$

Initially, the mass is at rest. Thus $x(-\varepsilon) = \dot{x}(-\varepsilon) = 0$. Since x is a continuous function, the integral in Eq. (1.33) approaches zero as ε goes to zero. Considering the initial condition $x(0) = 0$, the limiting case as $\varepsilon \rightarrow 0$ gives

$$m\dot{x}(0) = I \quad (1.34)$$

This is the second initial condition. The first, $x(0) = 0$, is given by (1.29). With $\dot{x}(0) = v_0 = I/m$ the motion of the mass is according to Eqs. (1.31) and (1.34)

$$x(t) = e^{-\beta t} \frac{I}{m\omega_r} \sin \omega_r t \quad (1.35)$$

where as before

$$\beta = \frac{c}{2m}, \quad \omega_r = \sqrt{\frac{k_0}{m} - \left(\frac{c}{2m}\right)^2} = \sqrt{\omega_0^2 - \beta^2}$$

The response to a unit pulse at $t = 0$, i.e., $I = 1$ is defined as:

$$h(t) = e^{-\beta t} \frac{1}{m\omega_r} \sin \omega_r t \quad (1.36)$$

This result can form the basis for the solution to the general problem when an external time-dependent force $F(t)$ excites the mass.

The equation of motion for the general case is

$$m\ddot{x} + c\dot{x} + k_0x = F(t) \quad (1.37)$$

where

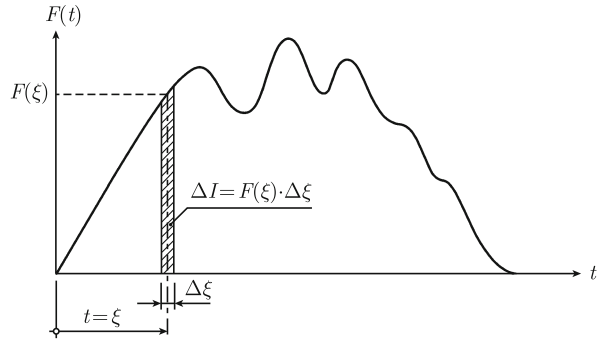
$$F(t) = 0 \quad \text{for } t < 0$$

The force acting on the mass is shown in Fig. 1.10 as function of time. At the time $t = \xi$, the system is given an impulse $\Delta I = \Delta \xi \cdot F(\xi)$. According to Eq. (1.36), the resulting deflection Δx caused by the impulse ΔI is

$$\Delta x = \Delta I \cdot h(t - \xi) = \Delta \xi \cdot F(\xi) \cdot h(t - \xi)$$

The total response at time t is the sum of all separate impulses up to that time. In integral form, the result to Eq. (1.37) is

Fig. 1.10 Force as function of time and fractional impulse at $t = \xi$



$$x(t) = \int_0^t d\xi \cdot F(\xi) \cdot h(t - \xi) \quad (1.38)$$

Since $F(\xi) = 0$ for $\xi < 0$, Eq. (1.37) can also be written as

$$x(t) = \int_{-\infty}^t d\xi \cdot F(\xi) \cdot h(t - \xi)$$

Since $h(t - \xi) = 0$ for $\xi \geq t$ it follows that the upper limit of the integral can be extended to plus infinity. The integral is the convolution of the input $F(t)$ with the impulse response $h(t)$ or

$$x(t) = \int_{-\infty}^{\infty} d\xi \cdot F(\xi) \cdot h(t - \xi) \quad (1.39)$$

Symbolically this result is often written

$$x(t) = F(t) * h(t)$$

This expression can be written again in an alternative way by a change of variables or by introducing the parameter τ as $\tau = t - \xi$. Thus

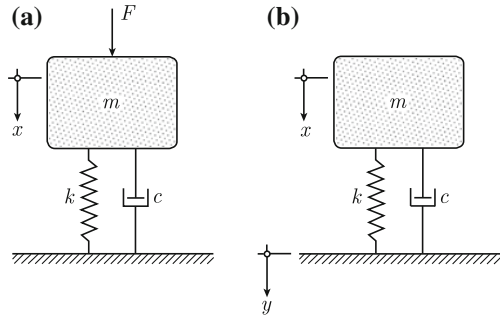
$$x(t) = \int_{-\infty}^{\infty} d\tau \cdot F(t - \tau) \cdot h(\tau)$$

This result can be achieved in alternative way as suggested by Green and demonstrated in Problem 1.12. The starting point are the two equations

$$m\ddot{h} + c\dot{h} + k_0h = \delta(t - \tau), \quad m\ddot{x} + c\dot{x} + k_0x = F(t)$$

The solution to the first is given by Eq. (1.36). By multiplying the first equation by x and the second by h and integrating the resulting equations with respect to t ,

Fig. 1.11 Excitation of a mass due to **a** external force
b motion of foundation



the displacement $x(t)$ is obtained in integral form as shown in Problem 1.12. The procedure proposed by Green is also used in Sect. 6.2 to determine the response of a beam excited by a point force. Compare also Sect. 7.3.

For an ideal mass–spring system, the impulse excitation of the mass can basically be caused by a sudden motion of the foundation or by an external force acting on a mass mounted resiliently on a firm foundation as shown in Fig. 1.11.

The equations describing the motion of the mass in the two examples are

$$\text{Case A} \quad m\ddot{x} + c\dot{x} + k_0x = F(t) \quad (1.40)$$

$$\text{Case B} \quad m\ddot{x} + c(\dot{x} - \dot{y}) + k_0(x - y) = 0 \quad (1.41)$$

In the last expression, the substitution $z = x - y$ can be made. This leads to the following expressions

$$m\ddot{z} + c\dot{z} + k_0z = -m\ddot{y} = F_f(t) \quad (1.42)$$

The general solutions to Eqs. (1.40) and (1.41) are according to Eq. (1.38)

$$\text{Case A} \quad x(t) = \int_0^t F(\xi) \cdot h(t - \xi) \cdot d\xi$$

$$\text{Case B} \quad x(t) = y(t) + \int_0^t d\xi \cdot F_f(\xi) \cdot h(t - \xi) \quad (1.43)$$

$$= y(t) - \int_0^t d\xi \cdot m\ddot{y}(\xi) \cdot h(t - \xi) \quad (1.44)$$

The function $h(t)$ is defined in Eq. (1.36). Two basic types of transient excitation—a step and pulse displacement of the foundation are discussed below.

In the first case, the foundation is given the displacement

$$y = A(1 - e^{-\gamma t}) \quad (1.45)$$

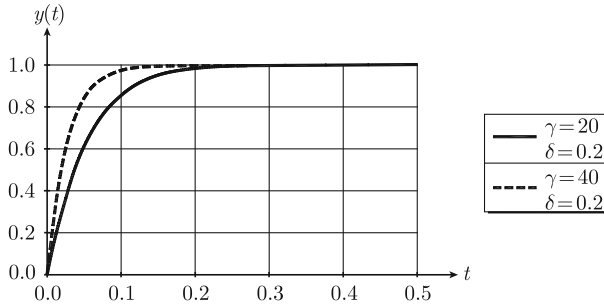


Fig. 1.12 Step displacement of foundation

Consequently as the parameter γ is increased, the gradient of the displacement curve increases as shown in Fig. 1.12. According to Eq. (1.44), the response $x(t)$ of the mass due to the motion of the foundation is given by

$$x(t) = A \left[1 - \exp(-\gamma t) + m\gamma^2 \int_0^t h(t - \xi) \cdot \exp(-\gamma \xi) \cdot d\xi \right]$$

where

$$h(t - \xi) = \frac{e^{-\beta(t-\xi)}}{m\omega_r} \sin \omega_r(t - \xi) \quad (1.46)$$

The integral is solved by means of partial integration. The result is:

$$x(t) = A \left[1 - \exp(-\gamma t) + \frac{\gamma^2 \Gamma(t)}{\omega_r [(\beta - \gamma)^2 + \omega_r^2]} \right]$$

$$\Gamma(t) = \omega_r e^{-\gamma t} - (\beta - \gamma) e^{-\beta t} \sin \omega_r t - \omega_r e^{-\beta t} \cos \omega_r t \quad (1.47)$$

From Eq. (1.47), the velocity and acceleration as well as the maximum deflection, velocity, and acceleration can be calculated.

In Fig. 1.13, the response x is presented for two different values of γ . The other parameters m , c , k_0 and A are constant. The figure shows that the maximum amplitude is increased when γ is increased, i.e., as the slope of the deflection curve for the foundation is increased. As time goes to infinity, the deflection of the mass approaches A , which is also the final deflection for the foundation. In Fig. 1.14, the deflection of the mass is shown for two different damping ratios. When the damping is increased by a factor 2.5, the amplitude of the mass is decreasing more rapidly as a function of time. Despite this, the maximum amplitude is just slightly reduced.

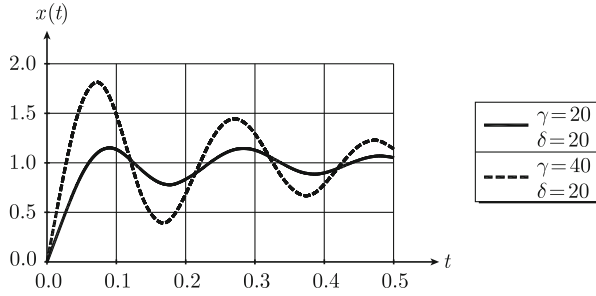


Fig. 1.13 Response of a mass caused by a step displacement of foundation

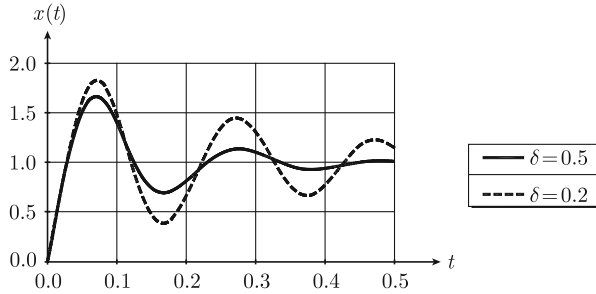


Fig. 1.14 Response of a mass with respect to time for two damping ratios, $\gamma = 40$

In the second example, the displacement y of the foundation is defined as

$$\begin{aligned} y(t) &= A \sin \omega t \quad \text{for } 0 \leq t \leq t_0 \\ y(t) &= 0 \quad \text{for } t < 0 \text{ and } t > t_0 \end{aligned} \quad (1.48)$$

where $t_0 = \pi/\omega$. The motion of the mass is again described by Eq. (1.44) and is

$$x(t) = A \left[\sin \omega t + m\omega^2 \int_0^t h(t - \xi) \sin \omega \xi \cdot d\xi \right] \quad (1.49)$$

where again $h(t)$ is defined in Eq. (1.36). Note that the upper limit t for the integral cannot exceed t_0 as $y(t)$ is only defined in the time interval $0 \leq t \leq t_0$. For $0 \leq t \leq t_0$, the solution to Eq. (1.49) is

$$\begin{aligned} x(t) &= A \left[\sin \omega t + \frac{\omega^2}{\omega_r} (H_1 - H_2) \right] \\ H_1 &= \frac{\beta \cos \omega t + (\omega + \omega_r) \sin \omega t - \beta e^{-\beta t} \cos \omega_r t + (\omega + \omega_r) e^{-\beta t} \sin \omega_r t}{2[(\omega + \omega_r)^2 + \beta^2]} \\ H_2 &= \frac{\beta \cos \omega t + (\omega - \omega_r) \sin \omega t - \beta e^{-\beta t} \cos \omega_r t - (\omega - \omega_r) e^{-\beta t} \sin \omega_r t}{2[(\omega - \omega_r)^2 + \beta^2]} \end{aligned} \quad (1.50)$$

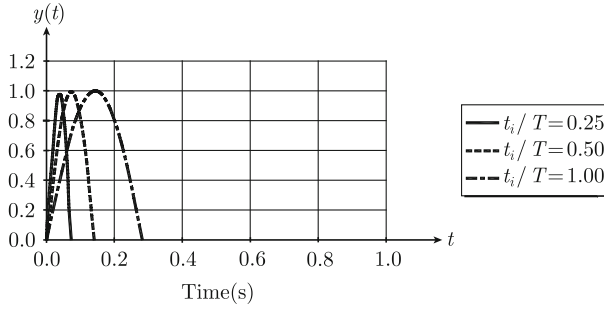


Fig. 1.15 Displacement $y(t)$ of foundation

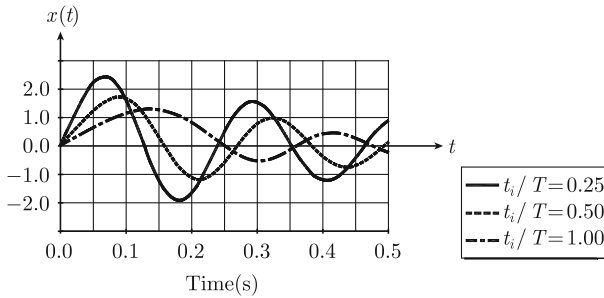


Fig. 1.16 Response of mass caused by displacement $y(t)$ of foundation

From these expressions, the deflection $x_0 = x(t_0)$ and velocity $v_0 = \dot{x}(t_0)$ can be calculated. For $t > t_0$, no external force is acting on the system thus the motion of the mass is determined by free vibrations. According to Eq. (1.16), the motion of the mass for $t \geq t_0$ is

$$x(t) = e^{-\beta(t-t_0)} \left\{ x_0 \cos [\omega_r(t - t_0)] + \frac{v_0 + \beta x_0}{\omega_r} \sin [\omega_r(t - t_0)] \right\} \quad (1.51)$$

In Fig. 1.15, the deflection of the foundation is shown as a function of time for three different values of ω , i.e., for three different pulse lengths t_0 .

The corresponding response $x(t)$ for the mass is shown in Fig. 1.16. It is evident that the response very much depends on the length of time, t_0 , of the exciting pulse with respect to the time T for one cycle corresponding to free vibrations of the mass–spring system. The peak amplitude A of the pulse is constant in the example. For a short pulse, the acceleration of the foundation is initially large. This results in a large early displacement of the mass. The resulting amplitude is thus a function of the slope of the curve defining the displacement of the foundation as well as the length of the pulse. The importance of the pulse length can be illustrated by considering a 1-DOF system mounted on a fixed foundation and excited by an external force $F(t)$ corresponding to Case A discussed above. For a resiliently mounted mass excited by

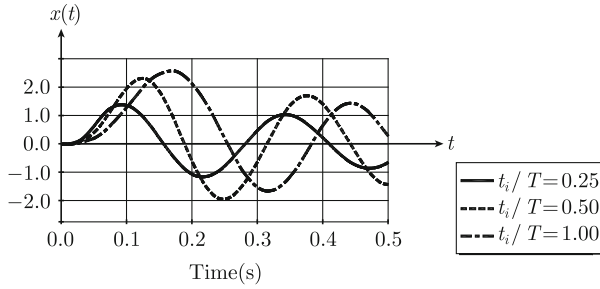


Fig. 1.17 Response of mass excited by a force $F(t) = y(t)$

a force with the time dependence of a half sine wave, the response is obtained from the Eq. (1.43) and by comparing the results (1.49) and (1.50). Thus, let a force $F(t)$ excite the mass. The force is defined as

$$\begin{aligned} F(t) &= F_0 \sin(\omega t) \text{ for } 0 \leq t \leq t_0 \\ F(t) &= 0 \text{ for } t < 0 \text{ and } t > t_0 \end{aligned} \quad (1.52)$$

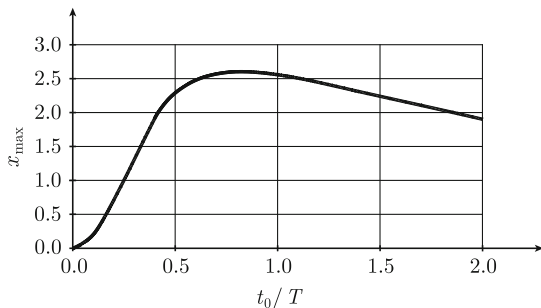
where $t_0 = \pi/\omega$. The response $x(t)$ of the 1-DOF system is for a fixed foundation, $y = 0$, equal to

$$x(t) = F_0 \frac{H_1(t) - H_2(t)}{m\omega_r} \text{ for } 0 \leq t \leq t_0 \quad (1.53)$$

The functions H_1 and H_2 are defined in Eq. (1.50). For $t > t_0$, i.e., for free vibrations, the response is given by Eq. (1.51). The parameters x_0 and v_0 are as before the displacement and velocity at $t = t_0$. In Fig. 1.17, the response due to a force in the shape of a half sine wave is shown. The duration or pulse length of the half sine wave is set equal to $T/4$, $T/2$, and T as in the previous case. The force functions have the same time dependence as the displacements $y(t)$ shown in Fig. 1.15. The resulting response of the mass due to this type of force excitation is illustrated in Fig. 1.17. The initial slopes of the response curves are different as compared to the previous case (motion of foundation). For force excitation of the mass, its initial velocity is equal to zero. The response of the mass again depends on the duration of the pulse exciting the system. The maximum displacement of the mass can be calculated from Eq. (1.53). In Fig. 1.18, the maximum amplitude of the response is shown as function of t_0/T or the ratio between the pulse length and the time corresponding to one free oscillation of the system. The maximum amplitude increases for increasing pulse lengths up to $t_0 \approx 0.8T$ for half sine wave excitation. For other types of excitation pulses, the maximum displacement is obtained for other ratios between t_0 and T . See Problem 1.6.

One final example is of interest in connection with forced excitation discussed in the next section. Assume that the mass at time $t = 0$ is started to be excited by a harmonic force $F(t) = F_0 \cdot \sin(\omega t)$. The resulting displacement of the mass for

Fig. 1.18 Maximum amplitude as function of pulse length



$t \geq 0$ is obtained from Eq. (1.43). The calculations are somewhat laborious but still straightforward. The result is

$$x(t) = \frac{F_0[(\omega_0^2 - \omega^2) \sin(\omega t) - 2\omega\beta \cos(\omega t)]}{m[(\omega_0^2 - \omega^2)^2 + (2\beta\omega)^2]} - e^{-\beta t} \frac{F_0[(\omega_0^2 - \omega^2 - 2\beta^2) \sin(\omega_r t)(\omega/\omega_r) - 2\omega\beta \cos(\omega_r t)]}{m[(\omega_0^2 - \omega^2)^2 + (2\beta\omega)^2]} \quad (1.54)$$

The result indicates that as time goes to infinity or rather when $\exp(-\beta t) \ll 1$, the time dependence is predominately determined by the time dependence of the force. In other words, if a periodic force is applied to a damped mass–spring system, the motion of the mass shows the same periodicity as the force once the transients can be neglected. If for example $\beta t \approx 2.5$, the energy of the transient motion is of the order 1/10 of the energy of the stationary motion. After twice this time, i.e., for $\beta t \approx 5$ the ratio is 1/100. For this case, the transient vibrations can be neglected.

Clearly, the response of a dynamic system strongly depends on the rise time of the force exciting the system. The sharper the rise, the more violent is the response of the system. The maximum amplitude of the system depends primarily on the rise time rather than on the losses of the system. In noise control engineering, the rise time of any force acting on a noise radiating structure should be made as long as possible. The response of a system excited by an impulse depends not only on the rise time of the pulse but also on its duration.

For more complicated dynamic systems, transient solutions are most easily obtained by using Laplace transforms. See for example Ref. [5]. Transient vibrations of dynamic systems are discussed at length in for example Ref. [3].

1.4 Forced Harmonic Vibrations

When a harmonic force excites a damped dynamic system, the system tends to vibrate at the same frequency as that of the force. Initially, when the force is applied, the total motion is composed of transient as well as forced vibrations. The result is as shown

in Eq. (1.54). However, there are always losses in a dynamic system. Consequently the free vibrations, which are proportional to $\exp(-\beta t)$ will die out as shown in the previous section. After a certain time, depending on the losses, the forced motion will dominate completely. Transient vibrations are therefore neglected whenever a system is excited by a stationary force.

Periodic forces are typically induced by rotating machinery. A periodic force could, for example, be caused by a rotor imbalance. For each turn of the rotor, the time history of the force is repeated.

If a force $F(t)$ is repeated after the time or period T , i.e., if

$$F(t) = F(t + T) \quad (1.55)$$

then the force is said to be periodic with the period T . An example of a periodic force $F(t)$, period T , is

$$F(t) = F_0 \sin \omega t$$

where the angular frequency $\omega = 2\pi/T$. This is a harmonic force, which is the simplest type of periodic force. The force is stationary since angular frequency and amplitude are constant.

The equation of motion for the simple mass–spring system with a harmonic force applied to the mass is

$$m\ddot{x} + c\dot{x} + k_0x = F_0 \sin \omega t \quad (1.56)$$

The solution describing the forced motion must be of the form

$$\begin{aligned} x(t) &= A_1 \sin \omega t + A_2 \cos \omega t = A_0 \sin(\omega t + \varphi) \\ &= A_0 \sin \omega t \cos \varphi + A_0 \cos \omega t \sin \varphi \end{aligned} \quad (1.57)$$

In both cases, there are two unknown quantities. In the first case, A_1 and A_2 and in the second case A_0 and φ . An identification of the coefficients in Eq. (1.57) yields

$$A_0 = \sqrt{A_1^2 + A_2^2}, \quad \tan \varphi = A_2/A_1 \quad (1.58)$$

The general solution to Eq. (1.56) must also include the free vibration solution corresponding to the case when $F(t) = 0$. However due to the losses in the system, this solution can be neglected as time goes to infinity. In fact, the transient response can in most practical cases be neglected after some minute after the force have been turned on as discussed in Sect. 1.3.

If the first expression in Eq. (1.57) is inserted in Eq. (1.56) the result is

$$[A_1(k_0 - m\omega^2) - c\omega A_2] \sin \omega t + [A_2(k_0 - m\omega^2) + c\omega A_1] \cos \omega t = F_0 \sin \omega t \quad (1.59)$$

For this equation to be valid at any time t , the expression inside the bracket in front of the cosine term must be zero. Thus,

$$A_2 = -A_1 \frac{c\omega}{k_0 - m\omega^2} = -A_1 \frac{2\beta\omega}{\omega_0^2 - \omega^2}$$

where

$$\beta = \frac{c}{2m}, \quad \omega_0^2 = \frac{k_0}{m}.$$

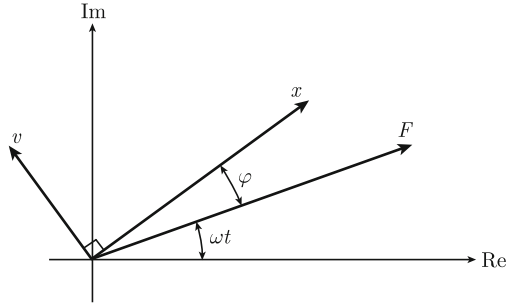
In addition, the expression in front of the sine term on the left hand side of the equation must equal F_0 . The parameters A_1 , A_2 , A_0 and φ are consequently obtained as

$$\begin{aligned} A_1 &= \frac{F_0(\omega_0^2 - \omega^2)}{m[(\omega_0^2 - \omega^2)^2 + (2\beta\omega)^2]} \\ A_2 &= -\frac{F_0 2\omega\beta}{m[(\omega_0^2 - \omega^2)^2 + (2\beta\omega)^2]} \\ A_0 &= \frac{F_0}{m[(\omega_0^2 - \omega^2)^2 + (2\beta\omega)^2]^{1/2}} \\ \tan \varphi &= -\frac{2\beta\omega}{\omega_0^2 - \omega^2} \end{aligned} \tag{1.60}$$

The same result is obtained from Eq. (1.54) when t approaches infinity. The displacement or the amplitude A_0 in (1.60) has a maximum for the denominator having a minimum. For small losses, this maximum amplitude or resonance is found when the frequency of the force exciting the system nearly coincides with the natural frequency of the system or rather when $\omega = \sqrt{\omega_0^2 - 2\beta^2}$ whereas the natural angular frequency is $\omega_r = \sqrt{\omega_0^2 - \beta^2}$. In general, the two expressions are almost equal since the losses are small or rather $\beta \ll 1$.

According to the second expression in Eq. (1.57), there is a phase difference φ between force and amplitude. The magnitude of this phase angle depends on the losses and the relative difference between the angular frequencies for the force and the undamped resonance ω_0 for the system. Thus for a force described by $F(t) = F_0 \sin \omega t$ the displacement of the mass is $x(t) = A_0 \sin(\omega t + \varphi)$ and its velocity $\dot{x}(t) = \omega A_0 \cos(\omega t + \varphi) = \omega A_0 \sin(\omega t + \varphi + \pi/2)$. These quantities can be drawn in a phase diagram as shown in Fig. 1.19. The time dependence of the functions is obtained by the projections of the various vectors on the vertical axis in the diagram. If the force is of the form $\cos \omega t$, velocity and displacement are equal to the projection of the corresponding vectors on the horizontal axis.

Fig. 1.19 Phase difference between force, displacement, and velocity



For the simple 1-DOF system excited by the force $F_0 \sin \omega t$, the time average of the velocity squared is given by

$$\begin{aligned}
 \bar{v}^2 &= \bar{\dot{x}}^2 \\
 &= \frac{1}{T} \int_0^T A_0^2 \omega^2 \cos^2(\omega t + \varphi) dt \\
 &= \frac{\omega^2 A_0^2}{2} \\
 &= \frac{\omega^2 F_0^2}{2m^2 [(\omega_0^2 - \omega^2)^2 + (2\beta\omega)^2]} \quad (1.61)
 \end{aligned}$$

Since x and thus \dot{x} are periodic, it is sufficient to take the average over only one period $T = 2\pi/\omega$.

The time average of the kinetic energy for the 1-DOF system is

$$\bar{T} = \frac{m\bar{v}^2}{2} = \frac{\omega^2 F_0^2}{4m[(\omega_0^2 - \omega^2)^2 + (2\beta\omega)^2]} \quad (1.62)$$

In a similar way, the time average of the potential energy is

$$\bar{V} = \frac{1}{T} \int_0^T dt \cdot k_0 \frac{x^2}{2} = \frac{\omega_0^2 F_0^2}{4m[(\omega_0^2 - \omega^2)^2 + (2\beta\omega)^2]} \quad (1.63)$$

For vibrations induced by a simple harmonic force described by $F_0 \sin \omega t$, the time averages of the potential and kinetic energies are not equal except when the angular frequency ω of the force is equal to ω_0 . For free vibrations, equality holds when there are no losses, or in practice when the losses are small.

The average power $\bar{\Pi}$ fed into the system during one period—or rather, the time average of the power input—is defined as

$$\begin{aligned}
 \bar{\Pi} &= \frac{1}{T} \int_0^T dt \cdot F(t) \cdot v(t) \\
 &= \frac{1}{T} \int_0^T dt \cdot F_0 \sin \omega t [A_1 \omega \cos \omega t - A_2 \omega \sin \omega t] \\
 &= -\frac{\omega A_2 F_0}{2} \\
 &= \frac{\beta \omega^2 F_0^2}{m[(\omega_0^2 - \omega^2)^2 + (2\beta\omega)^2]} \quad (1.64)
 \end{aligned}$$

From Eqs. (1.61) and (1.64) it follows that

$$\bar{\Pi} = 2\bar{v}^2 m\beta \quad \text{or} \quad \bar{v}^2 = \frac{\bar{\Pi}}{2m\beta} = \frac{\bar{\Pi}}{c} \quad (1.65)$$

This important relationship means that the average velocity squared is inversely proportional to the losses in the system if the power input to the system is constant.

1.5 Fourier Series

The response of a simple 1-DOF system is readily determined whenever the system is excited by a harmonic force. The straight forward solutions discussed in the previous section can be extended to include any 1-DOF system excited by a periodic force. Any periodic function or force can be expanded in a Fourier series. Thus if $F(t) = F(t + T)$, then the function $F(t)$ can be written as

$$F(t) = \frac{a_0}{2} + \sum_{n=1}^{\infty} (a_n \cdot \cos \omega_n t + b_n \cdot \sin \omega_n t) \quad (1.66)$$

where $\omega_n = 2\pi n/T$ for $n = 1, 2, \dots$. The coefficients a_n and b_n are derived as demonstrated in Problem 1.8. For $n = 0, 1, 2, \dots$, the coefficients a_n and b_n are

$$a_n = \frac{2}{T} \int_0^T F(t) \cos \omega_n t \cdot dt, \quad b_n = \frac{2}{T} \int_0^T F(t) \sin \omega_n t \cdot dt \quad (1.67)$$

There are alternative ways of expanding the function $F(t)$ in the time interval $0 \leq t \leq T$. This is demonstrated by first defining a new function $G_1(t)$ as:

$$G_1(t) = F(t) \quad \text{for } 0 \leq t \leq T, \quad G_1(t) = -F(-t) \quad \text{for } -T \leq t < 0$$

The function $G_1(t)$ is assumed to be periodic with the period $T_0 = 2T$. A Fourier expansion of $G_1(t)$ in the time interval $-T \leq t \leq T$ as given by Eq. (1.66) yields:

$$G_1(t) = \sum_{n=1}^{\infty} b_n \cdot \sin(\omega_n t/2)$$

However, $G_1(t) = F(t)$ for $0 \leq t \leq T$. Thus in this time interval $F(t)$ is obtained as

$$F(t) = \sum_{n=1}^{\infty} b_n \cdot \sin(\omega_n t/2) = \sum_{n=1}^{\infty} b_n \cdot \sin(n\pi t/T) \quad (1.68)$$

The coefficients b_n are given by Eq. (1.67) as

$$b_n = \frac{2}{T} \int_0^T dt \cdot F(t) \sin(n\pi t/T) \quad (1.69)$$

Yet another possibility to expand $F(t)$ in a series is obtained by defining a function $G_2(t)$ as

$$G_2(t) = F(t) \text{ for } 0 \leq t \leq T, \quad G_2(t) = F(-t) \text{ for } -T \leq t < 0$$

A Fourier expansion of $G_2(t)$ in the time interval $-T \leq t \leq T$ yields:

$$G_2(t) = \frac{a_0}{2} + \sum_{n=1}^{\infty} a_n \cdot \cos(\omega_n t/2)$$

where $\omega_n = 2\pi n/T$ for $n = 1, 2, \dots$. However, $G_2(t) = F(t)$ for $0 \leq t \leq T$. Thus in this time interval $F(t)$ is obtained as

$$F(t) = \frac{a_0}{2} + \sum_{n=1}^{\infty} a_n \cdot \cos(\omega_n t/2) = \frac{a_0}{2} + \sum_{n=1}^{\infty} a_n \cdot \cos(n\pi t/T) \quad (1.70)$$

The coefficients a_n are given by Eq. (1.67) as

$$a_n = \frac{2}{T} \int_0^T F(t) \cos(n\pi t/T) \cdot dt \quad (1.71)$$

In general, any of the three methods could be used to expand $F(t)$ in a series. However, the rate of convergence could differ considerably between the methods.

The response of a mass, which is excited by a periodic force, can also be expanded in a Fourier series. If the force is periodic, then the forced motion is also periodic with the same period as the force. Consequently, the response $x(t)$ of such a forced system can be written as

$$\begin{aligned}
 x(t) &= \frac{A_0}{2} + \sum_{n=1}^{\infty} (A_n \cdot \cos \omega_n t + B_n \cdot \sin \omega_n t) \\
 &= \frac{A_0}{2} + \sum_{n=1}^{\infty} C_n \cdot \cos(\omega_n t + \varphi_n)
 \end{aligned} \tag{1.72}$$

Each amplitude A_n and B_n can be solved as described for the simple harmonic force. In a similar way, the total amplitude C_n and the phase angle φ_n are determined for each ω_n or frequency component.

The time average of the velocity squared is as before given by

$$\bar{v}^2 = \frac{1}{T} \int_0^T \dot{x}^2 \cdot dt$$

This can be expressed by means of the components A_n and B_n of the Fourier series as:

$$\bar{v}^2 = \frac{1}{2} \sum_{n=1}^{\infty} \omega_n^2 (A_n^2 + B_n^2) = \frac{1}{2} \sum_{n=1}^{\infty} \omega_n^2 C_n^2 \tag{1.73}$$

This result is obtained since

$$\frac{1}{T} \int_0^T dt \cdot \sin \omega_n \cdot \sin \omega_k = \frac{1}{2} \text{ for } n = k \text{ and equal to zero for } n \neq k.$$

The time average of the velocity squared can be illustrated in the frequency domain as a line spectrum. The amplitude at $\omega = \omega_n$ is $\omega_n^2 (A_n^2 + B_n^2)/2$. The frequency domain of a signal and its significance are discussed in Chap. 2.

1.6 Complex Notation

For harmonic excitation, it is often convenient to assume that the force applied to the system can be expressed in the form $F_0 \exp(i\omega t)$. Since a physical quantity must be real, it can be assumed that the real force is equal to

$$F(t) = \text{Re} \left(F_0 e^{i\omega t} \right) = F_0 \cos \omega t.$$

If on the other hand, the force is given by a sine function then

$$F(t) = \text{Im} \left(F_0 e^{i\omega t} \right) = F_0 \sin \omega t.$$

The expressions above Re and Im define the real and imaginary parts of the force, respectively. In the phase diagram, Fig. 1.19, the axes can now be identified with the real and imaginary parts of a force vector in the complex plane.

If now the force is given by $F_0 \exp(i\omega t)$, then the resulting forced displacement of the mass in the 1-DOF system must be expressed in the form $x = x_0 \exp(i\omega t)$. With these expressions for F and x inserted in the basic equation of motion $m\ddot{x} + c\dot{x} + k_0x = F$, the amplitude x_0 is obtained as

$$\begin{aligned} x_0 &= \frac{F_0}{-m\omega^2 + i\omega c + k_0} \\ &= \frac{F_0}{m[(\omega_0^2 - \omega^2) + 2i\omega\beta]} \\ &= \frac{F_0[(\omega_0^2 - \omega^2) - 2i\omega\beta]}{m[(\omega_0^2 - \omega^2)^2 + (2\omega\beta)^2]} \end{aligned} \quad (1.74)$$

If the force is given by $F(t) = F_0 \cos \omega t = \text{Re}(F_0 e^{i\omega t})$, the solution is

$$\begin{aligned} x(t) &= \text{Re}(x_0 e^{i\omega t}) = \text{Re}(x_0 \cos \omega t + i x_0 \sin \omega t) \\ &= \frac{F_0[(\omega_0^2 - \omega^2) \cos \omega t + 2\omega\beta \sin \omega t]}{m[(\omega_0^2 - \omega^2)^2 + (2\omega\beta)^2]} \end{aligned} \quad (1.75)$$

For the case where the force is described by $F(t) = F_0 \sin \omega t = \text{Im}(F_0 e^{i\omega t})$, the solution is

$$x(t) = \text{Im}(x_0 e^{i\omega t}) = \frac{F_0[(\omega_0^2 - \omega^2) \sin \omega t - 2\omega\beta \cos \omega t]}{m[(\omega_0^2 - \omega^2)^2 + (2\omega\beta)^2]} \quad (1.76)$$

The last result is the same as that given by the Eqs. (1.57) and (1.60) and obtained in the traditional way. The general solution (1.74) can be expressed in an alternative way as

$$x = |x_0| \cdot \exp[i(\omega t + \varphi)] \quad (1.77)$$

where

$$|x_0| = \frac{F_0}{m[(\omega_0^2 - \omega^2)^2 + (2\omega\beta)^2]^{1/2}}, \quad \tan \varphi = -\frac{2\omega\beta}{\omega_0^2 - \omega^2}$$

So again if the force acting on the mass is described by $F(t) = F_0 \sin \omega t$, then

$$x = \text{Im}\{|x_0| \cdot \exp[i(\omega t + \varphi)]\} = |x_0| \cdot \sin(\omega t + \varphi)$$

This expression is identical to the solution given by the Eqs. (1.57) and (1.60). Compare Fig. 1.19.

Physical quantities of interest for the description of the response of a mechanical system are velocity squared, kinetic energy, potential energy, and power input and the time averages of these quantities. These quantities are real and nonnegative. In order to consider this, a convention with respect to the complex notation must be adopted.

The convention can be made that, when a complex number is to be squared, the complex number is multiplied by its complex conjugate. Further, the average value of the square of a quantity represented by the complex function $x(t) = A \exp(i\omega t)$ is equal to one-half of the square of the magnitude A .

This convention can be compared to results obtained when just using sine and cosine functions. For example, if a function $x(t)$ is written as $x(t) = A \cos(\omega t + \varphi)$ then

$$\bar{x}^2 = \frac{1}{T} \int_0^T A^2 \cos^2(\omega t + \varphi) \cdot dt = \frac{A^2}{2} \text{ since } \omega T = 2\pi$$

Alternatively, $x(t)$ is expressed as

$$x(t) = A \cdot \exp[i(\omega t + \varphi)]$$

According to the convention above, the average of x squared is defined as

$$\bar{x}^2 = \frac{xx^*}{2} = \frac{1}{2} A \exp[i(\omega t + \varphi)] A^* \exp[-i(\omega t + \varphi)] = \frac{|A|^2}{2} \quad (1.78)$$

In a similar way,

$$\dot{x}(t) = i\omega A \cdot \exp[i(\omega t + \varphi)], \quad \bar{\dot{x}}^2 = \frac{\omega^2 |A|^2}{2} \quad (1.79)$$

The time average of the input power is also a nonnegative and real quantity. With $F(t) = F_0 \exp(i\omega t)$ and $x(t) = x_0 \exp(i\omega t)$ where x_0 is given in Eq. (1.74), then in accordance with the discussion above the average input power is defined as:

$$\begin{aligned} \bar{\Pi} &= \frac{1}{2} \text{Re}(F \cdot \dot{x}^*) = \frac{1}{2} \text{Re}[F_0 e^{i\omega t} \cdot (-i\omega) x_0^* e^{-i\omega t}] \\ &= \frac{\omega}{2} \text{Im}(F_0 x_0) = \frac{\beta \omega^2 |F_0|^2}{m[(\omega_0^2 - \omega^2)^2 + (2\beta\omega)^2]} \end{aligned} \quad (1.80)$$

This expression is the same as that derived in Eq. (1.64). It is, however, much more convenient to derive the required results by means of the complex notation than through solutions which are a combination of sine and cosine functions and which eventually have to be integrated with respect to time. In addition, the complex amplitudes F_0 and x_0 have a very significant meaning which will be discussed in Chap. 2. Compare also Sect. 2.9.

The simple equation of motion for a linear damped 1-DOF system is for $c = 2\beta m$ and $F = F_0 \exp(i\omega t)$ and according to Eq. (1.56) given by

$$m\ddot{x} + 2m\beta\dot{x} + k_0x = F_0 \cdot e^{i\omega t}$$

The parameters m , β and k_0 are real quantities. If the solution $x = x_0 \exp(i\omega t)$ is assumed the result is, neglecting the transient response and omitting the time-dependent term $\exp(i\omega t)$, equal to

$$x_0(-m\omega^2 + 2i\omega m\beta + k_0) = F_0$$

This can be rewritten as:

$$x_0[-m\omega^2 + k_0(1 + i\delta_0)] = F_0 \quad (1.81)$$

where

$$\delta_0 = \frac{2\omega\beta}{\omega_0^2}$$

Thus for harmonic excitation of a 1-DOF system, the equation of motion is, using complex notation

$$m\ddot{x} + kx = F \quad (1.82)$$

where

$$k = k_0(1 + i\delta_0)$$

The spring constant k is thus complex. The real parameter δ_0 is equal to the ratio between the imaginary part of the spring constant and its real part. The parameter δ_0 is quite simply referred to as the loss factor of the spring.

From Eq. (1.81), the response of the mass is also written

$$x(t) = \frac{F_0 e^{i\omega t}}{k_0(1 + i\delta) - m\omega^2} = \frac{F_0 e^{i\omega t}}{m(2\pi)^2[f_0^2(1 + i\delta) - f^2]}$$

For free vibrations, the same technique cannot be used directly. The result described in Eq. (1.81) is only valid as long as the displacement of the mass is harmonic. Free oscillations of a damped 1-DOF system are not harmonic, i.e., the velocity is not given by $i\omega$ times the displacement. However, if the losses are very small, the free vibrations are approximately harmonic within a period.

For $\beta \ll 1$, the free vibrations of a 1-DOF system are, according to Eq. (1.15), described by

$$x(t) = e^{-\beta t} \cdot [C \cos \omega_r t + D \sin \omega_r t]$$

According to Eq. (1.81), $\beta = \omega_0 \delta_0 / 2$ since $\omega_r \approx \omega_0$ for $\beta \ll 1$. The free oscillations of a lightly damped 1-DOF system can therefore be approximated by the expression

$$x(t) = \exp(-\omega_0 \delta_0 t / 2) \cdot [C \cos \omega_r t + D \sin \omega_r t] \quad (1.83)$$

The total energy or the time average of the kinetic or potential energy is thus decaying as

$$\mathcal{E}(t) = \mathcal{E}(0) \cdot \exp(-\omega_0 \delta_0 t) \quad (1.84)$$

where $\mathcal{E}(0)$ is the energy at $t = 0$. Compare Eqs. (1.23) and (1.26). For standard solids, the loss factor decreases as the frequency is increased. However, there are notable exceptions, for example rubber and some composite structures as discussed in Chap. 3.

Problems

1.1 Determine the energy dissipated over one period for a simple mass–spring system if the losses are (a) viscous and (b) hysteretic. Assume that the displacement of the mass is described by $x(t) = x_0 \sin(\omega t)$.

1.2 The displacement of the mass of a simple mass–spring system is given by $x(t) = x_0 \sin(\omega t)$. Determine the force required to maintain this motion if the damping force is due to (i) viscous losses and (ii) frictional losses. In a diagram, show the force as function of displacement. Make some appropriate assumption concerning the magnitude of the properties m , k_0 , c and F_d .

1.3 The mass in Fig. 1.20 is excited and is thereafter left to oscillate freely. Determine the displacement as function of time if the losses are assumed to be frictional. Assume that the displacement is x_0 and the velocity zero at time $t = 0$.

1.4 Show that for a critically damped system, the displacement can be zero for time t being finite and that this can only happen at one instance.

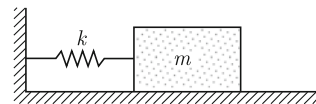
1.5 The mass of a simple mass–spring system is excited by an impulse I at time intervals T . Determine the response of the mass. Consider only harmonic solutions, i.e., assume that the excitation process was started at $t = -\infty$. The system is lightly damped.

1.6 A mass–spring system is at rest for $t < 0$. The mass is excited by a force $F(t)$ at $t = 0$. The force is given by $F(t) = F_0$ for $0 \leq t \leq T$; $F(t) = 0$ for $t < 0$ and $t > T$.

Determine the response of the mass. In particular, consider the cases for which the product $\omega_r T$ is equal to $\pi/2$, π and 2π with ω_r defined in Eq. (1.14). Assume that $\beta T \ll 1$. For definitions, see Sect. 1.2.

1.7 For the problem described in Example 1.6 determine the maximum amplitude as function of T .

Fig. 1.20 Mass-spring system with frictional losses



1.8 A function $x(t)$ is expanded in a Fourier series as

$$x(t) = \frac{a_0}{2} + \sum_{n=1}^{\infty} (a_n \cos \omega_n t + b_n \sin \omega_n t); \quad \omega_n = 2\pi n/T; \quad n = 1, 2, \dots$$

Show that the coefficients a_n and b_n are

$$a_n = \frac{2}{T} \int_0^T x(t) \cos(\omega_n t) dt; \quad b_n = \frac{2}{T} \int_0^T x(t) \sin(\omega_n t) dt$$

1.9 A harmonic force $F(t)$ with the period T is exciting the mass of a simple 1-DOF system. Determine the displacement of the mass if

$$F(t) = F(t + T) = G_0/2 + \sum_{n=1}^{\infty} G_n \cos(\omega_n t) + \sum_{n=1}^{\infty} H_n \sin(\omega_n t); \quad \omega_n = 2\pi n/T$$

Assume the losses to be viscous.

1.10 Solve Problem 1.5 by expanding the force and response in Fourier series.

1.11 A 1-DOF system is excited by a force $F(t) = F_0 \cdot e^{i\omega t}$. Determine the time averages of kinetic and potential energies as well as the time average of the input power to the system. Assume that the equation governing the motion of the system is

$$m\ddot{x} + kx = F; \quad k = k_0(1 + i\delta)$$

According to Eq. (1.81), $\delta = 2\omega m\beta/k_0$. Since $\beta = c/(2m)$ δ is written $\delta = c\omega/k_0$. Discuss the difference between viscous and structural damping.

1.12 A 1-DOF system is governed by the equation $m\ddot{x} + c\dot{x} + k_0x = F(t)$. A function $h(t - \tau)$ satisfies the equation $m\ddot{h} + c\dot{h} + k_0h = \delta(t - \tau)$ show that $x(t)$ is given by

$$x(t) = \int_{-\infty}^t d\tau F(\tau) h(t - \tau).$$

1.13 The displacement of a 1-DOF system can be described in two different ways as

- (i) $m\ddot{x} + kx = F; \quad k = k_0(1 + i\delta)$
- (ii) $m\ddot{x} + c\dot{x} + k_0x = F$

Assume $F = F_0 \cdot e^{i\omega t}$ and $x = x_0 \cdot e^{i\omega t}$ and derive the input power to the system for both cases. Show in the first case that the input power is proportional to the potential energy of the system and in the second case to the kinetic energy.

Chapter 2

Frequency Domain

The time response of a complicated structure which is exposed to a number of forces is often extremely difficult to interpret. However, if the behavior of a linear mechanical system is studied in the frequency domain, it is possible to attribute the response at a certain frequency to a particular force or a resonance in the system. In this chapter some of the basic tools like Fourier transforms, frequency response and mobility functions used for analysis of signals are introduced. The response of simple systems excited by periodic as well as random forces are discussed. The simple one degree of freedom system is used to illustrate the basic procedures, when changing from the time to the frequency domain. The concepts discussed are later used for analysis of continuous systems. Some techniques for determining loss factors are also introduced.

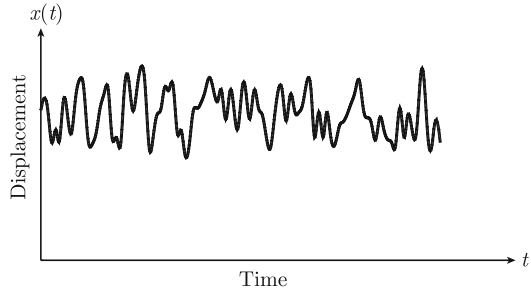
2.1 Introduction

The time functions hereto considered could be called deterministic. In other words, a mathematical expression can be formulated giving the instantaneous value of displacement, etc., of a mechanical system. The excitation of a linear 1-DOF system by means of a periodic force results in a response which in turn is periodic. This response can be expanded in a Fourier series. Each term in the series corresponds to a certain frequency. In the frequency domain this is equivalent to a line spectrum. Each line corresponds to a component in the Fourier series.

A force, response, or any other function could also be random. If a random function is stationary then the average

$$\bar{x} = \frac{1}{T} \int_{t_0}^{t_0+T} x(t) dt \quad (2.1)$$

Fig. 2.1 The time response of a 1-DOF system excited by a random force



is independent of t_0 . The same should be true for all statistical properties of the signal. If a random process is stationary: its statistical properties do not vary, when computed over different samples, then the random process is ergodic. For a random process in general, it is not meaningful to consider the time history of the response. Figure 2.1 shows the time response of a 1-DOF system, excited by a random force. A direct interpretation of the time history is not easily deduced. However, the frequency response of the same signal can contain vital information within the mechanical system.

The actual excitation of typical mechanical systems is often due to a combination of harmonic and random forces. The discrete frequency spectrum of a periodic function becomes a continuous spectrum if the period T is extended to infinity. This means in the usual way that the Fourier series is transformed to a Fourier integral. Thus the function $x(t)$ can be expressed as

$$x(t) = \frac{1}{2\pi} \int_{-\infty}^{\infty} \hat{x}(\omega) \cdot e^{i\omega t} d\omega \quad (2.2)$$

where $\hat{x}(\omega)$ is the FT (Fourier transform) of $x(t)$. Inversely $\hat{x}(\omega)$ can be defined as

$$\hat{x}(\omega) = \int_{-\infty}^{\infty} x(t) \cdot e^{-i\omega t} dt \quad (2.3)$$

The result (2.3) is a consequence of the identity

$$\delta(\omega - \omega_0) = \frac{1}{2\pi} \int_{-\infty}^{\infty} e^{it(\omega_0 - \omega)} dt \quad (2.4)$$

This is a very useful equality which is often utilized in the transformation from the time to the frequency domain and vice versa. The proofs of Eqs. (2.2) and (2.3) are left for Problem 2.13.

In principle, a signal $x(t)$ must be known in the entire time domain, i.e., from minus to plus infinity, for its Fourier transform to be defined. However, the signal

can be redefined as being equal to $x(t)$ in the time domain $-T/2 \leq t \leq T/2$ and zero elsewhere. Thereafter the necessary operations or transforms can be carried out. A certain error is introduced by means of this method. In practice, the so-called Fast Fourier Transform (FFT) technique is used for processing of signals. By means of this technique only a certain time history of a signal is used for calculation of the Fourier transform of the signal. The FFT technique leads to certain errors. However, it is well understood how to estimate and suppress any possible errors. Signal analysis in theory and practice is discussed in Refs. [6–9] and random vibrations in Refs. [10, 11].

2.2 Frequency Response

According to Eq. (1.39) the response $x(t)$ of a linear system, excited by a force $F(t)$ is given by the convolution integral

$$x(t) = \int_{-\infty}^{\infty} d\tau \cdot h(\tau) F(t - \tau) \quad (2.5)$$

where $h(t)$ is the response function of the system caused by a unit impulse at $t = 0$. Further, $F(t) = 0$ for $t < 0$.

The functions $h(t)$ and $x(t)$ have the Fourier transforms $H(\omega)$ and $\hat{F}(\omega)$, respectively. Thus,

$$H(\omega) = \int_{-\infty}^{\infty} dt \cdot e^{-i\omega t} \cdot h(t), \quad \hat{F}(\omega) = \int_{-\infty}^{\infty} dt \cdot e^{-i\omega t} \cdot F(t) \quad (2.6)$$

The function $F(t - \tau)$ can according to Eq. (2.2) be written as

$$F(t - \tau) = \frac{1}{2\pi} \int_{-\infty}^{\infty} \hat{F}(u) \cdot e^{iu(t-\tau)} du \quad (2.7)$$

The FT of $x(t)$ as defined in Eq. (2.5) is

$$\hat{x}(\omega) = \int_{-\infty}^{\infty} dt \cdot e^{-i\omega t} \cdot \int_{-\infty}^{\infty} d\tau \cdot h(\tau) F(t - \tau) \quad (2.8)$$

The definition (2.7) can now be inserted into Eq. (2.8). The order of integration is changed and the result (2.4), i.e., the FT of a Dirac function, is utilized as follows:

$$\begin{aligned}
\hat{x}(\omega) &= \int_{-\infty}^{\infty} dt \cdot e^{-i\omega t} \cdot \int_{-\infty}^{\infty} d\tau \cdot h(\tau) \frac{1}{2\pi} \int_{-\infty}^{\infty} du \cdot \hat{F}(u) \cdot e^{iu(t-\tau)} \\
&= \int_{-\infty}^{\infty} d\tau \cdot h(\tau) \int_{-\infty}^{\infty} du \cdot \hat{F}(u) \cdot e^{-iu\tau} \frac{1}{2\pi} \int_{-\infty}^{\infty} dt \cdot e^{it(u-\omega)} \\
&= \int_{-\infty}^{\infty} d\tau \cdot h(\tau) \int_{-\infty}^{\infty} du \cdot \hat{F}(u) \cdot e^{-iu\tau} \delta(\omega - u) \\
&= \int_{-\infty}^{\infty} d\tau \cdot h(\tau) \hat{F}(\omega) \cdot e^{-i\omega\tau} \\
&= \hat{F}(\omega) \int_{-\infty}^{\infty} d\tau \cdot h(\tau) \cdot e^{-i\omega\tau} = \hat{F}(\omega) H(\omega)
\end{aligned} \tag{2.9}$$

The result means that for a linear mechanical system the FT of the response is equal to the product between the FT of the force and the FT of the response function. This last transform $H(\omega)$ is referred to as the frequency response function (FRF), or the transfer function of the mechanical system being excited.

The FRF of a 1-DOF system can be derived based on the equation of motion for the system. Returning to the time domain the equation of motion for a 1-DOF system excited by a unit pulse at $t = 0$ is

$$m\ddot{h} + c\dot{h} + k_0h = \delta(t) \tag{2.10}$$

where $h(t)$ is the response of a damped 1-DOF system excited by a unit pulse. The Fourier transform of $h(t)$ is defined in Eq. (2.6).

The equation of motion for the 1-DOF system, Eq. (2.10), is multiplied by $e^{-i\omega t}$ and integrated over time resulting in

$$\begin{aligned}
m \int_{-\infty}^{\infty} \ddot{h}(t) e^{-i\omega t} dt + c \int_{-\infty}^{\infty} \dot{h}(t) e^{-i\omega t} dt + k_0 \int_{-\infty}^{\infty} h(t) e^{-i\omega t} dt \\
= \int_{-\infty}^{\infty} \delta(t) e^{-i\omega t} dt
\end{aligned} \tag{2.11}$$

The last integral on the left-hand side is according to definition equal to $k_0 H(\omega)$. The integral on the right-hand side is equal to unity. The first and the second integrals on the left-hand side are integrated by parts. Starting with the second integral the result is

$$\int_{-\infty}^{\infty} \dot{h}(t) e^{-i\omega t} dt = \left[h(t) e^{-i\omega t} \right]_{-\infty}^{\infty} + i\omega \int_{-\infty}^{\infty} h(t) e^{-i\omega t} dt = i\omega H(\omega) \tag{2.12}$$

The function $h(t)$ is defined as being equal to zero for $t < 0$. The system has losses, consequently $h(t)$ approaches zero as $t \rightarrow \infty$. Therefore, the expression inside the bracket is equal to zero at both time limits. In a similar way the FT of $\ddot{h}(t)$ is found to be

$$\int_{-\infty}^{\infty} \ddot{h}(t) e^{-i\omega t} dt = (i\omega)^2 H(\omega) = -\omega^2 H(\omega)$$

Thus, based on the results defining the FTs of $h(t)$ and its time derivatives the frequency response function $H(\omega)$ is obtained as

$$H(\omega) = \frac{1}{-m\omega^2 + i\omega c + k_0} = \frac{1}{m(\omega_0^2 - \omega^2 + 2i\beta\omega)} \quad (2.13)$$

whereas before $\omega_0^2 = k_0/m$ and $\beta = c/(2m)$. For a forced linear 1-DOF system the equation of motion is

$$m\ddot{x} + c\dot{x} + k_0x = F(t) \quad (2.14)$$

The Fourier transform of $x(t)$ is, according to Eq. (2.9), given by $\hat{x} = \hat{F}H(\omega)$ or

$$\hat{x}(\omega) = \hat{F}(\omega)H(\omega) = \frac{\hat{F}(\omega)}{m(\omega_0^2 - \omega^2 + 2i\beta\omega)} \quad (2.15)$$

It is interesting now to note that exactly the same result is obtained by making the following substitutions in Eq. (2.14)

$$x(t) \rightarrow \hat{x}(\omega) \cdot e^{i\omega t}, \quad F(t) \rightarrow \hat{F}(\omega) \cdot e^{i\omega t} \quad (2.16)$$

Consequently, if for a linear system, it is assumed that the time dependence for force and displacement is $\exp(i\omega t)$, then the resulting amplitude of the displacement is identical to the FT of the displacement if the amplitude of the force is equal to its FT.

The basic Eq. (2.10) can according to the discussion in Sect. 1.6, Eq. (1.82), also be written as

$$m\ddot{h} + kh = \delta(t), \quad k = k_0(1 + i\delta_0)$$

The frequency response function $H(\omega)$ is for this case obtained as

$$H(\omega) = \frac{1}{-m\omega^2 + k} = \frac{1}{m[(\omega_0^2 - \omega^2) + i\omega_0^2\delta_0]} \quad (2.17)$$

where $\omega_0^2 = k_0/m$. The lossfactor is in Eq. (1.81) given as $2\omega\beta/\omega_0^2$. Since the quantities β and ω_0^2 are real and positive, the loss factor δ_0 must be negative for $\omega < 0$. This change of sign is of importance whenever $H(\omega)$ or any other function of δ_0 is part of a Fourier integral. This is demonstrated in Problem 2.3.

In conclusion, the FT of the response of a 1-DOF system is readily defined if the FT of the force exciting the system is known. Thus, if for a 1-DOF system the equation of motion is $m\ddot{x} + kx = F(t)$, then by making the substitutions $x(t) \rightarrow \hat{x}(\omega) \cdot e^{i\omega t}$ and $F(t) \rightarrow \hat{F}(\omega) \cdot e^{i\omega t}$ the FT of the response is

$$\hat{x}(\omega) = \hat{F}(\omega)H(\omega) = \frac{\hat{F}(\omega)}{-m\omega^2 + k} = \frac{\hat{F}(\omega)}{m[(\omega_0^2 - \omega^2) + i\omega_0^2\delta_0]} \quad (2.18)$$

The FT of the response is the product of two functions, one, the frequency response function $H(\omega)$, depends on the frequency and the material parameters of the system. The other function, \hat{F} , is determined by the characteristics and time history of the force.

2.3 Correlation Functions

The correlation functions are of great importance when dealing with random and other stationary processes. If for example a structure is excited by several forces, then the response clearly depends on how these forces are correlated. Furthermore, the characteristics of any stationary signal can be determined by correlating the signal at one instant with the same signal at another time.

The autocorrelation function $R_{xx}(\tau)$ for the signal $x(t)$ is defined as the time average of the product of the signal at time t and the same signal at time $t + \tau$ or

$$R_{xx}(\tau) = \lim_{T \rightarrow \infty} \frac{1}{T} \int_{-T/2}^{T/2} x(t)x(t + \tau)dt \quad (2.19)$$

This integral can be symbolized by

$$R_{xx}(\tau) = E [x(t)x(t + \tau)]$$

The symbol E stands for the expected value of the expression inside the bracket. In a similar way the cross-correlation function $R_{xy}(\tau)$ between the signals $x(t)$ and $y(t)$ is defined as

$$R_{xy}(\tau) = \lim_{T \rightarrow \infty} \frac{1}{T} \int_{-T/2}^{T/2} x(t)y(t + \tau)dt = E [x(t)y(t + \tau)] \quad (2.20)$$

As a first example, consider the autocorrelation function for a random signal. If the mean value of this random signal $x(t)$ is zero, then for large values of τ the autocorrelation must be zero; because of the random nature of the signal, $x(t)$ and $x(t + \tau)$ are quite unrelated. The product of the two signals is sometimes positive and at other times negative. The total average over time is therefore equal to zero. For the other extreme case, $\tau = 0$, the definition (2.19) gives

$$R_{xx}(0) = E[x^2(t)] \quad (2.21)$$

This is quite simply the mean square value of x . This function is not equal to zero. In order to satisfy these requirements the autocorrelation function for an ideally random signal is defined as

$$R_{xx}(\tau) = a \cdot \delta(\tau) \quad (2.22)$$

where a is a positive nonzero constant. Thus, $R_{xx}(\tau) = 0$ for $\tau \neq 0$ for an ideal random signal. The significance of the parameter a is discussed in connection with the derivation of Eq. (2.39).

For the harmonic function $x(t) = A \sin \omega t$ the autocorrelation function is obtained from Eq. (2.19) as

$$R_{xx}(\tau) = \frac{A^2}{T} \int_0^T \sin \omega t \cdot \sin[\omega(t + \tau)] dt = \frac{A^2}{2} \cos \omega \tau \quad (2.23)$$

For a harmonic function it is sufficient to take a time average over one period T where $\omega T = 2\pi$. For the signal $x(t) = A \cos \omega t$ the autocorrelation function is the same as for the sine function. Thus, the autocorrelation function of a harmonic signal is a harmonic function with the same period as the signal.

If a signal is composed of the random function $\xi(t)$ with a mean value equal to zero and, say, a harmonic function $h(t)$ then for $x(t) = h(t) + \xi(t)$ the autocorrelation function is

$$\begin{aligned} R_{xx}(\tau) &= E[x(t)x(t + \tau)] = E[h(t)h(t + \tau)] \\ &\quad + E[\xi(t)h(t + \tau)] + E[h(t)\xi(t + \tau)] + E[\xi(t)\xi(t + \tau)] \\ &= R_{hh}(\tau) + R_{\xi\xi}(\tau) = R_{hh}(\tau) + a \cdot \delta(\tau) \end{aligned} \quad (2.24)$$

The time average of the product between a random and a harmonic function is equal to zero. The cross terms in Eq. (2.24) are consequently eliminated.

For two stationary processes $x(t)$ and $y(t)$, random or harmonic, the cross-correlation function can be written in two ways

$$R_{xy}(\tau) = E[x(t)y(t + \tau)] \quad \text{or} \quad R_{xy}(\tau) = E[x(t - \tau)y(t)] \quad (2.25)$$

The derivatives with respect to τ should be the same for the two expressions. This means that

$$R'_{xy} = \frac{dR_{xy}(\tau)}{d\tau} = E[x(t)y'(t + \tau)] = E[-x'(t - \tau)y(t)]$$

For $\tau = 0$ the last two expressions give

$$E[x(t)y'(t)] = E[-x'(t)y(t)] \quad \text{or} \quad E[x\dot{y}] + E[\dot{x}y] = 0$$

If $x(t) = y(t)$ this result can only be satisfied if

$$E [x(t)\dot{x}(t)] = 0 \quad (2.26)$$

In a similar way it can be shown that

$$E [\dot{x}(t)\ddot{x}(t)] = 0 \quad (2.27)$$

If $x(t)$ is stationary and describes the displacement of a structure and $\dot{x}(t)$ is the velocity at that point, then the time average of the product between velocity and displacement is equal to zero. The time average of the velocity and acceleration at that same point is also equal to zero. These relationships are important when dealing with statistical energy methods. It should be noted that the time average of the product between displacement and acceleration in general is different from zero. The average of this product can be written as

$$E [x(t)\ddot{x}(t)] = \left[\frac{d^2 R_{xx}(\tau)}{d\tau^2} \right]_{\tau=0} \quad (2.28)$$

The time average of the velocity squared is

$$E [\dot{x}^2(t)] = - \left[\frac{d^2 R_{xx}(\tau)}{d\tau^2} \right]_{\tau=0} \quad (2.29)$$

The derivation of the last expression is left for Problem 2.14.

2.4 Spectral Density

A transfer from the time domain to the frequency domain naturally leads to the FT of the correlation functions. Starting with the cross-correlation function $R_{xy}(\tau)$ its FT is according to Eqs. (2.3) and (2.20)

$$\begin{aligned} FT \{R_{xy}(\tau)\} &= \int_{-\infty}^{\infty} d\tau \cdot e^{-i\omega\tau} E[x(t)y(t+\tau)] \\ &= \lim_{T \rightarrow \infty} \frac{1}{T} \int_{-\infty}^{\infty} d\tau \cdot e^{-i\omega\tau} \int_{-T/2}^{T/2} dt x(t)y(t+\tau) \\ &= \lim_{T \rightarrow \infty} \frac{1}{T} \int_{-\infty}^{\infty} d\tau \int_{-T/2}^{T/2} dt \cdot e^{i\omega t} x(t) e^{-i\omega\tau - i\omega t} y(t+\tau) \\ &= \lim_{T \rightarrow \infty} \frac{1}{T} \int_{-\infty}^{\infty} dt \cdot e^{i\omega t} x(t) \int_{-T/2}^{T/2} d\xi \cdot e^{-i\xi t} y(\xi) \\ &= \lim_{T \rightarrow \infty} \frac{\hat{x}^*(\omega)\hat{y}(\omega)}{T} \end{aligned} \quad (2.30)$$

In deriving the result ξ has been set to $\xi = t + \tau$. Further, the FT of $x(t)$ is given by $\hat{x}(\omega)$ as defined in Eq. (2.3). According to the same expression it follows that

$$\hat{x}^*(\omega) = \int_{-\infty}^{\infty} dt \cdot x(t) \cdot e^{i\omega t} \quad (2.31)$$

This expression is utilized to derive Eq. (2.30). The result given in Eq. (2.30) is again obtained using the expression $R_{xy}(\tau) = E[x(t)y(t + \tau)] = E[x(t - \tau)y(t)]$.

The FT of the cross-correlation function is referred to as the cross-spectral density $S_{xy}(\omega)$ and is defined as

$$S_{xy}(\omega) = S_{xy}(2\pi f) = \lim_{T \rightarrow \infty} \frac{\hat{x}(\omega)\hat{y}^*(\omega)}{T} \quad (2.32)$$

where f is the frequency. The FT of the autocorrelation function is immediately obtained by substituting $y(t + \tau)$ by $x(t + \tau)$ into Eq. (2.30). Thus,

$$S_{xx}(\omega) = FT \{R_{xx}(\tau)\} = \lim_{T \rightarrow \infty} \frac{|\hat{x}(\omega)|^2}{T} \quad (2.33)$$

The quantity $S_{xx}(\omega)$ is the power spectral density or autospectral density of the signal $x(t)$.

The results can be summarized as

$$\begin{aligned} R_{xx}(\tau) &= \frac{1}{2\pi} \int_{-\infty}^{\infty} S_{xx}(\omega) e^{i\omega\tau} d\omega \\ S_{xx}(\omega) &= \int_{-\infty}^{\infty} R_{xx}(\tau) e^{-i\omega\tau} d\tau \\ R_{xy}(\tau) &= \frac{1}{2\pi} \int_{-\infty}^{\infty} S_{xy}(\omega) e^{i\omega\tau} d\omega \\ S_{xy}(\omega) &= \int_{-\infty}^{\infty} R_{xy}(\tau) e^{-i\omega\tau} d\tau \end{aligned} \quad (2.34)$$

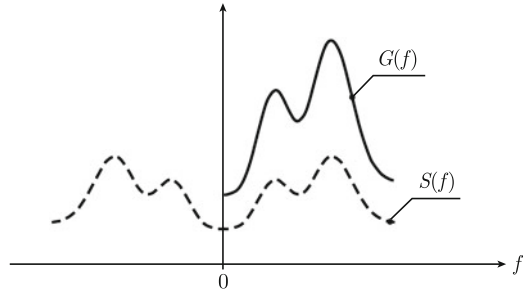
The spectral densities have some properties which are useful in various mathematical manipulations. From the hypothesis of a stationary process it follows that the correlation functions satisfy the equalities

$$R_{xx}(\tau) = R_{xx}(-\tau), \quad R_{xy}(\tau) = R_{yx}(-\tau) \quad (2.35)$$

From these symmetry properties for the stationary correlation functions and the results (2.33) and (2.34) it follows that

$$S_{xx}(\omega) = S_{xx}(-\omega), \quad S_{xy}(\omega) = S_{yx}(-\omega) \quad (2.36)$$

Fig. 2.2 One-sided and two-sided spectral density functions



Consequently $S_{xx}(\omega)$ is an even function. It is therefore possible to define the physically realizable one-sided spectral density $G_{xx}(\omega)$ as

$$G_{xx}(\omega) = 2S_{xx}(\omega) \text{ for } \omega \geq 0 \text{ otherwise zero} \quad (2.37)$$

The one-sided and two sided spectral densities are illustrated in Fig. 2.2. In a similar way the physically realizable one-sided cross-spectral density $G_{xy}(\omega)$ is defined as

$$G_{xy}(\omega) = 2S_{xy}(\omega) \text{ for } \omega \geq 0 \text{ otherwise zero}$$

However, $G_{xy}(\omega)$ is not a real function which is the case for $G_{xx}(\omega)$. The real part of $G_{xy}(\omega)$ is symmetric. The importance of the real part of $G_{xy}(\omega)$ will later be demonstrated. For future reference the definitions above yield for $\omega \geq 0$

$$\text{Re}[G_{xy}(\omega)] = 2\text{Re}[S_{xy}(\omega)] = 2\text{Re}[S_{yx}(\omega)] \quad (2.38)$$

2.5 Examples of Spectral Density

It has previously been pointed out that the autocorrelation function for a completely stationary random signal $x(t)$ or white noise can be written as $R_{xx}(\tau) = a \cdot \delta(\tau)$. Thus, the corresponding power spectral density for the signal is obtained from Eq. (2.34) as

$$S_{xx}(\omega) = \int_{-\infty}^{\infty} a \cdot \delta(\tau) e^{-i\omega\tau} d\tau = a \text{ for all } \omega, \quad G_{xx}(\omega) = 2a \text{ for } \omega \geq 0 \quad (2.39)$$

The power spectral density for a completely random signal is constant and thus independent of frequency. This is the definition of white noise—every frequency component is equally represented. However, this type of signal can not be physically reproduced. For a completely random signal $x(t)$, the time average of $x^2(t)$,

or $R_{xx}(\tau) = a \cdot \delta(\tau)$ is infinite for $\tau = 0$. The energy required to reproduce a completely random signal would be infinite. All physically generated “random” signals have in fact only a random character within a certain frequency band. Still, in most mathematical formulations, the definitions (2.22) and (2.39) are preferably used.

For a harmonic signal $x(t) = A \cdot \sin \omega_0 t$ or $x(t) = A \cdot \cos \omega_0 t$ the autocorrelation function is given by Eq. (2.23) as

$$R_{xx}(\tau) = \frac{A^2}{2} \cos \omega_0 \tau \quad (2.40)$$

According to definition the power spectral density of this signal is

$$\begin{aligned} S_{xx}(\omega) &= \frac{A^2}{2} \int_{-\infty}^{\infty} \cos \omega_0 \tau \cdot e^{-i\omega \tau} d\tau \\ &= \frac{A^2}{4} \int_{-\infty}^{\infty} d\tau (e^{i\omega_0 \tau - i\omega \tau} + e^{-i\omega \tau - i\omega_0 \tau}) \\ &= \frac{\pi A^2}{2} [\delta(\omega - \omega_0) + \delta(\omega + \omega_0)] \end{aligned} \quad (2.41)$$

The two-sided power spectral density of a harmonic signal, angular frequency ω_0 , has two frequency components corresponding to $\omega = \pm \omega_0$. The one-sided spectral density is

$$G_{xx}(\omega) = \pi A^2 \delta(\omega - \omega_0) \text{ for } \omega \geq 0 \quad (2.42)$$

The expression (2.42) can also be written as

$$G_{xx}(2\pi f) = A^2/2 \cdot \delta(f - f_0) \text{ for } f \geq 0$$

This is a consequence of $\delta(kt - kt_0) = \delta(t - t_0)/k$.

For a harmonic signal of the form

$$x(t) = \frac{a_0}{2} + \sum_{n=1}^{\infty} (a_n \cos \omega_n t + b_n \sin \omega_n t), \quad \omega_n = \frac{2\pi n}{T}$$

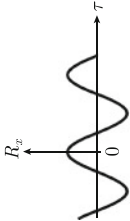
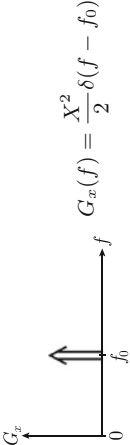
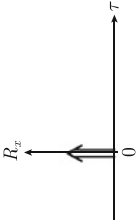
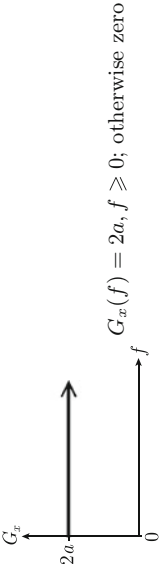
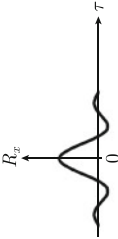
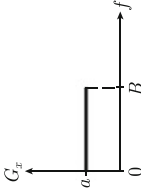
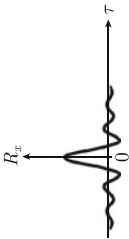
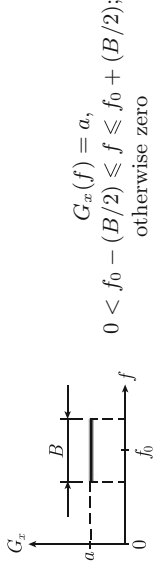
the autocorrelation function is

$$R_{xx}(\tau) = \left(\frac{a_0}{2}\right)^2 + \sum_{n=1}^{\infty} \left(\frac{a_n^2 + b_n^2}{2}\right) \cos(\omega_n \tau) \quad (2.43)$$

Based on the results Eqs. (2.39) and (2.40) the one-sided power spectral density of the signal is

$$G_{xx}(\omega) = \frac{\pi a_0^2}{2} \cdot \delta(\omega) + \sum_{n=1}^{\infty} \pi (a_n^2 + b_n^2) \delta(\omega - \omega_n) \quad (2.44)$$

Table 2.1 Some special stationary autocorrelation function and related one side spectral density function

Types	Autocorrelation Function	(One-Sided) Power Spectral Density Function
Sine wave	 $R_x(\tau) = \frac{X^2}{2} \cos(2\pi f_0 \tau)$	 $G_x(f) = \frac{X^2}{2} \delta(f - f_0)$
White noise	 $R_x(\tau) = a\delta(\tau)$	 $G_x(f) = 2a, f \geq 0; \text{ otherwise zero}$
Low-pass, white noise	 $R_x(\tau) = aB \frac{\sin(2\pi B \tau)}{2\pi B \tau}$	 $G_x(f) = a, 0 \leq f \leq B; \text{ otherwise zero}$
Band-pass, white noise	 $R_x(\tau) = aB \frac{\sin(\pi B \tau)}{\pi B \tau} \cos(2\pi f_0 \tau)$	 $G_x(f) = a, 0 < f_0 - (B/2) \leq f \leq f_0 + (B/2); \text{ otherwise zero}$

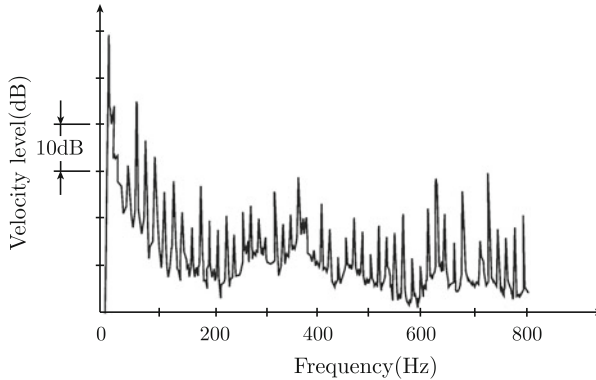


Fig. 2.3 Measured velocity level on foundation of a Diesel engine

The result is a line spectrum as opposed to the continuous spectrum shown in Fig. 2.2. In the spectrum there is a line for $f = \omega_n/(2\pi) = n/T$, where $n = 0, 1, 2, \dots$. Table 2.1 presents some special stationary autocorrelation functions and related one sided spectral density functions. The autocorrelation functions for low-pass and band-pass white noise are discussed in Problem 2.5.

A spectrum from a real source and in particular, a source like a machine rotating at a constant rpm. is generally built up of continuous and line spectra. One example is shown in Fig. 2.3. The power spectral density of the velocity is G_{vv} . A reference function is given by G_{ref} . The velocity level L_v in dB or rather $L_v = 10 \cdot \log(G_{vv}/G_{\text{ref}})$ is shown as function of frequency. The velocity level is measured on the foundation on which a ship Diesel engine is resiliently mounted. The engine is running at 960 rpm. Corresponding to a rotation frequency of 16 Hz. Distinct peaks or lines are shown in the spectrum for the frequencies $f_n = n \cdot 16$ Hz for n an integer.

Even a simple measured noise spectrum can often be used to identify the contributions from various noise sources. If at a certain position away from a large vibrating structure the sound pressure induced by a number of sources is analyzed with a good frequency resolution, the main noise sources could be identified based on a knowledge of the operation of the source. One example is illustrated in Fig. 2.4. The noise was radiated from the hull of a catamaran into the water. The sound pressure level, or rather the quantity $L_p = 10 \cdot \log(G_{pp}/G_{\text{ref}})$, has been recorded at a position in the water. The one-sided power spectral density of the pressure is given by G_{pp} . As in the previous case the rpm of the main engine is 960, corresponding to 16 cycles/s. The first five harmonics, denoted ME₁ through ME₅, are quite distinct in the spectrum as shown in Fig. 2.4.

The auxiliary engine is running at 1460 rpm. The first few harmonics, AE₁, etc., are approximately at $n \times 24$ Hz. The rpm of the six-bladed pump wheel of the water jet is 455, with the first, WJ₁, and second, WJ₂, harmonics at 46 and 92 Hz respectively. The frequency of the first harmonic is given by the number of rounds per second of the shaft times the number of propeller blades. The second harmonics AE₂ induced

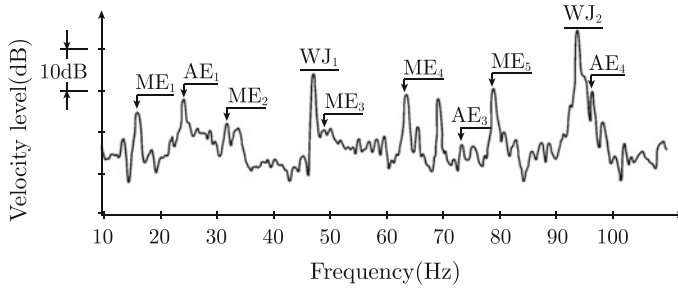


Fig. 2.4 Sound pressure level measured in the water close to a catamaran

by the auxiliary engine cannot clearly be distinguished from the dominating first harmonic WJ_1 from the water jet.

In the high frequency region, the higher harmonics of the various sources tend to merge and the sources cannot be readily identified by this simple technique, more sophisticated methods must be used. For multiple-input linear systems, the so-called partial coherence function gives a quantitative indication of the degree of linear dependence between, for example, the vibration velocity of a source and the measured sound pressure level at a certain point. The method is described in for example Ref. [8].

2.6 Coherence

The so-called coherence function $\gamma_{xy}^2(\omega)$ can be used as a measure of the quality of two observations $x(t)$ and $y(t)$. The coherence function is defined as

$$\gamma_{xy}^2(\omega) = \frac{|G_{xy}(\omega)|^2}{G_{xx}(\omega)G_{yy}(\omega)} \quad (2.45)$$

The coherence function is always real and positive and can vary between zero and unity. If the coherence function is equal to zero for $\omega = \omega_0$ the signals $x(t)$ and $y(t)$ are said to be incoherent or uncorrelated at the frequency $f = \omega_0/(2\pi)$. For the coherence function to be equal to unity $x(t)$ and $y(t)$ must be fully coherent or correlated. This, for example, is the case if $y(t) = q \cdot x(t)$, where q is a constant.

The applicability of the coherence function can be demonstrated by considering a linear 1-DOF system. A force $F(t)$ is exciting the mass of the system. However, the response of the mass is not only determined by the force $F(t)$, but is also influenced by a secondary force $K(t)$. The FT of the response $x(t)$ of the mass is determined by the frequency response function $H(\omega)$. Thus,

$$\hat{x} = (\hat{F} + \hat{K})H \quad (2.46)$$

The power spectral density of the response is according to the definition (2.33) equal to

$$\begin{aligned} S_{xx}(\omega) &= \lim_{T \rightarrow \infty} \frac{|\hat{x}(\omega)|^2}{T} = \lim_{T \rightarrow \infty} \frac{(\hat{F} + \hat{K})(\hat{F}^* + \hat{K}^*) |H(\omega)|^2}{T} \\ &= (S_{FF} + S_{FK} + S_{KF} + S_{KK}) |H|^2 \end{aligned}$$

If the forces K and F are completely uncorrelated then the cross-spectral densities S_{FK} and S_{KF} are equal to zero. In this case

$$S_{xx}(\omega) = (S_{FF} + S_{KK}) \cdot |H|^2 \quad \text{and} \quad G_{xx}(\omega) = (G_{FF} + G_{KK}) \cdot |H|^2 \quad (2.47)$$

The cross-power spectral density G_{Fx} is equal to $G_{FF}H$. The coherence function with respect to the force $F(t)$ and the displacement $x(t)$ is thus,

$$\begin{aligned} \gamma_{Fx}^2(\omega) &= \frac{|G_{Fx}(\omega)|^2}{G_{xx}(\omega)G_{FF}(\omega)} = \frac{|G_{FF}|^2 |H|^2}{(G_{FF} + G_{KK})G_{FF} |H|^2} \\ &= \frac{|G_{FF}|^2}{(G_{FF} + G_{KK})G_{FF}} < 1 \end{aligned} \quad (2.48)$$

The spectral densities G_{FF} and G_{KK} are positive and real. The coherence function is consequently equal to unity only if G_{KK} is zero. Otherwise the coherence function is less than unity. This is the case whenever:

- (i) The measurements are influenced by extraneous noise;
- (ii) The system is not linear;
- (iii) The response is due to an input $F(t)$ as well as other inputs.

The coherence function is thus a measure of the quality of two observations.

2.7 Time Averages of Power and Energy

It is often of great interest to determine the time averages of kinetic and potential energies of a mechanical system. These energies can be determined as functions of the FT of displacement and velocity. The time average of the square of a signal $x(t)$ is according to Eq. (2.34) equal to

$$E[x^2] = R_{xx}(0) = \frac{1}{2\pi} \int_{-\infty}^{\infty} S_{xx}(\omega) d\omega = \frac{1}{2\pi} \int_0^{\infty} G_{xx}(\omega) d\omega \quad (2.49)$$

The time average of the power input to a system is equal to the average of the product between force and velocity, or in a general way, between the signals $x(t)$ and $y(t)$. Thus,

$$E[xy] = R_{xy}(0) = \frac{1}{2\pi} \int_{-\infty}^{\infty} S_{xy}(\omega) d\omega$$

From Eqs. (2.36) and (2.32) it follows that

$$S_{xy}(-\omega) = S_{yx}(\omega) \quad \text{and} \quad S_{yx}(\omega) = S_{xy}^*(\omega)$$

Consequently,

$$\begin{aligned} E[xy] &= R_{xy}(0) = \frac{1}{2\pi} \int_0^{\infty} [S_{xy}(\omega) + S_{yx}(\omega)] d\omega \\ &= \frac{1}{\pi} \operatorname{Re} \int_0^{\infty} S_{xy}(\omega) d\omega = \frac{1}{2\pi} \operatorname{Re} \int_0^{\infty} G_{xy}(\omega) d\omega \end{aligned} \quad (2.50)$$

It can be stated that the functions $G_{xx}(\omega)$ and $G_{xy}(\omega)$ represent the time averages $E[x^2]$ and $E[xy]$ in the frequency domain.

Again returning to the simple mass-spring system, the transfer function $H(\omega)$ is from Eq. (2.17)

$$H(\omega) = \frac{1}{-m\omega^2 + k} = \frac{1}{m[(\omega_0^2 - \omega^2) + i\omega_0^2\delta_0]} \quad (2.51)$$

The FT of the force is $\hat{F}(\omega)$, consequently and according to Eq. (2.15) the FT of the response is $\hat{x} = \hat{F}H$. The power spectral density of the displacement is

$$S_{xx}(\omega) = \lim_{T \rightarrow \infty} \frac{|\hat{x}|^2}{T} = \lim_{T \rightarrow \infty} \frac{|H|^2 |\hat{F}|^2}{T} = |H|^2 S_{FF}(\omega) \quad (2.52)$$

As defined the FT of the resulting velocity is $\hat{x} = i\omega\hat{x} = \hat{v}$. Thus,

$$S_{vv}(\omega) = \omega^2 |H|^2 S_{FF}(\omega) \quad \text{or} \quad G_{vv}(\omega) = \omega^2 |H|^2 G_{FF}(\omega) \quad (2.53)$$

For a force defined by $F(t) = F_0 \sin \omega_1 t$ the corresponding power spectral density of the force is $G_{FF}(\omega) = \pi F_0^2 \cdot \delta(\omega - \omega_1)$. Consequently the spectral density has only one frequency component. The force is exciting a 1-DOF system, represented by the frequency response function $H(\omega)$. The resulting time average of the velocity squared is

$$\begin{aligned} \bar{v}^2 &= R_{vv}(0) \\ &= \frac{1}{2\pi} \int_0^{\infty} G_{vv}(\omega) d\omega \\ &= \frac{1}{2} \int_0^{\infty} |\omega H(\omega)|^2 \cdot F_0^2 \cdot \delta(\omega - \omega_1) d\omega \end{aligned}$$

$$\begin{aligned}
&= |\omega_1 H(\omega_1)|^2 \frac{F_0^2}{2} \\
&= \frac{\omega_1^2 F_0^2}{2m^2[(\omega_0^2 - \omega_1^2)^2 + (\omega_0^2 \delta_0)^2]}
\end{aligned} \tag{2.54}$$

This is the same result as obtained in Sect. 1.4.

The time average of the power input to the system is—compare Eq. (2.50)

$$\bar{\Pi} = E[F(t)v(t)] = R_{Fv}(0) = \frac{1}{2\pi} \text{Re} \int_0^\infty G_{Fv}(\omega) d\omega \tag{2.55}$$

The cross-spectral density G_{Fv} is

$$G_{Fv}(\omega) = \lim_{T \rightarrow \infty} 2 \frac{\hat{F}^* \hat{v}}{T} = \lim_{T \rightarrow \infty} 2 \frac{\hat{F}^*(i\omega) \hat{x}}{T} = 2i\omega S_{Fx} = i\omega G_{Fx} \tag{2.56}$$

The FT of the response is $\hat{x} = \hat{F}H$. For a force defined by $F(t) = F_0 \sin \omega_1 t$ and $G_{FF}(\omega) = \pi F_0^2 \cdot \delta(\omega - \omega_1)$, the cross-power spectral density between force and velocity is

$$G_{Fv}(\omega) = \lim_{T \rightarrow \infty} 2 \frac{\hat{F}^* \hat{v}}{T} = \lim_{T \rightarrow \infty} 2 \frac{|\hat{F}|^2 (i\omega) H(\omega)}{T} = i\omega G_{FF} H(\omega) \tag{2.57}$$

The frequency response function for the simple mass-spring system is defined in Eq. (2.17). Thus,

$$\begin{aligned}
\text{Re} G_{Fv}(\omega) &= \text{Re} \left\{ \frac{i\omega G_{FF}(\omega)}{m[(\omega_0^2 - \omega^2) + i\omega_0^2 \delta_0]} \right\} \\
&= \frac{\pi \omega_0^2 \omega \delta_0 F_0^2}{m[(\omega_0^2 - \omega^2)^2 + (\omega_0^2 \delta_0)^2]} \delta(\omega - \omega_1)
\end{aligned} \tag{2.58}$$

From Eq. (2.55) it follows that

$$\bar{\Pi} = \frac{\omega_0^2 \omega_1 \delta_0 F_0^2}{2m[(\omega_0^2 - \omega_1^2)^2 + (\omega_0^2 \delta_0)^2]} \tag{2.59}$$

The same procedure can be repeated for white noise excitation of the mass of the simple mass-spring system. For white noise excitation the autocorrelation function and the power spectral densities are

$$R_{FF}(\tau) = a \cdot \delta(\tau)$$

where

$$a = \lim_{T \rightarrow \infty} \frac{|\hat{F}|^2}{T} = S_{FF}(\omega)$$

$$G_{FF}(\omega) = 2a$$

Following the discussion above this means that

$$\begin{aligned} \bar{v}^2 &= \frac{1}{2\pi} \int_0^\infty G_{vv}(\omega) d\omega = \frac{1}{2\pi} \int_0^\infty \omega^2 G_{FF}(\omega) |H(\omega)|^2 d\omega \\ &= \frac{1}{2\pi} \int_0^\infty d\omega \frac{\omega^2 G_{FF}(\omega)}{m^2[(\omega_0^2 - \omega^2)^2 + (\omega_0^2 \delta_0)^2]} = \frac{a}{\pi m^2} \cdot I \end{aligned} \quad (2.60)$$

where

$$I = \int_0^\infty d\omega \frac{\omega^2}{[(\omega_0^2 - \omega^2)^2 + (\omega_0^2 \delta_0)^2]}$$

This type of integral appears quite often in analysis of dynamic problems. For future reference it is convenient to formulate a general solution to this type of integral. Thus, consider the contour integral

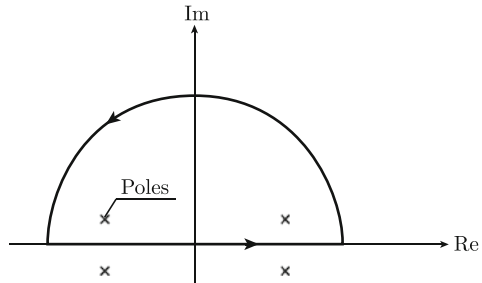
$$J = \oint \frac{g(z) dz}{(z^2 - \omega_0^2)^2 + (\omega_0^2 \delta_0)^2} = \oint \frac{g(z) dz}{h(z)}$$

The integration in the complex plane is along the path shown in Fig. 2.5.

The function $g(z)$ is analytic and regular in the domain. The integrand has two poles, $z_1 = \omega_0(1 + i\delta/2)$ and $z_2 = -\omega_0(1 - i\delta/2)$, in the upper half of the complex plane. It is assumed that $0 < \delta_0 \ll 1$. According to the theorem of residues and Cauchy's theorem—see Ref. [5]—the integral J is equal to

$$J = \oint \frac{g(z) dz}{h(z)} = 2\pi i \sum_n \frac{g(z_n)}{h'(z_n)} = 2\pi i \sum_n \frac{g(z_n)}{4z_n(z_n^2 - \omega_0^2)} \quad (2.61)$$

Fig. 2.5 Path of integration in complex plane



The summation is made over all poles inside the closed path shown in Fig. 2.5. For $\delta_0 \ll 1$ the result is for $g(\omega) = g(-\omega)$ quite simply equal to

$$J = \frac{\pi g(\omega_0)}{\omega_0^3 \delta_0} \quad (2.62)$$

The result is the sum of the integral along the real axis and along the semicircle C , or

$$J = \oint \frac{g(z)dz}{h(z)} = \int_{-\infty}^{\infty} \frac{g(z)dz}{h(z)} + \int_C \frac{g(z)dz}{h(z)}$$

If the functions $g(z)$ and $h(z)$ are such that the integral along the path C goes to zero as the radius of the circle goes to infinity, i.e., for $z = R \cdot \exp(i\varphi)$ and $R \rightarrow \infty$, then for $\delta_0 \ll 1$

$$J = \int_{-\infty}^{\infty} d\omega \frac{g(\omega)}{[(\omega_0^2 - \omega^2)^2 + (\omega_0^2 \delta_0)^2]} = \frac{\pi \cdot g(\omega_0)}{\omega_0^3 \delta_0} \quad (2.63)$$

Returning to Eq. (2.60) the integral I is now readily solved. For $g(\omega) = \omega^2$ the result given by Eqs. (2.60) and (2.63) is $I = \pi / (2\omega_0 \delta_0)$. Thus, for white noise excitation the time average of the velocity squared, Eq. (2.60), is

$$\begin{aligned} \bar{v}^2 &= \frac{a}{2m^2 \omega_0 \delta_0} \\ &= \frac{G_{FF}}{4m^2 \omega_0 \delta_0} \end{aligned} \quad (2.64)$$

The time average of the kinetic energy is consequently

$$\bar{T} = \frac{m \bar{v}^2}{2} = \frac{G_{FF}}{8m \omega_0 \delta_0} \quad (2.65)$$

The time average of the potential energy for the mass-spring system is, for white noise excitation and based on Eq. (2.63), equal to

$$\begin{aligned} \bar{U} &= \frac{\bar{x}^2 k_0}{2} \\ &= \frac{1}{2\pi} \int_{-\infty}^{\infty} d\omega \frac{k_0 S_{FF}}{2m^2 [(\omega_0^2 - \omega^2)^2 + (\omega_0^2 \delta_0)^2]} \\ &= \frac{S_{FF}}{4m \omega_0 \delta_0} \\ &= \frac{G_{FF}}{8m \omega_0 \delta_0} \end{aligned} \quad (2.66)$$

For white noise excitation of a 1-DOF system \bar{T} and \bar{U} are equal. This is not the case for harmonic excitation. In this case equality holds only at resonance.

The time average of the power input to the linear 1-DOF system is according to Eqs. (2.55) and (2.58) equal to

$$\bar{\Pi} = -\frac{1}{2\pi} \int_{-\infty}^{\infty} d\omega \cdot \omega S_{FF}(\omega) \cdot \text{Im}H(\omega)$$

The frequency response function $H(\omega)$ can be defined as in Eq. (2.13) or in (2.17). In the last case $\text{Im}H$ is

$$\text{Im}H(\omega) = -\frac{\omega_0^2 \delta_0}{m[(\omega_0^2 - \omega^2)^2 + (\omega_0^2 \delta_0)^2]}$$

The loss factor δ_0 is equal to $2\omega\beta/\omega_0^2$ as defined in Eq. (1.81). According to this definition, δ_0 is negative for $\omega < 0$ and positive for $\omega > 0$. Considering this, the time average of the power input to the system can be solved by means of a contour integration of the expression above. Compare the discussion at the end of Sect. 2.2. The alternative approach for solving the integral is to use Eq. (2.17) defining $H(\omega)$ as demonstrated in Problem 2.12. In the first case the time average of the input power for white noise excitation of the system is

$$\begin{aligned} \bar{\Pi} &= -\frac{1}{2\pi} \int_{-\infty}^{\infty} d\omega \cdot \omega S_{FF}(\omega) \text{Im}H(\omega) \\ &= S_{FF} \int_{-\infty}^{\infty} \frac{1}{2\pi} \cdot \frac{\omega \omega_0^2 \delta_0}{m[(\omega_0^2 - \omega^2)^2 + (\omega_0^2 \delta_0)^2]} d\omega \\ &= \frac{S_{FF}}{2m} \\ &= \frac{G_{FF}}{4m} \end{aligned} \tag{2.67}$$

Considering the results shown in Eqs. (2.65)–(2.67) the following important result is obtained:

$$\bar{\Pi} = \omega_0 \delta_0 (\bar{T} + \bar{U}) = m \bar{v}^2 \omega_0 \delta_0 \tag{2.68}$$

Thus, for white noise excitation of a linear mechanical system, the time average of the total energy of the system is proportional to the time average of the input power to the system and inversely proportional to its losses. The same result is not valid for harmonic excitation since for that case equality does not hold for the kinetic and potential energies. However, as in the case with white noise excitation the average velocity squared of the system is proportional to the input power and inversely proportional to the losses as demonstrated in Eq. (1.65). The last part of the expression (2.68) can be written in an alternative way since $\omega_0^2 = k_0/m$. Thus,

$$\bar{v}^2 = \frac{\bar{\Pi}}{\delta_0 \sqrt{mk_0}} \quad (2.69)$$

For a fixed power input to a system the velocity of the mass can be decreased if the stiffness, mass, or lossfactor is increased. In most practical cases it can be more or less impossible to increase mass or stiffness due to some other constraints. However, the losses can in general be altered as discussed in Chap. 5. These conclusions are somewhat deceptive since the input power to a system seldom is constant. If a 1-DOF system is excited by a harmonic force the average velocity squared is almost independent of the losses if the frequency of the harmonic force is somewhat different from the natural frequency of the system as shown in Eq. (2.54). Consequently, for this particular case added losses to the system do not significantly decrease the velocity of the mass. However, for white noise excitation the time average of the velocity squared is inversely proportional to the loss factor, Eq. (2.64). For this case added losses will always decrease the velocity of the mass.

2.8 Frequency Response and Point Mobility Functions

From Eq. (2.17) the frequency response function $H(\omega)$ for a linear 1-DOF system or quite simply a mass-spring system is

$$\begin{aligned} H(\omega) &= \frac{1}{m[(\omega_0^2 - \omega^2) + i\omega_0^2\delta_0]} \\ &= \frac{(\omega_0^2 - \omega^2) - i\omega_0^2\delta_0}{m[(\omega_0^2 - \omega^2)^2 + (\omega_0^2\delta_0)^2]} = |H(\omega)| e^{i\varphi_1} \end{aligned} \quad (2.70)$$

where

$$|H(\omega)| = \frac{1}{m[(\omega_0^2 - \omega^2)^2 + (\omega_0^2\delta_0)^2]^{1/2}}, \quad \varphi_1 = -\arctan \left[\frac{\omega_0^2\delta_0}{(\omega_0^2 - \omega^2)} \right] \quad (2.71)$$

The loss factor δ_0 can be a function of frequency as previously discussed. For example, if the losses are viscous then $\delta_0 = c\omega/k_0$, where c and k_0 are constants as defined in Chap. 1. For viscous losses $|H|$ has a maximum for $\omega = \sqrt{\omega_0^2 - (c/m)^2/2}$. In most practical cases the losses are small, which means that with a sufficient degree of accuracy the maximum of the absolute value of the frequency response function is obtained for $\omega = \omega_0$. If the loss factor is independent of frequency, then the maximum value is obtained exactly for $\omega = \omega_0$ and the value is

$$|H(\omega)|_{\max} = \frac{1}{m\omega_0^2\delta_0}$$

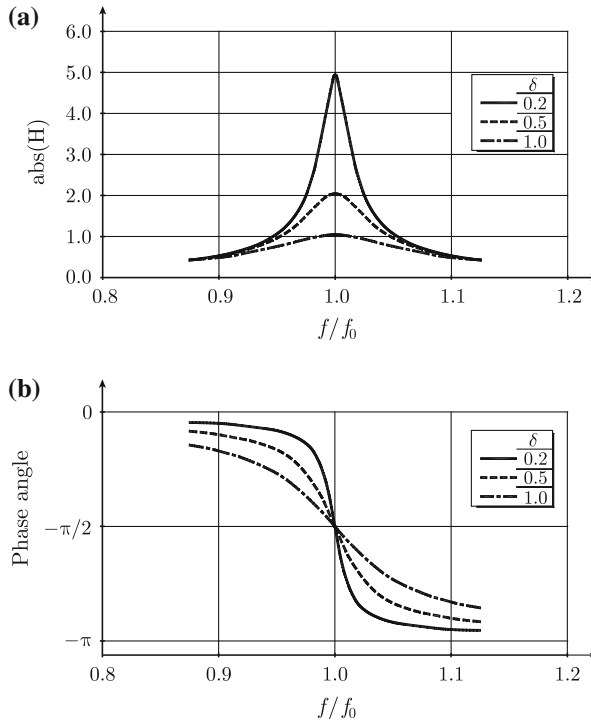


Fig. 2.6 Absolute value of frequency response function and phase angle for different loss factors

In Fig. 2.6 the function $|H|$ and φ_1 are shown for some different values of δ_0 . The limiting values are

$$\begin{aligned} |H(\omega)| &\rightarrow 1/k_0, & \varphi_1 &\rightarrow 0 & \text{as } \omega &\rightarrow 0 \\ |H(\omega)| &\rightarrow |H(\omega)|_{\max}, & \varphi_1 &\rightarrow -\pi/2 & \text{as } \omega &\rightarrow \omega_0 \end{aligned}$$

$$|H(\omega)| \rightarrow 1/(m\omega^2), \quad \varphi_1 \rightarrow -\pi \quad \text{as } \omega \rightarrow \infty$$

For a loss factor δ_0 of the order 0.1 the maximum at resonance is not very distinct. However, a loss factor of 0.1 is fairly high. Typical loss factors for various materials are presented in Chap. 3. Based on measurements of frequency response functions the resonance frequency for a heavily damped system is most readily determined from a phase diagram as shown in Fig. 2.6. The resonance is at the frequency for which the phase shift is $-\pi/2$.

The frequency response function has an interesting characteristic which is apparent if the function is plotted in a Nyquist diagram i.e. the imaginary part of H is plotted as a function of the real part of H . According to Eq. (2.70)

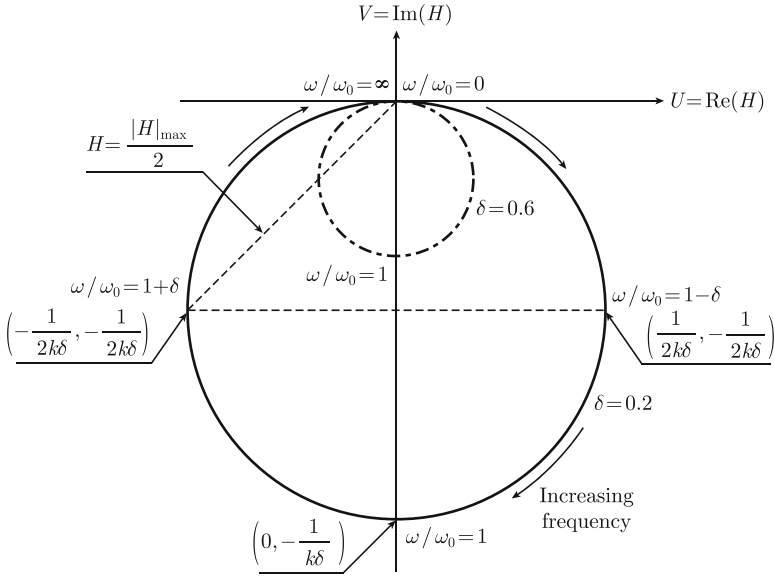


Fig. 2.7 Two Nyquist plots of transfer functions

$$\begin{aligned} \operatorname{Re} H(\omega) = U &= \frac{(\omega_0^2 - \omega^2)}{m[(\omega_0^2 - \omega^2)^2 + (\omega_0^2 \delta_0)^2]} \\ \operatorname{Im} H(\omega) = V &= \frac{-\omega_0^2 \delta_0}{m[(\omega_0^2 - \omega^2)^2 + (\omega_0^2 \delta_0)^2]} \end{aligned} \quad (2.72)$$

The parameters U and V fulfil the equation for a circle, i.e.,

$$U^2 + (V + V_0)^2 = V_0^2, \quad V_0 = \frac{1}{2m\omega_0^2 \delta_0} = \frac{1}{2k_0 \delta_0} \quad (2.73)$$

The radius of the circle is inversely proportional to the loss factor. Two examples of Nyquist diagrams of H are given in Fig. 2.7. For systems with several degrees of freedom similar curves but not exact circles are obtained for frequencies at and very close to each resonance frequency. The distortion of the circular shape for a multi-degree of freedom system depends on how close the resonance frequencies are. For a large spacing the shape of the curve is almost a perfect circle. Note that when $|H| = |H|_{\max}/2$ then $U = \pm V$ as indicated in Fig. 2.7.

The point mobility function $Y(\omega)$ is related to the frequency response function. If a force F , FT \hat{F} , is applied to a certain point of a dynamical system and if the resulting FT of the velocity in that particular point is \hat{v} , then the point mobility $Y(\omega)$ is defined as:

$$Y(\omega) = \frac{\hat{v}(\omega)}{\hat{F}(\omega)} \quad (2.74)$$

It has already been shown that the FT of the deflection of the point at which a force F , FT \hat{F} , is applied is given by $\hat{x} = \hat{F}H$. It has also been demonstrated that the FT of the velocity in that point is $\hat{v} = i\omega\hat{x}$. Based on these two expressions and Eq. (2.74) the point mobility is written as

$$Y(\omega) = \frac{\hat{v}(\omega)}{\hat{F}(\omega)} = \frac{i\omega\hat{x}(\omega)}{\hat{F}(\omega)} = i\omega H(\omega) \quad (2.75)$$

Accordingly, for a simple mass-spring system mounted on an infinitely stiff foundation the point mobility of the mass is obtained from Eqs. (2.75) and (2.70)

$$\begin{aligned} Y(\omega) &= \frac{i\omega}{m[(\omega_0^2 - \omega^2) + i\omega_0^2\delta_0]} \\ &= \frac{\omega\omega_0^2\delta_0 + i\omega(\omega_0^2 - \omega^2)}{m[(\omega_0^2 - \omega^2)^2 + (\omega_0^2\delta_0)^2]} = |Y(\omega)| e^{i\varphi_2} \end{aligned} \quad (2.76)$$

The absolute value of the mobility and the phase angle are

$$\begin{aligned} |Y(\omega)| &= \frac{|\omega|}{m[(\omega_0^2 - \omega^2)^2 + (\omega_0^2\delta_0)^2]^{1/2}}, \\ \varphi_2 &= -\arctan \left[\frac{(\omega^2 - \omega_0^2)}{\omega_0^2\delta_0} \right] = \varphi_1 + \frac{\pi}{2} \end{aligned} \quad (2.77)$$

In Fig. 2.8 the point mobility and phase angle are given for a few cases for which the loss factor has been varied. Compare the corresponding results for the frequency response function, Fig. 2.6.

Again, some limiting values

$$\begin{aligned} |Y(\omega)| &\rightarrow \omega/k_0, & \varphi_2 &\rightarrow \pi/2 & \text{as } \omega &\rightarrow 0 \\ |Y(\omega)| &\rightarrow |Y(\omega)|_{\max}, & \varphi_2 &\rightarrow 0 & \text{as } \omega &\rightarrow \omega_0 \\ |Y(\omega)| &\rightarrow 1/(m\omega), & \varphi_2 &\rightarrow -\pi/2 & \text{as } \omega &\rightarrow \infty \end{aligned}$$

In the first case, $\omega \rightarrow 0$, the absolute value of the point mobility can be said to be stiffness controlled. In the second case, i.e., in the high frequency region $|Y(\omega)|$ is mass controlled. When the mass and the stiffness of the spring approach infinity, the point mobility tends to zero.

The point mobility of a mass-spring system or, in fact, any system is a very important parameter, which determines the power input to the system. Returning to Eqs. (2.55) and (2.56) it is demonstrated that the cross-power spectral density G_{Fv} is

$$G_{Fv}(\omega) = \lim_{T \rightarrow \infty} 2 \frac{\hat{F}^* \hat{v}}{T}$$

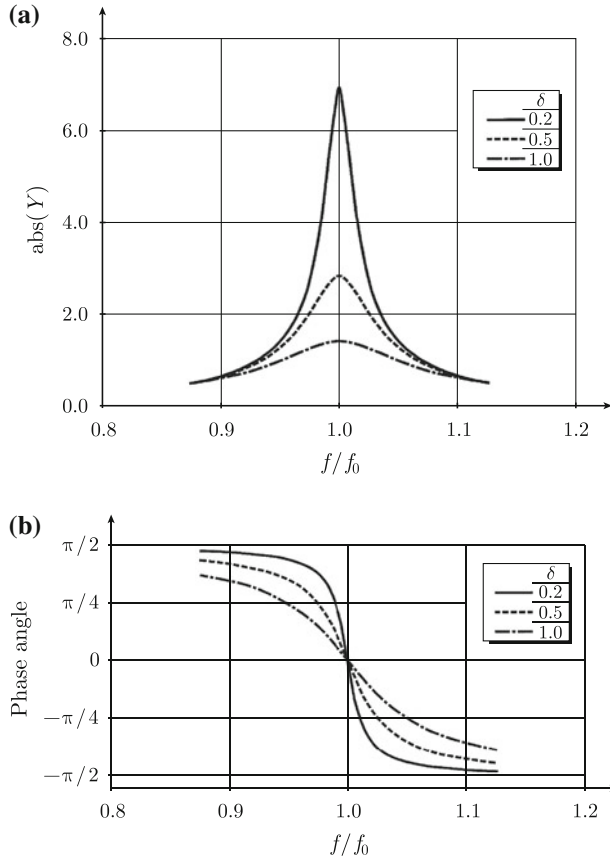


Fig. 2.8 Absolute value of point mobility and corresponding phase angle as function of frequency for different loss factors

However, $\hat{v} = \hat{F}Y$. Thus,

$$G_{Fv}(\omega) = \lim_{T \rightarrow \infty} 2 \frac{\hat{F}^* \hat{v}}{T} = \lim_{T \rightarrow \infty} 2 \frac{\hat{F}^* \hat{F} Y}{T} = G_{FF} Y \quad (2.78)$$

This expression is the same as Eq.(2.57) considering that $Y = i\omega H$. The time average of the power input to the system is according to Eq.(2.55) given by

$$\bar{\Pi} = \frac{1}{2\pi} \text{Re} \int_0^\infty G_{Fv}(\omega) d\omega = \frac{1}{2\pi} \int_0^\infty \text{Re} Y \cdot G_{FF}(\omega) d\omega \quad (2.79)$$

Thus, the time average of the power input to a system is a function of the real part of the point mobility of the structure at the excitation point.

In all the previous examples it has been assumed that the point mobility of the foundation on which a mass-spring system is mounted is equal to zero, i.e., the foundation is infinitely stiff. If however this point mobility is known from measurements or calculations, the resulting motion of the mass can be derived as functions of the mobility at the point on the foundation where the spring is mounted.

Thus, consider the system shown in Fig. 1.11. The equation of motion for the mass m is

$$m\ddot{x} + k(x - y) = F \quad (2.80)$$

The force on the foundation is $F_f = k(x - y)$. The spring constant k is complex or $k = k_0(1 + i\delta_0)$. In the equation above the deflections of mass and foundation are x and y respectively. The problem is solved by making the following transformations:

$$x \rightarrow \hat{x} \cdot e^{i\omega t}, \quad y \rightarrow \hat{y} \cdot e^{i\omega t}, \quad F \rightarrow \hat{F} \cdot e^{i\omega t}$$

This type of transformation was discussed in Sect. 2.2. Consequently \hat{x} is the FT of x and so on. The velocity of the foundation depends on the force F exciting it and the point mobility at the excitation point. The FT of the velocity of the foundation is

$$\hat{y} = i\omega \hat{y} = \hat{F}_f \cdot Y = kY(\hat{x} - \hat{y}) \quad (2.81)$$

where Y is its point mobility of the foundation. The displacements of mass and foundation are given by two equations

$$\hat{x}(-m\omega^2 + k) - k\hat{y} = \hat{F} \quad \text{and} \quad i\omega \hat{y} = kY(\hat{x} - \hat{y}) \quad (2.82)$$

These equations are obtained after inserting the transformations above in Eq. (2.80). From Eq. (2.82) the FTs of the displacements \hat{x} and \hat{y} are

$$\hat{x} = \frac{\hat{F}(kY + i\omega)}{-m\omega^2 kY + i\omega k - i\omega^3 m}, \quad \hat{y} = \frac{\hat{F}kY}{-m\omega^2 kY + i\omega k - i\omega^3 m} \quad (2.83)$$

In the limiting case for an infinitely stiff foundation $Y = 0$, the standard solution for \hat{x} is obtained. With no foundation at all, Y is infinite and $\hat{x} = -\hat{F}/(m\omega^2)$. This is also the response of a completely free mass.

From Eq. (2.83) it is obvious that the resonance frequencies for the system are functions of Y . Depending on the point mobility the system can now have multi degrees of freedom. For $\text{Re}Y > 0$ there is an energy flow to the foundation that increases the losses of the mass-spring system. Point and transfer mobilities for beams and plates are discussed in subsequent chapters.

2.9 Loss Factor

The loss factor for a mechanical system is clearly a very important parameter. Detailed knowledge of this factor is essential in order to describe the motion and energy balance of any system. The loss factor is often measured by means of either of four methods:

- (i) half band width;
- (ii) reverberation time;
- (iii) power injection;
- (iv) Nyquist plot.

The last technique was reviewed in Sect. 2.8. In addition, the modal analysis method can be used as discussed in Ref. [12].

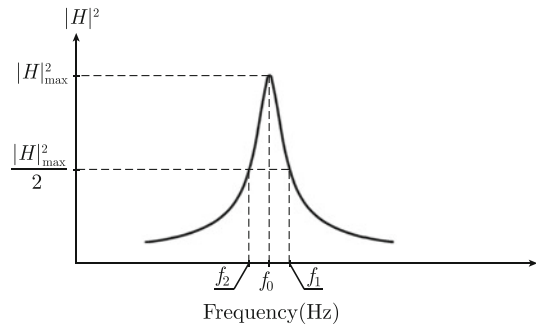
For a hypothetical 1-DOF system the four methods are straightforward. So let us again return to the simple mass-spring system with mass m and complex spring constant $k = k_0(1 + i\delta)$. The frequency response function H for a 1-DOF system relating force and displacement can be determined from measurements of the cross-spectral density G_{Fx} between force and displacement and the power spectral density G_{FF} of the force function. According to definition the frequency response function is obtained as

$$H(\omega) = \frac{G_{Fx}(\omega)}{G_{FF}(\omega)} \quad (2.84)$$

One example of a frequency response function or $|H| = |\hat{x}/\hat{F}|$ is shown in Fig. 2.9. Compare also Fig. 2.6. The resonance frequency f_0 , angular frequency $\omega_0 = 2\pi f_0$, is the frequency for which $|H|$ has a maximum and when the phase angle is equal to $-\pi/2$ as shown in Fig. 2.6. The energy of a 1-DOF system is proportional to $|H|^2$. A frequently used concept for the characterization of a system is to define the angular frequencies ω_1 and ω_2 for which

$$|H(\omega_1)|^2 = |H(\omega_2)|^2 = |H(\omega_0)|^2 / 2 = |H|_{\max}^2 \quad (2.85)$$

Fig. 2.9 Determination of loss factor based on the half band method



These angular frequencies satisfying Eq. (2.85) can be derived from Eq. (2.71) by considering the denominator in the expression for $|H(\omega)|$. Thus,

$$(\omega_0^2 - \omega_{1,2}^2)^2 + (\omega_0^2 \delta_0)^2 = 2(\omega_0^2 \delta_0)^2$$

The roots are $\omega_{1,2} = \omega_0 \sqrt{1 \pm \delta_0}$. For $\delta \ll 1$, which is generally the case, the roots can be simplified as

$$\omega_1 = \omega_0(1 + \delta_0/2), \quad \omega_2 = \omega_0(1 - \delta_0/2) \quad (2.86)$$

Consequently

$$\delta_0 = \frac{\omega_1 - \omega_2}{\omega_0} = \frac{f_1 - f_2}{f_0} \quad (2.87)$$

The frequency difference $\Delta f = f_1 - f_2$ is often referred to as the half bandwidth of the resonance peak.

Thus, if the frequency response function for a system can be determined through measurements as function of frequency, then the resonance frequency and the loss factor can be estimated. The half bandwidth of the resonance peak is equal to the width of the peak when the maximum absolute value of the frequency response function is reduced by a factor $\sqrt{2}$. The loss factor obtained from Eq. (2.87) is the loss factor at the frequency f_0 . The quality of the estimate depends on the resolution of the frequency analyser used. For continuous systems or in fact real structures excited by a force there are an infinite number of resonances. The various resonance peaks can be extremely difficult to separate even in the low frequency region. The half bandwidth technique is best suited for simple systems like beams. Even so, only approximately the first ten resonances can usually be identified. For a plate, resonances are very close or even coinciding making the technique less useful.

It is interesting to return to the Nyquist diagram of the frequency response function shown in Fig. 2.6. The angular frequencies for which $\text{Re}H = \pm \text{Im}H$ are equal to ω_1 and ω_2 given in Eq. (2.86). This follows directly from the discussion in Sect. 2.3. The Nyquist plot can be used also for continuous systems. However, the proximity of resonance frequencies makes the determination of loss factors difficult.

The reverberation time method is based on the fact that free vibrations of a system decay with time. If a system is excited by a constant force which at a certain time is turned off or if the system is excited by an impulse, for example a hammer blow, then the motion of the system is determined by free vibrations. For lightweight structures a gentle knock by the fist is often sufficient to excite the structures. For heavy solid structures a hammer blow might be required. At other times a shaker is needed. The response of a 1-DOF system excited by an impulse is given by Eq. (1.79). The kinetic energy of the system is decaying as $\exp(-\omega_0 \delta_0 t)$ as shown in Eq. (1.80). Thus,

$$\bar{v}^2 = C \cdot e^{-\omega_0 \delta_0 t} \quad (2.88)$$

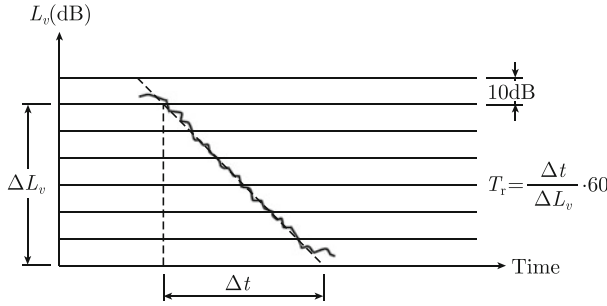


Fig. 2.10 Decay curve for measurement of reverberation time

where C is some constant. The velocity level of the mass as a function of time is

$$L_v(t) = 10 \log \left(\frac{\bar{v}^2}{v_{\text{ref}}^2} \right) = L_v(0) - 10\omega_0\delta_0 t \log e \quad (2.89)$$

The velocity level at $t = 0$ is $L_v(0)$. An example of a measured decay curve is given in Fig. 2.10. The decay curve is fairly smooth if ω_0 is sufficiently large. The reverberation time T_r in seconds is defined as the time during which the velocity level is decreased 60 dB. Thus, from Eq. (2.89) $10\omega_0\delta_0 T_r \log e = 60$.

The loss factor is consequently given by

$$\delta_0 = \frac{6}{2\pi f_0 T_r \log e} \approx \frac{2.2}{f_0 T_r} \quad (2.90)$$

Very often it is not possible to record the decay for 60 dB. This could for example be due to noise in the system or a broken decay curve as shown in Fig. 2.11. The general procedure is therefore to measure the time for the velocity level to decrease from say the 5 dB level to the 20 dB level below the maximum. The reverberation time is

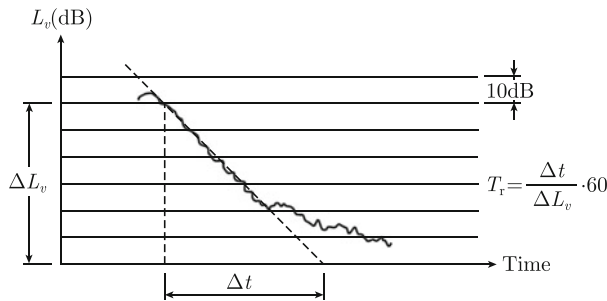


Fig. 2.11 Broken decay curve

thereafter obtained through extrapolation. The reverberation time and thus the loss factor can only be determined at a natural frequency of the system. For continuous systems the reverberation time and loss factors are determined for frequency bands, typically 1/3 octave bands. The resulting loss factor then represents some frequency average over the band width since each band could include a number of natural frequencies.

The power injection method has already been discussed in Sect. 2.7. If a constant force is acting on a mass of a mass-spring system the resulting velocity of the mass is a function of the loss factor. The result given in Eq. (2.68) means that if the time average of the input power $\bar{\Pi}$ and the time average of the velocity squared \bar{v}^2 are known then for a 1-DOF system

$$\delta_0 = \frac{\bar{\Pi}}{m\omega_0\bar{v}^2} \quad (2.91)$$

From Eq. (2.54) the power spectral density G_{vv} for the velocity is given as

$$G_{vv} = |H|^2 \omega^2 G_{FF}$$

The real part of the cross-spectral density G_{Fv} is according to Eq. (2.57) equal to

$$\text{Re}G_{Fv} = -\omega G_{FF} \text{Im}H$$

According to Eq. (2.17) the imaginary part of the frequency response function H for a 1-DOF system is

$$\begin{aligned} \text{Im}H(\omega) &= \text{Im} \frac{1}{m[(\omega_0^2 - \omega^2) + i\omega_0^2\delta_0]} \\ &= \frac{-\omega_0^2\delta_0}{m[(\omega_0^2 - \omega^2)^2 + (\omega_0^2\delta_0)^2]} = -m\omega_0^2\delta_0 |H|^2 \end{aligned}$$

From these expressions it follows that

$$\delta_0 = \frac{\omega}{m\omega_0^2} \cdot \frac{\text{Re}G_{Fv}}{G_{vv}} \quad (2.92)$$

The methods discussed above can also be used to determine the loss factors for systems with multidegrees of freedom. For plate structures the half bandwidth method is difficult to use in the high frequency range since the resonance peaks can be closely linked or spaced. It can therefore be impossible to determine the necessary frequencies f_0 , f_1 and f_2 for all but a few resonances.

The reverberation time technique is more versatile, when as is generally the case, an average loss factor is required for a certain frequency band. The structure is excited by white noise within a frequency band while the time decay of the velocity

level within this frequency band is recorded. This band could contain one or several resonances. This could result in a broken decay curve of the type shown in Fig. 2.10. In a case like this the upper part of the decay curve should always be used, in order to get a proper average of the losses within the band. It is consequently of great importance to have a visual display of the reverberation curve.

The power injection method can always be used for any type of structure as long as this structure is not connected to any other construction. If this is the case the vibrating mass can not be determined. The resulting loss factor includes losses to adjoining structures. However, this is always the case whenever loss factors are measured. Detailed studies indicate that the use of the reverberation time technique ensures the most reliable results as compared to the other three procedures.

2.10 Response of a 1-DOF System, A Summary

A number of different representations have been used to describe the response of a simple 1-DOF system. For the sake of completeness it is therefore appropriate to make a comparison between the different techniques.

1. Harmonic force excitation

A 1-DOF system is excited by a harmonic force $F(t) = F_0 \sin \omega_1 t$. The equation of motion of the system is

$$m\ddot{x} + c\dot{x} + k_0x = F_0 \sin \omega_1 t$$

According to Eq. (1.57) the response of the mass is given by

$$\begin{aligned} x(t) &= A_1 \sin \omega_1 t + A_2 \cos \omega_1 t = A_0 \sin(\omega_1 t + \varphi) \\ &= \frac{F_0[(\omega_0^2 - \omega_1^2) \sin \omega_1 t - (\omega_0^2 \delta_0) \cos \omega_1 t]}{m[(\omega_0^2 - \omega_1^2)^2 + (\omega_0^2 \delta_0)^2]} \end{aligned} \quad (2.93)$$

where A_0 , A_1 and A_2 and φ are defined in Eq. (1.60). The time average, over the period T , of the velocity squared is

$$\bar{v}^2 = \frac{1}{T} \int_0^T dt \dot{x}^2 = \frac{\omega_1^2 F_0^2}{2m^2[(\omega_0^2 - \omega_1^2)^2 + (\omega_0^2 \delta_0)^2]} \quad (2.94)$$

The time average of the force squared is $\bar{F}^2 = |F_0|^2 / 2$. Thus, Eq. (2.94) can also be written as

$$\bar{v}^2 = \bar{F}^2 \frac{\omega_1^2}{m^2[(\omega_0^2 - \omega_1^2)^2 + (\omega_0^2 \delta_0)^2]} \quad (2.95)$$

The time average of the input power to the system is

$$\begin{aligned}\bar{\Pi} &= \frac{1}{T} \int_0^T dt F \dot{x} = \frac{\omega_1 \omega_0^2 \delta_0 F_0^2}{2m[(\omega_0^2 - \omega_1^2)^2 + (\omega_0^2 \delta_0)^2]} \\ &= \bar{F}^2 \frac{\omega_1 \omega_0^2 \delta_0}{m[(\omega_0^2 - \omega_1^2)^2 + (\omega_0^2 \delta_0)^2]}\end{aligned}\quad (2.96)$$

2. Harmonic force excitation, complex notation

The equation of motion for the system is given by Eq. (1.82) as

$$m\ddot{x} + kx = F(t)$$

where

$$F(t) = F_0 \exp(i\omega_1 t), \quad k = k_0(1 + i\delta)$$

The response, having the same time dependence as the force, is

$$x = x_0 e^{i\omega_1 t} = \frac{F_0 e^{i\omega_1 t}}{k - m\omega_1^2} = \frac{F_0 e^{i\omega_1 t}}{m[\omega_0^2(1 + i\delta_0) - \omega_1^2]} \quad (2.97)$$

The time average of the absolute value of the force squared is $|\bar{F}|^2 = |\bar{F}_0|^2/2$ and the time average of the absolute value of the velocity squared is

$$\begin{aligned}|\bar{v}^2| &= \frac{|\dot{x}|^2}{2} = \frac{|F_0|^2 \omega_1^2}{2m^2[(\omega_0^2 - \omega_1^2)^2 + (\omega_0^2 \delta_0)^2]} \\ &= \bar{F}^2 \frac{\omega_1^2}{m^2[(\omega_0^2 - \omega_1^2)^2 + (\omega_0^2 \delta_0)^2]}\end{aligned}\quad (2.98)$$

The time average of the input power to the system is

$$\begin{aligned}\bar{\Pi} &= \frac{1}{2} \text{Re}(F \cdot v^*) = \frac{|F_0|^2 \omega_1 \omega_0^2 \delta_0}{2m[(\omega_0^2 - \omega_1^2)^2 + (\omega_0^2 \delta_0)^2]} \\ &= \frac{|\bar{F}|^2 \omega_1 \omega_0^2 \delta_0}{m[(\omega_0^2 - \omega_1^2)^2 + (\omega_0^2 \delta_0)^2]}\end{aligned}\quad (2.99)$$

Thus, as in the previous case, Eq. (2.98) is identical to Eq. (2.95) and Eq. (2.99) to (2.96).

Equation (2.99) can also be written as

$$\bar{\Pi} = \frac{1}{2} \text{Re}(F \cdot v^*) = \frac{|F_0|^2}{2} \text{Re} Y \quad (2.100)$$

where Y is the mobility at the excitation point.

3. Fourier transform

In the time domain the equation of motion of the system is as before written as

$$m\ddot{x} + kx = F(t)$$

where

$$F(t) = F_0 \exp(i\omega t), \quad k = k_0(1 + i\delta)$$

By making the substitutions $F \rightarrow \hat{F}e^{i\omega t}$ and $x \rightarrow \hat{x}e^{i\omega t}$ in the equation of motion, then if \hat{F} is the Fourier transform of $F(t)$, it follows that \hat{x} is the FT of x as discussed in Sect. 2.2. Thus

$$\hat{x} = \frac{\hat{F}}{k - m\omega^2} = \frac{\hat{F}}{m[\omega_0^2(1 + i\delta_0) - \omega^2]} = \hat{F} \cdot H(\omega) \quad (2.101)$$

The Fourier transform of the velocity is $\hat{v} = i\omega\hat{x} = i\omega\hat{F}H$. Thus, the power spectral density of the velocity is obtained as

$$\begin{aligned} S_{vv}(\omega) &= \lim_{T \rightarrow \infty} \frac{|\hat{v}|^2}{T} = \lim_{T \rightarrow \infty} \frac{\omega^2 |\hat{F}|^2 |H|^2}{T} = S_{FF}(\omega) \omega^2 |H|^2 \\ &= S_{FF}(\omega) \frac{\omega^2}{m^2[(\omega_0^2 - \omega^2)^2 + (\omega_0^2 \delta_0)^2]} \end{aligned} \quad (2.102)$$

For harmonic excitation $F(t) = F_0 \sin \omega_1 t$ the power spectral density of the force is

$$S_{FF}(\omega) = \frac{\pi F_0^2 \cdot [\delta(\omega - \omega_1) + \delta(\omega + \omega_1)]}{2} \quad (2.103)$$

The time average of the velocity squared is obtained from Eqs. (2.101) and (2.103) as

$$|\bar{v}|^2 = \frac{1}{2\pi} \int_{-\infty}^{\infty} S_{vv}(\omega) d\omega = \frac{\omega_1^2 F_0^2}{2m^2[(\omega_0^2 - \omega_1^2)^2 + (\omega_0^2 \delta_0)^2]} \quad (2.104)$$

The time average of the force squared is

$$|\bar{F}|^2 = \frac{1}{2\pi} \int_{-\infty}^{\infty} S_{FF}(\omega) d\omega = \frac{|F_0|^2}{2}$$

Thus,

$$|\bar{v}|^2 = \frac{\omega_1^2 |\bar{F}|^2}{m^2[(\omega_0^2 - \omega_1^2)^2 + (\omega_0^2 \delta_0)^2]} \quad (2.105)$$

The power spectral density of the input power is given as

$$G_{\Pi} = G_{FF} \text{Re}(i\omega H) = G_{FF} \text{Re}(Y) = G_{FF} \frac{\omega_0^2 \omega_1 \delta_0}{m[(\omega_0^2 - \omega_1^2)^2 + (\omega_0^2 \delta_0)^2]} \quad (2.106)$$

The time average of the power in put is

$$\bar{\Pi} = \frac{1}{2\pi} \int_{-\infty}^{\infty} G_{\Pi}(\omega) d\omega = \frac{|\bar{F}|^2 \omega_0^2 \omega_1 \delta_0}{m[(\omega_0^2 - \omega_1^2)^2 + (\omega_0^2 \delta_0)^2]} \quad (2.107)$$

Thus, using any of the three methods the results are the same with respect to the time averages of velocity squared and input power. The results support the convention introduced in Sect. 1.6 with respect to complex notations.

Problems

2.1 Determine the FT of the function

$$\begin{aligned} h(t) &= \exp(-\beta t) \cdot \sin(\omega_n t) / (m\omega_n) \text{ for } t \geq 0 \\ h(t) &= 0 \text{ for } t < 0 \end{aligned}$$

where $\omega_n^2 = \omega_0^2 - \beta^2$ and $\beta = \omega_0^2 \delta / (2\omega) > 0$.

2.2 A periodic signal $x(t) = x(t + T)$ is a function of time as

$$x(t) = A \text{ for } 0 \leq t \leq T/2 \text{ and } x(t) = 0 \text{ for } T/2 < t < T$$

Determine the autocorrelation function and power spectral density of the signal.

2.3 The frequency response function $H(\omega)$ of a 1-DOF system is

$$H(\omega) = \frac{1}{-m\omega^2 + k} = \frac{1}{m[(\omega_0^2 - \omega^2) + i\omega_0^2 \delta]}$$

Show that the inverse FT of H is equal to

$$h(t) = \exp(-\omega_0 t \delta / 2) \cdot \sin(\omega_0 t) / (m\omega_0)$$

2.4 The mass of a mass-spring system is excited by the force defined in example 2.2. Determine the time average of the velocity squared for the mass m . The spring constant is

$$k = k_0(1 + i\delta).$$

2.5 Determine the autocorrelation functions for band-pass white noise and low-pass white noise. In the first case $G_{xx}(f) = a$ for $0 \leq f_0 - B/2 \leq f \leq f_0 + B/2$ and in the second case $G_{xx}(f) = a$ for $0 \leq f \leq B$.

2.6 A force $F(t)$ is applied to the mass m of a mass-spring system. The complex spring constant is given by $k = k_0(1 + i\delta)$. The force is $F(t) = A \sin(\omega_1 t) + \xi(t)$, where $\xi(t)$ is a random signal with the one sided power spectral density $G_{\xi\xi} = A^2/(2\omega_0)$ where $\omega_0^2 = k_0/m$. Determine the time average of the velocity squared of the mass.

2.7 Determine the time averages of the potential and kinetic energies of a mass-spring system for which the mass is excited by a force $F(t) = F_0 \cdot \sin(\omega_1 t)$.

2.8 Determine the time average of the velocity squared of the mass of a lightly damped mass-spring system excited by a force characterized by an exponential autocorrelation function, i.e., having a one-sided power spectral density

$$G_{FF}(\omega) = \frac{4a}{a^2 + \omega^2}.$$

2.9 A mass-spring system is mounted on a foundation as shown in Fig. 1.1. The point mobility of the foundation is Y_f . Determine the point mobility Y in the excitation point.

2.10 For the system described in Problem 2.9 determine the one sided power spectral density of the power transmitted to the foundation. The power spectral density of the force exciting the mass is constant and equal to G_{FF} . The point mobility of the foundation is Y_f . Determine also the time average of the power input to the foundation if Y_f is real and much smaller than unity and in addition independent of frequency.

2.11 The mass of a mass-spring system is excited by a force $F(t)$, with the one-sided power spectral density G_{FF} . The response of the mass is $z(t) = x(t) + y(t)$ where $y(t)$ is due to extraneous and random noise. The one-sided power spectral density of the random signal y is G_{yy} . The response x due to the force can be written as $x = HF$ where H is the frequency response function for the system. Determine the coherence function between the force F and the displacement z .

2.12 Determine the time average of the power input

$$\bar{\Pi} = -\frac{1}{2\pi} \int_{-\infty}^{\infty} d\omega \cdot S_{FF}(\omega) \cdot \text{Im}(H)$$

when the frequency response function is defined according to Eq. (2.17) as

$$H(\omega) = \frac{1}{-m\omega^2 + i\omega c + k_0} = \frac{1}{m(\omega_0^2 - \omega^2 + 2i\beta\omega)}$$

2.13 A function $x(t)$ is written $x(t) = \frac{a_0}{2} + \sum_{n=1}^{\infty} (a_n \cos \omega_n t + b_n \sin \omega_n t)$ in the time interval $-T/2 \leq t \leq T/2$. Show that as $T \rightarrow \infty$ the function can be written in integral form as

$$x(t) = \frac{1}{2\pi} \int_{-\infty}^{\infty} d\omega \cdot \hat{x}(\omega) e^{i\omega t} \quad \text{where} \quad \hat{x}(\omega) = \int_{-\infty}^{\infty} dt \cdot x(t) e^{-i\omega t}$$

2.14 Show that $E[\dot{x}^2(t)] = - \left[\frac{d^2 R_{xx}}{d\tau^2} \right]_{\tau=0}$.

Chapter 3

Waves in Solids

The energy flow in structures is caused by various types of waves. The description and understanding of the character of these waves are therefore essential. In this chapter, the basic differential equations governing the one-dimensional propagation of longitudinal, transverse, torsional, and bending waves are discussed. The equations are derived based on the concept of strains and stresses in beam-like structures. Thereafter, flexural waves in thin plates are considered. General solutions to the various wave equations are introduced. Based on these solutions, expressions for kinetic and potential energies are derived. The energy flow and the intensity concept in plates and beams are also discussed.

Later in Chap. 4, the so-called generalized wave equation is derived and discussed. The general wave equation governs all wave types discussed in this chapter and in fact all elastic motions of a solid. It could therefore be argued that it would have been sufficient just to include the generalized wave equation in this chapter. However, the derivations of the more simple one-dimensional equations improve the physical understanding of the generalized case.

3.1 Stresses and Strains

A solid, which is exposed to external forces, is deformed. For example, consider a bar with a rectangular cross section being stretched. The bar is submitted to a normal stress σ_x in the direction of its main axis, which coincides with the x -axis of a Cartesian coordinate system as shown in Fig. 3.1.

Due to the stress σ_x the bar will be elongated but at the same time, the dimensions of the cross section will be decreased due to contraction. For an isotropic material, the resulting strains in the direction of the main coordinate axes are

$$\varepsilon_x = \sigma_x/E, \quad \varepsilon_y = -\nu\sigma_x/E, \quad \varepsilon_z = -\nu\sigma_x/E. \quad (3.1)$$

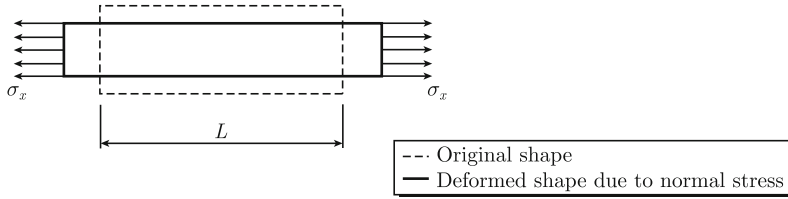


Fig. 3.1 Deformation of bar due to normal stress along main axis

In these expressions, E is the Young's modulus of elasticity and ν the Poisson's ratio. Inasmuch as experience shows that hydrostatic compression induces reduction of volume, $\nu = 0.5$ is an upper limit of the Poisson's ratio for isotropic materials. The lower theoretical limit is zero.

If the displacements along the three coordinate axes x , y , and z are defined as ξ , η , and ζ , respectively, the resulting strains are

$$\varepsilon_x = \frac{\partial \xi}{\partial x}, \quad \varepsilon_y = \frac{\partial \eta}{\partial y}, \quad \varepsilon_z = \frac{\partial \zeta}{\partial z}. \quad (3.2)$$

Equations (3.1) and (3.2) defining ε_x give

$$\frac{\partial \xi}{\partial x} = \frac{\sigma_x}{E}.$$

The length of the bar shown in Fig. 3.1 is L when the bar is not exposed to any external forces. The total deflection is obtained by the integration of the expression above over the entire length of the bar. Assuming σ_x constant along the length of the element the result is

$$\xi = L\sigma_x/E.$$

The force F_x stretching the bar at each end is

$$F_x = S\sigma_x, \quad (3.3)$$

where S is the area of the cross section of the uniform bar. The strain is assumed to be constant over the cross-sectional area. Consequently based on these assumptions, the total displacement or elongation ξ of the bar due to the force F_x is

$$\xi = \frac{F_x L}{SE}. \quad (3.4)$$

The elongation of the bar is proportional to the force and the initial length of the bar. This is Hooke's law.

If on the other hand the element shown in Fig. 3.1 is exposed to normal stresses in all three directions, i.e., along the three main axes x , y , and z , the resulting strains are

$$\begin{aligned}\varepsilon_x &= [\sigma_x - \nu(\sigma_y + \sigma_z)]/E, & \varepsilon_y &= [\sigma_y - \nu(\sigma_x + \sigma_z)]/E, \\ \varepsilon_z &= [\sigma_z - \nu(\sigma_x + \sigma_y)]/E.\end{aligned}\quad (3.5)$$

Based on these expressions, the stresses can be derived as functions of the strains. The result is

$$\begin{aligned}\sigma_x &= \frac{E}{1+\nu} \left[\varepsilon_x + \frac{\nu}{1-2\nu} (\varepsilon_x + \varepsilon_y + \varepsilon_z) \right] \\ \sigma_y &= \frac{E}{1+\nu} \left[\varepsilon_y + \frac{\nu}{1-2\nu} (\varepsilon_x + \varepsilon_y + \varepsilon_z) \right] \\ \sigma_z &= \frac{E}{1+\nu} \left[\varepsilon_z + \frac{\nu}{1-2\nu} (\varepsilon_x + \varepsilon_y + \varepsilon_z) \right]\end{aligned}\quad (3.6)$$

If in an infinite medium or solid, the strain can vary in one direction only—let say in the x -direction—then $\varepsilon_y = \varepsilon_z = 0$ assuming no cross-sectional contraction. If these boundary conditions are inserted in Eq.(3.6) the result is

$$\sigma_x = \varepsilon_x \frac{E(1-\nu)}{(1+\nu)(1-2\nu)} = \varepsilon_x E_x. \quad (3.7)$$

The parameter E_x is quite simply the ratio between the stress and the strain in the x -direction. For ν approaching 0.5, the stress σ_x required to achieve a finite strain ε_x is becoming increasingly large as given by Eq.(3.7). In the limiting case, $\nu = 0.5$, the solid is incompressible. For certain rubber materials Poisson's ratio can be close to 0.5.

For a plate, which is oriented in the x - y plane, the stress σ_z perpendicular to the plate is equal to zero on the two surfaces of the plate. For a sufficiently thin plate, σ_z is set equal to zero throughout the plate. If the strain can only vary in the x -direction in the plane of the plate, then $\varepsilon_y = 0$. The boundary conditions $\sigma_z = 0$ and $\varepsilon_y = 0$ inserted in Eq.(3.5) yield

$$\sigma_x = \varepsilon_x \frac{E}{(1-\nu^2)} = \varepsilon_x E_x. \quad (3.8)$$

For these boundary conditions, $\sigma_z = 0$ and $\varepsilon_y = 0$, a strain in the z -direction is also induced. According to Eq.(3.5), $\sigma_y = \nu\sigma_x$ and $\varepsilon_z = -\nu(\sigma_x + \sigma_y)/E$. These expressions in combination with Eq.(3.8) lead to $\varepsilon_z = -\nu\varepsilon_x/(1-\nu)$.

Finally for a bar with its length along the x -axis and a small and constant cross-sectional area exposed to a force along its length the stresses σ_y and σ_z are zero. Thus for $\sigma_y = \sigma_z = 0$, Eq.(3.5) gives

$$\sigma_x = E\varepsilon_x = E_x\varepsilon_x. \quad (3.9)$$

For these boundary conditions, corresponding to a bar or rather a slender beam, strains in the z - and y -directions are induced. According to Eq.(3.5) these strains are $\varepsilon_y = \varepsilon_z = -\nu\varepsilon_x$.

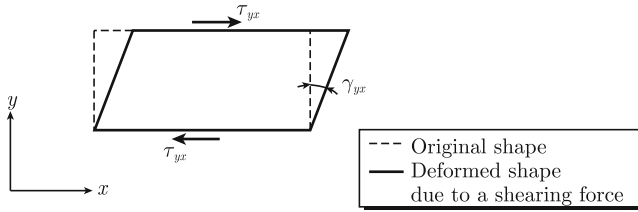


Fig. 3.2 Deformation of an element due to a shear force

The results relating normal stress and strain along the x -axis or the center line of a beam, plate or infinite body can be summarized in tabular form as follows:

Structure	$E_x = \sigma_x / \varepsilon_x$
Infinite body	$E(1 - \nu) / ((1 + \nu)(1 - 2\nu))$
Thin plate	$E / (1 - \nu^2)$
Slender beam	E

In addition to normal stresses, a volume element of a solid can also be exposed to a shearing stress. A simple case of a shearing deformation is shown in Fig. 3.2.

The shear stress τ_{xy} is proportional to the shear angle γ_{xy} as $\tau_{xy} = G\gamma_{xy}$, where G is the shear modulus of the material. If as before the deformation in the x -direction is given by ξ then for the one-dimensional case the shear angle is $\gamma_{yx} = \partial\xi / \partial y$. The shear modulus G is directly related to the E modulus as

$$G = \frac{E}{2(1 + \nu)}. \quad (3.10)$$

It is now of interest to consider in two dimensions the possible displacements and strains of a small element. The displacements in the x and y directions are given by ξ and η , respectively. In the first case, illustrated in Fig. 3.3a, the element is exposed to pure normal stresses in the x and y directions. The resulting strains are

$$\varepsilon_x = \frac{\partial\xi}{\partial x}, \quad \varepsilon_y = \frac{\partial\eta}{\partial y}.$$

In the second case, Fig. 3.3b, the element is deformed due to shear along the x - and y -axes. For pure shear, the angles γ_1 and γ_2 are equal, thus $\gamma_1 = \gamma_2 = \gamma/2$ and

$$\gamma_1 = \frac{\partial\xi}{\partial y}, \quad \gamma_2 = \frac{\partial\eta}{\partial x}.$$

The shear angle γ in the x - y plane is denoted γ_{xy} . According to the definitions of γ_1 and γ_2 it follows that

$$\gamma_{xy} = \gamma_1 + \gamma_2 = \frac{\partial\xi}{\partial y} + \frac{\partial\eta}{\partial x} = \gamma_{yx}.$$

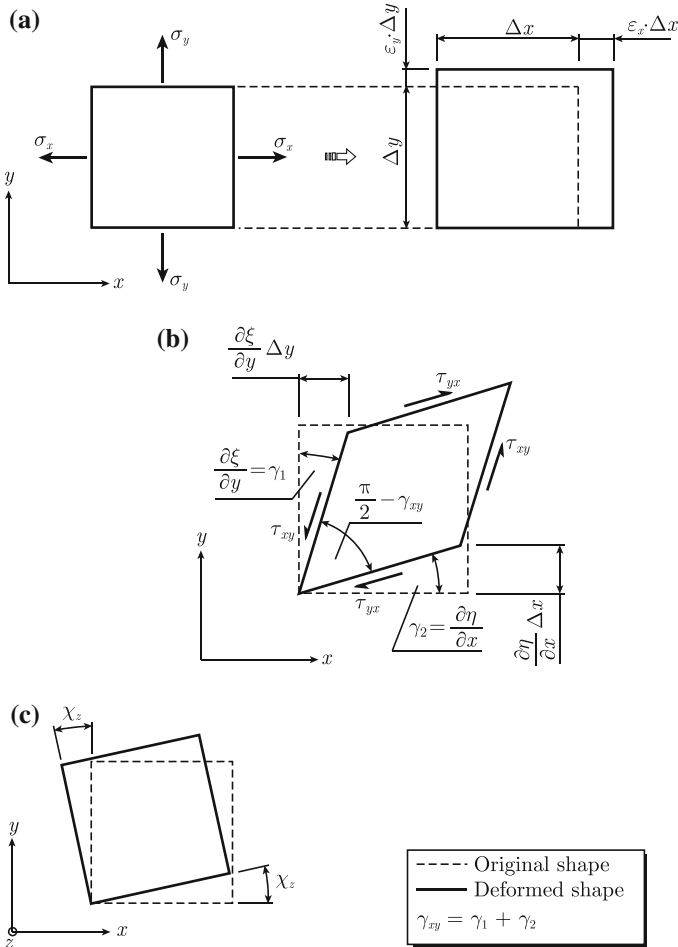


Fig. 3.3 Deformation in two dimensions **a** pure extension. **b** Pure shear. **c** Pure rotation

In the third case, Fig. 3.3c, the element is rotated about the z -axis. The element is not exposed to any stress—the displacement is due to pure rotation. The rotational angle is χ_z and in terms of the displacements ξ and η given as

$$\chi_z = \frac{1}{2} \left(\frac{\partial \eta}{\partial x} - \frac{\partial \xi}{\partial y} \right).$$

The index z identifies the axis around which the rotation takes place.

For the general three-dimensional case with displacements ξ , η , and ζ along the x , y , and z -axes the strains, shear and rotational angles are

$$\begin{aligned}
\varepsilon_x &= \frac{\partial \xi}{\partial x}, \quad \varepsilon_y = \frac{\partial \eta}{\partial y}, \quad \varepsilon_z = \frac{\partial \zeta}{\partial z} \\
\gamma_{xy} = \gamma_{yx} &= \frac{\partial \xi}{\partial y} + \frac{\partial \eta}{\partial x}, \quad \gamma_{xz} = \gamma_{zx} = \frac{\partial \xi}{\partial z} + \frac{\partial \zeta}{\partial x}, \quad \gamma_{yz} = \gamma_{zy} = \frac{\partial \eta}{\partial z} + \frac{\partial \zeta}{\partial y} \\
\chi_z &= \frac{1}{2} \left(\frac{\partial \eta}{\partial x} - \frac{\partial \xi}{\partial y} \right), \quad \chi_y = \frac{1}{2} \left(\frac{\partial \xi}{\partial z} - \frac{\partial \zeta}{\partial x} \right), \quad \chi_x = \frac{1}{2} \left(\frac{\partial \zeta}{\partial y} - \frac{\partial \eta}{\partial z} \right) \quad (3.11)
\end{aligned}$$

The shear stresses are $\tau_{xy} = G\gamma_{xy}$, $\tau_{xz} = G\gamma_{xz}$, and $\tau_{yz} = G\gamma_{yz}$. The stress-strain relationship is in matrix form written as

$$\begin{Bmatrix} \sigma_x \\ \sigma_y \\ \sigma_z \\ \tau_{xy} \\ \tau_{xz} \\ \tau_{yz} \end{Bmatrix} = \frac{E}{(1+\nu)(1-2\nu)} [Q] \begin{Bmatrix} \varepsilon_x \\ \varepsilon_y \\ \varepsilon_z \\ \gamma_{xy} \\ \gamma_{xz} \\ \gamma_{yz} \end{Bmatrix},$$

where

$$[Q] = \begin{bmatrix} (1-\nu) & \nu & \nu & 0 & 0 & 0 \\ \nu & (1-\nu) & \nu & 0 & 0 & 0 \\ \nu & \nu & (1-\nu) & 0 & 0 & 0 \\ 0 & 0 & 0 & (1-2\nu)/2 & 0 & 0 \\ 0 & 0 & 0 & 0 & (1-2\nu)/2 & 0 \\ 0 & 0 & 0 & 0 & 0 & (1-2\nu)/2 \end{bmatrix} \quad (3.12)$$

Since $\gamma_{xy} = \gamma_{yx}$ it follows that $\tau_{xy} = \tau_{yx}$. The Eqs. (3.6) and (3.12) together constitute Hooke's generalized law. For an isotropic material there are two independent elastic coefficients, either E and G , E and ν or G and ν . Test methods for determining the main elastic parameters are described in for example Ref. [78].

The various stress components are illustrated in Fig. 3.4. The equations governing the simple wave types can be derived based on the concepts concerning stresses and strains discussed above.

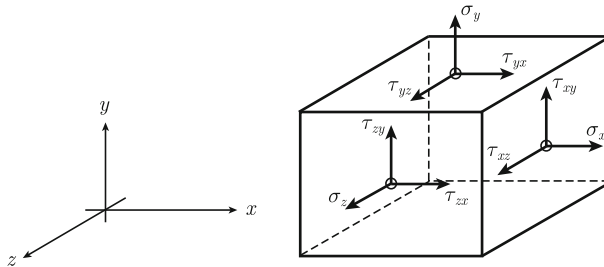


Fig. 3.4 Stresses acting on a volume element. The positive directions are indicated

The strain–stress relation is also given by means of the compliance matrix, the inverse of the matrix in Eq. (3.12). For future reference, this relationship is also given in matrix form.

$$\begin{Bmatrix} \varepsilon_x \\ \varepsilon_y \\ \varepsilon_z \\ \gamma_{xy} \\ \gamma_{xz} \\ \gamma_{yz} \end{Bmatrix} = \begin{bmatrix} 1/E & -\nu/E & -\nu/E & 0 & 0 & 0 \\ -\nu/E & 1/E & -\nu/E & 0 & 0 & 0 \\ -\nu/E & -\nu/E & 1/E & 0 & 0 & 0 \\ 0 & 0 & 0 & 1/G & 0 & 0 \\ 0 & 0 & 0 & 0 & 1/G & 0 \\ 0 & 0 & 0 & 0 & 0 & 1/G \end{bmatrix} \begin{Bmatrix} \sigma_x \\ \sigma_y \\ \sigma_z \\ \tau_{xy} \\ \tau_{xz} \\ \tau_{yz} \end{Bmatrix} \quad (3.13)$$

The shear modulus G is $G = E/[2(1 + \nu)]$.

According to Eqs. (3.6) and (3.12), stresses and strains can be related by means of the independent material parameters ν and E . In the literature various other parameters are often introduced. This can in many cases be convenient, but at times also rather confusing when results from different sources are compared. The shear modulus G is a parameter, which is a function of the two basic parameters ν and E . Some other examples are

$$\begin{aligned} \text{Bulk modulus } K &= \frac{E}{3(1 - 2\nu)} \\ \text{Lamé constant } \lambda &= \frac{\nu E}{(1 + \nu)(1 - 2\nu)}. \end{aligned}$$

In fact both G and λ are referred to as the Lamé constants. In some literature G is denoted μ . However, throughout this text, only the parameters E , G , and ν are used.

Many problems in the field of vibro-acoustics are most easily solved by means of various types of energy methods. This is discussed in subsequent sections and chapters. However, for future reference it is therefore now convenient to derive the energy stored in a solid as function of the strains. The potential energy \mathcal{U}_v and kinetic energy \mathcal{T}_v stored per unit volume of a solid can be derived from the basic equations relating stresses and strains. The potential energy \mathcal{U}_v per unit volume of the solid is

$$\mathcal{U}_v = \int (\sigma_x d\varepsilon_x + \sigma_y d\varepsilon_y + \sigma_z d\varepsilon_z + \tau_{xy} d\gamma_{xy} + \tau_{xz} d\gamma_{xz} + \tau_{yz} d\gamma_{yz}). \quad (3.14)$$

The stresses σ and τ are given in Eqs. (3.6) and (3.12). However, the various strain components are not independent functions. This means that terms on the form $\varepsilon_x d\varepsilon_y$ cannot be evaluated separately. This problem can be overcome if instead the contribution due to the normal stresses, the first part of the integral, is written

$$\mathcal{U}_{v1} = \frac{E}{1 + \nu} \int [\varepsilon_x d\varepsilon_x + \varepsilon_y d\varepsilon_y + \varepsilon_z d\varepsilon_z + \frac{\nu}{1 - 2\nu} (\varepsilon_x + \varepsilon_y + \varepsilon_z) d(\varepsilon_x + \varepsilon_y + \varepsilon_z)].$$

This result is obtained by inserting Eq. (3.6) in (3.14). The integration of the expression above is now straight forward. The result is

$$\mathcal{U}_{v1} = \frac{E}{2(1+\nu)} \left[\varepsilon_x^2 + \varepsilon_y^2 + \varepsilon_z^2 + \frac{\nu}{1-2\nu} (\varepsilon_x + \varepsilon_y + \varepsilon_z)^2 \right]. \quad (3.15)$$

The components of the shear stresses are given in Eq. (3.12). The stored potential energy due to shear is thus

$$\mathcal{U}_{v2} = \int (\tau_{xy} d\gamma_{xy} + \tau_{xz} d\gamma_{xz} + \tau_{yz} d\gamma_{yz}) = \frac{G}{2} (\gamma_{xy}^2 + \gamma_{xz}^2 + \gamma_{yz}^2). \quad (3.16)$$

The total stored potential energy \mathcal{U}_v per unit volume is consequently

$$\begin{aligned} \mathcal{U}_v = \mathcal{U}_{v1} + \mathcal{U}_{v2} = G & \left[\varepsilon_x^2 + \varepsilon_y^2 + \varepsilon_z^2 \right. \\ & \left. + \frac{\nu}{1-2\nu} (\varepsilon_x + \varepsilon_y + \varepsilon_z)^2 + \frac{1}{2} (\gamma_{xy}^2 + \gamma_{xz}^2 + \gamma_{yz}^2) \right] \end{aligned} \quad (3.17)$$

The kinetic energy \mathcal{T}_v per unit volume is

$$\mathcal{T}_v = \frac{\rho}{2} \left[\left(\frac{\partial \xi}{\partial t} \right)^2 + \left(\frac{\partial \eta}{\partial t} \right)^2 + \left(\frac{\partial \zeta}{\partial t} \right)^2 \right]. \quad (3.18)$$

As before ξ , η and ζ are the displacements along the main coordinate axes.

If in a closed volume V_0 the total energy is varying with time there will be a net flow of energy through the surface S_0 enclosing the volume. If the intensity vector due to this flow is \mathbf{I} , then considering the conservation of energy and in the absence of a source inside the volume

$$\int_{S_0} \mathbf{I} \cdot \mathbf{n} dS + \int_{V_0} \frac{\partial}{\partial t} (\mathcal{U}_v + \mathcal{T}_v) dV = 0.$$

Considering the Stoke theorem the integral equation is equivalent to

$$\nabla \cdot \mathbf{I} + \frac{\partial}{\partial t} (\mathcal{U}_v + \mathcal{T}_v) = 0.$$

The intensity induced by normal and shear stresses in a solid can be written in vector form as $\mathbf{I} = (I_x, I_y, I_z)$. The components of the intensity vector are derived in Chap. 5. However, the result is already now summarized as

$$\begin{aligned} I_x &= -\sigma_x \dot{\xi} - \tau_{xy} \dot{\eta} - \tau_{xz} \dot{\zeta}, & I_y &= -\sigma_y \dot{\eta} - \tau_{xy} \dot{\xi} - \tau_{yz} \dot{\zeta}, \\ I_z &= -\sigma_z \dot{\zeta} - \tau_{xz} \dot{\xi} - \tau_{yz} \dot{\eta} \end{aligned} \quad (3.19)$$

The stresses are defined in Eqs. (3.6) and (3.12). The intensity induced by various wave types is discussed in subsequent sections. The intensity is a very important quantity for the mapping of energy flow between structural elements. However, unlike the acoustical intensity, the structural intensity is extremely difficult to measure.

3.2 Losses in Solids

The damping in solids is due to the internal friction of materials. Hooke's law, i.e., proportionality between force and displacement, cannot be completely verified in practice. It was proposed by Boltzman [13] that there is an elastic delay in solids. The deformation of a solid is delayed with respect to the force. The deformation depends on not only the stress applied at one particular instant but also on the stresses applied at any previous instant. The stress-strain relationship is explained by means of a memory or relaxation function as

$$\sigma(t) = \int_{-\infty}^t C(t - \tau) \frac{d\varepsilon(\tau)}{d\tau} d\tau. \quad (3.20)$$

The memory function $C(t - \tau)$ is only defined as long as $(t - \tau) \geq 0$. For $(t - \tau) < 0$ the function $C(t - \tau)$ is set to equal zero. The integral in Eq. (3.20) can thus be integrated from minus to plus infinity. A partial integration of Eq. (3.20) yields

$$\begin{aligned} \sigma(t) &= [C(t - \tau)\varepsilon(\tau)]_{-\infty}^t + \int_{-\infty}^t c(t - \tau)\varepsilon(\tau) d\tau \\ &= C(0)\varepsilon(t) + \int_{-\infty}^t c(t - \tau)\varepsilon(\tau) d\tau \end{aligned} \quad (3.21)$$

where $c(t) = dC(t)/dt$. The strain $\varepsilon(t)$ tends to be zero as t approaches minus infinity. Equation (3.20) gives the stress-strain relationship according to classic theory proposed by Volterra [14], and also discussed in Refs. [15, 16].

The function $c(t)$ in Eq. (3.21) is experimentally found to be a negative monotone increasing function of time. As a first approximation the functions $C(t)$ and its derivative $c(t)$ are written as

$$C(t) = A_0 + A_1 \cdot e^{-\alpha_1 t}, \quad c(t) = -\alpha_1 \cdot A_1 \cdot e^{-\alpha_1 t}. \quad (3.22)$$

The parameters A_0 , A_1 , and α_1 are positive and real. Equation (3.22) inserted in Eq. (3.21) yields

$$\sigma(t) = C(0)\varepsilon(t) - \alpha_1 \cdot A_1 \cdot e^{-\alpha_1 t} \int_{-\infty}^t e^{\alpha_1 \tau} \varepsilon(\tau) d\tau. \quad (3.23)$$

A derivation with respect to t gives

$$\dot{\sigma}(t) = C(0)\dot{\varepsilon}(t) + \alpha_1^2 \cdot A_1 \cdot e^{-\alpha_1 t} \int_{-\infty}^t e^{\alpha_1 \tau} \varepsilon(\tau) d\tau - \alpha_1 \cdot A_1 \cdot \varepsilon(t). \quad (3.24)$$

By multiplying Eq. (3.23) by α_1 and by adding Eq. (3.24) to this result the integral is eliminated. The result is

$$\alpha_1 \sigma + \dot{\sigma} = [\alpha_1 \cdot C(0) - \alpha_1 \cdot A_1] \varepsilon(t) + C(0) \dot{\varepsilon}(t). \quad (3.25)$$

The parameter $C(0)$ is according to Eq. (3.22) equal to $A_0 + A_1$. The expression (3.25) is rewritten as

$$\sigma + \dot{\sigma}/\alpha_1 = E(\varepsilon + \dot{\varepsilon}/\beta), \quad (3.26)$$

with $E = A_0$ and $1/\beta = (1 + A_1/A_0)/\alpha_1$. The parameter β is positive since A_0 , A_1 , and α_1 all are positive. Equation (3.26) is often referred to as the standard linear model giving the stress–strain relationship. For the static case, $\dot{\sigma} = \dot{\varepsilon} = 0$, Eq. (3.26) is reduced to Hooke's law as given by the first part of Eq. (3.1). Equation (3.26) represents a more complex relationship than given by the simple viscous model

$$\sigma = E(\varepsilon + \nu \dot{\varepsilon}). \quad (3.27)$$

The parameter ν is determined by the viscous losses in the material. The model (3.27), referred to as the Kelvin-Voigt model, can be compared to Eq. (1.7) in Sect. 1.1, describing the motion of a simple mass-spring system with viscous losses. In the example (1.7), the force on the mass caused by the spring is $kx + c\dot{x}$, where x is the displacement of the mass.

Yet another frequently used model was proposed by Maxwell and is given by

$$E \cdot \dot{\varepsilon} = \dot{\sigma} + \sigma/\nu. \quad (3.28)$$

The added complexity of Eq. (3.26) as compared to the simple Hooke's law can be overcome if only simple harmonic oscillations are considered. For this particular case the stress–strain relationship given by Eq. (3.26) can be much simplified. It is assumed that σ and ε vary with time as $\exp(i\omega t)$, i.e., $\dot{\sigma} = i\omega\sigma$ and $\dot{\varepsilon} = i\omega\varepsilon$. For this case Eq. (3.26) is reduced to

$$\sigma(1 + i\omega/\alpha_1) = E\varepsilon(1 + i\omega/\beta).$$

Thus

$$\frac{\sigma}{\varepsilon} = E \left[\frac{1 + \omega^2/(\alpha_1\beta) + i\omega(1/\beta - 1/\alpha_1)}{1 + (\omega/\alpha_1)^2} \right]. \quad (3.29)$$

By defining this ratio or complex modulus as

$$\frac{\sigma}{\varepsilon} = E_0 [1 + i\eta_0], \quad (3.30)$$

where E_0 and η_0 are real, it is found that

$$\left| \frac{\sigma}{\varepsilon} \right| = E \left[\frac{1 + (\omega/\beta)^2}{1 + (\omega/\alpha_1)^2} \right]^{1/2}, \quad E_0 = E \left[\frac{1 + \omega^2/(\alpha_1\beta)}{1 + (\omega/\alpha_1)^2} \right],$$

$$\eta_0 = \frac{\omega(1/\beta - 1/\alpha_1)}{1 + (\omega/\alpha_1)^2}. \quad (3.31)$$

According to Eq. (3.26) $1/\beta > 1/\alpha_1$ resulting in the loss factor being positive. The absolute value of the complex modulus or $|\sigma/\varepsilon|$ as well as the loss factor η_0 are shown in Figs. 3.5 and 3.6, respectively. The loss factor, or rather the internal loss factor for a viscoelastic material, has a maximum when $\omega = \sqrt{\alpha_1\beta}$. In the same frequency range there is transition of the ratio $|\sigma/\varepsilon|$ from E to $E\alpha_1/\beta > E$.

The variation of the absolute value of the shear modulus as function of frequency for two materials, plexiglas and a certain type of rubber, is shown in Figs. 3.7 and 3.8 from the Refs. [17, 18], respectively.

For certain materials the memory function must be defined as a sum of exponentials as

Fig. 3.5 Absolute value of complex modulus as function of angular frequency, Eq. (3.31)

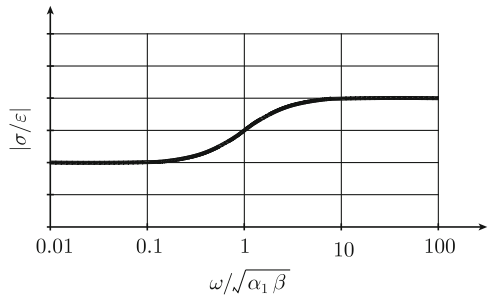


Fig. 3.6 Loss factor as function of angular frequency as given by Eq. (3.31)

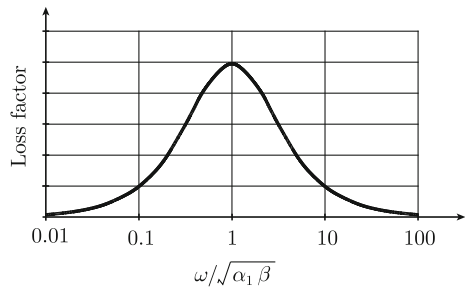


Fig. 3.7 Relative magnitude of complex shear modulus for plexiglas, from Ref. [17]

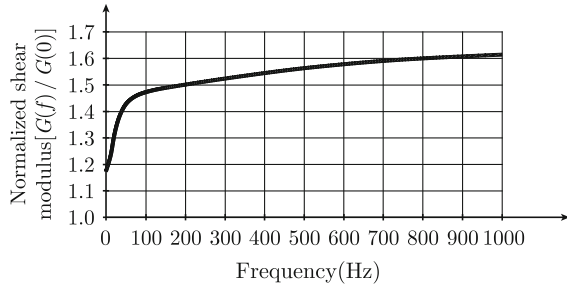
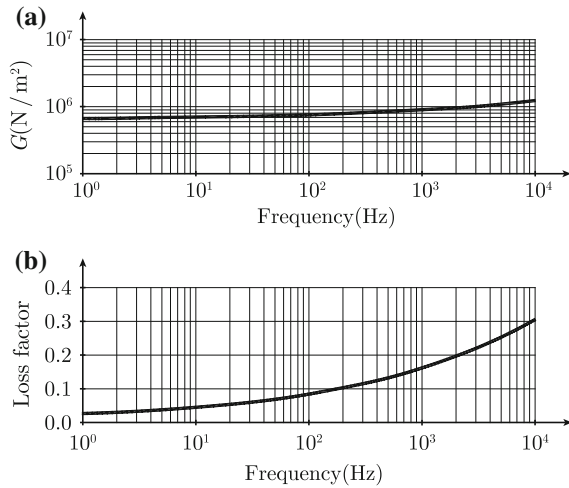


Fig. 3.8 Complex shear modulus and loss factor for a rubber material, from Ref. [18]



$$C(t) = \sum_{n=0}^N A_n \cdot e^{-\alpha_n t}.$$

Again assuming a periodic displacement the loss factor can be obtained as a function of frequency. The resulting loss factor exhibits a number of peaks, which can be attributed to certain physical phenomena as discussed in Refs. [15, 16]. Thermodynamic effects can be included as suggested for example by Lesieutre [19] and summarized by Dovstam [20].

For plexiglas the shear modulus and thus the E -modulus starts to level out in the midfrequency region as shown in Fig. 3.7. For rubber the quantity $\sqrt{\alpha_1 \beta}$ defined in Eq. (3.31) is very high. Consequently the shear modulus and loss factor are steadily increasing up to very high frequencies. For simple linear solids exposed to harmonic oscillations and normal conditions with respect strain, stress, and temperature, the real part of the E -modulus can be considered to be constant in the frequency range of general interest within the field of sound and vibration. The E -modulus for a number of simple linear solids is given in Table 3.1 in Sect. 3.3. The magnitudes of the internal loss factors are also indicated. The internal or material loss factor is decreasing for

Table 3.1 Mechanical properties of some materials under standard conditions

Material	Density ρ (kg/m ³)	Young's modulus E (N/m ²)	Poisson's ratio ν	Phase velocity L-waves c_l (m/s)
Aluminum	2700	0.72×10^{11}	0.34	5200
Lead	11300	0.17×10^{11}	0.43	1250
Iron	7800	2×10^{11}	0.30	5050
Steel	7800	2.1×10^{11}	0.31	5100
Magnesium	1740	0.43×10^{11}	0.29	5000
Brass	8500	0.95×10^{11}	0.33	3200
Tin	7280	0.04×10^{11}	0.39	780
Concrete*	2400	0.28×10^{11}	0.25	3400
Light-weight concrete*	600	0.014×10^{11}		1550
Chipboard*	440	0.012×10^{11}		1650
Glass*	2400	0.6×10^{11}	0.24	5000

The properties of the materials marked by * can vary considerably. The phase velocity is given for longitudinal waves propagating in bars, Eq. (3.53). The internal loss factor is $(0.2 - 3) \times 10^{-4}$ for steel and $(0.3 - 10) \times 10^{-5}$ for aluminum. For lead the internal loss factor is much higher or $(5 - 30) \times 10^{-2}$.

increasing frequencies for $\omega \gg \sqrt{\alpha_1 \beta}$. For coupled structures, the internal losses are very small as compared to the losses due to the energy transfer from one structure to another. However, the application of damping layers on the structure can change this as discussed in Sect. 5.5.

3.3 Transverse Waves

There are two wave types, which can be classified as in-plane waves. These are transverse and longitudinal waves. When these waves propagate in a thin plate, both the directions of the waves and their displacements are in the same plane as the plate.

Starting with transverse or shear waves, consider a small element of a thin homogeneous and isotropic plate. The element is located in the x - y plane as shown in Fig. 3.9. The stress τ_{xy} is independent of z since the plate is assumed to be thin. The shear causes a deflection ξ along the x -axis. At a distance Δy from the x -axis the displacement is $\Delta \xi$. According to the geometry shown in Fig. 3.9, $\Delta \xi$ depends on the shear angle γ_{xy} as $\Delta \xi = \Delta y \cdot \gamma_{xy}$. In the limiting case

$$\gamma_{xy} = \frac{\partial \xi}{\partial y}. \quad (3.32)$$

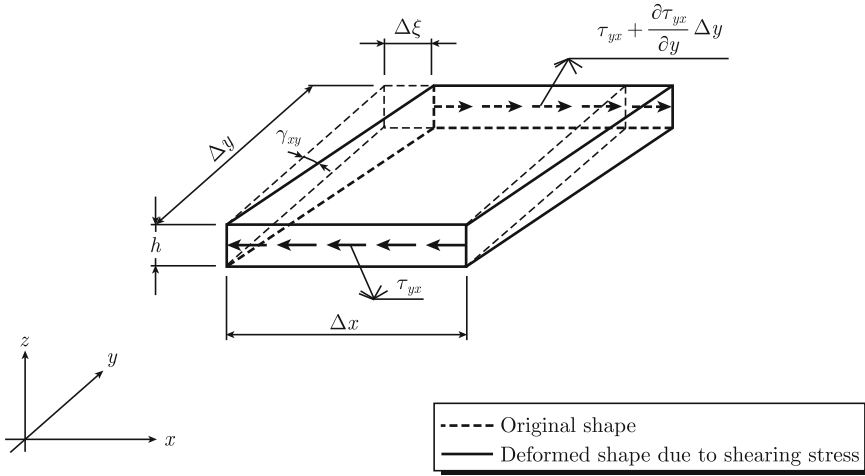


Fig. 3.9 Shear deformation of a plate element

The shear stress τ_{yx} , on the near surface of the element shown in Fig. 3.9, is proportional to the shear angle or

$$\tau_{xy} = G\gamma_{xy} = G \frac{\partial \xi}{\partial y}. \quad (3.33)$$

On the opposite surface, for $y = \Delta y$, the shear stress is $\tau_{yx}(\Delta y) \approx \tau_{yx}(0) + \Delta y \cdot \partial\tau_{yx}/\partial y$. Let $\Delta S = h \cdot \Delta x$ be the area of the near as well as the opposite surface with h being the thickness of the plate. The total force ΔF acting on the plate element in the x -direction is from Fig. 3.9

$$\Delta F = \Delta S \left(\tau_{yx} + \frac{\partial \tau_{yx}}{\partial y} \Delta y - \tau_{yx} \right) = h \Delta x \cdot \Delta y \frac{\partial \tau_{yx}}{\partial y} = h \Delta x \cdot \Delta y \cdot G \frac{\partial^2 \xi}{\partial y^2}. \quad (3.34)$$

The mass Δm of the element is

$$\Delta m = \Delta x \cdot \Delta y \cdot h \cdot \rho, \quad (3.35)$$

where ρ is the density of the material. The displacement caused by the shear is ξ . Thus according to Newton's second law

$$\Delta F = \Delta m \cdot \frac{\partial^2 \xi}{\partial t^2}. \quad (3.36)$$

Equations (3.34) and (3.35) inserted in Eq. (3.36) give as $\Delta x \rightarrow 0$

$$\frac{\partial^2 \xi}{\partial y^2} - \frac{\rho}{G} \cdot \frac{\partial^2 \xi}{\partial t^2} = 0. \quad (3.37)$$

This is the one-dimensional wave equation for transverse waves propagating in a plate. The general solution of a second-order differential shown in Eq. (3.37) is

$$\xi(y, t) = f(y - c_t \cdot t) + g(y + c_t \cdot t), \quad (3.38)$$

where f and g are two arbitrary functions. For the function $f(y - c_t \cdot t)$ to be constant, the quantity $(y - c_t \cdot t)$ must be constant as well. This means that a disturbance described by $f(y - c_t \cdot t)$ seems to be traveling along the positive y -axis since as t is increased, the distance y must also be increased as $c_t t$ for the function $f(y - c_t \cdot t)$ is constant. The expression $(y - c_t \cdot t) = C$ where C is a constant gives $\dot{y} = c_t$ which is the phase velocity of the disturbance. Using the same argument the disturbance $g(y + c_t \cdot t)$ is traveling along the negative y -axis with the speed c_t . The phase velocity is obtained by inserting (3.38) in (3.37). The result is

$$c_t = \sqrt{\frac{G}{\rho}} = \sqrt{\frac{E}{2\rho(1 + \nu)}}. \quad (3.39)$$

Equations (3.38) and (3.29) constitute the so-called classical D'Alembert solution to the wave Eq. (3.37). The phase velocity c_t is a function of the material parameters E , ν , and ρ . These parameters are for some materials given in Table 3.1. Note that if—as in this example—the wave is propagating along the y -axis, the resulting deflection is along the x -axis.

For this simple case of a one-dimensional wave propagating in a thin plate with thickness h the kinetic energy \mathcal{T}_S per plate area is

$$\mathcal{T}_S = \frac{\rho h}{2} \left(\frac{\partial \xi}{\partial t} \right)^2. \quad (3.40)$$

This expression is only valid if the displacements η and ζ along the y and z axes are equal to zero. For the same one-dimensional wave the potential energy \mathcal{U}_S per plate area is

$$\mathcal{U}_S = h \int \tau_{xy} d\gamma_{xy} = \frac{hG}{2} \gamma_{xy}^2 = \frac{hG}{2} \cdot \left(\frac{\partial \xi}{\partial y} \right)^2. \quad (3.41)$$

This expression is obtained from Eq. (3.16). For a one-dimensional shear wave propagating along the y -axis the normal strains, σ_x , σ_y and σ_z , and the shear angles γ_{xz} and γ_{yz} are equal to zero. If the displacement ξ is assumed to have a time dependence $\exp(i\omega t)$ then the solution to the wave equation (3.37) must be of the form

$$\xi(y, t) = A \cdot \exp[i(\omega t - k_t y)] + B \cdot \exp[i(\omega t + k_t y)], \quad (3.42)$$

where

$$k_t = \omega/c_t \quad (3.43)$$

is the wavenumber-unit m^{-1} —for transverse waves. In Eq. (3.42) A is the amplitude of the wave propagating along the positive y -axis. B is the corresponding amplitude for the wave propagating in the opposite direction. If the complex notation is used, the time averages of the kinetic and potential energies must be expressed as

$$\bar{T}_S = \frac{\rho h}{4} \left| \frac{\partial \xi}{\partial t} \right|^2, \quad \bar{U}_S = \frac{hG}{4} \cdot \left| \frac{\partial \xi}{\partial y} \right|^2. \quad (3.44)$$

These energies are really equivalent to the time averages over one cycle as previously discussed.

The intensity of a plane transverse wave traveling along the positive y -axis with the displacement ξ in the direction of the x -axis is according to Eq. (3.19) equal to

$$I_y = -\tau_{yx} \cdot \dot{\xi} = -G \frac{\partial \xi}{\partial y} \cdot \frac{\partial \xi}{\partial t}. \quad (3.45)$$

Using the complex notation the time average of the intensity is

$$\bar{I}_y = -\frac{G}{2} \text{Re} \left[\frac{\partial \xi}{\partial y} \left(\frac{\partial \xi}{\partial t} \right)^* \right]. \quad (3.46)$$

3.4 Longitudinal Waves

The longitudinal wave is yet another in-plane wave type. Consider a small element shown in Fig. 3.10. The element is part of a solid and is exposed to only normal stress in the x -direction. The total force ΔF acting on the element is

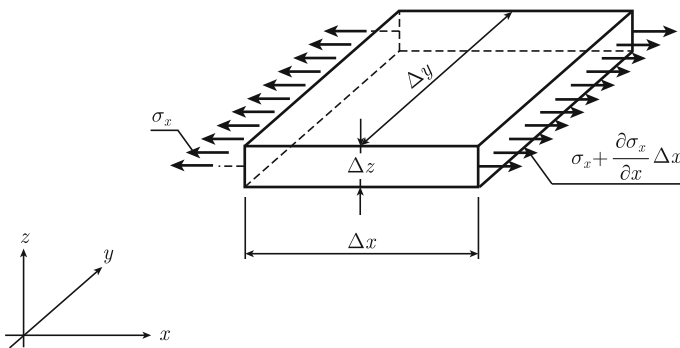


Fig. 3.10 Deformation due to pure extension

$$\Delta F = \Delta y \cdot \Delta z \left(\sigma_x + \Delta x \cdot \frac{\partial \sigma_x}{\partial x} - \sigma_x \right) = \Delta y \cdot \Delta z \cdot \Delta x \cdot \frac{\partial \sigma_x}{\partial x}. \quad (3.47)$$

If the resulting displacement along the x -axis is ξ , then

$$\sigma_x = E_x \frac{\partial \xi}{\partial x}. \quad (3.48)$$

The factor E_x is proportional to the modulus of elasticity as discussed in Sect. 3.1 and depends on whether the element is part of a beam, plate or an infinite body.

The force acting on the element gives rise to an acceleration or according to Newton's second law

$$\Delta F = \Delta m \frac{\partial^2 \xi}{\partial t^2}, \quad (3.49)$$

where the mass is

$$\Delta m = \Delta x \cdot \Delta y \cdot \Delta z \cdot \rho. \quad (3.50)$$

A combination of the Eqs. (3.47)–(3.50) gives, when $\Delta x \rightarrow 0$

$$\frac{\partial \sigma_x}{\partial x} - \rho \frac{\partial^2 \xi}{\partial t^2} = 0 \quad \text{or} \quad \frac{\partial}{\partial x} \left(E_x \frac{\partial \xi}{\partial x} \right) - \rho \frac{\partial^2 \xi}{\partial t^2} = 0.$$

For a homogeneous material E_x is constant and the second part of the differential equation is reduced to

$$\frac{\partial^2 \xi}{\partial x^2} - \frac{\rho}{E_x} \cdot \frac{\partial^2 \xi}{\partial t^2} = 0. \quad (3.51)$$

This is the wave equation governing the propagation of longitudinal waves in a homogeneous solid.

The general solution to Eq. (3.51) can again according to D'Alembert be written as

$$\xi(x, t) = f(x - c_1 t) + g(x + c_1 t),$$

where f and g are two arbitrary functions. The first expression corresponds to a wave propagating along the positive x -axis. Following the discussion in the previous section, this corresponds to waves propagating along the x -axis with a phase velocity $c_1 = \sqrt{E_x/\rho}$. The second expression corresponds to a wave propagating in the opposite direction, again with the speed c_1 . Assuming a time dependence $\exp(i\omega t)$ the solution to the wave equation is

$$\xi(x, t) = A \cdot \exp[i(\omega t - k_1 x)] + B \cdot \exp[i(\omega t + k_1 x)], \quad k_1 = \frac{\omega}{c_1}. \quad (3.52)$$

The wavenumber for longitudinal waves is denoted k_1 . The amplitudes of the waves propagating in the positive and negative directions of the x -axis are A and B . Note that for longitudinal waves the displacement is in the same direction as the propagation.

The parameter E_x depends on the shape or rather on the boundary conditions of the elements. This means that the phase velocity of longitudinal waves also depends on the shape of the solid. Thus according to Sect. 3.1

$$\begin{aligned}
 \text{infinite homogeneous body} \quad c_1 &= \sqrt{\frac{E(1-\nu)}{(1+\nu)(1-2\nu)\rho}} \\
 \text{thin homogeneous plate} \quad c_1 &= \sqrt{\frac{E}{(1-\nu^2)\rho}} \\
 \text{slender homogeneous bar} \quad c_1 &= \sqrt{\frac{E}{\rho}}.
 \end{aligned} \tag{3.53}$$

Contrary to longitudinal waves, the phase velocity of transverse waves is constant or independent of the shape of the solid. The phase velocity c_1 for longitudinal waves propagation along a bar is given in Table 3.1 for some solids. Longitudinal waves are always traveling faster than transverse waves. For $\nu = 0.3$ the ratio between the velocity for transverse and the velocity of longitudinal waves propagating in a beam is equal to

$$\frac{c_t}{c_l} = \frac{1}{\sqrt{2(1+\nu)}} \approx 0.62.$$

A longitudinal wave propagating along a beam or in the plane of a plate will, because of contraction, also cause a deflection perpendicular to the direction of propagation. For a beam, its orientation along the x -axis, the strains in the y and z directions induced by a longitudinal wave propagating along the beam are

$$\varepsilon_y = \varepsilon_z = -\frac{\nu\sigma_x}{E} = -\nu \cdot \frac{\partial \xi}{\partial x}.$$

The deformation of the beam due to a longitudinal wave propagating in the x -direction is shown in Fig. 3.11. This type of wave is often referred to as a quasi-longitudinal wave. Because of contraction shear is induced.

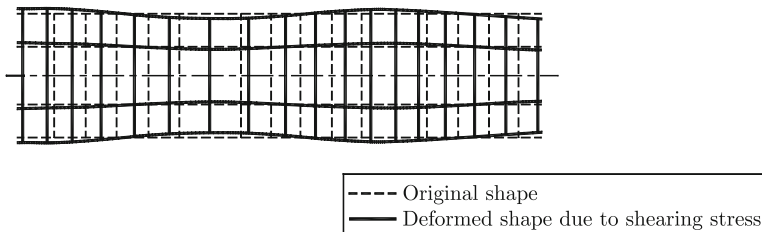


Fig. 3.11 A quasi-longitudinal wave

For a longitudinal wave propagating in a plate with thickness h the kinetic energy \mathcal{T}_S per plate area is, neglecting contraction

$$\mathcal{T}_S = \frac{h\rho}{2} \left(\frac{\partial \xi}{\partial t} \right)^2. \quad (3.54)$$

The corresponding potential energy \mathcal{V}_S per plate area is

$$\mathcal{V}_S = h \int \sigma_x d\varepsilon_x = \frac{hE_x \varepsilon_x^2}{2} = \frac{hE}{2(1-\nu^2)} \cdot \left(\frac{\partial \xi}{\partial x} \right)^2. \quad (3.55)$$

The intensity I_x in the x -direction is

$$I_x = -\sigma_x \cdot v_x = -\frac{E}{(1-\nu^2)} \cdot \frac{\partial \xi}{\partial x} \cdot \frac{\partial \xi}{\partial t}. \quad (3.56)$$

Using complex notations the time averages of the corresponding quantities are

$$\begin{aligned} \bar{\mathcal{T}}_S &= \frac{h\rho}{4} \left| \frac{\partial \xi}{\partial t} \right|^2, \quad \bar{\mathcal{V}}_S = \frac{hE}{4(1-\nu^2)} \cdot \left| \frac{\partial \xi}{\partial x} \right|^2, \\ \bar{I}_x &= -\frac{E}{2(1-\nu^2)} \cdot \operatorname{Re} \left[\frac{\partial \xi}{\partial x} \cdot \left(\frac{\partial \xi}{\partial t} \right)^* \right]. \end{aligned} \quad (3.57)$$

For a beam oriented along the x -axis and with a cross section area S the corresponding energies and intensity are

$$\bar{\mathcal{T}}_l = \frac{S\rho}{4} \left| \frac{\partial \xi}{\partial t} \right|^2, \quad \bar{\mathcal{V}}_l = \frac{SE}{4} \cdot \left| \frac{\partial \xi}{\partial x} \right|^2, \quad \bar{I}_x = -\frac{E}{2} \cdot \operatorname{Re} \left[\frac{\partial \xi}{\partial x} \cdot \left(\frac{\partial \xi}{\partial t} \right)^* \right]. \quad (3.58)$$

The subscript l denotes energy per unit length of the beam.

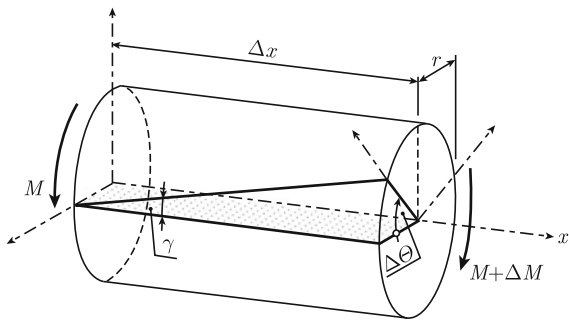
3.5 Torsional Waves

An additional wave type of interest is the torsional wave. The equation describing this wave type is particularly simple for waves traveling along the axis of an axisymmetric pipe, beam or shaft. One example is illustrated in Fig. 3.12.

A pure torsional moment is acting on a homogeneous shaft. The torsional angle γ can from the figure be related to the angular displacement $\Delta\theta$ as $\Delta x \cdot \gamma = r \cdot \Delta\theta$. In the limiting case as $\Delta x \rightarrow 0$ the torsional angle is $\gamma = r \partial\theta / \partial x$. The induced torsion τ is equal to

$$\tau = G\gamma = Gr \frac{\partial \theta}{\partial x}. \quad (3.59)$$

Fig. 3.12 Rotation and shear of an axisymmetric shaft



The torsional moment is

$$M_x = \int_0^R 2\pi r^2 \tau dr = \frac{\pi R^4 G}{2} \cdot \frac{\partial \Theta}{\partial x}. \quad (3.60)$$

The resulting torsional moment is equal to the moment of inertia. Thus

$$M_x + \Delta M_x - M_x = \Delta x \cdot \int_0^R 2\pi r \rho r (r \ddot{\Theta}) dr = \Delta x \cdot \frac{\pi R^4}{2} \ddot{\Theta}.$$

In the limiting case as $\Delta x \rightarrow 0$

$$\frac{\partial M_x}{\partial x} = \frac{\pi R^4 \rho}{2} \cdot \ddot{\Theta}. \quad (3.61)$$

Consequently—from Eq. (3.60) and assuming the shear modulus to be constant

$$\frac{\partial^2 \Theta}{\partial x^2} - \frac{\rho}{G} \cdot \frac{\partial^2 \Theta}{\partial t^2} = 0. \quad (3.62)$$

Comparing the discussion in Sect. 3.3 the phase velocity for a torsional wave propagating along an axisymmetric shaft is $c_{t0} = \sqrt{G/\rho}$. Thus for an axisymmetric pipe, beam or shaft the phase velocity is the same as for transverse waves. The wave equation (3.62) applies to torsional waves propagating along homogeneous bars as well as pipes with circular cross sections and constant wall thickness. For beams with other than circular or elliptical cross sections, the torsional moment or torque is not readily derived. Exact solutions for beams with elliptical cross sections are for example discussed in Ref. [16]. Numerical results for beams with rectangular cross sections are evaluated in Ref. [21]. The wave equation for torsional waves propagating symmetrically around the axis of a beam, height h and width b , can according to Ref. [21] be written as

Table 3.2 Form function f and phase velocity c_{to} compared to c_t for various ratios h/b

h/b	1.00	1.25	1.50	2.00	3.00	4.00	5.00	10.0	∞
$f(h/b)$	0.422	0.515	0.587	0.686	0.790	0.842	0.874	0.937	1.00
c_{to}/c_t	0.919	0.897	0.850	0.741	0.562	0.445	0.367	0.193	0

$$\Xi \cdot \frac{\partial^2 \Theta}{\partial x^2} - I\rho \cdot \frac{\partial^2 \Theta}{\partial t^2} = 0, \quad I = \frac{bh^3 + b^3h}{12}, \quad \Xi = G \cdot f(h/b) \cdot \frac{hb^3}{3}. \quad (3.63)$$

The moment of inertia is $I\rho$. The form function $f(h/b)$ can be calculated numerically. The phase velocity of torsional waves is a function of the geometry of the structure. For a beam with a rectangular cross section the phase velocity c_{to} is

$$c_{to} = \sqrt{\frac{\Xi}{I\rho}} = 2c_t \sqrt{\frac{f(h/b)}{1 + (h/b)^2}},$$

where c_t is the speed of propagation for transverse waves. The phase velocity of torsional waves traveling along a beam with a rectangular cross section is given in Table 3.2. The results are from Ref. [21].

For a shaft with a rectangular cross section, the phase velocity decreases as the ratio between height and width increases. The twisting of a shaft with a rectangular cross section not only causes pure torsion but also warping. This is discussed in more detail in for example Ref. [22].

The time averages of kinetic and potential energies per unit length of a uniform shaft are using complex notation

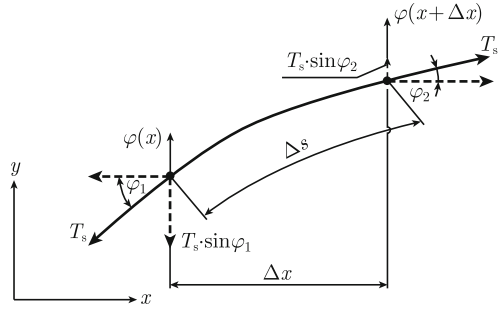
$$\bar{T}_l = \frac{I\rho}{4} \left| \frac{\partial \Theta}{\partial t} \right|^2, \quad \bar{U}_s = \frac{\Xi}{4} \cdot \left| \frac{\partial \Theta}{\partial x} \right|^2.$$

3.6 Waves on a String

A string is an idealized structure and is supposed to be completely limp and having no bending stiffness. When at rest the string is assumed to be stretched along the x -axis. The tension in the string is T_s and its mass per unit length is m' . The string is given a small displacement w perpendicular to its length. The resulting forces acting on a small element Δs are shown in Fig. 3.13. For small deflections the total force ΔF_y on the element Δs is

$$\Delta F_y = T_s \cdot \sin \varphi_2 - T_s \cdot \sin \varphi_1 \approx T_s (\varphi_2 - \varphi_1).$$

Fig. 3.13 Deflection of a string



The angles φ_1 and φ_2 are

$$\varphi_1 = \frac{\partial w(x)}{\partial x}, \quad \varphi_2 = \frac{\partial w(x + \Delta x)}{\partial x} \approx \frac{\partial w(x)}{\partial x} + \Delta x \frac{\partial^2 w(x)}{\partial x^2}.$$

Thus

$$\Delta F_y = T_s \Delta x \frac{\partial^2 w(x)}{\partial x^2}.$$

According to Newton's second law

$$\Delta F_y = m' \Delta s \cdot \ddot{w}.$$

The length of the string element is $\Delta s \approx \Delta x \cdot \cos[(\varphi_1 + \varphi_2)/2] \approx \Delta x$. In the limit as $\Delta x \rightarrow 0$ the two expressions giving the force result in the simple differential equation governing the displacement as

$$\frac{\partial^2 w}{\partial x^2} - \frac{m'}{T_s} \cdot \frac{\partial^2 w}{\partial t^2} = 0. \quad (3.64)$$

Considering the approximations made it is evident that Eq.(3.64) only is valid for small displacements i.e., as long as $\varphi \ll 1$. The general solution to Eq.(3.64) is

$$w(x, t) = f(x - c_s t) + g(x + c_s t), \quad c_s = \sqrt{T_s/m'}. \quad (3.65)$$

The phase velocity c_s is consequently a function of the tension in the string as well as of its mass per unit length.

The wave types discussed so far are all governed by second-order differential equations. For transverse waves, torsional waves, and waves on a string the displacement is perpendicular to the direction of propagation. For longitudinal waves the displacement and the direction of propagation are parallel. When longitudinal and transverse waves are traveling in a thin plate, the displacements as well as the direction of propagation are in the plane of the plate. These waves are therefore often referred to as in-plane waves.

3.7 Bending or Flexural Waves-Beams

The theories describing pure bending of beams and plates are based on the same assumptions. The bending theory for plates is often ascribed to Kirchhoff, whereas the bending theory for beams is referred to as the Euler or Euler-Bernoulli equation.

The Euler beam equation is valid as long as

- (i) The shape of the cross section of the beam is not deformed by bending;
- (ii) The normal stresses in the plane of the beam are zero at the middle surface of the beam i.e., in the neutral plane of the beam; and
- (iii) The radius of curvature due to bending is much larger than the thickness of the beam.

Figure 3.14 shows a segment of a beam under bending. The cross sections normal to the axis are plane under flexure. The bending takes place in the x - z plane. The deflection due to bending is given by w with the positive direction along the positive z -axis. In the one-dimensional case, corresponding to the bending of a beam, the deflection w only depends on the x -coordinate and time. The external force ΔF_0 is due to a force F' per unit length of the beam and acting in the direction of the positive z -axis. Thus

$$\Delta F_0 = F' \Delta x. \quad (3.66)$$

According to Newton's second law the equation giving the motion of the element shown in Fig. 3.14 is

$$\Delta F + \Delta F_0 = \Delta x \cdot m' \cdot \frac{\partial^2 w}{\partial t^2}. \quad (3.67)$$

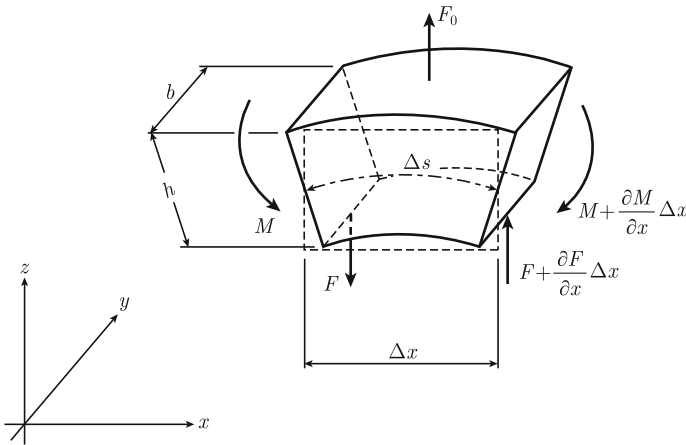


Fig. 3.14 Deformation due to bending of a beam element

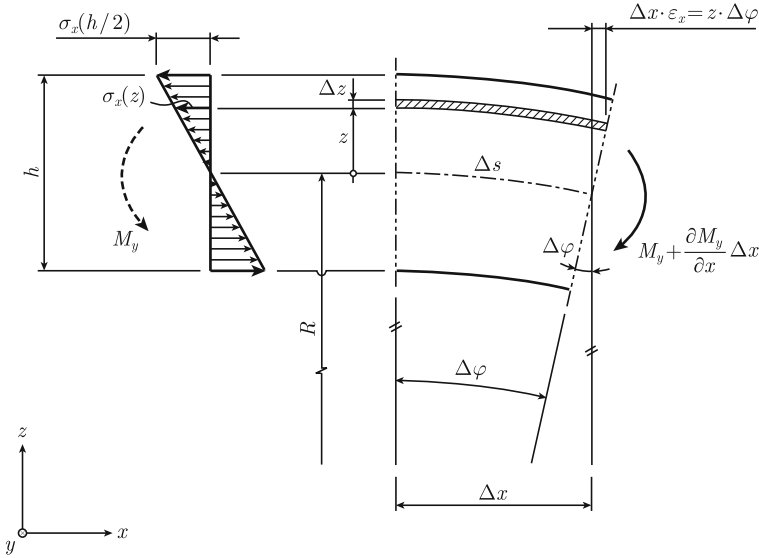


Fig. 3.15 Curvature and strain due bending of a beam element

The mass per unit length of the homogeneous beam is $m' = \rho b h$ where b is the width of the beam and h its height and ρ the density of the homogeneous material. In the limiting case, $\Delta x \rightarrow 0$, Eq. (3.67) yields,

$$F' + \frac{\partial F}{\partial x} = m' \frac{\partial^2 w}{\partial t^2}. \quad (3.68)$$

When the beam is being bent, part of it is compressed and part of it is elongated as shown in Fig. 3.15. The strain is zero along the neutral axis—the dashed line in Fig. 3.15.

The length of the neutral axis for the element shown in the figure is equal to Δx . The radius of curvature R is

$$R = -1 / \left(\frac{\partial^2 w}{\partial x^2} \right). \quad (3.69)$$

The angle $\Delta\varphi$ giving the curvature is

$$\Delta\varphi = \frac{\Delta x}{R} = -\Delta x \cdot \frac{\partial^2 w}{\partial x^2}. \quad (3.70)$$

The strain ε_x varies with the distance z from the neutral or symmetry axis since the cross section of the beam is plane during bending as initially assumed. Compare Eq. (4.56) and the discussion in Sect. 4.4. Based on the geometry shown in Fig. 3.15 the displacement at the distance z from the neutral axis can be written as $\varepsilon_x \cdot \Delta x$ or

$z \cdot \Delta\varphi z$. Thus

$$\varepsilon_x \cdot \Delta x = z \cdot \Delta\varphi. \quad (3.71)$$

This expression in combination with Eq. (3.70) gives

$$\varepsilon_x = -z \frac{\partial^2 w}{\partial x^2}, \quad \sigma_x = E\varepsilon_x = -zE_x \frac{\partial^2 w}{\partial x^2}. \quad (3.72)$$

The bending moment M_y around the y -axis is obtained as

$$M_y = b \int_{-h/2}^{h/2} \sigma_x z dz = -bE_x \frac{\partial^2 w}{\partial x^2} \int_{-h/2}^{h/2} z^2 dz = -E_x \frac{bh^3}{12} \frac{\partial^2 w}{\partial x^2} = -E_x I \frac{\partial^2 w}{\partial x^2}. \quad (3.73)$$

The moment of inertia I is equal to $bh^3/12$ for a beam with a rectangular cross section, height h and width b . The bending stiffness D' of the beam is defined as

$$D' = E_x I = \frac{Ebh^3}{12}. \quad (3.74)$$

For a beam E_x is equal to E as discussed in Sect. 3.1. The bending stiffness is occasionally and in particular in German literature denoted B .

Again returning to Fig. 3.14, the sum of the bending moments acting around the y -axis through the left-hand side of the neutral axis must be zero. Thus

$$M + \Delta M - M = (F + \Delta F)\Delta x + \Delta F_0 \Delta x/2.$$

In the limiting case, $\Delta x \rightarrow 0$, the result relating F and M is obtained as

$$F = \frac{\partial M}{\partial x} = -\frac{\partial}{\partial x} \left(D' \frac{\partial^2 w}{\partial x^2} \right). \quad (3.75)$$

More appropriately, this equation is written

$$F_z = \frac{\partial M_y}{\partial x}.$$

In this way, the directions of the force and bending moment are indicated by means of the subscripts.

Equation (3.75) inserted in Eq. (3.68) gives the Euler equation for bending waves on beams as

$$\frac{\partial^2}{\partial x^2} \left(D' \frac{\partial^2 w}{\partial x^2} \right) + m' \frac{\partial^2 w}{\partial t^2} = F'. \quad (3.76)$$

For a constant cross section and a constant E -modulus along the beam and with m' as the mass per unit length of the beam the result is

$$\frac{\partial^4 w}{\partial x^4} + \frac{m'}{D'} \cdot \frac{\partial^2 w}{\partial t^2} = \frac{F'}{D'}, \quad m' = bh\rho, \quad D' = \frac{Ebh^3}{12}. \quad (3.77)$$

This is a fourth-order differential equation. For longitudinal torsional and transverse waves the corresponding wave equations are of the second order. For the case that no external force F' acting on the beam and for a time dependence $\exp(i\omega t)$ the general solution to Eq. (3.77) is

$$w(x, t) = \begin{cases} e^{i\omega t} (A_1 \cdot e^{-i\kappa x} + A_2 \cdot e^{i\kappa x} + A_3 \cdot e^{-\kappa x} + A_4 \cdot e^{\kappa x}), & \kappa = \left[\frac{m'\omega^2}{D'} \right]^{1/4} \\ e^{i\omega t} (B_1 \cdot \sin \kappa x + B_2 \cdot \cos \kappa x + B_3 \cdot \sinh \kappa x + B_4 \cdot \cosh \kappa x) \end{cases} \quad (3.78)$$

The parameter κ is the wavenumber for flexural or bending waves. The amplitudes A_i and B_i are determined by the boundary conditions. In the first expression of Eq. (3.78) A_1 is the amplitude of a wave propagating along the positive x -axis. A_2 is the amplitude of a wave propagating in the opposite direction. A_3 and A_4 are the amplitudes of the evanescent waves. These “waves” are rapidly decaying to the right and left respectively along the x -axis.

A propagating wave traveling along the positive x -axis can be written as

$$w(x, t) = A \cdot \exp[i(\omega t - \kappa x)] \text{ or } w(x, t) = B \cdot \sin(\omega t - \kappa x). \quad (3.79)$$

The sine function could even be replaced by a cosine function. The velocity corresponding to a constant phase—or quite simply the phase velocity, is in these expressions given by

$$c_b = \frac{\omega}{\kappa} = \sqrt{\omega} \cdot \left(\frac{D'}{m'} \right)^{1/4}. \quad (3.80)$$

The wavenumber κ is given in Eq. (3.78). The result (3.80) means—contrary to the case with longitudinal and transverse waves—that the phase velocity for flexural waves is a function of frequency. Flexural waves are for this reason termed dispersive. The result (3.80) is based on two assumptions listed at the beginning of Sect. 3.7. These assumptions are violated in the high frequency range or rather when the wavelength of flexural waves is small as compared to the thickness of a plate or beam. In Chap. 4 it is demonstrated that the phase velocity of flexural waves has a finite upper limit. The result (3.80) is valid for “thin” beams as defined in Chap. 4 and only up to a certain frequency limit.

A consequence of the dispersive character of flexural waves is that a wave of a certain shape is distorted while traveling along a beam. In a loss-free medium transverse and longitudinal traveling waves have the same shape independent of time. This is also true for waves traveling on a string. Transverse traveling waves on a string and flexural waves in a beam are compared in Sect. 3.8.

In addition to a phase velocity also a group velocity can be defined for flexural waves. Consider two flexural waves with the same amplitude but with slightly dif-

ferent frequencies. The waves travel along the positive x -axis. The total disturbance of the two waves is

$$\begin{aligned} w(x, t) &= \sin(\omega t - \kappa x) + \sin[t(\omega + \Delta\omega) - x(\kappa + \Delta\kappa)] \\ &= 2 \sin[(\omega + \Delta\omega/2)t - (\kappa + \Delta\kappa/2)x] \cos(\Delta\omega t/2 - \Delta\kappa x/2). \end{aligned}$$

The sine wave can be called the carrier wave and the cosine wave the disturbed wave. The velocity for the carrier wave is

$$\frac{\omega + \Delta\omega/2}{\kappa + \Delta\kappa/2} \rightarrow \frac{\omega}{\kappa} = c_b = \kappa \cdot \sqrt{\frac{D'}{m'}}.$$

The limit is obtained when $\Delta\omega$ and thus also $\Delta\kappa$ approaches zero. For the disturbed wave the velocity or rather group velocity c_g is

$$\frac{\Delta\omega}{\Delta\kappa} \rightarrow \frac{\partial\omega}{\partial\kappa} = c_g.$$

But from the result above $\omega = \kappa^2 \sqrt{D'/m'}$, thus

$$c_g = 2\kappa \sqrt{\frac{D'}{m'}} = 2c_b. \quad (3.81)$$

The group velocity is twice as high as the phase velocity as long as the beam can be considered as “thin.” In the high frequency limit the group velocity c_g approaches c_b as demonstrated in Chap. 4. The group and phase velocities are the same for longitudinal and transverse waves.

For flexural waves traveling in a beam the kinetic energy per unit length of the beam is

$$\mathcal{T}_1 = \frac{m'}{2} \left(\frac{\partial w}{\partial t} \right)^2. \quad (3.82)$$

Based on the complex notation the time average of the kinetic energy is

$$\bar{\mathcal{T}}_1 = \frac{m'}{4} \left| \frac{\partial w}{\partial t} \right|^2. \quad (3.83)$$

The potential energy per unit length of a beam, height h and width b as shown in Fig. 3.15, is

$$\mathcal{V}_1 = b \int_{-h/2}^{h/2} dz \int d\varepsilon_x \sigma_x = \frac{b}{2} E_x \int_{-h/2}^{h/2} dz \varepsilon_x^2.$$

According to Eq. (3.73) and the definition of the bending stiffness D' , this integral is equal to

$$\mathcal{U}_1 = \frac{E_x b}{2} \int_{-h/2}^{h/2} dz \cdot z^2 \left(\frac{\partial^2 w}{\partial x^2} \right)^2 = \frac{E_x b h^3}{24} \left(\frac{\partial^2 w}{\partial x^2} \right)^2 = \frac{D'}{2} \left(\frac{\partial^2 w}{\partial x^2} \right)^2. \quad (3.84)$$

Using complex notations the time average of the potential energy is

$$\bar{\mathcal{U}}_1 = \frac{D'}{4} \left| \frac{\partial^2 w}{\partial x^2} \right|^2. \quad (3.85)$$

As an example, consider a wave moving along an infinite beam in the direction of the positive x -axis. The displacement including the evanescent motion is

$$w(x, t) = e^{i\omega t} (A \cdot e^{-i\kappa x} + B \cdot e^{-\kappa x}).$$

The amplitude of the traveling wave is A and of the evanescent wave B . The kinetic energy per unit length of the beam is obtained from Eq. (3.83) as

$$\bar{\mathcal{T}}_1 = \frac{m' \omega^2}{4} [|A|^2 + |B|^2 \cdot e^{-2\kappa x} + 2e^{-\kappa x} \operatorname{Re}(AB^* e^{-i\kappa x})].$$

The corresponding result for the potential energy is—compared with Eq. (3.85),

$$\bar{\mathcal{U}}_1 = \frac{\kappa^4 D'}{4} \bar{\mathcal{T}}_1 = \frac{m' \omega^2}{4} [|A|^2 + |B|^2 \cdot e^{-2\kappa x} - 2e^{-\kappa x} \operatorname{Re}(AB^* e^{-i\kappa x})].$$

The total energy per unit length of the beam is

$$\bar{\mathcal{T}}_1 + \bar{\mathcal{U}}_1 = \frac{m' \omega^2}{2} [|A|^2 + |B|^2 \cdot e^{-2\kappa x}]. \quad (3.86)$$

The energy flow Π in the beam is equal to the intensity in the direction of the beam times the area of the cross section of the beam. The energy flow is determined by two effects. The first Π_F is caused by the translatory motion of the beam and the second Π_M is caused by the rotational motion.

The force F_z and moment M_y acting at a cross section of a beam are shown in Fig. 3.16. The displacement, velocity, and rotation are denoted by w , v_z , and ω_y . The energy flow from beam 1 to beam 2 is given by

$$\Pi = \Pi_F + \Pi_M. \quad (3.87)$$

If w is a real quantity then

$$\Pi_F = -F_z \dot{w} = -F_z v_z, \quad \Pi_M = M_y \omega_y. \quad (3.88)$$

If on the other hand, the complex notation is used then

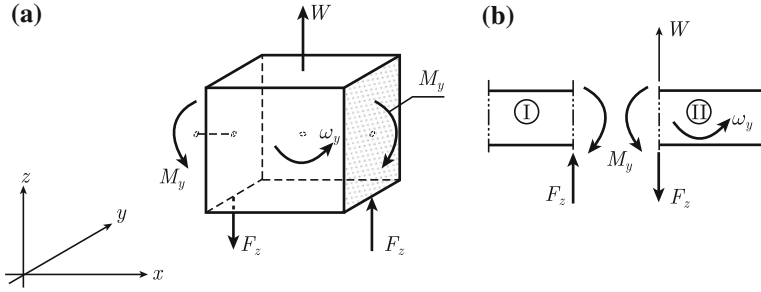


Fig. 3.16 Forces and moments acting on a small element (a) and at a cross section (b)

$$\bar{\Pi}_F = -\frac{1}{2}\text{Re}[F_z \dot{w}^*], \quad \bar{\Pi}_M = \frac{1}{2}\text{Re}[M_y \omega_y^*]. \quad (3.89)$$

The minus sign for Π_F is obtained since the positive directions of the force and displacement are defined along the negative and positive z -axis, respectively.

The forces, moments, etc. in Fig. 3.16 are defined as

$$v_z = \frac{\partial w}{\partial t}, \quad \omega_y = \frac{\partial}{\partial x} \left(\frac{\partial w}{\partial t} \right), \quad M_y = -D' \frac{\partial^2 w}{\partial x^2}, \quad F_z = -D' \frac{\partial^3 w}{\partial x^3}. \quad (3.90)$$

For a wave described by

$$w(x, t) = e^{i\omega t} (A \cdot e^{-i\kappa x} + B \cdot e^{-\kappa x}),$$

the resulting time average of the energy flow is

$$\bar{\Pi} = \omega D' \kappa^3 |A|^2 = \frac{\omega^3 m'}{\kappa} |A|^2. \quad (3.91)$$

The result shows that the energy flow is caused by the traveling wave with the amplitude A . An evanescent wave cannot generate an energy flow in a loss free medium. The time average of the total energy, kinetic and potential, per unit length of the beam induced by the traveling wave with the amplitude A is according to Eq. (3.86)

$$\bar{\mathcal{T}}_1 + \bar{\mathcal{U}}_1 = \frac{m' \omega^2}{2} |A|^2.$$

The time average of the energy flow from Eq. (3.91) is thus

$$\bar{\Pi} = 2 \frac{\omega}{\kappa} (\bar{\mathcal{T}}_1 + \bar{\mathcal{U}}_1) = 2c_b (\bar{\mathcal{T}}_1 + \bar{\mathcal{U}}_1). \quad (3.92)$$

The result shows that the energy flow due to a traveling flexural wave is equal to the group velocity $c_g = 2c_b$ times the energy per unit length of the beam. The energy induced by the evanescent waves is neglected as long as $\kappa x \gg 1$. Compare Eq. (3.86).

It can be shown as Ref. [79] that the time average of the energy flow $\bar{\Pi}$ induced by a plane wave propagating in a solid is

$$\bar{\Pi} = \frac{\partial \omega}{\partial \kappa} (\bar{\mathcal{T}}_1 + \bar{\mathcal{U}}_1),$$

where $\partial \omega / \partial \kappa$ is the group velocity. If the energy is carried by a flexural wave, the group velocity is twice the phase velocity. For a longitudinal wave the phase and group velocities are the same.

3.8 Waves on Strings and Beams—A Comparison

The governing equation for waves propagating on a string is given by a second-order differential equation as shown in Eq. (3.64). For flexural waves on a beam the corresponding equation is of the fourth order—see Eq. (3.77). In the first case, the speed of propagation is constant. In the second case, for flexural waves, the phase velocity is frequency dependent. An initial disturbance is therefore varying as function of time in different ways for the two cases. This is demonstrated first by considering an infinite string oriented along the x -axis. The initial disturbance is $w(x, 0)$ and given by a normal distribution around $x = 0$. The string is at rest for $t < 0$. At $t = 0$ the string is released. The initial conditions are

$$w(x, 0) = \exp[-(x/2a)^2], \quad \dot{w}(x, 0) = 0. \quad (3.93)$$

The parameter a is a positive constant. The general solution to the wave equation is according to Eq. (3.65)

$$w(x, t) = f(x - c_s t) + g(x + c_s t).$$

The velocity is consequently

$$\dot{w}(x, t) = -c_s [f'(x - c_s t) - g'(x + c_s t)].$$

At $t = 0$ the velocity is equal to zero. This means that $f'(x) = g'(x)$ or $f(x) = g(x)$ considering the symmetry. The deflection at $t = 0$ is

$$w(x, 0) = f(x) + g(x) = 2f(x) = \exp[-(x/2a)^2].$$

Based on these results it follows that the displacement of the string is

$$w(x, t) = \frac{\exp[-(x - c_s t)^2 / (2a)^2] + \exp[-(x + c_s t)^2 / (2a)^2]}{2}. \quad (3.94)$$

A general solution to the wave equation governing flexural waves on a beam cannot be formulated in a similar way. By replacing the string by an infinite beam the equation for flexural waves is for no external force, according to Eq. (3.77), given by

$$\frac{\partial^4 w}{\partial x^4} + \frac{m'}{D'} \cdot \frac{\partial^2 w}{\partial t^2} = 0. \quad (3.95)$$

The displacement perpendicular to the beam is given by $w(x, t)$, the bending stiffness by D' and mass per unit length by m' . The initial conditions are the same as for the string given in Eq. (3.93). In Chap. 2 temporal Fourier transforms were introduced. In a similar way the displacement in one dimension can be expressed as a spatial Fourier transform, or

$$w(x, t) = \frac{1}{2\pi} \int_{-\infty}^{\infty} \tilde{w}(k, t) e^{ikx} dk. \quad (3.96)$$

The spatial one-dimensional Fourier transform of w is

$$\tilde{w}(k, t) = \int_{-\infty}^{\infty} w(x, t) e^{-ikx} dx. \quad (3.97)$$

Spatial Fourier transform in one, two, and three dimensions is discussed further in Chap. 5. In analogy with the use of the temporal FT, the introduction of the spatial FT in the wave equation (3.95) gives

$$k^4 \tilde{w} + \frac{m'}{D'} \cdot \frac{\partial^2 \tilde{w}}{\partial t^2} = 0. \quad (3.98)$$

The general solution to this second-order differential equation is

$$\tilde{w}(k, t) = A \sin(\Omega t) + B \cos(\Omega t),$$

where

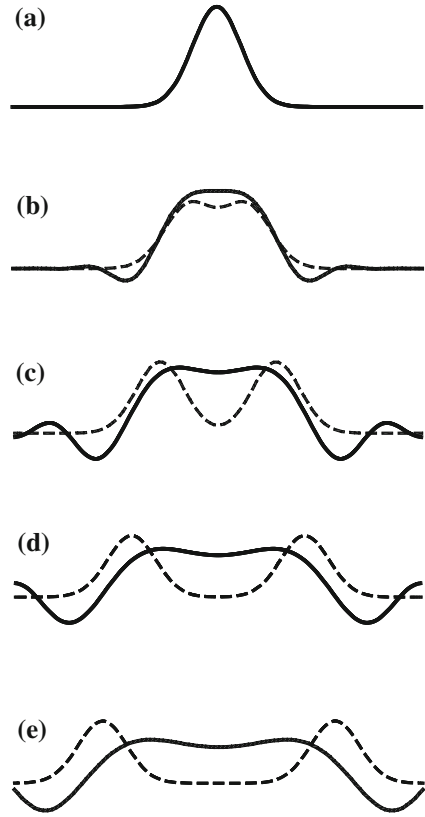
$$\Omega = k^2 \sqrt{D'/m'}. \quad (3.99)$$

The parameters A and B are determined by the initial conditions. For the same initial conditions as for the string—Eq. (3.93)—it follows that $\dot{w}(x, 0) = 0 \Rightarrow \tilde{\dot{w}}(k, 0) = 0$.

In order to satisfy this part of the initial conditions the amplitude A in the general solution Eq. (3.99) must be equal to zero. The remaining parameter B is thus given by

$$B = \tilde{w}(k, 0) = \int_{-\infty}^{\infty} w(x, 0) e^{-ikx} dx = \int_{-\infty}^{\infty} dx \exp[-(x/2a)^2 - ikx]$$

Fig. 3.17 Comparison between the displacements of flexural waves on a beam (solid line) and on a string (dashed line), From Ref. [23]



$$= 2a\sqrt{\pi} \cdot \exp[-(ka)^2] \quad (3.100)$$

The displacement $w(x, t)$ is according to Eqs. (3.99) and (3.96) equal to

$$w(x, t) = \frac{1}{2\pi} \int_{-\infty}^{\infty} dk \cdot B \cos(\Omega t) \cdot e^{ikx}. \quad (3.101)$$

The parameter Ω is a function of k . The evaluation of the integral is discussed in connection with Problem 3.8 of this chapter. Introducing the parameter β as $\beta = \sqrt{D'/m'}$, the end result giving the displacement of the beam is

$$w(x, t) = \frac{\exp\left[-\frac{a^2 x^2}{4(a^4 + t^2 \beta^2)}\right]}{\left(1 + \frac{t^2 \beta^2}{a^4}\right)^{1/4}} \cdot \cos\left[\frac{x^2 t \beta}{4(a^4 + t^2 \beta^2)} - \frac{1}{2} \arctan(t \beta / a^2)\right]. \quad (3.102)$$

The displacements for the two cases can, as demonstrated in Ref. [23], be illustrated as shown in Fig. 3.17.

The two displacement curves for the beam and the string are in the figure given at certain fixed time intervals. The displacement of the string is composed of two Gaussian curves. One is moving to the right and the other to the left on the infinite string. Each displacement curve is moving with the constant velocity c_s . Similar results can be obtained for plane longitudinal, transverse, or torsional waves or in fact for any wave type governed by a second-order differential equation. The difference between these wave types is the speed of propagation and the direction and character of the displacement.

The displacement curve for the beam shown in Fig. 3.17 illustrates that the initial shape of the disturbance is changing continuously as function of time. This is always the case for waves propagating in dispersive media. It is therefore not meaningful to define the speed of propagation in the time domain for flexural waves since the speed depends on frequency.

3.9 Flexural Waves-Plates

The wave equation governing the transverse vibrations of thin homogeneous and flat plates is derived based on assumptions attributed to Kirchhoff. These basic assumptions are as follows:

- (i) A straight line initially normal to the surface of the plate remains straight and normal to the surface of the plate under bending, shear neglected;
- (ii) The normal stresses in the plane of the plate are zero at the middle surface of the plate i.e. in the neutral plane of the plate; and
- (iii) The radius of curvature due to bending is much larger than the thickness of the plate.

These assumptions correspond to the hypotheses discussed in connection with the derivation of the wave equation governing the vibrations of beams.

In Fig. 3.18 the forces and moments acting on a plate element under bending are shown. The plate is isotropic and homogeneous. The plate with the thickness h is extended in the x - y plane. The moment M'_x per unit width of the plate is due to normal stress in the x -direction whereas M'_{yx} is caused by the torsional stress τ_{yx} . The symbol M' denotes a bending moment per unit width of the plate. For a thin plate, the stress σ_z is set to equal zero. The normal stresses σ_x and σ_y are, for $\sigma_z = 0$, obtained from Eq. (3.6). The result is

$$\sigma_x = \frac{E}{1 - \nu^2}(\varepsilon_x + \nu\varepsilon_y), \quad \sigma_y = \frac{E}{1 - \nu^2}(\varepsilon_y + \nu\varepsilon_x). \quad (3.103)$$

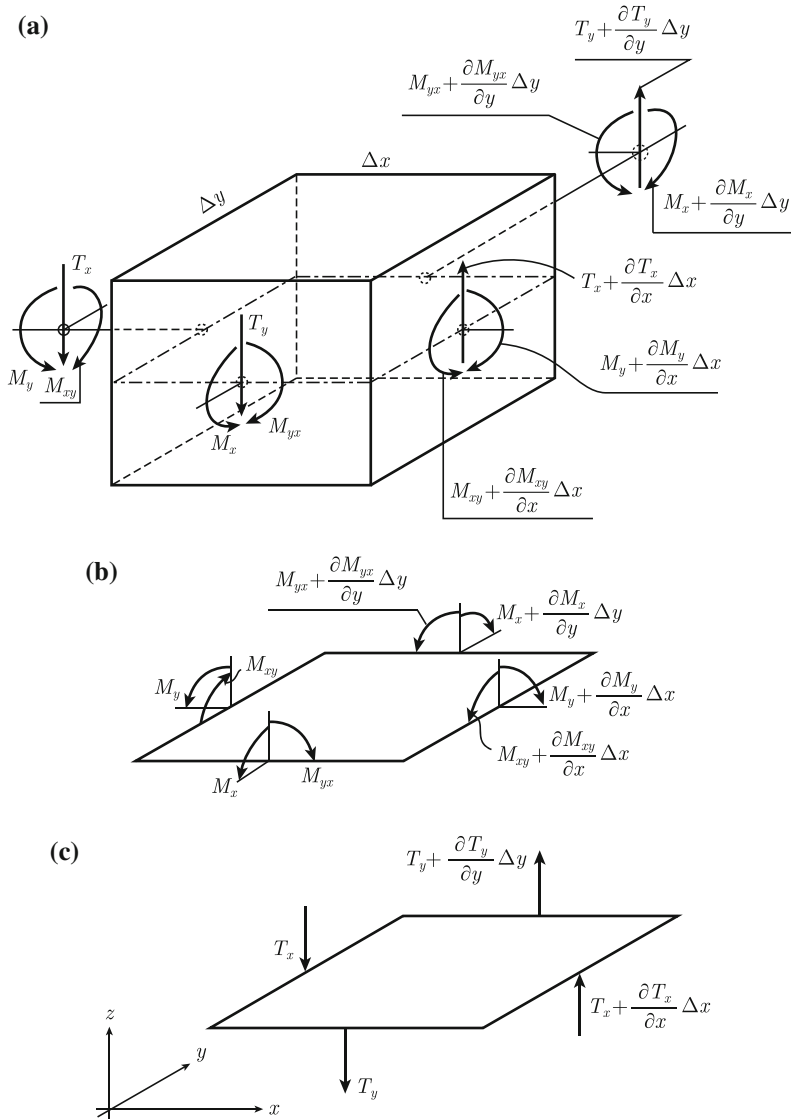


Fig. 3.18 Forces and moments acting on a plate element under bending **a** moments and forces. **b** Moments. **c** Forces

In Sect. 3.7, the strain in a beam was found to be a function of the distance from the neutral axis and the curvature of the beam. The result is given in Eq. (3.72). In a similar way the strains in the x and y directions of a plate are

$$\varepsilon_x = -z \cdot \frac{\partial^2 w}{\partial x^2}, \quad \varepsilon_y = -z \cdot \frac{\partial^2 w}{\partial y^2}. \quad (3.104)$$

In these expressions, w is the displacement of the plate along the positive z -axis. The bending moment M'_y around the y -axis is per unit width of the plate

$$\begin{aligned} M'_y &= \int_{-h/2}^{h/2} \sigma_x z dz = - \int_{-h/2}^{h/2} \frac{E}{1-\nu^2} \left(\frac{\partial^2 w}{\partial x^2} + \nu \frac{\partial^2 w}{\partial y^2} \right) z^2 dz \\ &= -D \left(\frac{\partial^2 w}{\partial x^2} + \nu \frac{\partial^2 w}{\partial y^2} \right). \end{aligned} \quad (3.105)$$

This result should be compared to Eq. (3.74) derived for a beam. The bending stiffness D for a plate is defined as

$$D = \frac{E h^3}{12(1-\nu^2)}. \quad (3.106)$$

Note the difference as compared to the bending stiffness $D' = b h^3 E / 12$ for a beam with a rectangular cross section, height h , and width b . Following the procedure leading up to Eq. (3.105) the moment M'_x is obtained as

$$M'_x = -D \left(\frac{\partial^2 w}{\partial y^2} + \nu \frac{\partial^2 w}{\partial x^2} \right). \quad (3.107)$$

The shear stress τ_{xy} is according to Eqs. (3.10) and (3.11) equal to

$$\tau_{xy} = G \gamma_{xy} = \frac{E}{2(1+\nu)} \left(\frac{\partial \xi}{\partial y} + \frac{\partial \eta}{\partial x} \right). \quad (3.108)$$

As before ξ and η are the deflections along the x - and y -axis, respectively. The strain ε_x can be written in two ways—as the derivative of the displacement ξ in the x -direction as given in Eq. (3.2) and as a function of the distance z from the neutral plane and the curvature of the plate in the x -direction, Eq. (3.104). Thus

$$\varepsilon_x = \frac{\partial \xi}{\partial x} = -z \cdot \frac{\partial^2 w}{\partial x^2}.$$

An integration with respect to x of the last two expressions gives ξ as

$$\xi = -z \cdot \frac{\partial w}{\partial x}. \quad (3.109)$$

In a similar way

$$\eta = -z \cdot \frac{\partial w}{\partial y}. \quad (3.110)$$

These two expressions, Eqs. (3.109) and (3.110), inserted in Eq. (3.108) yield

$$\tau_{xy} = \tau_{yx} = -\frac{E}{1+\nu} \cdot z \cdot \frac{\partial^2 w}{\partial x \partial y}, \quad \gamma_{xy} = \gamma_{yx} = -2 \cdot z \cdot \frac{\partial^2 w}{\partial x \partial y}. \quad (3.111)$$

The last part of these expressions is obtained using the equality $\tau_{xy} = G\gamma_{xy}$. The resulting bending moment M'_{xy} is

$$M'_{xy} = \int_{-h/2}^{h/2} \tau_{xy} z dz = - \int_{-h/2}^{h/2} \frac{E}{1+\nu} z^2 \frac{\partial^2 w}{\partial x \partial y} dz = -D(1-\nu) \frac{\partial^2 w}{\partial x \partial y}. \quad (3.112)$$

The shear forces T'_x and T'_y per unit width of the plate defined in Fig. 3.18 are for D constant across the plate equal to

$$\begin{aligned} T'_x &= \frac{\partial M'_y}{\partial x} + \frac{\partial M'_{yx}}{\partial y} = -D \left(\frac{\partial^3 w}{\partial x^3} + \frac{\partial^3 w}{\partial x \partial y^2} \right) = -D \frac{\partial}{\partial x} (\nabla^2 w) \\ T'_y &= \frac{\partial M'_x}{\partial y} + \frac{\partial M'_{xy}}{\partial x} = -D \left(\frac{\partial^3 w}{\partial y^3} + \frac{\partial^3 w}{\partial x^2 \partial y} \right) = -D \frac{\partial}{\partial y} (\nabla^2 w). \end{aligned} \quad (3.113)$$

The equation of motion for the element shown in Fig. 3.18, mass $\mu = \rho h$ per unit area, is

$$\frac{\partial T'_y}{\partial y} + \frac{\partial T'_x}{\partial x} = \mu \frac{\partial^2 w}{\partial t^2}. \quad (3.114)$$

Using Eq. (3.113) the result is

$$D \left(\frac{\partial^4 w}{\partial x^4} + 2 \frac{\partial^4 w}{\partial x^2 \partial y^2} + \frac{\partial^4 w}{\partial y^4} \right) + \mu \frac{\partial^2 w}{\partial t^2} = 0.$$

This can be written in a more compact form as

$$D \nabla^2 (\nabla^2 w) + \mu \frac{\partial^2 w}{\partial t^2} = 0, \quad \nabla^2 = \frac{\partial^2}{\partial x^2} + \frac{\partial^2}{\partial y^2}, \quad (3.115)$$

where ∇^2 is the two-dimensional Laplace operator. For a pressure $p(x, y, t)$ exciting the plate in the direction of the positive z -direction the resulting wave equation is

$$D \nabla^2 (\nabla^2 w) + \mu \frac{\partial^2 w}{\partial t^2} = p. \quad (3.116)$$

A plane bending wave with the displacement w and propagating along the positive x -axis of a plate can be expressed as $w(x, t) = A \cdot \exp[i(\omega t - \kappa x)]$ with A being the amplitude of the wave. For this expression to satisfy the wave equation (3.115),

the wavenumber κ must be equal to

$$\kappa = \left(\frac{\mu\omega^2}{D} \right)^{1/4} = \left[\frac{12\rho(1-\nu^2)\omega^2}{Eh^2} \right]^{1/4}. \quad (3.117)$$

This is the wavenumber for bending or flexural waves propagating along a thin and homogeneous plate. Except for the factor $(1-\nu^2)$ the expression is equal to the wavenumber for bending waves traveling along a beam. The phase and group velocities for the dispersive bending waves are again defined as $c_b = \omega/\kappa$ and $c_g = \partial\omega/\partial\kappa = 2c_b$ for thin plates. The interpretation of “thin” plates and “slender” beams is discussed in Sect. 4.4.

The boundary conditions for rectangular plates depend not only on the shear forces T'_x and T'_y and moments M'_x and M'_y but also on the torsional moments M'_{xy} and M'_{yx} . The total shear force at an edge is determined by transverse shear as well as the effect of the torsional moment in the cross section area at the edge. The total shear force F'_x per unit length along an edge $x = 0$ or $x = L_x$ of a rectangular plate is, following the definitions in Fig. 3.18, obtained as,

$$\begin{aligned} F'_x &= T'_x + \frac{\partial M'_{yx}}{\partial y} \\ &= -D \left(\frac{\partial^3 w}{\partial x^3} + \frac{\partial^3 w}{\partial x \partial y^2} \right) - D(1-\nu) \frac{\partial^3 w}{\partial x \partial y^2} \\ &= -D \left[\frac{\partial^3 w}{\partial x^3} + (2-\nu) \frac{\partial^3 w}{\partial x \partial y^2} \right]. \end{aligned} \quad (3.118)$$

In a similar way the total shear force F'_y per unit length along the edge $y = 0$ or $y = L_y$ is given by

$$F'_y = -D \left[\frac{\partial^3 w}{\partial y^3} + (2-\nu) \frac{\partial^3 w}{\partial x^2 \partial y} \right]. \quad (3.119)$$

For a rectangular plate oriented in the x - y plane with edges defined by the lines $x = 0$, $x = L_x$, $y = 0$, and $y = L_y$ the boundary conditions for simply supported, free, and clamped edges are given in Table 3.3.

The wave equations for flexural waves in beams and plates have been derived assuming rather vaguely that the thickness of the structure is small compared to the radius of curvature. In Chap. 4 it is shown that the error for the wavenumber κ is less than 10 % as long as

$$\kappa h < 1. \quad (3.120)$$

The potential energy stored in a vibrating plate can be calculated based on the general formula (3.16) derived in Sect. 3.1. For a thin plate, it is as before assumed that the stress σ_z normal to the plate surface is equal to zero. According to Eq. (3.6) the

Table 3.3 Boundary conditions for rectangular isotropic plates*Simply supported edge*

$$x = 0; \quad x = L_x, \quad w = 0; \quad M'_y = -D \left(\frac{\partial^2 w}{\partial x^2} + \nu \frac{\partial^2 w}{\partial y^2} \right) = 0$$

$$y = 0; \quad y = L_y, \quad w = 0; \quad M'_x = -D \left(\frac{\partial^2 w}{\partial y^2} + \nu \frac{\partial^2 w}{\partial x^2} \right) = 0$$

Clamped edge

$$x = 0; \quad x = L_x, \quad w = 0; \quad \frac{\partial w}{\partial x} = 0$$

$$y = 0; \quad y = L_y, \quad w = 0; \quad \frac{\partial w}{\partial y} = 0$$

Free edge

$$x = 0; \quad x = L_x; \quad M'_y = -D \left(\frac{\partial^2 w}{\partial x^2} + \nu \frac{\partial^2 w}{\partial y^2} \right) = 0, \quad F'_x = -D \left[\frac{\partial^3 w}{\partial x^3} + (2 - \nu) \frac{\partial^3 w}{\partial x \partial y^2} \right] = 0$$

$$y = 0; \quad y = L_y; \quad M'_x = -D \left(\frac{\partial^2 w}{\partial y^2} + \nu \frac{\partial^2 w}{\partial x^2} \right) = 0, \quad F'_y = -D \left[\frac{\partial^3 w}{\partial y^3} + (2 - \nu) \frac{\partial^3 w}{\partial x^2 \partial y} \right] = 0$$

corresponding normal strain ε_z is obtained as

$$\varepsilon_z = -\frac{\nu(\varepsilon_x + \varepsilon_y)}{1 - \nu} \quad (3.121)$$

Further, for a thin plate the shear stress is equal to zero on the plate surface. This means

$$\gamma_{xz} = \gamma_{yz} = 0. \quad (3.122)$$

The potential energy can, based on the general expression (3.17) and the additional conditions given by the Eqs. (3.121) and (3.122), be written as

$$\mathcal{U}_v = \frac{E}{2(1 - \nu^2)} \left(\varepsilon_x^2 + \varepsilon_y^2 + 2\nu\varepsilon_x\varepsilon_y + \frac{1 - \nu}{2} \gamma_{xy}^2 \right). \quad (3.123)$$

The normal strains are defined in Eq. (3.104) and the shear stress in Eq. (3.111). Based on these expressions in combination with Eq. (3.123) the potential energy \mathcal{U}_S per unit area is obtained as

$$\begin{aligned} \mathcal{U}_S &= \int_{-h/2}^{h/2} \mathcal{U}_v dz \\ &= \frac{EI}{2(1 - \nu^2)} \left[\left(\frac{\partial^2 w}{\partial x^2} \right)^2 + \left(\frac{\partial^2 w}{\partial y^2} \right)^2 \right. \\ &\quad \left. + 2\nu \left(\frac{\partial^2 w}{\partial x^2} \right) \left(\frac{\partial^2 w}{\partial y^2} \right) + 2(1 - \nu) \left(\frac{\partial^2 w}{\partial x \partial y} \right)^2 \right]. \end{aligned} \quad (3.124)$$

The moment of inertia I in the expression above is given as

$$I = \int_{-h/2}^{h/2} z^2 dz = \frac{h^3}{12}.$$

The bending stiffness D is

$$D = \frac{Eh^3}{12(1 - \nu^2)}.$$

The displacement of the plate is predominantly in the z -direction. The kinetic energy per unit area for a plate with the thickness h is thus

$$\mathcal{T}_S = \frac{\mu}{2} \left(\frac{\partial w}{\partial t} \right)^2. \quad (3.125)$$

If a complex notation is used the expressions (3.124) and (3.125) must be modified as previously discussed.

3.10 Orthotropic Plates

So far, it has been assumed that the elastic properties of a material are the same in all directions. Such materials are isotropic. Typical examples of isotropic materials are metals. However, certain other materials have different elastic properties in different directions and are called anisotropic. Natural anisotropic materials are for example wood and plywood. Other materials or rather structures can be manufactured in such a way as to exhibit an anisotropic character. Examples of such materials are steel-reinforced concrete, metal plates with stiffeners or ribs and various types of composite materials.

If a homogeneous material has three perpendicular planes of symmetry with respect to its elastic properties, the plate is orthogonally anisotropic and is said to be orthotropic. Twelve elastic properties are required to relate stresses and strains in this type of material as discussed in for example Refs. [16, 77]. These twelve properties are not independent, meaning that the number required can be reduced to nine independent properties. For such a case, the compliance matrix is Ref. [77].

$$\begin{Bmatrix} \varepsilon_x \\ \varepsilon_y \\ \varepsilon_z \\ \gamma_{xy} \\ \gamma_{xz} \\ \gamma_{yz} \end{Bmatrix} = [C] \begin{Bmatrix} \sigma_x \\ \sigma_y \\ \sigma_z \\ \tau_{xy} \\ \tau_{xz} \\ \tau_{yz} \end{Bmatrix}$$

$$[C] = \begin{bmatrix} 1/E_x & -\nu_{yx}/E_y & -\nu_{zx}/E_z & 0 & 0 & 0 \\ -\nu_{xy}/E_x & 1/E_y & -\nu_{zy}/E_z & 0 & 0 & 0 \\ -\nu_{xz}/E_x & -\nu_{yz}/E_z & 1/E_z & 0 & 0 & 0 \\ 0 & 0 & 0 & 1/G_{xy} & 0 & 0 \\ 0 & 0 & 0 & 0 & 1/G_{xz} & 0 \\ 0 & 0 & 0 & 0 & 0 & 1/G_{yz} \end{bmatrix} \quad (3.126)$$

It can be shown that the matrix is symmetric. Thus, $\nu_{xy}/E_x = \nu_{yx}/E_y$ etc. The number of independent coefficients is thereby reduced to 9. For a thin anisotropic plate oriented in the x - y -plane, $\sigma_z = \tau_{yz} = \tau_{xz} = 0$. With only two directions of orthotropy along the x - and y -axes, five elastic properties are required to determine the bending of the plate. The matrix system (3.126) is therefore reduced to Ref. [25]

$$\begin{Bmatrix} \varepsilon_x \\ \varepsilon_y \\ \gamma_{xy} \end{Bmatrix} = \begin{bmatrix} 1/E_x & -\nu_{yx}/E_y & 0 \\ -\nu_{xy}/E_x & 1/E_y & 0 \\ 0 & 0 & 1/G_{xy} \end{bmatrix} \begin{Bmatrix} \sigma_x \\ \sigma_y \\ \tau_{xy} \end{Bmatrix} \quad (3.127)$$

The inverse relationship is

$$\begin{Bmatrix} \sigma_x \\ \sigma_y \\ \tau_{xy} \end{Bmatrix} = \frac{1}{1 - \nu_{xy}\nu_{yx}} \begin{bmatrix} E_x & \nu_{yx}E_x & 0 \\ \nu_{xy}E_y & E_y & 0 \\ 0 & 0 & G_{xy}(1 - \nu_{xy}\nu_{yx}) \end{bmatrix} \begin{Bmatrix} \varepsilon_x \\ \varepsilon_y \\ \gamma_{xy} \end{Bmatrix} \quad (3.128)$$

The shear modulus G_{xy} of this type of orthotropic material is, Ref. [25], approximately given by

$$G_{xy} \approx \frac{\sqrt{E_x E_y}}{2(1 + \sqrt{\nu_x \nu_y})}. \quad (3.129)$$

For thin plates, the strains are functions of the curvature of the plate under bending as given by Eq. (3.104). Thus

$$\varepsilon_x = -z \frac{\partial^2 w}{\partial x^2}, \quad \varepsilon_y = -z \frac{\partial^2 w}{\partial y^2},$$

where w again, as in Sect. 3.9, is the displacement of the plate. The bending moments M'_x and M'_y per unit width of the plate are obtained from Eq. (3.105) as

$$M'_x = -D_y \left(\frac{\partial^2 w}{\partial y^2} + \nu_x \frac{\partial^2 w}{\partial x^2} \right), \quad M'_y = -D_x \left(\frac{\partial^2 w}{\partial x^2} + \nu_y \frac{\partial^2 w}{\partial y^2} \right). \quad (3.130)$$

The bending stiffness D_x and D_y for a thin plate with a constant thickness h are

$$D_x = \frac{E_x h^3}{12(1 - \nu_x \nu_y)}, \quad D_y = \frac{E_y h^3}{12(1 - \nu_x \nu_y)}. \quad (3.131)$$

The additional bending moment induced by shear is

$$M'_{xy} = -\sqrt{D_x D_y} (1 - \sqrt{\nu_x \nu_y}) \cdot \frac{\partial^2 w}{\partial x \partial y}. \quad (3.132)$$

This expression is obtained according to the procedure outlined in Sect. 3.9 and leading up to the result (3.112). The equation of motion governing the flexural motion of an orthotropic plate element with a geometry shown in Fig. 3.18 is derived by first combining the Eqs. (3.113) and (3.114) into the expression

$$\frac{\partial^2 M'_y}{\partial x^2} + 2 \frac{\partial^2 M'_{xy}}{\partial x \partial y} + \frac{\partial^2 M'_x}{\partial y^2} = \mu \frac{\partial^2 w}{\partial t^2}. \quad (3.133)$$

This expression in combination with the Eqs. (3.130) and (3.132) results in the differential equation governing the bending of thin orthotropic plates. This reads

$$D_x \frac{\partial^4 w}{\partial x^4} + 2B \frac{\partial^4 w}{\partial x^2 \partial y^2} + D_y \frac{\partial^4 w}{\partial y^4} = \mu \frac{\partial^2 w}{\partial t^2}$$

$$B = \sqrt{D_x D_y} (1 - \sqrt{\nu_x \nu_y}) + D_x \nu_y / 2 + D_y \nu_x / 2. \quad (3.134)$$

The parameter B is the effective torsional rigidity of the plate. This expression can be simplified since according to Betti's reciprocal theorem $D_x \nu_y = D_y \nu_x$. The torsional rigidity is simplified to

$$B = \sqrt{D_x D_y}. \quad (3.135)$$

This expression is not exact since it is based on the approximate expression (3.129) giving the shear modulus. The result (3.134) in combination with Eq. (3.135) can also be used to model the vibrations of frame reinforced plates. A number of examples are given in Ref. [25]. The basic theory of laminated anisotropic plates is discussed in Ref. [26].

3.11 Energy Flow

The energy flow in a thin isotropic beam can be determined by longitudinal, transverse, torsional, and bending waves. The displacement due to bending and shear could be in any direction perpendicular to the axis of the beam. The complete description of the energy flow in a solid results in a rather massive expression as given by Achenbach [80]. Thus for simplicity consider first a homogeneous beam oriented along the

x -axis. The height of the beam is h and its width is b . Displacement due to bending is in the z -direction only. Torsion, i.e., rotation around the axis of the beam is neglected. The energy flow in a beam due to longitudinal waves is equal to bhI_x where the intensity I_x is given in Eq. (3.56). The corresponding expression for the energy flow due to bending waves is defined in Eqs. (3.89) and (3.90). The beam is assumed to be thin. Therefore, the energy flow due to shear waves is neglected. The total energy flow due to one-dimensional longitudinal and bending waves in a beam is

$$\Pi_x = -Ebh \frac{\partial \xi}{\partial x} \cdot \frac{\partial \xi}{\partial t} + \frac{Ebh^3}{12} \frac{\partial^3 w}{\partial x^3} \cdot \frac{\partial w}{\partial t} - \frac{Ebh^3}{12} \frac{\partial^2 w}{\partial x^2} \cdot \frac{\partial^2 w}{\partial x \partial t}. \quad (3.136)$$

The displacement due to bending is w . In order to measure this energy flow in a simple structure like a beam the in-plane strain ξ its spatial derivative and velocity must be measured. This requires two transducers. For the transverse displacement w the first, second, and third derivatives as well as velocity must be recorded. Despite this apparently monumental task, very promising results have been reported. In all these cases, the strains have been measured by means of optical techniques. For the sake of completeness, also the energy flow in a thin plate is given in Eq. (3.137). Flexural waves and longitudinal and transverse in-plane waves are included in the expression. The plate is in the x - y plane. The displacements ξ , η , and w are in the x , y , and z directions, respectively. The energy flow Π'_x per unit width of the plate propagating along the x -axis is equal to the intensity times the thickness of the plate. The displacements induced by longitudinal and transverse waves propagating along the x -axis are ξ and η . The displacement due to flexural waves is w . The energy flow per unit width of the plate is

$$\begin{aligned} \Pi'_x = I_x h = & -\frac{Eh}{1-\nu^2} \left(\frac{\partial \xi}{\partial x} + \nu \frac{\partial \eta}{\partial y} \right) \frac{\partial \xi}{\partial t} \\ & - \frac{Eh}{2(1+\nu)} \left(\frac{\partial \xi}{\partial y} + \frac{\partial \eta}{\partial x} \right) \frac{\partial \eta}{\partial t} - \frac{Eh^3}{12(1-\nu^2)} \left[\nabla^2 w \frac{\partial^2 w}{\partial x \partial t} - \frac{\partial}{\partial x} (\nabla^2 w) \frac{\partial w}{\partial t} \right. \\ & \left. + (1-\nu) \left(\frac{\partial^2 w}{\partial x \partial y} \frac{\partial^2 w}{\partial t \partial y} - \frac{\partial^2 w}{\partial y^2} \frac{\partial^2 w}{\partial t \partial x} \right) \right]. \end{aligned} \quad (3.137)$$

For a plane flexural wave traveling along the x -axis with the displacement $w(x, t)$ normal to the plate the energy flow per unit width of the plate is

$$\Pi'_{x, \text{flexural}} = -\frac{Eh^3}{12(1-\nu^2)} \left(\frac{\partial^2 w}{\partial x^2} \frac{\partial^2 w}{\partial x \partial t} - \frac{\partial^3 w}{\partial x^3} \frac{\partial w}{\partial t} \right). \quad (3.138)$$

The corresponding energy flow in a plate caused by a plane longitudinal wave with the displacement $\xi(x, t)$ is

$$\Pi'_{x, \text{longitudinal}} = -\frac{Eh}{(1-\nu^2)} \frac{\partial \xi}{\partial x} \frac{\partial \xi}{\partial t}. \quad (3.139)$$

For a plane transverse wave, displacement $\eta(x, t)$ the energy flow is

$$\Pi'_{x, \text{transverse}} = -\frac{Eh}{2(1+\nu)} \frac{\partial \eta}{\partial x} \frac{\partial \eta}{\partial t}. \quad (3.140)$$

Intensity and energy flow are discussed in Refs. [27–30].

The use of primitive measurement techniques have been attempted in order to determine the energy flow in thin beams and for that matter even on plates. For these measurements, two closely spaced accelerometers are often used. In order to do this too many simplifications are made. All evanescent waves as well as the in-plane waves are neglected. This type of measurement can only to a certain degree indicate the direction of the energy flow but not its magnitude.

Problems

3.1 An infinite beam is oriented along the x -axis in a coordinate system. The displacement along the x -axis is $\xi = A \cdot \sin(\omega t - k_l x)$, where k_l is the wave number for quasi-longitudinal waves. The width of the beam is b and its height h . Determine the displacement perpendicular to the x -axis of the beam. Assume that σ_y and σ_z are equal to zero in the beam.

3.2 Determine the resulting kinetic energy in the beam of Problem 3.1. Consider only the effects due to quasi-L-waves.

3.3 An L-wave is propagating in an infinite and homogeneous beam oriented along the x -axis of a coordinate system. The resulting displacement is defined by $f(x - c_l t)$. Determine the kinetic and potential energies plus the energy flow due to this wave.

3.4 A semi-infinite and homogeneous beam with constant cross section area S is oriented along the x -axis of a coordinate system. At $x = 0$ the beam is excited by a force $F(t)$ in the direction of the positive x -axis. Determine the displacement in the beam. Consider only L-waves. As an example let the force be given by $F(t) = F_0 \sin \omega t$.

3.5 Torsional waves are propagating in an infinite cylindrical and homogeneous shaft with radius R . Due to the wave motion the torsional angle Θ varies as $\Theta = \Theta_0 \sin(k_t x - \omega t)$. Determine the potential and kinetic energies per unit length of the shaft as well as the energy flow in the shaft which is oriented along the x -axis of a coordinate system.

3.6 Flexural waves are propagating in an infinite and homogeneous beam oriented along the x -axis of a coordinate system. The displacement of the beam is given by $w(x, t)$. Determine the potential energy per unit length of the beam based on the general expression Eq. (3.17) and the definition of the strain in Eq. (3.72). Neglect shear effects.

3.7 The deflection η of an infinite and homogeneous string oriented along the x -axis is at $t = 0$ equal to $\eta(x, 0) = \cos(\pi x/L)$ for $-L/2 < x < L/2$ otherwise zero.

The string is at rest at $t = 0$. Determine the displacement of the string when it is released at $t = 0$. Neglect the losses.

3.8 A thin, infinite, and homogeneous beam is oriented along the x -axis in a coordinate system. The mass per unit length is m' and its bending stiffness D' . For $t < 0$ the beam is at rest having the lateral displacement $\exp[-(x/2a)^2]$. The beam is released at $t = 0$. Determine the displacement of the beam for $t > 0$. Compare the discussion in Sect. 3.8.

3.9 An attempt is made to measure the energy flow in a thin homogeneous beam by means of just one accelerometer. The material and geometrical parameters of the beam are known.

The bending stiffness and wavenumber are denoted D' and κ . Losses are neglected. In the first case the lateral displacement of the beam, which is oriented along the x -axis of a coordinate system, is equal to $w(x, t) = A \cdot \exp[i(\omega t - \kappa x)]$. Determine the energy flow in the beam as function of the time average of the velocity squared measured at the point $x = x_0$.

In the second case the near field can not be neglected. The displacement is $w(x, t) = A \cdot \exp(i\omega t) \cdot [\exp(-i\kappa x) - i \cdot \exp(-\kappa x)]$. Determine the ratio between the actual energy flow and the energy flow estimated by means of the velocity squared measured by means of the accelerometer at the point $x = x_0$.

In the third case the near field but not a reflected field can be neglected. The displacement is given by $w(x, t) = A \cdot \exp(i\omega t) \cdot [\exp(-i\kappa x) + X \cdot \exp(i\kappa x)]$. Again calculate the ratio between the actual and measured energy flows at the point $x = x_0$.

3.10 Show that the bending moment per unit length induced by shear in an orthotropic plate is given by Eq. (3.132) as

$$M'_{xy} = -\sqrt{D_x D_y} \cdot (1 - \sqrt{\nu_x \nu_y}) \cdot \frac{\partial^2 w}{\partial x \partial y}.$$

The plate is oriented in the x - y -plane of a coordinate system.

3.11 An L-wave is propagating in an infinite beam oriented along the x -axis of a coordinate system. The displacement is $\xi(x, t) = A \cdot \exp[i(\omega t - k_l x)]$. Show that the time average of the energy flow Π is $\bar{\Pi} = c_l \bar{E}_l$, where \bar{E}_l is the time average of the total energy per unit length of the beam and c_l the phase velocity of the wave.

3.12 Show that the intensity of L-waves propagating in the beam of Problem 3.11 is given by $I_x = -\sigma_x \cdot \partial \xi / \partial t$ where ξ is the displacement in the beam. Start by considering the total energy per unit volume of the beam.

Chapter 4

Interaction Between Longitudinal and Transverse Waves

The simple differential equations, describing the bending of plates and beams derived in the previous chapter, are only valid as long as the structures can be considered as “thin.” In this chapter, this limitation is studied in more detail. The basis for the discussion is the general wave equation. It is found that bending can be described, by means of the interaction of longitudinal and transverse waves. The bending of thick beams and composite structures are derived, based on these assumptions.

In the first part of the chapter, the generalized wave equation is derived. Based on the result, some coupling effects between longitudinal and transverse waves are illustrated. Thereafter the generalized wave equation is utilized to describe the bending of thick plates, sandwich beams, and I-beams.

4.1 Generalized Wave Equation

The wave equations governing flexural waves in beams and plates were derived based on a number of assumptions in Chap. 3. Bending moments, etc., were determined based on stresses due to longitudinal waves only. Shear effects were neglected. A more detailed analysis of bending shows that the simplified fourth-order differential wave equation governing bending of thin beams and plates can be described by two coupled second-order differential equations. One of these describes the propagation of longitudinal waves and the other transverse waves. The basis for a more complete description of bending is the generalized wave equation.

In a solid, the strain along the x -axis can be caused by longitudinal waves traveling in the x -direction or by transverse waves traveling in either the y - or z -direction. For just longitudinal waves propagating along the x -axis, the stress σ_x and the displacement ξ satisfy Eq. (3.51), or

$$\frac{\partial \sigma_x}{\partial x} = \rho \frac{\partial^2 \xi}{\partial t^2}.$$

For pure transverse waves propagating in the y -direction the corresponding expression is from Eq. (3.37)

$$\frac{\partial \tau_{xy}}{\partial y} = \rho \frac{\partial^2 \xi}{\partial t^2}.$$

Similarly, for pure transverse waves propagating in the z -direction the resulting shear τ_{xz} creates an acceleration component along the x -axis as

$$\frac{\partial \tau_{xz}}{\partial z} = \rho \frac{\partial^2 \xi}{\partial t^2}.$$

If all three waves are present at the same time the total force is equal to the sum of the forces due to each wave. Consequently, if all waves are present, Newton's second law gives

$$\frac{\partial \sigma_x}{\partial x} + \frac{\partial \tau_{xy}}{\partial y} + \frac{\partial \tau_{xz}}{\partial z} = \rho \frac{\partial^2 \xi}{\partial t^2}. \quad (4.1)$$

The stresses σ_x , τ_{xy} , and τ_{xz} are defined in the Eqs. (3.6) and (3.11). If, as before, the deflections due to the waves are given by ξ , η , and ζ in the directions of the axes x , y , and z then Eq. (4.1) can, with $G = E/[2(1 + \nu)]$, be written as

$$G \left[\nabla^2 \xi + \frac{1}{(1 - 2\nu)} \cdot \frac{\partial}{\partial x} \left(\frac{\partial \xi}{\partial x} + \frac{\partial \eta}{\partial y} + \frac{\partial \zeta}{\partial z} \right) \right] = \rho \frac{\partial^2 \xi}{\partial t^2}. \quad (4.2)$$

Similar expressions can be derived describing the forces and displacements along the y and z axes. These expressions can be written in compact form if the displacement vector \mathbf{r} is introduced as

$$\mathbf{r} = (\xi, \eta, \zeta). \quad (4.3)$$

The result is

$$G \left[\nabla^2 \mathbf{r} + \frac{1}{(1 - 2\nu)} \mathbf{grad}(\text{div } \mathbf{r}) \right] = \rho \frac{\partial^2 \mathbf{r}}{\partial t^2}. \quad (4.4)$$

This is the general differential equation, which all elastic oscillatory motions in the interior of a solid must satisfy. It has previously been pointed out that in a solid there can be rotation due to transverse waves and also a rotational-free motion due to longitudinal waves. It is therefore natural to assume that the total field consists of a divergence-free field and a rotational-free field. In fact, any continuous vector field can be separated into one irrotational and one divergence-free part. The rotational-free field is defined as a function of a scalar potential ϕ . The resulting vector field is given by $\mathbf{grad } \phi$ and is irrotational since

$$\mathbf{curl}(\mathbf{grad } \phi) = 0.$$

The divergence-free field is given as a function of a vector potential $\boldsymbol{\psi} = (\psi_x, \psi_y, \psi_z)$. A vector field $\mathbf{F} = \mathbf{curl} \boldsymbol{\psi}$ is said to be source or divergence free within a volume V if the net flow out of the surface S enclosing the volume is zero. This can be expressed by means of Gauss' theorem as

$$\int \mathbf{F} \cdot \mathbf{n} dS = \int \text{div } \mathbf{F} dV = 0.$$

For the net flow or the volume integral to be zero, $\text{div}(\mathbf{F})$ must also be equal to zero. This condition is satisfied since

$$\text{div}(\mathbf{curl} \boldsymbol{\psi}) = 0.$$

Considering these arguments, the displacement vector \mathbf{r} in a solid is defined as a function of a scalar potential ϕ and a vector potential $\boldsymbol{\psi}$ or

$$\mathbf{r} = (\xi, \eta, \zeta) = \mathbf{grad} \phi + \mathbf{curl} \boldsymbol{\psi}$$

$$\xi = \frac{\partial \phi}{\partial x} + \frac{\partial \psi_z}{\partial y} - \frac{\partial \psi_y}{\partial z}, \quad \eta = \frac{\partial \phi}{\partial y} + \frac{\partial \psi_x}{\partial z} - \frac{\partial \psi_z}{\partial x}, \quad \zeta = \frac{\partial \phi}{\partial z} + \frac{\partial \psi_y}{\partial x} - \frac{\partial \psi_x}{\partial y}. \quad (4.5)$$

Inserting the definition of \mathbf{r} —the first expression in Eqs. (4.4)–(4.5)—the result is

$$\begin{aligned} G \left\{ \nabla^2(\mathbf{grad} \phi) + \nabla^2(\mathbf{curl} \boldsymbol{\psi}) + \frac{1}{1-2\nu} \mathbf{grad}[\text{div}(\mathbf{grad} \phi)] \right\} \\ = \rho \frac{\partial^2}{\partial t^2} [\mathbf{grad} \phi + \mathbf{curl} \boldsymbol{\psi}]. \end{aligned} \quad (4.6)$$

However,

$$\nabla^2(\mathbf{grad} \phi) = \mathbf{grad}(\nabla^2 \phi) \text{ and } \nabla^2(\mathbf{curl} \boldsymbol{\psi}) = \mathbf{curl}(\nabla^2 \boldsymbol{\psi}).$$

Considering these alternative expressions, Eq. (4.6) is rewritten as

$$\mathbf{grad} \left(G \nabla^2 \phi + \frac{G}{1-2\nu} \nabla^2 \phi - \rho \frac{\partial^2 \phi}{\partial t^2} \right) + \mathbf{curl} \left(G \nabla^2 \boldsymbol{\psi} - \rho \frac{\partial^2 \boldsymbol{\psi}}{\partial t^2} \right) = 0. \quad (4.7)$$

This equation is satisfied if the expressions inside the two brackets are equal to a constant. However, for vibrations around some state of equilibrium this constant can be set to equal zero. Compare the discussion in Sect. 1.1. Thus for Eq. (4.7) to be satisfied it follows that

$$\frac{E(1-\nu)}{(1+\nu)(1-2\nu)} \nabla^2 \phi - \rho \frac{\partial^2 \phi}{\partial t^2} = 0, \quad G \nabla^2 \boldsymbol{\psi} - \rho \frac{\partial^2 \boldsymbol{\psi}}{\partial t^2} = 0. \quad (4.8)$$

The first expression is the three-dimensional wave equation for longitudinal waves in solids. The speed of propagation c_l is

$$c_l = \sqrt{\frac{E(1-\nu)}{\rho(1+\nu)(1-2\nu)}}.$$

The result is the same as previously derived for longitudinal waves propagating in an infinite solid, compare Eqs. (3.51) and (3.53). As pointed out in Sect. 3.4, pure longitudinal waves can only propagate in an infinite solid. In beams and plates, strains perpendicular to the direction of propagation lead to shearing effects. This means that both longitudinal and transverse waves must exist. However, if the plates and beams are “thin,” the effect of the transverse waves is negligible. In this type of structure, the “longitudinal waves” are called quasi-longitudinal waves. The speed of these waves depends on the geometry of the structure as discussed in Sect. 3.4.

The wave equation governing quasi-longitudinal waves propagating in a “thin” beam oriented along the x -axis is

$$E \frac{\partial^2 \phi}{\partial x^2} - \rho \frac{\partial^2 \phi}{\partial t^2} = 0. \quad (4.9)$$

The displacement ξ along the x -axis is given by $\xi = \partial\phi/\partial x$.

For quasi-longitudinal waves propagating in a thin plate oriented in the x - y plane the corresponding wave equation is

$$\frac{E}{1-\nu^2} \left(\frac{\partial^2 \phi}{\partial x^2} + \frac{\partial^2 \phi}{\partial y^2} \right) - \rho \frac{\partial^2 \phi}{\partial t^2} = 0. \quad (4.10)$$

The displacement vector \mathbf{r} due to quasi-longitudinal waves in a plate is

$$\mathbf{r} = \mathbf{grad} \phi = \left(\frac{\partial \phi}{\partial x}, \frac{\partial \phi}{\partial y}, 0 \right).$$

The general three-dimensional wave equation for pure longitudinal waves in a solid is defined in Eq. (4.8). The displacement vector \mathbf{r} due to longitudinal waves in a solid is

$$\mathbf{r} = \mathbf{grad} \phi = \left(\frac{\partial \phi}{\partial x}, \frac{\partial \phi}{\partial y}, \frac{\partial \phi}{\partial z} \right).$$

The second expression of Eq. (4.8) defines the wave equation for transverse waves in three dimensions. The differential equation really consists of three equations—one for each component of the vector ψ . The speed of propagation is the same as defined in Sect. 3.3 irrespective of the geometry of the solid. Thus

$$c_t = \sqrt{\frac{E}{2\rho(1+\nu)}}.$$

In a beam oriented along the x -axis the displacement, due to transverse waves propagating in the direction of the length of the beam, can be in the y and z directions. This shows that the components of the vector potential ψ are functions of x only. Indicating, according to Eq. (4.5), that the resulting displacements are

$$\eta = -\frac{\partial\psi_z}{\partial x}, \quad \zeta = \frac{\partial\psi_y}{\partial x}.$$

The corresponding wave equations are

$$G \frac{\partial^2 \psi_y}{\partial x^2} - \rho \frac{\partial^2 \psi_y}{\partial t^2} = 0, \quad G \frac{\partial^2 \psi_z}{\partial x^2} - \rho \frac{\partial^2 \psi_z}{\partial t^2} = 0. \quad (4.11)$$

For transverse waves, propagating in the x - y plane of a thin plate with the displacements in the plane of the plate, the displacement in the z -direction is equal to zero. According to Eq. (4.5) the components ψ_x and ψ_y must therefore be equal to zero. The remaining component ψ_z is a function of the coordinates x and y defining the plane of the plate. The wave equation governing in plane transverse waves propagating in the x - y plane is thus from Eq. (4.8)

$$G \left(\frac{\partial^2 \psi_z}{\partial x^2} + \frac{\partial^2 \psi_z}{\partial y^2} \right) - \rho \frac{\partial^2 \psi_z}{\partial t^2} = 0. \quad (4.12)$$

The resulting displacements are from Eq. (4.5) obtained as

$$\xi = \frac{\partial\psi_z}{\partial y}, \quad \eta = -\frac{\partial\psi_z}{\partial x}.$$

For any solid, the two equations in Eq. (4.8) can be used to describe deflections in the solid, as long as the appropriate boundary conditions are known i.e., if the stresses on the surfaces of the solid are known. Consequently, any deflection of a solid can be described by means longitudinal and transverse waves. Demonstrating that the wave equations in Eq. (4.8) are sufficient to describe “flexural waves” on a beam or plate, which is not necessarily thin compared to the wavelength. However, before proceeding with thick plates, the coupling between in plane longitudinal and transverse waves is investigated for a more simple case, a semi-infinite plate.

4.2 Intensity

The energy flow in beams and plates was discussed in Sect. 3.11. It was assumed that the intensity and thus the energy flow were induced by longitudinal, transverse, and bending waves. The energy flow was derived as functions of measurable quantities on the surfaces of beams and plates. However, bending waves are really a combination of

longitudinal and transverse waves as discussed in Sect. 4.1. Thus, the intensity I_x in the direction of the x -axis of a coordinate system can be induced by longitudinal and transverse waves traveling along the positive x -axis. The normal stress σ_x caused by the longitudinal wave is parallel to the direction of the wave. The intensity component due to the longitudinal wave is $(I_x)_l = -\sigma_x \cdot \dot{\xi}$ where, as in Sect. 4.1, ξ is the displacement along the x -axis. The stress and velocity are defined positive in different directions resulting in a minus sign, see Fig. 3.4. The shear or transverse waves traveling along the x -axis can have the displacement η in the y -direction resulting in the shear stress τ_{xy} in the same direction. There could also be a displacement in the z -direction causing the shear stress τ_{xz} . The intensity component $(I_x)_t$ induced by transverse waves is consequently $(I_x)_t = -\tau_{xy}\dot{\eta} - \tau_{xz}\dot{\zeta}$. The total intensity component I_x is $I_x = (I_x)_l + (I_x)_t$. Repeating the same discussion for the intensity components I_y and I_z the intensity vector is $\mathbf{I} = (I_x, I_y, I_z)$ where

$$\begin{aligned} I_x &= -\sigma_x \dot{\xi} - \tau_{xy} \dot{\eta} - \tau_{xz} \dot{\zeta} \\ I_y &= -\sigma_y \dot{\eta} - \tau_{xy} \dot{\xi} - \tau_{yz} \dot{\zeta} \\ I_z &= -\sigma_z \dot{\zeta} - \tau_{xz} \dot{\xi} - \tau_{yz} \dot{\eta}. \end{aligned} \quad (4.13)$$

The stresses and strains are defined in Eqs. (3.6) and (3.11). In Sect. 3.1, it was concluded that the divergence of the intensity vector and the total energy per unit volume of the solid are, in the absence of a source, related as

$$\nabla \cdot \mathbf{I} + \frac{\partial}{\partial t} (\mathcal{U}_v + \mathcal{T}_v) = 0, \quad (4.14)$$

where \mathcal{U}_v and \mathcal{T}_v are defined in Eqs. (3.17) and (3.18). The general wave equation (4.4) is also obtained from the expression (4.14).

4.3 Coupling Between Longitudinal and Transverse Waves

In plate structures the L (longitudinal)- and T (transverse)-waves are in general well coupled. If for example an L-wave is induced in a thin plate, other wave types can be excited at the edges or the boundaries of the plate. This can be demonstrated by considering a thin semi-infinite plate as shown in Fig. 4.1. The plate is located in the x - y plane for $x \leq 0$. The edge of the plate is defined by the line $x = 0$. A plane longitudinal wave is incident on the edge. The plate is assumed to be thin meaning that the wave is propagating in the x - y plane only. The angle of incidence is α , i.e., the angle between the normal to the edge and the direction of the wave is equal to α . The incident wave is traveling between the positive directions of the x - and y -axis.

The scalar potential ϕ describing the incident L-wave must therefore be of the form

$$\phi(x, y, t) = \exp[i(\omega t - k_x x - k_y y)]. \quad (4.15)$$

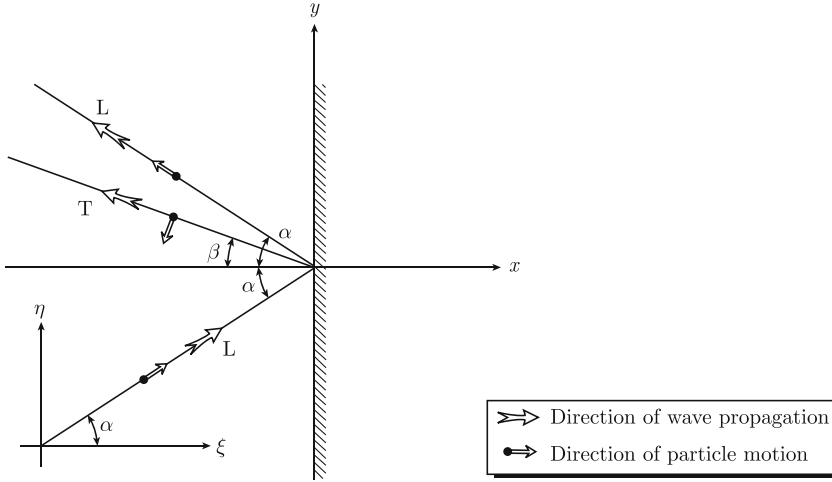


Fig. 4.1 A plane L-wave incident on an edge. L- and T-waves reflected

The displacement ξ in the x -direction is

$$\xi = \frac{\partial \phi}{\partial x} = -ik_x \cdot \phi.$$

The corresponding displacement η along the y -axis is

$$\eta = \frac{\partial \phi}{\partial y} = -ik_y \cdot \phi.$$

For a plane wave with the angle of incidence α , the ratio between η and ξ must, according to Fig. 4.1, be $\eta/\xi = \tan \alpha$. Consequently

$$k_y/k_x = \tan \alpha. \quad (4.16)$$

In addition, the expression (4.15) must satisfy the wave equation (4.10). Thus

$$k_x^2 + k_y^2 = k_l^2 = \frac{\omega^2}{c_l^2} = \frac{\omega^2 \rho (1 - \nu^2)}{E}. \quad (4.17)$$

In this expression c_l is the velocity of quasi-longitudinal waves propagating in a plate. The corresponding wavenumber is k_l . The solution to Eqs. (4.16) and (4.17) is

$$k_x = k_l \cdot \cos \alpha, \quad k_y = k_l \cdot \sin \alpha. \quad (4.18)$$

At the edge, the reflected L-wave must have the same dependence on y as the incident wave in order to fulfill the boundary conditions at the edge for every y .

The reflected L-wave must also obey the wave equation. The reflected wave travels between the negative x -axis and the positive y -axis and must therefore be of the form

$$\phi(x, y, t) = R_{LL} \cdot \exp[i(\omega t + k_x x - k_y y)]. \quad (4.19)$$

It is assumed that the incident wave has unit amplitude and the reflected L-wave the amplitude R_{LL} . The first and second subscripts indicate that the incident and reflected waves are both L-waves.

For a thin plate, i.e., waves are propagating only in the x - y plane, two boundary conditions must be satisfied at the edge. For a free edge, the normal and shear stresses must be zero. If on the other hand, the plate is connected to a structure with an infinite impedance, the displacements perpendicular and parallel to the edge must be zero. The two boundary conditions cannot in general be satisfied by an incident and a reflected wave. There is only one unknown parameter R_{LL} , but for each edge condition, two conditions or requirements must be met. The consequence is that at the edge a transverse wave is induced. This wave also travels in the same quadrant, as the reflected longitudinal wave. The displacement due to this wave must be in the x - y plane, since the plate is assumed to be thin and any displacement in the z -direction is neglected. Demonstrating that the vector potential ψ , describing the fields for the transverse waves, is of the form

$$\psi = (0, 0, \psi_z).$$

If the induced T-wave travels away from the edge at an angle β with the normal to the edge, the z -component of the vector potential must be of the form

$$\psi_z(x, y, t) = R_{LT} \cdot \exp[i(\omega t + k_t \cdot \cos \beta \cdot x - k_t \cdot \sin \beta \cdot y)]. \quad (4.20)$$

The amplitude of the T-wave induced by an incident L-wave is given by R_{LT} as indicated by the subscripts. In Eq. (4.20) k_t is the wavenumber for transverse waves i.e., $k_t = \omega/c_t$. The function ψ_z satisfies the wave equation for transverse waves given by Eq. (4.12).

In order to satisfy the boundary conditions at the edge for every y , the angle β must fulfill the following condition

$$k_t \cdot \sin \beta = k_l \cdot \sin \alpha \quad \text{or} \quad \frac{\sin \alpha}{\sin \beta} = \frac{c_l}{c_t}. \quad (4.21)$$

The total scalar potential and the z -component of the vector potential can thus be written as

$$\phi = \exp[i(\omega t - k_l \cdot \cos \alpha \cdot x - k_l \cdot \sin \alpha \cdot y)] + R_{LL} \cdot \exp[i(\omega t + k_l \cdot \cos \alpha \cdot x - k_l \cdot \sin \alpha \cdot y)]$$

$$\psi_z = R_{LT} \cdot \exp[i(\omega t + \Lambda \cdot x - k_l \cdot \sin \alpha \cdot y)], \quad (4.22)$$

where

$$\Lambda = k_t \cdot \cos \beta = \sqrt{k_t^2 - k_l^2 \sin^2 \beta} = \sqrt{k_t^2 - k_l^2 \sin^2 \alpha}. \quad (4.23)$$

The last expression follows directly from Eq. (4.21). The parameter Λ is real since $k_t > k_l$. The unknown amplitudes R_{LL} and R_{LT} are determined by the boundary conditions. If the plate is connected to an infinitely stiff structure, i.e., with infinite impedance, the deflections ξ and η in the x - and y -directions must be zero. According to Eq. (4.5) the boundary conditions for this case are

$$\xi = \frac{\partial \phi}{\partial x} + \frac{\partial \psi_z}{\partial y} = 0, \quad \eta = \frac{\partial \phi}{\partial y} - \frac{\partial \psi_z}{\partial x} = 0 \quad \text{for } x = 0. \quad (4.24)$$

The insertion of the expressions given in Eq. (4.22) in the boundary conditions yields

$$\begin{aligned} -ik_l \cdot \cos \alpha \cdot (1 - R_{LL}) - ik_l \cdot \sin \alpha \cdot R_{LT} &= 0 \\ -ik_l \cdot \sin \alpha \cdot (1 + R_{LL}) - i\Lambda R_{LT} &= 0 \end{aligned} \quad (4.25)$$

The parameters R_{LL} and R_{LT} are obtained from these equations as

$$R_{LL} = \frac{\Lambda \cos \alpha - k_l \sin^2 \alpha}{\Lambda \cos \alpha + k_l \sin^2 \alpha}, \quad R_{LT} = -\frac{k_l \sin 2\alpha}{\Lambda \cos \alpha + k_l \sin^2 \alpha}. \quad (4.26)$$

For normal incidence, $\alpha = 0$, Eq. (4.26) gives $R_{LL} = 1$ $R_{LT} = 0$. For normal incidence the amplitude of the reflected L-wave is the same as the amplitude of the incident wave. No transverse wave is generated. This is also the case for grazing incidence when $\alpha = \pi/2$. However, at this angle the amplitude of the reflected L-wave is equal to -1 . The total field is thus equal to zero. At one angle, the incident L-wave is completely transformed into a T-wave. The amplitudes R_{LL} and R_{LT} are shown in Fig. 4.2 as functions of the angle of incidence. Note that the amplitudes R_{LL} and R_{LT} are only functions of the angle of incidence and not the frequency. This is evident when making the substitution $k_l = \omega/c_l$ in Eq. (4.26).

The angle β for the reflected T-wave is always smaller than α , the angle of the incident L-wave. However, if instead the incident wave is a T-wave with the angle of incidence α , an L- and a T-wave are induced and reflected. The reflected L-wave is of the form

$$\phi \propto \exp[i(\omega t + \Lambda x - k_t \cdot \sin \alpha \cdot y)],$$

where

$$\Lambda = \sqrt{k_l^2 - k_t^2 \sin^2 \alpha}.$$

For $\sin \alpha > k_l/k_t = c_t/c_l$ the parameter Λ is complex, which means that the amplitude of the induced L-wave decays exponentially with the distance from the

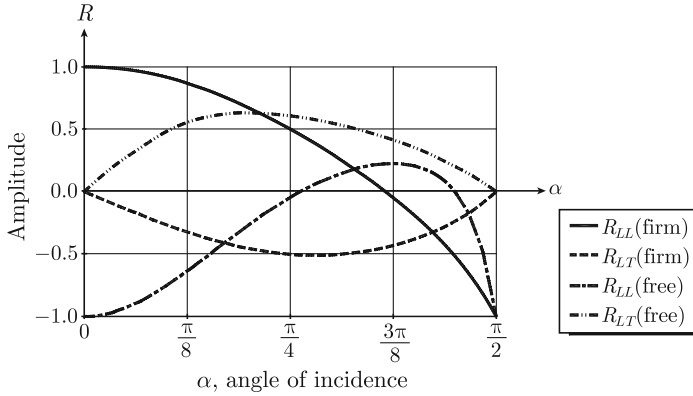


Fig. 4.2 Amplitudes of waves reflected at a free or a firm edge. An L-wave, unit amplitude, is incident on the edge. The amplitudes of the reflected L- and T-waves are denoted R_{LL} and R_{LT} , respectively

edge. The intensity of the induced L-wave is zero. The particulars are left for Problem 4.1.

In the second example considered, the edge of the semi-infinite plate is assumed to be completely free. Indicating that the normal and shear stresses at the edge must be zero. According to Eq. (3.6) the normal stress σ_x for a thin plate located in the x - y plane is given by

$$\sigma_x = \frac{E}{1-\nu^2}(\varepsilon_x + \nu\varepsilon_y) = \frac{E}{1-\nu^2} \left(\frac{\partial \xi}{\partial x} + \nu \frac{\partial \eta}{\partial y} \right).$$

The corresponding shear stress τ_{xy} is given by Eq. (3.11) as

$$\tau_{xy} = G \left(\frac{\partial \xi}{\partial y} + \frac{\partial \eta}{\partial x} \right).$$

The displacements ξ and η can as before be described by the velocity potential ϕ and the stream function component ψ_z . Equation (4.24), defining the displacements as functions of ϕ and ψ_z in combination with the expressions defining the stresses, give the boundary conditions for a free edge as

$$\begin{aligned} \frac{\partial^2 \phi}{\partial x^2} + \nu \frac{\partial^2 \phi}{\partial y^2} + (1-\nu) \frac{\partial^2 \psi_z}{\partial x \partial y} &= 0 \text{ for } x = 0 \\ 2 \frac{\partial^2 \phi}{\partial x \partial y} + \frac{\partial^2 \psi_z}{\partial y^2} - \frac{\partial^2 \psi_z}{\partial x^2} &= 0 \text{ for } x = 0 \end{aligned} \quad (4.27)$$

The general expressions (4.22) describing the incident and reflected L-wave and the induced T-wave are inserted in the boundary conditions in order to solve the unknown

amplitudes R_{LL} and R_{LT} . The result is

$$R_{LL} = \frac{X_1 - X_2}{X_1 + X_2}, \quad R_{LT} = \frac{2}{X_1 + X_2}, \quad (4.28)$$

where

$$X_1 = \frac{(1 - \nu) \Lambda k_l \sin \alpha}{(k_l \cos \alpha)^2 + \nu(k_l \sin \alpha)^2}, \quad X_2 = \frac{\Lambda^2 - (k_l \sin \alpha)^2}{k_l \sin 2\alpha}.$$

The amplitudes R_{LL} and R_{LT} are shown in Fig. 4.2 as functions of the angle of incidence. As in the previous case, the resulting amplitudes are independent of frequency. For normal incidence $\alpha = 0$, the amplitude of the induced T-wave is again equal to zero. However, the amplitude of the reflected L-wave is for normal incidence equal to -1 . This means that the phase angle between the incident and reflected wave is equal to π .

The following conclusions can be made:

- (i) If the impedance at the edge is infinite, an incident L- or T-wave at normal incidence is reflected in-phase as an L- or T-wave, respectively;
- (ii) For a free edge—normal incidence—the reflected L- or T-wave is in antiphase with the incident L- or T- wave respectively; and
- (iii) Except for normal incidence, L-waves generate T-waves or vice versa at an edge.

4.4 Bending of Thick Beams/Plates

It has previously been pointed out that the Bernoulli–Euler theory for beams and the Kirchhoff theory for plates are valid only as long as the beam or plate can be considered to be thin compared to the wavelength or rather when

$$\kappa h < 1 \quad \text{or} \quad \lambda = 2\pi/\kappa > 2\pi h \approx 6h, \quad (4.29)$$

where λ is the wave length, κ is the corresponding wavenumber for bending waves and h is the thickness of the beam. The apparent bending of thick plates or beams can be described by means of the generalized wave equation. The deflection of the structure is then completely determined by longitudinal and transverse waves. The procedure is just an extension of the discussion in the previous section. The possible solutions are restricted to some idealized cases corresponding to the bending of thick infinite plates or to the bending of thick beams with a negligible width. However, before the discussion of this general method, a widely used approximate procedure should be mentioned.

For the bending of thick beams, rotation as well as shear must be considered. Timoshenko Ref. [22] has formulated an approximate method based on a variational technique. Consider a beam with constant cross section area S . The mass m' per

unit length of the beam is $m' = \rho S$ where ρ is the density of the beam. For a homogeneous beam, width b and thickness h , the mass moment of inertia is $I_\omega = \rho I = \rho b h^3 / 12 = \rho S h^2 / 12$. The bending stiffness is $D' = b h^3 E / 12$. The differential equation governing the bending of this type of beam is by Timoshenko given as

$$\frac{D'}{m'} \frac{\partial^4 w}{\partial x^4} + \frac{\partial^2 w}{\partial t^2} - \left(\frac{D'}{G_e S} + \frac{I_\omega}{m'} \right) \frac{\partial^4 w}{\partial x^2 \partial t^2} + \frac{I_\omega}{G_e S} \frac{\partial^4 w}{\partial t^4} = 0. \quad (4.30)$$

The effective shear modulus G_e is written $G_e = T_b G$ where T_b is the so-called Timoshenko constant. The dimensionless parameter T_b is a shear coefficient introduced to account for the fact that shear is not uniformly distributed over the cross section of the beam. In the Timoshenko differential equation the fourth term is due to the rotation of a segment of the beam. The third term depends on shear effects. The Timoshenko wave equation plus forced excitation and the formulation of some boundary conditions are discussed in Sect. 9.5.

The parameter T_b introduced in the Timoshenko equation depends on the geometry of the cross section of the beam. The parameter T_b was initially defined by Timoshenko, see Ref. [22], as the ratio between the average shear stress on the section of the structure and the product of the shear modulus and the shear strain at the neutral axis. According to this definition, T_b is equal to $2/3$ as discussed at the end of this section. However, it has been observed that for $T_b = 2/3$ the response of a beam is not adequately described in the high frequency region. Alternative definitions of the shear coefficient T_b have therefore been discussed. It is frequently suggested, see for example Ref. [70], that the shear coefficient or Timoshenko constant should be $5/6$ for a rectangular cross section assuming $\nu = 0$ and 0.850 for $\nu = 0.3$. For a circular cross section and for $\nu = 0.3$, T_b is given as 0.886 . Shear coefficients for other geometries are given in Ref. [70]. Various definitions of the Timoshenko constant are discussed in Refs. [71, 72]. In principal, the shear coefficient should be a function of frequency. Compare also problem 4.9.

For a “bending wave” propagating along a thick beam the displacement can be written as $w(x, t) = A \cdot \exp[i(\omega t - k_x x)]$. For this expression to satisfy the Timoshenko differential equation, k_x is the solution to the equation

$$k_x^4 - k_x^2(k_l^2 + k_t^2/T_b) - (\kappa^4 - k_l^2 k_t^2/T_b) = 0$$

$$k_l = \omega \sqrt{\frac{\rho}{E}}, \quad k_t = \omega \sqrt{\frac{\rho}{G}} = \omega \sqrt{\frac{2\rho(1+\nu)}{E}}, \quad \kappa = \left[\frac{m' \omega^2}{D'} \right]^{1/4}, \quad (4.31)$$

where k_l , k_t , and κ are the wavenumbers for longitudinal, transverse, and flexural waves, respectively. There are four solutions to the wavenumber equation. These are

$$k_x = \pm \sqrt{\frac{1}{2} \left[(k_l^2 + k_t^2/T_b) \pm \sqrt{4\kappa^4 + (k_l^2 - k_t^2/T_b)^2} \right]}. \quad (4.32)$$

In the low frequency region $\kappa \gg k_t$ and the solutions approach $\pm\kappa$ and $\pm i\kappa$ for decreasing frequencies. For high frequencies k_t and k_l are much larger than κ . The high frequency asymptotes are consequently $k_x = \pm k_l$ and $k_x = \pm k_l/\sqrt{T_b}$.

The bending of thin homogeneous and flat plates is discussed in Sect. 3.9. In deriving the wave equation governing the flexural vibration of plates the influence of shear and rotary inertia was neglected. Mindlin, Ref. [73], have included these effects for plates in flexure in a similar way as Timoshenko described the bending of thick beams. This is discussed in Sect. 9.6.

However, as an alternative to approximate methods, the general wave equation can be used to describe the bending of a thick infinite plate or a beam with negligible width. In the first case the starting point is the plate. For simplicity, it is assumed that the waves can only propagate in the x - y plane as shown in Fig. 4.3. The strain ε_z is consequently set equal to zero.

The deflections of the plate can be described by L- and T-waves. Due to these waves the horizontal surfaces—i.e., for $y = h/2$ and $y = -h/2$ appear to bend. This apparent bending wave propagates along the x -axis as described by the expression $\exp[i(\omega t - k_x x)]$ where k_x is the as yet unknown wavenumber for the “bending” waves. The wave equation governing the velocity potential ϕ describing the L-waves and the stream function or vector potential ψ describing the T-waves are defined in Eq. (4.8). The scalar potential is of the form

$$\phi(x, y, t) = \exp[i(\omega t - k_x x)] \cdot (A_1 \cdot e^{-i\lambda_1 y} + A_2 \cdot e^{i\lambda_1 y}). \quad (4.33)$$

A_1 is the amplitude of the wave propagating towards the upper boundary at $y = h/2$. A_2 is consequently the amplitude of the wave propagating towards the lower boundary at $y = -h/2$. The potential ϕ must satisfy the wave equation for longitudinal waves. Consequently

$$\lambda_1 = \sqrt{k_l^2 - k_x^2}, \quad (4.34)$$

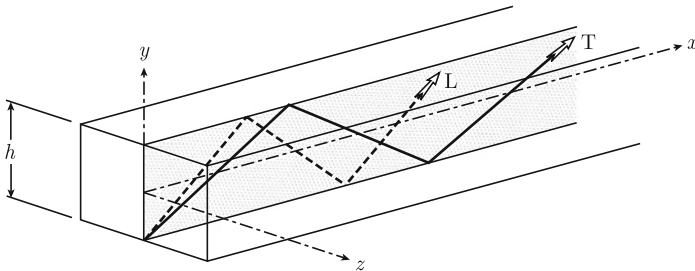


Fig. 4.3 L- and T-waves propagating in the x - y plane of a plate element

where as before k_l is the wavenumber for L-waves i.e.,

$$k_l^2 = \frac{\omega^2 \rho}{E} \frac{(1 + \nu)(1 - 2\nu)}{(1 - \nu)} = k_0^2 \frac{(1 + \nu)(1 - 2\nu)}{(1 - \nu)}. \quad (4.35)$$

The corresponding vector potential or rather its z -component, which describes the propagation of the T-waves in the x - y plane, is of the form:

$$\psi_z(x, y, t) = \exp[i(\omega t - k_x x)] \cdot (A_3 \cdot e^{-i\lambda_2 y} + A_4 \cdot e^{i\lambda_2 y}). \quad (4.36)$$

Again, the wave equation—this time for T-waves—must be satisfied. Thus:

$$\lambda_2 = \sqrt{k_t^2 - k_x^2},$$

where

$$k_t^2 = \frac{2(1 + \nu)\omega^2 \rho}{E} = k_0^2 \cdot 2(1 + \nu). \quad (4.37)$$

It can be expected that in the low frequency region and for thin plates the wavenumber k_x approaches the wavenumber for pure bending waves, defined in Sect. 3.7. Consequently it is assumed that

$$k_x \approx \kappa > k_l.$$

The parameter λ_1 is therefore imaginary in the low frequency range. In order to somewhat simplify the discussion the parameter α is introduced as

$$\alpha = i\lambda_1 = \sqrt{k_x^2 - k_t^2}. \quad (4.38)$$

The general solution (4.33) can now be rewritten as

$$\phi(x, y, t) = \exp[i(\omega t - k_x x)] \cdot [B_1 \cdot \sinh(\alpha y) + B_2 \cdot \cosh(\alpha y)]. \quad (4.39)$$

The corresponding vector potential or rather its z -component, which describes the propagation of the T-waves in the x - y plane, can in a similar way be written as

$$\psi_z(x, y, t) = \exp[i(\omega t - k_x x)] \cdot [C_1 \cdot \sinh(\beta y) + C_2 \cdot \cosh(\beta y)], \quad (4.40)$$

where

$$\beta = \sqrt{k_x^2 - k_t^2}.$$

The expression for ψ_z must satisfy the wave equation for the stream function, which governs the propagation of the transverse waves.

The displacements ξ and η along the positive x and y axes are for $\psi_x = \psi_y = 0$ according to Eq. (4.5) equal to

$$\xi = \frac{\partial \phi}{\partial x} + \frac{\partial \psi_z}{\partial y}, \quad \eta = \frac{\partial \phi}{\partial y} - \frac{\partial \psi_z}{\partial x}. \quad (4.41)$$

The subscript z for the stream function is henceforth omitted.

The general solutions (4.39) and (4.40) are composed of two solutions. One corresponds to the inphase and the other to the antiphase motion of the free surfaces of the plate. The inphase motion represents the bending of the plate. For bending, the displacements normal to the free surfaces, at $y = \pm h/2$, are the same. However, in the x -direction there is contraction at one surface and elongation at the other. Thus for the inphase motion corresponding to the bending mode

$$\xi_+(x, y, t) = -\xi_+(x, -y, t), \quad \eta_+(x, y, t) = \eta_+(x, -y, t). \quad (4.42)$$

The corresponding results for the antiphase motion are

$$\xi_-(x, y, t) = \xi_-(x, -y, t), \quad \eta_-(x, y, t) = -\eta_-(x, -y, t). \quad (4.43)$$

The expression (4.43) means that the surfaces of the plate are moving in opposite directions—equivalent to the displacement due to a quasi-longitudinal wave. The subscripts $+$ and $-$ in the Eqs. (4.42) and (4.43) identify the inphase and antiphase motions, respectively. The inphase and antiphase motions are shown in Fig. 4.4.

Based on the definition of the displacements, Eq. (4.42), the general solutions (4.39) and (4.40) can also be given by two functions, one representing the inphase and the other the antiphase motion. In the first case

$$\begin{aligned} \phi_+(x, y, t) &= \exp[i(\omega t - k_x x)] \cdot B_1 \cdot \sinh(\alpha y) \\ \psi_+(x, y, t) &= \exp[i(\omega t - k_x x)] \cdot C_2 \cdot \cosh(\beta y) \end{aligned} \quad (4.44)$$

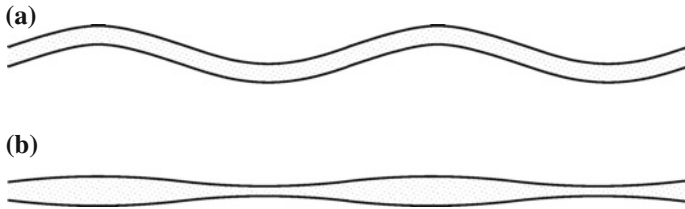


Fig. 4.4 The *top figure (a)* shows the inphase or bending motion of a plate. The *bottom figure (b)* shows the antiphase motion or longitudinal mode

For the antiphase motion the corresponding results are

$$\begin{aligned}\phi_{-}(x, y, t) &= \exp[i(\omega t - k_x x)] \cdot B_2 \cdot \cosh(\alpha y) \\ \psi_{-}(x, y, t) &= \exp[i(\omega t - k_x x)] \cdot C_1 \cdot \sinh(\beta y)\end{aligned}\quad (4.45)$$

For free boundaries and for $\varepsilon_z = 0$, then, according to Eq. (3.6), the normal stress σ_y is

$$\sigma_y = \frac{E}{(1 + \nu)} \left[\varepsilon_y + \frac{\nu}{(1 - 2\nu)} (\varepsilon_x + \varepsilon_y) \right] = 0 \quad \text{for } y = \pm h/2.$$

The shear stress τ_{yx} is from Eq. (3.11) equal to

$$\tau_{yx} = G \left(\frac{\partial \xi}{\partial y} + \frac{\partial \eta}{\partial x} \right) = 0 \quad \text{for } y = \pm h/2.$$

For $\varepsilon_x = \partial \xi / \partial x$ and ξ and η defined as in Eq. (4.5) and with $\psi_x = \psi_y = 0$, the boundary conditions for $y = \pm h/2$ yield

$$\begin{aligned}\sigma_y &= \frac{E}{(1 + \nu)(1 - 2\nu)} \left[\nu \frac{\partial^2 \phi}{\partial x^2} + (1 - \nu) \frac{\partial^2 \phi}{\partial y^2} - (1 - 2\nu) \frac{\partial^2 \psi}{\partial x \partial y} \right] = 0 \\ \tau_{yx} &= G \left(2 \frac{\partial^2 \phi}{\partial x \partial y} + \frac{\partial^2 \psi}{\partial y^2} - \frac{\partial^2 \psi}{\partial x^2} \right) = 0.\end{aligned}\quad (4.46)$$

The general solution (4.44) for the inphase motion in combination with Eq. (4.46) gives for $y = \pm h/2$

$$\begin{aligned}B_1 \sinh(\alpha h/2) [k_x^2 - k_0^2(1 + \nu)] + i k_x \beta C_2 \sinh(\beta h/2) &= 0 \\ -2i k_x \alpha B_1 \cosh(\alpha h/2) + 2C_2 \cosh(\beta h/2) [k_x^2 - k_0^2(1 + \nu)] &= 0\end{aligned}\quad (4.47)$$

The parameters B_1 and C_2 are readily eliminated from Eq. (4.47). The result is

$$\tanh(\alpha h/2) [k_x^2 - k_0^2(1 + \nu)]^2 = k_x^2 \alpha \beta \tanh(\beta h/2). \quad (4.48)$$

The dispersion Eq. (4.48) gives the wavenumber k_x for the inphase motion or bending mode for the plate. In a similar way the dispersion equation for the antiphase motion is obtained as

$$\tanh(\beta h/2) [k_x^2 - k_0^2(1 + \nu)]^2 = k_x^2 \alpha \beta \tanh(\alpha h/2). \quad (4.49)$$

One solution to Eq. (4.48) is $\alpha = 0$. However, returning to the basic Eqs. (4.44) and (4.47), it is evident that this solution only satisfies the basic equations if at the same time the amplitudes B_1 and C_2 are equal to zero. The solution $\alpha = 0$ is consequently without any physical meaning. The solution k_x to Eq. (4.48) should, as h decreases, approach the wavenumber κ previously derived for flexural waves

propagating in thin plates. For h small, the expression (4.48) can be expanded in a Taylor series. However, the expansion of a tanh function is converging slowly. It is therefore advantageous to rearrange Eq. (4.48) as

$$\begin{aligned} & \{\sinh[(\alpha + \beta)h/2] + \sinh[(\alpha - \beta)h/2]\} [k_x^2 - k_0^2(1 + \nu)]^2 \\ & = k_x^2 \alpha \beta \{\sinh[(\alpha + \beta)h/2] - \sinh[(\alpha - \beta)h/2]\} \end{aligned} \quad (4.50)$$

The sinh functions can now be expanded in Taylor series as

$$\sinh x = x + x^3/6 + x^5/120 + \dots$$

For thin plates i.e., for h small, a Taylor expansion of the sinh terms in Eq. (4.50), including the first two expansion terms only, gives

$$k_x^4 = k_0^2 \frac{12(1 - \nu^2)}{h^2} + 2k_x^2 k_0^2 (2 + \nu - \nu^2) + k_0^4 (1 + \nu)^2 (5 - 4\nu)/2. \quad (4.51)$$

The first term on the right-hand side of the equation becomes very large as h approaches zero. The limiting value is

$$\lim_{h \rightarrow 0} |k_x| = \left[\frac{12k_0^2(1 - \nu^2)}{h^2} \right]^{1/4} = \left[\frac{12\omega^2 \rho(1 - \nu^2)}{Eh^2} \right]^{1/4} = \kappa. \quad (4.52)$$

The solution to Eq. (4.51) is thus $k_x = \pm \kappa$ and $k_x = \pm i\kappa$ as the thickness of the plate approaches zero. This is the same result or wavenumber as previously derived in Chap. 3 for flexural waves propagating on thin infinite plates. The result (4.51) can also be used to estimate the deviation between k_x and κ as the plate thickness h is increased. For an error in κ of less than 10%, or a 46% error in κ^4 , the second term in Eq. (4.51) should satisfy the inequality

$$2k_x^2 k_0^2 (2 + \nu - \nu^2) < 0.46 \cdot k_0^2 (1 - \nu^2) 12/h^2.$$

Setting Poisson's ratio equal to 0.3 this inequality is approximately given by $k_x h \approx \kappa h < 1$. A plate of thickness h can be considered as "thin" as long as h and the wavenumber κ predicted according to the Kirchhoff theory satisfy the inequality

$$\kappa h < 1. \quad (4.53)$$

The error in κ is less than 10% when the condition (4.53) is satisfied. The inequality (4.53) also holds for bending waves in beams satisfying Eq. (3.77). The same limit is usually derived from Timoshenko's approximate formula. This is for example shown in Ref. [31]. The criterion (4.53) is the standard definition of a "thin" plate or beam.

In Table 4.1 below the maximum thickness h_{\max} satisfying the inequality (4.53) is given as function of frequency for three materials.

Table 4.1 Maximum thickness for “thin” plates

f (Hz)	h_{\max} (mm)					
	500	1000	2000	4000	8000	16000
Steel	477	238	119	60	30	15
Aluminum	474	237	119	59	30	15
Concrete	314	157	78	39	20	10

Showing that plates can be treated as thin for typical aircraft and car structures in the entire audible frequency range. In ships, the hull and deck plating is usually less than 18 mm. There are exceptions, for example submarines and ships built for arctic waters. The plate thickness of engine foundations on ships can however be of the order 40 mm. A standard thickness of concrete floors in buildings is 180 mm.

Based on the expressions (4.44) and (4.47) the potentials ϕ and ψ can be described everywhere in the interior of the plate. This means that the normal and shear stresses and displacements can also be determined as functions of the coordinates x and y . The expressions given in Eq. (4.41) define the displacements ξ and η . The normal stress σ_x is defined in (3.6). Thus for $\varepsilon_z = 0$

$$\sigma_x = \frac{E}{(1 + \nu)(1 - 2\nu)} \left[(1 - \nu) \frac{\partial^2 \phi}{\partial x^2} + \nu \frac{\partial^2 \phi}{\partial y^2} - (1 - 2\nu) \frac{\partial^2 \psi}{\partial x \partial y} \right]. \quad (4.54)$$

The shear stress τ_{yx} is based on Eq. (3.11) obtained as

$$\tau_{yx} = G \left[2 \frac{\partial^2 \phi}{\partial x \partial y} + \frac{\partial^2 \psi}{\partial y^2} - \frac{\partial^2 \psi}{\partial x^2} \right] = 0. \quad (4.55)$$

For thin plates the stresses and displacements are functions of the coordinate y or rather the distance to the neutral axis of the plate. For a thin plate oriented in the x - z plane with the boundaries at $y = \pm h/2$, a plane flexural wave propagating along the x -axis will induce the following displacements and stresses

$$\eta = w(x, t), \quad \xi = -y \frac{\partial w}{\partial x}, \quad \sigma_y = 0$$

$$\tau_{xy} = - \left(\frac{h^2}{4} - y^2 \right) \frac{E}{2(1 - \nu^2)} \frac{\partial^3 w}{\partial x^3}, \quad \sigma_x = -y \frac{E}{(1 - \nu^2)} \frac{\partial^2 w}{\partial x^2}. \quad (4.56)$$

The details are left for Problem 4.8. The displacements and stresses presented in Eq. (4.56) are valid as long as $\kappa h < 1$ for a plate under flexure. The normal stress σ_x given in Eq. (4.56) forms the basis for the derivation of the bending wave equation for thin beams and plates as discussed in Chap. 3. For a beam, the quantity $E/(1 - \nu^2)$ is replaced by E in Eq. (4.56). The general assumptions made in Sect. 3.9 concerning

the bending of thin plates are thus verified by means of the results (4.56) derived from the generalized wave equation. It can be concluded that the bending of plates is described completely by means of longitudinal and transverse waves.

The bending M'_z per unit width of the plate and the force T'_y per unit width are obtained as

$$M'_z = \int_{-h/2}^{h/2} \sigma_x y dy, \quad T'_y = \int_{-h/2}^{h/2} \tau_{xy} dy,$$

where σ_x and τ_{xy} are defined in the Eqs. (4.54) and (4.55). For a thin plate the normal and shear stresses can be approximated by the expressions given by Eq. (4.56) resulting in

$$M'_z = -\frac{Eh^3}{12(1-\nu^2)} \frac{\partial^2 w}{\partial x^2}, \quad T'_y = -\frac{Eh^3}{12(1-\nu^2)} \frac{\partial^3 w}{\partial x^3}.$$

In deriving these expressions, it is assumed that the “bending” wave only propagates in the x -direction. A more general case is discussed in Sect. 3.9, compare Eqs. (3.105) and (3.113) while remembering the different orientations of the coordinate systems for the two cases. The forces and bending moments derived for thin plates and beams are again obtained from the general wave equation as long as $\kappa h < 1$.

The lateral vibrations of a so-called Timoshenko beam were discussed earlier in this section. The Timoshenko constant T_b introduced in the equation of motion for the beam is defined as the ratio between the average shear stress over the cross section of the structure and the shear stress at the neutral axis. According to Eq. (4.56) the average shear stress for the plate is

$$\begin{aligned} \bar{\tau}_{xy} &= \frac{1}{h} \int_{-h/2}^{h/2} dy \tau_{xy} = -\frac{1}{h} \int_{-h/2}^{h/2} dy \left(\frac{h^2}{4} - y^2 \right) \frac{E}{2(1-\nu^2)} \frac{\partial^3 w}{\partial x^3} \\ &= -\frac{Eh^2}{12(1-\nu^2)} \frac{\partial^3 w}{\partial x^3} \end{aligned}$$

The shear stress along the neutral axis, $y = 0$, is

$$\tau_{xy}(0) = -\frac{Eh^2}{8(1-\nu^2)} \frac{\partial^3 w}{\partial x^3}.$$

The Timoshenko constant T_b for a homogeneous plate with a constant cross section is obtained as

$$T_b = \frac{\bar{\tau}_{xy}}{\tau_{xy}(0)} = \frac{2}{3}.$$

This result is also used for homogeneous beams with rectangular cross sections.

The shear stress in a plate under flexure has, as shown in Eq. (4.56), a maximum at the center line of the plate. At the boundaries, $y = \pm h/2$ the shear stress is equal to zero as required. The displacement normal to center plane of the plate is, as a

first approximation for thin plates, constant over the cross section of the plate. The intensity traveling in the x -direction of the plate is for $\zeta = 0$ given by Eq. (3.18) as

$$I_x = -\sigma_x \dot{\xi} - \tau_{xy} \dot{\eta}.$$

The results of Eq. (4.56) inserted in this expression yields

$$I_x = - \left[\frac{E}{1 - \nu^2} \right] \left[y^2 \frac{\partial^2 w}{\partial x^2} \cdot \frac{\partial^2 w}{\partial x \partial t} - \frac{1}{2} \left(\frac{h^2}{4} - y^2 \right) \frac{\partial^3 w}{\partial x^3} \frac{\partial w}{\partial t} \right].$$

The intensity due to shear, the second term in the expression above, is, as the shear stress, equal to zero at the surfaces of the plate, i.e., for $y = \pm h/2$. The intensity in the x -direction caused by shear is in fact proportional to $(h/2)^2 - y^2$. Revealing that the intensity, defined in Eq. (3.18), which is caused by shear, has a maximum along the neutral axis, $y = 0$, in the plate. The intensity induced by longitudinal waves, the first term in the expression, has maxima at $y = \pm h/2$ and is proportional to y^2 . This is shown in Problem 4.7. The energy flow Π'_x per unit width of the plate is given by

$$\Pi'_x = \int_{-h/2}^{h/2} I_x dy = -D \left(\frac{\partial^2 w}{\partial x^2} \frac{\partial^2 w}{\partial x \partial t} - \frac{\partial^3 w}{\partial x^3} \frac{\partial w}{\partial t} \right).$$

This energy flow is due to “bending” only and is equal to the result of Eq. (3.138). The first term of Eq. (3.137) is induced by longitudinal waves only.

The dispersion relation (4.48) can also be used to estimate the wavenumber as the plate thickness is increased. For α and β real and positive, the tanh functions in Eqs. (4.48) and (4.49) tend to be unity as the plate thickness goes to infinity. At the limit the wavenumber k_x for the inphase and antiphase motion of the plate must satisfy the dispersion equation

$$[k_x^2 - k_0^2(1 + \nu)]^2 = k_x^2 \alpha \beta.$$

This is an equation of the third order in k_x^2 . Only one solution satisfies the prerequisites on α and β , i.e., α and β should be real. For a propagating wave the limiting wavenumber for plates with infinite thickness can be written as

$$k_x = k_r = X_r \omega \sqrt{\frac{\rho}{E}} = X_r k_0. \quad (4.57)$$

The parameter X_r is a function only of Poisson's ratio. The resulting wave type is referred to as a Rayleigh wave, discussed in more detail in Sect. 4.6. The parameter X_r and the speed of sound c_r as compared to the wave velocity c_t for transverse waves are given as function of ν in Table 4.2.

Based on the discussion above, it can be expected that the wavenumber for the bending mode for decreasing frequencies approaches the wavenumber derived for

Table 4.2 The parameter X_r from Eq. (4.57) and the ratio between the speed of sound c_r for Rayleigh and c_t for transverse waves

ν	0.00	0.05	0.10	0.15	0.20	0.25	0.30	0.35	0.40	0.45	0.50
X_r	1.62	1.64	1.66	1.68	1.70	1.72	1.74	1.76	1.78	1.79	1.81
c_r/c_t	0.87	0.88	0.89	0.90	0.91	0.92	0.93	0.94	0.94	0.95	0.96

thin plates. In the very high frequency region—for h large—the asymptotic value $X_r k_0$ for Rayleigh waves should be reached.

As an example, the wavenumber k_x for the first inphase propagating bending mode is shown in Fig. 4.5 as function of frequency. The structure is a 400 mm thick concrete plate with an E -modulus of 3×10^{10} Pa and a density of 2300 kg/m^3 . Poisson’s ratio is 0.15. For comparison the wavenumbers k_f , k_l , k_t , and k_r for flexural (Kirchhoff theory), longitudinal (thin plate), transverse, and Rayleigh waves are also shown in the figure. It is evident that the wavenumber k_x , calculated from Eq. (4.48), starts to deviate from the thin plate approximation k_f in the low frequency range. For high frequencies k_x coincides asymptotically with the wavenumber k_r , which is valid for infinitely thick plates. At the limit, the wavelength is small compared to the plate thickness.

The wavenumbers for traveling bending waves are illustrated in Fig. 4.6 for concrete plates with varying thickness. In the high frequency limit, all the wavenumbers approach the wavenumber for Rayleigh waves. The wavenumbers are obtained from Eq. (4.48). In Fig. 4.6 only the wavenumbers for the first propagating mode are shown. There is an infinite number of solutions to Eq. (4.48). In the low frequency region there are only two solutions defining propagating waves. These solutions have the same absolute value but opposite signs and correspond to the first propagating mode. These wavenumbers or solutions represent plane waves propagating along the positive and negative x -axes. Other solutions to Eq. (4.48) are imaginary, representing near field solutions. For increasing frequencies, a second solution defining

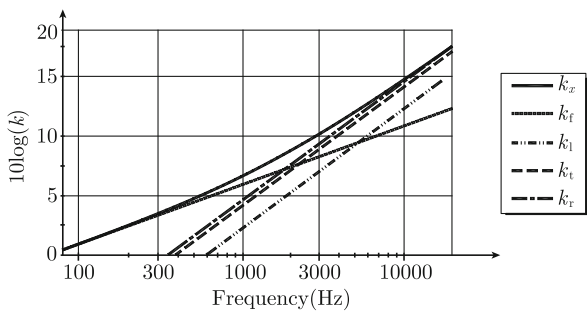


Fig. 4.5 Wavenumbers $k(\text{m}^{-1})$ for some wave types propagating in a 400 mm thick concrete plate. k_x -first propagating bending wave, general wave equation; k_f -bending waves, simple theory; k_l -longitudinal waves, simple theory; k_t - transverse waves; k_r -Rayleigh waves

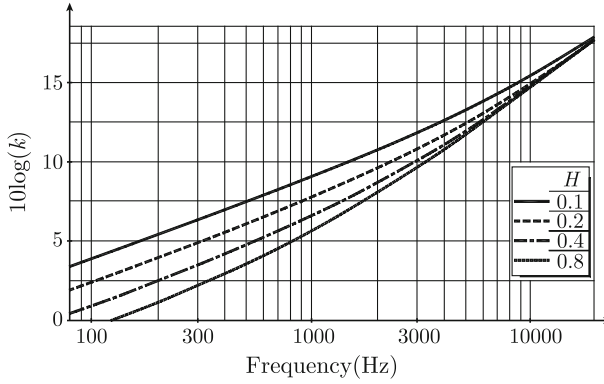


Fig. 4.6 Wavenumbers $k(\text{m}^{-1})$ for bending waves propagating in a concrete plate of thickness $H(\text{m})$. k_x -first propagating bending wave, general wave equation. Results obtained from general wave equation

propagating waves is obtained. The resulting wavenumbers correspond to the second propagating mode. The number of solutions describing propagating waves increases with increasing frequency.

The phase and group velocities for bending waves are defined in Eqs. (3.80) and (3.81). For an infinite plate, the wavenumber k_x for the bending mode of the plate is given by Eq. (4.48). The phase velocity, $c_b = \omega/k_x$, and the group velocity, $c_g = \partial\omega/\partial k_x$, are shown in Fig. 4.7 for a 400 mm thick concrete plate, the same as used in the example illustrated in Fig. 4.5. The phase velocities c_l , c_t , c_f , and c_r for longitudinal, transverse, flexural (Kirchhoff theory), and Rayleigh waves are also shown in Fig. 4.7. In the low frequency region, the group velocity is equal to twice the phase velocity as predicted from the Kirchhoff theory. For increasing frequencies,

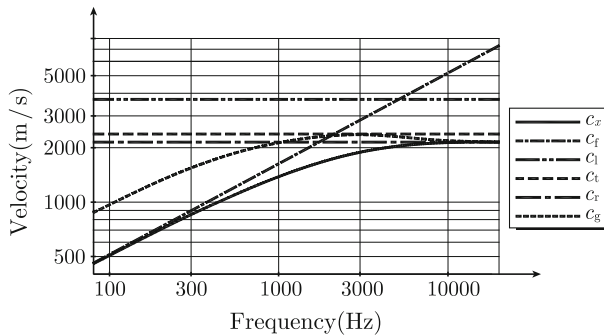


Fig. 4.7 Phase and group velocity of bending waves, first propagating mode, in a 400 mm thick concrete plate. c_x and c_g phase and group velocities from general wave equation. The phase velocities c_l , c_t , c_f , and c_r for longitudinal, transverse, flexural (Kirchhoff theory), and Rayleigh waves are also shown

both the group and phase velocities are converging towards the velocity of Rayleigh waves. Thus, as previously pointed out, the phase and group velocities for bending waves are finite and equal in the high frequency limit.

The ratio η/ξ , between the deflections normal and parallel to the free surface of a plate under flexure, can be calculated based on the expressions (4.44) and (4.47). In Fig. 4.8 the velocity level difference $\Delta L_v = 20 \log |\dot{\eta}/\dot{\xi}|$ is calculated for a 100 mm thick concrete plate. In the low frequency region the ratio between the deflections is given by

$$|\eta/\xi| = 2/(\kappa h), \quad (4.58)$$

where κ is the wavenumber for pure bending. This has a practical implication when the normal velocity of a thick plate is measured by means of accelerometers. The reason is that a typical accelerometer has a certain sensitivity to displacements perpendicular to its axis. In the low frequency region, this is not a problem, since the ratio between the accelerations in the normal and in plane directions is very large. However, for thick plates and high frequencies this effect should be considered.

The discussion above was devoted to the apparent bending of infinite plates. A similar discussion can be carried out for the other limiting and idealized case—the bending of a thick beam with a negligible width. In doing so, some of the basic equations, which are valid for the plate, have to be modified. To start with, let the beam be extended along the x -axis in a Cartesian coordinate system. The height of the beam is h . The upper and lower boundaries for the beam are at $y = \pm h/2$ in the same way as for the plate shown in Fig. 4.3. The width of the beam is assumed to be small. This leads to the assumption that $\sigma_z = 0$. The wavenumber k_l for longitudinal waves propagating in the beam or rather the plate segment is now

$$k_l^2 = \frac{\omega^2 \rho (1 - \nu^2)}{E} = k_0^2 (1 - \nu^2).$$

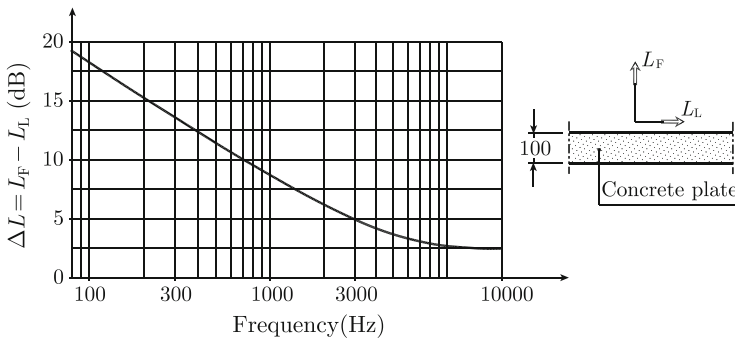


Fig. 4.8 Velocity level difference L_v (dB) between flexural and longitudinal waves at the surface of a 100 mm thick concrete plate

Equation (4.35) gives the corresponding wavenumber, which is valid for infinite plate as previously discussed.

The normal stresses σ_x and σ_y are for $\sigma_z = 0$ obtained from Eqs. (3.6) and (4.41) as

$$\sigma_x = \frac{E}{1 - \nu^2} \left[\frac{\partial^2 \phi}{\partial x^2} + \nu \frac{\partial^2 \phi}{\partial y^2} - (1 - \nu) \frac{\partial^2 \psi}{\partial x \partial y} \right]$$

$$\sigma_y = \frac{E}{1 - \nu^2} \left[\nu \frac{\partial^2 \phi}{\partial x^2} + \frac{\partial^2 \phi}{\partial y^2} - (1 - \nu) \frac{\partial^2 \psi}{\partial x \partial y} \right].$$

The shear stresses τ_{yx} and τ_{xy} are as before given by Eq. (3.11). The wavenumber for the bending of a thick beam with a negligible width can now be derived following the same procedure as for the plate.

4.5 Quasi-Longitudinal Waves in Thick Plates

The antiphase motion of a plate, as illustrated in Fig. 4.4, is caused by the propagation of a quasi-longitudinal wave in the plate. The dispersion equation defining the wavenumbers for this type of displacement is given in Eq. (4.49). The approximate wavenumber for the first propagating mode is obtained from the dispersion equation by means of a Taylor expansion of the sinh functions. The procedure is the same as discussed in connection with the derivation of Eq. (4.51). Neglecting terms of the second and higher orders, the resulting wavenumber k_x for the quasi-longitudinal wave is obtained as

$$k_x^2 = k_0^2(1 - \nu^2) + \nu^2 h^2 k_0^2(1 + \nu)^2/12 + \dots \quad (4.59)$$

Including the first two terms only, the wavenumber can be written as

$$k_x = k_l \sqrt{1 + \frac{(\nu h k_l)^2}{12(1 - \nu^2)}}, \quad (4.60)$$

where

$$k_l = k_0 \sqrt{1 - \nu^2}.$$

The wavenumber is, as for bending waves, a function of the plate thickness and frequency. For $h \rightarrow 0$, $k_x \rightarrow k_0 \sqrt{1 - \nu^2}$, which is the wavenumber for quasi-longitudinal waves propagating in a thin plate. As the thickness h of the plate increases the second and higher order terms can no longer be neglected. For an error in k_l of less than 10% the wavenumber k_l and plate thickness h should satisfy the inequality

$$\nu h k_l < 1.6. \quad (4.61)$$

A plate can be considered as “thin” with respect to the propagation of longitudinal waves as long as this condition is satisfied.

The result (4.60) can be interpreted by identifying the apparent density ρ_a of the plate as

$$\rho_a = \rho \left[1 + \frac{(\nu h k_l)^2}{12(1 - \nu^2)} \right]. \quad (4.62)$$

The apparent density is thus a function of plate thickness and frequency. The ratio ρ_a/ρ is larger than unity indicating that the displacement is not only in the direction of the main axis but also perpendicular to this. The two-dimensional motion increases the inertia and thus the apparent mass if only the one-dimensional motion is considered. The wavenumber k_l for quasi-longitudinal waves propagating in a plate can as a first approximation be written as

$$k_l = \omega \sqrt{\frac{\rho_a(1 - \nu^2)}{E}}. \quad (4.63)$$

The result shown in Eq. (4.62) can be obtained in a more straightforward way as formulated by first Rayleigh and later by Love. A quasi-longitudinal wave propagating in a plate deforms the plate parallel and perpendicular to the main axis of the plate. This effect was discussed in Chap. 3 and illustrated in Fig. 3.11. For an L-wave, propagating in a plate oriented in x - y plane it is assumed that $\varepsilon_y = \sigma_z = 0$ as discussed in Sect. 3.1. The strain ε_z is obtained from Eq. (3.5) as

$$\varepsilon_z = -\frac{\nu}{1 - \nu} \cdot \varepsilon_x.$$

For $\varepsilon_z = \partial\zeta/\partial z$ and $\varepsilon_x = \partial\xi/\partial x$, the displacement ζ is

$$\zeta = \int dz \varepsilon_z = - \int dz \frac{\nu}{1 - \nu} \frac{\partial\xi}{\partial x} = -z \frac{\nu}{1 - \nu} \frac{\partial\xi}{\partial x}. \quad (4.64)$$

For an L-wave propagating in a plate, wavenumber $k_l = k_0\sqrt{1 - \nu^2}$, along the positive x -axis, the displacement ξ can be defined as $\xi = A \exp[i(\omega t - k_l x)]$. The resulting strain is consequently

$$\varepsilon_x = \frac{\partial\xi}{\partial x} = -ik_l \xi.$$

The kinetic energy per unit area of the plate is

$$\bar{T}_s = \frac{1}{4} \int_{-h/2}^{h/2} dz \rho \left[|\dot{\xi}|^2 + |\dot{\zeta}|^2 \right]. \quad (4.65)$$

The particle velocity $\dot{\xi}$ in the z -direction is obtained from Eq. (4.64). The kinetic energy induced in the plate is consequently equal to

$$\bar{T}_s = \frac{h\rho}{4} |\dot{\xi}|^2 \left[1 + \frac{(\nu h k_l)^2}{12(1 - \nu^2)} \right] = \frac{h\rho_a}{4} |\dot{\xi}|^2, \quad (4.66)$$

where

$$\rho_a = \rho \left[1 + \frac{(\nu h k_l)^2}{12(1 - \nu^2)} \right].$$

The apparent density ρ_a obtained in this way is identical to the expression (4.62) derived by a Taylor expansion of the exact result and neglecting higher order terms.

In the previous section it was found that the wavenumber for the first propagating bending wave mode in thick plates has low and high frequency asymptotes. The first asymptote is given by the “thin plate” approximation. The high frequency limit is defined by the wavenumber for Rayleigh waves. In a similar way, there are two asymptotes for L-waves propagating in thick plates. The low frequency asymptote is given by the “thin plate” approximation defining the wavenumber as $k_l = \omega \sqrt{\rho(1 - \nu^2)/E}$. The high frequency asymptote is obtained from Eq. (4.49). For high frequencies, short wavelengths or large plate thicknesses, the Eqs. (4.48) and (4.49) are identical. In both cases the tanh functions approach unity as the products αh and βh increase to infinity. In the limit, as thickness or frequency approaches infinity, the Eqs. (4.48) and (4.49) are identical. The high frequency asymptote is in both cases given by the wavenumber k_r for Rayleigh waves.

Exact wavenumbers, calculated from Eq. (4.49), for the first propagating longitudinal mode in a 400 mm thick concrete slab is shown in Fig. 4.9. The wavenumber calculated according to Eq. (4.63), Rayleigh correction, as well as the low and high frequency asymptotes are shown in the graph. The agreement between the exact and the approximate solutions is rather poor in the high frequency range. For high frequencies the wavenumber predicted according to Love/Rayleigh is even increas-

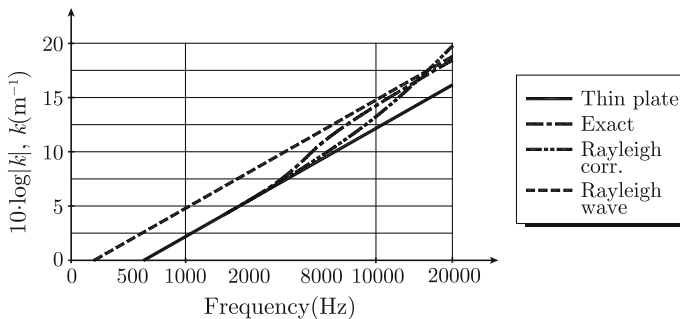


Fig. 4.9 Wavenumber for L-waves propagating in a 400 mm thick concrete slab. The figure shows the exact and approximate results as well as high and low frequency asymptotes

ing with frequency f as f^2 whereas the exact solution is increasing as f in the very high frequency region. Despite this, the Rayleigh or Love approximation is frequently used for the determination of the propagation of longitudinal waves in resilient mounts as discussed in Chap. 10. Except for this very important application, it is hardly ever necessary to correct the wavenumbers for L-waves with respect to plate thickness.

4.6 Rayleigh Waves

In the preceding section, it was shown that when the thickness of a plate is increased to infinity then the deflection of the plate is determined by surface or Rayleigh waves. A more general description of this wave type is achieved by starting from Eq. (4.44). This expression defines the inphase motion of a plate with thickness h . For simplicity let the upper surface of the plate in Fig. 4.3 be shifted to $y = 0$ through the transformation

$$y_1 \rightarrow y - h/2.$$

After this coordinate transformation and for h large, the expressions in Eq. (4.44) become

$$\begin{aligned}\phi_+(x, y, t) &= \exp[i(\omega t - k_x x)] \cdot B_1 \cdot \exp[\alpha(y_1 + h/2)]/2 \\ \psi_+(x, y, t) &= \exp[i(\omega t - k_x x)] \cdot C_2 \cdot \exp[\beta(y_1 + h/2)]/2 \\ k_x &= k_r.\end{aligned}\quad (4.67)$$

The approximation $\sinh x \approx \cosh x \approx \exp x/2$, which is valid for x large, has been used to obtain Eq. (4.67). The wavenumber k_r for Rayleigh waves is given in Eq. (4.57). At the free surface σ_y and τ_{xy} must be equal to zero. These boundary conditions lead to the expressions given in Eq. (4.46) that must be equal to zero for $y_1 = 0$. These boundary conditions give the results presented in Eq. (4.47). The last expression in Eq. (4.47) can, after replacing the sinh and cosh functions by an exponential function as discussed above, be written as

$$C_2/B_1 = i \cdot \exp[h(\alpha - \beta)/2][k_r^2 - k_0^2(1 + \nu)]/(k_r\beta).$$

Neglecting the subscript of y , this expression and Eq. (4.67) yield for $y = 0$

$$\begin{aligned}\phi_+(x, y, t) &= \Gamma \cdot e^{\alpha y} \exp[i(\omega t - k_r x)], \\ \psi_+(x, y, t) &= i\Gamma e^{\beta y} \exp[i(\omega t - k_r x)] \cdot [k_r^2 - k_0^2(1 + \nu)]/(k_r\beta) \\ \beta &= \sqrt{k_r^2 - k_t^2}, \quad \alpha = \sqrt{k_r^2 - k_l^2}, \quad \Gamma = B_1 e^{h\alpha/2}/2.\end{aligned}\quad (4.68)$$

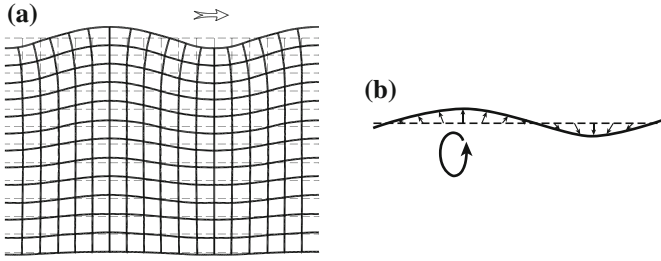


Fig. 4.10 Deformation due to Rayleigh waves in a semi-infinite structure

The deflections ξ and η in the solid are obtained from Eq. (4.41). The velocity potential and the stream function defined in Eq. (4.68) decay exponentially as the distance from the surface increases. The function α is larger than β . Indicating that the influence of the longitudinal waves decays faster than the effect of the transverse waves. The deformation, due to a propagating Rayleigh wave in a semi-infinite solid, is shown in Fig. 4.10. At the surface, the ratio between the relative displacements perpendicular and parallel to the surface is

$$\left| \frac{\eta}{\xi} \right| = \frac{k_r^2 - k_0^2(1 + \nu)}{k_r \sqrt{k_r^2 - 2k_0^2(1 + \nu)}}. \quad (4.69)$$

For $\nu = 0.3$ this ratio is 1.52 and for $\nu = 0.15$ the corresponding value is 1.38. The last value or rather $20\log(1.38)$ gives the asymptotic level in Fig. 4.8 in the high frequency region for the concrete plate. The reason is that a plate of finite thickness in the high frequency range and for short wave lengths seems to be of infinite thickness.

4.7 Sandwich Plates-General

In Sect. 4.4, it was pointed out that, in general, plates can be considered as thin with the notable exception of concrete constructions in buildings. However, for composite structures like sandwich constructions, the thin plate theory can no longer be applied. The term “sandwich construction” here refers to a structure in the form of a lightweight core with thin laminates bonded to each side of the core as shown in Fig. 4.11. This type of structure combines a low weight with a high strength. With respect to material and building costs, sandwich constructions can compare very favorably with other lightweight materials like aluminum.

The number of applications for sandwich panels is steadily increasing. One reason for the growing interest is that today it is possible to manufacture high-quality laminates for many applications. The materials used in the laminates are often made of carbon fiber or glass-reinforced plastic, abbreviated GRP. The composition of a

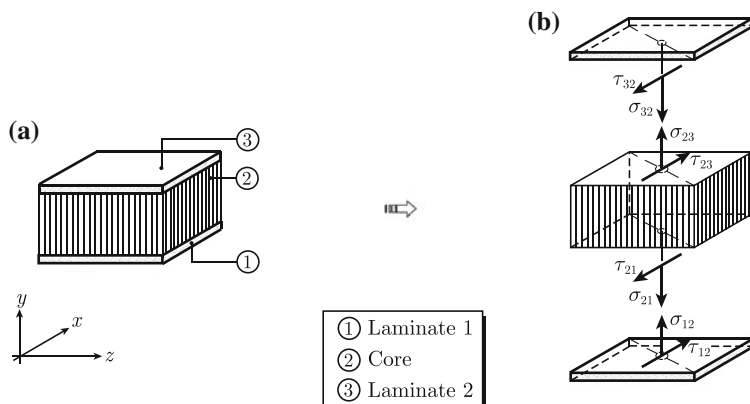


Fig. 4.11 Sandwich element and resulting stress components

laminate and thus its material parameters can be varied considerably in the manufacturing process. Various types of core materials are commercially available. The technique of bonding core materials and laminates as well as different plate structures is well understood, although still developing.

In the shipbuilding industry in particular, the use of sandwich materials is well established. Small and very fast passenger vessels have for many years been built in sandwich materials. For these vessels, weight and strength are of vital importance. For navy vessels, and especially for minesweepers, GRP sandwich constructions offer some additional advantages. Sandwich plates and similar elements are also used for the construction of railroad cars and sections of aircraft.

In the building industry special types of sandwich plates have been introduced. These plates can, for example, consist of a lightweight core bonded to plates of lightweight concrete. It is often stated that sandwich elements compare favorably to some traditional construction materials with respect to cost, weight, strength, and thermal insulation. However, for certain types of sandwich plates the acoustic properties can be very poor. The lack of acoustic qualities can severely restrict the use of sandwich elements.

A GRP laminate is built up of a number of layers: consequently, its dynamical properties can be very complex. A number of papers and textbooks on applications, measurements, and theories concerning laminated plates have been published: Refs. [32–35] are just a few examples. The finite element method is widely used for the prediction of the non-linear response of orthotropic laminated plates (see Refs. [36–38]). However, for many applications the laminates are constructed in such a way that they, as a first approximation, can be considered as isotropic. The amplitude of a plate excited by an extended force or an acoustical field is so small in the audio frequency range that any major non-linear effects can, in general, be neglected.

The core in a sandwich construction can be described as a thick plate. In Sect. 4.4, the shear and rotation effects in this type of plate were described. The wave fields in a thick plate can be derived as functions of the boundary conditions at each side of the plate. Consequently, the coupled motion of several plates joined together can be described if the boundary conditions at the junction between two plates are considered.

The laminates in sandwich panels frequently used in, for example, the shipbuilding industry are comparatively thin, of the order 3-6 mm. The laminates can therefore be treated as thin plates according to classical theory in the frequency range up to 16 kHz. Below this frequency limit, the description of the coupled motion between laminates and core can be simplified, as compared to the general method described in Ref. [39]. This simplified approach is pursued in what follows for symmetric and asymmetric three-layered sandwich plates.

4.8 Bending of Sandwich Plates

In order to determine the response of a sandwich plate excited by an acoustic field or any force acting perpendicular to the plate the wavenumbers in the structure must be known. In particular, this applies to the waves, which basically determine the lateral motion or apparent bending of a plate.

In the low frequency limit, the wavenumber is equal to

$$\kappa_b = \left(\frac{\mu \omega^2}{D_0} \right)^{1/4}. \quad (4.70)$$

In this expression μ is the total mass per unit area and D_0 the bending stiffness of the plate. The suffix b to the wavenumber denotes that only bending is considered.

The bending stiffness D_0 of a structure shown in Fig. 4.11 is in the low frequency limit given by

$$D_0 = \int_0^{y_3} E(y)(y - y_0)^2 dy. \quad (4.71)$$

The coordinate y_0 defines the neutral axis and is according to standard procedure obtained from

$$\int_0^{y_3} E(y)(y - y_0) dy = 0. \quad (4.72)$$

$E(y)$ is equal to the apparent modulus of elasticity of the various plate elements or layers in the construction. For increasing frequencies the apparent bending stiffness decreases as discussed below.

4.9 Equations Governing Bending of Sandwich Plates

The geometry of the type of sandwich panel considered here is shown in Fig. 4.11. In general, the construction is symmetric with respect to the center line. The thickness of the lightweight core is typically of the order 10–75 mm. In general, the thickness of the laminate could vary between 1 and 8 mm. The E-modulus for a laminate is high and much higher than the corresponding modulus for the core. Each laminate is built up of a number of layers. The reinforcing fibers in these layers are oriented in such a way that the strength of the plate, at least as a first approximation, is independent of direction in the plane of the panel. The laminates are therefore assumed to be isotropic. Within the frequency range of interest i.e., below 16 kHz, the deflection of the laminates can be described by means of the theory for thin plates.

According to Eq. (4.53) a plate can be treated as thin as long as the wavelength for pure bending waves in the structure is larger than six times the thickness of the plate. For the lateral motion or the bending of the entire sandwich construction, it is assumed that the displacement of a laminate is determined by flexural and longitudinal waves.

For the rather thick core, the displacements must be described by means of the general wave equation. Thus bending, rotation and shear as well as longitudinal deflection should be included in the model for the core. The entire deflection of the core can be described, by means of a combination of longitudinal and shear waves. The core materials discussed below can be considered as being isotropic.

For laminate 1 in the structure shown in Fig. 4.11, the displacements in the directions of the x - and y -axes are given by ξ_1 and η_1 , respectively. The governing equations for bending and longitudinal deflection can be written as

$$\frac{\partial^4 \eta_1}{\partial x^4} - \kappa_1^4 \eta_1 = \left(\frac{\sigma_{21}}{D_1} \right)_{y=0} \quad (4.73)$$

$$\frac{\partial^2 \xi_1}{\partial x^2} + k_{l1}^2 \xi_1 = - \left[\frac{\tau_{21}(1 - \nu_1^2)}{t_1 E_1} \right]_{y=0}. \quad (4.74)$$

The time dependence of $\exp(i\omega t)$ has been omitted throughout. In the equations thickness, density, Poisson's ratio, and Young's modulus are denoted by t_1 , ρ_1 , ν_1 and E_1 , respectively. The stress components τ_{21} and σ_{21} are indicated in Fig. 4.11. In Eqs. (4.73) and (4.74) the following notations are introduced for bending and longitudinal wavenumbers and bending stiffness

$$\kappa_1 = \left(\frac{\mu_1 \omega^2}{D_1} \right)^{1/4}, \quad E'_1 = \frac{E_1}{1 - \nu_1^2}, \quad D_1 = \frac{E'_1 t_1^3}{12}, \quad k_{l1} = \omega \sqrt{\frac{\rho_1}{E'_1}}.$$

The mass per unit area of the laminate 1 is μ_1 .

In Eqs. (4.73) and (4.74) the laminate is assumed to be thin compared to the core. The neutral axis of laminate 1 is now given by $y = 0$. An exact description according

to Fig.4.11 should mean that the neutral axis is located at $y = t_1/2$. The interface between laminate and core should be at $y = t_1$. This discrepancy can to a certain degree be compensated, by setting the core thickness equal to $h + (t_1 + t_3)/2$. In this way, the core thickness in any prediction model is defined as the distance between the neutral axes of the laminates.

For laminate 3 the corresponding wave equations are

$$\frac{\partial^4 \eta_3}{\partial x^4} - \kappa_3^4 \eta_3 = - \left(\frac{\sigma_{23}}{D_3} \right)_{y=h} \quad (4.75)$$

$$\frac{\partial^2 \xi_3}{\partial x^2} + k_{I3}^2 \xi_3 = \left[\frac{\tau_{23}(1 - \nu_3^2)}{t_3 E_3} \right]_{y=h}. \quad (4.76)$$

Wavenumber, etc., for plate 3 are defined in a similar way as for laminate 1.

The normal and the shear stresses in the core can be written as

$$\sigma_y = \sigma_{21} = \sigma_{23} = \frac{E_2(1 - \nu_2)}{(1 + \nu_2)(1 - 2\nu_2)} \left(\frac{\partial \eta_2}{\partial y} + \frac{\nu_2}{1 - \nu_2} \frac{\partial \xi_2}{\partial x} \right) \quad (4.77)$$

$$\tau_{yx} = \tau_{21} = \tau_{23} = \frac{E_2}{2(1 + \nu_2)} \left(\frac{\partial \xi_2}{\partial y} + \frac{\partial \eta_2}{\partial x} \right). \quad (4.78)$$

The displacements ξ and η along the two main axes are determined by transverse and longitudinal waves propagating in the core. These wave types are expressed as functions of a scalar function ϕ and a velocity potential ψ_z as discussed in Sect.4.4. The subscript z is omitted in the text below. Consequently the displacements 2 along the x - and y -axes can be written as

$$\xi_2 = \frac{\partial \phi}{\partial x} + \frac{\partial \psi}{\partial y}, \quad \eta_2 = \frac{\partial \phi}{\partial y} - \frac{\partial \psi}{\partial x}. \quad (4.79)$$

The velocity or scalar potential ϕ , which determines the propagation of longitudinal waves in a medium without cross sectional contraction, must satisfy the wave equation

$$\nabla^2 \phi + \omega^2 \rho_2 \phi / E_2' = 0, \quad (4.80)$$

where

$$E_2' = \frac{E_2(1 - \nu_2)}{(1 + \nu_2)(1 - 2\nu_2)}.$$

The transverse waves in the core are given by the stream function ψ . The governing differential equation for this function is

$$\nabla^2 \psi + \omega^2 \rho_2 \psi / G_2 = 0, \quad (4.81)$$

where

$$G_2 = \frac{E_2}{2(1 + \nu_2)}.$$

The displacements along the two main axes are continuous at the two junctions between laminates and core. This implies that

$$\begin{aligned} \eta_1 &= \eta_2, \quad \xi_1 = \xi_2 \quad \text{for } y = 0 \\ \eta_2 &= \eta_3, \quad \xi_2 = \xi_3 \quad \text{for } y = h. \end{aligned} \quad (4.82)$$

With respect to forced propagation of waves in the x -direction in the sandwich construction, it is assumed that all wave types are governed by the overall propagation constant k and a time dependence of $\exp(i\omega t)$. The flexural waves propagating along the positive x -axis in the laminates can, omitting the time dependence, be written as

$$\eta_n = A_n \cdot \exp(-ikx) \quad \text{for } n = 1, 3 \quad (4.83)$$

The corresponding expression for the longitudinal wave is

$$\xi_n = B_n \cdot \exp(-ikx) \quad \text{for } n = 1, 3. \quad (4.84)$$

The stream function and the velocity potential describing the transverse and longitudinal waves must satisfy respective differential equation in the core i.e., for $0 < y < h$. Considering the boundary conditions (4.82), the propagation constant in the x -direction for the waves in the core must be the same, as the wavenumbers describing the wave motion in the adjoining plates.

The general expression for the longitudinal waves in the core is of the form

$$\phi = e^{-ikx} (A_2 \cdot e^{-i\lambda_l y} + A_4 \cdot e^{i\lambda_l y}) \quad (4.85)$$

This expression must fulfill the wave Eq. (4.80). Thus

$$\lambda_l = \sqrt{\omega^2 \rho_2 / E_2' - k^2}. \quad (4.86)$$

The corresponding expression defining the transverse waves is

$$\psi = e^{-ikx} (B_2 \cdot e^{-i\lambda_t y} + B_4 \cdot e^{i\lambda_t y}). \quad (4.87)$$

From Eq. (4.78) λ_t is obtained as

$$\lambda_t = \sqrt{\omega^2 \rho_2 / G_2 - k^2}. \quad (4.88)$$

These basic equations are sufficient to solve k as described in Ref. [40].

4.10 Wavenumbers of Sandwich Plates

Some predicted wavenumbers for a symmetric sandwich plate are shown in Fig. 4.12. The dimensions and material parameters for the plate are shown in Table 4.3.

Laminates and core are assumed to be isotropic. In Fig. 4.12 two parallel lines are indicated. The lower line corresponds to the wavenumber for pure bending of the entire construction. The upper line represents the wavenumber for flexural waves propagating in an uncoupled laminate. It is found that, the wavenumber for the first propagating mode, for the inphase lateral motion of the laminates, asymptotically approaches the lower curve for decreasing frequencies. In the high frequency range, the upper curve is the asymptote. Thus, as should be expected, the lateral motion of the laminates is mainly determined by pure bending of the entire construction in the low frequency region and by the bending stiffness of one laminate in the high frequency range. In the mid-frequency region, the predicted curve starts to deviate from the lower asymptote when rotation and shear effects become important. For frequencies just above 2 kHz the second propagating mode for the inphase motion of the laminates can be excited. The consecutive modes are excited for even higher frequencies.

The purely imaginary wavenumbers, corresponding to the near field solutions or the evanescent waves for the inphase motion, have two branches in the low frequency region. One solution has in the limit the same absolute value as the wavenumber

Fig. 4.12 Predicted wavenumbers k (m^{-1}) for a symmetric sandwich plate. The thick solid lines are valid for propagating waves. The lower straight line is the wavenumber predicted based on simple bending theory for the entire structure. The upper straight line is the corresponding value for one laminate

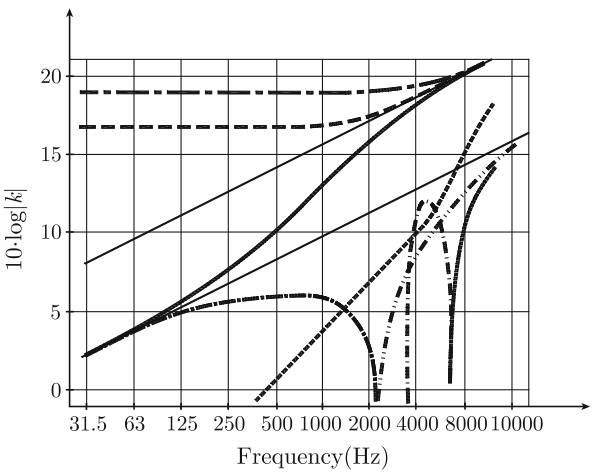


Table 4.3 Dimensions and material parameters

	Thickness (mm)	E (N/m ²)	ρ (kg/m ³)	ν
Laminates	5	1.67×10^{10}	1760	0.3
Core	50	0.013×10^{10}	130	0.3

for the first propagating mode. The other solution is constant in the low frequency region and thereafter approaches a limit, determined by the material parameters for the laminates. If the thickness of the core is decreased, the level of this branch is increased in the low frequency range.

For the antiphase motion, there is one solution, which up to approximately 6 kHz, is determined by quasi-longitudinal waves propagating in the structure. Nonpropagating modes change to propagating modes at just above 2 kHz for the inphase motion and at 6 kHz for the antiphase motion. The incipience of the propagating mode of the antiphase motion of the laminates at about 6 kHz coincides with the eigenfrequency f_r related to the mass-spring-mass system of the plate. For a sandwich plate with a lightweight core, the laminates are roughly equivalent to these masses and the core to the spring. The resonance or dilatation frequency f_r is given by the expression

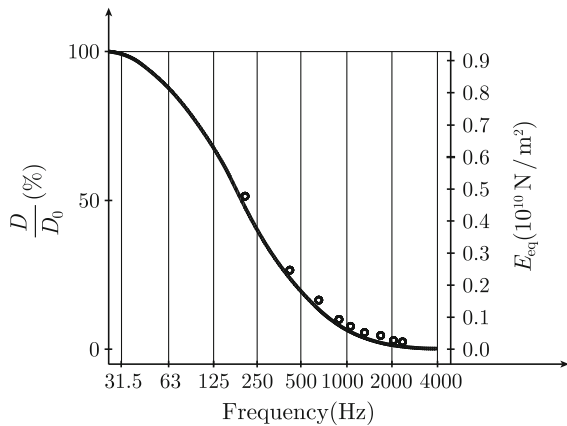
$$f_r = \frac{1}{2\pi} \left[\frac{(\rho_1 t_1 + \rho_3 t_3) E_2}{\rho_1 t_1 \rho_3 t_3 h} \right]^{1/2}. \quad (4.89)$$

The number of solutions in k , defining propagating modes, increases with increasing frequencies.

4.11 Bending Stiffness of Sandwich Plates

The predicted and measured bending stiffness for one plate are shown in Fig. 4.13. The material parameters for the plate are presented in the table in Sect. 4.4. The apparent bending stiffness D or the bending stiffness corresponding to the first propagating mode is compared to the low frequency limit D_0 —from Eq. (4.65)—which is equal to 1.17×10^5 Nm. In addition, the equivalent or apparent E -modulus for the entire structure is given on the vertical axis on the right-hand side of the graph.

Fig. 4.13 Measured (circles) and predicted (solid line) bending stiffness and equivalent E -modulus for a sandwich element



It is evident that the bending stiffness of the structure declines rapidly for increasing frequencies. At and above 1 kHz, the bending stiffness of the plate is just a few percent of the value in the low frequency limit. Some of the main acoustic and dynamic properties of sandwich elements can in most cases, with a sufficient degree of accuracy, be described by means of rather simple models. For plates with thin laminates, 3–6 mm, and a thick core, 25–75 mm, which can be assumed to be isotropic, the shear effects in the core are of major importance, particularly, in the frequency range from 200 to 4000 Hz. The rotational effects are of less importance. This is discussed in Chap. 9.

In the very low frequency range, the lateral motion of a sandwich plate is determined by pure bending of the entire construction. The corresponding limit in the high frequency range is given by the flexural motion of the seemingly uncoupled laminates. Consequently, the apparent bending stiffness of the entire construction is strongly dependent on frequency, while to a certain limit decreases with increasing frequency.

The apparent bending stiffness of sandwich beams is also found to depend on the boundary conditions of the structure. For clamped edges shear effects in the core tend to decrease the apparent bending stiffness. For a 1.2 m long beam with the geometry and the material parameters shown in the table in Sect. 4.10 the apparent bending stiffness is decreased by approximately 25 % at 100 Hz when the boundary conditions are changed from free to clamped as reported in Ref. [41].

If sandwich plates are to be parts of a large construction, certain requirements, with respect to weight and strength are often formulated. Even so, the material parameters and the geometry of the plates can be varied in such a way that the acoustic properties of the plate can be optimized in the frequency range of interest. Sandwich and honeycomb plates are discussed further in Chap. 9.

4.12 Bending of I-Beams

The simple one-dimensional bending of I-beams or plates reinforced with frames can be described in the same way as the bending of sandwich plates or beams. The basic configuration of a reinforced plate or an I-beam is shown in Fig. 4.14. The structure extends along the x -axis and consists of parallel sections. Only the apparent bending waves propagating along the x -axis are considered. Plates reinforced with frames are typical building elements in many large constructions and in particular for ship structures.

The beam or a strip of the structure in Fig. 4.14 is limited by the lines $z = \pm b_1/2$. The thicknesses of the plate elements 1–3 are given by t_1 , t_2 , and t_3 and are assumed to be small as compared to the other dimensions, i.e., each plate element is considered “thin.” Only wave motions, parallel to the x – y plane, corresponding to the fundamental propagating mode are being considered. No twisting or any other

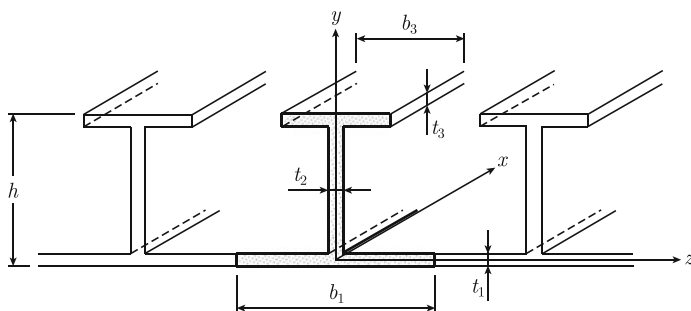
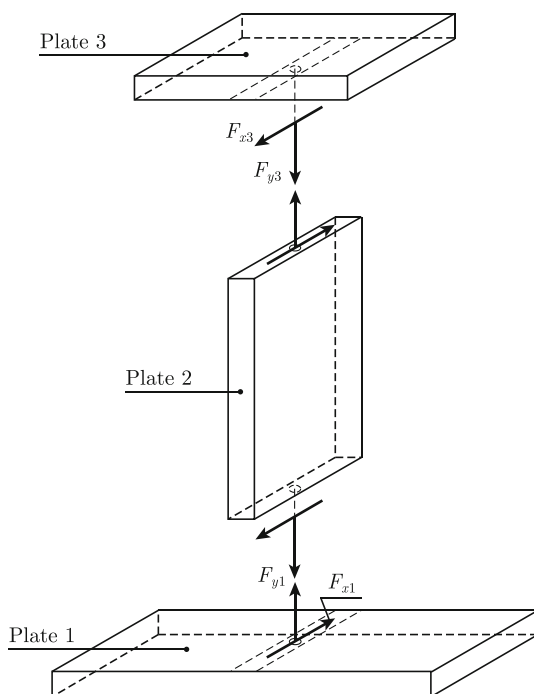


Fig. 4.14 Plate with reinforcing beams

motion in the z -direction is included in the model. Based on these assumptions, the following wave motions must be considered: flexural and longitudinal waves in the horizontal plates and longitudinal and transverse waves in the vertical plate shown in Fig. 4.15. As compared to the sandwich plate, the horizontal plates in the figure correspond to the laminates and the vertical plate to the core.

Fig. 4.15 Resulting forces at the boundaries between elements due to normal and shear stresses in plate 2



The forces acting on the various elements are shown in Fig. 4.15. These forces are

$$\begin{aligned} F_{x1} &= t_2 \tau_{y=0} = b_1 \tau_{21}, & F_{x3} &= t_2 \tau_{y=h} = b_3 \tau_{23} \\ F_{y1} &= t_2 \sigma_{y=0} = b_1 \sigma_{21}, & F_{y3} &= t_2 \sigma_{y=h} = b_3 \sigma_{23}. \end{aligned} \quad (4.90)$$

In these expressions τ and σ are the shear and normal stresses, respectively. The normal stresses in the vertical element should be defined as discussed in the last part of Sect. 4.4. The stresses τ_{21} , σ_{21} , etc., can be considered as average stresses if the forces are smeared out over the entire widths of the horizontal elements. This simplification follows from the assumption that the deflection of the elements is independent of the z -coordinate. Thus, the governing wave equations for an I-beam are obtained, if in the Eqs. (4.73) and (4.76), which are valid for the sandwich plate, the following substitutes are made

$$\begin{aligned} \sigma_{21} &\rightarrow t_2 \sigma_{y=0}/b_1, & \sigma_{23} &\rightarrow t_2 \sigma_{y=h}/b_3 \\ \tau_{21} &\rightarrow t_2 \tau_{y=0}/b_1, & \tau_{23} &\rightarrow t_2 \tau_{y=h}/b_3. \end{aligned} \quad (4.91)$$

These expressions are obtained directly from Eq. (4.90).

If the structure is an I-beam made of the same material then

$$E'_1 = E_1, \quad E'_3 = E_3. \quad (4.92)$$

If however element 1 is part of a plate structure as in Fig. 4.14, then

$$E'_1 = E_1/(1 - \nu_1^2). \quad (4.93)$$

Based on these substitutions, the wavenumbers for “bending” waves propagating along the x -axis can be solved as described in Sect. 4.4. A more complete derivation is presented in Ref. [42].

The predicted wavenumber for the first propagating bending mode is shown in Fig. 4.16. The structure is a steel I-beam with the dimensions: $b_1 = 0.6$ m, $b_3 = 0.2$ m, $h = 0.6$ m, $t_1 = t_2 = t_3 = 12$ mm. Three curves are shown in the figure. The solid line represents the wavenumber calculated as described above. Demonstrating that shear and rotational effects in element 2 are included. The straight bottom line is calculated, based on the simple Euler theory discussed in Chap. 3. The dashed line corresponds to the Timoshenko model—discussed in Sect. 4.4—with the so-called Timoshenko constant equal to $1/2.2$. It is obvious that the simple Euler theory is only applicable in the very low frequency range. The Timoshenko theory is, for this particular construction, useful up to approximately 1 kHz. It is interesting to note that the wavenumber for waves excited in element 1 approaches the wavenumber for pure bending of element 1 in the high frequency range. For this type of wave motion the reinforcing frame—elements 2 and 3—do not influence the propagation of “bending” waves in the high frequency region.

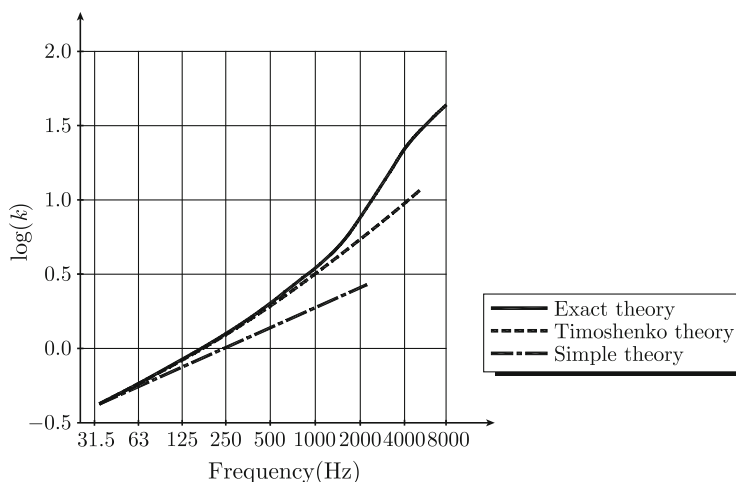


Fig. 4.16 Predicted wavenumber $k(\text{m}^{-1})$ corresponding to the bending of a beam

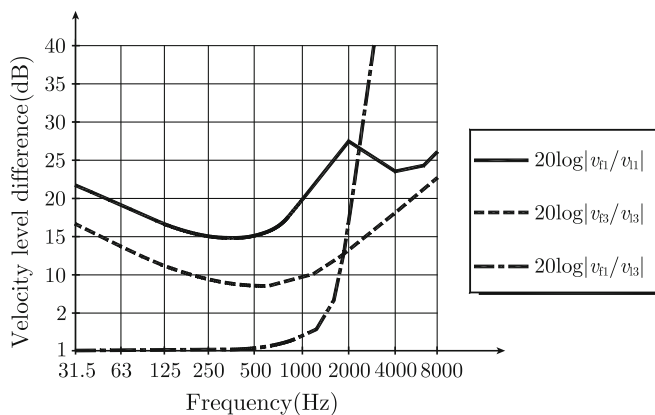


Fig. 4.17 Relative velocities of I-beam

In Fig. 4.17, the relative velocities of the elements 1 and 3 of the I-beam previously discussed are compared. The velocities v_{f1} , v_{l1} , v_{f3} and v_{l3} are defined in the same figure. In the low frequency region—up to approximately 1 kHz—the elements 1 and 3 are moving inphase with almost the same velocity. For higher frequencies, the velocity v_{f1} of the larger element becomes much higher than for the smaller plate-element 3. As mentioned above, the Timoshenko theory breaks down in this same frequency range. If a bending wave is excited in element 1, then the velocity v_{f3} of element 3 decreases with increasing frequencies. This shows again that at the high frequency limit, element 1 bends independently of the remainder of the structure.

Problems

- 4.1** A T-wave is for $x < 0$ traveling in a thin semi-infinite plate. The plate is in the x - y -plane. The wave is traveling towards a straight edge at $x = 0$. The angle of incidence is β . The impedance of the edge is infinite. Determine the relative amplitudes of the reflected L- and T-waves at the edge.
- 4.2** Two semi-infinite plates are oriented in the x - y plane. The junction between the plates is defined by the line $x = 0$. Plate 1 has the thickness h and plate 2 the thickness H . An L-wave is in plate 1 traveling towards the junction. The angle of incidence is α . Determine the ratio between the incident power and the power transmitted to plate 2.
- 4.3** Use Eq. (4.51) to determine the wavenumber for traveling and evanescent bending waves in a plate with thickness h . Include second-order terms. Determine also the energy flow due to a plane traveling bending wave in the plate. Include second-order terms in h .
- 4.4** Use Eq. (4.49) to determine the wavenumber for quasi-longitudinal waves traveling in a plate. Include only terms of the first order as the plate thickness approaches zero.
- 4.5** Determine the low and high frequency limits for the wave number describing flexural waves propagating in a sandwich plate. Geometrical and material parameters are given in the table of Sect. 4.10.
- 4.6** A bending wave, $w(x, t)$ is propagating in a plate. Use Eq. (4.56) to show that the resulting bending moment per unit width of the plate is $-D\partial^2 w/\partial x^2$ and the corresponding shear force $-D\partial^3 w/\partial x^3$. The plate is oriented in the x - y plane.
- 4.7** A bending wave, $w(x, t) = \eta_0 \exp[i(\omega t - \kappa x)]$ is propagating in a plate with the thickness h . Determine the intensity in the plate. Use Eq. (4.56) in combination with the definition of the intensity. The plate is oriented in the x - y plane.
- 4.8** Determine the shear stress in a plate with thickness h as function of the distance y from the neutral plane of the plate. Use the result (4.44).
- 4.9** The wavenumber k_x for a wave propagating along a so called Timoshenko beam is in Eq. (4.32) given as

$$k_x = \pm \sqrt{\frac{1}{2} \left[(k_l^2 + k_t^2/T_b) \pm \sqrt{4\kappa^4 + (k_l^2 - k_t^2/T_b)^2} \right]}.$$

In the high frequency limit k_x should approach k_r , the wavenumber for Rayleigh waves. Determine the coefficient T_b for

$$\lim_{\omega \rightarrow \infty} k_x = k_r.$$

4.10 According to Sect. 4.6 a Rayleigh wave propagating along the x -axis in a semi-infinite solid can for $y \leq 0$ be described by the potentials

$$\phi = B_1 \exp[\alpha(y + h/2)] \exp[i(\omega t - k_r x)]/2$$

$$\psi_z = C_2 \exp[\beta(y + h/2)] \exp[i(\omega t - k_r x)]/2,$$

where

$$C_2/B_1 = i \cdot \exp[h/2(\alpha - \beta)][k_r^2 - k_0^2(1 + \nu)]/(k_r \beta)$$

and k_r is the wavenumber for Rayleigh waves. The parameters α and β are

$$\beta = \sqrt{k_r^2 - k_t^2}, \quad \alpha = \sqrt{k_r^2 - k_l^2}.$$

Show that $\sigma_y = 0$ and $\tau_{xy} = 0$ for $y = 0$, i.e., on the surface of the semi-infinite solid.

4.11 Indicate a procedure to determine the intensity induced by a Rayleigh wave traveling in a semi-infinite solid. Use Eq. (4.68).

Chapter 5

Wave Attenuation Due to Losses and Transmission Across Junctions

In large building constructions like ships, cars, houses, etc., the energy flows from a mechanical source—for example an engine—to other structures is mainly determined by longitudinal, transverse, and flexural waves. In particular, this is the case, if the total construction is mainly built-up by plate elements. However, torsional waves must also be considered if beams, frames, stringers, shafts, etc., are part of the entire structure. It is obvious that if all wave types are included in a theoretical model describing the energy flow, then the resulting model can be exceedingly complex. It is therefore a very sound policy to estimate experimentally or otherwise the importance of various wave types for the energy flow in a certain construction. Based on the results, a theoretical model can be greatly simplified.

The energy flow in a structure is not only influenced by junctions and other discontinuities but also by losses in the structure itself. A standard method of decreasing the vibration levels of a construction is to artificially increase the losses of the structural elements. Some methods for estimating the effect of added damping are discussed. Measured and predicted loss factors are presented.

In the previous chapter, it was demonstrated that the so-called in plane waves, i.e., longitudinal and transverse waves, are well coupled. In addition, L- and T-waves can be induced by flexural waves and vice versa. If a pure bending wave impinges on a junction between two semi-infinite plates, inplane as well as flexural waves are reflected and transmitted at the junction. In this chapter, it is shown for some simple cases that the energy transfer from one wave type to another depends on material parameters, geometries, and frequency. A joint between structural elements if properly designed can effectively reduce the energy flow in large built-up structures. Some examples of special junctions are presented at the end of the chapter.

5.1 Excitation and Propagation of L-waves

In any real structure, there are losses. So far, these structural losses have not been included in various wave equations derived in the previous chapters. However, losses in solids were discussed in Sect. 3.2. The one-dimensional stress–strain relationship

including losses is according to the standard linear model of Eq. (3.26) equal to

$$\sigma_x + \dot{\sigma}_x/\alpha_1 = E_x(\varepsilon_x + \dot{\varepsilon}_x/\beta) \quad (5.1)$$

The subscript x indicates the direction of the strain and stress. For the static case, $\dot{\sigma}_x = \dot{\varepsilon}_x = 0$, Eq. (5.1) is reduced to Hooke's law as given in Eq. (3.1).

Deriving the equation governing the propagation of longitudinal waves in beams, it was found, as given in Eq. (3.51), that a variation of the stress in a beam induces an acceleration $\ddot{\xi}$ as given in

$$\frac{\partial \sigma_x}{\partial x} = \rho \frac{\partial^2 \xi}{\partial t^2} \quad (5.2)$$

A derivation with respect to time plus a multiplication by a factor $1/\alpha_1$ gives

$$\frac{1}{\alpha_1} \frac{\partial \dot{\sigma}_x}{\partial x} = \frac{\rho}{\alpha_1} \frac{\partial^3 \xi}{\partial t^3} \quad (5.3)$$

By adding the Eqs. (5.2) and (5.3), the result is

$$\frac{\partial}{\partial x}(\sigma_x + \dot{\sigma}_x/\alpha_1) = \rho \frac{\partial^2 \xi}{\partial t^2} + \frac{\rho}{\alpha_1} \frac{\partial^3 \xi}{\partial t^3} \quad (5.4)$$

The expression inside the bracket on the left-hand side is in Eq. (5.1) given as function of ε_x or $\varepsilon_x = \partial \xi / \partial x$. Thus a combination of the Eqs. (5.1) and (5.4) give

$$E_x \frac{\partial^2 \xi}{\partial x^2} + \frac{E_x}{\beta} \frac{\partial^3 \xi}{\partial x^2 \partial t} = \rho \frac{\partial^2 \xi}{\partial t^2} + \frac{\rho}{\alpha_1} \frac{\partial^3 \xi}{\partial t^3} \quad (5.5)$$

This is the wave equation including losses for longitudinal waves as derived from the standard linear model (3.26) giving the relationship between stress and strain. For simple harmonic displacement with ξ varying with time as $\exp(i\omega t)$, Eq. (5.5) is reduced to

$$E_x \left(1 + \frac{i\omega}{\beta}\right) \frac{\partial^2 \xi}{\partial x^2} + \omega^2 \rho \left(1 + \frac{i\omega}{\alpha_1}\right) \xi = 0 \quad (5.6)$$

Following the results given in Eq. (3.31) this expression can be modified to

$$\begin{aligned} E_0 (1 + i\eta) \frac{\partial^2 \xi}{\partial x^2} + \omega^2 \rho \xi &= 0 \\ E_0 = E_x \cdot \frac{1 + \omega^2/(\alpha_1 \beta)}{1 + \omega^2/\alpha_1}, \quad \eta &= \frac{\omega(1/\beta - 1/\alpha_1)}{1 + (\omega/\alpha_1)^2} \end{aligned} \quad (5.7)$$

where E_0 and η are real and positive as defined in Eq. (3.31). For solids like those listed in Table 3.1, the modulus of elasticity can be considered as constant as discussed in Sect. 3.2.

The effect of a complex E -modulus on the propagation of L-waves in a beam is demonstrated by considering the excitation of a semi-infinite beam oriented along the x -axis. The wave equation governing the propagation of L-waves in the beam is given by

$$\frac{\partial^2 \xi}{\partial x^2} - \frac{\rho}{E} \frac{\partial^2 \xi}{\partial t^2} = 0 \quad (5.8)$$

where ξ is the displacement. The E -modulus is complex or defined as $E = E_0(1 + i\eta)$ as in Eq. (5.7). Let the beam be semi-infinite and extend from $x = 0$ to infinity. The cross section of the beam is constant and equal to S . All material parameters are constant along the length of the beam. A force $F(t) = F_0 \cdot \exp(i\omega t)$ is applied to the end of the beam at $x = 0$ in the direction of the positive x -axis as shown in Fig. 5.1. The force generates an L-wave traveling along the x -axis. Since the beam is assumed to be infinite, no reflected waves are induced. The L-wave, or rather its displacement along the beam, can therefore be described by

$$\xi = A \cdot e^{i(\omega t - k_1 x)} \quad (5.9)$$

The displacement must have the same time dependence as the driving force, if only the stationary solution is of interest. The expression Eq. (5.9) inserted in the wave Eq. (5.8) yields

$$k_1^2 = \frac{\rho \omega^2}{E} = \frac{\rho \omega^2}{E_0(1 + i\eta)}, \quad k_1 = \frac{k_{01}}{\sqrt{1 + i\eta}}, \quad k_{01} = \omega \sqrt{\frac{\rho}{E_0}} \quad (5.10)$$

A series expansion of the terms including the loss factor gives

$$\frac{1}{\sqrt{1 + i\eta}} = 1 - i\eta/2 + 3\eta^2/4 + \dots$$

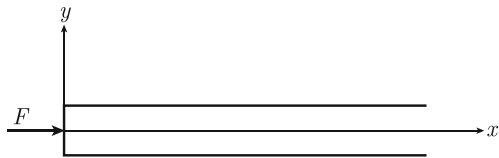
For sufficiently small η , terms of the second and higher orders of η can be neglected. Consequently,

$$k_1 = k_{10}(1 - i\eta/2) \text{ for } \eta \ll 1 \quad (5.11)$$

Thus for free waves propagating in a medium with losses, the wave number is complex.

Returning to the semi-infinite beam, the force acting on the structure induces a stress in the beam. It is assumed that the stress is constant over a cross section of the

Fig. 5.1 Excitation of L-waves in a semi-infinite beam



beam. The positive direction of the stress is according to Sect. 3.3 defined along the negative x -axis for the end section. Thus the boundary condition is

$$F = -S\sigma = -SE \frac{\partial \xi}{\partial x} \text{ at } x = 0 \quad (5.12)$$

The general expression (5.9) in combination with the boundary condition determines the unknown amplitude A . For $x = 0$, the result reads

$$F = F_0 e^{i\omega t} = -SE \frac{\partial \xi}{\partial x} = ik_1 SE A \cdot e^{i\omega t} \quad (5.13)$$

The amplitude A is for $\eta \ll 1$ obtained from Eq. (5.13) as

$$A = \frac{F_0}{ik_1 SE} = -i \cdot \frac{F_0}{k_{10}(1 - i\eta/2)SE_0(1 + i\eta)} \approx -i \cdot \frac{F_0}{k_{10}SE_0}(1 - i\eta/2) \quad (5.14)$$

The displacement due to the force at $x = 0$ is then obtained from the Eqs. (5.9), (5.11) and (5.14). The result is

$$\xi = -i \cdot \frac{F_0}{k_{10}E_0S}(1 - i\eta/2) \exp[i(\omega t - k_{10}x) - k_{10}x\eta/2] \quad (5.15)$$

The structural losses indicate that the absolute value of the amplitude of the displacement decays exponentially with increasing distance from the end section of the beam. In mathematical terms,

$$|\xi| = \frac{F_0}{k_{10}E_0S} e^{-k_{10}\eta x/2} \quad (5.16)$$

Again, terms of the second order of η have been neglected. In fact, this will be the general procedure throughout the remainder of the text. As previously pointed out, both the wave number and loss factor are functions of frequency.

The time average of the intensity I_x in the beam in the x -direction is according to Eq. (3.56) equals to

$$\bar{I}_x = -\frac{1}{2} \text{Re} \left[E \frac{\partial \xi}{\partial x} \left(\frac{\partial \xi}{\partial t} \right)^* \right] \quad (5.17)$$

From Eq. (5.9), the strain and velocity are found to be

$$\frac{\partial \xi}{\partial x} = -ik_1 \xi = -ik_{10}(1 - i\eta/2)\xi, \quad \frac{\partial \xi}{\partial t} = i\omega \xi$$

These expressions in combination with Eqs. (5.16) and (5.17) give

$$\bar{I}_x = \frac{1}{2} \omega k_{10} |\xi|^2 E_0 = \frac{1}{2} \frac{\omega |F_0|^2}{S^2 k_{10} E_0} e^{-k_{10}\eta x} \quad (5.18)$$

The time average of the energy flow in the x -direction is

$$\bar{\Pi}_x = S \bar{I}_x = \frac{1}{2} \frac{\omega |F_0|^2}{S k_{10} E_0} e^{-k_{10} \eta x} \quad (5.19)$$

The energy flow decays exponentially with distance. However, the attenuation of energy, due to the losses in a beam, is very small. For example, for a steel beam with a loss factor of 0.002 at 1000 Hz, the attenuation of the energy is just 0.01 dB/m.

Based on the expressions given above, the point mobility Y for a semi-infinite beam, is readily derived. The point mobility is as before defined as the ratio between the Fourier transform of the velocity and the Fourier transform of the force exciting the structure at the same point—in this case the end section of the beam and along the axis of the beam. It is assumed that the deflection and thus the velocity is the same over the cross section of the beam. From Eq. (5.15), the velocity at the end section of the beam at $x = 0$ is

$$v(0, t) = \frac{\omega F_0}{k_{10} E_0 S} (1 - i\eta/2) \exp(i\omega t) \quad (5.20)$$

Following the discussion in Sect. 2.2, the FT of the velocity $v(0, t)$ is given as function of the FT of the force $F(t)$ if in the time-dependent equations the following substitutions are made

$$F(t) \rightarrow \hat{F}(\omega) \cdot e^{i\omega t} \quad \text{and} \quad v(0, t) \rightarrow \hat{v}(0, \omega) \cdot e^{i\omega t}$$

Thus $F_0 \rightarrow \hat{F}(\omega)$ in Eq. (5.20). The FT of the velocity is

$$\hat{v}(0, \omega) = \frac{\omega \hat{F}(\omega)}{k_{10} E_0 S} \cdot (1 - i\eta/2)$$

For this particular case, the point mobility Y at $x = 0$ or rather $Y(0, \omega)$ is

$$Y(0, \omega) = \frac{\hat{v}(0, \omega)}{\hat{F}(\omega)} = \frac{\omega}{k_{10} E_0 S} \cdot (1 - i\eta/2) \quad (5.21)$$

In a similar way, the transfer mobility $Y(0, x_2, \omega)$ is defined as the ratio between the FT of the velocity observed at the point x_2 and the FT of the force exciting the beam at $x = 0$. Thus

$$Y(0, x_2, \omega) = \frac{\hat{v}(x_2, \omega)}{\hat{F}(\omega)} = \frac{\omega}{k_{10} E_0 S} \cdot (1 - i\eta/2) \cdot \exp[-k_{10} x_2 (i + \eta/2)]$$

The FRF H_{12} , frequency response function, between a force at an excitation point at $x_1 = 0$ and the response at x_2 is given by

$$H_{12}(x_1, x_2) = \frac{\hat{\xi}(x_2, \omega)}{\hat{F}(x_1, \omega)} = -i \cdot \frac{(1 - i\eta/2)}{k_{10} E_0 S} \cdot \exp[-ik_{10}x_2(1 - i\eta/2)] \quad \text{for } x_1 = 0 \quad (5.22)$$

In subsequent chapters, it will be demonstrated that reciprocity holds or that $Y(x_1, x_2) = Y(x_2, x_1)$ and $H_{12} = H_{21}$.

5.2 Excitation and Propagation of F-Waves

The structural losses for flexural waves, or for that matter any type of wave, can be incorporated in the wave equation by defining the E -modulus as a complex parameter, as discussed in Sect. 5.1. The wave equation for one-dimensional F-waves in a homogenous beam, which is oriented along the x -axis, is

$$\frac{\partial^4 w}{\partial x^4} + \frac{m'}{D'} \frac{\partial^2 w}{\partial t^2} = 0 \quad (5.23)$$

The displacement perpendicular to the beam is given by w . The beam has the width b and height h . Thus the mass m' per unit length of the beam is

$$m' = \rho b h \quad (5.24)$$

The bending stiffness is

$$D' = \frac{bh^3 E}{12} = \frac{bh^3}{12} E_0(1 + i\eta) = D'_0(1 + i\eta) \quad (5.25)$$

The E -modulus is made complex by introducing $E = E_0(1 + i\eta)$ as discussed in Sect. 5.1. Both E_0 and η are real quantities.

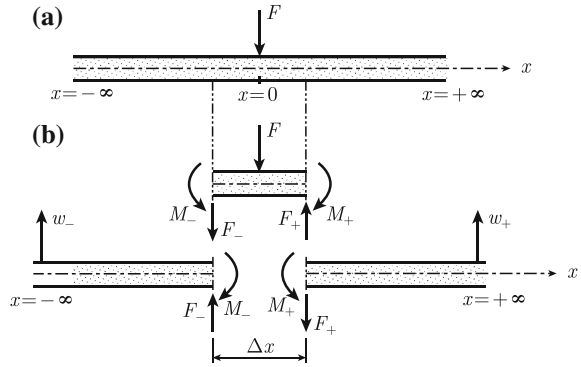
A force $F(t) = F_0 \cdot \exp(i\omega t)$ is applied to the infinite beam at $x = 0$ as shown in Fig. 5.2. The force will excite F-waves traveling along the positive and negative x -axes as well as decaying waves extending in both directions. Since the beam is assumed to be infinite, there are no reflected waves. The general solution to the wave equation can be written as

$$\begin{aligned} w_+ &= (A_1 \cdot e^{-i\kappa x} + B_1 \cdot e^{-\kappa x}) \cdot e^{i\omega t} \quad \text{for } x \geq 0 \\ w_- &= (A_2 \cdot e^{i\kappa x} + B_2 \cdot e^{\kappa x}) \cdot e^{i\omega t} \quad \text{for } x \leq 0 \end{aligned} \quad (5.26)$$

Because of the symmetry $A_1 = A_2 = A$ and $B_1 = B_2 = B$, the expressions given in Eq. (5.26) must satisfy the wave Eq. (5.23). Thus

$$\kappa^4 = \frac{m'\omega^2}{D'} \quad (5.27)$$

Fig. 5.2 Excitation of flexural waves in an infinite beam



However, the bending stiffness is complex as defined in Eq. (5.25). For small η , a Taylor expansion of the wavenumber yields

$$\kappa = \left[\frac{m'\omega^2}{D'_0(1+i\eta)} \right]^{1/4} \approx \left[\frac{m'\omega^2}{D'_0} \right]^{1/4} (1 - i\eta/4) = \kappa_0(1 - i\eta/4) \quad (5.28)$$

According to standard procedure, second and higher order terms of η have been neglected.

The boundary conditions at $x = 0$ require that the displacement and slope of the beam are continuous across the excitation point. This leads to

$$w_+ = w_-, \quad \frac{\partial w_+}{\partial x} = \frac{\partial w_-}{\partial x} \quad \text{at } x = 0 \quad (5.29)$$

In addition, the bending moments at each side of the force must be identical or

$$M_+ = -D' \frac{\partial^2 w_+}{\partial x^2} = -D' \frac{\partial^2 w_-}{\partial x^2} = M_- \quad (5.30)$$

The first and third boundary conditions are immediately satisfied from the symmetry condition, i.e., $A_1 = A_2 = A$ and $B_1 = B_2 = B$. The second boundary condition gives

$$-i\kappa A - B\kappa = i\kappa A + B\kappa \quad \text{or} \quad B = -iA \quad (5.31)$$

For obtaining equilibrium, the external force F must be equal to

$$F = F_+ - F_- = F_0 \cdot e^{i\omega t} \quad (5.32)$$

where

$$\begin{aligned} F_+ &= -D' \frac{\partial^3 w_+}{\partial x^3} = -iD'\kappa^3(A + iB) \cdot e^{i\omega t} = -2iD'\kappa^3 A \cdot e^{i\omega t} \\ F_- &= 2iD'\kappa^3 A \cdot e^{i\omega t}. \end{aligned} \quad (5.33)$$

The Eqs. (5.32) and (5.33) give

$$A = -\frac{F_0}{4i\kappa^3 D'} = \frac{iF_0(1 - i\eta/4)}{4\kappa_0^3 D'_0} \quad (5.34)$$

The solution or displacement of the beam excited by a point force $F_0 e^{i\omega t}$ at $x = 0$ is thus

(i) for $x \geq 0$.

$$w_+ = \frac{iF_0(1 - i\eta/4)}{4\kappa_0^3 D'_0} \cdot \{\exp[i(\omega t - \kappa_0 x) - \kappa_0 \eta x/4] - i \exp[i(\omega t + \kappa_0 \eta x/4) - \kappa_0 x]\}$$

(ii) for $x \leq 0$.

$$w_- = \frac{iF_0(1 - i\eta/4)}{4\kappa_0^3 D'_0} \cdot \{\exp[i(\omega t + \kappa_0 x) + \kappa_0 \eta x/4] - i \exp[i(\omega t - \kappa_0 \eta x/4) + \kappa_0 x]\} \quad (5.35)$$

Each solution is composed of two parts. The first part corresponds to a traveling wave. Due to the losses in the structure, the amplitude of this wave decays exponentially with increasing distance from the excitation point. The second part corresponds to the near-field solution. This solution rapidly decays for increasing distances from the excitation point. The amplitude of the near-field solution is approximately 2/1000 of the amplitude of the traveling wave, one wavelength away from the excitation point, i.e., at $|x| = 2\pi/\kappa_0$.

The time average of the energy flow Π_+ along the positive x -axis is obtained from Eq. (3.138) as

$$\bar{\Pi}_+ = \frac{1}{2} \text{Re} \left[D' \left(\frac{\partial^3 w}{\partial x^3} \right) \left(\frac{\partial w_+}{\partial t} \right)^* - D' \left(\frac{\partial^2 w}{\partial x^2} \right) \left(\frac{\partial^2 w_+}{\partial x \partial t} \right)^* \right]$$

Considering that the bending stiffness is complex, or $D' = D'_0(1 + i\eta)$, the energy flow in the positive x -direction can, based on the definition above and on Eq. (5.35), be obtained as

$$\begin{aligned} \bar{\Pi}_+(x) &= \frac{|F_0|^2 \kappa_0}{16\omega m'} \\ &\times \left\{ e^{-\kappa_0 \eta x/2} + \frac{\eta}{4} e^{-2\kappa_0 x} + \frac{\eta}{\sqrt{2}} e^{-\kappa_0 x(1 + \eta/4)} \cdot \sin[\kappa_0 x(1 + \eta/4)] - \pi/4 \right\} \end{aligned} \quad (5.36)$$

The first term inside the bracket is due to the propagating wave. The second part is caused by the near-field solution. The last part is the result of the interaction of the two wave types. The near-field, i.e., the second part of the solution (5.36), induces a decaying energy flow in the positive direction. The amplitude of this energy flow is proportional to the loss factor. The last term inside the bracket, the result of the combined effect of the evanescent and traveling waves, could be both positive and negative. The additional effect of the evanescent waves could either increase or decrease the energy flow caused by just the traveling waves. It should be noted that the near-field solution for $x \geq 0$ is, according to Eq. (5.35), a function of $\exp[i(\omega t + \kappa_0 \eta x/4) - \kappa_0 x]$. The imaginary time and space-dependent term $\exp[i(\omega t + \kappa_0 \eta x/4)]$ could indicate that the evanescent wave is traveling toward the negative x -axis. However, the only true indicator of the direction of propagation for a wave is the energy flow or intensity of the wave.

The total flow traveling to the right from the excitation point is from (5.36) equal to

$$\bar{\Pi}_+(0) = \frac{|F_0|^2 \kappa_0}{16\omega m'}(1 - \eta/4)$$

Considering the symmetry, the flow in the negative direction from the excitation point is equal to the flow in the positive direction. The total power induced in the beam is thus

$$\bar{\Pi}(0) = \bar{\Pi}_+(0) + \bar{\Pi}_-(0) = \frac{|F_0|^2 \kappa_0}{8\omega m'}(1 - \eta/4) \quad (5.37)$$

This expression is only valid as long as $\eta \ll 1$. The power induced in a loss free beam is consequently somewhat higher than the corresponding power in a beam with losses. Further, the evanescent waves transmit energy when losses are not neglected. The direction of this flow could vary as indicated by Eq. (5.36).

The attenuation of the energy flow carried by flexural waves in solids is in general very small. For a 6 mm thick strip of a steel plate with a loss factor of 0.002 at 1 kHz, the attenuation of the energy is of the order 0.02 dB/m.

Based on the expression (5.35) and the discussion in Sect. 5.1, the FT of the velocity at the excitation point is a function of the FT of the force as

$$\hat{v}(0, \omega) = \hat{w}_+(0, \omega) = -\frac{\hat{F}(1-i)(1-i\eta/4)\kappa_0}{4\omega m'} \quad (5.38)$$

The point mobility Y of an infinite and homogenous beam with a constant cross-sectional area, excited by a point force perpendicular to the extension of the beam is given as

$$Y = -\frac{\hat{v}(0, \omega)}{\hat{F}(\omega)} = \frac{(1-i)(1-i\eta/4)\kappa_0}{4\omega m'} \quad (5.39)$$

The minus sign is due to that force and displacement in Fig. 5.2 are defined positive in different directions.

The power induced by the point force in the beam is given as

$$\bar{\Pi}(0) = \frac{1}{2} \operatorname{Re} (F \cdot v^*) = \frac{1}{2} \operatorname{Re} (F \cdot F^* Y^*) = \frac{|F|^2}{2} \operatorname{Re} (Y^*) = \frac{|F_0|^2 \kappa_0}{8\omega m'} (1 - \eta/4)$$

This expression is identical to the result (5.37). Compare Sect. 2.10 and Eq. (2.100). The significance of point mobilities is discussed in a subsequent section, in connection with the coupling and interaction of structures.

5.3 Point Excited Infinite Plate

In the previous section, the excitation of flexural waves on an infinite beam was discussed. It is natural to extend the analysis also to include “point” excited flexural waves on a thin plate. Thus, consider a thin infinite plate. The plate is excited at the origin by a harmonic force $F(t) = F_0 \cdot \exp(i\omega t)$. The excitation force is such that the waves induced are axisymmetric, i.e., only depend on the distance from force and not the cylindrical angle. The resulting displacement is $w(r, t)$ where r is the distance to the origin. At the origin, the displacement is $w(0, t) = w_0 \cdot \exp(i\omega t)$. The equation governing free flexural waves outside the area of excitation is according to Eq. (3.115)

$$\nabla^2(\nabla^2 w) - \kappa^4 w = 0$$

A time dependence $\exp(i\omega t)$ is assumed. The displacement is given as $w(r, t) = w(r) \cdot \exp(i\omega t)$. The wave number for flexural waves is κ . The wave equation can also be written as

$$(\nabla^2 + \kappa^2)(\nabla^2 - \kappa^2)w = 0 \quad (5.40)$$

This equation can be replaced by two second order differential equations on the form

$$\nabla^2 w_1 + \kappa^2 w_1 = 0, \quad \nabla^2 w_2 - \kappa^2 w_2 = 0 \quad (5.41)$$

If one of these equations is satisfied then the solution also satisfies the original wave equation. The total solution w to Eq. (5.40) is thus $w = w_1 + w_2$.

In cylindrical coordinates, the operator ∇^2 is equal to

$$\nabla^2 = \frac{\partial^2}{\partial r^2} + \frac{1}{r} \frac{\partial}{\partial r} + \frac{1}{r^2} \frac{\partial^2}{\partial \varphi^2}$$

For symmetric excitation, the solution w is also symmetric and thus independent of the cylindrical angle φ .

The general solution to the first equation in the expression (5.41) can according to standard procedure—see Refs. [5, 23]—be written as a combination of two linearly independent solutions of the Bessel function $J_0(\kappa r)$ and the Neumann function

$Y_0(\kappa r)$. The solution to the first equation is

$$w_1(r) = A_1 \cdot J_0(\kappa r) + A_2 \cdot Y_0(\kappa r) \quad (5.42)$$

The amplitudes A_1 and A_2 are determined by the boundary conditions. The solution can also be written as combination of the linearly independent Hankel functions of the first and second kind since

$$H_0^{(1)}(z) = J_0(z) + iY_0(z), \quad H_0^{(2)}(z) = J_0(z) - iY_0(z) \quad (5.43)$$

where z can be an arbitrary complex number. The Bessel and Neumann functions can, according to Ref. [43], for small z , be expanded as

$$\begin{aligned} J_0(z) &= 1 - \frac{z^2}{4} + \frac{z^4}{64} + \dots \\ Y_0(z) &= \frac{2}{\pi} \left[\ln\left(\frac{z}{2}\right) + \gamma \right] J_0(z) + \frac{2}{\pi} \frac{z^2}{4} - \frac{3}{2} \frac{z^4}{64} + \dots \end{aligned} \quad (5.44)$$

In this expression, the so-called Euler constant γ is equal to $0.577 \dots$. The results given in Eq. (5.44) show that $J_0(z)$ is finite as z tends to zero, whereas $Y_0(z)$ tends to infinity. For increasingly large z , the Bessel, Neumann, and Hankel functions asymptotically approach some simple expressions. The asymptotic solutions as $z \rightarrow \infty$ are according to Ref. [43] equal to

$$\begin{aligned} J_0(z) &= \sqrt{\frac{2}{\pi z}} \cdot \cos(z - \pi/4) \\ Y_0(z) &= \sqrt{\frac{2}{\pi z}} \cdot \sin(z - \pi/4) \\ H_0^{(1)}(z) &= \sqrt{\frac{2}{\pi z}} \cdot \exp[i(z - \pi/4)] \\ H_0^{(2)}(z) &= \sqrt{\frac{2}{\pi z}} \cdot \exp[-i(z - \pi/4)] \end{aligned} \quad (5.45)$$

For an infinite plate, the waves induced must propagate away from the area of excitation, i.e., the displacement must be a function of $\exp[i(\omega t - \kappa r)]$. This condition can only be satisfied by the solution $H_0^{(2)}(\kappa r)$ or the Hankel function of the second kind. The solution to the first equation of the expression (5.41) is thus

$$w_1(r, t) = C_1 \cdot H_0^{(2)}(\kappa r) \cdot \exp(i\omega t) \quad (5.46)$$

The solution to the second equation of (5.41), must be of the same form as the solution to the first. Possible solutions can be obtained, by replacing κr by $i\kappa r$ or $-i\kappa r$ in the result (5.46). However, considering the asymptotic expansions of the Hankel functions, it follows that the only physically realizable solutions are either

$H_0^{(1)}(i\kappa r)$ or $H_0^{(2)}(-i\kappa r)$. The reason is that only these solutions result in finite amplitudes as $r \rightarrow \infty$. The second solution is chosen as the basis for the subsequent derivations. However, the final result is independent of the choice of which one of the solutions $H_0^{(1)}(i\kappa r)$ or $H_0^{(2)}(-i\kappa r)$ is used. The solution to the second differential equation of the expression (5.41) is written on the form

$$w_2(r, t) = C_2 H_0^{(2)}(-i\kappa r) \cdot \exp(i\omega t) \quad (5.47)$$

Consequently, the total solution to Eq. (5.40) is,

$$w(r, t) = \left[C_1 \cdot H_0^{(2)}(\kappa r) + C_2 \cdot H_0^{(2)}(-i\kappa r) \right] \cdot \exp(i\omega t) \quad (5.48)$$

The solution must be finite as $r \rightarrow 0$ or in fact equal to $w_0 \cdot \exp(i\omega t)$. For small r , the Hankel function of the second kind is dominated by the Neumann function which is infinite for $r = 0$. The Bessel function is finite for $r = 0$. For small r , the solution (5.48) can as $r \rightarrow 0$ and omitting the time dependence, be expanded as

$$\begin{aligned} w &\rightarrow C_1[-iY_0(\kappa r)] + C_2[-iY_0(-i\kappa r)] \\ &= -\frac{2i}{\pi}[\ln(\kappa r) + \gamma - \ln 2]C_1 - \frac{2i}{\pi}[\ln(\kappa r) - \frac{\pi i}{2} + \gamma - \ln 2]C_2 \\ &= -\frac{2i}{\pi}(C_1 + C_2)[\ln(\kappa r) + \gamma - \ln 2] - C_2 \end{aligned} \quad (5.49)$$

The equality $\ln(-i\kappa r) = \ln(\kappa r) - (\pi i/2)$ has been used to obtain this expression. For w to be finite at $r = 0$, $C_1 = -C_2$, the total solution is thus reduced to

$$w(r, t) = C_1[H_0^{(2)}(\kappa r) - H_0^{(2)}(-i\kappa r)] \cdot \exp(i\omega t)$$

From Eq. (5.49), it follows that in the limit, $r = 0$, the displacement is given by $w = -C_2$. However, for $r = 0$ the displacement should be equal to w_0 . Thus, $C_1 = -C_2 = w_0$. The results can be summarized as

$$w(r, t) = w_0[H_0^{(2)}(\kappa r) - H_0^{(2)}(-i\kappa r)] \cdot e^{i\omega t} \quad (5.50)$$

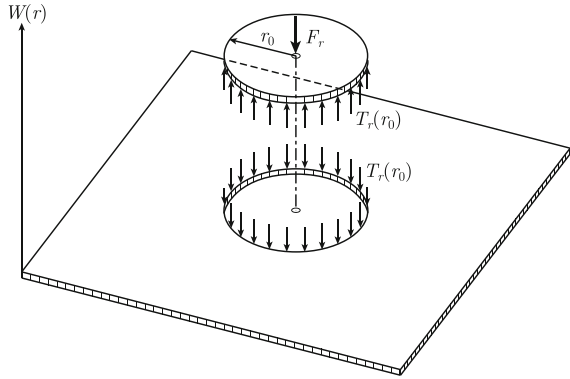
The far-field solution as $r \rightarrow \infty$ is

$$w(r, t) = w_0 \sqrt{\frac{2}{\pi \kappa r}} \left(\frac{1+i}{\sqrt{2}} \cdot e^{-i\kappa r} - i \cdot e^{-\kappa r} \right) \cdot e^{i\omega t}$$

It can be shown—Ref. [31]—that the exact solution is sufficiently well described by the far-field solution (5.51) for $\kappa r > 4$.

The shear force T_r' per unit length acting on the periphery of a circle around the origin or the excitation point as shown in Fig. 5.3, is, based on Eq. (3.113), given by

Fig. 5.3 Shear force due point excitation of plate



$$\begin{aligned}
 T'_r &= -D \frac{\partial}{\partial r} (\nabla^2 w) = -D w_0 \frac{\partial}{\partial r} \left\{ \nabla^2 [H_0^{(2)}(\kappa r) - H_0^{(2)}(-i\kappa r)] \right\} \cdot e^{i\omega t} \\
 &= -D \kappa^2 w_0 \frac{\partial}{\partial r} \left[H_0^{(2)}(\kappa r) + H_0^{(2)}(-i\kappa r) \right] \cdot e^{i\omega t} \quad (5.51)
 \end{aligned}$$

For $r \rightarrow 0$, the Hankel function of the second kind approaches infinity as

$$H_0^{(2)}(\kappa r) \rightarrow \frac{2i}{\pi} \ln(\kappa r), \quad H_0^{(2)}(i\kappa r) \rightarrow \frac{2i}{\pi} \ln(i\kappa r) = -i + \frac{2i}{\pi} \ln(\kappa r)$$

From this it follows that the shear force T'_r for $r = r_0 \ll 1$ tends to

$$(T'_r)_{r=r_0} \rightarrow -D \kappa^2 w_0 \left[\frac{4i}{\pi} \frac{\partial}{\partial r} \ln(\kappa r) \right]_{r=r_0} \cdot e^{i\omega t} = -\frac{4i}{\pi r_0} D \kappa^2 w_0 \cdot e^{i\omega t} \quad (5.52)$$

The shear force T'_r approaches infinity as r approaches zero. In order to overcome this apparent anomaly, it must be assumed that the excitation force is equally distributed along a circle with radius $r = r_0$. The total force is thus equal to

$$F_0 \cdot e^{i\omega t} = 2 \pi r_0 (T'_r)_{r=r_0} = -8i \kappa^2 D w_0 \cdot e^{i\omega t} = -8 \kappa^2 D v_0 / \omega \cdot e^{i\omega t} \quad (5.53)$$

The velocity of the plate at the excitation point is given by v_0 . Following the discussion in Sect. 5.1, it follows that the point mobility Y at $r = 0$ is equal to

$$Y = -\frac{\hat{v}}{\hat{F}} = \frac{\omega}{8 \kappa^2 D} = \frac{1}{8 \sqrt{\mu D}} = \frac{1 - i\eta/2}{8 \sqrt{\mu D_0}} \quad (5.54)$$

The minus sign is due to the fact, that the force and displacement are defined positive in opposite directions. In the expression (5.54), μ is the mass per unit area of the plate and the bending stiffness is $D = E h^3 / [12(1 - \nu^2)]$.

The time average of the energy flow per unit length, at the circumference of a circle, with the radius r around the excitation point, is

$$\bar{\Pi}'_r(r) = \frac{1}{2} \text{Re} \left[D \left(\frac{\partial}{\partial r} \nabla^2 w \right) \left(\frac{\partial w}{\partial t} \right)^* - D \left(\nabla^2 w \right) \left(\frac{\partial^2 w}{\partial r \partial t} \right)^* \right] \quad (5.55)$$

This expression can be somewhat more easy to handle if the displacement w is as before written as the sum of the two solutions w_1 and w_2 . By means of Eq. (5.41), the expression (5.55) is simplified. Further, the losses in the plate can be included by writing the bending stiffness and the wavenumber as $D = D_0(1 + i\eta)$ and $\kappa = \kappa_0(1 - i\eta/4)$. In the far-field, the time average of the energy flow per unit width is for $\eta \ll 1$

$$\bar{\Pi}'_r(r) = \frac{2\omega D_0 \kappa_0^2 |w_0|^2}{\pi r} \cdot e^{-\kappa_0 r \eta/2} \quad (5.56)$$

If the losses in the plate are neglected, the total power $\bar{\Pi}_{\text{tot}}$ fed into the plate can be calculated since the energy flow integrated along a circle enclosing the excitation point is equal to the power induced in the plate by the force. The time average of the total power $\bar{\Pi}_{\text{tot}}$ fed into the plate is consequently

$$\bar{\Pi}_{\text{tot}} = 2 \pi r \bar{\Pi}'_r(r) = 4\omega D_0 \kappa_0^2 |w_0|^2 \quad (5.57)$$

The amplitude of the waves can also be expressed as function of an excitation force by means of the point mobility Y as demonstrated in Problem 5.8.

In practice, the excitation area has certain extension. The force distribution within the excitation area can also influence the response of a plate and its mobility. The force distribution depends on whether the forcing structure is hard or soft, for example made of steel or rubber. A number of these problems are discussed in Ref. [44]. It can be concluded that the power forced into a plate can be reduced if the force is distributed over a large area. Further, the difference in power input to a plate, between rigid and soft body excitation, can be of the order 4–5 dB in the high-frequency range.

The derivation above, of the point mobility, was based on the thin plate theory. For thick plates, a more detailed analysis must be carried out. This is for example discussed in Refs. [31, 44]. Alternative methods for predicting mobilities are discussed in the following section.

5.4 Spatial Fourier Transforms

The temporal Fourier transform was introduced in Sect. 2.1. By means of a temporal FT, any problem can be transferred from the time domain to the frequency domain or vice versa. In a similar way, a spatial Fourier transform transfer a function from the space to the wavenumber domain and back. The technique is very powerful tool in

particular when solving problems related to structures of infinite extent; for example, infinite beams and plates. It will be demonstrated later, that in certain important cases a finite plate or beam can be treated as were it an infinite structure. The calculation of the point impedance of an infinite beam or an infinite plate is two examples well suited for exercising spatial Fourier transforms. Mathematically, it can be advantageous to describe coupling effects between structures and fluids by means of spatial Fourier transforms. This is later discussed in Chap. 12.

The definition and application of spatial FTs follows the discussion in Sect. 2.1 on temporal FTs. Starting with a one-dimensional case, let $u(x)$ be a function defined along the entire x -axis or rather for all x . The function can be defined through its spatial FT $\tilde{u}(k)$ as

$$u(x) = \frac{1}{2\pi} \int_{-\infty}^{\infty} \tilde{u}(k) \cdot e^{ikx} dk \quad (5.58)$$

Inversely, the function $\tilde{u}(k)$ is defined as

$$\tilde{u}(k) = \int_{-\infty}^{\infty} u(x) \cdot e^{-ikx} dx \quad (5.59)$$

The expressions (5.58) and (5.59) lead to the identity

$$\delta(k - k_0) = \frac{1}{2\pi} \int_{-\infty}^{\infty} e^{ix(k_0 - k)} dx \quad (5.60)$$

The expressions (5.58)–(5.60) are analogous to the temporal transforms given in Eqs. (2.2)–(2.4).

Spatial FTs can be generalized to more than one dimension. In two dimensions, the transforms are

$$\tilde{u}(k_x, k_y) = \int_{-\infty}^{\infty} \int_{-\infty}^{\infty} u(x, y) \cdot e^{-i(k_x x + k_y y)} dx dy$$

or

$$\tilde{u}(\mathbf{k}) = \int_{-\infty}^{\infty} u(\mathbf{r}) \cdot e^{-i\mathbf{k} \cdot \mathbf{r}} d^2 \mathbf{r}$$

$$u(x, y) = \frac{1}{(2\pi)^2} \int_{-\infty}^{\infty} \int_{-\infty}^{\infty} \tilde{u}(k_x, k_y) \cdot e^{i(k_x x + k_y y)} dk_x dk_y$$

or

$$u(\mathbf{r}) = \frac{1}{(2\pi)^2} \int_{-\infty}^{\infty} \tilde{u}(\mathbf{k}) \cdot e^{i\mathbf{k} \cdot \mathbf{r}} d^2 \mathbf{k}$$

$$\delta(\mathbf{k} - \mathbf{k}_0) = \frac{1}{(2\pi)^2} \int_{-\infty}^{\infty} e^{i\mathbf{r} \cdot (\mathbf{k}_0 - \mathbf{k})} d^2 \mathbf{k} \quad (5.61)$$

where $\mathbf{r} = (x, y)$ and $\mathbf{k} = (k_x, k_y)$. Finally in three-dimensional space the transforms are

$$\begin{aligned}\tilde{u}(\mathbf{k}) &= \int_{-\infty}^{\infty} u(\mathbf{r}) \cdot e^{-i\mathbf{k}\mathbf{r}} d^3\mathbf{r} \\ u(\mathbf{r}) &= \frac{1}{(2\pi)^3} \int_{-\infty}^{\infty} \tilde{u}(\mathbf{k}) \cdot e^{i\mathbf{k}\mathbf{r}} d^3\mathbf{k} \\ \delta(\mathbf{k} - \mathbf{k}_0) &= \frac{1}{(2\pi)^3} \int_{-\infty}^{\infty} e^{i\mathbf{r}(\mathbf{k}_0 - \mathbf{k})} d^3\mathbf{k}\end{aligned}\quad (5.62)$$

where $\mathbf{r} = (x, y, z)$ and $\mathbf{k} = (k_x, k_y, k_z)$.

The calculation of the point mobility for an infinite homogeneous beam can illustrate the versatility of the spatial Fourier transforms. Let a beam be oriented along the x -axis of a coordinate system. The beam is excited by a point force at $x = 0$ as shown in Fig. 5.2a. The equation governing flexural vibrations of the beam is

$$\frac{\partial^4 w}{\partial x^4} + \frac{m'}{D'} \frac{\partial^2 w}{\partial t^2} = \frac{F \cdot \delta(x)}{D'} \quad (5.63)$$

The notations are defined in Sect. 5.2. The displacement w and the force F have the temporal FTs $\hat{w}(x, \omega)$ and $\hat{F}(\omega)$, respectively. The temporal FT of Eq. (5.63) yields

$$\frac{\partial^4 \hat{w}}{\partial x^4} - \kappa^4 \hat{w} = \frac{\hat{F} \cdot \delta(x)}{D'} \quad (5.64)$$

The temporal FT of the velocity is $\hat{v} = i\omega \hat{w}$. Introducing this in Eq. (5.64) gives

$$\frac{\partial^4 \hat{v}}{\partial x^4} - \kappa^4 \hat{v} = \frac{i\omega \hat{F} \cdot \delta(x)}{D'}, \quad \kappa^4 = \frac{m'\omega^2}{D'} = \frac{m'\omega^2}{D'_0} (1 - i\eta) \quad (5.65)$$

The spatial FT of \hat{v} is \tilde{v} . Thus

$$\hat{v}(x, \omega) = \frac{1}{2\pi} \int_{-\infty}^{\infty} \tilde{v}(k, \omega) \cdot e^{ikx} dk \quad (5.66)$$

The spatial FT of the force function is

$$\tilde{\hat{F}} = \int_{-\infty}^{\infty} \hat{F} \cdot \delta(x) \cdot e^{-ikx} dx = \hat{F} \quad (5.67)$$

Taking the spatial FT of Eq. (5.65) results in

$$\int_{-\infty}^{\infty} \left[\tilde{v}(k^4 - \kappa^4) - \frac{i\omega \hat{F}}{D'} \right] e^{ikx} dk = 0$$

The expression inside the bracket gives

$$\tilde{v}(k^4 - \kappa^4) = \frac{i\omega \hat{F}}{D'} \quad (5.68)$$

The Eqs. (5.66) and (5.68) give

$$\hat{v}(0, \omega) = \frac{1}{2\pi} \int_{-\infty}^{\infty} \tilde{v}(k, \omega) dk = \frac{1}{2\pi} \int_{-\infty}^{\infty} \frac{i\omega \hat{F}}{D'(k^4 - \kappa^4)} dk \quad (5.69)$$

The equation can be solved by means of contour integral in the upper part of the complex plain as shown in Fig. 5.4. By setting $z = k$, the contour integral is

$$\hat{v}(0, \omega) = \frac{i\omega \hat{F}}{2\pi D'} \oint \frac{dz}{z^4 - \kappa^4} \quad (5.70)$$

The integral along the semicircle tends to zero as $|z| \rightarrow \infty$. There are four poles, namely $z = \pm\kappa = \pm\kappa_0(1 - i\eta/4)$ and $z = \pm i\kappa = \pm i\kappa_0(1 - i\eta/4)$. Two of the poles are in the upper part of the complex plain. These are $z_1 = -\kappa_0(1 - i\eta/4)$ and $z_2 = i\kappa_0(1 - i\eta/4)$.

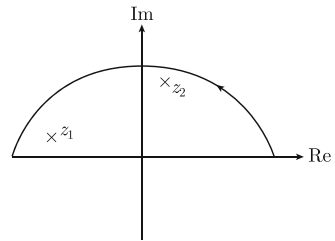
According to the theorem of residues and Cauchy's theorem, Ref. [5], a contour integral J has the solution

$$J = \oint \frac{g(z)dz}{h(z)} = 2\pi i \sum_n \frac{g(z_n)}{h'(z_n)} \quad (5.71)$$

The summation is made over all poles inside a closed path. For Eq. (5.70) the solution is

$$\begin{aligned} \hat{v}(0, \omega) &= \frac{i\omega \hat{F}}{2\pi D'} \oint \frac{dz}{z^4 - \kappa^4} = \frac{-\omega}{D'} \hat{F} \left(\frac{1}{4z_1^3} + \frac{1}{4z_2^3} \right) \\ &= \frac{(1-i)\hat{F}}{4D'\kappa^3} = \frac{(1-i)(1-i\eta/4)\hat{F}}{4D'\kappa^3} \end{aligned} \quad (5.72)$$

Fig. 5.4 Integration path for Eq. (5.70)



The point mobility is consequently

$$Y = \frac{\hat{v}(0, \omega)}{\hat{F}} = \frac{(1-i)(1-i\eta/4)\kappa_0}{4m'\omega} \quad (5.73)$$

This is the same result as given by Eq. (5.39).

The same procedure can be followed to calculate the point mobility of a homogeneous and infinite plate with the mass per unit area μ and the bending stiffness D . The wavenumber for flexural waves propagating along the plate is consequently $\kappa = (\mu\omega^2/D)^{1/4}$. A point force F is exciting the plate at origin. The displacement and the force are positive in the same direction. Compare Fig. 5.3. The equation governing flexural vibrations of the plate is

$$\nabla^2(\nabla^2 w) + \frac{\mu}{D} \frac{\partial^2 w}{\partial t^2} = \frac{F \cdot \delta(\mathbf{r})}{D} \quad (5.74)$$

The displacement w and the force F have the temporal FTs $\hat{w}(x, \omega)$ and $\hat{F}(\omega)$, respectively. The temporal FT of Eq. (5.63) yields

$$\nabla^2(\nabla^2 \hat{w}) - \kappa^4 \hat{w} = \frac{\hat{F} \cdot \delta(\mathbf{r})}{D} \quad (5.75)$$

The temporal FT of the velocity is $\hat{v} = i\omega \hat{w}$. Introducing this in Eq. (5.75) gives

$$\nabla^2(\nabla^2 \hat{v}) - \kappa^4 \hat{v} = \frac{i\omega \hat{F} \cdot \delta(\mathbf{r})}{D}, \quad \kappa^4 = \frac{\mu\omega^2(1-i\eta)}{D} \quad (5.76)$$

The spatial FT of \hat{v} is \tilde{v} . Thus

$$\hat{v}(x, y, \omega) = \frac{1}{(2\pi)^2} \int_{-\infty}^{\infty} \int_{-\infty}^{\infty} \tilde{v}(k_x, k_y, \omega) \cdot e^{i(k_x x + k_y y)} dk_x dk_y \quad (5.77)$$

By changing from Cartesian to cylindrical coordinates through the transforms $x = r \cos \varphi$, $y = r \sin \varphi$, $k_x = k \cos \varphi$, and $k_y = k \sin \varphi$ Eq. (5.77) is according to standard procedure reduced to

$$\hat{v}(r, \omega) = \frac{1}{(2\pi)^2} \int_0^{\infty} \tilde{v}(k, \omega) \cdot e^{ikr} 2\pi k dk \quad (5.78)$$

Note that the limits for the integration now are zero and infinity following the definition of k_x and k_y . The spatial FT of the force function is

$$\begin{aligned}
\tilde{\hat{F}} &= \int_{-\infty}^{\infty} \hat{F} \delta(\mathbf{r}) e^{-i(k_x x + k_y y)} d\mathbf{r} \\
&= \int_{-\infty}^{\infty} \hat{F} \delta(x) e^{-ik_x x} dx \int_{-\infty}^{\infty} \delta(y) e^{-ik_y y} dy \\
&= \hat{F}
\end{aligned} \tag{5.79}$$

Taking the spatial FT of Eq. (5.76) results in

$$\tilde{v}[(k_x^2 + k_y^2)^2 - \kappa^4] = \frac{i\omega \hat{F}}{D}, \quad \tilde{v} = \frac{i\omega \hat{F}}{D(k^4 - \kappa^4)} \tag{5.80}$$

Equation (5.80) inserted in (5.78) gives for $r = 0$

$$\hat{v}(0, \omega) = \frac{1}{2\pi} \frac{i\omega \hat{F}}{D} \int_0^{\infty} \frac{k dk}{k^4 - \kappa^4}$$

Thus, the point mobility is

$$Y = \frac{\hat{v}}{\hat{F}} = \frac{i\omega}{2\pi D} \int_0^{\infty} \frac{k dk}{k^4 - \kappa^4}$$

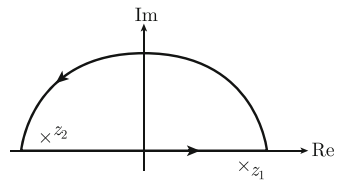
The integral cannot immediately be made into a contour integral as in the previous case since the integrand is not an even function. However, this problem is overcome by setting $k^2 = \varsigma$. In this way, the integration can be made from minus infinity to plus infinity instead of from zero to infinity. Since $k^2 = \varsigma$ then $k dk = d\varsigma/2$ and the integral is transformed into

$$Y = \frac{\hat{v}}{\hat{F}} = \frac{i\omega}{2\pi D} \frac{1}{4} \int_{-\infty}^{\infty} \frac{d\varsigma}{\varsigma^2 - \kappa^4} \tag{5.81}$$

The integral can now be solved by means of a contour integral in upper part of the complex plain as shown in Fig. 5.5. The contour integral is

$$Y = \frac{\hat{v}}{\hat{F}} = \frac{i\omega}{8\pi D} \oint \frac{dz}{z^2 - \kappa^4} \tag{5.82}$$

Fig. 5.5 Integration path for Eq. (5.82)



The integral along the semicircle tends to zero as the radius increased. There are two poles, $z_1 = \kappa^2 = \kappa_0^2(1 - i\eta/2)$ and $z_2 = -\kappa^2 = -\kappa_0^2(1 - i\eta/2)$. One pole, z_2 , is in the upper half plane. The contour integration gives according to (5.71)

$$Y = \frac{i\omega}{8\pi D} \cdot 2\pi i \left(\frac{1}{2z_2} \right) = \frac{1}{8D\kappa^2} = \frac{1 - i\eta/2}{8\sqrt{\mu}D_0} \quad (5.83)$$

This is the same result as (5.54). It could be claimed that the result (5.83) is derived in a mathematically more concise way.

The displacement of the structure is obtained by making an inverse FT of the spatial transform. As an example, consider again the point excited beam. The spatial FT of the velocity of the beam is given in Eq. (5.68). The spatial FT \tilde{w} is consequently

$$\tilde{w}(k, \omega) = \frac{\tilde{v}(k, \omega)}{i\omega} = \frac{\hat{F}}{D'(k^4 - \kappa^4)} \quad (5.84)$$

According to the definition (5.66), the displacement $\hat{w}(x, \omega)$ is given by

$$\hat{w}(x, \omega) = \frac{\hat{F}}{2\pi D'} \int_{-\infty}^{\infty} \frac{e^{ikx}}{k^4 - \kappa^4} dk$$

For $x \geq 0$, the integral can be solved by means of a contour integration in the upper half part of the complex plane along the curve shown in Fig. 5.4. The contour integral is

$$\hat{w}(x, \omega) = \frac{\hat{F}}{2\pi D'} \oint \frac{e^{izx}}{z^4 - \kappa^4} dz \quad (5.85)$$

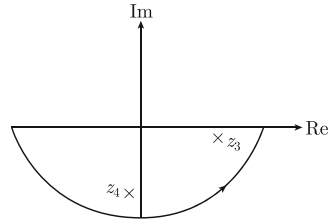
The integral along the semi circle approaches zero as $|z| \rightarrow \infty$ since the imaginary part of z is positive. For $x \geq 0$ and $\text{Im } z > 0$, $\exp(izx) \rightarrow 0$ as $|z| \rightarrow \infty$. The two poles in the upper half plane are $z_1 = -\kappa_0(1 - i\eta/4)$ and $z_2 = i\kappa_0(1 - i\eta/4)$. The result of the contour integration is following (5.71) for $x \geq 0$

$$\begin{aligned} \hat{w}(x, \omega) &= \frac{\hat{F}}{2\pi D'} 2\pi i \left[\frac{e^{ixz_1}}{4z_1^3} + \frac{e^{ixz_2}}{4z_2^3} \right] \\ &= \frac{i\hat{F}(1 - i\eta/4)}{4\kappa_0^3 D'_0} [e^{-i\kappa_0 x(1 - i\eta/4)} - ie^{-\kappa_0 x(1 - i\eta/4)}] \end{aligned} \quad (5.86)$$

For $x \leq 0$, the contour integral must be made along a path in the lower part of the complex plane to ensure that the integral along the semicircle tends to zero as the radius increases. See Fig. 5.6. This gives for $x \leq 0$

$$\hat{w}(x, \omega) = -\frac{\hat{F}}{2\pi D'} \oint \frac{e^{izx}}{z^4 - \kappa^4} dz$$

Fig. 5.6 Integration path for $x \leq 0$



Note the minus sign. A contour integration is always made anticlockwise. The poles in the lower part of the complex plane are $z_3 = \kappa_0(1 - i\eta/4)$ and $z_4 = -i\kappa_0(1 - i\eta/4)$. The response for $x \leq 0$ is thus

$$\hat{w}(x, \omega) = -\frac{\hat{F}}{2\pi D'} 2\pi i \left[\frac{e^{ixz_3}}{4z_3^3} + \frac{e^{ixz_4}}{4z_4^3} \right] = \frac{i\hat{F}(1 - i\eta/4)}{4\kappa_0^3 D'_0} [e^{i\kappa_0 x(1 - i\eta/4)} - i e^{\kappa_0 x(1 - i\eta/4)}] \quad (5.87)$$

Compare the result (5.35).

5.5 Added Damping

The losses in a structure will influence the attenuation of structure-borne sound in solids. More importantly, the frequency average of the energy of a finite structure excited by white noise is inversely proportional to the losses in the system. At a resonance, the energy is even inversely proportional to the square of the loss factor. However, for harmonic excitation of a structure, damping is only of importance if the frequency of the force exciting the structure is close to one of its natural frequencies. For finite systems or in fact any real system, the effect of increasing the damping can drastically reduce the energy of the system. The loss factors for most metals like steel and aluminum and for building materials like concrete are fairly low. It can therefore often be of importance to increase the losses in a structure artificially to reduce vibrations and thus noise radiated from the structure. Although the internal loss factor of most solids is very low, transmission losses at the boundaries of an element can be high. To be effective, the added damping must be significantly higher than the total damping of the system to which it is applied.

The structural damping can, in particular for plates, be increased considerably by the addition of so-called viscous and elastic materials. These materials are often high polymers with high loss factors. When stretched and thereafter released, this type of material regains its original shape very slowly. This is due to the viscous losses. The shear modulus and loss factor for typical viscoelastic materials depend not only on frequency but also on temperature.

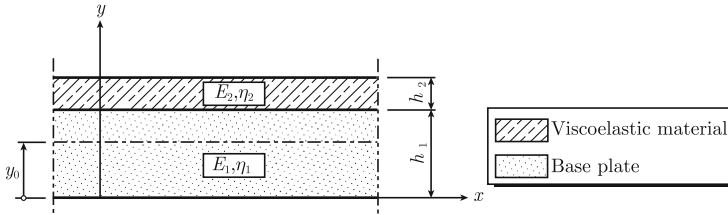


Fig. 5.7 Viscoelastic layer on a plate

The most simple but not necessarily the most effective way of increasing the damping of a structure is to apply a viscoelastic layer on the structure as shown in Fig. 5.7. When the structure or in this case the plate is exposed to bending there is also an expansion and contraction in the layer. The displacement within the layer will transform the potential and kinetic energy into heat. This energy transfer will cause the losses.

The added layer will also increase the bending stiffness and weight of the basic structure. The increased stiffness and weight can often be factors limiting the additional damping, which can be achieved. The reason is that due to the change of weight and stiffness, the dynamic properties and thus the natural frequencies of the structure are changed.

Consider a homogeneous base plate with constant thickness. A layer of viscoelastic material is applied to the plate as shown in Fig. 5.7. The material parameters as well as the thicknesses of plate and layer are indicated in the figure. The subscripts 1 and 2 refer to the base plate and layer, respectively. Due to the stiffness of the layer, the neutral axis, with the y -coordinate y_0 , will be shifted away from the center of the base plate. The coordinate for the neutral axis is obtained from the expression

$$\int_0^{h_1} E_{01}(y - y_0)dy + \int_{h_1}^{h_1+h_2} E_{02}(y - y_0)dy = 0 \quad (5.88)$$

The E -moduli E_1 and E_2 for the plate and layer are complex and defined as

$$E_1 = E_{01}(1 + i\eta_1), \quad E_2 = E_{02}(1 + i\eta_2) \quad (5.89)$$

where η_n is the loss factor for structure n . Equation (5.88) means that the sum of the expanding and contracting stresses on each side of the neutral axis is equal to zero. From Eq. (5.88), the coordinate y_0 for the neutral axis, is obtained as

$$y_0 = \frac{E_{01}h_1^2 + E_{02}(h_2^2 + 2h_1h_2)}{2(E_{01}h_1 + E_{02}h_2)} \quad (5.90)$$

The complex bending stiffness D for the entire construction is

$$\begin{aligned}
 D &= E_1 \int_0^{h_1} (y - y_0)^2 dy + E_2 \int_{h_1}^{h_1+h_2} (y - y_0)^2 dy \\
 &= E_1 \left(\frac{h_1^3}{3} - h_1^2 y_0 + h_1 y_0^2 \right) \\
 &\quad + E_2 \left[\frac{3h_1^2 h_2 + 3h_1 h_2^2 + h_2^3}{3} - y_0(h_2^2 + 2h_1 h_2) + y_0^2 h_2 \right]
 \end{aligned} \quad (5.91)$$

The total loss factor for the damped plate is

$$\eta_{\text{tot}} = \frac{\text{Im} D}{\text{Re} D} \quad (5.92)$$

In general, $E_1 \gg E_2$, $h_1 \gg h_2$ and $\eta_2 \gg \eta_1$. For this particular case, the following approximations are obtained

$$y_0 = h_1/2, \quad D = E_1 h_1^3/12 + E_2 h_1^2 h_2/4, \quad \eta_{\text{tot}} = \frac{3\eta_2 h_2 E_{02}}{h_1 E_{01}} \quad (5.93)$$

The effect of the damping layer can be improved if a spacer is placed in between the base plate and the viscoelastic layer as discussed in Ref. [45]. In this case, again based on the assumptions leading up to Eq. (5.93), the total loss factor with a spacer height h_0 shown in Fig. 5.8, is

$$\eta_{\text{tot}} = \frac{12\eta_2 h_2 a^2 E_{02}}{h_1^3 E_{01}}, \quad a = \frac{h_1 + h_2}{2} + h_0 \quad (5.94)$$

The total loss factors discussed above are valid for bending only. For longitudinal waves propagating along the x -axis in the plate construction shown in Fig. 5.4 the total loss factor is obtained as

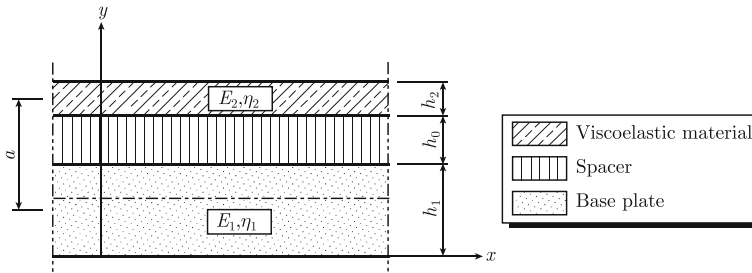


Fig. 5.8 Viscoelastic layer with a spacer

$$\eta_{\text{tot}} = \frac{\eta_1 h_1 E_{01} + \eta_2 h_2 E_{02}}{h_1 E_{01} + h_2 E_{02}} \quad (5.95)$$

By comparing Eqs. (5.93) and (5.95), it is evident that the losses for longitudinal and flexural waves propagating in the same structure are quite different. This is also true for various wave types propagating in coupled structures as discussed in Sect. 5.12. Consequently, the loss factor is not a material parameter or constant but depends on wave type and adjoining structures.

The total loss factor η as a function of the thickness ratio h_2/h_1 for a construction consisting of a steel plate, thickness h_1 , and a damping layer, thickness h_2 , is shown in Fig. 5.9. The loss factor as a function of temperature is for the same material shown in Fig. 5.10 for the ratio $h_2/h_1 = 1$. In both cases, the losses are due to bending. The damping layer is of type SWEDAC/SD. The results are obtained from the SWEDAC product catalog, Ref. [46]. The loss factor of most viscoelastic materials strongly depends on temperature.

The effect of the damping treatment can be greatly improved, if a constraining layer is mounted on top of the damping material, as shown in Fig. 5.11. When the plate is being bent, a shear stress is induced in the layer between the plates. The shear adds to the total damping. Compare the difference of the deformation of the viscoelastic layer, with and without a constraining layer, as shown in Figs. 5.7 and 5.11.

The resulting bending stiffness and loss factor of the entire construction can be calculated by considering the pure shear forces acting on the base plate and constraining layer. The procedure is described in Sect. 9.5. See also, for example, Refs. [45, 47].

Fig. 5.9 Loss factor for a steel plate, thickness h_1 , with a layer of damping material, thickness h_2 , Ref. [46]

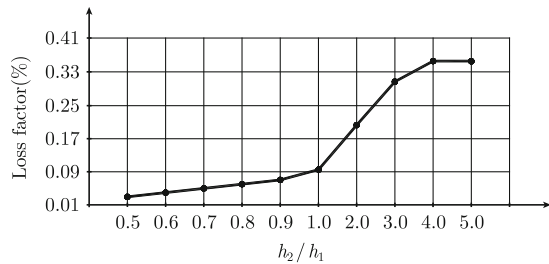
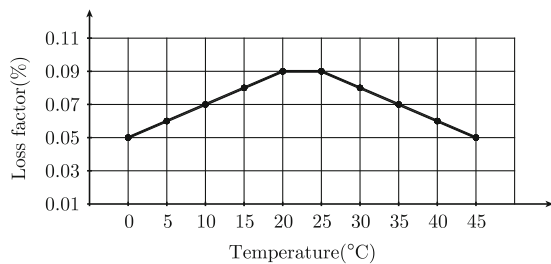


Fig. 5.10 Temperature dependence of loss factor, Ref. [46]



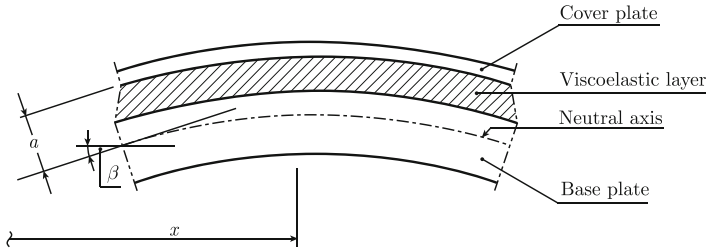


Fig. 5.11 Deformation of plate with constrained viscoelastic layer

Let the base plate of the structure shown in Fig. 5.11 have the Young's modulus E_1 , density ρ_1 and thickness h_1 . The bending stiffness or rather the real part of it, is

$$D_{01} = \frac{E_{01}h_1^3}{12(1 - \nu_1^2)} \quad (5.96)$$

In this type of structure, the losses for the base plate can be neglected in comparison with the losses in the interlayer of viscoelastic material. The material and geometrical parameters for the constraining layer are identified in a similar way by a subscript 3.

The complex bending stiffness D_x for a composite structure consisting of base plate, viscoelastic layer, and constraining layer can, as discussed in Sect. 9.5, be described as

$$D_x = (D_1 + D_3) \left(1 + \frac{\gamma Z}{k_x^2 + Z} \right) \quad (5.97)$$

where

$$Z = \frac{G}{h_2} \left(\frac{E_1 h_1 + E_3 h_3}{E_1 h_1 E_3 h_3} \right), \quad \gamma = \frac{[h_2 + (h_1 + h_3)/2]^2}{(D_1 + D_3)} \left(\frac{E_1 h_1 E_3 h_3}{E_1 h_1 + E_3 h_3} \right) \quad (5.98)$$

The thickness of the damping layer is h_2 . The shear modulus of the viscoelastic layer is $G = G_0(1 + i\eta_2)$. The wavenumber for flexural waves propagating along the structure is denoted k_x and is defined as

$$k_x = \left(\frac{\mu_0 \omega^2}{D_x} \right)^{1/4} \quad (5.99)$$

where $\mu_0 = \rho_1 h_1 + \rho_2 h_2 + \rho_3 h_3 \approx \rho_1 h_1 + \rho_3 h_3$.

The total loss factor η_{tot} of the plate is given by

$$\eta_{\text{tot}} = \frac{\text{Im}(D_x)}{\text{Re}(D_x)} \quad (5.100)$$

By assuming that $\eta_2 \gg \eta_1$ and $\eta_2 \gg \eta_3$ and by introducing \mathcal{X} as $\mathcal{X} = \mathcal{Z}/k_x^2$, the total loss factor is obtained as

$$\eta_{\text{tot}} = \frac{\eta_2 \mathcal{X}_0 \gamma}{1 + (2 + \gamma) \mathcal{X}_0 + (1 + \gamma)(1 + \eta_2^2) \mathcal{X}_0^2} \quad (5.101)$$

Since $\eta_2 \gg \eta_1$ and $\eta_2 \gg \eta_3$ the parameters E_1 and E_3 can be replaced by E_{01} and E_{03} in Eq. (5.98). The real part of \mathcal{X} is defined as \mathcal{X}_0 and approximated by the expression

$$\mathcal{X}_0 = \frac{G_0}{k_{x0}^2 h_2} \left(\frac{E_{01} h_1 + E_{03} h_3}{E_{01} h_1 E_{03} h_3} \right) \quad (5.102)$$

The real part, k_{x0} , of the wavenumber k_x is a function of the bending stiffness which in turn is a function of the shear parameter \mathcal{X} and thus also of the wavenumber. The parameter, $\mathcal{X} = \mathcal{Z}/k_x^2$, Eq. (5.97), must therefore be solved by iteration. The initial value for \mathcal{X}_0 could be set to equal 0.5. Thereafter D_x is calculated. This value gives k_x which in turn is inserted in the expression for \mathcal{X}_0 and so on.

The maximum value of γ is equal to 3. If the base plate and constraining layer are of the same material γ_{max} is obtained for $h_1 = h_3$. If the shear modulus is very large, then \mathcal{X} is also large and the total bending stiffness is the same as if the base plate and constraining layer were firmly connected. If $E_1 = E_3$, then for both G and \mathcal{X} being large, the bending stiffness for the entire construction is

$$D_0 = \frac{(h_1 + h_3)^3 E_{01}}{12(1 - \nu_1^2)} \quad (5.103)$$

If on the other hand the shear modulus is very low, then the total bending stiffness of the plate is $D_0 = D_{01} + D_{03}$.

In most practical cases, it is necessary to limit the total weight of a construction, while at the same time maintaining a required stiffness. Due to these considerations, it is not always possible to achieve an optimal damping. For a damping layer, the shear modulus is fairly low as compared to the E -moduli of the connected plates. This means that the shear parameter is also small. For optimal damping, this would mean that h_3 approximately should be equal to h_1 . This would double the weight of the structure. This might be quite unacceptable. Due to weight considerations, the thickness ratio is in practice often chosen to be of the order 1/3.

Some elastic properties of a few viscoelastic materials are listed in Ref. [48]. However, a large number of different viscoelastic materials is continuously being produced. For most applications, it is often possible to find a viscoelastic material with the right properties within the required temperature and frequency ranges. Relevant and up-to-date databases should always be consulted.

The influence of the thickness ratio on the loss factor is shown in Fig. 5.12. In the example, the base plate is a 6 mm steel plate. The interlayer consists of a 1 mm Polysulfide rubber. The constraining plate is made of steel. The calculations are made for three thicknesses—2, 4, and 6 mm—of the constraining layer. Clearly, the thickest

Fig. 5.12 Influence on loss factor of thickness ratio between constraining layer and base plate

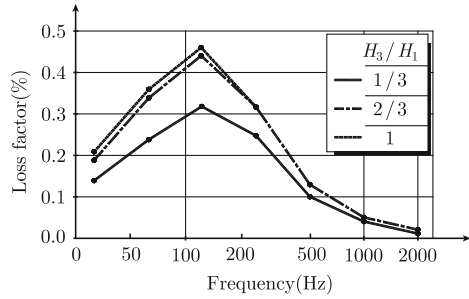
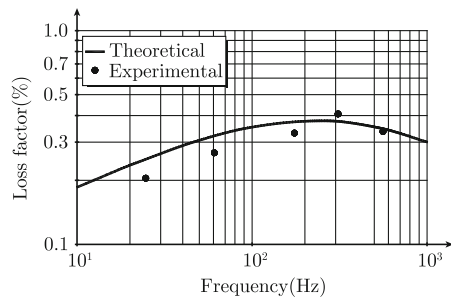


Fig. 5.13 Comparison between predicted and measured loss factor



constraining layer gives the highest loss factor. But still, even for the thickness ratio $1/3$, the resulting loss factor is very high, as compared to an untreated panel for which the loss factor is much less than 1% . In Fig. 5.13, predicted and measured loss factors are compared. The damping of plates and bars by means of viscoelastic layers can be made in a great number of ways as discussed in Ref. [45].

5.6 Losses in Sandwich Plates

A plate with a constrained viscoelastic layer has certain similarities to a sandwich construction as defined in Sect. 4.7. In deriving loss factors for a plate and a constrained layer, only shear forces on the plate elements are included, as discussed in Sect. 9.4. For the sandwich construction, the normal stresses on the elements applied to the core are also considered. Further, a viscoelastic layer is assumed to be “thin.” This is not necessarily the case for a core in a sandwich element. The basic models describing the bending of plates with constrained viscoelastic layers and the bending of sandwich or honeycomb panels are discussed in Sects. 9.3 and 9.4.

In a sandwich element, laminates and core have losses. These can be included in the model discussed in Chap. 4 or Sect. 9.3 and by introducing a complex E -modulus for each structure. According to standard procedure, the E modulus for the various layers n can be written as

$$E_n = E_{0n}(1 + i\eta_n) \quad (5.104)$$

In this expression, η_n represents the losses or rather the loss factor in the structure. Thus, if the losses are known for the laminates as well as the core, then by introducing these by means of the expression (5.104) in the wave equations governing the bending of sandwich elements, the total loss factor for the entire structure is obtained. The resulting wavenumber k for propagating “bending” waves, derived in Sect. 4.8, is thus also complex. The apparent and complex bending stiffness of the structure is for the first mode for propagating waves on a symmetric three-layered plate given by

$$D = \mu_{\text{tot}} \omega^2 / k^4 = D_0 (1 + i \eta_{\text{tot}}) \quad (5.105)$$

where μ_{tot} is equal to the total mass per unit area of the sandwich plate. The real part of the bending stiffness is D_0 and the total loss factor for the structure is η_{tot} .

Figure 5.14 shows the calculated total loss factors for a symmetric 5-50-5 mm sandwich plate for three different cases. In the examples, the loss factor for the core is set to equal 2%. The loss factors for the laminates for the three cases are 1.5, 3, and 6%. The remaining parameters are given in the Table 4.3 in Sect. 4.10.

In the low-frequency region, the lateral motion of the structure is determined by pure bending. Consequently, the total losses are more or less determined through expansion and contraction of the laminates. For increasing frequencies, the lateral motion of the entire construction is influenced by rotation and shear in the core. In particular, this additional deflection in the core increases the total loss factor of the structure with the laminates with the lowest loss factor, as shown in Fig. 5.14. If the losses for the laminates are doubled, the maximum total loss factor is increased just by, approximately, 10%, since the loss factor for the core is unchanged. When the losses for the laminates are increased even further, the total loss factor has a minimum in the frequency range, where shear and rotation in the core is of main importance. In this frequency domain, deflections in the core mainly contribute to the total losses. In

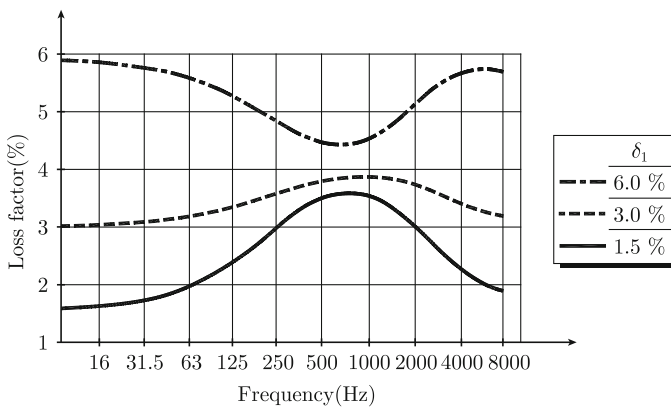
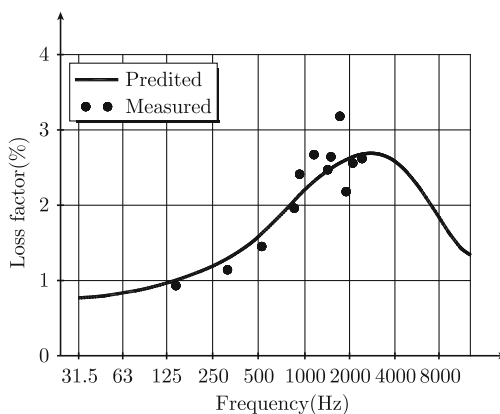


Fig. 5.14 Predicted loss factors for a sandwich plate. Losses in core are constant and equal to 2%. The losses δ_1 in both laminates varied

Fig. 5.15 Loss factor for a sandwich plate



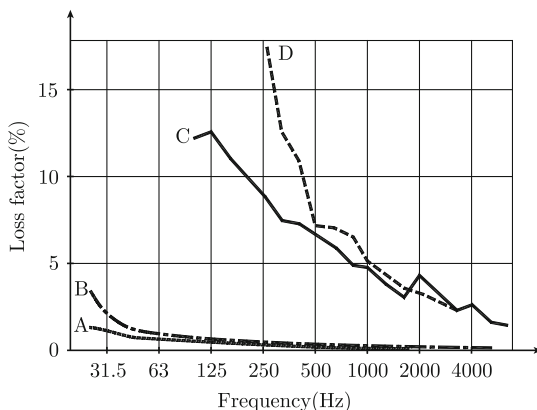
the high frequency range, the motion is dominated by flexural waves in the laminates. The total loss factor again, therefore, approaches the loss factors for each laminate.

For typical sandwich plates, the total loss factor is primarily determined by the losses of the laminates in the high- and low-frequency ranges. In the mid-frequency domain, the shear and rotational effects in the core have a dominating effect. Thus, for these frequencies, the losses in the core considerably influence the total loss factor for the lateral motion of the sandwich plate.

In Fig. 5.15 predicted and measured loss factors are compared for the same sandwich panel. In the prediction model, the loss factors for core and laminates have been set to 1.5 and 0.7 % respectively. These values are based on measurements for the first few resonances of each separate structure. It would perhaps be expected that these loss factors should be frequency dependent. However, this could not be verified. For this reason, the losses for each separate structure are assumed to be constant in the prediction model. The agreement between predicted and measured total loss factors is satisfactory for most applications.

The loss factor for a typical sandwich plate is of the order 100 times higher than for a free steel or aluminum plate. It is well known that the losses for a plate which in part of a large construction, are much higher than for free plates. This is due to the additional losses at junctions. In Fig. 5.16 loss factors for some typical deck constructions on ships are compared. In the figure, loss factors measured in situ are given for: (A) a bare 6 mm steel deck; (B) 6 mm steel deck plus a thin layer of a 2–4 mm standard type of leveling compound; (C) steel deck plus damping layer and leveling compound as constraining layer; (D) a 60 mm standard sandwich plate. The results indicate that the losses for a standard sandwich plate by far exceed the losses of other, typically damped and undamped deck-structures. On ships, structure-borne noise is of dominating importance. Consequently, the high loss factor for a sandwich construction makes such a panel a suitable building material for small and fast vessels for which weight, strength, and noise are of major concern.

Fig. 5.16 Full-scale measurements of loss factors for some typical deck constructions *A* 6 mm steel deck; *B* 6 mm steel deck plus 2–4 mm leveling compound; *C* steel plate plus constrained viscoelastic layer; *D* 60 mm sandwich plate



5.7 Coupling Between Flexural and Inplane Waves

Flexural waves can be coupled to the inplane waves, i.e., L- and T- waves. This happens, for example, at junctions where plates or beams are connected at a certain angle. This coupling effect can be illustrated by a simple case with two semi-infinite plates connected at a right angle as shown in Fig. 5.17. A plane incident flexural wave travels in plate 1 along the positive x -axis toward the plate junction, which is perpendicular to the x -axis. Due to the incident wave, a bending moment is induced around the junction. No other external forces or moments are applied to the junction. The bending at the junction will in turn induce an F-wave in plate 2 and also a reflected F-wave in plate 1. The incident and reflected F-waves in plate 1 create a force acting on plate 2 along the y -axis. Due to this inplane force, a longitudinal wave is induced in plate 2. No transverse waves are created as long as the incident F-wave is traveling perpendicular to the junction. Compare Sect. 4.2. In a similar way, the F-wave in plate 2 creates a reflected L-wave in plate 1.

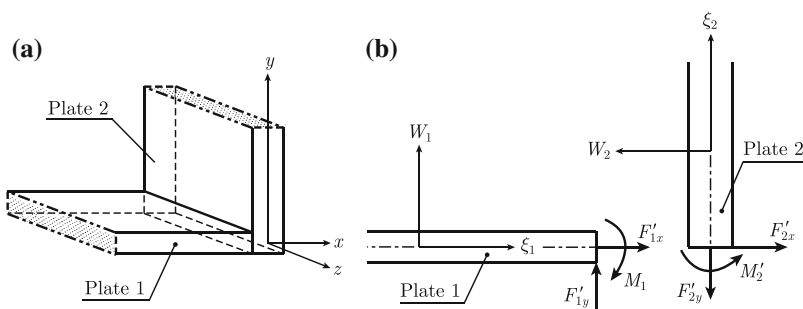


Fig. 5.17 Two coupled plates. Incident F-wave. L- and F-waves transmitted and reflected

If it is assumed that the plates are of equal thickness and made of the same material, the general expressions for the waves can, omitting the time dependence $\exp(i\omega t)$, be given as

Plate 1

$$\text{Incident F-wave } w_{\text{in}} = e^{-i\kappa x}$$

$$\text{Reflected F-wave } w_{\text{re}} = A_1 \cdot e^{i\kappa x} + A_2 \cdot e^{\kappa x}$$

$$\text{Reflected L-wave } \xi_1 = A_3 \cdot e^{ikx}$$

$$\text{Sum of F-waves } w_1 = w_{\text{in}} + w_{\text{re}} = e^{-i\kappa x} + A_1 \cdot e^{i\kappa x} + A_2 \cdot e^{\kappa x}$$

Plate 2

$$\begin{aligned} \text{Transmitted F-wave } w_2 &= A_4 \cdot e^{-i\kappa y} + A_5 \cdot e^{-\kappa y} \\ \text{Transmitted L-wave } \xi_2 &= A_6 \cdot e^{-iky} \end{aligned} \quad (5.106)$$

The parameter κ is the wavenumber for flexural waves in a plate and k the wavenumber for L-waves in the same plate. Thus

$$\kappa = \left[\frac{12\rho\omega^2(1-\nu^2)}{Eh^2} \right]^{1/4}, \quad k = \sqrt{\frac{\rho\omega^2(1-\nu^2)}{E}}$$

The thickness of the two identical and homogeneous plates is h .

The amplitude of the incident F-wave is unity. The parameters A_1, A_2 , etc., are the amplitudes of the other wave components. In all, there are six unknown amplitudes, which must be determined by means of six boundary conditions. The displacements, forces, and moments for the plates are shown in Fig. 5.17.

The displacements in the x - and y -directions must be the same for both plates at the junction. According to the definitions in Fig. 5.17 this means

$$\xi_1 = -w_2, \quad \xi_2 = w_1 \quad \text{for } x = 0 \text{ and } y = 0 \quad (5.107)$$

At the junction, the angle between the plates is assumed to be constant even during bending. This means that the rotation of plate 1 at the junction is equal to the rotation of plate 2. Consequently,

$$\frac{\partial w_1}{\partial x} = \frac{\partial w_2}{\partial y} \quad \text{for } x = 0 \text{ and } y = 0 \quad (5.108)$$

Further, the total bending moment around the junction is zero, or according to the defined directions in Fig. 5.17, which according to Eq. (3.105) is formulated as

$$M'_1 = -D \frac{\partial^2 w_1}{\partial x^2} = -D \frac{\partial^2 w_2}{\partial y^2} = M'_2 \quad \text{for } x = 0 \text{ and } y = 0 \quad (5.109)$$

where D is the bending stiffness per unit width of the plate.

Likewise, the sum of the forces per unit width acting in the x - and y -directions, respectively, must be zero, or from Fig. 5.17

$$F'_{1x} + F'_{2x} = 0, \quad F'_{1y} = F'_{2y} \quad \text{for } x = 0 \text{ and } y = 0 \quad (5.110)$$

The forces per unit width of the plate are from Eq. (3.118) obtained as

$$\begin{aligned} F'_{1x} &= \frac{hE}{1 - \nu^2} \frac{\partial \xi_1}{\partial x} \\ F'_{2x} &= -D \frac{\partial^3 w_2}{\partial y^3} \\ F'_{1y} &= -D \frac{\partial^3 w_1}{\partial x^3} \\ F'_{2y} &= \frac{hE}{1 - \nu^2} \frac{\partial \xi_2}{\partial y} \end{aligned} \quad (5.111)$$

In all, there are six boundary conditions and six unknown parameters. It is straight forward but somewhat cumbersome to determine the amplitudes. As suggested in Ref. [31] it is convenient to introduce the parameter β as

$$\beta = \frac{D\kappa^3(1 - \nu^2)}{Ehk} = \frac{c_b}{c_l} = \left[\frac{\rho\omega^2 h^2(1 - \nu^2)}{12E} \right]^{1/4} \quad (5.112)$$

The parameter β is equal to the ratio between the phase velocities for bending and longitudinal waves. The wave fields and boundary conditions above have been derived assuming that the plates are thin or $\kappa h < 1$. This requirement is equivalent to $\beta < 1/\pi$.

After some algebraic exercises the amplitudes can be expressed as

$$\begin{aligned} A_1 &= \frac{\beta - i(1 - \beta^2)}{1 - \beta^2 + i(1 + 3\beta + \beta^2)} \\ A_4 &= \frac{1 - \beta^2 + 2i\beta}{1 - \beta^2 + i(1 + 3\beta + \beta^2)} \\ A_2 &= \frac{\beta - 1 - A_1(1 + \beta)}{1 + i\beta} \\ A_3 &= A_4 \frac{\beta(1 - i)}{1 + i\beta} \\ A_5 &= -A_4 \frac{1 + \beta}{1 + i\beta} \\ A_6 &= \frac{\beta + i\beta - A_1(\beta - i\beta)}{1 + i\beta} \end{aligned} \quad (5.113)$$

The energy flow per unit width of the plate is for F-waves given in Eq. (3.138). The corresponding flow caused by the L-waves is defined in Eq. (3.139). The time averages of the energy flows are per unit width given by

F-waves

$$\begin{aligned}
\text{Incident} \quad & \bar{\Pi}'_{\text{fin}} = \omega D_0 \kappa_0^3 \\
\text{Reflected} \quad & \bar{\Pi}'_{\text{fre}} = \omega D_0 \kappa_0^3 |A_1|^2 = \rho_{\text{ff}} \cdot \bar{\Pi}_{\text{fin}} \\
\text{Transmitted} \quad & \bar{\Pi}'_{\text{ftr}} = \omega D_0 \kappa_0^3 |A_4|^2 = \tau_{\text{ff}} \cdot \bar{\Pi}_{\text{fin}}
\end{aligned} \tag{5.114a}$$

L-waves

$$\begin{aligned}
\text{Reflected} \quad & \bar{\Pi}'_{\text{lre}} = \frac{\omega k_{10} E_0 h}{2(1 - \nu^2)} |A_3|^2 = \rho_{\text{fl}} \cdot \bar{\Pi}_{\text{fin}} \\
\text{Transmitted} \quad & \bar{\Pi}'_{\text{ltr}} = \frac{\omega k_{10} E_0 h}{2(1 - \nu^2)} |A_6|^2 = \tau_{\text{fl}} \cdot \bar{\Pi}_{\text{fin}}
\end{aligned} \tag{5.114b}$$

The parameter ρ_{ff} can be termed as the reflection coefficient with respect to the incident energy flow. The subscripts ff indicate that the reflection is from an F-wave to an F-wave. The corresponding transmission coefficient is denoted τ_{ff} , etc. According to the definitions Eqs. (5.112) and (5.114) the various transmission and reflection coefficients can be written as

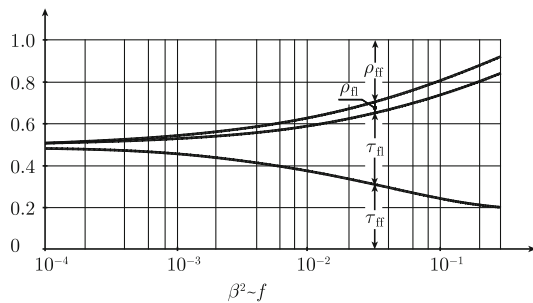
$$\rho_{\text{ff}} = |A_1|^2, \quad \tau_{\text{ff}} = |A_4|^2, \quad \rho_{\text{fl}} = |A_3|^2 / (2\beta), \quad \tau_{\text{fl}} = |A_6|^2 / (2\beta) \tag{5.115}$$

Considering the conservation of energy, it follows that

$$\rho_{\text{ff}} + \tau_{\text{ff}} + \rho_{\text{fl}} + \tau_{\text{fl}} = 1$$

In Fig. 5.18 the transmission and reflection coefficients are shown as functions of β . The parameters are calculated for the case that the plates are equal. If the average velocity levels of the two plates are compared the error if the energy flow carried by L-waves is neglected is less than 0.5 dB for frequencies below 3150 Hz for 3 mm steel plates. The corresponding frequency limits for 6 and 12 mm steel plates are 1600 and 800 Hz, respectively.

Fig. 5.18 Energy distribution between reflected and transmitted waves caused by an incident flexural wave incident on an L junction shown in Fig. 5.1. From Ref. [31]



For decreasing frequencies, β approaches zero. For this limit, the incident energy flow is equally transmitted and reflected as flexural waves—no longitudinal waves are induced. This means that the junction between the plates only rotates—no translatory motion takes place. For increasing frequencies, the importance of the longitudinal waves increases. If however, it is assumed that the junction can only rotate, i.e., the incident F-wave is only reflected and transmitted as F-waves, then $\rho_{ff} = \tau_{ff} = 0.5$ independently of frequency. The error due to this simplification can be fairly small, in particular, if the velocity levels measured perpendicular to the plate surfaces are compared. The error for the velocity level difference is less than 1 dB if instead of $\rho_{ff} = \tau_{ff} = 0.5$ these parameters are equal to 0.4. An error of less than 1 dB is obtained as long as $\beta^2 < 6/1000$ or whenever the plate parameters or frequency satisfy the inequality $hf/\sqrt{E_0/\rho} < 2/1000$ given by Eq. (5.112).

The transmission of flexural waves across a junction between thin plates can, in the low-frequency region, be sufficiently well described even assuming no translatory motion of the junction. By making this assumption, the complexity of the calculations is drastically reduced without incurring unnecessarily large errors. This conclusion is based on results obtained for a junction freely suspended in space. For real built-up structures, all junctions are part of an assembly of structural elements. The translatory motion of a junction, which is part of a large structure, is therefore very restricted. For the prediction of energy flow across junctions between thin plates, it is reasonable to assume that the junction only is allowed to rotate. This is a valid approximation in the low-frequency region. This approach much simplifies any calculation procedure.

If the incident flexural wave is not traveling perpendicular to the junction then in order to satisfy the boundary conditions allowing translatory motion, transverse waves must also be included. This will naturally increase the complexity of the problem considerably. Examples are given in Refs. [31, 49] for a number of plate configurations. Transmission across junctions between plates or beams at angles different from 90° are discussed in Ref. [49]. However, if the junction is such that its translatory motion can be neglected then not only longitudinal but also transverse waves can be neglected assuming an incident F-wave.

However, the important conclusion is that an F-wave or an inplane wave, which is incident on a junction allowing translatory motion, generates reflected and transmitted F and inplane waves.

5.8 Transmission of F-Waves Across Junctions, Diffuse Incidence

The method outlined in the previous section can be used to calculate the transmission across most types of junctions between flat infinite plates. Although valid for semi-infinite plates, the transmission coefficients so derived can be of great importance for estimating the energy balance between finite coupled plates. One such procedure is the statistical energy analysis (SEA) technique.

For a complete description of the energy flow across a junction, all wave types must be considered. For certain, special cases like normal incidence simplifications can be made. However, as demonstrated in the previous section, the transmission of flexural waves across a junction between thin plates can, in the low frequency region, be sufficiently well described even assuming no translatory motion of the junction.

As an example of this procedure, neglecting inplane waves, consider two thin, semi-infinite, and flat plates joined together as shown in Fig. 5.19. A plane flexural wave is incident on the junction. The angle of incidence is α . The translatory motion of the junction is neglected. Reflected and transmitted inplane waves are therefore excluded. The energy transmission across the junction is caused by the bending moment and the rotation around the junction. Both these quantities are independent of the angle between the plates. In the example, the plates are in the same plane. However, considering the assumptions the results derived are also valid for an L-junction or for any angle between the two semi-infinite plates. The example is illustrated in Fig. 5.19. The plates are in the x - y -plane. The junction is along the line $x = 0$. The thickness, bending stiffness, and mass per unit area is for plate 1 given by h_1 , D_1 and μ_1 . The wavenumber for flexural waves is $\kappa_1 = (\mu_1 \omega^2 / D_1)^{1/4}$. For the other plate, the corresponding quantities have the subscript 2.

A flexural wave with unit amplitude is in plate 1 propagating toward the junction as shown in Fig. 5.19. The angle of incidence is α . The wave is given by

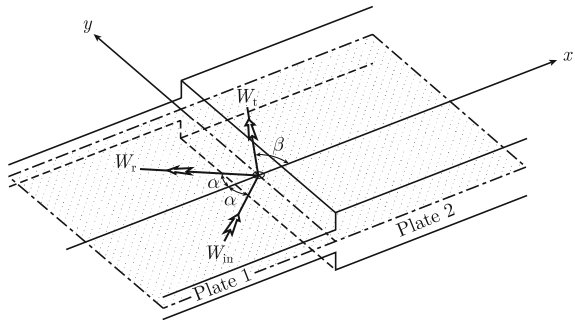
$$w_{\text{in}}(x, y, t) = \exp[i(\omega t - \kappa_1 x \cos \alpha - \kappa_1 y \sin \alpha)] \quad (5.116)$$

The lateral displacement w_{in} satisfies Eq. (3.115) governing the bending of thin plates. The reflected field with amplitude R must be of the form

$$w_{\text{re}}(x, y, t) = R \cdot \exp[i(\omega t + \lambda_1 x \cos \alpha - \kappa_1 y \sin \alpha)]$$

The y -dependence is the same as for the incident wave to satisfy all boundary conditions for any y along the junction $x = 0$. The reflected field must satisfy the wave Eq. (3.115) giving

Fig. 5.19 Two thin semi-infinite plates joined along $x = 0$. A plane F-wave, angle of incidence α , propagates toward the junction



$$(\lambda_1 \cos \alpha)^4 + 2\lambda_1^2 \kappa_1^2 (\sin \alpha \cdot \cos \alpha)^2 + (\kappa_1 \sin \alpha)^4 - \kappa_1^4 = 0$$

The solutions are

$$\lambda_1 = \pm \kappa_1, \quad \lambda_1 = \pm i \kappa_1 \frac{\sqrt{1 + \sin^2 \alpha}}{\cos \alpha}$$

The first two solutions correspond to propagating waves and the last two to near-field solutions. For waves reflected toward the negative x -axis, the positive signs must be chosen in each case. The reflected field is thus composed of the two solutions as

$$\begin{aligned} w_{\text{re}} = & \exp[i(\omega t - \kappa_1 y \sin \alpha)] \cdot [R \cdot \exp(i \kappa_1 x \cos \alpha) \\ & + Q_1 \cdot \exp(\kappa_1 x \sqrt{1 + \sin^2 \alpha})] \end{aligned} \quad (5.117)$$

where R is the amplitude of the reflected propagating wave and Q_1 is the amplitude corresponding to the near-field solution. The total field in plate 1 is thus

$$\begin{aligned} w_1 = & w_{\text{in}} + w_{\text{re}} \\ = & \exp[i(\omega t - \kappa_1 y \sin \alpha)] \cdot [\exp(-i \kappa_1 x \cos \alpha) \\ & + R \cdot \exp(i \kappa_1 x \cos \alpha) + Q_1 \cdot \exp(\kappa_1 x \sqrt{1 + \sin^2 \alpha})] \end{aligned} \quad (5.118)$$

In a similar way the displacement of plate 2 is, following the notations in Fig. 5.19, given by

$$\begin{aligned} w_2 = & \exp[i(\omega t - \kappa_2 y \sin \beta)] \cdot [T \exp(-i \kappa_2 x \cos \beta) \\ & + Q_2 \cdot \exp(-\kappa_2 x \sqrt{1 + \sin^2 \beta})] \end{aligned} \quad (5.119)$$

Any boundary condition must be satisfied for any y along the junction $x = 0$. This implies that the y -dependence of the functions w_1 and w_2 must be the same, meaning that

$$\kappa_1 \cdot \sin \alpha = \kappa_2 \cdot \sin \beta \quad (5.120)$$

A similar condition was discussed in Sect. 4.3, Eqs. (4.19) and (4.21), in connection with the derivation of coupling effects between longitudinal and transverse waves. From Eq. (5.120), it follows that the angle β , defining the direction of the transmitted wave, is a function of the angle of incidence α and the wavenumbers κ_1 and κ_2 . The x -component of the wavenumber for the transmitted wave is given by the condition (5.120) as

$$\kappa_{2x} = \kappa_2 \cos \beta = \kappa_2 \sqrt{1 - \sin^2 \beta} = \kappa_2 \sqrt{1 - (\kappa_1 / \kappa_2)^2 \sin^2 \alpha} \quad (5.121)$$

As shown in Fig. 5.20, for $\sin \alpha > (\kappa_2 / \kappa_1)$ the x -component κ_{2x} is imaginary resulting in that no waves are propagating away from the junction in plate 2. The

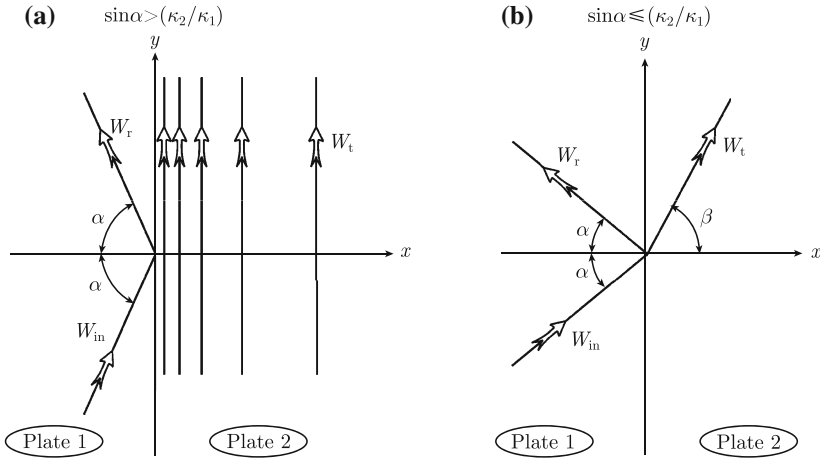


Fig. 5.20 Transmission and reflection at the junction shown in Fig. 5.19 for **a** $|\sin \alpha| > (\kappa_2/\kappa_1)$ and **b** $|\sin \alpha| \leq (\kappa_2/\kappa_1)$

resulting displacement of plate 2 is for $\sin \alpha > (\kappa_2/\kappa_1)$ determined by two wave fields. The amplitude of these waves are both decaying exponentially as the distance to the junction is increased. Both wave fields represent near-field solutions. For $\sin \alpha > (\kappa_2/\kappa_1)$ the displacement of plate 2 is obtained from Eqs. (5.119) and (5.121) as

$$\begin{aligned}
 w_2 = & \exp[i(\omega t - \kappa_2 y \sin \beta)] \\
 & \times \left\{ T \exp \left[-\kappa_2 x \sqrt{(\kappa_1/\kappa_2)^2 \sin^2 \alpha - 1} \right] \right. \\
 & \left. + Q_2 \cdot \exp \left[-\kappa_2 x \sqrt{(\kappa_1/\kappa_2)^2 \sin^2 \alpha + 1} \right] \right\} \quad (5.122)
 \end{aligned}$$

The amplitudes R , T , Q_1 , and Q_2 are determined from the boundary conditions between the plates. The amplitude of the incident wave is unity. Assuming only rotation around the junction, thus neglecting any translatory motion, the angle between the plates being fixed during rotation, the boundary conditions for $x = 0$ are formulated as

$$w_1 = 0, \quad w_2 = 0, \quad \frac{\partial w_1}{\partial x} = \frac{\partial w_2}{\partial x}, \quad M'_{y1} = M'_{y2} \quad (5.123)$$

The bending moments M'_{y1} and M'_{y2} are according to Eq. (3.130) given by

$$M'_{y1} = -D_1 \left(\frac{\partial^2 w_1}{\partial x^2} + \nu \frac{\partial^2 w_1}{\partial y^2} \right), \quad M'_{y2} = -D_2 \left(\frac{\partial^2 w_2}{\partial x^2} + \nu \frac{\partial^2 w_2}{\partial y^2} \right)$$

Since $w_1 = w_2$ along the junction it follows that $\partial^2 w_n / \partial y^2$ is zero for both plates. The condition $M'_{y1} = M'_{y2}$ for $x = 0$ is thus equivalent to

$$D_1 \left(\frac{\partial^2 w_1}{\partial x^2} \right) = D_2 \left(\frac{\partial^2 w_2}{\partial x^2} \right) \quad (5.124)$$

The boundary conditions (5.123) give four equations to solve the four unknown amplitudes R , T , Q_1 , and Q_2 . These amplitudes are the solutions to

$$1 + R + Q_1 = 0, \quad T + Q_2 = 0$$

$$\begin{aligned} & \kappa_1 (\cos \alpha - R \cdot \cos \alpha + i Q_1 \cdot \sqrt{1 + \sin^2 \alpha}) \\ &= \kappa_2 \cdot [T \sqrt{1 - (\kappa_1 / \kappa_2)^2 \sin^2 \alpha} - i Q_2 \cdot \sqrt{1 + (\kappa_1 / \kappa_2)^2 \sin^2 \alpha}], \\ & D_1 \kappa_1^2 [\cos^2 \alpha (1 + R) - Q_1 \cdot (1 + \sin^2 \alpha)] \\ &= D_2 \kappa_2^2 \left\{ T \left[1 - \left(\frac{\kappa_1 \sin \alpha}{\kappa_2} \right)^2 \right] + Q_2 \left[1 + \left(\frac{\kappa_1 \sin \alpha}{\kappa_2} \right)^2 \right] \right\} \end{aligned}$$

By introducing

$$\begin{aligned} Y &= \frac{D_2 \kappa_2^2}{D_1 \kappa_1^2} \\ Z &= \frac{\kappa_2}{\kappa_1} \\ U_1 &= \sqrt{Z^2 + \sin^2 \alpha} + Y \sqrt{1 + \sin^2 \alpha} \\ U_2 &= \sqrt{Z^2 - \sin^2 \alpha} + Y \cos \alpha \\ U_3 &= \sqrt{Z^2 - \sin^2 \alpha} - Y \cos \alpha \end{aligned} \quad (5.125)$$

the resulting amplitudes are

$$\begin{aligned} T &= -\frac{2i \cos \alpha}{U_1 - i U_2} \\ R &= \frac{U_1 - i U_3}{U_1 - i U_2} \\ Q_1 &= -(1 + R) \\ Q_2 &= -T \end{aligned} \quad (5.126)$$

The time average of the energy flow per unit width of the plate along the path of the incident wave is from Eq. (3.91) obtained as $\bar{\Pi}'_{\text{in}} = \omega D_1 \kappa_1^3$. The reflected energy flow in the direction of the reflected wave is $\bar{\Pi}'_{\text{re}} = \omega D_1 \kappa_1^3 |R|^2$. The transmitted energy flow in the direction defined by β is $\bar{\Pi}'_{\text{tr}} = \omega D_2 \kappa_2^3 |T|^2$. The exponentially decaying fields give no contribution to the energy flow as discussed in Sect. 3.7. The x -components of the energy flows per unit width of the plate are for $Z > \sin \alpha$

$$\begin{aligned}
\bar{\Pi}'_{\text{xin}} &= \omega D_1 \kappa_1^3 \cos \alpha \\
\bar{\Pi}'_{\text{xre}} &= -\omega D_1 \kappa_1^3 |R|^2 \cos \alpha \\
\bar{\Pi}'_{\text{xtr}} &= \omega D_2 \kappa_2^3 |T|^2 \cos \beta = \omega D_2 \kappa_2^3 |T|^2 \sqrt{Z^2 - \sin^2 \alpha}
\end{aligned}$$

For $Z < \sin \alpha$ no waves propagate out from the junction in plate 2 and there is no energy flow in the x -direction in plate 2. The energy flow incident on the junction is reflected completely, rendering the absolute value of R to equal unity. Compare Problem 5.10. The energy flows per unit width are for $Z < |\sin \alpha|$

$$\bar{\Pi}'_{\text{xin}} = -\bar{\Pi}'_{\text{xre}} = \omega D_1 \kappa_1^3 \cos \alpha, \quad \bar{\Pi}'_{\text{xtr}} = 0 \quad (5.127)$$

Note that the reflected energy flow is written as negative quantity since it is propagating along the negative x -axis. For a flexural wave propagating toward a junction with the angle of incidence α , part of the incident energy flow can be transmitted. This transmitted flow is

$$\bar{\Pi}'_{\text{tr}} = \bar{\Pi}'_{\text{in}} + \bar{\Pi}'_{\text{re}} = \bar{\Pi}'_{\text{in}} (1 - |R|^2) = \bar{\Pi}'_{\text{in}} \cdot \tau(\alpha) \quad (5.128)$$

where $\tau(\alpha)$ is the transmission coefficient for a flexural wave propagating toward a junction with an angle of incidence α . Thus for $Z < \sin \alpha$, Eqs. (5.125) and (5.126) yield

$$\tau(\alpha) = (1 - |R|^2) = |T|^2 Y Z \cos \beta / \cos \alpha = |T|^2 Y \sqrt{(Z^2 - \sin^2 \alpha)} / \cos \alpha \quad (5.129)$$

The derivation of the last part of the expression is left for Problem 5.11. The transmission coefficient $\tau(\alpha)$ is also equal to the ratio $\bar{\Pi}'_{\text{xtr}}/\bar{\Pi}'_{\text{xin}}$. For $Z < \sin \alpha$, $\tau(\alpha) = 0$ as given by Eq. (5.127).

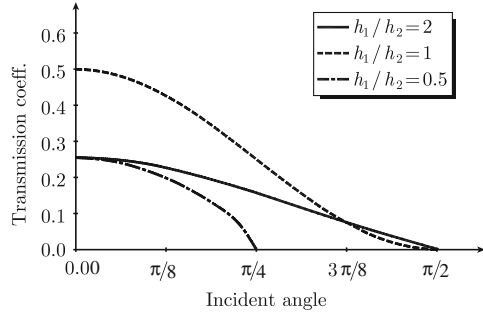
For illustrating the transmission across a junction shown in Fig. 5.19, allow the material parameters for the two plates to be the same, the thickness of plate 1 being h_1 and of plate $2h_2$. For this particular case, the parameters Y and Z are

$$Z = \sqrt{\frac{h_1}{h_2}}, \quad Y = \left(\frac{h_2}{h_1}\right)^2 \quad \text{for } E_1 = E_2, \rho_1 = \rho_2 \text{ and } \nu_1 = \nu_2$$

In Fig. 5.21, the transmission coefficient $\tau(\alpha)$ is shown for three ratios between the plate thicknesses or for h_1/h_2 equal to 2, 1, and 1/2. For $h_1/h_2 = 1/2$ there is no energy flow across the junction if $\sin \alpha > Z = \sqrt{1/2}$ or if $\alpha > \pi/4$. In all three cases, the transmission has a maximum at normal incidence. The transmission coefficient is steadily decreasing for increasing angles of incidence.

Two cases relating to normal incidence and to a diffuse incident field are of special interest. The first case, $\alpha = 0$, corresponds to the transmission across a junction between two beams. As before in this section, the translatory motion of the junction

Fig. 5.21 Transmission coefficient as function of angle of incidence for problem shown in Fig. 5.19. The transmission coefficient is given for three ratios between the plate thicknesses



is neglected. For the two legs, being of the same material and width but with the thicknesses h_1 and h_2 the transmission coefficient is for $\alpha = 0$ obtained from Eqs. (5.126) and (5.129) as

$$\tau(0) = \frac{2Z^5}{(Z^5 + 1)^2} \quad \text{for } Z = \sqrt{\frac{h_1}{h_2}} \quad (5.130)$$

It is convenient to introduce the parameter R as

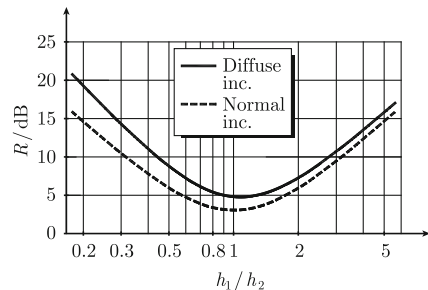
$$R = 10 \log(\bar{\Pi}'_{\text{xin}}/\bar{\Pi}'_{\text{xtr}}) = 10 \log(1/\tau) \quad (5.131)$$

The parameter R is equal to the level difference between the incident and transmitted energy flow across the junction. The transmission coefficient $\tau(0)$ or rather $R_0 = 10 \log[1/\tau(0)]$ is shown in Fig. 5.22 as function of the ratio h_1/h_2 . The transmission coefficient is symmetric with respect to $Z = 1$ implying that the transmission across the junction is the same whether the incident wave travels in plate 1 or 2 assuming the energy flow of the incident wave to be the same in both cases.

In a diffuse field, it is assumed that the intensity or energy flow is the same in every direction or for any α , i.e., $\bar{\Pi}'_{\text{in}}(\alpha) = \bar{\Pi}'$ where $\bar{\Pi}'$ is a constant. The energy flow out from the junction in plate 2 is

$$\bar{\Pi}'_{\text{xtr}} = \bar{\Pi}'_{\text{tr}} \cdot \cos \beta = \bar{\Pi}'_{\text{in}} \cdot \cos \alpha \cdot \tau(\alpha) = \bar{\Pi}' \cdot \cos \alpha \cdot \tau(\alpha)$$

Fig. 5.22 Level difference between incident and transmitted energy flow for two cases: normal incidence and diffuse incidence. Flexural waves only. Plate configuration shown in Fig. 5.19



The total transmitted flow per unit area is for diffuse incidence

$$\int_0^{\pi/2} \bar{\Pi}'_{xtr} d\alpha = \int_0^{\pi/2} \bar{\Pi}' \cdot \cos \alpha \cdot \tau(\alpha) d\alpha = \int_0^{\pi/2} \bar{\Pi}' \cdot \cos \alpha \cdot \tau_d \cdot d\alpha \quad (5.132)$$

The transmission coefficient averaged over all angles of incidence is introduced as τ_d and is from Eq. (5.132) given by

$$\tau_d = \left(\int_0^{\pi/2} \tau(\alpha) \cos \alpha \cdot d\alpha \right) / \left(\int_0^{\pi/2} \cos \alpha \cdot d\alpha \right) = \int_0^{\pi/2} \tau(\alpha) \cos \alpha \cdot d\alpha \quad (5.133)$$

The average transmission coefficient τ_d through $R = 10 \log(1/\tau_d)$ as well as $R_0 = 10 \log[1/\tau(0)]$ corresponding to normal incidence are shown in Fig. 5.22 as functions of the ratio h_1/h_2 . The coefficient $\tau(0)$ is symmetric around $h_1/h_2 = 1$. For an L-junction between two identical plates, the transmission coefficient is $\tau(\alpha) = \cos^2 \alpha/2$. According to Eq. (5.133), the average transmission coefficient for diffuse incidence is $\tau_d = 1/3$. Defining the average transmission coefficient from plate 1 to 2 as τ_{d12} and from plate 2 to 1 as τ_{d21} these are related as

$$\tau_{d12} \cdot \left(\frac{\rho_1}{E_1 h_1^2} \right)^{1/4} = \tau_{d21} \cdot \left(\frac{\rho_2}{E_2 h_2^2} \right)^{1/4} \quad (5.134)$$

This asymmetry for a diffuse incident field is in fact a condition necessary for ensuring reciprocity with respect to energy for two plates coupled by a junction. For one-dimensional structures, reciprocity is achieved for transmission coefficients being symmetric with respect to the ratio h_1/h_2 . This is discussed in more detail in a subsequent chapter on energy methods. For finite plates, a field incident on a junction can never be completely diffuse. In addition, the modeling of a junction is incomplete since generally, certain approximations are made. It can therefore be argued, as in Ref. [31], that for many engineering purposes it is sufficient to use a transmission coefficient determined for normal incidence. The energy flow across a junction will in this way be slightly overestimated while reducing the complexity of the calculations.

5.9 Transmission of F-Waves Across Junctions, Normal Incidence

The method outlined in Sect. 5.8 can be used to calculate the transmission of flexural waves across various types of junctions. A number of examples are presented in Refs. [31, 49, 67]. Three results from Ref. [31] are presented in the Figs. 5.23, 5.24 and 5.25. The results are based on the following assumptions:

Fig. 5.23 Attenuation of flexural waves across an L-junction. Longitudinal waves not included. From Ref. [31]

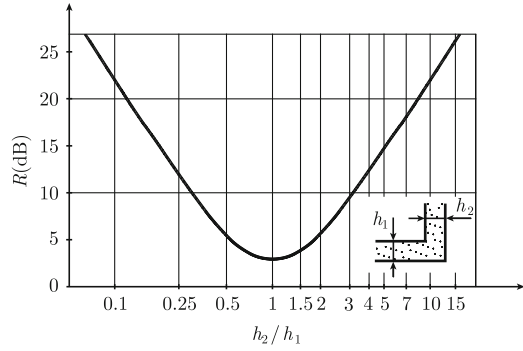


Fig. 5.24 Attenuation of flexural waves across a T-junction. L-waves not included. From Ref. [31]

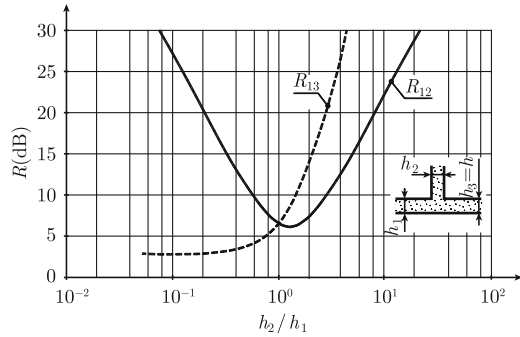
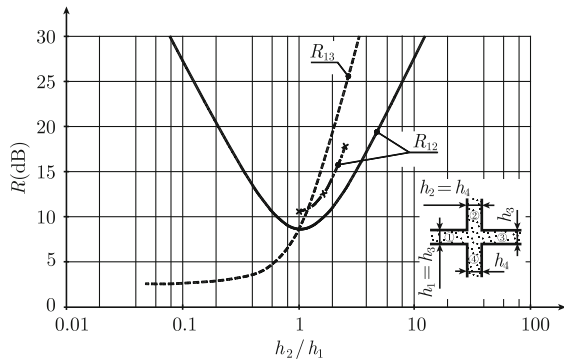


Fig. 5.25 Attenuation of flexural waves across an X-junction. L-waves not included, Ref. [31]. The inserted curve is valid for random incidence, Ref. [67]



- (i) the plates are thin, semi-infinite, and made of the same material;
- (ii) the incident wave is an F-wave traveling perpendicular toward the junction;
- (iii) longitudinal waves are neglected, i.e., no translatory motion of the junction.

The attenuation R_{ij} given in the figures is defined as:

$$R_{ij} = 10 \log(\bar{\Pi}'_i / \bar{\Pi}'_j) (\text{dB}) \quad (5.135)$$

where $\bar{\Pi}'_i$ is the time average of the incident energy flow per unit width of the plate and $\bar{\Pi}'_j$ the time average of the transmitted energy flow per unit width to plate j . If the plates are of equal thickness, the attenuation over an L-junction is 3 dB, over a T-junction 6.5 dB and over an X-junction 9 dB. Since the translatory motion of the junction is neglected, the angles between the plate elements are of no consequence for the results.

It is very straight forward to determine the attenuation across a junction consisting of n semi-infinite identical plates. It is assumed that a flexural wave propagates in one plate toward the junction. The angle of incidence is normal to the junction. Only rotation is allowed at the junction. Consequently, longitudinal waves are neglected. The angles between the plates can be arbitrary but constant during rotation of the junction. If the incident wave is propagating in element i , the attenuation of the energy flow to any of the other plates j is obtained as

$$R_{ij} = 10 \log(n^2/2)(\text{dB})$$

The details are left to Problem 5.3.

5.10 Attenuation Due to Change of Cross Section

Any type of wave traveling in a beam or plate is partly reflected and transmitted, if there is a discontinuity in the structure. A junction between structures is one type of discontinuity. Another could be created by a change of cross section.

The effect of changing the cross section of a beam is illustrated by considering two beams joined together as shown in Fig. 5.26. The beams are of the same material with the modulus of elasticity E and density ρ . The beams have the same width but different thicknesses— h_1 and h_2 for beam 1 and 2, respectively. An incident F-wave of amplitude 1 travels in beam 1 toward the junction is described by

$$w_{in} = \exp[i(\omega t - \kappa_1 x)]$$

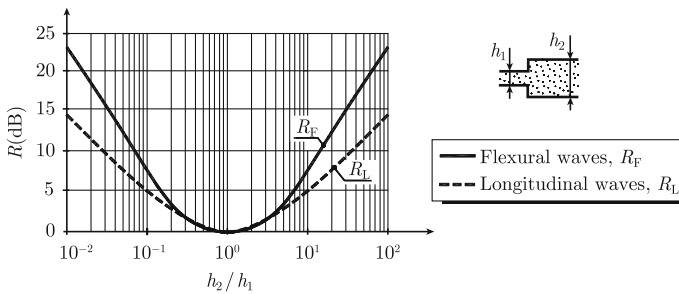


Fig. 5.26 Attenuation due to change of cross section area. From Ref. [31]

where κ_1 is the wave number for flexural waves traveling in beam 1. The incident F-wave does not create any force in the direction of the beam. Consequently, only F-waves are transmitted and reflected. Despite the difference in thickness between the beams, it is assumed that the bending moment caused by one beam at the junction, is uniformly transferred to the second beam across the entire junction.

The reflected F-wave must be of the form

$$w_{\text{re}} = \left(A_1 \cdot e^{i\kappa_1 x} + A_2 \cdot e^{\kappa_1 x} \right) \cdot e^{i\omega t}$$

The total field in beam 1 is thus

$$w_1 = \left(e^{-i\kappa_1 x} + A_1 \cdot e^{i\kappa_1 x} + A_2 \cdot e^{\kappa_1 x} \right) \cdot e^{i\omega t} \quad (5.136)$$

The transmitted F-wave is given by

$$w_2 = \left(A_3 \cdot e^{-i\kappa_2 x} + A_4 \cdot e^{-\kappa_2 x} \right) \cdot e^{i\omega t} \quad (5.137)$$

The wave number for F-waves in plate 2 is given by κ_2 .

At the junction, $x = 0$, there must be continuity with respect to displacement and rotation. The junction can be displaced. Further, the bending moments and forces at the ends of the beams must be equal. The boundary conditions at $x = 0$ are

$$\begin{aligned} w_1 &= w_2, \quad \frac{\partial w_1}{\partial x} = \frac{\partial w_2}{\partial x}, \quad M_1 = -D'_1 \frac{\partial^2 w_1}{\partial x^2} = -D'_2 \frac{\partial^2 w_2}{\partial x^2} = M_2 \\ F_{1y} &= -D'_1 \frac{\partial^3 w_1}{\partial x^3} = -D'_2 \frac{\partial^3 w_2}{\partial x^3} = F_{2y} \end{aligned} \quad (5.138)$$

The resulting system of equations is

$$\begin{aligned} 1 + A_1 + A_2 &= A_3 + A_4 \\ -i\kappa_1(1 - A_1 + iA_2) &= -i\kappa_2(A_3 - iA_4) \\ D'_1 \kappa_1^2(1 + A_1 - A_2) &= D'_2 \kappa_2^2(A_3 - A_4) \\ -iD'_1 \kappa_1^3(1 - A_1 - iA_2) &= -iD'_2 \kappa_2^3(A_3 + iA_4) \end{aligned} \quad (5.139)$$

The bending stiffness and the wave number are functions of the beam thickness. It is readily shown that with $\vartheta^4 = h_1/h_2$ the ratios between wave numbers, etc., can be written as

$$\frac{\kappa_1}{\kappa_2} = \frac{1}{\vartheta^2}, \quad \frac{D'_1 \kappa_1^2}{D'_2 \kappa_2^2} = \vartheta^8, \quad \frac{D'_1 \kappa_1^3}{D'_2 \kappa_2^3} = \vartheta^6 \quad (5.140)$$

The time average of incident and reflected energy flows, $\bar{\Pi}_{\text{in}}$ and $\bar{\Pi}_{\text{tr}}$ are, according to Eq. (3.91) equal to

$$\bar{\Pi}_{\text{in}} = \omega D'_1 \kappa_1^3, \quad \bar{\Pi}_{\text{tr}} = \omega D'_2 \kappa_2^3 |A_3|^2$$

The attenuation in dB of the energy flow due to a change of cross section, is

$$R = 10 \log (\bar{\Pi}_{\text{in}} / \bar{\Pi}_{\text{tr}}) = 10 \log \left(\vartheta^6 / |A_3|^2 \right) \quad (5.141)$$

After some effort the result is written

$$R = 20 \log \left(\frac{1}{2} \cdot \frac{1/\vartheta^8 + 2/\vartheta^2 + 2 + 2\vartheta^2 + \vartheta^8}{1/\vartheta^5 + 1/\vartheta^3 + \vartheta^3 + \vartheta^5} \right) \text{ (dB)} \quad (5.142)$$

The resulting attenuation R is fairly small. For $\vartheta^4 = h_1/h_2 = 2$ or 0.5 , R is 0.14 dB. For $h_1/h_2 = 10$ or 0.1 , the corresponding attenuation over the area jump is 3.6 dB. The area change must therefore be considerable, in order to cause any appreciable attenuation.

If instead of an F-wave, the incident wave is an L-wave, both the reflected and transmitted waves are L-waves. The reason is that there is no bending moment around the junction to excite any F-waves. The junction is not fixed.

The L-waves in beam 1—an incident with the amplitude 1 and a reflected with the amplitude B_1 —are described by

$$\xi_1 = \left(e^{-ikx} + B_1 \cdot e^{ikx} \right) \cdot e^{i\omega t} \quad (5.143)$$

The wave number for longitudinal waves is given by k . The transmitted wave in beam 2 is

$$\xi_2 = B_2 \cdot e^{i(\omega t - kx)} \quad (5.144)$$

The wave number k is the same for both beams, as long as the beams are made of the same material. The displacements in the beams are the same at the junction. Thus

$$\xi_1 = \xi_2 \text{ for } x = 0 \quad (5.145)$$

This is a simplification, since it can be expected that the vertical end section of the thicker beam is slightly deformed, by the pressure from the thinner beam. However, this is only a secondary effect, which is of no consequence in the low-frequency range. The total force in the x -direction on beam 2 should be equal to the force acting on beam 1 or for $x = 0$

$$bh_1 E \frac{\partial \xi_1}{\partial x} = bh_2 E \frac{\partial \xi_2}{\partial x} \quad (5.146)$$

Both beams having the width b . There are two unknown parameters and two boundary conditions. The resulting system of equations is

$$1 + B_1 = B_2, \quad h_1(1 - B_1) = h_2 B_2$$

From these expressions, the amplitude of the transmitted wave becomes

$$B_2 = 2h_1/(h_1 + h_2)$$

According to (3.58), the time average of the incident and transmitted energy flows are

$$\bar{\Pi}_{\text{in}} = \frac{bh_1\omega k_0 E_0}{2}, \quad \bar{\Pi}_{\text{tr}} = \frac{bh_2\omega k_0 E_0 |B_2|^2}{2}$$

The attenuation over the area jump is for L-waves

$$R = 10 \log (\bar{\Pi}_{\text{in}}/\bar{\Pi}_{\text{tr}}) = 10 \log \left[\frac{(h_1 + h_2)^2}{4h_1h_2} \right] \quad (5.147)$$

For h_1/h_2 equals 2 or 0.5, R is 0.5 dB and for $h_1/h_2 = 10$ or 0.1 the attenuation is 4.8 dB. These values are slightly lower than the corresponding values obtained for the case with the incident F-wave as shown in Fig. 5.26. The attenuation due to an area jump is fairly modest even if the ratio between the areas of the two cross sections is considerable.

5.11 Some Other Methods to Increase Attenuation

It is often desirable to increase the attenuation of structure-borne sound in the propagation path between a source and receiver. One method is to use elastic interlayers in the structure as shown in Fig. 5.27. The predicted attenuation—from Ref. [31]—of an incident L-wave and an incident F-wave are also given in the figure.

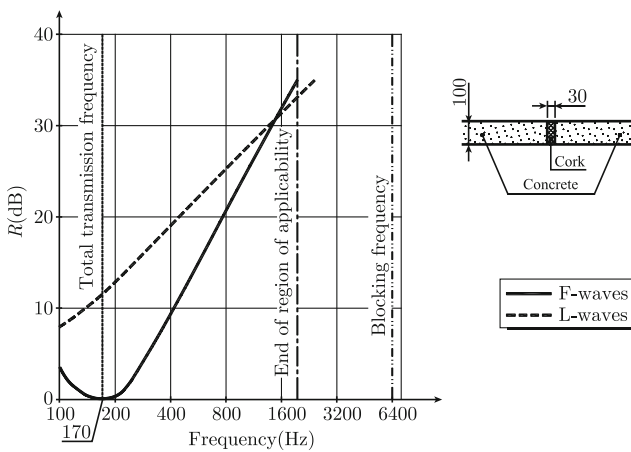


Fig. 5.27 Attenuation due to an elastic interlayer. From Ref. [31]

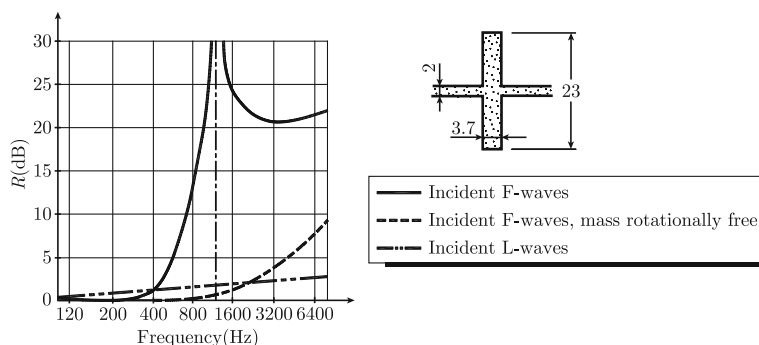


Fig. 5.28 Transmission loss due to a rib. From Ref. [31]

The attenuation depends on the bending stiffness of the adjoining structures and also on the geometries of these and the resilient interlayer. The shear modulus of the material in the gap between the structures is naturally also a very significant parameter. The attenuation of F-waves due to this type of interlayer can be very poor in the important mid-frequency region. A good attenuation is really only achieved in the high-frequency region. Many sources like engines and other rotating machinery are running at a fairly low rpm. The resulting disturbances are therefore concentrated in the low-frequency region. The effect of an elastic interlayer could consequently be moderate. Another disadvantage is that the strength of the construction is decreased due to the inclusion of an elastic interlayer.

An alternative method is to use so-called blocking masses in the transmission path. An example from Ref. [31] is shown in Fig. 5.28. A blocking mass can for certain frequencies attenuate F-waves quite considerably. However, the effect on L-waves is fairly small. The attenuation is determined by the geometries of the blocking mass and the beam or plate to which the mass is attached. The attenuation effect can be calculated as described in Ref. [31]. However, it is always advisable to test a configuration, in either full or model scale, before the device is implemented in a real construction.

5.12 Velocity Level Differences and Transmission Losses

It is often of interest to estimate the velocity level difference between two coupled plates, one of which is being excited. The lateral velocity of a plate or rather its velocity level due to flexural waves is readily measured, whereas the measurement of the energy flow in a plate or beam requires a very elaborate technique as indicated in Sect. 3.11. Returning to the problem concerning coupled semi-infinite plates discussed in Sect. 5.7, the displacement of plate 1 is given in Eq. (5.118) and of plate 2 by Eq. (5.119). The near-field solutions decay rapidly as the distance to the junction

increases. For sufficiently large distances or rather a few wavelengths away from the junction, the contribution from the near-field solutions to the overall velocity level can be neglected. The time average of the velocity squared of plate 1 is

$$|\bar{v}_1|^2 = \frac{\omega^2}{2} \left\{ 1 + |R|^2 + 2 \cdot \text{Re}[R \cdot \exp(2i\kappa x \cdot \cos \alpha)] \right\} \quad (5.148)$$

The expression $\exp(2i\kappa x \cdot \cos \alpha)$ has an average with respect the distance x to the junction which is equal to zero. The distance to the junction should be compared to the wavelength λ of the F-wave. The space average of the velocity squared is for $|x| > 2\lambda$ approximately given by

$$\langle |\bar{v}_1|^2 \rangle \approx \frac{\omega^2}{2} (1 + |R|^2) = \frac{\omega^2}{2} [2 - \tau(\alpha)]$$

The last part of the expression is a consequence of the result (5.129). In a similar way, the space and time averages for $|x| > 2\lambda$ is for plate 2 obtained as

$$\langle |\bar{v}_2|^2 \rangle \approx \frac{\omega^2}{2} |T|^2 = \frac{\omega^2 \cos \alpha \cdot \tau(\alpha)}{2 \cos \beta \cdot Y \cdot Z}$$

If in plate 1 a plane flexural wave, angle of incidence α , propagates toward a junction characterized by a transmission coefficient $\tau(\alpha)$ for flexural waves the resulting average velocity level difference between the coupled plates is

$$\Delta L_v(\alpha) = 10 \log \left(\frac{\langle |\bar{v}_1|^2 \rangle}{\langle |\bar{v}_2|^2 \rangle} \right) = 10 \log \left\{ \frac{[2 - \tau(\alpha)] \cos \beta \cdot Z \cdot Y}{\cos \alpha \cdot \tau(\alpha)} \right\}$$

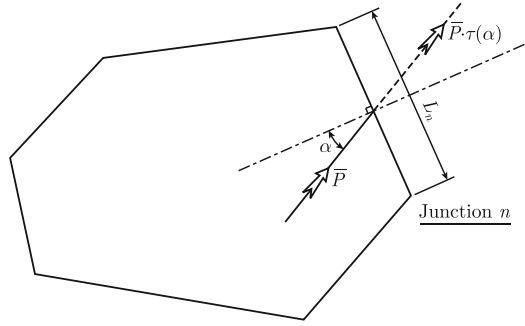
For a diffuse incident field, an integration over all angles of incidence must be performed. Thus

$$\Delta L_v(\text{diffuse}) = 10 \log \left(\frac{\Gamma_1}{\Gamma_2} \right)$$

$$\Gamma_1 = \int_{-\pi/2}^{\pi/2} [2 - \tau(\alpha)] d\alpha, \quad \Gamma_2 = \int_{-\pi/2}^{\pi/2} \frac{\tau(\alpha) \cdot \cos \alpha}{\cos \beta \cdot Z \cdot Y} d\alpha \quad (5.149)$$

For a vibrating plate, there are certain internal losses in the material itself as discussed in Chap. 3 but more importantly, there are also losses at the boundaries due to energy flow from the plate across the junction and to the adjoining plate. These losses at the boundaries can be estimated from the transmission coefficients representing each individual junction of the plate. The energy flow across a junction represents a loss of energy for the plate itself. The transmission coefficient for normal incidence is slightly higher than for a diffuse incident field. One example is shown in Fig. 5.22 where R is given as $10 \log(1/\tau)$ for random and normal incidence. The result shown in Fig. 5.22 implies that the losses for normal incidence tend to be higher than for

Fig. 5.29 Energy flow across junction n of length L_n



random incidence. Thus considering a diffuse incident field on a junction, Fig. 5.29, the time average of the power lost due to the transmission across a junction n of length L_n and with an average transmission coefficient τ_n is, using Eq. (5.133)

$$(\bar{\Pi}_{tr})_n = \int_{-\pi/2}^{\pi/2} \bar{\Pi}' \cdot \tau(\alpha) \cdot \cos \alpha \cdot L_n d\alpha = 2\bar{\Pi}'\bar{\tau}_n L_n \quad (5.150)$$

The energy flow per unit width of the panel is $\bar{\Pi}'$, etc.

The total power lost at all junctions is the sum of the lost power at each junction or

$$\bar{\Pi}_{total} = \sum_n (\bar{\Pi}_{tr})_n = \sum_n 2\bar{\Pi}'\bar{\tau}_n L_n \quad (5.151)$$

For a plane flexural wave, energy flow $\bar{\Pi}'$ per unit width, propagating in a plate the resulting time average of the total energy per unit area of plate is given by $\bar{\mathcal{E}}_S = \bar{\Pi}'/c_g$, where c_g is the group velocity of the wave. Compare Eq. (3.92) which is valid for a beam in flexure. For a diffuse field, the energy flow in every direction being $\bar{\Pi}'$, the total energy per unit area is obtained from the principle of superpositioning or by integrating the energy flow over all angles from 0 to 2π . Thus the time average of the total energy per unit area of the plate is

$$\bar{\mathcal{E}}_S = \frac{\bar{\mathcal{E}}}{S} = \frac{1}{c_g} \int_0^{2\pi} \bar{\Pi}' d\alpha = \frac{2\pi \bar{\Pi}'}{c_g} \quad (5.152)$$

where $\bar{\mathcal{E}}$ is the time average of the total energy of the plate and S the area of the plate. The energy flow can be expressed as $\bar{\Pi}' = c_g \bar{\mathcal{E}}_S / (2\pi S)$ which inserted in Eq. (5.151) yields

$$\bar{\Pi}_{total} = \sum_n (\bar{\Pi}_{tr})_n = \frac{c_g \bar{\mathcal{E}}}{\pi S} \sum_n \bar{\tau}_n L_n \quad (5.153)$$

The power $\bar{\Pi}_d$ lost due to the internal losses is, based on Eq. (2.68), equal to $\bar{\Pi}_d = \omega \eta_d \bar{E}$. Assuming a power input $\bar{\Pi}_{in}$ due to an external force acting on the system this power is lost due to internal or transmission losses or it will change the energy of the system. The power balance requires that

$$\bar{\Pi}_{in} = \omega \eta_d \bar{E} + \frac{\bar{E} c_g}{\pi S} \sum_n \bar{\tau}_n L_n + \frac{d\bar{E}}{dt} \quad (5.154)$$

Here \bar{E} represents the time average of the energy over one cycle of oscillation assuming the losses to be small as discussed in Sect. 2.9. For a steady-state condition, $d\bar{E}/dt = 0$, Eq. (5.154) gives

$$\bar{\Pi}_{in} = \omega \eta_{tot} \bar{E}, \quad \eta_{tot} = \eta_d + \frac{c_g}{\omega \pi S} \sum_n \bar{\tau}_n L_n \quad (5.155)$$

The total loss factor is thus determined by the internal losses and the transmission losses. For no input power to the system, the energy balance requires that $\omega \eta_{tot} \bar{E} + d\bar{E}/dt = 0$. The energy of the system is thus decaying as

$$\bar{E}(t) = \bar{E}(0) \cdot \exp(-\omega \eta_{tot} t) \quad \text{for } t \geq 0 \quad (5.156)$$

The loss factor can be measured by means of reverberation time measurements as discussed in Chap. 2. The total loss factor η_{tot} is a function of reverberation time T and frequency f as $\eta_{tot} = 2.2/(f \cdot T)$.

The importance of the transmission losses is appreciated by considering an example. Let a 1 mm steel plate with the dimensions $0.7 \times 1.2 \text{ m}^2$ be mounted in such a way that the junctions to adjoining plates are allowed only to rotate. The adjoining plates are also 1 mm steel plates. The average transmission coefficient is of the order 1/3, which corresponds to the transmission coefficient between two equal and semi-infinite plates. The internal loss factor for a steel plate is according to Table 3.1 less than 3×10^{-4} . The transmission losses are from Eq. (5.155) obtained as 0.02, 0.015 and 0.007 at the frequencies 500, 1000 and 5000 Hz, respectively. Although resulting from a rough estimate, the transmission losses are found to be much higher than the internal losses. In fact, for many undamped structures the internal losses can be neglected as compared to the transmission losses. For damping treatment to be effective, the added damping must be significantly higher than the transmission losses.

Whenever the complex E -modulus of an element, which is part of a built-up structure, is used, the ratio between the imaginary and real parts is equal to the total loss factor of the element. Thus by defining the E -modulus as $E = E_0(1 + i\eta)$ for an element, the parameter η is equal to the total loss factor for the element.

A transmission coefficient not only depends on type of junction and material parameters but also on the type of wave propagating toward the junction. The transmission coefficient for flexural waves is different from the transmission coefficient

for longitudinal waves propagating across the same type of junction. The loss factors for flexural and longitudinal or for that matter any other wave type are in fact different.

Junctions between plates or any other structures can also have losses. For plates with this type of junction with losses, the total loss factor of the plate as given by Eq. (5.155) must be modified. The average transmission coefficient $\bar{\tau}_n$ should be replaced by $1 - \bar{\rho}_n$ where $\bar{\rho}_n$ is the average reflection coefficient at the junction. The energy flow not reflected is absorbed by the junction or transmitted across. Compare also the discussion in Sect. 5.13.

5.13 Measurements on Junctions Between Beams

The transmission of flexural waves across junctions is of great importance with respect to the energy flow in large built-up structures like cars, ships, aircraft, trains, etc. The losses of each individual structural element depend on the transmission coefficients for the junctions of the element as discussed in Sect. 5.12. For a plate excited by a mechanical source, the ideal junctions of the plate should be such that the transmission of energy across any junction is minimal while the losses of the plate are maintained high. To a certain extent, these requirements are contradictory since a high loss factor without added damping requires a high transmission coefficient. However, the performance of a junction could be such that energy is lost due to friction or other mechanisms in the joint itself. All joints discussed so far have been treated as conservative systems meaning that the energy flow incident on the junction was either reflected or transmitted. For real junctions energy is also dissipated in the junction itself. If properly designed for obtaining low transmission coefficients and high losses, large benefits with respect to low noise and vibration levels can be achieved. The integrity or “strength” of the structure is often the limiting factor for achieving an acoustically optimized design.

It can be difficult or even impossible to mathematically model real junctions. Even if modeling tools should be available, material data for joints are in general inadequate for making any reliable predictions. The alternative to a prediction method is a measurement procedure. The transmission and reflection of energy flow across a junction depend on the angle of incidence of the incoming wave. The transmission coefficient for diffuse incidence on a junction between to identical plates was in Sect. 5.8 found to be 2/3 of the transmission coefficient for normal incidence. See also Problem 5.11. These results imply that the acoustic properties valid for normal incidence on a junction can be indicative of the performance of the same junction when exposed to a diffuse incident field. Measurements on junctions between coupled beams—normal incidence—can to a certain extent be used to classify the acoustic performance of junctions. Various measurements for classifying joints between beams or plates are compared and discussed by Feng in Ref. [50].

A method for the measurement of transmission, reflection, and absorption properties of junctions between aligned beam elements is presented in Ref. [51]. The

method is based on a technique initially developed by Åbom and Bodén, Ref. [52], for sound propagation problems in ducts. Only flexural waves are considered in Ref. [51]. The test arrangement is shown in Fig. 5.30. Two coupled straight beams have their ends embedded in sand. One beam element is excited by a shaker. The response of each beam element is measured at two positions. The response is given as the frequency response function between the displacement at the observation point and the force induced by the shaker. The measurement technique is not subjected to any restrictions concerning the mounting of the coupled beams. However, the quality of the measurements is much improved when the reflections from the end sections are suppressed. One way of ensuring low reflection from the ends is to embed them in sand as shown in Fig. 5.30.

The incident field on the junction is induced by a shaker connected to beam 1 as indicated in Fig. 5.30. The resulting wave field in beam 1 is composed of waves propagating in both directions along the beam plus evanescent waves decaying from the excitation point, both ends of the beam and the junction. At a distance of two wavelengths away from the excitation point or any discontinuity, the amplitude of any evanescent wave is sufficiently small to be neglected. Thus, if the response of the beam is recorded at a distance greater than two wavelengths away from any discontinuity the wave field in beam 1 is primarily determined by one flexural wave propagating along the positive x -axis and one in the opposite direction as illustrated in Fig. 5.30. The wave field in beam 2 is decomposed in a similar way.

The displacement w_1 due to flexural waves propagating in beam 1 is, neglecting the evanescent waves, given as

$$w_1(x, t) = \left(A_+ \cdot e^{-i\kappa_1 x} + A_- \cdot e^{i\kappa_1 x} \right) \cdot e^{i\omega t} \quad (5.157)$$

The wave number for flexural waves in beam 1 is κ_1 . The amplitude of the wave traveling toward the junction is A_+ and the amplitude of the wave traveling the opposite direction is A_- . The displacement of beam 2 is, based on the same assumptions, defined by

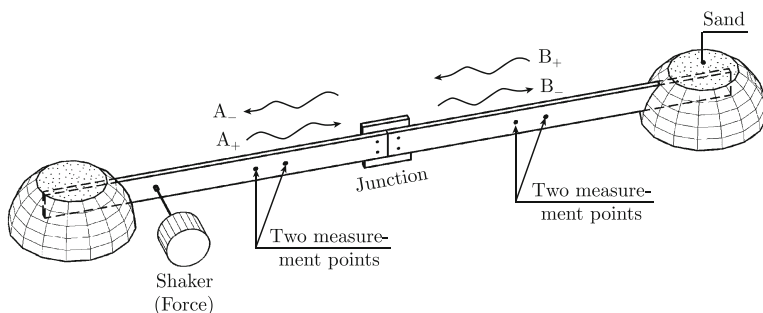


Fig. 5.30 Test arrangement for measurement of acoustic properties of joints

$$w_2(x, t) = \left(B_+ \cdot e^{i\kappa_2 x} + B_- \cdot e^{-i\kappa_2 x} \right) \cdot e^{i\omega t} \quad (5.158)$$

B_+ is again the amplitude of the wave traveling toward the junction and B_- the amplitude of the wave traveling in the opposite direction in beam 2. The wavenumber is κ_2 . The amplitude B_- is determined by the transmission of the incident wave in beam 1 and the reflection of the incident wave in beam 2. Defining the ratio between the amplitudes of the wave transmitted to beam 2 and the wave incident on the junction in beam 1 as T_a and the ratio between reflected and incident waves in beam 2 as R_b the amplitude B_- of the wave traveling away from the junction in beam 2 is

$$B_- = T_a \cdot A_+ + R_b \cdot B_+ \quad (5.159)$$

In a similar way, the amplitude A_- is determined by the amplitude of the incident wave in beam 1 and the reflection ratio R_a and the transmission ratio T_b from the incident wave in beam 2 and the wave transmitted to beam 1. Thus

$$A_- = T_b \cdot B_+ + R_a \cdot A_+ \quad (5.160)$$

For identical beams and complete symmetry around the junction the transmission ratio from beam 1 to beam 2 must be identical to the transmission ratio from beam 2 to 1. The same holds for the reflection ratios. Thus $T_a = T_b = T$ and $R_a = R_b = R$. For the symmetric case the Eqs. (5.129) and (5.130) can be written in matrix form as

$$\begin{Bmatrix} A_- \\ B_- \end{Bmatrix} = \begin{bmatrix} A_+ & B_+ \\ B_+ & A_+ \end{bmatrix} \begin{Bmatrix} R \\ T \end{Bmatrix} \quad (5.161)$$

The reflection and transmission ratios are from Eq. (5.161) obtained as

$$\begin{Bmatrix} R \\ T \end{Bmatrix} = \begin{bmatrix} A_+ & B_+ \\ B_+ & A_+ \end{bmatrix}^{-1} \begin{Bmatrix} A_- \\ B_- \end{Bmatrix} \quad (5.162)$$

If the ratios between the amplitudes are known the parameters R and T can be calculated. These ratios are determined from measurements of four frequency response functions between the excitation point and observation points as shown in Fig. 5.31. The coordinates for the observation points are $x_1 = -d$, $x_2 = -d - s$, $x_3 = d$, and $x_4 = d + s$. The center point of the symmetric joint is at $x = 0$. The FT of the displacement $\hat{w}_1(x_1)$ at x_1 is $\hat{w}_1(x_1) = \hat{F} H_{F1}$ where \hat{F} the FT of the force, exciting

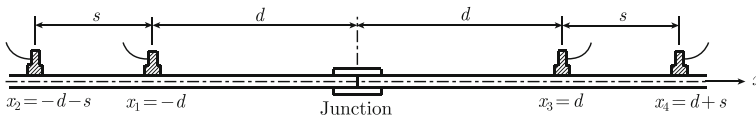


Fig. 5.31 Measurement points on beams

the coupled beams is and H_{F1} is the frequency response function or transfer function measured between the excitation point and the observation point 1.

In a similar way, the FT of responses at x_2 , x_3 and x_4 are obtained as $\hat{w}_1(x_2) = \hat{F} H_{F2}$, $\hat{w}_2(x_3) = \hat{F} H_{F3}$ and $\hat{w}_2(x_4) = \hat{F} H_{F4}$. These expressions in combination with the basic Eqs. (5.157) and (5.158) defining the displacement of the two beam elements give

$$\begin{aligned}\hat{F} \cdot H_{F1} &= A_+ \cdot e^{i\kappa d} + A_- \cdot e^{-i\kappa d} \\ \hat{F} \cdot H_{F2} &= A_+ \cdot e^{i\kappa(d+s)} + A_- \cdot e^{-i\kappa(d+s)} \\ \hat{F} \cdot H_{F3} &= B_+ \cdot e^{i\kappa d} + B_- \cdot e^{-i\kappa d} \\ \hat{F} \cdot H_{F4} &= B_+ \cdot e^{i\kappa(d+s)} + B_- \cdot e^{-i\kappa(d+s)}\end{aligned}\quad (5.163)$$

The amplitudes are obtained from these expressions as

$$\begin{aligned}A_+ &= \frac{\hat{F} \cdot e^{-i\kappa d}}{2i \cdot \sin(\kappa s)} \cdot G_1, \quad G_1 = H_{F2} - H_{F1} \cdot e^{-i\kappa s} \\ A_- &= \frac{\hat{F} \cdot e^{i\kappa d}}{2i \cdot \sin(\kappa s)} \cdot G_2, \quad G_2 = H_{F1} \cdot e^{i\kappa s} - H_{F2} \\ B_+ &= \frac{\hat{F} \cdot e^{-i\kappa d}}{2i \cdot \sin(\kappa s)} \cdot G_3, \quad G_3 = H_{F4} - H_{F3} \cdot e^{-i\kappa s} \\ B_- &= \frac{\hat{F} \cdot e^{i\kappa d}}{2i \cdot \sin(\kappa s)} \cdot G_4, \quad G_4 = H_{F3} \cdot e^{i\kappa s} - H_{F4}\end{aligned}\quad (5.164)$$

For κs approaching $n\pi$, the denominator giving the amplitude is becoming small and any measurement errors are amplified. In Ref. [53], it was demonstrated that the value of κs should be between 0.1π and 0.8π to limit the errors. Another potential error occurs when A_+ and A_- are approximately equal or for that matter when B_+ and B_- are of the same magnitude. When this is the case, the inversion of the matrix in Eq. (5.162) is numerically unstable. This particular problem is avoided by embedding the ends of the coupled beams in sand thus reducing the reflections from the ends resulting in that A_+ and A_- differ significantly.

The results (5.164) inserted in Eq. (5.162) yield

$$\begin{Bmatrix} R \\ T \end{Bmatrix} = e^{2i\kappa d} \cdot \begin{bmatrix} G_1 & G_3 \\ G_3 & G_1 \end{bmatrix}^{-1} \begin{Bmatrix} G_2 \\ G_4 \end{Bmatrix}\quad (5.165)$$

For the symmetric case, the transmission coefficient τ and the reflection coefficient ρ are defined as

$$\tau = \bar{\Pi}_{tr}/\bar{\Pi}_{in} = |T|^2, \quad \rho = \bar{\Pi}_{re}/\bar{\Pi}_{in} = |R|^2\quad (5.166)$$

where $\bar{\Pi}_{tr}$, $\bar{\Pi}_{in}$ and $\bar{\Pi}_{re}$ are the time averages of the transmitted, incident, and reflected energy flows. The junction dissipates the energy flow not transmitted or reflected. The dissipation coefficient δ is defined as $\delta = \bar{\Pi}_d/\bar{\Pi}_{in}$ where $\bar{\Pi}_d$ is the energy flow

dissipated by the junction. Since $\bar{\Pi}_{in} = \bar{\Pi}_{tr} + \bar{\Pi}_{re} + \bar{\Pi}_d$ it follows that

$$\delta = \bar{\Pi}_d / \bar{\Pi}_{in} = 1 - \tau - \rho = 1 - |T|^2 - |R|^2 \quad (5.167)$$

If only the quantities $|R|^2$ and $|T|^2$ are to be calculated, the phase factor $\exp(2i\kappa d)$ can be neglected in Eq. (5.165) by setting $d = 0$. Thus the transmission, reflection and dissipation coefficients can be determined for a symmetric joint if four transfer functions are measured at two positions at each beam symmetrically located with respect to the joint. The transfer functions should preferably be measured by optical means to avoid mass loading effects of accelerometers. The distance s between the two observation points should be such that $0.1\pi < \kappa s < 0.8\pi$. It is assumed that the waves primarily propagate along the axis of the beams. The first cross mode is generated for $\kappa b = 4.73$ where b is the width of the beam. This is discussed in Chap. 7. For ensuring normal incidence on the junction $\kappa b < 4.73$. A technique for measurement of transmission across asymmetric joints is presented in Ref. [51]. The technique is again based on the studies presented in Ref. [52].

Some examples of measured transmission coefficients or rather transmission losses R defined as $R = 10 \log(\bar{\Pi}_{in}/\bar{\Pi}_{tr}) = 10 \log(1/\tau)$ are presented in Figs. 5.32, 5.33 and 5.34. In all these examples, two 2 mm thick and 35 mm wide steel beams are bolted together. In the first figure, two bolts are used resulting in a substantial transmission loss at approximately 1.3 kHz.

Increasing the number of bolts to four the transmission loss is much improved over a large frequency range as shown in Fig. 5.33. An improvement can also be achieved by adding a viscoelastic layer between the beams. The configuration and the result are presented in Fig. 5.34.

Results presented in Refs. [54, 55, 56] clearly show that significant transmission losses can be achieved from bolted, riveted and spot welded joints. For coupled plate structures the spacing between bolts, welds, etc., are of importance for the

Fig. 5.32 Transmission loss across a two-bolt junction

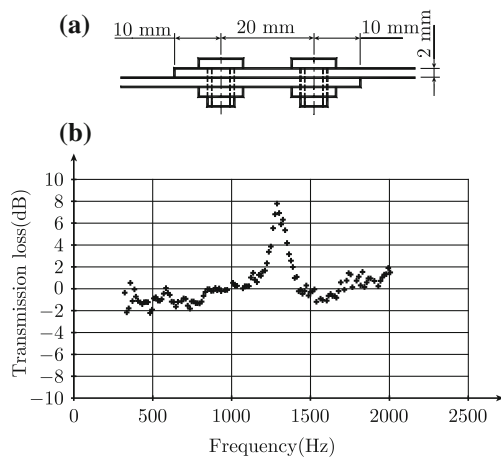


Fig. 5.33 Transmission loss across a four-bolt junction

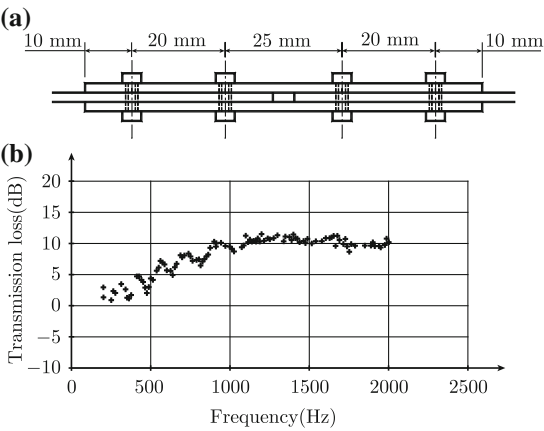
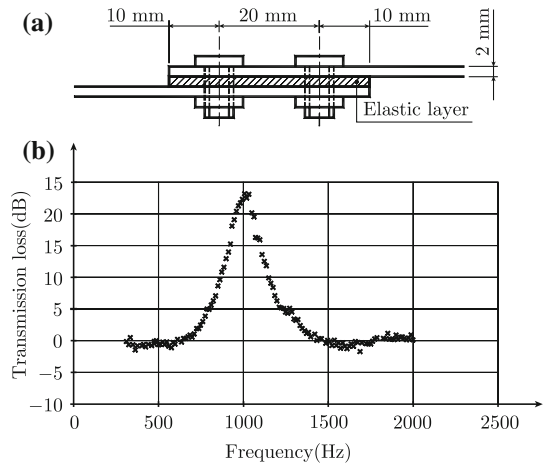


Fig. 5.34 Transmission loss across a two-bolt junction with a rubber interlayer



performance of the joint. In general, the transmission loss is increased as the spacing increases.

The transmission loss across a junction depends on the geometry and the joining technique. Losses due to so-called air pumping are negligible as shown in Ref. [54]. The integration of viscoelastic materials in a joint can be made in many different ways to increase the losses as suggested in Ref. [57]. Some examples are given in Figs. 5.35 and 5.36.

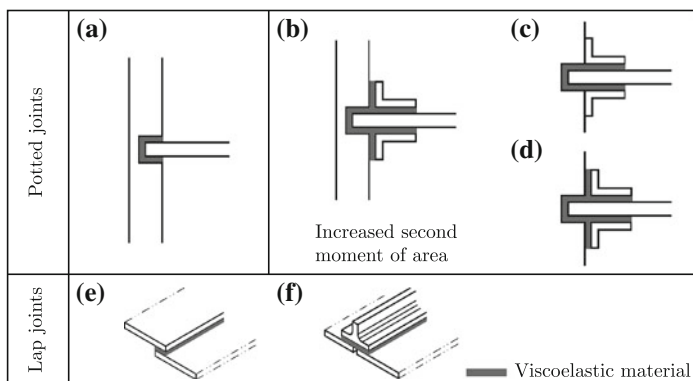


Fig. 5.35 Joints with viscoelastic materials

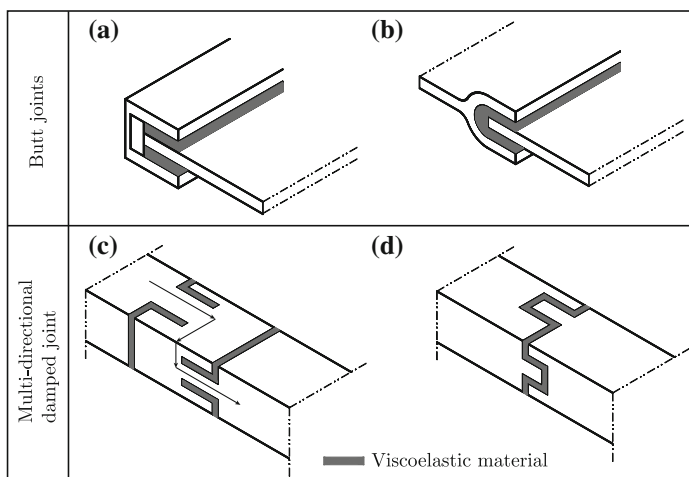


Fig. 5.36 Some additional joints with viscoelastic materials

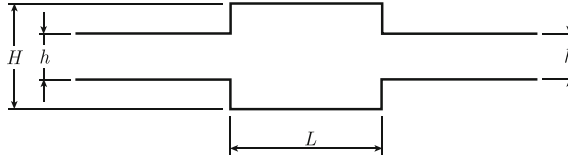
Problems

5.1 Two semi-infinite beams are connected at right angles. The junction between the beams is hinged, i.e., no bending moment can be transferred from one beam to the other. A longitudinal wave is incident on the junction in beam 1. Determine the transmitted and reflected energy flows as function of the incident energy flow. The two beams are identical, width b , height h , Young's modulus E , Poisson's ratio ν , and density ρ .

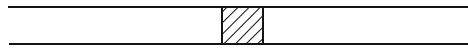
5.2 The incident wave in Problem 5.1 is a flexural wave. Determine the transmitted and reflected energy flows.

5.3 At a junction n , identical semi-infinite plates are connected along a straight line. In one of the plates, a plane flexural wave is incident on the junction (normal incidence). Determine the attenuation of the energy flow to any of the other plates. Neglect the translatory motion of the junction.

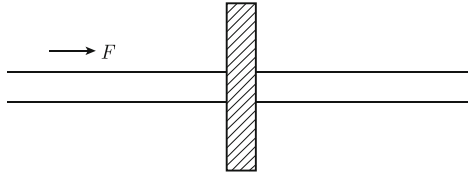
5.4 A longitudinal wave is incident on the discontinuity shown in the figure. Determine the ratio between the incident and transmitted energy flows.



5.5 Two semi-infinite beams oriented along the same axis are connected by means of an elastic interlayer as shown in the figure. A longitudinal wave is incident on the interlayer. Determine the attenuation across the junction. Consider only longitudinal waves.



5.6 A flexural wave is propagating in a beam toward a blocking mass as shown in the figure. A flexural wave is transmitted across the blocking mass. Determine the ratio between incident and transmitted energy flows. It is sufficient to define incident and transmitted waves and the boundary conditions necessary for solving the problem. Assume the blocking mass to be rigid. Its mass is M and its rotational mass moment of inertia J . The width of the beam is b and its height h .



5.7 An evanescent flexural wave on a beam is described by

$$w(x, t) = A \cdot \exp[i(\omega t + \kappa_0 \eta x / 4) - \kappa_0 x]$$

where κ_0 is the real part of the wave number and η the loss factor. Determine the energy flow in the beam due to this wave.

5.8 A thin infinite plate is excited at the origin by a point force $F = F_0 \cdot \exp(i\omega t)$. Determine the far-field displacement of the resulting flexural wave.

5.9 An infinite plate is excited by a point force. The displacement in the far-field is given by the result of Example 5.8. Neglecting the losses in the plate show that the power transmitted to the far-field is equal to power input at the excitation point.

5.10 Two semi-infinite plates are joined together along a straight line. The joint is allowed to rotate only. A flexural plane wave, unit amplitude, is incident on the junction. Determine the amplitude R of the reflected wave and show that $|R| = 1$ when no propagating wave is transmitted across the junction.

5.11 Two semi-infinite and equal plates are joined together along a straight line. The joint is allowed to rotate only. A flexural plane wave is incident on the junction. Show that the transmission coefficient for transmission across the junction is given by Eq. (5.129).

5.12 Two semi-infinite and equal plates are joined together along a straight line. The joint is allowed to rotate only. A flexural plane wave is incident on the junction. Show that the transmission coefficient for diffuse incidence is two-third of the transmission coefficient for normal incidence.

Chapter 6

Longitudinal Vibrations of Finite Beams

In Sect. 1.2, the free vibration of a simple mass-spring system was discussed. It was shown that the time dependence of the free vibrations was determined by the natural frequency or eigenfrequency of the system plus the losses. In a similar way, free longitudinal waves in a finite structure oscillate only at certain frequencies or eigenfrequencies. For a continuous finite system, there is an infinite number of eigenfrequencies. Each frequency is associated with a certain mode shape or eigenfunction. In this chapter, it is shown how these eigenfunctions can be used to determine the forced response of a beam. An alternative method, based on Green's function, is also discussed.

The mobility concept is used to determine the response of a mass mounted on rod, which, to a certain extent, can be considered as a homogeneous spring. The resonances in the rod are shown to have a major influence on the transmissibility through the "spring." The transfer matrix is introduced to describe the coupling between a set of beams.

6.1 Free Longitudinal Vibrations in Finite Beams

As an illustration of waves in a finite structure, consider a homogeneous beam with constant cross section with the area S . The length of the beam is L . The length L should at least be ten times the largest dimension of the cross section of the structure. The beam is oriented along the x -axis. In this coordinate system, the ends of the beam are at $x = 0$ and $x = L$. The beam is assumed to be freely suspended. At time $t = 0$, the longitudinal waves are excited in the beam parallel to the x -axis, for example by a hammer blow. For $t > 0$, no external forces are applied to the beam. The displacement $\xi(x, t)$ in the beam must for $t > 0$ satisfy the wave equation for L-waves. Thus

$$\frac{\partial^2 \xi}{\partial x^2} - \frac{\rho}{E} \frac{\partial^2 \xi}{\partial t^2} = 0 \quad (6.1)$$

The E -modulus is complex as defined in Sect. 5. It is convenient now to make a separation of variables or to define the displacement $\xi(x, t)$ as

$$\xi(x, t) = g(t) \cdot \varphi(x) \quad (6.2)$$

This expression is inserted in the wave Eq. (6.1), which is thereafter divided by $\xi = g\varphi$ resulting in

$$\frac{1}{\varphi} \frac{d^2 \varphi}{dx^2} = \frac{\rho}{E} \frac{1}{g} \frac{d^2 g}{dt^2}$$

If the left-hand side of this expression is set to equal $-k^2$ the right-hand side of the equation must also equal $-k^2$. The functions $g(t)$ and $\varphi(x)$ must now satisfy the equations

$$\frac{d^2 \varphi}{dx^2} + k^2 \varphi = 0, \quad \frac{d^2 g}{dt^2} + k^2 \frac{E}{\rho} g = 0 \quad (6.3)$$

Thus, if these two differential equations are satisfied, the wave Eq. (6.1) is also satisfied. The general solution to the first part of Eq. (6.3) is

$$\varphi(x) = A_1 \cdot e^{-ikx} + B_1 \cdot e^{ikx} \quad (6.4)$$

or alternatively

$$\varphi(x) = A_2 \cdot \sin kx + B_2 \cdot \cos kx \quad (6.5)$$

The two general solutions are analogous. However, for finite structures, the expression (6.5) should be preferred.

The function $\varphi(x)$ must satisfy the boundary conditions for the beam. For a freely suspended beam, there are no constraining forces acting on the ends of the beam. Thus for a free-free beam, the stresses at the two ends of the beam must be zero or

$$\sigma = E \frac{\partial \xi}{\partial x} = 0 \quad \text{for } x = 0 \quad \text{and } x = L \quad (6.6)$$

Considering the definition of the displacement given in Eq. (6.2), this boundary condition is equivalent to

$$\frac{d\varphi}{dx} = 0 \quad \text{for } x = 0 \quad \text{and } x = L \quad (6.7)$$

For the general solution given in Eq. (6.5) to satisfy these boundary conditions it follows that

$$A_2 = 0, \quad B_2 \sin(kL) = 0 \quad (6.8)$$

For a nontrivial solution, i.e., for $B_2 \neq 0$, the boundary conditions can only be satisfied if $\sin(kL) = 0$. This condition is fulfilled for an infinite number of solutions in k or rather for

$$k = k_n = \frac{n\pi}{L}, \quad n = 0, 1, 2, 3, \dots \quad (6.9)$$

There is consequently also an infinite number of solutions, one solution $\varphi_n(x)$ for each k_n . The solutions or eigenfunctions satisfying the differential Eq. (6.3) for $k = k_n$ and the boundary condition (6.6) are

$$\varphi_n(x) = \cos(k_n x), \quad k_n = \frac{n\pi}{L} \quad \text{for } n = 0, 1, 2, 3, \dots \quad (6.10)$$

As yet the amplitude of the eigenfunction is unity. According to the basic assumption (6.3), each pair of the eigenfunction φ_n and the corresponding eigenvalue k_n satisfies the equation

$$\frac{d^2 \varphi_n}{dx^2} + k_n^2 \varphi_n = 0 \quad (6.11)$$

The eigenfunction and the corresponding eigenvalue depend on the boundary conditions. For a beam with clamped ends, the boundary conditions are $\xi = 0$ for $x = 0$ and $x = L$. For $\xi(x, t) = g(t) \cdot \varphi(x)$, these boundary conditions are equivalent to $\varphi = 0$ for $x = 0$ and $x = L$. As in the previous case there is an infinite number of solutions. These or rather the resulting eigenfunctions are

$$\varphi_n(x) = \sin(k_n x), \quad k_n = \frac{n\pi}{L} \quad \text{for } n = 1, 2, 3, \dots \quad (6.12)$$

Another boundary condition of general interest corresponds to a beam with one end free at $x = L$ and the other end clamped at $x = 0$. The resulting eigenfunctions are

$$\varphi_n(x) = \sin(k_n x), \quad k_n = \frac{\pi(n + 1/2)}{L} \quad \text{for } n = 0, 1, 2, 3, \dots \quad (6.13)$$

Compare the solutions to the Problems 6.1–6.3.

Solutions to free and forced vibration problems can readily be formulated if the motion of the structure can be described by means of orthogonal eigenfunctions. In these cases, the solutions can be expressed as infinite sums over the relevant eigenfunctions. The procedure is discussed below in this section for free vibrations and in Sect. 6.3 for forced vibrations. The eigenfunctions $\varphi_m(x)$ and $\varphi_n(x)$ are orthogonal if

$$\int_0^L \varphi_m(x) \cdot \varphi_n(x) dx = C_{mn} \cdot \delta_{mn}$$

where the Kronecker delta δ_{mn} is unity for $m = n$ and zero for $m \neq n$. For $C_{mn} = 1$ the eigenfunctions $\varphi_m(x)$ and $\varphi_n(x)$ are said to be orthonormal. The requirements to boundary conditions satisfied by orthogonal eigenfunctions can be formulated from

the basic equations governing the eigenfunctions. Thus, consider the two eigenfunctions $\varphi_m(x)$ and $\varphi_n(x)$ with the eigenvalues k_m and k_n , respectively. The eigenfunction $\varphi_n(x)$ satisfies Eq. (6.11). This equation is multiplied by $\varphi_m(x)$ and integrated with respect to x . The result is

$$\int_0^L \varphi_m(x) \cdot \frac{d^2 \varphi_n}{dx^2} dx + k_n^2 \int_0^L \varphi_m(x) \cdot \varphi_n(x) dx = 0 \quad (6.14)$$

The first expression can be integrated by parts. Thus

$$\int_0^L \varphi_m(x) \cdot \frac{d^2 \varphi_n}{dx^2} dx = \left[\varphi_m \frac{d\varphi_n}{dx} - \frac{d\varphi_m}{dx} \varphi_n \right]_0^L + \int_0^L \frac{d^2 \varphi_m}{dx^2} \cdot \varphi_n(x) dx$$

This result replaces the first integral of Eq. (6.14), which is rewritten as

$$k_n^2 \int_0^L \varphi_m(x) \cdot \varphi_n(x) dx + \int_0^L \frac{d^2 \varphi_m}{dx^2} \cdot \varphi_n(x) dx = - \left[\varphi_m \frac{d\varphi_n}{dx} - \frac{d\varphi_m}{dx} \varphi_n \right]_0^L \quad (6.15)$$

From Eq. (6.11) it follows that φ_m and k_m should satisfy

$$\frac{d^2 \varphi_m}{dx^2} = -k_m^2 \varphi_m$$

This result inserted in the second integral of Eq. (6.15) gives

$$(k_n^2 - k_m^2) \int_0^L \varphi_m(x) \cdot \varphi_n(x) dx = - \left[\varphi_m \frac{d\varphi_n}{dx} - \frac{d\varphi_m}{dx} \varphi_n \right]_0^L$$

For $m \neq n$, the corresponding eigenvalues are unequal or $k_m \neq k_n$. Thus, the eigenfunctions φ_m and φ_n are orthogonal if the expression on the right-hand side of this equation is equal to zero. In a more general way, the eigenfunctions φ_m and φ_n are orthogonal as defined by

$$\int_0^L \varphi_m(x) \cdot \varphi_n(x) dx = 0 \quad \text{for } m \neq n \quad (6.16)$$

if at the same time the eigenfunctions φ_m and φ_n satisfy the condition

$$\left[\varphi_m \frac{d\varphi_n}{dx} - \frac{d\varphi_m}{dx} \varphi_n \right]_0^L = 0 \quad (6.17)$$

For certain boundary conditions, the expression (6.15) is equal to zero. The corresponding eigenfunctions are consequently orthogonal. Some boundary conditions satisfying Eq. (6.17) for any m or n are:

(i) Both ends clamped.

$$\varphi_n = 0 \quad \text{for } x = 0 \text{ and } x = L$$

(ii) Both ends free.

$$\frac{d\varphi_n}{dx} = 0 \quad \text{for } x = 0 \text{ and } x = L$$

(iii) Both ends resiliently mounted by identical springs.

$$\frac{d\varphi_n}{dx} = -q\varphi_n \quad \text{for } x = L, \quad \frac{d\varphi_n}{dx} = q\varphi_n \quad \text{for } x = 0$$

(iv) Periodicity.

$$\varphi_n(0) = \varphi_n(L), \quad \left(\frac{d\varphi_n}{dx} \right)_{x=0} = \left(\frac{d\varphi_n}{dx} \right)_{x=L}$$

The first three boundary conditions are illustrated in Fig. 6.1.

Orthogonal eigenfunctions are also obtained for mixed boundary conditions, for example beams with one end fixed and the other free. Other combinations are fixed and resilient ends and free and resilient. The last condition, (iv) periodicity, can not be combined with any of the others since the boundary conditions at one end must be related to the boundary conditions at the other end of the beam.

For boundary condition (iii), the ends of a beam are connected via an ideal spring with a spring constant k_0 to an infinitely stiff structure as shown in Fig. 6.2. For a displacement ξ of one end of the beam, the force on the beam due to the elongation of the spring is equal to $k_0\xi$. The resulting stress at the end of the beam is $\sigma = E \cdot \partial\xi/\partial x$ and is assumed constant over the cross section. For a beam with a cross-section area S , it follows that for $x = 0$

$$k_0\xi = S\sigma = SE \frac{\partial\xi}{\partial x}$$

For $\xi(x, t) = \varphi(x) \cdot g(t)$, the boundary conditions can be reformulated as

Fig. 6.1 Boundary conditions satisfied by orthogonal eigenfunctions. L-waves only

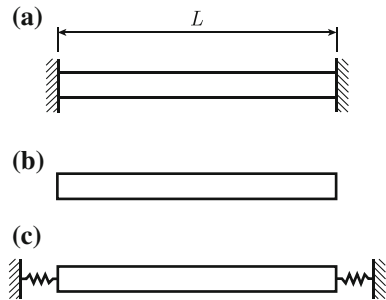
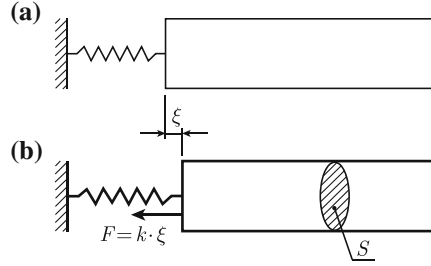


Fig. 6.2 Displacement and forces at the end of a resiliently mounted beam



$$k_0 \varphi = SE \frac{d\varphi}{dx} \quad \text{or} \quad \frac{d\varphi_n}{dx} = q \varphi_n \quad \text{for } x = 0$$

At the other end of the beam, the boundary conditions are

$$k_0 \varphi = -SE \frac{d\varphi}{dx} \quad \text{or} \quad \frac{d\varphi_n}{dx} = -q \varphi_n \quad \text{for } x = L$$

These boundary conditions satisfy Eq. (6.17) resulting in that the eigenfunctions are orthogonal for this condition. Compare Problem 6.3 and the discussion leading up to the result (6.110) in Sect. 6.7.

For a beam satisfying the boundary conditions (i) or (ii) or for a beam with one clamped and one free end there is no energy flow away from the beam. The intensity in the beam, L- waves only, is obtained from Eq. (3.19) as

$$I_x = -\sigma_x \cdot \dot{\xi} = -E \cdot \frac{\partial \xi}{\partial x} \cdot \dot{\xi}$$

There is no energy flow across a boundary if ξ or $\partial \xi / \partial x$ equals zero at this section of the beam. For condition (iii), there is an oscillating energy flow to the spring. The time average of this energy flow is zero since there is no energy transfer to the infinitely stiff foundation. If the spring is considered as an integral part of the beam, the total energy of the beam–spring system is constant. In the fourth case, there can be an energy flow across one junction away from the beam. However, due to the periodicity of the boundary conditions, the energy flow to the beam across the other junction is the same as the flow away from the beam at the opposite end. Thus, even for this case, the total energy of a dynamic system for which the eigenfunctions are orthogonal is constant.

In order to separate the various time-dependent solutions corresponding to each eigenfunctions φ_n and eigenvalue k_n each such solution is given the subscript n . The time-dependent solution g_n must satisfy the first part of Eq. (6.3) as

$$\frac{d^2 g_n}{dt^2} + \frac{E}{\rho} \cdot k_n^2 g_n = 0 \quad (6.18)$$

The E -modulus is complex. For small losses it is convenient to introduce the parameter

$$\omega_n = k_n \cdot \sqrt{\frac{E_0}{\rho}} \cdot (1 + i\eta/2), \quad \omega_n = \omega_{n0}(1 + i\eta/2) \quad (6.19)$$

The problem defined in Eq. (6.18) is now similar to the one presented in Sect. 1.6 for free vibrations of a lightly damped 1-DOF system. The solution, according to Eq. (1.83), is consequently on the form

$$g_n(t) = [D_{1n} \cdot \sin(\omega_{0n}t) + D_{2n} \cdot \cos(\omega_{0n}t)] \cdot \exp(-\omega_{0n}\eta t/2) \quad (6.20)$$

The total solution describing the displacement $\xi(x, t)$ is the sum of all the separate solutions or modes, given by

$$\begin{aligned} \xi(x, t) &= \sum_{n=0}^{\infty} \varphi_n(x) \cdot g_n(t) \\ &= \sum_{n=0}^{\infty} \varphi_n(x) [D_{1n} \cdot \sin(\omega_{0n}t) + D_{2n} \cdot \cos(\omega_{0n}t)] \cdot \exp(-\omega_{0n}\eta t/2) \end{aligned}$$

where

$$\varphi_n(x) = \cos\left(\frac{n\pi x}{L}\right), \quad \omega_{0n} = \frac{n\pi}{L} \sqrt{\frac{E_0}{\rho}} \quad (6.21)$$

For $n = 0$, ω_{0n} is also equal to zero and the corresponding eigenfunctions $\varphi_0(x) = 1$. The contribution to the solution for $n = 0$ is just the constant D_{20} , which gives the displacement at equilibrium as time goes to infinity. The result (6.19) is analogous to the solution for the 1-DOF problem discussed in Chap. 1. However, for a continuous system like a finite beam, there are an infinite number of eigenfrequencies. These eigenfrequencies are

$$f_n = \frac{\omega_{0n}}{2\pi} = \frac{k_n}{2\pi} \sqrt{\frac{E_0}{\rho}} = \frac{n}{2L} \sqrt{\frac{E_0}{\rho}}, \quad n = 1, 2, 3, \dots \quad (6.22)$$

The results (6.21) and (6.22) are valid for a beam with free ends. For all the boundary conditions discussed so far, clamped and free etc., the eigenfrequency f_n for mode n is

$$f_n = \frac{\omega_{0n}}{2\pi} = \frac{k_n}{2\pi} \sqrt{\frac{E_0}{\rho}} \quad (6.23)$$

where k_n is the eigenvalue corresponding to certain boundary conditions. For some natural boundary conditions, the resulting orthogonal eigenfunctions and the corresponding eigenfrequencies are listed in Table 6.1. Compare also Problems 6.1 and 6.2.

Table 6.1 Boundary conditions satisfied by some orthogonal eigenfunctions φ_n with eigenvalue k_n and eigenfrequency f_n

(i) Both ends clamped
$\varphi_n(x) = 0$ for $x = 0$ and $x = L$
$\varphi_n(x) = \sin(k_n x)$, $k_n = n\pi/L$, $f_n = n/(2L) \cdot \sqrt{E_0/\rho}$
(ii) Both ends free
$d\varphi_n/dx = 0$ for $x = 0$ and $x = L$
$\varphi_n(x) = \cos(k_n x)$, $k_n = n\pi/L$, $f_n = n/(2L) \cdot \sqrt{E_0/\rho}$
(iii) Both ends resiliently mounted
$d\varphi_n/dx = q\varphi_n$ for $x = 0$, $d\varphi_n/dx = -q\varphi_n$ for $x = L$
$\varphi_n(x) = \sin(k_n x + \gamma_n)$, $\tan(\gamma_n) = k_n/q$
$\tan(k_n L) = (2k_n/q)/[(k_n/q)^2 - 1]$, $f_n = k_n/(2\pi) \cdot \sqrt{E_0/\rho}$
(iv) One end clamped, the other free
$\varphi_n(x) = 0$ for $x = 0$, $d\varphi_n/dx = 0$ for $x = L$
$\varphi_n(x) = \sin(k_n x)$, $k_n = (n + 1/2)\pi/L$, $f_n = (n + 1/2)/(2L) \cdot \sqrt{E_0/\rho}$
(v) Periodic structure
$\varphi_n(0) = \varphi_n(L)$, $[d\varphi_n/dx]_{x=0} = [d\varphi_n/dx]_{x=L}$
$\varphi_n(x) = \sin(k_n x + \beta_n)$, β_n arbitrary
$k_n = 2n\pi/L$, $f_n = n/L \cdot \sqrt{E_0/\rho}$

The eigenfunctions given in the table, with one exception, satisfy the conditions

$$\int_0^L \varphi_n(x) \cdot \varphi_m(x) dx = \frac{L}{2}, \quad \int_0^L \varphi_m(x) \cdot \varphi_n(x) dx = 0 \quad \text{for } m \neq n$$

In these cases, the norm of the eigenfunctions is said to be equal to $L/2$. For the free-free boundary condition, and only for this condition, the norm is equal to L for $n = 0$. For $n > 0$ the norm is equal to $L/2$.

For the boundary conditions i), ii) and iv) the spacing Δf between two consecutive eigenfrequencies is

$$\Delta f = f_{n+1} - f_n = \frac{1}{2L} \sqrt{\frac{E_0}{\rho}}$$

The modal density \mathcal{N}_f is defined as the number of modes per frequency interval. In the frequency interval Δf , there is one eigenfrequency. Consequently, the modal density is

$$\mathcal{N}_f = \frac{1}{\Delta f} = 2L \sqrt{\frac{\rho}{E_0}} \quad (6.24)$$

Table 6.2 First three eigenfrequencies f_n (Hz) for L-waves in beams of length L (m)

Material/boundary condition	$f_1 \cdot L$	$f_2 \cdot L$	$f_3 \cdot L$
<i>Steel/aluminum</i>			
Free-free	2628	5256	7884
Clamped-clamped	2628	5256	7884
Clamped-free	1314	3942	6570
<i>Concrete</i>			
Free-free	1708	3415	5123
Clamped-clamped	1708	3415	5123
Clamped-free	854	2561	4269

The modal density is thus independent of the boundary conditions and frequency, depending only on the length of the beam and its material parameters. However, for the very special periodic case, the modal density is only $L\sqrt{\rho/E_0}$.

For typical materials like aluminum, steel, and concrete used in large constructions the first few eigenfrequencies are fairly high for longitudinal vibrations of beams. Some examples are given in Table 6.2 for the products between length L and the natural- or eigenfrequency f_n for steel, aluminum and concrete beams. For steel and aluminum, the ratio between E -modulus and density is approximately the same. The eigenfrequencies for an aluminum and a steel bar of the same length and with the same boundary conditions are therefore, according to Eq. (6.23), also approximately equal. In Table 6.2 f_n is in Hz and the length L in m.

The usefulness of representing the response by means of orthogonal eigenvectors can be illustrated by a simple example. Consider a beam for which the displacement is given by the function $u(x)$ along the x -axis, which also corresponds to the axis of the beam. At time $t = 0$, the beam is released with the boundary conditions free-free. For $t > 0$, the general expression for the displacement ξ is given in Eq. (6.21). The velocity is zero for $t = 0$ which means $D_{1n} = 0$. The resulting displacement for $t \geq 0$ is thus, with $D_{1n} = 0$ in Eq. (6.21), equal to

$$\xi(x, t) = \sum_{n=0}^{\infty} \varphi_n(x) \cdot D_{2n} \cdot \cos(\omega_{0n}t) \cdot \exp(-\omega_{0n}t/2) \quad (6.25)$$

For a free-free beam $\varphi_n(x) = \cos(n\pi x/L)$. At $t = 0$ the displacement in the beam must be equal to $u(x)$, i.e.,

$$u(x) = \sum_{n=0}^{\infty} \varphi_n(x) \cdot D_{2n} \quad (6.26)$$

The expression (6.26) is now multiplied by $\varphi_m(x)$ and integrated over the length of the beam. The result is

$$\int_0^L \varphi_m(x) u(x) dx = \sum_{n=0}^{\infty} D_{2n} \cdot \int_0^L \varphi_m(x) \varphi_n(x) dx$$

The eigenfunctions are orthogonal thus

$$D_{2n} = \frac{\int_0^L u(x) \varphi_n(x) dx}{\int_0^L \varphi_n^2(x) dx} = \frac{2}{L \varepsilon_n} \int_0^L u(x) \varphi_n(x) dx \quad (6.27)$$

The parameter ε_n is defined as $\varepsilon_n = 2$ for $n = 0$ and $\varepsilon_n = 1$ for $n > 0$. This is a consequence of the value of the norm of the eigenfunctions for free ends being L for $n = 0$ and $L/2$ for $n > 0$.

The spatial average of the velocity squared is for $\eta \ll 1$ obtained as

$$\langle v^2 \rangle = \frac{1}{L} \int_0^L \xi^2(x, t) dx = \frac{1}{2} \sum_{n=1}^{\infty} D_{2n}^2 \omega_{0n}^2 \sin^2(\omega_{0n} t) \cdot \exp(-\omega_{0n} \eta t) \quad (6.28)$$

The summation can be made from $n = 1$ since for $n = 0$ the parameter ω_{0n} is equal to zero. The time average over one period of the spatial average of the velocity squared is

$$\langle \bar{v}^2 \rangle = \frac{1}{T} \int_0^T \langle v^2 \rangle dt = \frac{1}{4} \sum_{n=1}^{\infty} D_{2n}^2 \omega_{0n}^2 \cdot \exp(-\omega_{0n} \eta t) \quad (6.29)$$

As was the case for the simple mass spring system, the average over a period of the modal kinetic energy decays as $\exp(-\omega_{0n} \eta t)$. Indicating the energy of the modes decay at varying rates, since loss factors at different frequencies are in general different. Loss factors at each resonance or eigenfrequency can be determined by means of the half band width method or from reverberation time measurements as discussed in Sect. 2.8. If for reverberation time measurements there are several eigenfrequencies within a frequency band, the loss factor is eventually determined by the decay rate of the most lightly damped mode. If the loss factor varies significantly for various modes, reverberation time measurements in frequency bands including several modes can give misleading results. The reverberation time T_r corresponding to a decay of 60 dB of the velocity squared gives the loss factor as

$$\eta = \frac{2.2}{f_n \cdot T_r} \quad (6.30)$$

This expression gives the loss factor at the eigenfrequency f_n . However, if the losses can be described as viscous, the loss factor is inversely proportional to frequency. This means that the product $f_n \eta$ is constant. For this particular case, the decay rate is the same for every mode.

6.2 Forced Longitudinal Vibrations in Finite Beams

The wave equation for L-waves discussed in Sect. 3.4 was derived without considering any external forces. Consider again a homogenous beam with a constant cross section with the area S . The beam with length L is oriented along the x -axis between $x = 0$ and $x = L$. The deflection ξ of the beam is defined positive along the positive x -axis. A force $F'(x, t)$ per unit length of the beam is acting on the structure along the positive x -axis. The external force $F' \Delta x$ and the internal force $S \cdot \partial \sigma / \partial x$ will act on the mass $\rho S \Delta x$. Returning to Sect. 3.4, ΔF in Eq. (3.49) is for forced excitation replaced by $(F' + S \cdot \partial \sigma / \partial x) \Delta x$. The sum of the internal and external forces, according to Newton's second law result in the wave equation

$$\frac{\partial^2 \xi}{\partial x^2} - \frac{\rho}{E} \frac{\partial^2 \xi}{\partial t^2} = -\frac{F'}{SE} \quad (6.31)$$

This is the governing equation for forced excitation of L-waves in a beam where $F' = F'(x, t)$ is the external force per unit length of the beam. For a point force $F_0 \cdot \exp(i\omega t)$ applied to the structure at $x = x_1$, the function $F'(x, t)$ is

$$F'(x, t) = F_0 \cdot \delta(x - x_1) \cdot \exp(i\omega t) \quad (6.32)$$

In this expression $\delta(x - x_1)$ is the Dirac function with the dimension one over unit length. The example is illustrated in Fig. 6.3. The force acts on the beam in such a way, that the resulting stress is constant over the cross section of the beam at $x = x_1$. As in the previous section it is assumed that the ends of the beam are free, i.e., the stress in the beam is zero for $x = 0$ and $x = L$. For the forced vibration of the beam, the displacement must have the same time dependence as the driving force. The solution to the problem can be obtained by considering the wave fields to the right and left of the driving force. The wave fields are thereafter matched by means of the boundary conditions at the point where the force is applied. For forced vibrations, the time dependence for the force is $\exp(i\omega t)$, the displacement ξ is defined as

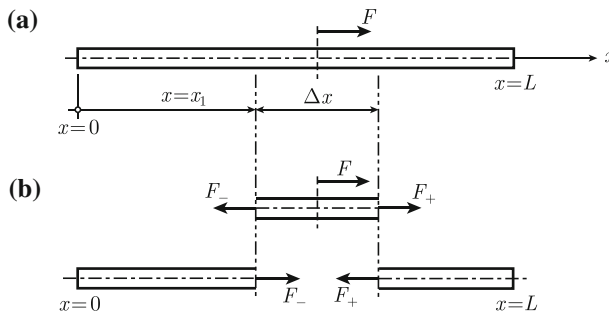


Fig. 6.3 External force applied to a beam along its axis

$$\xi(x, t) = h(x) \cdot e^{i\omega t} \quad (6.33)$$

This means that, except at $x = x_1$, the function $h(x)$ must satisfy the differential equation

$$\frac{d^2 h}{dx^2} + k_1^2 h = 0 \quad \text{for } x \neq x_1 \quad (6.34)$$

The complex wave number k_1 for L-waves is defined in Eqs. (5.10) and (5.11).

For $0 \leq x < x_1$, i.e., to the left of the force, the general solution to Eq. (6.34) is

$$h_-(x) = A_1 \cdot \sin(k_1 x) + B_1 \cdot \cos(k_1 x) \quad (6.35)$$

The corresponding solution on the other side of the force, i.e., for $L \geq x > x_1$, is

$$h_+(x) = A_2 \cdot \sin[k_1(L - x)] + B_2 \cdot \cos[k_1(L - x)] \quad (6.36)$$

This function could also be written as

$$h_+(x) = D_1 \cdot \sin(k_1 x) + D_2 \cdot \cos(k_1 x)$$

The first expression (6.36) ensures a certain symmetry as compared to Eq. (6.35) with respect to the distance to nearest end of the beam. This symmetry can somewhat simplify the calculations. Either approach leads to the correct solution.

For a beam with free ends, the resulting stress is zero at these positions. These boundary conditions lead to

$$\frac{dh_-}{dx} = 0 \quad \text{for } x = 0, \quad \frac{dh_+}{dx} = 0 \quad \text{for } x = L \quad (6.37)$$

The displacement along the beam is continuous at $x = x_1$ or

$$h_- = h_+ \quad \text{for } x = x_1 \quad (6.38)$$

The final boundary condition concerns the equilibrium of the forces at the position $x = x_1$ as illustrated in Fig. 6.3. The equilibrium of forces leads to

$$F_0 = -F_+ + F_- = -SE \left(\frac{dh_+}{dx} - \frac{dh_-}{dx} \right)_{x=x_1} \quad (6.39)$$

The first two boundary conditions (6.37) in combination with the general solutions Eqs. (6.35) and (6.36) yield

$$A_1 = A_2 = 0 \quad (6.40)$$

This result and the continuity condition (6.38) give

$$B_1 \cdot \cos(k_1 x_1) = B_2 \cdot \cos[k_1(L - x_1)] \quad (6.41)$$

In a similar way, the last boundary condition (6.39) results in

$$-\frac{F_0}{SEk_1} = B_1 \cdot \sin(k_1 x_1) + B_2 \cdot \sin[k_1(L - x_1)] \quad (6.42)$$

The unknown parameters B_1 and B_2 are obtained from Eqs. (6.41) and (6.42) as

$$B_1 = -\frac{F_0}{SEk_1} \frac{\cos[k_1(L - x_1)]}{\sin(k_1 L)}, \quad B_2 = -\frac{F_0}{SEk_1} \frac{\cos(k_1 x_1)}{\sin(k_1 L)} \quad (6.43)$$

The general solution to Eq. (6.31) with the force defined in Eq. (6.32) is thus

$$\begin{aligned} \xi(x, t) &= G(x|x_1) \cdot F_0 \cdot e^{i\omega t} \\ G(x|x_1) &= G_1(x|x_1) = -\frac{1}{SEk_1} \frac{\cos(k_1 x_1) \cos[k_1(L - x)]}{\sin(k_1 L)} \quad \text{for } 0 \leq x_1 \leq x \\ G(x|x_1) &= G_2(x|x_1) = -\frac{1}{SEk_1} \frac{\cos(k_1 x) \cos[k_1(L - x_1)]}{\sin(k_1 L)} \quad \text{for } x \leq x_1 \leq L \end{aligned} \quad (6.44)$$

The first solution, $G_1(x|x_1)$, is valid for any excitation point x_1 on the beam as long as this point is to the left of the observation point x or rather for $0 \leq x_1 \leq x$. The other solution $G_2(x|x_1)$ is valid for $x \leq x_1 \leq L$. The expression $G(x|x_1)$ is referred to as Green's function.

The displacement $\xi(x, t)$ of the beam is large when the term $\sin(k_1 L)$ is small. As long as the losses are not neglected, this term is never equal to zero. According to the definition of the complex wave number (5.28), the sine term is, including the losses, equal to

$$\sin(k_1 L) = \sin(k_{10} L - ik_{10} L \eta / 2) \quad (6.45)$$

If the imaginary part inside the bracket is small, the sine term can be expanded in a Taylor series as

$$\sin(k_1 L) = \sin(k_{10} L) - ik_{10} L \eta / 2 \cdot \cos(k_{10} L) + \dots \quad (6.46)$$

For viscous losses, the product $k_{10} \eta$ is constant. However, if the quantity $k_{10} L \eta / 2$ is not small, the expression (6.45) is written

$$\sin(k_1 L) = \sin(k_{10} L) \cosh(k_{10} L \eta / 2) - i \cdot \cos(k_{10} L) \sinh(k_{10} L \eta / 2)$$

The amplitude of the displacement has for small losses a maximum when

$$k_{10}L = \omega L \sqrt{\frac{\rho}{E_0}} = n\pi, \quad n = 1, 2, 3, \dots \quad (6.47)$$

Comparing Eq. (6.21), these maxima occur when the frequency of the driving force coincides with any of the eigenfrequencies of the system resulting in a resonance at that particular frequency.

The result presented in Eq. (6.44) has an important property of reciprocity. The displacement at a point $x = x_2$ caused by a point force $F_0 \exp(i\omega t)$ at $x = x_1$ where $x_2 > x_1$ is

$$\xi(x_2, t) = F_0 \cdot e^{i\omega t} G_1(x_2|x_1) = -\frac{F_0 e^{i\omega t}}{SEk_1} \frac{\cos(k_1 x_1) \cos[k_1(L - x_2)]}{\sin(k_1 L)} \quad (6.48)$$

If on the other hand the force is applied at $x = x_2$, the displacement at $x = x_1$ is

$$\xi(x_1, t) = F_0 \cdot e^{i\omega t} G_2(x_1|x_2) = -\frac{F_0 e^{i\omega t}}{SEk_1} \frac{\cos(k_1 x_1) \cos[k_1(L - x_2)]}{\sin(k_1 L)} \quad (6.49)$$

Thus

$$G_1(x_2|x_1) = -\frac{\cos(k_1 x_1) \cos[k_1(L - x_2)]}{SEk_1 \sin(k_1 L)},$$

$$G_2(x_1|x_2) = -\frac{\cos(k_1 x_1) \cos[k_1(L - x_2)]}{SEk_1 \sin(k_1 L)}$$

The resulting displacement is the same for the two cases or $G(x_1|x_2) = G(x_2|x_1)$. The result can be generalized as the theorem of reciprocity:

A force acting on a linear system in a position i , gives a certain displacement of the system in position j . The same displacement is obtained at position i , if the same force is applied at position j .

The principle of reciprocity can be useful for experimental work. For example, if the frequency response function between excitation and response points is to be measured. For practical reasons it might not be possible to mount the exciter at the desired position, whereas the response point is more accessible. Excitation and response points can therefore be interchanged, for the measurement of the desired transfer function. The quality of an FRF measurement can be verified by making reciprocal measurements, i.e., by exchanging excitation and observation points. If not the same result is obtained, either the measurements are not correct or the system can not be considered linear.

Green's function can be used to solve Eq. (6.31), i.e., to derive the response of a beam excited by any harmonic force function. The result is obtained by superposition. As before let the distributed force be given by $F'(x) \cdot \exp(i\omega t)$. At $x = \zeta$, the force acting on an element with the length $\Delta\zeta$ is $F'(\zeta) \cdot \Delta\zeta$. The response $\Delta\xi$ due to this force is

$$\Delta \xi = \Delta \zeta \cdot F'(\zeta) G(x|\zeta)$$

A summation or rather integration of the contributions from each part of the beam gives

$$\xi(x, t) = e^{i\omega t} \int_0^L F'(\zeta) G(x|\zeta) d\zeta \quad (6.50)$$

Green's function is given by $G_1(x|\zeta)$ for $0 \leq \zeta \leq x$ and by $G_2(x|\zeta)$ for $x \leq \zeta \leq L$. The response is consequently

$$\xi(x, t) = e^{i\omega t} \left[\int_0^x F'(\zeta) G_1(x|\zeta) d\zeta + \int_x^L F'(\zeta) G_2(x|\zeta) d\zeta \right] \quad (6.51)$$

For a beam with free ends and constant cross section, the result is according to Eq. (6.44)

$$\begin{aligned} \xi(x, t) = & -\frac{e^{i\omega t}}{SEk_1 \sin(k_1 L)} \\ & \times \left\{ \cos[k_1(L-x)] \int_0^x F'(\zeta) \cos(k_1 \zeta) d\zeta + \cos(k_1 x) \int_x^L F'(\zeta) \cos[k_1(\zeta-L)] d\zeta \right\} \end{aligned} \quad (6.52)$$

Green's function can be derived for other boundary conditions. For a clamped-clamped beam Green's function is

$$\begin{aligned} G_1(x|x_1) = & -\frac{\sin(k_1 x_1) \sin[k_1(x-L)]}{SEk_1 \cdot \sin(k_1 L)} \quad \text{for } 0 \leq x_1 \leq x \\ G_2(x|x_1) = & -\frac{\sin(k_1 x) \sin[k_1(x_1-L)]}{SEk_1 \cdot \sin(k_1 L)} \quad \text{for } x \leq x_1 \leq L \end{aligned} \quad (6.53)$$

The corresponding result for a beam with a free end at $x = L$ and a clamped end at $x = 0$ is

$$\begin{aligned} G_1(x|x_1) = & \frac{\sin(k_1 x_1) \cos[k_1(L-x)]}{SEk_1 \cdot \cos(k_1 L)} \quad \text{for } 0 \leq x_1 \leq x \\ G_2(x|x_1) = & \frac{\sin(k_1 x) \cos[k_1(x_1-L)]}{SEk_1 \cdot \cos(k_1 L)} \quad \text{for } x \leq x_1 \leq L \end{aligned} \quad (6.54)$$

The response of the beam due to forced excitation is thereafter obtained from Eq. (6.51). The approach of finding the displacement of a beam exposed to forced excitation by using Green's function can be illustrated in an alternative way. Green's function $G(x|x_1)$ is the solution to the equation

$$SE \frac{\partial^2 G}{\partial x^2} + \omega^2 S \rho G = -\delta(x - x_1) \quad (6.55)$$

This follows from Eqs. (6.31) and (6.32) by setting $F_0 = 1$ and by replacing ξ by G . For a beam excited by the force $F'(x) \cdot \exp(i\omega t)$ per unit length, the forced response is $\xi(x) \cdot \exp(i\omega t)$ where ξ should satisfy the equation

$$SE \frac{\partial^2 \xi}{\partial x^2} + \omega^2 S \rho \xi = -F'(x) \quad (6.56)$$

Equation (6.55) is multiplied by ξ and Eq. (6.56) by G . The results are subtracted giving

$$SE \left[\xi \frac{\partial^2 G}{\partial x^2} - G \frac{\partial^2 \xi}{\partial x^2} \right] = -\xi(x) \delta(x - x_1) + F'(x) G(x|x_1) \quad (6.57)$$

This expression is integrated with respect to x over the length of the beam. Thus

$$SE \int_0^L dx \left[\xi \frac{\partial^2 G}{\partial x^2} - G \frac{\partial^2 \xi}{\partial x^2} \right] = -\xi(x_1) + \int_0^L dx F'(x) G(x|x_1) \quad (6.58)$$

The expression on the left-hand side of this equation is denoted K . After partial integration the expression K reads

$$K = SE \left[\xi \frac{\partial G}{\partial x} - G \frac{\partial \xi}{\partial x} \right]_0^L \quad (6.59)$$

The functions ξ and G must satisfy the same boundary conditions. If these are identical to any of the natural boundary conditions the expression K is equal to zero since either ξ and G or $\partial \xi / \partial x$ and $\partial G / \partial x$ are zero at the boundaries. For the periodic and resilient mounting conditions, K is also equal to zero. The displacement ξ of the beam is obtained by setting the left-hand side of Eq. (6.57) equal zero. Since $G(x|x_1)$ is symmetric with respect to x and x_1 the result of Eq. (6.57) is after exchanging x by ζ and x_1 by x given by

$$\xi(x) = \int_0^L d\zeta F'(\zeta) G(x|\zeta) \quad (6.60)$$

This is result given by Eq. (6.50) omitting the time dependence $\exp(i\omega t)$.

6.3 The Mode Summation Technique

In Sect. 6.1, it was established that free or transient longitudinal vibrations in a finite beam can be expressed as a sum over the appropriate orthogonal eigenfunctions. The amplitude corresponding to each eigenfunction is determined by the initial conditions. Forced excitation of a structure is really just a summation of an infinite number of transient excitations. This simple argument leads to the conclusion that even the

response of a structure—or rather a linear system—due to forced excitation, can be expressed as a sum over the appropriate orthogonal eigenfunctions. In fact, any continuous function can be expanded in a series of orthogonal eigenfunctions, or any other set of orthogonal functions, if the series converges uniformly. This statement is based on Bessel's Inequality and the Completeness Relation. These theorems are perhaps best described by Courant and Hilbert in Ref. [58].

Having considered these very fundamental issues, a return to the basic problem is made. The general differential equation governing the forced excitation of L-waves in a beam is given in Eq. (6.31). For

$$\xi(x, t) = \xi(x) \cdot e^{i\omega t}, \quad F'(x, t) = F'(x) \cdot e^{i\omega t}$$

the Eq. (6.31) is simplified to

$$\frac{d^2 \xi}{dx^2} + k_l^2 \xi = -\frac{F'}{SE} \quad (6.61)$$

The time dependence is omitted. Let $\varphi_n(x)$ be a complete set of orthogonal eigenfunctions. The displacement of the beam, which for a continuous beam is also a continuous function, can according to the introduction be expanded in a series as

$$\xi(x) = \sum_{n=0}^{\infty} C_n \cdot \varphi_n(x) \quad (6.62)$$

In this sum, the expansion coefficients C_n are as yet unknown. In order to determine these coefficients, the differential Eq. (6.61) is multiplied by φ_n . The resulting expression is integrated over the length of the beam. The result is

$$\int_0^L \varphi_n \frac{d^2 \xi}{dx^2} dx + k_l^2 \int_0^L \varphi_n \xi dx = -\frac{1}{SE} \int_0^L \varphi_n F' dx \quad (6.63)$$

The first integral is integrated by parts. Thus

$$\int_0^L \varphi_n \frac{d^2 \xi}{dx^2} dx = \left[\varphi_n \frac{d\xi}{dx} - \frac{d\varphi_n}{dx} \xi \right]_0^L + \int_0^L \frac{d^2 \varphi_n}{dx^2} \xi dx \quad (6.64)$$

If φ_n and ξ both satisfy one of the so-called closed boundary conditions listed in Sect. 6.1, the expression corresponding to the bracket in Eq. (6.64) is equal to zero. Since φ_n satisfies the same boundary condition as ξ , which is assumed to be one of those listed in Sect. 6.1, and then φ_n is an orthogonal eigenfunction. According to Eq. (6.11) k_n and φ_n are related as $d^2 \varphi_n / dx^2 = -k_n^2 \varphi_n$. By inserting this condition in Eq. (6.64) and by setting the bracket in the same expression equal to zero for any of the natural boundary conditions, Eq. (6.64) is reduced to

$$\int_0^L \varphi_n \frac{d^2 \xi}{dx^2} dx = -k_n^2 \int_0^L \varphi_n \xi dx \quad (6.65)$$

This result in combination with Eq. (6.63) gives

$$(k_1^2 - k_n^2) \langle \varphi_n | \xi \rangle = -\frac{1}{SE} \langle \varphi_n | F' \rangle \quad (6.66)$$

The general interpretation of the expressions enclosed by the triangular brackets is

$$\langle f | g \rangle = \int_0^L f(x)g(x)dx$$

The general solution (6.62) is now multiplied by φ_m and integrated over x or the length of the beam. The result is

$$\langle \varphi_m | \xi \rangle = \sum_{n=0}^{\infty} C_n \langle \varphi_m | \varphi_n \rangle$$

The eigenfunctions φ_m and φ_n are orthogonal. Thus the product $\langle \varphi_m | \varphi_n \rangle$ is only different from zero for $m = n$. The infinite sum is consequently reduced to a single term, namely $C_m \langle \varphi_m | \varphi_m \rangle$. The equation above is therefore equal to

$$\langle \varphi_m | \xi \rangle = C_m \langle \varphi_m | \varphi_m \rangle \quad (6.67)$$

For $m = n$ the Eqs. (6.66) and (6.67) give

$$C_n = -\frac{\langle \varphi_n | F' \rangle}{SE \langle \varphi_n | \varphi_n \rangle (k_1^2 - k_n^2)} \quad (6.68)$$

The expressions (6.62) and (6.68) give the complete solution to the Eq. (6.61). The norm $\langle \varphi_m | \varphi_m \rangle$ of the eigenvectors is equal to $L/2$ except for the mode $n = 0$ for the boundary condition corresponding to free ends as discussed in Sect. 6.1. The solution to Eq. (6.61) is consequently

$$\xi(x, t) = \xi(x)e^{i\omega t} = -\sum_{n=0}^{\infty} \frac{\langle \varphi_n | F' \rangle \varphi_n(x)e^{i\omega t}}{SE \langle \varphi_n | \varphi_n \rangle (k_1^2 - k_n^2)} \quad (6.69)$$

As an example, consider a beam which is clamped at $x = 0$. The other end, at $x = L$, is free. The cross-sectional area of the beam is constant and equal to S . The beam is excited by a harmonic force at $x = x_1$ as shown in Fig. 6.4. The force function F' and the eigenfunctions satisfying the appropriate boundary conditions are

$$F'(x, t) = F_0 \delta(x - x_1) e^{i\omega t}, \quad \varphi_n(x) = \sin(k_n x), \quad k_n = (n + 1/2)\pi/L \quad (6.70)$$

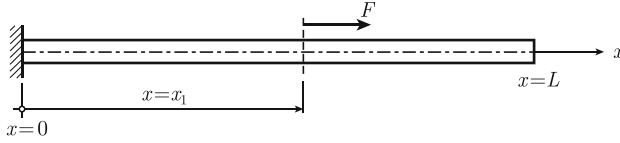


Fig. 6.4 A finite beam excited by a harmonic force at $x = x_1$. The beam is clamped at $x = 0$ and free at $x = L$

Compare Table 6.1. The response of the beam is given by Eq. (6.69). The product between the force, omitting the time-dependent function, and the eigenfunction defined in (6.60) is

$$\langle F' \mid \varphi_n \rangle = F_0 \int_0^L \sin(k_n x) \delta(x - x_1) dx = F_0 \sin(k_n x_1) \quad (6.71)$$

The norm of the eigenfunction is $L/2$. The response is consequently

$$\begin{aligned} \xi(x, t) &= \frac{2F_0}{SEL} \sum_{n=0}^{\infty} \frac{\sin(k_n x_1) \sin(k_n x)}{(k_n^2 - k_1^2)} \cdot e^{i\omega t} \\ &= \frac{2F_0}{SL\rho(2\pi)^2} \sum_{n=0}^{\infty} \frac{\sin(k_n x_1) \sin(k_n x)}{[f_n^2(1 + i\eta) - f^2]} \cdot e^{i\omega t} \end{aligned} \quad (6.72)$$

The general definition of the wave number $k_l^2 = (2\pi f)^2 \rho / [E_0(1 + i\eta)]$ plus the expression (6.23) defining f_n have been inserted in the first part of Eq. (6.72) to obtain the final expression. The coefficients in front of the eigenfunction $\sin(k_n x)$ under the summation sign converge, as n goes to infinity as required, to make this type of expansion of the displacement. The E -modulus and the wave number k_1 are complex quantities. The result (6.72) is equivalent to the expression previously derived in Sect. 6.2 and given by Green's function. The result in Sect. 6.2 is in closed form, whereas the result (6.72) is expressed as an infinite sum. If the first result is expanded by means of the orthogonal eigenfunctions φ_n given in Eq. (6.70) the two results are identical. Again it is evident that the amplitude of ξ is large, when the real part of the wavenumber is equal to any eigenvalue k_n or rather when the forced frequency is equal to a natural frequency of the system. The result (6.72) clearly illustrates the reciprocity concept. The response $\xi(x, t)$ due to a point force at $x = x_1$ is identical to the response $\xi(x_1, t)$ due to a force applied at x .

Returning to the very simple 1-DOF system, the response $x = x_0 \cdot \exp(i\omega t)$ due to a force $F = F_0 \cdot \exp(i\omega t)$ is according to Eq. (1.81)

$$x(t) = \frac{F_0 e^{i\omega t}}{k_0(1 + i\delta) - m\omega^2} = \frac{F_0 e^{i\omega t}}{m(2\pi)^2 [f_0^2(1 + i\delta) - f^2]}$$

The similarity to the result (6.72) is evident when considering that the mass m of the beam is $m = \rho SL$ rendering Eq. (6.72) into

$$\xi(x, t) = \frac{2F_0}{m(2\pi)^2} \sum_{n=0}^{\infty} \frac{\sin(k_n x_1) \sin(k_n x)}{[f_n^2(1 + i\eta) - f^2]} \cdot e^{i\omega t} \quad (6.73)$$

Each mode of the continuous system is vibrating like a simple 1-DOF system. The similarities between a 1-DOF and a continuous system are even more apparent after an introduction of modal parameters like modal mass, modal stiffness and modal force. This is discussed in Sect. 7.4.

6.4 Kinetic Energy of Vibrating Beam

For a force with the time dependence $\exp(i\omega t)$ exciting a beam, the resulting forced displacement must also be a function of $\exp(i\omega t)$ as long as the transients are neglected. In Chap. 2 it was pointed out that the amplitudes of the force and displacement with this time dependence can be interpreted as their respective Fourier transforms $\hat{\xi}$ and \hat{F} . For a beam clamped at $x = 0$ and free at $x = L$ and excited by a force with the FT \hat{F} at $x = x_1$ the FT of the displacement is according to Eq. (6.72) given by

$$\hat{\xi}(x, \omega) = \frac{2\hat{F}(\omega)}{SEL} \sum_{n=0}^{\infty} \frac{\sin(k_n x_1) \sin(k_n x)}{(k_n^2 - k_1^2)} \quad (6.74)$$

The wavenumber k_1 is a function of ω . The FT of the velocity is according to Eq. (2.42) given by $\hat{v} = i\omega \hat{\xi}$. The transfer mobility between the velocity at the position x and the force at $x = x_1$ is consequently

$$Y(x, x_1, \omega) = \frac{\hat{v}(x, \omega)}{\hat{F}(x_1, \omega)} = \frac{2i\omega}{SEL} \sum_{n=0}^{\infty} \frac{\sin(k_n x_1) \sin(k_n x)}{(k_n^2 - k_1^2)} \quad (6.75)$$

The two-sided power spectral densities for displacement and velocity are $S_{\xi\xi}(\omega)$ and $S_{vv}(\omega)$, respectively. These spectral densities are related as $S_{vv} = \omega^2 S_{\xi\xi}$. The spectral density $S_{vv}(\omega)$ can, according to the general definition (2.33) and in combination with Eq. (6.74), be expressed as a function of the two-sided power spectral density S_{FF} of the force as

$$S_{vv}(\omega) = S_{FF}(\omega) \left| \frac{2\omega}{SEL} \sum_{n=0}^{\infty} \frac{\sin(k_n x_1) \sin(k_n x)}{(k_n^2 - k_1^2)} \right|^2 \quad (6.76)$$

The time average of the total kinetic energy for the beam with the cross-sectional area S and the density ρ is

$$\bar{T} = \frac{1}{2} \int_0^L \rho S |\bar{v}|^2 dx = \frac{1}{2} \int_0^L \rho S dx \int_{-\infty}^{\infty} \frac{1}{2\pi} S_{vv}(\omega) d\omega$$

The power spectral density includes the square of an infinite sum. When this quantity is integrated with respect to x , it is reduced to a single infinite sum. This is due to the orthogonality of the eigenfunctions $\sin(k_n x)$. The time average of the kinetic energy is thus

$$\bar{T} = \frac{1}{4\pi} \sum_{n=0}^{\infty} \int_{-\infty}^{\infty} \frac{2\omega^2 \rho S L \sin^2(k_n x_1)}{|SEL|^2 |k^2 - k_n^2|^2} S_{FF}(\omega) d\omega \quad (6.77)$$

For white noise excitation $S_{FF}(\omega)$ is constant. The denominator under the summation sign in Eq. (6.73) can be written as

$$|SEL(k^2 - k_n^2)|^2 = (2\pi)^4 (SL\rho)^2 [(f^2 - f_n^2)^2 + (\eta f_n^2)^2] \quad (6.78)$$

The eigenfrequency f_n corresponds to the eigenfunction φ_n as given in the table in Sect. 6.1. The mass of the beam is $m = SL\rho$. The time average of the kinetic energy for white noise excitation is thus

$$\bar{T} = \sum_{n=0}^{\infty} S_{FF} \int_{-\infty}^{\infty} \frac{f^2 \sin^2(k_n x_1)}{(2\pi)^2 m [(f^2 - f_n^2)^2 + (\eta f_n^2)^2]} df \quad (6.79)$$

This type of integral was solved in Chap. 2, Eq. (2.63). The solution to Eq. (6.79) is consequently

$$\bar{T} = \sum_{n=0}^{\infty} S_{FF} \frac{\sin^2(k_n x_1)}{4\pi m f_n \eta} = \sum_{n=0}^{\infty} G_{FF} \frac{\sin^2(k_n x_1)}{8\pi m f_n \eta} \quad (6.80)$$

For viscous losses, the product ηf_n is constant. If in addition, the force is randomly distributed over the length of the beam, then the space average of the function $\sin^2(k_n x_1)$ is equal to $1/2$. The time average of the kinetic energy for this case is

$$\bar{T} = \sum_{n=0}^{\infty} \bar{T}_n, \quad \bar{T}_n = \frac{S_{FF}}{8\pi m f_n \eta} = \frac{G_{FF}}{16\pi m f_n \eta} \quad (6.81)$$

This means that the contribution from each mode to the total kinetic energy is the same. Or in other words, if a random force in space and time excites a linear system with viscous losses, then the kinetic energy of each mode is the same. This is often referred to as the equipartition of energy between modes. These conclusions are valid as long as the beam satisfies any of the closed boundary conditions listed in

Sect. 6.1. These boundary conditions give orthogonal eigenfunctions, a requirement for obtaining the result (6.81).

In Chap. 5, the influence of losses on the attenuation of L-waves propagating in an infinite beam was found to be very small. For finite beams, the magnitude of the loss factor is of great importance. As shown in Eq. (6.81), the time average of the kinetic energy is inversely proportional to the loss factor for white noise excitation. If the losses are increased, as discussed in Chap. 5, the kinetic energy can be drastically reduced. However, as discussed before, this is true only for white noise excitation. For harmonic excitation added damping is only efficient close to a resonance.

The summation and integration in Eq. (6.79) can, without loss of generality, be interchanged resulting in

$$\bar{T} = \int_{-\infty}^{\infty} df \sum_{n=0}^{\infty} S_{FF}(\omega) \frac{f^2 \sin^2(k_n x_1)}{(2\pi)^2 m [(f^2 - f_n^2)^2 + (\eta f_n^2)^2]} \quad (6.82)$$

The angular frequency ω is as always $\omega = 2\pi f$. According to the general definition of average energy as a function of spectral densities given in Eq. (2.49), this energy \bar{T} can also be written as

$$\bar{T} = \frac{1}{2\pi} \int_{-\infty}^{\infty} S_T(\omega) d\omega = \frac{1}{2\pi} \int_0^{\infty} G_T(\omega) d\omega \quad (6.83)$$

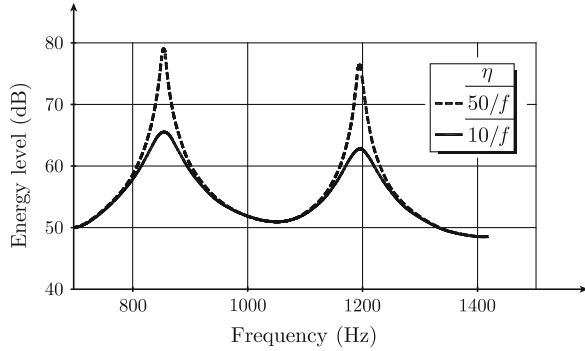
In these expressions, $G_T(\omega)$ and $S_T(\omega)$ are the one- and two-sided spectral densities representing the kinetic energy. The expression after the summation sign in Eq. (6.82) is according to Eq. (6.83) equal to the two-sided spectral density for the kinetic energy. The one-sided spectral density is consequently

$$G_T(\omega) = \sum_{n=0}^{\infty} G_{FF}(\omega) \frac{f^2 \sin^2(k_n x_1)}{(2\pi)^2 m [(f^2 - f_n^2)^2 + (\eta f_n^2)^2]} \quad (6.84)$$

The function $G_{FF}(\omega)$ is for white noise excitation constant. The function $G_T(\omega)$ or rather the level $10 \log G_T(\omega)$ in dB with respect to some reference level is shown in Fig. 6.5.

In this example, the beam is assumed to be made of concrete, $E = 2.8 \times 10^{10} \text{ N/m}^2$ and $\rho = 2400 \text{ kg/m}^3$. The length of the beam is 5 m. The x -coordinate x_1 , defining the excitation point, is set to equal $0.64 \times L$. The energy density level is shown in the octave band with the center frequency 1 kHz. The relative amplitudes of the maxima are determined by the coordinate x_1 , the eigenfrequency f_n and thus also k_n as well as the loss factor. In Fig. 6.5, the result is given for two loss factors. In one case, the product between frequency and loss factor is equal to 10, while in the other case the same product is 50. This means that the losses are assumed to be viscous. There are two resonances within the frequency band. It is evident that the energy level is only influenced by the loss factor close to a resonance. At a resonance, the level is

Fig. 6.5 The one-sided power spectral density of the kinetic energy given as $10 \log G_T(\omega)$ in the 1 kHz octave band. The beam is excited by white noise. The result is given for two loss factors: $\eta = 50/f$, $\eta = 10/f$



15–30 dB above the level in between resonances. The total level in the frequency band is consequently determined mainly by the energy densities close to the resonances.

The time average of the kinetic energy within a certain frequency band Δf , defined as $\Delta f = f_u - f_l$, is

$$\bar{T}_{\Delta f} = \frac{1}{2\pi} \int_{\omega_l}^{\omega_u} G_T(\omega) d\omega = \int_{f_l}^{f_u} G_T(2\pi f) df \quad (6.85)$$

If the losses are small, the modes with eigenfrequencies well outside the frequency interval Δf do not significantly contribute to the kinetic energy within the band. The infinite sum of Eq. (6.80) can therefore be approximated by the terms for which the mode number n satisfies the inequality $n_l \leq n \leq n_u$ where n_l corresponds to the eigenfrequency f_u and n_l to f_l . The upper mode number is denoted n_u and the lower n_l . The average number of modes within the frequency band Δf is determined by the modal density \mathcal{N}_f , defined in Eq. (6.24). The total number N of modes within the band is approximately equal to

$$N = \Delta f \cdot \mathcal{N}_f \quad (6.86)$$

The time average of the modal energy is according to Eq. (6.80)

$$\bar{T}_n = G_{FF} \frac{\sin^2(k_n x_1)}{8\pi m f_n \eta}$$

For white noise excitation G_{FF} is constant. For viscous losses, the product ηf_n is also constant. The time average of the kinetic energy within the band is, if only the modes for which $n_l \leq n \leq n_u$, approximately equal to

$$\bar{T}_{\Delta f} = \sum_{n=n_l}^{n_u} \bar{T}_n = \frac{G_{FF}}{8\pi m f_n \eta} \sum_{n=n_l}^{n_u} \sin^2(k_n x_1) \quad (6.87)$$

The sine squared function varies for each mode. For a sufficiently large number of modes within the band, the sum is approximately equal to the number of modes within the frequency band, times the average of the sine squared function. The average with respect to the product $(k_n x_1)$ of the sine squared function is equal to 1/2. Considering this an approximate expression for the time average of the kinetic energy within the frequency band is, for white noise excitation, equal to

$$\bar{T}_{\Delta f} = N\bar{T}_n = \Delta f \cdot \mathcal{N}_f \cdot \bar{T}_n = \Delta f \cdot \mathcal{N}_f \cdot \frac{G_{FF}}{16\pi m f_n \eta} = \Delta f \cdot \frac{G_{FF}}{8\pi S f_n \eta \sqrt{\rho E_0}} \quad (6.88)$$

The parameter f_n can be set to equal the center frequency of the band, i.e., $f_n = \sqrt{f_l \cdot f_u}$. The loss factor can be determined by means of reverberation time measurements. The modal density \mathcal{N}_f is given in Eq. (6.24). The cross-sectional area of the beam is S .

For the boundary conditions i), ii), and iv) in Table 6.1, the modal density is independent of the boundary conditions of the beam. Thus, the time average of the kinetic energy of a beam excited by white noise distributed along the length of the beam is given by Eq. (6.88) for any of the boundary conditions i), ii) and iv) in Table 6.1. However, the frequency band Δf should be wide enough to include a number of natural frequencies.

The error, as compared to the exact solution, is small if there is a sufficient number of modes in the frequency band. In this particular case, for the concrete beam previously described, the accuracy of this approximate or statistical method is illustrated in Fig. 6.6. The coordinate for the excitation point is $0.64 \times L$. The kinetic energy is calculated in 1/1 octave bands by means of numerical integration of the exact expression, Eqs. (6.84) and (6.85), and from the corresponding approximate expression (6.88).

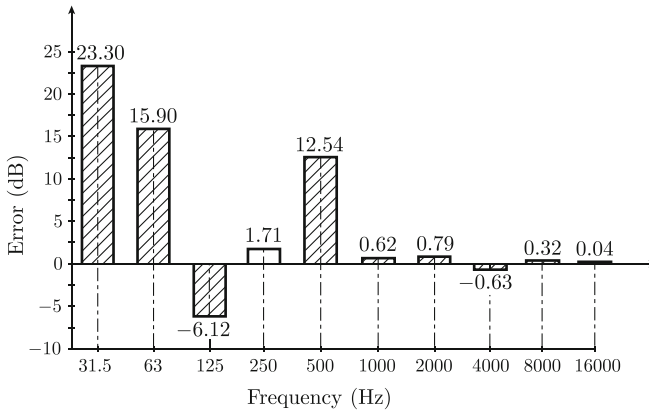


Fig. 6.6 Calculation of kinetic energy in beam excited by white noise. The error is the difference between exact and approximate results

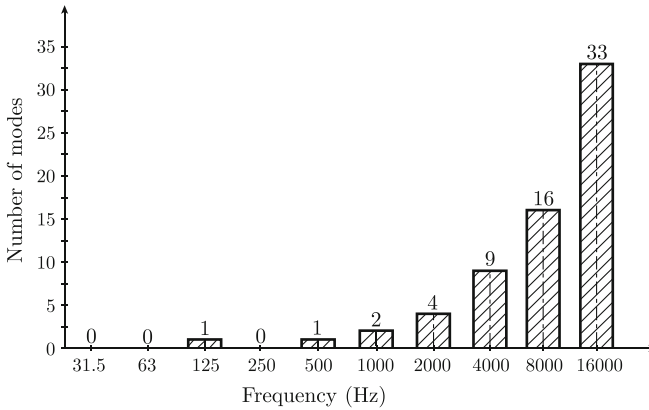


Fig. 6.7 Number of modes in octave bands for a 5 m long concrete beam

The number of modes in each octave band is shown in Fig. 6.7. In this particular case, the error shown in Fig. 6.6 is less than 1 dB if there are two or more modes in a band. The error very much depends on the number of modes in each frequency band. A large number of modes is required to ensure that the average of the sine squared term in Eq. (6.87) approximately is 1/2. As a general rule, there should be at least four resonances within a band for this type of analysis to be made. This statistical method can be very powerful for the estimation of energies in the high frequency regions. When the modal density is low, exact methods should be used. However, in the low frequency region only the first few modes have to be considered. This simplifies the analysis considerably.

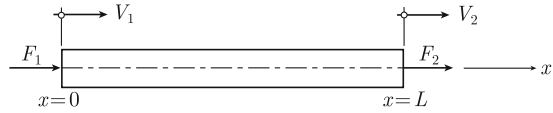
6.5 Mobilities

In Sect. 5.1—Eq. (5.21)—the point mobility for a semi infinite beam was derived. The point mobility was defined as the ratio between the Fourier transforms of velocity and force at the free end of the beam. The positive directions of force and velocity were defined along the same axis. This definition can be made more general by defining the transfer mobility Y_{ij} as the ratio between the FT of a force F_i in point i and the resulting FT of the velocity v_j in a point j as

$$Y_{ij} = \frac{\hat{v}_j}{\hat{F}_i} \quad (6.89)$$

For $i = j$, the expression above is equal to the point mobility at point i . Due to the reciprocity discussed in Sect. 6.2 it follows that for a linear system

Fig. 6.8 External forces applied to a beam and resulting velocities



$$Y_{ij} = Y_{ji} \quad (6.90)$$

By means of the expressions (6.48) and (6.49), the transfer mobilities are readily obtained for a beam with free ends. For other boundary conditions, the calculations follow the same procedure as those outlined in Sect. 6.2.

The transfer mobilities between the two ends of a beam are of special importance for the calculation of the response of coupled structures, partly consisting of beams. These mobilities are readily derived, based on the results (6.48) and (6.49). Thus, consider a beam with the length L and cross-sectional area S . The beam is oriented along the x -axis as shown in Fig. 6.8.

Two harmonic forces are applied to the beam, one at each end. The response or displacement ξ_2 anywhere along the beam due to the force $F_2 \cdot \exp(i\omega t)$ at $x_2 = L$ is obtained from Eq. (6.49). The result is

$$\xi_2(x, t) = -F_2 \cdot e^{i\omega t} \frac{\cos(k_1 x)}{SEk_1 \sin(k_1 L)}$$

The displacement ξ_1 due to the force F_1 at $x_1 = 0$ is

$$\xi_1(x, t) = -F_1 \cdot e^{i\omega t} \frac{\cos[k_1(L - x)]}{SEk_1 \sin(k_1 L)}$$

The total response caused by both forces is thus

$$\xi(x, t) = \xi_1(x, t) + \xi_2(x, t) = -\frac{e^{i\omega t}}{SEk_1 \sin(k_1 L)} \{F_1 \cos[k_1(L - x)] + F_2 \cos(k_1 x)\} \quad (6.91)$$

The velocity v_1 at $x = 0$ is thus

$$v_1 = \dot{\xi}(0, t) = -\frac{i\omega e^{i\omega t}}{SEk_1 \sin(k_1 L)} [F_1 \cos(k_1 L) + F_2] \quad (6.92)$$

The velocity v_2 at the other end is for $x = L$

$$v_2 = \dot{\xi}(L, t) = -\frac{i\omega e^{i\omega t}}{SEk_1 \sin(k_1 L)} [F_2 \cos(k_1 L) + F_1] \quad (6.93)$$

By making the substitutions $F_i \rightarrow \hat{F}_i \cdot e^{i\omega t}$ and $v_i \rightarrow \hat{v}_i \cdot e^{i\omega t}$ as discussed in Sect. 5.1 the Fourier transforms of the velocities are obtained as

$$\begin{aligned}\hat{v}_1 &= -\frac{i\omega}{SEk_1 \sin(k_1 L)} \left[\hat{F}_1 \cos(k_1 L) + \hat{F}_2 \right], \\ \hat{v}_2 &= -\frac{i\omega}{SEk_1 \sin(k_1 L)} \left[\hat{F}_2 \cos(k_1 L) + \hat{F}_1 \right]\end{aligned}\quad (6.94)$$

The wavenumber k_1 is complex due to the losses. The sine function in the denominator is therefore never equal to zero ensuring that \hat{v}_i is finite. The FT of the velocities can also be expressed by means of the transfer mobilities Y_{ij} as

$$\hat{v}_1 = \hat{F}_1 Y_{11} + \hat{F}_2 Y_{21}, \quad \hat{v}_2 = \hat{F}_2 Y_{22} + \hat{F}_1 Y_{12} \quad (6.95)$$

An identification of parameters in the Eqs. (6.94) and (6.95) gives

$$Y_{11} = Y_{22} = -\frac{i\omega}{SEk_1 \tan(k_1 L)}, \quad Y_{12} = Y_{21} = -\frac{i\omega}{SEk_1 \sin(k_1 L)} \quad (6.96)$$

In this particular case, the beam or rod is symmetric with respect to its midpoint. Therefore the point mobilities Y_{11} and Y_{22} are identical. If however, the beam had a conical shape, the area of one end being larger than the other, then Y_{11} and Y_{22} would not be equal. The transfer mobilities Y_{12} and Y_{21} are, for linear systems, always equal due to reciprocity. The parameters E and k_1 in Eq. (6.96) are complex due to the losses and defined as $E = E_0(1 + i\eta)$ and $k_1 = k_{10}(1 - i\eta/2)$ for $\eta \ll 1$. The trigonometric expressions in Eq. (6.96), can be rewritten as

$$\begin{aligned}\sin(k_1 L) &= \frac{1}{2i} \left[\exp(ik_{10}L + k_{01}L\eta/2) - \exp(-ik_{10}L - k_{01}L\eta/2) \right] \\ \cos(k_1 L) &= \frac{1}{2} \left[\exp(ik_{10}L + k_{01}L\eta/2) + \exp(-ik_{10}L - k_{01}L\eta/2) \right]\end{aligned}\quad (6.97)$$

The loss factor η is a positive quantity, consequently

$$\lim_{L \rightarrow \infty} \frac{1}{\sin(k_1 L)} = 0, \quad \lim_{L \rightarrow \infty} \frac{1}{\tan(k_1 L)} = i \quad (6.98)$$

This means that the point mobility for an infinite beam is obtained from Eqs. (6.95) and (6.98) as

$$\lim_{L \rightarrow \infty} Y_{11} = \frac{\omega}{SEk_1} = \frac{\omega(1 - i\eta/2)}{SE_0 k_{10}}$$

This is the same result as that derived in Sect. 5.1 for a semi-infinite beam. In a similar way, the limiting value for the transfer mobility Y_{12} is

$$\lim_{L \rightarrow \infty} Y_{21} = 0$$

For a sufficiently long beam, the force acting on the far end of the beam is insignificant as determined by Y_{21} . If for the sake of discussion it is argued that a finite beam can be treated as an infinite beam if

$$\left| \frac{Y_{21}}{Y_{11}} \right| < \frac{1}{10}$$

This condition would require that $k_{10}L\eta > 4.6$. For a steel beam with a loss factor of 0.01 the minimum length at 1 kHz would be of the order of 400 m.

6.6 Mass Mounted on a Rod

In Chap. 1 the response of a simple mass–spring system was discussed at length. A brief recapitulation of a typical problem. A stiff or solid mass m is mounted by means of a mass less spring on a solid foundation with a point mobility equal to zero. The mass is excited by a force $F = F_0 \cdot \exp(i\omega t)$. The spring constant k is defined as $k = k_0(1 + i\delta)$. The equation of motion of the mass is—compare Fig. 6.9— $m\ddot{x} + kx = F$.

The force F_2 acting on the foundation is for the stationary case

$$F_2 = kx = \frac{kF_0 \cdot e^{i\omega t}}{k - m\omega^2}$$

The absolute value of the ratio between the force on the foundation and the exciting force is obtained from

$$\left| \frac{F_2}{F} \right|^2 = \left| \frac{k}{k - m\omega^2} \right|^2 = \frac{f_0^4(1 + \delta^2)}{(f_0^2 - f^2)^2 + (\delta f_0^2)^2} \quad (6.99)$$

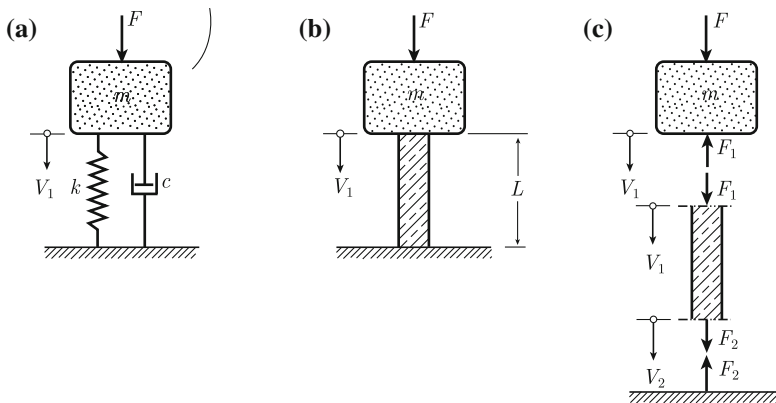


Fig. 6.9 Mass mounted on a spring and a rod. The foundation is infinitely stiff

The natural frequency f_0 of the system is $f_0 = 1/(2\pi)\sqrt{k_0/m}$. The static stiffness of a homogeneous rod or beam is obtained from Eq. (3.4). The force F acting on a rod compresses the rod $\xi = FL/(SE)$ where L is the length of the rod, $E = E_0(1 + i\eta)$ its Young's modulus and S its constant cross-sectional area. Since $F = kx$ it follows that

$$k_0 = \frac{SE_0}{L}, \quad \delta = \eta, \quad f_0 = \frac{1}{2\pi}\sqrt{\frac{k_0}{m}} = \frac{1}{2\pi}\sqrt{\frac{SE_0}{mL}} \quad (6.100)$$

From Eq. (6.99) it is evident that the ratio between the forces has a maximum when the frequency f is equal to the eigenfrequency f_0 of the system. The ratio $|F_2/F|$ in Eq. (6.99) is less than unity for $f > f_0 \cdot \sqrt{2}$. In this frequency range, the spring gives a positive insertion loss. For $f < f_0 \cdot \sqrt{2}$ the spring amplifies the force, i.e., the force on the foundation is larger than the force acting on the mass.

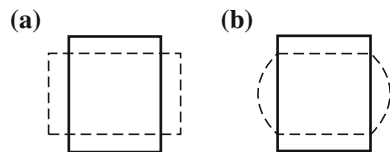
The compression of simple resilient mounts can, as a first approximation, be compared to the axial compression of a thin rod. However, the diameter of a cylindrical rubber mount is in general fairly large. A rod or a cylinder can be considered as thin if

$$\nu(1 + \nu)k_1\sqrt{S} < 1.6$$

where S is the cross-sectional area of the cylinder, $k_1 = \omega\sqrt{\rho/E}$ is the wave number for L-waves propagating in the cylinder and ν Poisson's ratio for the material. The inequality is a generalization of Eq. (4.61) which is valid for a plate with the thickness h being replaced by the characteristic cross-dimension \sqrt{S} of the cylinder. The shapes of a compressed ideal rod and a rubber element are not identical as indicated in Fig. 6.10. Under compression, the area of the cross-section of the rod does not vary along the length of the element. The ends of a real rubber element are generally fixed to some mounting device. Under compression, the area of the cross-section varies along the length of the element. Even without the mounting device, the frictional forces at the ends would cause the same type of deformation. Despite these limitations and differences, it is of interest to make the comparison between a mass mounted on a massless spring and on a simple rod. A resilient element is illustrated in Fig. 6.9 as a beam or a rod. The rod in the figure is assumed to be homogeneous with a constant cross-sectional area S . The forces are applied in such a way, that only L-waves are excited along the axis of the beam.

If instead of a massless spring, the resilient element is described as a rod, in which only L-waves can propagate in the direction of the axis, then the mobility concepts derived in the previous section can be used. The problem is illustrated in Fig. 6.9. The rod has a constant cross-sectional area S and the length L . The velocity of the

Fig. 6.10 Deformation of an ideal rod (a) and a rubber element (b)



upper end of the rod and thus also of the mass is v_2 . From Fig. 6.9 and Newton's second law and assuming a time dependence $\exp(i\omega t)$ it follows that

$$F = m\dot{v}_1 + F_1 = i\omega m \cdot v_1 + F_1 \quad (6.101)$$

The velocities v_1 and v_2 can be expressed as functions of the forces F_1 and F_2 as given in Eq. (6.94) or

$$v_1 = F_1 \cdot Y_{11} + F_2 \cdot Y_{21}, \quad v_2 = F_2 \cdot Y_{22} + F_1 \cdot Y_{12} \quad (6.102)$$

The functions v_1 , F_1 etc. in Eqs. (6.101) and (6.102) should be interpreted as the FT of the corresponding velocities and forces. If the foundation is infinitely stiff, its velocity is equal to zero, i.e., $v_2 = 0$. Thus from Eq. (6.102)

$$F_1 = -F_2 \cdot Y_{22}/Y_{12} \quad (6.103)$$

This result in combination with the first part of Eq. (6.102) gives

$$v_1 = F_2 \cdot \frac{(Y_{21} \cdot Y_{12} - Y_{22} \cdot Y_{11})}{Y_{12}} \quad (6.104)$$

The results (6.103) and (6.104) inserted in Eq. (6.101) yield

$$F = i\omega m F_2 \left[\frac{Y_{21} \cdot Y_{12} - Y_{22} \cdot Y_{11}}{Y_{12}} \right] - F_2 \cdot \frac{Y_{22}}{Y_{12}} \quad (6.105)$$

The transfer and point mobilities for a thin rod or beam are given in Eq. (6.96). Using this result in combination with Eq. (6.105), the ratio between the force on the foundation and the force on the mass is given as

$$\left| \frac{F_2}{F} \right|^2 = \left| \frac{SEk_1}{SEk_1 \cdot \cos(k_1 L) - m\omega^2 \sin(k_1 L)} \right|^2 \quad (6.106)$$

The Young's modulus of the rod is complex and according to standard procedure $E = E_0(1 + i\eta)$. The wave number for L-waves propagating in the rod is consequently also complex and given by $k_1 = k_{10}(1 - i\eta/2)$. The sine and cosine functions of the complex wavenumber in Eq. (6.106) can with $k_{10}L = \alpha$ be written as

$$\sin(k_1 L) = \sin(\alpha - i\alpha\eta/2) = \sin \alpha \cdot \cosh(\alpha\eta/2) - i \cdot \cos \alpha \cdot \sinh(\alpha\eta/2)$$

$$\cos(k_1 L) = \cos(\alpha - i\alpha\eta/2) = \cos \alpha \cdot \cosh(\alpha\eta/2) - i \cdot \sin \alpha \cdot \sinh(\alpha\eta/2)$$

The product SEk_1 is in a similar way written as

$$SEk_1 = SE_0 k_{10}(1 + i\eta/2)$$

These expressions in combination with Eq. (6.106) give the ratio between the force on the foundation and the external force. For small losses or rather when $k_{10}L\eta/2 \ll 1$ and with $X = SE_0k_{10}$ and $Z = m\omega^2$ the result (6.106) can be rewritten as

$$\left| \frac{F_2}{F} \right|^2 = \frac{X^2}{(X \cos \alpha - Z \sin \alpha)^2 + (\eta/2)^2 (Z \sin \alpha + X \alpha \sin \alpha + Z \alpha \cos \alpha)^2} \quad (6.107)$$

The ratio between the forces has maxima when, for small losses, the first parenthesis in the denominator is equal to zero, i.e., when

$$\tan \alpha = \tan(k_{10}L) = \frac{X}{Z} = \frac{SE_0k_{10}}{m\omega^2} \quad (6.108)$$

In the low frequency region, or when $k_{10}L \ll 1$, then $\tan(k_{10}L) \approx k_{10}L$ giving a maximum or resonance at the frequency f_0 where

$$f_0 = \frac{1}{2\pi} \sqrt{\frac{SE_0}{Lm}}$$

This is the same eigenfrequency which was derived for the simple mass-spring system. However, the Eq. (6.108) has an infinite number of solutions. In the high frequency range, the solutions approach

$$k_{10}L = n \cdot \pi, \quad n \text{ is an integer}$$

The transmissibility $\varepsilon = |F_2/F|$ is shown in Fig. 6.11 as function of f/f_0 where f is the frequency and f_0 the simple eigenfrequency given in Eq. (6.100). The parameter

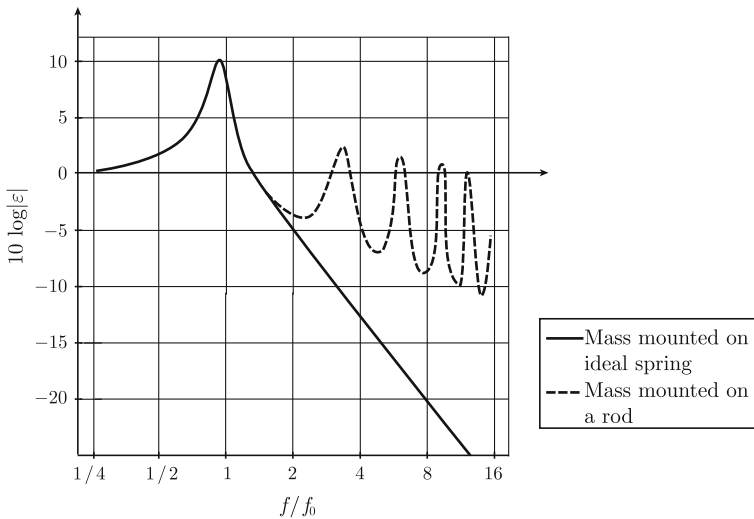


Fig. 6.11 Transmissibility

ε^2 is given in Eq. (6.99) for the simple theory and in Eq. (6.107) for the more complete solution.

It is clearly shown in Fig. 6.11 that the resonance phenomena in the rod drastically reduce the performance of the resilient element. At the first resonance of the mount, for $f/f_0 \approx 3.5$, the transmissibility predicted from the rod theory is 15 dB higher than the result obtained from the simple theory. The power transmitted to the foundation via the spring of the system shown in Fig. 6.9 is proportional to $|F_2|^2$ assuming a not completely stiff foundation. Consequently, for $f/f_0 \approx 3.5$, there is a difference of 30 dB between the power levels representing the power injected in the foundation as predicted by the two models. The discrepancies between the results from the two models can be very large in the frequency interval which is most significant with respect to the human sensation of annoyance.

The dimensions of an elastic element should always be chosen so that the first few eigenfrequencies of the system do not coincide with any major excitation at that particular frequency. Resilient mountings are also discussed in Chap. 10.

6.7 Transfer Matrices

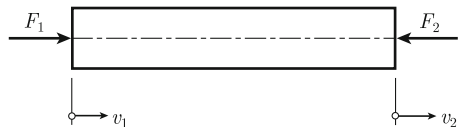
The response of beams coupled in the axial direction can readily be determined by means of so-called transfer matrices. The starting point is the by now standard beam shown in Fig. 6.12. The forces and the velocities at the ends of the beam are indicated in the figure. Note that the forces are defined positive when pointing towards the beam. It has been demonstrated in the previous sections, that if two of the quantities F_1 , F_2 , v_1 or v_2 are known then the two remaining quantities can be determined as functions of the two known quantities.

The basic expressions relating the Fourier transforms of forces and velocities are previously given in Eq. (6.94) as

$$v_1 = F_1 \cdot Y_{11} - F_2 \cdot Y_{21}, \quad v_2 = F_1 \cdot Y_{12} - F_2 \cdot Y_{22}$$

Note again that F_2 has a minus sign as compared to the previous case discussed in Sect. 6.5. The reason for this is that the positive direction of F_2 has been redefined. The quantities v_2 and F_2 can now be derived as functions of v_1 and F_1 as

Fig. 6.12 Forces acting on a rod



$$\begin{aligned}
 v_2 &= v_1 \frac{Y_{22}}{Y_{21}} + F_1 \left(\frac{Y_{12} \cdot Y_{21} - Y_{11} \cdot Y_{22}}{Y_{21}} \right) = a_{11}v_1 + a_{12}F_1 \\
 F_2 &= -v_1 \frac{1}{Y_{21}} + F_1 \frac{Y_{11}}{Y_{21}} = a_{21}v_1 + a_{22}F_1
 \end{aligned} \tag{6.109}$$

The mobilities for a simple rod were given in Eq. (6.96). The parameters a_{ij} are obtained from Eqs. (6.96) and (6.109) as

$$\begin{aligned}
 a_{11} &= \cos(k_1 L), \quad a_{12} = -\frac{i\omega \sin(k_1 L)}{SEk_1}, \\
 a_{21} &= -\frac{iSEk_1 \sin(k_1 L)}{\omega}, \quad a_{22} = \cos(k_1 L)
 \end{aligned} \tag{6.110}$$

In matrix form the result (6.110) is written

$$\begin{Bmatrix} v_2 \\ F_2 \end{Bmatrix}_n = [A]_n \cdot \begin{Bmatrix} v_1 \\ F_1 \end{Bmatrix}_n \tag{6.111}$$

The subscript n refers to beam n . The parameters k_1, L, S, E and loss factor which determine the elements a_{ij} of the matrix $[A]_n$ are specific for element n .

If now a number of beams are connected as shown in Fig. 6.13, then at the junction between the elements n and $n+1$ the following condition must be satisfied

$$\begin{Bmatrix} v_2 \\ F_2 \end{Bmatrix}_n = \begin{Bmatrix} v_1 \\ F_1 \end{Bmatrix}_{n+1}$$

where v_2 and F_2 are velocity and force at the end point on the right-hand side of beam n and v_1 and F_1 are the corresponding quantities on the left-hand side of beam $n+1$ as shown in Fig. 6.11. However based on Eq. (6.111)

$$\begin{Bmatrix} v_2 \\ F_2 \end{Bmatrix}_{n+1} = [A]_{n+1} \cdot \begin{Bmatrix} v_1 \\ F_1 \end{Bmatrix}_{n+1} = [A]_{n+1} \cdot \begin{Bmatrix} v_2 \\ F_2 \end{Bmatrix}_n = [A]_{n+1} \cdot [A]_n \cdot \begin{Bmatrix} v_1 \\ F_1 \end{Bmatrix}_n$$

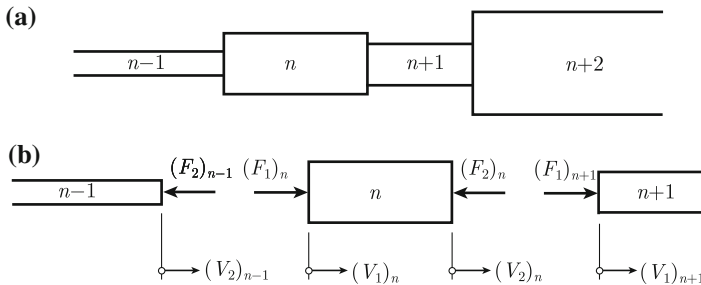


Fig. 6.13 Forces and velocities at junctions between coupled beams

By repeating this procedure for a chain of m elements or beams, the velocities and forces at the outer ends are related as

$$\begin{Bmatrix} v_2 \\ F_2 \end{Bmatrix}_m = [A]_m \cdot [A]_{m-1} \cdots [A]_1 \begin{Bmatrix} v_1 \\ F_1 \end{Bmatrix}_1 = [A]_{\text{tot}} \cdot \begin{Bmatrix} v_1 \\ F_1 \end{Bmatrix}_1 \quad (6.112)$$

So again, if two of the quantities F_1, F_2, v_1 or v_2 at the outer ends of the connected beams are known, then the two remaining quantities can be determined from Eq. (6.112). In a similar way, the force and velocity at any junction can be derived as discussed in Problem 6.13. The resulting eigenfrequencies for the set of coupled beams can be obtained from Eq. (6.112). If for example, the outer ends of the beam structure are fixed, the velocities $(v_2)_m$ and $(v_1)_1$ are equal to zero. For free ends, the external forces are zero etc. The resulting system of equations, given in matrix form in Eq. (6.107), gives the eigenfrequencies of the system. For the particular case $(v_2)_m = (v_1)_1 = 0$, the eigenfrequencies are the solutions to $a_{12} = 0$ where a_{12} is an element in the matrix $[A]_{\text{tot}}$ in Eq. (6.112). The transfer matrix concept can also be used for beams coupled to solid masses and mass less springs. For these elements, the transfer matrix can be simplified. The wavenumber k_1 in a beam is for L-waves equal to $\omega\sqrt{\rho/E}$. If either the density is low or the E-modulus high, the resulting wave number is small. In both cases, the sine and cosine functions in Eq. (6.110) can be expanded in a Taylor series. The results are, including only first order terms

$$a_{11} = a_{22} = 1, \quad a_{12} = -\frac{i\omega L}{SE}, \quad a_{21} = -\frac{iSEk_1^2 L}{\omega} = -i\omega SL\rho = -i\omega m \quad (6.113)$$

For an infinitely stiff mass, the E -modulus is infinite. The element a_{12} is equal to zero, and the element $a_{21} = -i\omega m$, where m is the total mass. The transfer matrix for a solid mass is thus

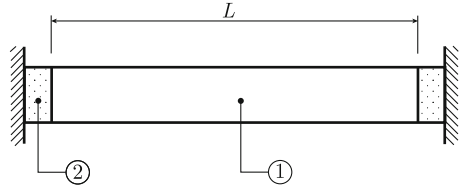
$$[A] = \begin{bmatrix} 1 & 0 \\ -i\omega m & 1 \end{bmatrix} \quad (6.114)$$

For a “mass less” spring, the density is equal to zero and $a_{21} = 0$. The spring constant k is $k = SE/L$. The corresponding result for a mass less spring, spring constant k , is

$$[A] = \begin{bmatrix} 1 & -i\omega/k \\ 0 & 1 \end{bmatrix} \quad (6.115)$$

The boundary condition corresponding to a “clamped” beam, requires that the beam is mounted to a structure with an infinite impedance or zero mobility. This condition is never quite encountered in reality. There is always a certain flexibility or mobility at the “clamped” ends. The effect of a finite resilience on the eigenfrequencies of the beam can be estimated, by assuming that there are resilient elements or springs, mounted between the ends of the beam and the structures to which is mounted. The problem is illustrated in Fig. 6.14.

Fig. 6.14 A finite beam ①, of length L mounted by means of resilient interlayers ② to infinitely stiff structures



Two elastic elements, each with a spring constant k , are mounted between the beam and the adjoining stiff structures. The transfer matrix for the spring elements is given in Eq. (6.115). The transfer matrices for the identical elements are $[A]_1$ and $[A]_3$. The transfer matrix for the beam is $[A]_2$ with the elements defined in Eq. (6.110).

The forces and velocities at the two ends of the complete beam including the spring elements is obtained from Eq. (6.102) as

$$\begin{Bmatrix} v_2 \\ F_2 \end{Bmatrix}_3 = [A]_3 \cdot [A]_2 \cdot [A]_1 \begin{Bmatrix} v_1 \\ F_1 \end{Bmatrix}_1 = [A]_{\text{tot}} \cdot \begin{Bmatrix} v_1 \\ F_1 \end{Bmatrix}_1 \quad (6.116)$$

The velocities $(v_2)_3$ and $(v_1)_1$ are equal to zero since the resilient elements are mounted to “stiff” structures. For $(v_2)_3$ and $(v_1)_1$ equal to zero, the system of equations can be satisfied only if the element a_{12} in the matrix $[A]_{\text{tot}}$ is equal to zero. This means that the wavenumber k_1 must satisfy the dispersion equation

$$\sin(k_1 L)[SEk_1/k - k/(SEk_1)] = 2 \cos(k_1 L) \quad (6.117)$$

For an infinitely soft ($k \rightarrow 0$) or hard ($k \rightarrow \infty$) spring, corresponding to free and clamped boundary conditions respectively, Eq. (6.117) is satisfied only if $k_1 L = n\pi$ as previously derived in Sect. 6.1. The resulting eigenfrequencies for intermediate values of the spring constant k are readily obtained from Eq. (6.117).

If the point mobilities Y_1 and Y_m of the structures to which the beam is mounted are known, then the Eq. (6.112) can be written as

$$\begin{Bmatrix} v_2 \\ F_2 \end{Bmatrix}_m = (F_2)_m \begin{Bmatrix} Y_m \\ 1 \end{Bmatrix}_m = [A]_{\text{tot}} \cdot \begin{Bmatrix} v_1 \\ F_1 \end{Bmatrix}_1 = [A]_{\text{tot}} \cdot \begin{Bmatrix} -Y_1 \\ 1 \end{Bmatrix}_1 (F_1)_1 \quad (6.118)$$

The minus sign in front of Y_1 is the result of force and velocity for the supporting structure 1 are defined positive in opposite directions. If the elements in the matrix $[A]_{\text{tot}}$ are a_{ij} the resulting dispersion equation giving the wavenumbers corresponding to a resonance is

$$Y_m(a_{22} - a_{21}Y_1) = a_{12} - a_{11}Y_1 \quad (6.119)$$

Forced excitation of coupled beams can also be described by means of transfer matrices. Figure 6.15 shows two coupled beams, denoted n and $n+1$. The beams are

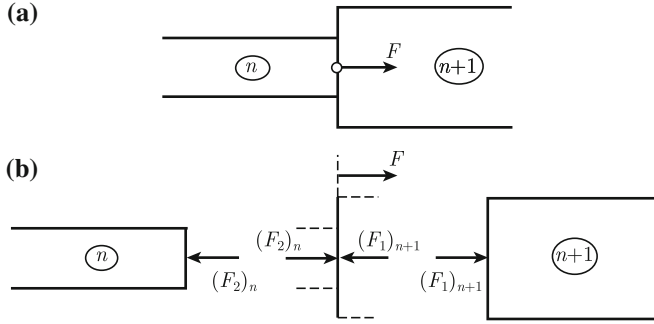


Fig. 6.15 Two coupled beams excited by a force at the junction

exited by a force, $FT F$, at the junction between the beams. Forces and velocities at the end sections of each beam are shown in Fig. 6.15.

For beam n forces and velocities are related as

$$\begin{Bmatrix} v_2 \\ F_2 \end{Bmatrix}_n = [A]_n \cdot \begin{Bmatrix} v_1 \\ F_1 \end{Bmatrix}_n \quad (6.120)$$

At the junction between the beams n and $n+1$ the boundary conditions are

$$(v_1)_{n+1} = (v_2)_n, \quad (F_1)_{n+1} = (F_2)_n + F \quad (6.121)$$

The velocity $(v_2)_{n+1}$ and the force $(F_2)_n$ at the right end section of the beam are following Eq. (6.120) given by

$$\begin{Bmatrix} v_2 \\ F_2 \end{Bmatrix}_{n+1} = [A]_{n+1} \cdot \begin{Bmatrix} v_1 \\ F_1 \end{Bmatrix}_{n+1} = [A]_{n+1} \cdot \left(\begin{Bmatrix} v_2 \\ F_2 \end{Bmatrix}_n + \begin{Bmatrix} 0 \\ F \end{Bmatrix} \right) \quad (6.122)$$

The boundary conditions (6.121) are used to arrive at the expression on the right-hand side of Eq. (6.122). By inserting Eq. (6.120) in (6.122) the result is

$$\begin{Bmatrix} v_2 \\ F_2 \end{Bmatrix}_{n+1} = [A]_{n+1} \cdot [A]_n \begin{Bmatrix} v_1 \\ F_1 \end{Bmatrix}_n + [A]_{n+1} \cdot \begin{Bmatrix} 0 \\ F \end{Bmatrix} \quad (6.123)$$

The procedure is illustrated in Problem 6.14.

Problems

If nothing else is stated, assume that the area of the cross section of the beam is S . Material parameters are $E = E_0(1 + i\eta)$ and ρ .

- 6.1** A beam is clamped at both ends at $x = 0$ and $x = L$. Determine the eigenfunctions and corresponding eigenfrequencies for longitudinal vibrations of the beam.
- 6.2** A beam is clamped at $x = 0$ and free at the other end at $x = L$. Determine the eigenfunctions and corresponding eigenfrequencies for longitudinal vibrations of the beam.
- 6.3** Determine the eigenfunctions and eigenfrequencies for a beam with resiliently mounted ends as shown in Fig. 6.1c. L-waves only.
- 6.4** Determine the eigenfunctions and eigenfrequencies for a beam with periodic boundary conditions. L-waves only.
- 6.5** Determine Green's function for a clamped beam. Consider only L-waves traveling along the axis of the beam.
- 6.6** A force $F'(x, t) = F/L \cdot \exp(i\omega t)$ per unit length excites a beam along its axis. The length of the beam is L . The beam is clamped at both ends. Determine the response of the beam by using the appropriate Green's function.
- 6.7** A force $F'(x, t) = F/L \cdot \sin(\pi x/L) \cdot \exp(i\omega t)$ per unit length is exciting a beam along its axis. The length of the beam is L . The beam is clamped at both ends. Determine the response of the beam by using the mode summation technique.
- 6.8** A beam is clamped at one end. A static force F is stretching the beam at the other end in the direction of its axis. At time $t = 0$ the beam is released. The beam is for $t > 0$ vibrating freely with one end clamped and the other free. Determine the displacement of the beam as function of time.
- 6.9** A beam is clamped at both ends and excited at midpoint by a harmonic force $F_0 \cdot \exp(i\omega t)$ along the axis of the beam. The frequency of the driving force is well below the first natural frequency of the beam. Determine the response of the beam. Use the mode summation technique.
- 6.10** Two straight beams, each with a length of L , are joined together along their axes. One beam has a cross-sectional area of S , the corresponding area for the other beam is $4S$. The thicker beam is clamped at one end. The other end of the construction is free. Determine the first eigenfrequency of the beam construction.
- 6.11** A beam, length L , is mounted in between two identical structures. The point mobility of the adjoining structures is Y at the mounting positions with respect to longitudinal vibrations of the beam. Determine the dispersion equation which gives the natural frequencies for the system. In particular consider the case when each of the adjoining structures is a rigid mass m .
- 6.12** A mass m is mounted on a rod, geometrical parameters S and L , material parameters E and ρ . The rod is in turn mounted to a plate with the point mobility Y . The mass is excited by a force $F_0 \cdot \exp(i\omega t)$. Determine the power transmitted to the plate.

6.13 Two beams are coupled. The axes of the beams coincide. Beam 1 (L_1, S_1, E_1, ρ_1) is clamped at one end and firmly coupled to beam 2 (L_2, S_2, E_2, ρ_2) at the other end. A force $F_0 \cdot \exp(i\omega t)$ is exciting the free end of beam 2 along its axis. Determine the velocity of the junction.

6.14 A beam, length L , is clamped at both ends. The beam is excited by a force $F \cdot \exp(i\omega t)$ at midpoint along the axis of the beam. Determine the response of the beam by using the matrix method.

6.15 Show that the eigenfunctions for a beam with both ends resiliently mounted are orthogonal. Longitudinal waves only.

6.16 Two homogeneous beams are coupled at the ends along a straight and vertical line. The cross-sectional area of beam 1, the upper beam, is S . The cross-sectional area of beam 2 is $2S$. The beams have the same length L and the same material parameters, Young's modulus E and density ρ . The upper end of the coupled beams is denoted 1 and the bottom end by 2. Determine the point and transfer mobilities Y_{11}, Y_{12}, Y_{21} and Y_{22} of the structure consisting of the two coupled beams. Consider only longitudinal waves propagating along the axes of the beams.

Chapter 7

Flexural Vibrations of Finite Beams

The methods discussed in the previous chapter are in this chapter extended to include the flexural vibrations of finite beams. It is demonstrated that the mode summation technique can be used to determine the forced response of a finite beam for certain natural boundary conditions. The eigenfunctions and eigenfrequencies corresponding to these boundary conditions are derived.

Comparisons are made between point mobilities for finite and infinite beams. This leads to the important conclusion that for certain cases the power input to a randomly excited finite beam can be determined as if the beams were infinite.

As in the previous chapter, transfer matrices are used to describe the coupling between a set of beams. The analysis is extended to include infinite periodic structures. A simple case illustrating the vibration of beams coupled by means of a resilient layer is also discussed. The example demonstrates the behavior of double wall structures excited by an acoustic field or a dynamic force.

7.1 Free Flexural Vibrations of Beams

It was shown in Sect. 6.1 that free longitudinal vibrations can only oscillate at certain frequencies or at the natural or eigenfrequencies of the system. Each natural frequency is coupled to a vibration mode, which determines the relative deflection along the beam at that particular frequency. The same applies to free flexural vibration of beams or, for that matter, any type of structure. For free vibrations of a homogeneous beam with constant cross section and orientated along the x -axis, the lateral displacement $w(x, t)$ must satisfy the wave Eq. (3.77) with the external force F' equal to zero.

Thus,

$$\frac{\partial^4 w}{\partial x^4} + \frac{m'}{D'} \frac{\partial^2 w}{\partial t^2} = 0. \quad (7.1)$$

For a beam with the height h and width b , the mass per unit length is $m' = bh\rho$ and the bending stiffness is $D' = bh^3E/12$. Due to losses the bending stiffness is complex. In analogy with the discussion in Sect. 6.1, the displacement is defined as the product between a time and an x dependent function. The displacement is given as

$$w(x, t) = g(t) \cdot \varphi(x). \quad (7.2)$$

The expression (7.2) inserted in Eq. (7.1) gives

$$g \frac{d^4 \varphi}{dx^4} + \frac{m'}{D'} \frac{d^2 g}{dt^2} \varphi = 0.$$

Let κ be an arbitrary constant, which satisfies the equation

$$\frac{d^4 \varphi}{dx^4} = \kappa^4 \varphi. \quad (7.3)$$

Equation (7.3) inserted in the previous expression leads to the function g satisfying the equation

$$\frac{m'}{D'} \frac{d^2 g}{dt^2} + \kappa^4 g = 0. \quad (7.4)$$

If solutions to Eqs. (7.3) and (7.4) can be found then also the wave equation (7.1) is satisfied. This is in analogy with the discussion in Sect. 6.1.

The free vibrations of a beam are readily determined for certain time independent boundary conditions. The most important of these conditions, or closed boundary conditions, are as follows:

(i) Clamped end

Displacement w and slope $\frac{\partial w}{\partial x}$ of displacement curve are zero.

Boundary conditions:

$$\varphi = \frac{d\varphi}{dx} = 0.$$

(ii) Simply supported end

Displacement w and bending moment $M = -D' \frac{\partial^2 w}{\partial x^2}$ zero

Boundary conditions:

$$\varphi = \frac{d^2 \varphi}{dx^2} = 0.$$

(iii) Free end

Force $F = -D' \frac{\partial^3 w}{\partial x^3}$ and bending moment $M = -D' \frac{\partial^2 w}{\partial x^2}$ zero

Boundary condition:

$$\frac{d^2\varphi}{dx^2} = \frac{d^3\varphi}{dx^3} = 0.$$

For finite beams, there are six possible combinations of the closed boundary conditions listed above. The ends can be clamped/clamped, clamped/free etc. Yet another case is discussed in Problem 7.1.

The general solution to Eq.(7.3) is

$$\varphi(x) = A_1 \sin \kappa x + A_2 \cos \kappa x + A_3 \sinh \kappa x + A_4 \cosh \kappa x. \quad (7.5)$$

For future reference, the first few derivatives of this solution are

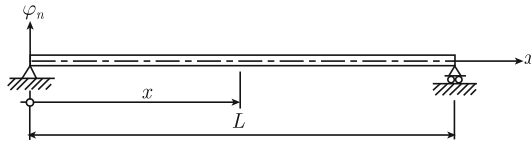
$$\frac{d\varphi}{dx} = \kappa[A_1 \cos \kappa x - A_2 \sin \kappa x + A_3 \cosh \kappa x + A_4 \sinh \kappa x] \quad (7.6)$$

$$\frac{d^2\varphi}{dx^2} = \kappa^2[-A_1 \sin \kappa x - A_2 \cos \kappa x + A_3 \sinh \kappa x + A_4 \cosh \kappa x] \quad (7.7)$$

$$\frac{d^3\varphi}{dx^3} = \kappa^3[-A_1 \cos \kappa x + A_2 \sin \kappa x + A_3 \cosh \kappa x + A_4 \sinh \kappa x]. \quad (7.8)$$

For each of the six closed boundary conditions, there are two conditions at each end, which must be satisfied. There are four unknown parameters namely the ratios between the amplitudes or A_2/A_1 , A_3/A_1 , and A_4/A_1 and the parameter κ .

Case A: A beam simply supported at both ends.



The length of the beam is L . The boundary conditions are

$$\varphi = \frac{d^2\varphi}{dx^2} = 0 \text{ for } x = 0 \text{ and } x = L$$

These boundary conditions in combination with the Eqs. (7.5) and (7.7) give

$$\begin{aligned} A_2 + A_4 &= 0, & -A_2 + A_4 &= 0 \\ A_1 \sin \kappa L + A_2 \cos \kappa L + A_3 \sinh \kappa L + A_4 \cosh \kappa L &= 0 \\ -A_1 \sin \kappa L - A_2 \cos \kappa L + A_3 \sinh \kappa L + A_4 \cosh \kappa L &= 0. \end{aligned}$$

The first two equations lead to $A_2 = A_4 = 0$. This result and the last two boundary conditions give

$$A_1 \sin \kappa L = 0, \quad A_3 \sinh \kappa L = 0.$$

However, $\sinh \kappa L > 0$ for κ real and positive. Consequently $A_3 = 0$. For a nontrivial solution i.e., for $A_1 \neq 0$ then the function $\sin \kappa L$ must be equal to zero. This condition, i.e., $\sin \kappa L = 0$, is satisfied for $\kappa L = n \cdot \pi$ where $n = 0, 1, 2, 3, \dots$. This means that there is an infinite series of functions or eigenfunctions $\varphi_n(x)$ which satisfy the boundary conditions. Each eigenfunction is associated with an eigenvalue κ_n . For a beam with simply supported ends these eigenfunctions and eigenvalues are

$$\varphi_n(x) = \sin \kappa_n x, \quad \kappa_n = n\pi/L \text{ for } n = 1, 2, 3, \dots \quad (7.9)$$

According to Eq. (7.3), φ_n and κ_n should satisfy the differential equation

$$\frac{d^4 \varphi_n}{dx^4} = \kappa_n^4 \varphi_n.$$

The time dependent solution must satisfy Eq. (7.4) for $\kappa = \kappa_n$. A similar problem was discussed in Sect. 6.1—compare the Eqs. (6.18)–(6.20). The function $g_n(t)$ is the solution to the equation

$$\frac{m'}{D'} \frac{d^2 g_n}{dt^2} + \kappa_n^4 g_n = 0.$$

Thus for

$$\omega_n = \kappa_n^2 \sqrt{\frac{D'}{m'}} = \kappa_n^2 \sqrt{\frac{D'_0}{m'}} (1 + i\eta/2) = \omega_{n0} (1 + i\eta/2), \quad (7.10)$$

the general time-dependent solution is of the form

$$g_n(t) = (C_{1n} \cdot e^{i\omega_{n0}t} + C_{2n} \cdot e^{-i\omega_{n0}t}) \cdot \exp(-\omega_{n0}\eta t/2)$$

or

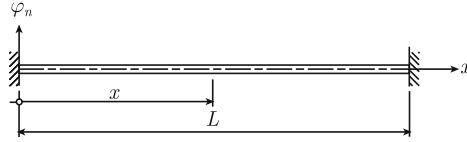
$$g_n(t) = [D_{1n} \cdot \cos(\omega_{n0}t) + D_{2n} \cdot \sin(\omega_{n0}t)] \cdot \exp(-\omega_{n0}\eta t/2). \quad (7.11)$$

The result is approximately correct if the losses are small resulting in an almost harmonic motion of the beam as discussed in Sect. 1.6. The concept of using a complex wavenumber is only exact for harmonic displacement. The parameters C_{1n} and C_{2n} or the parameters D_{1n} and D_{2n} in Eq. (7.11) are determined from the time-dependent initial conditions. Again this means that for free vibrations—no external force—the beam can oscillate only at certain natural frequencies f_n corresponding to the angular frequencies ω_{n0} or

$$f_n = \frac{\omega_{n0}}{2\pi} = \frac{\pi}{2} \left(\frac{n}{L}\right)^2 \sqrt{\frac{D'_0}{m'}} \quad (7.12)$$

Note that when the length of the beam is doubled the first natural frequency is reduced by a factor $1/4$. Further the second natural frequency ($n = 2$) is four times as high as the first ($n = 1$). This means that the natural frequencies are not equally spaced in the frequency domain as was the case for the L-waves propagating in a finite beam, see Eq. (6.22).

Case B: A beam clamped at both ends.



The boundary conditions are

$$\varphi = \frac{d\varphi}{dx} = 0 \text{ for } x = 0 \text{ and } x = L.$$

These conditions in combination with Eqs. (7.5) and (7.6) give

$$\begin{aligned} A_2 + A_4 &= 0, & A_1 + A_3 &= 0 \\ A_1 \sin \kappa L + A_2 \cos \kappa L + A_3 \sinh \kappa L + A_4 \cosh \kappa L &= 0 \\ A_1 \cos \kappa L - A_2 \sin \kappa L + A_3 \cosh \kappa L + A_4 \sinh \kappa L &= 0. \end{aligned} \quad (7.13)$$

The first two results in combination with the last two yield

$$\begin{aligned} A_1(\sin \kappa L - \sinh \kappa L) + A_2(\cos \kappa L - \cosh \kappa L) &= 0 \\ A_1(\cos \kappa L - \cosh \kappa L) - A_2(\sin \kappa L + \sinh \kappa L) &= 0. \end{aligned}$$

For A_1 and $A_2 \neq 0$ a solution can only be obtained if

$$\frac{\sin \kappa L - \sinh \kappa L}{\cos \kappa L - \cosh \kappa L} = -\frac{\cos \kappa L - \cosh \kappa L}{\sin \kappa L + \sinh \kappa L}.$$

This is equivalent to the requirement

$$\cos \kappa L \cdot \cosh \kappa L = 1. \quad (7.14)$$

There are an infinite number of solutions to this equation. Numerically computed solutions are

n	$\kappa_n L$
1	$3\pi/2 + 0.01765$
2	$5\pi/2 - 0.00078$
3	$7\pi/2 + 0.00003$

For subsequent n , the cosh function in Eq. (7.14) rapidly increases, which leads to

$$\cos \kappa_n L = 1 / \cosh \kappa_n L \approx 0, \quad \kappa_n L \approx \pi/2 + n\pi \text{ for } n \geq 4.$$

From Eq. (7.13) it follows that

$$A_2 = -A_4, \quad A_1 = -A_3 = -\frac{\cos \kappa_n L - \cosh \kappa_n L}{\sin \kappa_n L - \sinh \kappa_n L} \cdot A_4.$$

The eigenfunctions for a clamped-clamped beam are, consequently

$$\varphi_n(x) = A_4 \cdot \left[\cosh \kappa_n x - \cos \kappa_n x - \frac{\cos \kappa_n L - \cosh \kappa_n L}{\sin \kappa_n L - \sinh \kappa_n L} (\sinh \kappa_n x - \sin \kappa_n x) \right]. \quad (7.15)$$

For $n \geq 4$ the eigenfunctions can be approximated by some fairly simple expressions. For $\kappa_n L \approx (\pi/2 + n\pi) \gg 1$ the ratio inside the bracket in Eq. (7.15) is given as

$$\frac{\cos \kappa_n L - \cosh \kappa_n L}{\sin \kappa_n L - \sinh \kappa_n L} \approx 1 + 2 \sin \kappa_n L \cdot \exp(-\kappa_n L).$$

This approximate expression inserted in Eq. (7.15) gives

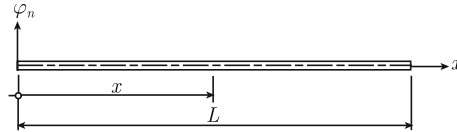
$$\varphi_n(x) \approx A_4 \{ \exp(-\kappa_n x) - \exp[-\kappa_n(L-x)] \cdot \sin \kappa_n L + \sin \kappa_n x - \cos \kappa_n x \}.$$

The exponential functions are decaying rapidly for $0 < x < L$. Along the central part of the beam the eigenfunction can therefore be written as

$$\varphi_n(x) \approx A_4 (\sin \kappa_n x - \cos \kappa_n x) = A_4 \sqrt{2} \sin(\kappa_n x - \pi/4),$$

for $\kappa_n L \approx (\pi/2 + n\pi) \gg 1$ and $n \geq 4$. For $A_4 = 1/\sqrt{2}$ the norm $\langle \varphi_n | \varphi_n \rangle$ of the eigenfunction is equal to the norm $L/2$ of the eigenfunction for the simply supported beam. For conformity reasons all eigenfunctions are set to have the same norm.

Case C: A beam with free ends.



Force and bending moment are equal to zero at the ends of the beam. The boundary conditions are

$$\frac{d^2 \varphi}{dx^2} = \frac{d^3 \varphi}{dx^3} = 0 \text{ for } x = 0 \text{ and } x = L.$$

These boundary conditions lead to the following equation for the eigenvalues

$$\cos \kappa_n L \cdot \cosh \kappa_n L = 1. \quad (7.16)$$

This expression is identical to the frequency equation derived for the clamped–clamped beam. The resulting eigenvalues are consequently the same for a free–free beam as for a clamped beam. However the eigenfunctions differ. For a free beam the eigenfunctions are

$$\varphi_n(x) = \frac{1}{\sqrt{2}} \cdot \left[\cosh \kappa_n x + \cos \kappa_n x - \frac{\cos \kappa_n L - \cosh \kappa_n L}{\sin \kappa_n L - \sinh \kappa_n L} (\sinh \kappa_n x + \sin \kappa_n x) \right]. \quad (7.17)$$

Again the amplitude of the eigenfunction has been chosen so as to give the norm $L/2$.

For the cases A, B and C plus two mixed boundary conditions clamped/simply supported and clamped/free, the main results are summarized in Tables 7.1, 7.2, 7.3, 7.4 and 7.5. For each case, the eigenfunctions and the characteristic equation giving the eigenvalues κ_n are stated. In addition, the value of the products $\kappa_n L$ are given for $1 \leq n \leq 5$. The eigenfrequency or natural frequency f_n corresponding to the eigenvector φ_n and the eigenvalue κ_n is always given by

$$f_n = \frac{\kappa_n^2}{2\pi} \sqrt{\frac{D'_0}{m'}}. \quad (7.18)$$

In practice, the boundary conditions for a beam, which is connected at both ends to other structures, could vary between simply supported and clamped. The boundary conditions are very critical for the occurrence of the first natural frequency. For a

Table 7.1 Beam, length L , with both ends simply supported at $x = 0$ and $x = L$

Eigenfunction $\varphi_n(x) = \sin \kappa_n x$

Eigenvalues $\kappa_n = n\pi/L$


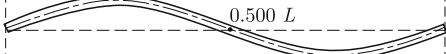
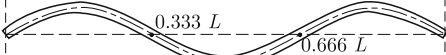


n	$\kappa_n L$	Characteristic modes of vibration
1	$1 \cdot \pi = 3.14159265$	
2	$2 \cdot \pi = 6.2831853$	
3	$3 \cdot \pi = 9.424778$	
4	$4 \cdot \pi = 12.5663706$	
5	$5 \cdot \pi = 15.7079633$	

Table 7.2 Beam, length L , with both ends clamped at $x = 0$ and $x = L$

Eigenfunction $\varphi_n(x) = \frac{1}{\sqrt{2}} \cdot \left[\cosh \kappa_n x - \cos \kappa_n x - \frac{\cos \kappa_n L - \cosh \kappa_n L}{\sin \kappa_n L - \sinh \kappa_n L} (\sinh \kappa_n x - \sin \kappa_n x) \right]$

Eigenvalues κ_n solutions to $\cos(\kappa_n L) \cdot \cosh(\kappa_n L) = 1$

n	$\kappa_n L$	Characteristic modes of vibration
1	$\frac{3 \cdot \pi}{2} + 0.0176519$ $= 4.7300408$	
2	$\frac{5 \cdot \pi}{2} - 0.0007769$ $= 7.8532046$	
3	$\frac{7 \cdot \pi}{2} + 0.0000337$ $= 10.9956078$	
4	$\frac{9 \cdot \pi}{2} + 0.0000012$ $= 14.1371655$	
5	$\frac{11 \cdot \pi}{2} + 0.0000003$ $= 17.2787596$	

Table 7.3 Beam, length L , with both ends free at $x = 0$ and $x = L$

Eigenfunction $\varphi_n(x) = \frac{1}{\sqrt{2}} \cdot \left[\cosh \kappa_n x + \cos \kappa_n x - \frac{\cos \kappa_n L - \cosh \kappa_n L}{\sin \kappa_n L - \sinh \kappa_n L} (\sinh \kappa_n x + \sin \kappa_n x) \right]$

Eigenvalues κ_n solutions to $\cos(\kappa_n L) \cdot \cosh(\kappa_n L) = 1$

n	$\kappa_n L$	Characteristic modes of vibration
1	$\frac{3 \cdot \pi}{2} + 0.0176519$ $= 4.7300408$	
2	$\frac{5 \cdot \pi}{2} - 0.0007769$ $= 7.8532046$	
3	$\frac{7 \cdot \pi}{2} + 0.0000337$ $= 10.9956078$	
4	$\frac{9 \cdot \pi}{2} - 0.0000012$ $= 14.1371655$	
5	$\frac{11 \cdot \pi}{2} + 0.0000003$ $= 17.2787596$	

Table 7.4 Beam, length L , one end clamped at $x = 0$ and one simply supported at $x = L$

$$\text{Eigenfunction } \varphi_n(x) = \frac{1}{\sqrt{2}} \cdot \left[\cosh \kappa_n x - \cos \kappa_n x - \frac{\cos \kappa_n L - \cosh \kappa_n L}{\sin \kappa_n L - \sinh \kappa_n L} (\sinh \kappa_n x - \sin \kappa_n x) \right]$$

Eigenvalues κ_n solutions to $\tan(\kappa_n L) = \tanh(\kappa_n L)$

n	$\kappa_n L$	Characteristic modes of vibration
1	$\frac{5 \cdot \pi}{4} + 0.0002884$ $= 3.9266023$	
2	$\frac{9 \cdot \pi}{4} - 0.0000006$ $= 7.0685827$	
3	$\frac{13 \cdot \pi}{4} + 0.0000002$ $= 10.2101761$	
4	$\frac{17 \cdot \pi}{4} - 0.0000003$ $= 13.3517688$	
5	$\frac{21 \cdot \pi}{4} + 0.0000003$ $= 16.4933614$	

Table 7.5 Beam, length L , one end clamped at $x = 0$ and one free at $x = L$

$$\text{Eigenfunction } \varphi_n(x) = \frac{1}{\sqrt{2}} \cdot \left[\cosh \kappa_n x - \cos \kappa_n x - \frac{\cos \kappa_n L + \cosh \kappa_n L}{\sin \kappa_n L + \sinh \kappa_n L} (\sinh \kappa_n x - \sin \kappa_n x) \right]$$

Eigenvalues κ_n solutions to $\cos(\kappa_n L) \cdot \cosh(\kappa_n L) = -1$

n	$\kappa_n L$	Characteristic modes of vibration
1	$\frac{\pi}{2} + 0.3043078$ $= 1.8751041$	
2	$\frac{3 \cdot \pi}{2} - 0.0182978$ $= 4.6940911$	
3	$\frac{5 \cdot \pi}{2} + 0.0007759$ $= 7.8547574$	
4	$\frac{7 \cdot \pi}{2} - 0.0000334$ $= 10.9955407$	
5	$\frac{9 \cdot \pi}{2} + 0.000017$ $= 14.1371684$	

clamped beam, the first natural frequency is approximately 2.25 times as high as the corresponding value for the same beam with simply supported ends.

For a simply supported beam, the wave number κ_n corresponding to mode n is

$$\kappa_n = \left[\frac{(2\pi f_n)^2 m'}{D'_0} \right]^{1/4} = \frac{n\pi}{L},$$

where $D'_0 = \frac{bh^3 E_0}{12}$, $m' = bh\rho$.

A simple derivation with respect to n of the first expression giving the wavenumber yields

$$\frac{\Delta f}{\Delta n} = \frac{\sqrt{2\pi f}}{L} \left[\frac{D'_0}{m'} \right]^{1/4}. \quad (7.19)$$

The subscript n for the frequency has been omitted. The result (7.19) can be interpreted in such a way that for $\Delta n = 1$, the spacing in the frequency domain between two subsequent natural frequencies is equal to Δf at the frequency f . The modal density \mathcal{N}_f , which is equal to the number of modes per frequency interval, is approximately equal to

$$\begin{aligned} \mathcal{N}_f &= \frac{\Delta n}{\Delta f} = \frac{L}{\sqrt{2\pi f}} \left[\frac{m'}{D'_0} \right]^{1/4} \\ &= \frac{L}{\sqrt{2\pi f h}} \left[\frac{12\rho}{E_0} \right]^{1/4} = \frac{\kappa_0 L}{2\pi f}. \end{aligned} \quad (7.20)$$

The modal density is consequently a function of frequency. The modal density decreases as the frequency increases. Further, the modal density is inversely proportional to \sqrt{h} and proportional to L . As a comparison it was shown in Chap. 6 that the modal density for longitudinal waves excited in a finite beam were independent of frequency.

For sufficiently high mode numbers, $n \geq 4$, the spacing with respect to wave number between two consecutive natural frequencies is, irrespective of boundary conditions, given by $\kappa_{n+1} - \kappa_n = \pi/L$. This means that the modal density for flexural waves excited in a finite beam of length L for any boundary condition is given by Eq. (7.20) for sufficiently high frequencies.

7.2 Orthogonality and Norm of Eigenfunctions

In Sect. 6.1, it was shown that a solution to a vibration problem, involving L-waves only, could be expressed as an infinite sum over the orthogonal eigenfunctions corresponding to any of the closed boundary conditions for the beam. A similar approach

can be used for F-waves once it has been proved that the eigenfunctions derived in Sect. 7.1 are orthogonal.

Thus, consider two eigenfunctions φ_m and φ_n which satisfy the same boundary conditions and the differential equation

$$\frac{d^4\varphi_i}{dx^4} = \kappa_i^4 \varphi_i, \quad (7.21)$$

where κ_m is the eigenvalue corresponding to φ_m and κ_n to φ_n . The expression (7.21) is for $i = m$ multiplied by φ_n and integrated over x as

$$\int_0^L \varphi_n \frac{d^4\varphi_m}{dx^4} dx - \kappa_m^4 \int_0^L \varphi_n \varphi_m dx = 0. \quad (7.22)$$

The first expression is integrated by parts as

$$\begin{aligned} \int_0^L \varphi_n \frac{d^4\varphi_m}{dx^4} dx = & \left[\varphi_n \frac{d^3\varphi_m}{dx^3} - \frac{d\varphi_n}{dx} \frac{d^2\varphi_m}{dx^2} + \frac{d^2\varphi_n}{dx^2} \frac{d\varphi_m}{dx} \right. \\ & \left. - \frac{d^3\varphi_n}{dx^3} \varphi_m \right]_0^L + \int_0^L \frac{d^4\varphi_n}{dx^4} \varphi_m dx. \end{aligned} \quad (7.23)$$

For any combination of the closed boundary conditions clamped/clamped, clamped/free, etc.—the expression corresponding to the bracket is zero. For example for a clamped/free beam, the boundary conditions making the bracket zero are

$$\varphi_i = \frac{d\varphi_i}{dx} = 0 \text{ for } x = 0 \text{ and } \frac{d^2\varphi_i}{dx^2} = \frac{d^3\varphi_i}{dx^3} = 0 \text{ for } x = L.$$

The original Eq. (7.22) can, for any of the closed boundary conditions, be rewritten as

$$\int_0^L \frac{d^4\varphi_n}{dx^4} \varphi_m dx - \kappa_m^4 \int_0^L \varphi_n \varphi_m dx = 0.$$

The eigenfunctions φ_n must also satisfy Eq. (7.21). Thus

$$\kappa_n^4 \int_0^L \varphi_n \varphi_m dx - \kappa_m^4 \int_0^L \varphi_n \varphi_m dx = (\kappa_n^4 - \kappa_m^4) \langle \varphi_n | \varphi_m \rangle = 0, \quad (7.24)$$

where as defined in Chap. 6

$$\langle \varphi_n | \varphi_m \rangle = \int_0^L \varphi_n \varphi_m dx.$$

Since in Eq. (7.24) $\kappa_m \neq \kappa_n$ for $m \neq n$, it follows that

$$\langle \varphi_n | \varphi_m \rangle = 0 \text{ for } m \neq n. \quad (7.25)$$

Consequently, the orthogonality condition is satisfied. For the eigenfunctions to be orthogonal the energy flow away from the beam is zero as given by the expression inside the bracket of Eq. (7.23). The norm or $\langle \varphi_n | \varphi_n \rangle$ is an important property for any eigenfunction. For a simply supported beam $\varphi_n(x) = \sin(n\pi x/L)$ and it is evident that

$$\langle \varphi_n | \varphi_n \rangle = L/2. \quad (7.26)$$

For clamped/clamped and free/free beams, the eigenfunctions are somewhat more complicated. However, after a certain computational effort, it can be shown that even for these boundary conditions the norm of the eigenfunctions is equal to $L/2$. In the Tables 7.1 through 7.5, the eigenfunctions and corresponding eigenvalues are listed for five cases. An additional case, one end simply supported and the other end free, is discussed in Problem 7.13. For all the cases listed, the norm of the eigenfunctions is equal to $L/2$. For certain applications, it is convenient if the norm of an eigenfunction is equal to unity. This is achieved by multiplying the eigenfunctions listed in Tables 7.1 through 7.5 by the factor $\sqrt{2/L}$. The resulting eigenfunctions are said to be orthonormal if orthogonal and having the norm 1. If φ_n is an orthogonal eigenfunction then also $C \cdot \varphi_n$ is an orthogonal eigenfunction to the same problem for C a constant. The norm of the eigenfunction is changed from $\langle \varphi_n | \varphi_n \rangle$ to $C^2 \langle \varphi_n | \varphi_n \rangle$.

Thus in summary: For flexural vibrations of a beam with a mounting corresponding to any of the closed boundary conditions, the resulting eigenfunctions are orthogonal. The norm of the eigenfunctions in Tables 7.1, 7.2, 7.3, 7.4 and 7.5 for both ends clamped, simply supported, free or any combination of these end conditions, the norm of the eigenfunctions is $L/2$ where L is the length of the beam. The deflection of the beam can, since the eigenfunctions are orthogonal and constitute a complete set, be expressed as

$$w(x, t) = \sum_{n=0}^{\infty} g_n(t) \cdot \varphi_n(x). \quad (7.27)$$

Once the function $w(x, t)$ is known, the functions $g_n(t)$ are obtained by multiplying the expression (7.27) by $\varphi_n(x)$. The result is thereafter integrated with respect to x over the length of the beam as described in Chap. 6. The result, considering the orthogonality of the eigenfunctions, is equal to

$$g_n = \frac{\langle w | \varphi_n \rangle}{\langle \varphi_n | \varphi_n \rangle}. \quad (7.28)$$

As an example, consider a simply supported beam of length L oriented along the x -axis of a system from $x = 0$ to $x = L$. The beam carries a static load F at midpoint

i.e., at $x = L/2$. The deflection $u(x)$ of the beam exposed to this force is obtained by means of the standard elastic line procedure as

$$u(x) = u_1(x) = \frac{F}{12D'_0}(x^3 - 3L^2x/4), \text{ for } 0 \leq x \leq L/2$$

$$u(x) = u_1(L - x) \quad \text{for } L/2 \leq x \leq L$$

The bending stiffness of the beam is D' . At time $t = 0$ the load is removed. For $t > 0$ the beam is vibrating freely. The displacement w is for $t > 0$ described by the general expression Eq. (7.11)

$$w(x, t) = \sum_{n=0}^{\infty} \varphi_n(x) [A_n \sin(\omega_{n0}t) + B_n \cos(\omega_{n0}t)] \exp(-\omega_{n0}\eta t/2),$$

where the eigenfunction for the simply supported beam is

$$\varphi_n(x) = \sin \kappa_n x = \sin(n\pi x/L), \quad \omega_{n0} = \kappa_n^2 \sqrt{D'_0/m'}.$$

The initial conditions are

$$w(x, 0) = u(x), \quad \dot{w}(x, 0) = 0.$$

The beam is at rest at $t = 0$; therefore, the velocity is zero when the beam is released. From the initial conditions it follows, for $\eta < 1$, that $A_n = 0$. For $t = 0$ the displacement is

$$w(x, 0) = u(x) = \sum_{n=0}^{\infty} \varphi_n(x) B_n, \quad B_n = \frac{\langle u | \varphi_n \rangle}{\langle \varphi_n | \varphi_n \rangle}.$$

The function $u(x)$ is symmetric around $x = L/2$. Consequently $B_n = 0$ for n even. For n odd the coefficients are

$$B_n = \frac{2}{L} \int_0^L u(x) \varphi_n(x) dx = \frac{2FL^3}{n^4\pi^4 D'}.$$

The average of the velocity squared over the length of the beam is

$$\langle v^2 \rangle = \frac{1}{L} \int_0^L \dot{w}^2 dx = \frac{1}{2} \sum_{n=0}^{\infty} \omega_{n0}^2 \cdot B_n^2 \cdot \sin^2(\omega_{n0}t) \cdot \exp(-\omega_{n0}\eta t).$$

The summation can be made from $n = 0$ since ω_{n0} is equal to zero for $n = 0$. The decay rate for the kinetic energy for each mode is thus $\exp(-\omega_{n0}\eta t)$. This means, as

discussed in Chap. 2, Eq. (2.75), that the loss factor can be determined by means of reverberation time measurements. For viscous losses the product $\omega_{n0}\eta$ is constant. For this special case the decay rate is independent of frequency.

7.3 Forced Excitation of F-Waves

In Sect. 6.2 the forced excitation of L-waves in a finite beam was discussed. A general expression defining the forced vibration was derived by means of Green's function. A similar approach can be used to describe forced flexural vibrations of a finite beam. Again the starting point is to determine the flexural response of a beam exposed to a point force.

Thus consider a point force $F_0 \cdot e^{i\omega t}$ applied to a simply supported beam at $x = x_1$ as shown in Fig. 7.1. The length of the beam is L . The forced motion of the beam is given by

$$w(x, t) = y(x) \cdot e^{i\omega t}. \quad (7.29)$$

The resulting differential equation, omitting the time-dependent function, is

$$\frac{d^4 y}{dx^4} - \kappa^4 y = \frac{F_0 \cdot \delta(x - x_1)}{D'}. \quad (7.30)$$

This follows directly from Eq. (3.77) if the force F' per unit length is replaced by $F_0 \cdot \delta(x - x_1)$. The force and displacement are defined positive in the same direction.

The by now familiar approach is to assume the following solutions

For $0 \leq x \leq x_1$

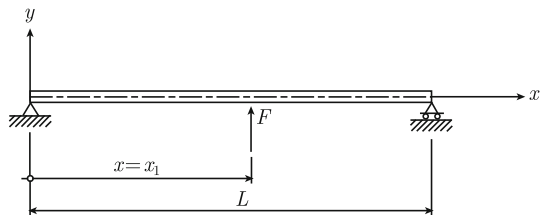
$$y_- = A_1 \sin \kappa x + A_2 \cos \kappa x + A_3 \sinh \kappa x + A_4 \cosh \kappa x. \quad (7.31)$$

For $x_1 \leq x \leq L$

$$y_+ = B_1 \sin[\kappa(L-x)] + B_2 \cos[\kappa(L-x)] + B_3 \sinh[\kappa(L-x)] + B_4 \cosh[\kappa(L-x)]. \quad (7.32)$$

Eight boundary conditions are needed to determine all the unknown parameters. The beam is simply supported at both ends. Thus

Fig. 7.1 Point excited simply supported beam



$$y_- = \frac{d^2 y_-}{dx^2} = 0 \text{ for } x = 0, \quad y_+ = \frac{d^2 y_+}{dx^2} = 0 \text{ for } x = L. \quad (7.33)$$

From these boundary conditions it follows immediately that

$$A_2 = A_4 = B_2 = B_4 = 0.$$

The displacement along the beam is continuous. Thus

$$y_- = y_+, \quad \frac{dy_-}{dx} = \frac{dy_+}{dx} \text{ for } x = x_1 \quad (7.34)$$

The bending moment $M = -D' \cdot \partial^2 w / \partial x^2$ is the same at both sides of the excitation point. This leads to

$$\frac{d^2 y_-}{dx^2} = \frac{d^2 y_+}{dx^2} \text{ for } x = x_1. \quad (7.35)$$

The condition concerning the balance of forces at $x = x_1$ yields

$$D' \left[\frac{d^3 y_+}{dx^3} - \frac{d^3 y_-}{dx^3} \right]_{x=x_1} = F_0. \quad (7.36)$$

Initially there were eight unknown parameters. There are four boundary conditions, which must be satisfied at the ends of the beam and four additional conditions at the excitation point. These last four conditions lead to the following system of equations when the parameters A_2 , A_4 , B_2 , and B_4 have been set to equal zero as given by Eq. (7.33)

$$A_1 \sin \kappa x_1 + A_3 \sinh \kappa x_1 = B_1 \sin[\kappa(L - x_1)] + B_3 \sinh[\kappa(L - x_1)]$$

$$A_1 \cos \kappa x_1 + A_3 \cosh \kappa x_1 = -B_1 \cos[\kappa(L - x_1)] - B_3 \cosh[\kappa(L - x_1)]$$

$$-A_1 \sin \kappa x_1 + A_3 \sinh \kappa x_1 = -B_1 \sin[\kappa(L - x_1)] + B_3 \sinh[\kappa(L - x_1)]$$

$$A_1 \cos \kappa x_1 - A_3 \cosh \kappa x_1 + B_1 \cos[\kappa(L - x_1)] + B_3 \cosh[\kappa(L - x_1)] = \frac{F_0}{D' \kappa^3}. \quad (7.37)$$

The solutions to Eq. (7.37) are

$$\begin{aligned} A_1 &= \frac{\sin[\kappa(L - x_1)]}{\sin \kappa L} \cdot \frac{F_0}{2D' \kappa^3}, \quad A_3 = -\frac{\sinh[\kappa(L - x_1)]}{\sinh \kappa L} \cdot \frac{F_0}{2D' \kappa^3} \\ B_1 &= \frac{\sin \kappa x_1}{\sin \kappa L} \cdot \frac{F_0}{2D' \kappa^3}, \quad B_3 = -\frac{\sinh \kappa x_1}{\sinh \kappa L} \cdot \frac{F_0}{2D' \kappa^3}. \end{aligned} \quad (7.38)$$

The response $w(x, t)$ is now obtained from the Eqs. (7.29), (7.31), (7.32) and (7.38) considering that $A_2 = A_4 = B_2 = B_4 = 0$. The result can be written in a compact

form as

$$w(x, t) = F_0 \cdot e^{i\omega t} \cdot G(x|x_1), \quad (7.39)$$

where $G(x|x_1)$ is Green's function with x the coordinate for the observation point and x_1 the coordinate for the excitation point. This function $G(x|x_1)$ is for a simply supported beam with the length L given as

$$\begin{aligned} &\text{For } 0 \leq x \leq x_1 \\ &G(x|x_1) = G_1(x|x_1) = \left\{ \frac{\sin[\kappa(L-x)] \sin(\kappa x_1)}{\sin \kappa L} \right. \\ &\quad \left. - \frac{\sinh[\kappa(L-x)] \sinh(\kappa x_1)}{\sinh \kappa L} \right\} \cdot \frac{1}{2D'\kappa^3} \\ &\text{For } x_1 \leq x \leq L \end{aligned} \quad (7.40)$$

$$\begin{aligned} &G(x|x_1) = G_2(x|x_1) = \left\{ \frac{\sin[\kappa(L-x_1)] \sin(\kappa x)}{\sin \kappa L} \right. \\ &\quad \left. - \frac{\sinh[\kappa(L-x_1)] \sinh(\kappa x)}{\sinh \kappa L} \right\} \cdot \frac{1}{2D'\kappa^3}. \end{aligned}$$

The Green's function for a simply supported beam has maxima when $\text{Re}(\kappa L) = n\pi$. Thus when the frequency of the driving force coincides with an eigenfrequency of the system there is a resonance.

Since $G(x|x_1) = G(x_1|x)$ the reciprocity relation holds. In other words, If a point force excites the beam at a position x_1 the response at a position x_2 is the same as the response in position x_1 if instead, the force excites the beam at position x_2 .

For the general case, a beam exposed to a force $F'(x)e^{i\omega t}$ per unit length of the beam, the displacement is $w(x, t) = y(x)e^{i\omega t}$, where $y(x)$ must satisfy the equation

$$\frac{d^4 y}{dx^4} - \kappa^4 y = \frac{F'}{D'}. \quad (7.41)$$

The response of the beam is

$$y(x) = \int_0^L F'(\varsigma) G(x|\varsigma) d\varsigma = \int_0^x F'(\varsigma) G_1(x|\varsigma) d\varsigma + \int_x^L F'(\varsigma) G_2(x|\varsigma) d\varsigma. \quad (7.42)$$

This is in accordance with the results discussed in Sect. 6.2—Eq. (6.51). Following the discussion in Sect. 6.2, the forced response of a simply supported beam in flexure can be derived in an alternative way. Omitting the time dependence $\exp(i\omega t)$, let the forced excitation $y(x)$ of a beam be governed by the differential equation

$$D' \frac{d^4 y}{dx^4} - m' \omega^2 y = F'.$$

The beam is assumed to satisfy one of the natural boundary conditions or any other boundary condition resulting in orthogonal eigenfunctions. The Green's function $G(x|x_1)$ is the solution to

$$D' \frac{d^4 G}{dx^4} - m' \omega^2 G = \delta(x - x_1),$$

with G satisfying the same boundary conditions as y . The two differential equations lead to

$$y(x) = \int_0^L F'(\varsigma) G(x|\varsigma) d\varsigma.$$

The proof is left for Problem 7.14.

As an example illustrating Green's method, consider a homogeneous beam of length L and simply supported at $x = 0$ and $x = L$. The force exciting the beam is equally distributed over the length of the beam i.e., $F'(x, t) = F \cdot \exp(i\omega t)/L$. The resulting response $w(x, t) = y(x) \exp(i\omega t)$ or rather the function $y(x)$ for the simply supported beam is according to Eqs. (7.40) and (7.39) given by

$$y(x) = \int_0^x d\varsigma \left\{ \frac{\sin[\kappa(L-x)] \sin(\kappa\varsigma)}{\sin \kappa L} - \frac{\sinh[\kappa(L-x)] \sinh(\kappa\varsigma)}{\sinh \kappa L} \right\} \cdot \frac{F}{2LD'\kappa^3} \\ + \int_x^L d\varsigma \left\{ \frac{\sin[\kappa(L-\varsigma)] \sin(\kappa x)}{\sin \kappa L} - \frac{\sinh[\kappa(L-\varsigma)] \sinh(\kappa x)}{\sinh \kappa L} \right\} \cdot \frac{F}{2LD'\kappa^3}. \quad (7.43)$$

The result is

$$y(x) = \frac{F}{m' L \omega^2} \left\{ \frac{\cos[\kappa(x - L/2)]}{\cos(\kappa L/2)} + \frac{\cosh[\kappa(x - L/2)]}{\cosh(\kappa L/2)} - 2 \right\}. \quad (7.44)$$

Green's function can also be derived for boundary conditions other than those discussed in this section.

For a static force F/L loading the same beam, the static deflection of the beam is also obtained from Eq. (7.44). As the frequency tends to zero the cosine and cosh functions in nominator and denominator of Eq. (7.44) can be expanded in a Taylor's series as

$$\cos \xi = 1 - \xi^2/2 + \xi^4/24 + \dots, \quad \cosh \xi = 1 + \xi^2/2 + \xi^4/24 + \dots$$

In the limit or for the static case, the displacement is

$$y(x) = \frac{F}{24LD'} (x^4 - 2Lx^3 + L^3x).$$

7.4 Mode Summation and Modal Parameters

The basic wave equation describing the forced excitation of F-waves on a uniform beam, with length L , bending stiffness D' and mass m' per unit length is as before

$$\frac{\partial^4 w}{\partial x^4} + \frac{m'}{D'} \frac{\partial^2 w}{\partial t^2} = \frac{F'(x, t)}{D'}. \quad (7.45)$$

The force $F'(x, t)$ per unit length and the displacement w are defined positive in the same direction perpendicular to the beam as shown in Fig. 7.1. It is assumed that the mounting of the beam can be described by one of the closed boundary conditions presented in Sect. 7.1. This means that there exists a complete set of orthogonal eigenfunctions $\varphi_n(x)$ satisfying the boundary conditions of the beam. Each eigenfunction has the eigenvalue κ_n . The displacement of the beam can now be expressed as an infinite sum over the eigenfunctions as

$$w(x, t) = \sum_{n=0}^{\infty} g_n(t) \cdot \varphi_n(x). \quad (7.46)$$

For harmonic excitation, the time-dependent expansion coefficients g_n are, considering the orthogonality of the eigenfunctions, given by

$$g_n(t) = \frac{\langle w(x, t) | \varphi_n(x) \rangle}{\langle \varphi_n(x) | \varphi_n(x) \rangle}. \quad (7.47)$$

If the displacement is not known, the coefficients g_n are obtained by first multiplying the wave Eq. (7.45) by φ_n . The result is then integrated over the length of the beam. Thus,

$$\int_0^L \varphi_n \frac{\partial^4 w}{\partial x^4} dx + \frac{m'}{D'} \int_0^L \varphi_n \frac{\partial^2 w}{\partial t^2} dx = \int_0^L \varphi_n \frac{F'}{D'} dx. \quad (7.48)$$

Since φ_n , with the eigenvalue κ_n , and w satisfy the same boundary conditions it follows that

$$\int_0^L \varphi_n \frac{\partial^4 w}{\partial x^4} dx = \int_0^L w \frac{\partial^4 \varphi_n}{\partial x^4} dx = \kappa_n^4 \int_0^L w \varphi_n dx. \quad (7.49)$$

The result is obtained by partial integration of the first integral as demonstrated in Eq. (7.23). The Eqs. (7.46) and (7.49) give

$$\int_0^L \varphi_n \frac{\partial^4 w}{\partial x^4} dx = \kappa_n^4 \langle \varphi_n | \varphi_n \rangle g_n. \quad (7.50)$$

The second integral in Eq. (7.48) can be rewritten as

$$\frac{m'}{D'} \int_0^L \varphi_n \frac{\partial^2 w}{\partial t^2} dx = \frac{m'}{D'} \int_0^L \varphi_n \left[\sum_{m=0}^{\infty} \frac{d^2 g_m}{dt^2} \varphi_m \right] = \frac{m'}{D'} \langle \varphi_n | \varphi_n \rangle \frac{d^2 g_n}{dt^2}. \quad (7.51)$$

Again this is a consequence of the orthogonality of the eigenfunctions. Considering the results (7.50) and (7.51) the basic Eq. (7.48) is reduced to

$$D' \kappa_n^4 \langle \varphi_n | \varphi_n \rangle g_n + m' \langle \varphi_n | \varphi_n \rangle \frac{d^2 g_n}{dt^2} = \langle \varphi_n | F' \rangle \quad (7.52)$$

Symbolically this equation can be written as

$$K_n g_n + M_n \frac{d^2 g_n}{dt^2} = F_n. \quad (7.53)$$

This is equivalent to the equation of motion for a 1-DOF system, displacement g_n , with the mass M_n and stiffness K_n and exposed to a force F_n . The generalized or modal parameters are defined as

Modal mass	$M_n = \int_0^L m' \varphi_n^2 dx$	
Modal stiffness	$K_n = \int_0^L D' \kappa_n^4 \varphi_n^2 dx$	
Modal force	$F_n = \int_0^L F' \varphi_n dx$	(7.54)

The mass per unit length and the bending stiffness can be allowed to vary along the length of the beam. For $E = E_0(1 + i\eta)$ the modal loss factor is defined as

$$\eta_n = \text{Im}(K_n)/\text{Re}(K_n) = \eta. \quad (7.55)$$

The modal parameters are not absolute quantities. The magnitude of a parameter depends on the norm $\langle \varphi_n | \varphi_n \rangle$ of the eigenfunction. However, the ratio between two modal parameters is independent of the norm of the eigenfunction. For forced harmonic excitation $F'(x, t) = F'(x) \cdot \exp(i\omega t)$ the expansion coefficient g_n in Eq. (7.46) are the solutions to Eq. (7.53) or for the stationary case given by

$$g_n(t) = \frac{F_n \cdot e^{i\omega t}}{K_n - \omega^2 M_n}, \quad (7.56)$$

where M_n , K_n , and F_n are defined in Eq. (7.54). The response w is consequently

$$w(x, t) = \sum_{n=0}^{\infty} g_n(t) \varphi_n(x) = \sum_{n=0}^{\infty} \frac{\langle F'(x) | \varphi_n(x) \rangle \varphi_n(x) e^{i\omega t}}{D'(\kappa_n^4 - \kappa^4) \langle \varphi_n(x) | \varphi_n(x) \rangle}, \quad (7.57)$$

where

$$\kappa^4 = \frac{m' \omega^2}{D'} = \frac{m' \omega^2}{D'_0} (1 - i\eta).$$

For a simply supported beam excited by a harmonic force $F'(x, t) = F_0 \cdot \delta(x - x_1) \cdot \exp(i\omega t)$ i.e., by a point force $F_0 \cdot \exp(i\omega t)$ at $x = x_1$, the response is, for $\varphi_n(x) = \sin \kappa_n x = \sin(n\pi x/L)$ and $0 \leq x \leq L$, equal to

$$w(x, t) = \sum_{n=1}^{\infty} \frac{2\varphi_n(x)\varphi_n(x_1)F_0 e^{i\omega t}}{LD'(\kappa_n^4 - \kappa^4)} = \sum_{n=1}^{\infty} \frac{2 \sin(n\pi x/L) \sin(n\pi x_1/L) F_0 e^{i\omega t}}{LD'[(n\pi/L)^4 - \kappa^4]}. \quad (7.58)$$

The expression is, as expected, symmetric with respect to x and x_1 . This again proves the reciprocity relation. The result (7.58) is equivalent to the previously derived expression (7.39) with the Green's function defined in Eq. (7.40) and can be obtained through expanding Eq. (7.40) in a sine-series. The quantity $n\pi/L$ can according to Eq. (7.13) be expressed as function of the natural frequency f_n . The wavenumber κ is a function of frequency. Thus

$$\left(\frac{n\pi}{L}\right)^4 = \frac{(2\pi)^2 m' f_n^2}{D'_0}, \quad \kappa^4 = \frac{(2\pi)^2 m' f^2}{D'} = \frac{(2\pi)^2 m' f^2}{D'_0(1 + i\eta)}.$$

These expressions inserted in Eq. (7.58) yield

$$w(x, t) = \sum_{n=1}^{\infty} \frac{2\varphi_n(x)\varphi_n(x_1)F_0 e^{i\omega t}}{Lm'(2\pi)^2[f_n^2(1 + i\eta) - f^2]}.$$

The response given above is on the same form as Eq. (6.73), which describes the response due to longitudinal point excitation of a finite clamped beam. In one case the total mass of the beam is $SL\rho$ and for the other case Lm' . The natural frequencies f_n are however different for the two cases. The derivations of kinetic energies etc. resulting from L- waves in finite beams discussed in Sect. 6.4 can now be repeated for beams in flexure. Modal parameters can also be defined for finite beams excited by a force in the longitudinal direction of the beam. The derivation of these modal parameters is left to Problem 7.4.

It is of interest now to compare the equation of motion for a simple mass-spring system and the modal equation given in (7.53). Assuming an excitation on the form $\exp(i\omega t)$ the equations for the two cases are

$$m\ddot{x} + kx = F, \quad k = k_0(1 + i\delta) \quad (7.59)$$

$$M_n\ddot{g}_n + K_ng_n = F_n, \quad K_n = K_{n0}(1 + i\eta).$$

For a mass-spring system described by the first expression in Eq. (7.59) it was shown in Chap. 2, Eq. (2.68), that the time average of the power input $\bar{\Pi}$ for white noise excitation is given by

$$\bar{\Pi} = E[Fv] = E[F\dot{x}] = m\bar{v}^2\omega_0\delta, \quad (7.60)$$

where \bar{v}^2 is the time average of the velocity squared. The angular frequency ω_0 corresponds to the natural frequency f_0 of the system or $\omega_0 = 2\pi f_0 = \sqrt{k_0/m'}$.

In Chap. 2, Eq. (2.64), the time average of the velocity squared of a mass-spring system excited by white noise, with the one sided spectral density G_{FF} was found to be

$$\bar{v}^2 = \frac{G_{FF}}{4m^2\omega_0\delta}. \quad (7.61)$$

Based on the results (7.60) and (7.61), the time average of the input power to a 1-DOF system is

$$\bar{\Pi} = \frac{G_{FF}}{4m}. \quad (7.62)$$

For white noise excitation the time averages of the kinetic and potential energies are equal. The time average of the total energy, kinetic plus potential, is thus for white noise excitation equal to twice the kinetic energy or

$$\bar{E} = m\bar{v}^2 = \frac{G_{FF}}{4m\omega_0\delta}. \quad (7.63)$$

Now returning to the beam, the time average of the input power is for mode n given by

$$\bar{\Pi}_n = E[Fv_n],$$

where v_n is the velocity of mode n at the excitation point $x = x_1$, or rather, $v_n = \dot{g}_n\varphi_n(x_1)$. The product Fv_n is thus equal to $\dot{g}_n\varphi_n(x_1)F$. The modal force F_n is equal to $\varphi_n(x_1)F$. The power input to mode n is thus

$$\bar{\Pi}_n = E[Fv_n] = E[F\varphi_n(x_1)\dot{g}_n] = E[F_n\dot{g}_n].$$

This result should be compared to the expression (7.60) defining the power input to a 1-DOF system. Thus the power input to mode n and in fact modal energies etc., can be derived as for a simple 1-DOF system by replacing mass, stiffness, loss factor, and force by the corresponding modal parameters defined in Eqs. (7.54) and (7.55).

If as before, the one sided spectral density of the point force F exciting the beam at $x = x_1$ is G_{FF} , then the corresponding spectral density of the modal force is

$$(G_{FF})_n = G_{FF}\varphi_n^2(x_1). \quad (7.64)$$

By comparing the basic expressions defining the equations of motion for the 1-DOF system and the modal equation for the beam and the expressions (7.62) and (7.63) defining the averages of power and energy for white noise excitation it is found that for each mode

$$\bar{\Pi}_n = \frac{G_{FF}\varphi_n^2(x_1)}{4M_n} = \frac{G_{FF}\varphi_n^2(x_1)}{2m'L} \quad (7.65)$$

$$\bar{E}_n = \frac{G_{FF}\varphi_n^2(x_1)}{4M_n\omega_{n0}\eta} = \frac{G_{FF}\varphi_n^2(x_1)}{2m'L\omega_{n0}\eta}, \quad (7.66)$$

where

$$\omega_{n0} = \sqrt{\frac{K_{n0}}{M_n}}.$$

The modal mass M_n is according to (7.54) equal to $M_n = m'L/2$. For white noise excitation, the time average of the total modal energy can also be written as the product between the total mass of the beam, $m'L$, and the spatial and time averages of the velocity squared $\langle \bar{v}_n^2 \rangle$. This leads to

$$\langle \bar{v}_n^2 \rangle = \frac{\bar{E}_n}{m'L} = \frac{G_{FF}\varphi_n^2(x_1)}{2(m'L)^2\omega_{n0}\eta} = \frac{G_{FF}\varphi_n^2(x_1)}{8M_n^2\omega_{n0}\eta}. \quad (7.67)$$

For any of the natural boundary conditions the modes are orthogonal. This means that the total energy is the sum of the modal energies and so forth. Thus,

$$\langle \bar{v}^2 \rangle = \sum_{n=1}^{\infty} \langle \bar{v}_n^2 \rangle = \sum_{n=1}^{\infty} \frac{G_{FF}\varphi_n^2(x_1)}{2(m'L)^2\omega_{n0}\eta} \quad (7.68)$$

$$\bar{\Pi} = \sum_{n=1}^{\infty} \bar{\Pi}_n = \sum_{n=1}^{\infty} \frac{G_{FF}\varphi_n^2(x_1)}{2(m'L)}. \quad (7.69)$$

By comparing the results, Eqs. (7.65)–(7.69), it is found that for white noise excitation

$$\bar{\Pi}_n = (m'L)\langle \bar{v}_n^2 \rangle\omega_{n0}\eta_n = \omega_{n0}\eta_n\bar{E}_n. \quad (7.70)$$

The time average of the total energy, kinetic plus potential energy, for mode n is \bar{E}_n . The relationship between power input and total energy as given in Eq. (7.70) is one of the basic assumptions used in the method referred to as the Statistical Energy Analysis or briefly SEA. For viscous losses, the product $\omega_{n0}\eta$ is constant being independent of frequency. Thus for the same input power to each mode having viscous losses the energy of each mode is the same—equipartition of energy. Further, the time average

of the power input to mode n for white noise excitation is proportional to the total mass of the beam and the temporal and spatial averages of the velocity squared. For a constant power input, the velocity squared for a mode is inversely proportional to the loss factor for that mode.

As previously pointed out the displacement due to longitudinal waves—Eq. (6.73)—and flexural waves—Eq. (7.58)—are on the same form. However, the natural frequencies for the two cases are different. Due to the similarity of the basic expressions, the kinetic energy induced by the flexural motion of the beam is identical to the corresponding expression for longitudinal waves. Thus from Eq. (6.79)

$$\bar{T} = \sum_{n=1}^{\infty} G_{FF} \int_0^{\infty} \frac{f^2 \varphi_n^2(x_1) df}{(2\pi)^2 m [(f^2 - f_n^2)^2 + (f_n^2 \eta)^2]} = \sum_{n=1}^{\infty} \bar{T}_n. \quad (7.71)$$

The total mass of the beam is $m = m' L$. For small losses the integrand has maxima for $f = f_n$. The main contribution to the integral is only obtained for frequencies very close to a resonance. The kinetic energy within a frequency band f is approximately equal to the sum of the kinetic energies for those modes with resonance frequencies within the band. The kinetic energy for mode n is

$$\bar{T}_n = G_{FF} \int_0^{\infty} \frac{f^2 \varphi_n^2(x_1) df}{(2\pi)^2 m [(f^2 - f_n^2)^2 + (f_n^2 \eta)^2]} = \frac{G_{FF} \sin^2(n\pi x_1/L)}{8\pi m f_n \eta}. \quad (7.72)$$

This means that the kinetic energy within the frequency band Δf approximately is equal to

$$\bar{T}_{\Delta f} = \sum_{n=n_1}^{n_u} \frac{G_{FF} \sin^2(n\pi x_1/L)}{8\pi m f_n \eta}. \quad (7.73)$$

The mode number for the highest mode within the band is n_u . The lowest mode is n_1 . The total number of modes N in the band is a function of the modal density \mathcal{N}_f , and is approximately equal to $N \approx \Delta f \cdot \mathcal{N}_f$. For viscous losses, the product $f\eta$ is constant. For white noise excitation, G_{FF} constant, the amplitude of the modal energy is just a function of the sine squared term. The average of this term, with respect to either n or x_1 , is $1/2$. Following the discussion in Sect. 6.3, the time average of the kinetic energy within the frequency band Δf and center frequency f is approximately equal to

$$\bar{T}_{\Delta f} = \mathcal{N}_f \cdot \Delta f \frac{G_{FF}}{16\pi m f_n \eta} = \Delta f \frac{\kappa_0 G_{FF}}{32\pi^2 m' f^2 \eta}, \quad (7.74)$$

where κ_0 is the real part of the wavenumber at the center frequency f . In a similar way, the time average of the power input within the band f for white noise excitation is

$$\bar{\Pi}_{\Delta f} = 2\bar{T}_{\Delta f} \omega \eta = \Delta f \cdot \frac{G_{FF} \kappa_0}{8\pi m' f}. \quad (7.75)$$

As discussed in Sect. 6.3 the accuracy of this approximate method depends on the number of modes within a frequency band. For an error to be sufficiently small the number of modes should at least be of order 4.

Considering the definition of the wavenumber κ_0 , the kinetic energy, Eq. (7.74), is written as

$$\bar{T}_{\Delta f} = \Delta f \frac{(m')^{1/4} \omega^{1/2} G_{FF}}{32\pi^2 (D')^{1/4} m' f^2 \eta} \propto \frac{1}{bh^{3/2} \eta}.$$

For the excitation and material parameters constant, the kinetic energy is decreased by increasing width b or height h of the beam or the loss factor. Maintaining the weight of the beam, the height of the beam should be increased and width decreased to reduce the kinetic energy of the structure.

7.5 Point Mobility and Power

The point mobility of a structure is an important quantity. First of all the response of the structure or rather the FT of the velocity at the excitation point is proportional to the point mobility. In addition the power injected into a structure by a force is proportional to the real part of the mobility at the excitation point.

The response or displacement of a uniform beam exposed to a point force can be defined in a closed form or as a sum over the eigenvectors. For a beam with the length L , simply supported at the ends at $x = 0$ and $x = L$ and exposed to a point force at $x = x_1$, the response of the structure is given in the Eqs. (7.39), (7.40) and (7.57). The mobility $Y(x_1)$ at the point where the force is applied is defined as the ratio between the FT of the velocity at the point and the FT of the force exciting the beam. Thus

$$Y(\omega, x_1) = \frac{\hat{v}(\omega, x_1)}{\hat{F}(\omega)} = \frac{i\omega \hat{w}(\omega, x_1)}{\hat{F}(\omega)}. \quad (7.76)$$

Based on the discussion in Sects. 2.2, 5.1, and 6.5, the FT of the velocity as function of the FT of the force is obtained by making the substitutions $F(t) \rightarrow \hat{F} \cdot \exp(i\omega t)$ and $w(x, t) \rightarrow \hat{w}(x) \cdot \exp(i\omega t)$ in the Eqs. (7.39) and (7.58). The FT of the velocity is $\hat{v} = i\omega \hat{w}$. Based on the results (7.39) and (7.58) the point mobility at $x = x_1$ can be written in two ways, closed form or as an infinite series, given by

$$Y(\omega, x_1) = \frac{i\omega}{2D'\kappa^3} \left\{ \frac{\sin(\kappa x_1) \sin[\kappa(L - x_1)]}{\sin(\kappa L)} - \frac{\sinh(\kappa x_1) \sinh[\kappa(L - x_1)]}{\sinh(\kappa L)} \right\}$$

$$Y(\omega, x_1) = \frac{2i\omega}{LD'} \sum_{n=1}^{\infty} \frac{\varphi_n^2(x_1)}{\kappa_n^4 - \kappa^4} = \frac{2i\omega}{LD'} \sum_{n=1}^{\infty} \frac{\sin^2(n\pi x_1/L)}{(n\pi/L)^4 - \kappa^4}. \quad (7.77)$$

The expressions given in Eq. (7.77) are valid for any x_1 as long as $0 \leq x_1 \leq L$. Due to the losses in the system the wavenumber κ is a complex quantity. Equation (7.77)

shows that the point mobility has maxima when the real part of the wavenumber is equal to $n\pi/L$ if $\sin(n\pi x_1/L) \neq 0$. The spectral density S_Π of the power injected into the beam is defined as

$$S_\Pi(\omega) = S_{Fv}(\omega) = \lim_{T \rightarrow \infty} \frac{\hat{F}^* \hat{v}}{T}. \quad (7.78)$$

This is a direct consequence of the result given in Eq. (2.56). However $\hat{v} = \hat{F}Y$, thus

$$S_\Pi(\omega) = S_{Fv}(\omega) = \lim_{T \rightarrow \infty} \frac{\hat{F}^* \hat{v}}{T} = \lim_{T \rightarrow \infty} \frac{\hat{F}^* \hat{F}Y}{T} = S_{FF}(\omega)Y. \quad (7.79)$$

The function S_{FF} is the power spectral density of the force. The time average of the power input Π is according to Eq. (2.55) equal to

$$\bar{\Pi} = \frac{1}{2\pi} \int_{-\infty}^{\infty} S_\Pi(\omega) d\omega = \frac{1}{2\pi} \int_0^{\infty} \text{Re} G_\Pi(\omega) d\omega. \quad (7.80)$$

From Eq. (7.79) it follows that

$$\text{Re} G_\Pi = \text{Re}(G_{FF}Y^*).$$

For white noise excitation G_{FF} is constant and real. Thus,

$$\text{Re} G_\Pi = G_{FF} \text{Re} Y.$$

The frequency average of the point mobility has some very interesting and important properties. In certain cases, the power input to a finite structure can regardless of boundary conditions be determined as if the structures were infinite. This can be demonstrated by considering a simply supported beam excited by a point force at $x_1 = L/2$. The point mobility at the center of the beam can according to Eq. (7.77) be written in two ways as

$$Y(\omega, L/2) = \frac{i\omega}{4D'\kappa^3} \left[\frac{\sin(\kappa L/2)}{\cos(\kappa L/2)} - \frac{\sinh(\kappa L/2)}{\cosh(\kappa L/2)} \right] \quad (7.81)$$

$$Y(\omega, L/2) = \frac{2i\omega}{LD'} \sum_{n=1}^{\infty} \frac{\sin^2(n\pi/2)}{(n\pi/L)^4 - \kappa^4} = \frac{2i\omega}{LD'} \sum_{n=0}^{\infty} \frac{1}{[(2n+1)\pi/L]^4 - \kappa^4}. \quad (7.82)$$

In the last expression and in the first summation, the terms for n even are equal to zero.

The product between wavenumber and the length is complex and can be written as

$$\kappa L/2 = \alpha = \kappa_0 L(1 - i\eta/4)/2 = \alpha_0(1 - i\eta/4), \quad (7.83)$$

where α_0 is a real quantity. The trigonometric functions in the first expression of Eq. (7.82) are consequently also complex but can readily be separated into a real and an imaginary part as

$$\begin{aligned}\sin \alpha &= \sin \alpha_0 \cos(i\alpha_0\eta/4) - \cos \alpha_0 \sin(i\alpha_0\eta/4) \\ &= \sin \alpha_0 \cosh(\alpha_0\eta/4) - i \cos \alpha_0 \sinh(\alpha_0\eta/4).\end{aligned}$$

In a similar way

$$\begin{aligned}\cos \alpha &= \cos \alpha_0 \cosh(\alpha_0\eta/4) + i \sin \alpha_0 \sinh(\alpha_0\eta/4) \\ \sinh \alpha &= \sinh \alpha_0 \cos(\alpha_0\eta/4) - i \cosh \alpha_0 \sin(\alpha_0\eta/4) \\ \cosh \alpha &= \cosh \alpha_0 \cos(\alpha_0\eta/4) - i \sinh \alpha_0 \sin(\alpha_0\eta/4).\end{aligned}$$

For $\alpha_0\eta/4 \ll 1$ the first expression in (7.82) approximately gives

$$\begin{aligned}\text{Re}Y(\omega, L/2) &= \frac{\omega\alpha_0\eta}{8D'_0\kappa_0^3} \left[\frac{1}{\cos^2 \alpha_0 + (\alpha_0\eta/4)^2 \sin^2 \alpha_0} \right. \\ &\quad \left. + \frac{1}{\cosh^2 \alpha_0 + (\alpha_0\eta/4)^2 \sinh^2 \alpha_0} \right].\end{aligned}\quad (7.84)$$

In order to obtain this expression $\sin(\alpha_0\eta/4)$ has been replaced by $(\alpha_0\eta/4)$ and so on. The second expression inside the bracket in (7.84) is much smaller than the first for $\kappa_0 L > 2$.

The second expression in Eq. (7.82) gives

$$Y(\omega, L/2) = \frac{2\omega\eta}{LD'_0} \sum_n \frac{\kappa_n^4}{(\kappa_n^4 - \kappa_0^4)^2 + (\eta\kappa_n^4)^2}.\quad (7.85)$$

The two equivalent expressions (7.84) and (7.85) are rapidly varying with frequency or wavenumber with maxima inversely proportional to η for $\alpha_0 = \kappa_0 L/2 = (n + 1/2)\pi$. For comparison, the point mobility for an infinite uniform beam is according to Eq. (5.39) a smoothly varying function given by

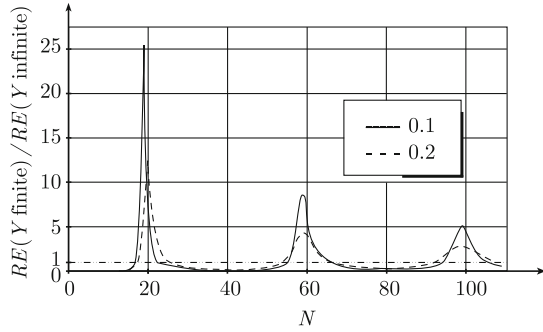
$$Y_\infty(\omega) = \frac{(1-i)(1+i\eta/4)\kappa_0}{4m'\omega}.$$

For small losses the real part of this point mobility is

$$\text{Re}Y_\infty = \frac{\kappa_0}{4m'\omega}.\quad (7.86)$$

In Fig. 7.2, the real part of the point mobility at $x = L/2$ for a simply supported beam of length L is compared to the real part of the point mobility for an infinite beam.

Fig. 7.2 Point mobility of a finite beam compared to the point mobility for an infinite beam. The product between wavenumber and length is $\kappa L = N\pi/20$, where N is given on the abscissa. The point mobilities are given for two loss factors 0.1 and 0.2



The figure shows the ratio $\text{Re } Y/\text{Re } Y_\infty$ as function of κ_0 . The ratio is plotted for two fairly high loss factors of 0.1 and 0.2. When the loss factor is increased the maximum amplitude is decreased. However, at the same time the base of the curve is widened considerably. The resonance frequency or rather the quantity α_0 resulting in a maximum is slightly increased as the losses are increased. For sufficiently small losses resonances are obtained for $\alpha_0 = \kappa_0 L/2 = n\pi + \pi/2$. The distance $\Delta\alpha_0$ between two peaks or maxima is π .

In the frequency domain, the difference $\Delta\alpha_0$ corresponds to Δf as $\Delta\alpha_0 = \Delta f \cdot d\alpha_0/df$. According to the definition (7.83) α_0 is equal to $\kappa_0 L/2$. Thus with $\alpha_0 = (L/2)[m'(2\pi f)^2/D_0']^{1/4}$ and $\Delta\alpha_0 = \pi$, the spacing Δf in the frequency domain between two maxima is

$$\Delta f = \frac{4\pi f}{L\kappa_0} = \frac{4\pi f_n}{L\kappa_0}, \quad (7.87)$$

where f_n is the frequency corresponding to the maximum order of n .

For white noise excitation at the midpoint of a simply supported beam, the time average of the power input to mode n is according to Eq. (7.65) equal to

$$\bar{\Pi}_n = \frac{G_{FF}\varphi_n^2(L/2)}{2m'L} = \frac{G_{FF}}{2m'L}. \quad (7.88)$$

The expression is valid for n odd. For n even $\varphi_n^2(L/2) = 0$. For a finite beam this is equal to the power input to the structure in the frequency range f_1 to $f_2 = f_1 + \Delta f$ corresponding to one maximum and where Δf is defined in Eq. (7.87) and is equal to the spacing between two maxima. For an infinite beam the spectral density of the power input is, comparing Eq. (7.86),

$$G_\Pi(\omega) = G_{FF}\text{Re } Y_\infty = \frac{G_{FF}\kappa_0}{4m'\omega}. \quad (7.89)$$

The power input over the same frequency range f_1 to $f_2 = f_1 + \Delta f$ with the centre frequency f_0 of the interval and with Δf given by Eq. (7.87) is for an infinite beam

$$\bar{\Pi}_{\Delta f} = \frac{1}{2\pi} \int_{f_1}^{f_2} G_{\Pi}(\omega) d\omega \approx G_{\Pi}(2\pi f_0) \Delta f = \frac{G_{FF}}{2m'L}. \quad (7.90)$$

This is the same result as given by Eq. (7.88). The result implies that the power input to a finite structure over a frequency range Δf including a resonance is the same as the power input to an infinite beam over the same frequency range, for white noise excitation. However, it has been assumed that the force is applied at the centre of the beam. The same result is obtained, if the excitation point of the force is randomly distributed in time over the length of the beam. This is a result of great importance. If a finite structure is excited by random forces in time and space, the power input to the structure can be calculated, as if the structures were infinite and excited at one point by a force with a power spectra density equal to the sum of the power spectra of all the sources acting on the finite structure.

The result (7.90) can also be obtained from the previously derived Eq. (7.75). This expression can be rewritten as

$$\bar{\Pi}_{\Delta f} = \Delta f \frac{G_{FF} \kappa_0}{8\pi m' f} = \Delta f \cdot G_{FF} \text{Re} Y_{\infty}.$$

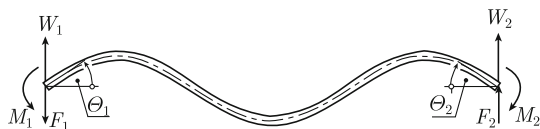
From this it follows, that if a beam is excited by white noise at one point, then the power input to the structure within a frequency band Δf containing a sufficient number of resonant modes, can be calculated as if the beam were infinite. This expression is valid for any boundary condition since the modal density is approximately independent of boundary conditions except for the first few modes.

7.6 Transfer Matrices for Bending of Beams

In Sect. 6.7 the transfer matrices for coupled beams excited by longitudinal waves were discussed. The transfer matrices were used to determine the response of a chain of coupled beams. In a similar way, the coupling between finite beams exposed to bending can be described by means of transfer matrices. The starting point is a single finite and uniform beam as illustrated in Fig. 7.3.

The displacement, rotation, bending moment, and force at one end of the beam can be expressed as functions of the corresponding quantities at the other end of the beam. The general expression giving the displacement $w(x)$ for flexural waves on the beam extended along the x -axis is, neglecting the time dependence $\exp(i\omega t)$, equal to

Fig. 7.3 Bending of beam element and resulting field parameters



$$w(x) = A_1 \sin \kappa x + A_2 \cos \kappa x + A_3 \sinh \kappa x + A_4 \cosh \kappa x. \quad (7.91)$$

The mass per unit length of the beam, bending stiffness, and wavenumber are given by m' , D' , and κ , respectively. The ends of the beam are located at $x = 0$ and $x = L$ where L is the length of the beam. The displacement, angular displacement, bending moment, and force at $x = 0$ are given by w_1 , Θ_1 , M_1 , and F_1 , respectively. The boundary conditions for $x = 0$ in combination with the general expression (7.91) yield

$$\begin{aligned} w_1 &= A_2 + A_4 \\ M_1 &= -D' \left[\frac{d^2 w}{dx^2} \right]_{x=0} = D' \kappa^2 (A_2 - A_4) \\ \Theta_1 &= \left[\frac{dw}{dx} \right]_{x=0} = \kappa (A_1 + A_3) \\ F_1 &= -D' \left[\frac{d^3 w}{dx^3} \right]_{x=0} = D' \kappa^3 (A_1 - A_3). \end{aligned} \quad (7.92)$$

The parameters A_1 – A_4 are obtained from Eq. (7.92) as

$$\begin{aligned} A_1 &= \frac{1}{2} \left(\frac{\Theta_1}{\kappa} + \frac{F_1}{D' \kappa^3} \right) \\ A_2 &= \frac{1}{2} \left(w_1 + \frac{M_1}{D' \kappa^2} \right) \\ A_3 &= \frac{1}{2} \left(\frac{\Theta_1}{\kappa} - \frac{F_1}{D' \kappa^3} \right) \\ A_4 &= \frac{1}{2} \left(w_1 - \frac{M_1}{D' \kappa^2} \right). \end{aligned} \quad (7.93)$$

These results imply that once the quantities w_1 , Θ_1 , M_1 , and F_1 at one end of the beam are known then the corresponding quantities can be obtained at any other position along the beam. At the other end of the beam i.e., for $x = L$ the resulting field quantities are for $\beta = \kappa L$ equal to

$$\begin{aligned} w_2 &= A_1 \sin \beta + A_2 \cos \beta + A_3 \sinh \beta + A_4 \cosh \beta \\ \Theta_2 &= \left[\frac{dw}{dx} \right]_{x=L} = \kappa [A_1 \cos \beta - A_2 \sin \beta + A_3 \cosh \beta + A_4 \sinh \beta] \\ M_2 &= -D' \left[\frac{d^2 w}{dx^2} \right]_{x=L} = \kappa^2 [-A_1 \sin \beta - A_2 \cos \beta + A_3 \sinh \beta + A_4 \cosh \beta] \\ F_2 &= -D' \left[\frac{d^3 w}{dx^3} \right]_{x=L} = D' \kappa^3 [A_1 \cos \beta - A_2 \sin \beta - A_3 \cosh \beta - A_4 \sinh \beta]. \end{aligned} \quad (7.94)$$

The amplitudes A_1 – A_4 are all linear functions of the field parameters w_1 , Θ_1 , M_1 , and F_1 . Consequently, the system of equations above can be expressed in matrix form as

$$\begin{Bmatrix} w_2 \\ \Theta_2 \\ M_2 \\ F_2 \end{Bmatrix} = [A] \cdot \begin{Bmatrix} w_1 \\ \Theta_1 \\ M_1 \\ F_1 \end{Bmatrix}$$

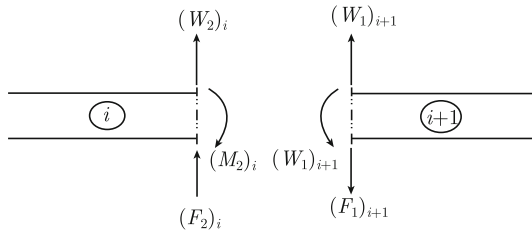
The elements a_{ij} in the matrix $[A]$ are

$$\begin{aligned} a_{11} &= \frac{1}{2}(\cos \beta + \cosh \beta) & a_{12} &= \frac{1}{2\kappa}(\sin \beta + \sinh \beta) \\ a_{13} &= \frac{1}{2D'\kappa^2}(\cos \beta - \cosh \beta) & a_{14} &= \frac{1}{2D'\kappa^3}(\sin \beta - \sinh \beta) \\ a_{21} &= \frac{\kappa}{2}(-\sin \beta + \sinh \beta) & a_{22} &= \frac{1}{2}(\cos \beta + \cosh \beta) \\ a_{23} &= \frac{1}{2D'\kappa}(-\sin \beta - \sinh \beta) & a_{24} &= \frac{1}{2D'\kappa^2}(\cos \beta - \cosh \beta) \\ a_{31} &= \frac{D'\kappa^2}{2}(\cos \beta - \cosh \beta) & a_{32} &= \frac{D'\kappa}{2}(\sin \beta - \sinh \beta) \\ a_{33} &= \frac{1}{2}(\cos \beta + \cosh \beta) & a_{34} &= \frac{1}{2\kappa}(\sin \beta + \sinh \beta) \\ a_{41} &= \frac{D'\kappa^3}{2}(-\sin \beta - \sinh \beta) & a_{42} &= \frac{D'\kappa^2}{2}(\cos \beta - \cosh \beta) \\ a_{43} &= \frac{\kappa}{2}(-\sin \beta + \sinh \beta) & a_{44} &= \frac{1}{2}(\cos \beta + \cosh \beta). \end{aligned} \quad (7.95)$$

At a junction between two adjoining beams denoted i and $i + 1$ shown in Fig. 7.4 the boundary conditions are

$$(w_2)_i = (w_1)_{i+1}, \quad (\Theta_2)_i = (\Theta_1)_{i+1}, \quad (M_2)_i = (M_1)_{i+1}, \quad (F_2)_i = (F_1)_{i+1}.$$

Fig. 7.4 Displacements, moments, and forces at a junction between two beam elements



This leads to

$$\begin{Bmatrix} w_1 \\ \Theta_1 \\ M_1 \\ F_1 \end{Bmatrix}_{i+1} = [A]_i \cdot \begin{Bmatrix} w_1 \\ \Theta_1 \\ M_1 \\ F_1 \end{Bmatrix}_i \quad (7.96)$$

The elements in the matrix $[A]$ are given in (7.95). The parameters D' , κ , and β are given an index i to indicate that they are valid for beam i . For a set of n beams the field parameters at the two extreme ends are coupled as

$$\begin{Bmatrix} w_2 \\ \Theta_2 \\ M_2 \\ F_2 \end{Bmatrix}_n = [\mathcal{A}] \cdot \begin{Bmatrix} w_1 \\ \Theta_1 \\ M_1 \\ F_1 \end{Bmatrix}_1, \quad [\mathcal{A}] = [A]_n \cdot [A]_{n-1} \cdots [A]_2 \cdot [A]_1 \quad (7.97)$$

Consider now the system shown in Fig. 7.5. A number of beams are joined together along their axes. A force $F \cdot \exp(i\omega t)$ is applied to the free end and perpendicular to the beam. The other end of the assembled beams is clamped to a structure with infinite impedance. Omitting the time dependence $\exp(i\omega t)$ the boundary conditions are

$$(w_2)_n = 0, \quad (\Theta_2)_n = 0, \quad (M_1)_1 = 0, \quad (F_1)_1 = F.$$

The remaining unknown field parameters can be solved based on the system of equations expressed in matrix form as

$$\begin{Bmatrix} 0 \\ 0 \\ M_2 \\ F_2 \end{Bmatrix}_n = [A]_n \cdot [A]_{n-1} \cdots [A]_2 \cdot [A]_1 \cdot \begin{Bmatrix} w_1 \\ \Theta_1 \\ 0 \\ F \end{Bmatrix}_1 = [\mathcal{A}] \cdot \begin{Bmatrix} w_1 \\ \Theta_1 \\ 0 \\ F \end{Bmatrix}_1$$

There are four unknown parameters $(w_1)_1$, $(\Theta_1)_1$, $(M_2)_n$, and $(F_2)_n$ and four equations. Once the unknown parameters have been solved the field parameters can be calculated at any junction. Then it follows that the displacement or any other field parameter can be calculated along any beam element by means of Eqs. (7.91) and (7.93).

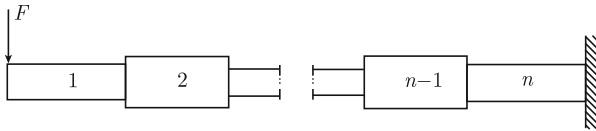


Fig. 7.5 A point force exciting a set of n coupled beams

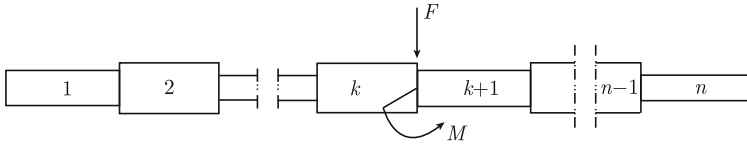


Fig. 7.6 A set of beams excited by a force and a bending moment at a junction

For a set of beams excited by a harmonic force F and a harmonic bending moment M at a junction between the elements k and $k + 1$ as shown in Fig. 7.6, the field parameters at the outer ends of the coupled beams are obtained from the equation

$$\begin{Bmatrix} w_2 \\ \Theta_2 \\ M_2 \\ F_2 \end{Bmatrix}_n = [A]_n \cdots [A]_1 \cdot \begin{Bmatrix} w_1 \\ \Theta_1 \\ M_1 \\ F_1 \end{Bmatrix}_1 + [A]_n \cdots [A]_{k+1} \cdot \begin{Bmatrix} 0 \\ 0 \\ M \\ F \end{Bmatrix} \quad (7.98)$$

Again, the time dependence $\exp(i\omega t)$ has been omitted. The boundary conditions for the ends must also be included to solve the resulting system of equations. For simply supported end w and M are zero.

7.7 Infinite Periodic Structures

In certain cases, periodic structures can be considered as infinite. A typical example is a railway track. The assumption, that a system is infinite, radically simplifies the solution of the dynamical problem. The method for solving these types of problems was formulated in physics by Bloch and in mathematics by Floquet. If an infinite structure, oriented along the x -axis of a coordinate system, is periodic with respect to the distance L , then according to Floquet the free vibrations of the structure are also periodic. For free vibrations this can be written as

$$\phi(x + nL) = e^{in\varphi} \cdot \phi(x). \quad (7.99)$$

The function $\phi(x)$ could describe the deflection due to any type of wave, for example flexural or longitudinal. The general method can be demonstrated by considering a simplified model of a railway track. The rail is modeled as an Euler beam. The beam is fastened at discrete equi-distant points as shown in Fig. 7.7.

The distance between each mounting is L . The mounting is assumed to be such that only a vertical force due to the mounting is reacting on the beam. The supports have a certain point mobility Y . The beam is “pinned” to these supports. This means that no bending moment is enforced by the supports on the beam. The displacement of the beam is assumed to be $w(x, t) = y(x) \cdot \exp(i\omega t)$. For harmonic flexural motion of the beam the force F_s reacting on the beam is $F_s = i\omega w/Y$. Neglecting

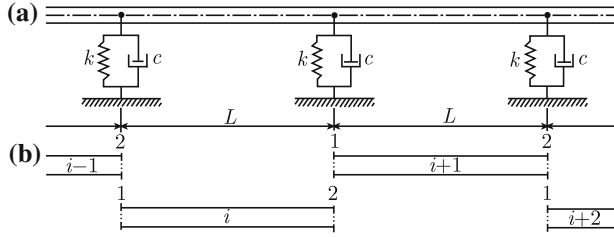


Fig. 7.7 Simple model of a rail or an infinite periodic beam structure

the time dependence $\exp(i\omega t)$ the equation of motion describing bending waves on the beam is

$$\frac{d^4 y}{dx^4} - \kappa^4 y = - \sum_{n=-\infty}^{\infty} i\omega y \delta(x - n \cdot L) / (D'Y). \quad (7.100)$$

The force on the rail at each support is given by the infinite sum. The locations of the support are at $x = nL$, where n is an integer. The beam is continuous across a support. The displacement of “segment i ” of the beam between two supports is given the subscript i . The field parameters at the left and right ends of a segment are defined by the subscripts 1 and 2 respectively as indicated in Fig. 7.7. The boundary conditions at a support are consequently

$$\begin{aligned} (y_2)_i &= (y_1)_{i+1} & \left(\frac{dy_2}{dx}\right)_i &= \left(\frac{dy_1}{dx}\right)_{i+1} \\ \left(\frac{d^2 y_2}{dx^2}\right)_i &= \left(\frac{d^2 y_1}{dx^2}\right)_{i+1} & \left(\frac{d^3 y_2}{dx^3}\right)_i &= \left(\frac{d^3 y_1}{dx^3}\right)_{i+1} + \frac{i\omega}{YD'}(y_1)_{i+1}. \end{aligned}$$

The boundary conditions correspond to equality between displacement, bending, and moment at each side of a support. The last condition is obtained from the balance of forces at a support. The boundary conditions above can also be written as

$$\begin{aligned} (w_2)_i &= (w_1)_{i+1} \\ (\Theta_2)_i &= (\Theta_1)_{i+1} \\ (M_2)_i &= (M_1)_{i+1} \\ (F_2)_i &= (F_1)_{i+1} - \frac{i\omega}{Y}(w_1)_{i+1}. \end{aligned} \quad (7.101)$$

If the field parameters at one end of the beam are known, the parameters at the other end can be determined by means of the matrix $[A]$ defined in Eq. (7.95). Thus

$$\begin{Bmatrix} w_2 \\ \Theta_2 \\ M_2 \\ F_2 \end{Bmatrix}_i = \begin{Bmatrix} w_1 \\ \Theta_1 \\ M_1 \\ F_1 - i\omega w_1/Y \end{Bmatrix}_{i+1} = [A]_i \cdot \begin{Bmatrix} w_1 \\ \Theta_1 \\ M_1 \\ F_1 \end{Bmatrix}_i$$

The four unknown field parameters with index $i + 1$ can be expressed as functions of the field parameters with index i . The parameter $(w_1)_{i+1}$ is according to Eq. (7.96) equal to $(w_1)_{i+1} = a_{11}(w_1)_i + a_{12}(\Theta_1)_i + a_{13}(M_1)_i + a_{14}(F_1)_i$. If this is inserted in the expression relating $(F_1 + i\omega w_1/Y)_{i+1}$ and $(F_1)_i$ it follows that

$$\begin{Bmatrix} w_1 \\ \Theta_1 \\ M_1 \\ F_1 \end{Bmatrix}_{i+1} = [A']_i \cdot \begin{Bmatrix} w_1 \\ \Theta_1 \\ M_1 \\ F_1 \end{Bmatrix}_i \quad (7.102)$$

The elements a'_{11} to a'_{34} in the matrix $[A']$ are identical to the corresponding elements a_{11} to a_{34} of matrix $[A]$. The elements in the last row are

$$\begin{aligned} a'_{41} &= a_{41} + i\omega a_{11}/Y \\ a'_{42} &= a_{42} + i\omega a_{12}/Y \\ a'_{43} &= a_{43} + i\omega a_{13}/Y \\ a'_{44} &= a_{44} + i\omega a_{14}/Y. \end{aligned} \quad (7.103)$$

According to Floquet there is a certain periodicity between the displacement of two adjoining elements. This means that $(w_1)_{i+1} = \exp(i\varphi)(w_1)_i$. The same periodicity holds for the derivatives of w_1 and thus also for the angular displacement, bending moment, and force. These conditions in combination with Eq. (7.102) yield

$$\begin{Bmatrix} w_1 \\ \Theta_1 \\ M_1 \\ F_1 \end{Bmatrix}_{i+1} = e^{i\varphi} \cdot \begin{Bmatrix} w_1 \\ \Theta_1 \\ M_1 \\ F_1 \end{Bmatrix}_i = [A']_i \cdot \begin{Bmatrix} w_1 \\ \Theta_1 \\ M_1 \\ F_1 \end{Bmatrix}_i$$

There is a solution to this expression if

$$\text{Det} \left[[A'] - e^{i\varphi} \mathbf{I} \right] = 0, \quad (7.104)$$

where \mathbf{I} is a 4×4 unit matrix. From Eq. (7.104) the phase angle φ can be solved.

The concept of infinite periodic structures can be illustrated by means of a special case of the problem discussed above. The most simple model of a railway track is based on the assumption that the supports are completely rigid, i.e., the mobility of the supports is equal to zero. The displacement of the rail or beam is consequently zero at a support. At the same time there is no constraining moment acting on the beam at a support. For $(w_1)_i = (w_1)_{i+1} = 0$ inserted in the basic Eq. (7.96), the system of equations becomes

$$\begin{aligned} a_{12}(\Theta_1)_i + a_{13}(M_1)_i + a_{14}(F_1)_i &= 0 \\ a_{12}(\Theta_1)_i + a_{13}(M_1)_i + a_{14}(F_1)_i &= (\Theta_1)_{i+1} \\ a_{32}(\Theta_1)_i + a_{33}(M_1)_i + a_{34}(F_1)_i &= (M_1)_{i+1}. \end{aligned}$$

The first expression gives $(F_1)_i$ as function of $(\Theta_1)_i$ and $(M_1)_i$. The result is thereafter inserted in the last two equations above. The reduced system of equations is written

$$\begin{Bmatrix} \Theta_1 \\ M_1 \end{Bmatrix}_{i+1} = [B] \cdot \begin{Bmatrix} \Theta_1 \\ M_1 \end{Bmatrix}_i \quad (7.105)$$

The elements b_{ij} of the matrix $[B]$ are obtained from Eq. (7.95) as

$$\begin{aligned} b_{11} &= \frac{a_{14}a_{22} - a_{12}a_{24}}{a_{14}} = \frac{\sin \beta \cosh \beta - \cos \beta \sinh \beta}{\sin \beta - \sinh \beta} \\ b_{12} &= \frac{a_{14}a_{23} - a_{13}a_{24}}{a_{14}} = -\frac{1}{D'\kappa} \frac{(1 - \cos \beta \cosh \beta)}{(\sin \beta - \sinh \beta)} \\ b_{21} &= \frac{a_{14}a_{32} - a_{12}a_{34}}{a_{14}} = -2D'\kappa \frac{\sin \beta \sinh \beta}{(\sin \beta - \sinh \beta)} \\ b_{22} &= \frac{a_{14}a_{33} - a_{13}a_{34}}{a_{14}} = \frac{\sin \beta \cosh \beta - \cos \beta \sinh \beta}{\sin \beta - \sinh \beta}. \end{aligned} \quad (7.106)$$

For an infinite periodic structure, the relative displacement between two adjoining segments is determined by the factor $\exp(i\varphi)$ as previously discussed. The phase angle φ is the solution to the equation

$$\text{Det} \left[[B] - e^{i\varphi} \mathbf{I} \right] = 0. \quad (7.107)$$

This can also be written as

$$e^{2i\varphi} - e^{i\varphi}(b_{11} + b_{22}) + (b_{11}b_{22} - b_{12}b_{21}) = 0.$$

By introducing the result (7.106) this expression becomes

$$e^{2i\varphi} - 2e^{i\varphi} \left(\frac{\sin \beta \cosh \beta - \cos \beta \sinh \beta}{\sin \beta - \sinh \beta} \right) + 1 = 0. \quad (7.108)$$

Multiplying this expression by $\exp(-i\varphi)$ the phase angle is obtained as the solution to

$$\cos \varphi = \left(\frac{\sin \beta \cosh \beta - \cos \beta \sinh \beta}{\sin \beta - \sinh \beta} \right) = Q. \quad (7.109)$$

The absolute value of Q can be larger than unity, making the phase angle complex. It is convenient to write the phase angle as $\varphi = u + iv$.

By setting $z = \exp(i\varphi)$ and by introducing Q from Eq. (7.109) in (7.108) the parameter z and thus also φ are solved. For $\varphi = u + iv$

$$\begin{aligned} z &= e^{i\varphi} = e^{-v}(\cos u + i \sin u) = Q \pm \sqrt{Q^2 - 1} \text{ for } |Q| \geq 1 \\ z &= e^{i\varphi} = e^{-v}(\cos u + i \sin u) = Q \pm i\sqrt{1 - Q^2} \text{ for } |Q| < 1. \end{aligned} \quad (7.110)$$

There can be no amplification of the amplitude of a free wave as it is progressing across a support. This means that $|\exp(i\varphi)| \leq 1$. When Q is larger than unity the minus sign in the first expression of (7.110) must be chosen. For Q negative with an absolute value larger than unity the plus sign should apply. For the absolute value of less than unity then according to the second expression $|\exp(i\varphi)| = 1$. For $|Q| < 1$ the solution $Q - i\sqrt{1 - Q^2}$ represents a wave propagating along the positive x -axis. The solution $Q + i\sqrt{1 - Q^2}$ corresponds to a wave propagating in the opposite direction. The real and imaginary part of φ are shown in Fig. 7.8 as functions of the product κL .

For $\pi/2 + n\pi \leq \kappa L \leq \pi + n\pi$ for n an integer, the wave motion is attenuated across each support. For $n\pi \leq \kappa L \leq \pi/2 + n\pi$, the imaginary part of φ , or v , is equal to zero. Consequently, in this frequency range there is no attenuation. The decay of the energy of the beam across one junction is given by the factor $\exp(-2v)$. This attenuation in dB is shown in Fig. 7.9. For $\beta = \kappa L \geq \pi$ the functions $\sinh \beta$ and $\cosh \beta$ are much larger than unity and approximately equal. This means that in this frequency interval, the parameter Q defined in Eq. (7.109) can be approximated as

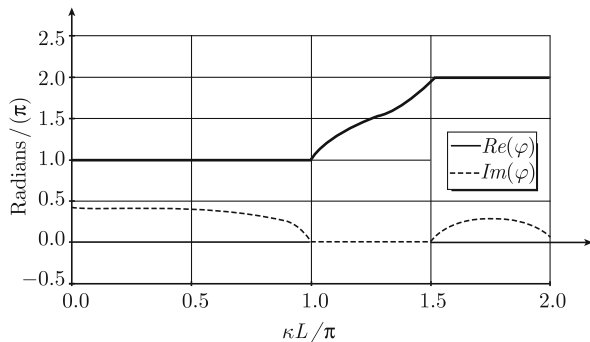
$$Q \approx \cos \beta - \sin \beta = \sqrt{2} \cos(\beta + \pi/4) \text{ for } \beta \geq \pi.$$

In the high frequency range, $\beta \geq \pi$, Q and thus also u and v are almost periodic, or

$$\begin{aligned} u &= \text{Re}[\varphi(\kappa L + n\pi)] \approx \text{Re}[\varphi(\kappa L)] + n\pi \\ v &= \text{Im}[\varphi(\kappa L + n\pi)] \approx \text{Im}[\varphi(\kappa L)]. \end{aligned}$$

It is interesting now to return to the single junction discussed in Sect. 5.9. In this section, it was shown that if a flexural wave is propagating in a semi-infinite beam towards a single “pinned” junction, 50 % of the incident intensity is transmitted across the junction to the adjoining and identical semi-infinite beam. The resulting 3 dB attenuation across this type of junction is independent of frequency. By comparison, the attenuation across one “pinned” junction of an infinite periodic structure can be zero for certain frequencies and for high frequencies, always less than 3 dB. The

Fig. 7.8 Real and imaginary parts of the phase angle φ as functions of $\kappa L/\pi$



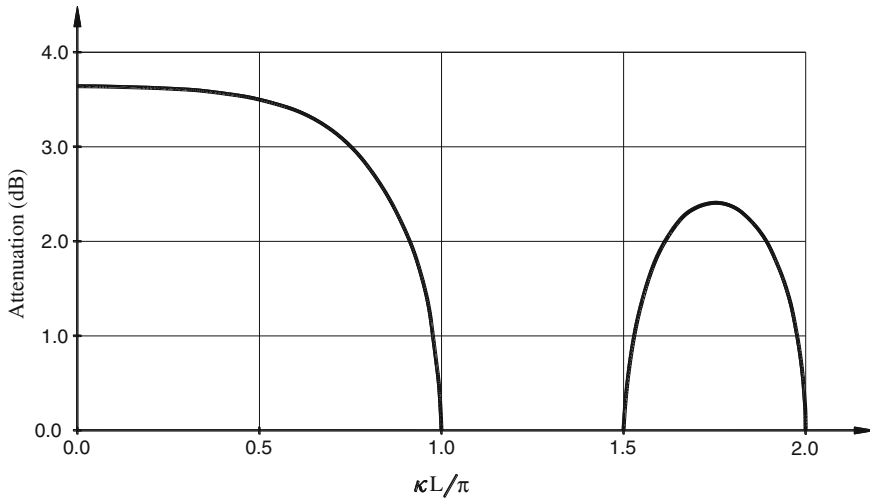


Fig. 7.9 Attenuation across a single-pinned junction of an infinite periodic structure

attenuation calculated for a single junction and semi-infinite structures should not be used for predicting the attenuation over a junction between finite beams, which in turn are connected to other structures.

Many of the fundamental ideas discussed above form the basis for the modeling of the vibration of railway rails. The response of a periodically supported track is discussed in for example Ref. [59]. The excitation of rails due to roughness on the wheel itself or on the rail is described by Thompson in Ref. [60]. The effects of randomly varying the distance between the sleepers supporting a rail have also been investigated as reported in Ref. [61].

7.8 Forced Vibration of Periodic Structures

The solutions derived in the previous section can form the basis for the solution of the corresponding forced problem. One example of such a problem is illustrated in Fig. 7.10. The basic structure is identical to the one discussed in Sect. 7.7. For simplicity, it is assumed that the force is exciting a beam segment at the midpoint between two supports at $x = -L/2$. In this way the symmetry can be utilized. The general procedure for solving the problem is the same irrespective of the excitation point. The force is assumed to be harmonic and equal to $F \cdot \exp(i\omega t)$. The beam is “pinned” to equi-distant supports. The distance between two supports is again equal to L .

Material parameters and geometry are constant along the length of the beam. The wavenumber for flexural waves is κ . The displacement of the beam in bay 0

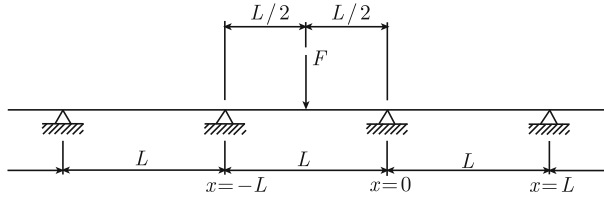


Fig. 7.10 Point excited infinite periodic beam structure

is symmetric with respect to the excitation point $x = -L/2$. The displacement of segment 0 is $y_0(x) \cdot \exp(i\omega t)$. For $-L < x < 0$ the governing equation describing flexural vibrations of the segment is

$$\frac{d^4 y_0}{dx^4} - \kappa^4 y_0 = \frac{F}{D'} \delta(x + L/2).$$

The displacement and force are defined positive in the same direction. The solution for $-L/2 < x < 0$ is

$$y_0(x) = A_0 \sin \kappa x + B_0 (\cos \kappa x - \cosh \kappa x) + C_0 \sinh \kappa x. \quad (7.111)$$

The expression (7.111) satisfies the boundary condition $y_0(0) = 0$. The displacement of the beam is symmetric around the coordinate $x = -L/2$. Due to this symmetry the boundary conditions at $x = -L/2$ are

$$\frac{dy_0}{dx} = 0, \quad \frac{d^3 y_0}{dx^3} = \frac{F}{2D'}.$$

For an infinite “pinned” periodic structure, the ratio between the deflection angle Θ and the bending moment M at each side of a support is given by Eq. (7.105). In this equation introduce $(\Theta_1)_i = \Theta$ and $(\Theta_1)_{i+1} = e^{i\varphi} \Theta$ and $(M_1)_i = M$. Thus

$$e^{i\varphi} \Theta = b_{11} \Theta + b_{12} M, \quad \Theta = \left[\frac{dy_0}{dx} \right]_{x=0}, \quad M = -D' \left[\frac{d^2 y_0}{dx^2} \right]_{x=0}.$$

By rearranging these expressions the result is

$$\begin{aligned} \left[\frac{d^2 y_0}{dx^2} \right]_{x=0} &= -\frac{1}{D'} \left(\frac{e^{i\varphi} - b_{11}}{b_{12}} \right) \left[\frac{dy_0}{dx} \right]_{x=0} = \kappa X \left[\frac{dy_0}{dx} \right]_{x=0} \\ X &= \frac{e^{i\varphi} (\sin \beta - \sinh \beta) - \sin \beta \cosh \beta + \cos \beta \sinh \beta}{1 - \cos \beta \cosh \beta}. \end{aligned} \quad (7.112)$$

For $\kappa L = \beta \gg 1$ the parameter X is obtained as $X = \pm\sqrt{-2 \tan \beta}$. This is a consequence of Q , as defined in Eq. (7.109), for $\kappa L = \beta \gg 1$ being $Q \approx \cos \beta - \sin \beta$. For simplicity two new parameters Z and α are defined as $Z = F/(2D'\kappa^3)$ and $\alpha = \beta/2$. Based on the boundary conditions and the general expression giving the displacement, the amplitudes A_0 , B_0 , and C_0 are found to equal

$$\begin{aligned} B_0 &= \frac{XZ(\cosh \alpha - \cos \alpha)}{2[2 \cosh \alpha \cos \alpha - X(\sin \alpha \cosh \alpha + \cos \alpha \sinh \alpha)]} \\ A_0 &= -\frac{B_0 \sin \alpha}{\cos \alpha} - \frac{Z}{2 \cos \alpha} \\ C_0 &= -\frac{B_0 \sinh \alpha}{\cosh \alpha} + \frac{Z}{2 \cos \alpha}. \end{aligned} \quad (7.113)$$

For $\kappa L = \beta \gg 1$ the amplitudes are approximately equal to

$$\begin{aligned} A_0 &\approx \frac{XZ - 2Z}{2[2 \cos \alpha - X(\sin \alpha + \cos \alpha)]} \\ B_0 &\approx -C_0 \approx \frac{XZ}{2[2 \cos \alpha - X(\sin \alpha + \cos \alpha)]}. \end{aligned} \quad (7.114)$$

The displacement of segment 1 can be written as

$$y_1(x) = A_1 \sin \kappa x + B_1(\cos \kappa x - \cosh \kappa x) + C_1 \sinh \kappa x. \quad (7.115)$$

This expression already satisfies one of the boundary conditions, i.e., $y_1(0) = 0$. Three additional boundary conditions are required to solve the unknown amplitudes. However, a large number of apparent boundary conditions can be formulated by considering the angular displacements and the bending moments at the junctions. The apparent boundary conditions are

$$\begin{aligned} (a) \quad & y_1(0) = 0 \\ (b) \quad & y_1(L) = 0 \\ (c) \quad & \left[\frac{dy_1}{dx} \right]_{x=L} = e^{i\varphi} \left[\frac{dy_0}{dx} \right]_{x=0} \\ (d) \quad & \left[\frac{d^2 y_1}{dx^2} \right]_{x=L} = e^{i\varphi} \left[\frac{d^2 y_0}{dx^2} \right]_{x=0} \\ (e) \quad & \left[\frac{dy_1}{dx} \right]_{x=0} = \left[\frac{dy_0}{dx} \right]_{x=0} \\ (f) \quad & \left[\frac{d^2 y_1}{dx^2} \right]_{x=0} = \left[\frac{d^2 y_0}{dx^2} \right]_{x=0}. \end{aligned} \quad (7.116)$$

Condition (a) is already satisfied by the expression (7.115). Some of the other requirements are identical. The conditions (c) and (d) are identical according to the Floquet assumption. The conditions (e) and (f) are also equivalent since according to

Eq. (7.112) the bending moment at a junction is proportional to the angular displacement for an infinite periodic structure. In order to solve the unknown parameters, the boundary conditions (b), (c), and (e) are sufficient. The phase angle φ is given in Eq. (7.119) and shown in Fig. 7.8. Based on these boundary conditions the unknown parameters are obtained as

$$\begin{aligned} B_1 &= -B_0 \frac{\sin \beta \cosh \beta + \sinh \beta \cos \beta + \sin \beta + \sinh \beta}{\sin \beta \cosh \beta - \cos \beta \sinh \beta - \exp(i\varphi)(\sin \beta - \sinh \beta)} \\ A_1 &= \frac{B_1[\exp(i\varphi) - \cos \beta]}{\sin \beta} \\ C_1 &= \frac{B_1[\cosh \beta - \exp(i\varphi)]}{\sinh \beta}. \end{aligned} \quad (7.117)$$

The displacement $y_n(x)$ of segment n for which $(n-1)L \leq x \leq nL$ is

$$y_n(x) = \exp[i(n-1)\varphi] \cdot y_1(x - nL + L). \quad (7.118)$$

The amplitudes A_0 , B_0 , and C_0 have maxima for

$$\operatorname{Re}[2 \cos \alpha - X(\sin \alpha + \cos \alpha)] = 0.$$

This is satisfied for

$$\operatorname{Re} \beta = \operatorname{Re}(2\alpha) = 3\pi/2 + 2n\pi \text{ and } \operatorname{Re} \beta = \pi + 2n\pi.$$

In the first case, each beam segment is vibrating as if clamped. The phase angle is obtained from Fig. 7.8 as $\varphi = 2n\pi$. The attenuation from one segment to another is equal to zero, since $|\exp(i\varphi)|$ is equal to unity. In the second case, each segment is vibrating as if the boundary conditions were simply supported. Again, for this case the attenuation is equal to zero. However there is a phase shift between two adjoining segments since $\varphi = \pi + 2n\pi$ and $\exp(i\varphi) = -1$. The two resonant modes are illustrated in Fig. 7.11.

The kinetic energy of a segment of the infinite beam is more or less determined by the response of the beam at resonances. At the resonance frequencies for the infinite

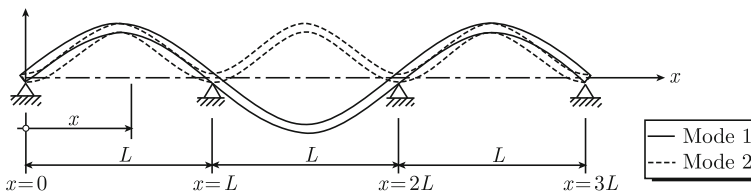


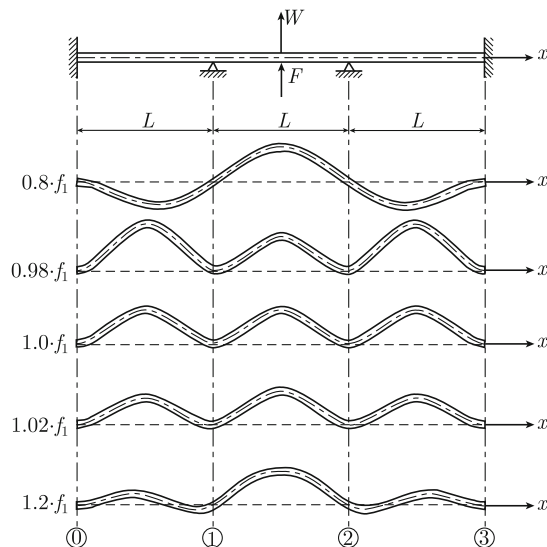
Fig. 7.11 Two resonant modes for an infinite beam with periodic mounts

periodic structure $|\exp(i\varphi)| = 1$. Indicating that the decay rate of the energy for each segment is low as the distance from the excitation point increases.

There is an interesting difference between the two resonant modes. For two subsequent segments vibrating out of phase, the simply supported mode, there is an energy flow between the segments since the angular displacement and bending moment are different from zero at each junction. For the other case, the clamped mode, the displacement as well as the angular displacement are equal zero at each junction. Consequently there is no energy flow between the beam segments. Can then the motion be maintained if losses are introduced in the system making the clamped mode an unstable solution? This question can be illustrated by considering a similar case. A beam, length $3L$, is clamped at each end and simply supported at two points as shown in Fig. 7.12. The beam is excited at its midpoint.

The resonance frequency corresponding to the clamped mode is given by f_1 . The response of the beam is in Fig. 7.12 shown for five excitation frequencies. These are: $0.8 \cdot f_1$, $0.98 \cdot f_1$, f_1 , $1.02 \cdot f_1$ and $1.2 \cdot f_1$. Well below the resonance frequency, for $f = 0.8 \cdot f_1$, the displacement is almost equal to the static deflection caused by a static upward force at midpoint. At $f = f_1$ the beam elements are vibrating in phase and as if they were clamped at each junction. As the frequency is varied the clamped mode shape is distorted. For $f \neq f_1$ energy can be transmitted across a junction. For $f = f_1$ this is not the case since both y and dy/dx are zero at each junction. For a beam with losses the perfectly clamped mode cannot exist. There must be an energy flow to the first and last elements to keep these vibrating. This can only be achieved if the mode shape is slightly distorted to allow $dy/dx \neq 0$. If the losses are small, the displacement is almost as if the beams were clamped. The clamped mode shape is stable and is developed by gradually increasing the frequency as shown in Fig. 7.12.

Fig. 7.12 A beam clamped at both ends and simply supported at two positions. The beam is excited at midpoint. The response of beam is given at five frequencies. The resonance frequency for the clamped mode is f_1



7.9 Finite Composite Beam

The bending theory of Euler or “thin” beams was treated in Sect. 3.6. The apparent bending of “thick” beams or plates was discussed in Sect. 4.3. The deflection of thick beams was in this section described by means of coupled longitudinal and transverse waves. Dispersion equations giving the wavenumbers defining the deflection of infinite I-beams and sandwich beams were also discussed. Based on these wavenumbers the deflection of finite beams exposed to external forces can be formulated. The general procedure is indicated in the proceeding text.

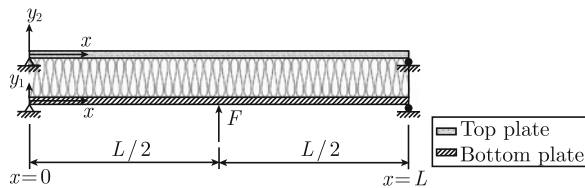
The general procedure of predicting the response of a finite I-beam or a composite structure can be demonstrated by means of a simplified case. The basic structure is illustrated in Fig. 7.13. Two thin beam elements are joined to a layer of a resilient material. In this case, the interlayer is mineral wool. The mechanical properties of the mineral wool are assumed to be equivalent to those of a locally reacting material. This type of material can be modeled as closely spaced mass-less spring elements. Each element is reacting locally or independently of any other element. The resilience of the layer or the mass-less springs is described by the spring constant s per unit length of the beam elements. Some material properties of mineral wool are listed in Sect. 8.11.

The displacements $w_1(x, t) = y_1(x) \cdot \exp(i\omega t)$ and $w_2(x, t) = y_2(x) \cdot \exp(i\omega t)$ of the two beam segments are defined positive along the positive y -axis as shown in Fig. 7.13. The reacting force on plate 1, due to the resilient layer and the displacement of the beam elements, is $s(y_1 - y_2) \exp(i\omega t)$. This reacting force is defined positive in the same direction as the displacement. The reacting force on element 2 is of the same magnitude but in the opposite direction. The bending of the “thin” beam elements satisfies the simple equation for flexural waves defined in Sect. 3.6. The wave number for flexural waves is defined in Eq. (3.65) as

$$\kappa_i = (m'_i \omega^2 / D'_i)^{1/4}.$$

The mass per unit length is m'_i and the bending stiffness D'_i for the beams. The index i is equal to 1 for the upper plate and equal to 2 for the bottom plate. The equations defining the motions of the beam elements are

Fig. 7.13 Two simply supported beam elements coupled by a resilient layer



$$\begin{aligned}\frac{d^4 y_1}{dx^4} - \kappa_1^4 y_1 &= -\frac{s}{D'_1} (y_1 - y_2) \\ \frac{d^4 y_2}{dx^4} - \kappa_2^4 y_2 &= \frac{s}{D'_2} (y_1 - y_2).\end{aligned}\tag{7.119}$$

Due to the losses in the system the parameters s , D'_i and thus κ_i are complex. The solutions to (7.119) are obtained in the standard way by assuming

$$y_1(x) = A_1 \cdot e^{\lambda x}, \quad y_2(x) = A_2 \cdot e^{\lambda x}.\tag{7.120}$$

The two functions must have the same dependence on x to satisfy the boundary conditions along the beams. For simplicity, it is assumed that the two plate elements are identical i.e., $\kappa_1 = \kappa_2 = \kappa$ etc. Equation (7.120) inserted in Eq. (7.119) gives, after the elimination of A_1 and A_2 ,

$$(\lambda^4 - \kappa^4 + s/D')^2 = (s/D)^2.$$

The solutions are obtained from

$$\lambda^4 = \kappa^4, \quad \lambda^4 = \kappa^4 - 2s/D' = \kappa^4 \left(1 - \frac{2s}{m'\omega^2}\right) = \kappa^4 \left(1 - \frac{\omega_0^2}{\omega^2}\right).$$

The angular frequency ω_0 corresponds to the natural frequency for a system consisting of two masses joined together by a mass-less spring. This angular frequency is equal to $\omega_0 = \sqrt{2s/m'}$ at resonance. The resulting eigenvalues and the corresponding wavenumbers are

$$\begin{aligned}\lambda &= \pm \kappa_x \text{ and } \pm i \kappa_x, \quad \kappa_x = \kappa \left(1 - \frac{\omega_0^2}{\omega^2}\right)^{1/4} \quad \text{for } A_1 = -A_2 \\ \lambda &= \pm \kappa \text{ and } \pm i \kappa \text{ for } A_1 = A_2.\end{aligned}\tag{7.121}$$

In the first case, $A_1 = -A_2$, the upper and lower beam elements move in opposite phase. In the second case, $A_1 = A_2$, the beams move in phase. It should be noted that κ_x is imaginary for $\omega < \omega_0$ if the losses are neglected.

The wavenumbers derived can now be used to determine the forced response of a finite composite beam of the type described above and illustrated in Fig. 7.13. At the ends of the structure, shown in Fig. 7.13, each beam element is assumed to be simply supported. Indicating that the spacing between the beams is constant and equal to H at the ends. The bottom beam is excited by a harmonic point force $F = F_0 \cdot \exp(i\omega t)$ at the center of the beam. The equations of motion for the two beams are

$$\begin{aligned}\frac{d^4 y_1}{dx^4} - \kappa^4 y_1 + \frac{s}{D'} y_1 &= \frac{s}{D'} y_2 + \frac{F_0}{D'} \cdot \delta(x - L/2) \\ \frac{d^4 y_2}{dx^4} - \kappa^4 y_2 + \frac{s}{D'} y_2 &= \frac{s}{D'} y_1.\end{aligned}\quad (7.122)$$

The solutions are composed of two parts, one symmetric solution $f(x)$ and one asymmetric $g(x)$. These functions have according to Eq.(7.121) the eigenvalues κ and κ_x respectively i.e.,

$$\frac{d^4 f}{dx^4} - \kappa^4 f = 0 \text{ and } \frac{d^4 g}{dx^4} - \kappa_x^4 g = 0. \quad (7.123)$$

The solutions defining the displacements of the upper and lower beams are

$$y_1(x) = f(x) + g(x) \text{ and } y_2(x) = f(x) - g(x). \quad (7.124)$$

Both solutions are symmetric around the excitation point $x = L/2$. Considering this, the boundary conditions for the simply supported beam elements are

$$\begin{aligned}y_1 &= \frac{d^2 y_1}{dx^2} = 0 \text{ for } x = 0 \\ \frac{dy_1}{dx} &= 0 \text{ for } x = L/2 \\ y_2 &= \frac{d^2 y_2}{dx^2} = 0 \text{ for } x = 0 \\ \frac{dy_2}{dx} &= 0 \text{ for } x = L/2.\end{aligned}\quad (7.125)$$

The additional boundary conditions at the excitation point are obtained by integrating the basic equations with respect to x from $L/2 - \varepsilon$ to $L/2 + \varepsilon$ according to the procedure outlined in Sect. 7.3. Considering the symmetry around the excitation point, the resulting boundary conditions are, as ε approaches zero

$$\frac{d^3 y_1}{dx^3} = -\frac{F_0}{2D'} \text{ and } \frac{d^3 y_2}{dx^3} = 0 \text{ for } x = L/2. \quad (7.126)$$

The corresponding boundary conditions for the functions f and g are readily obtained from the Eqs. (7.124) to (7.126) as

$$f = \frac{d^2 f}{dx^2} = g = \frac{d^2 g}{dx^2} = 0 \text{ for } x = 0, \quad \frac{d^3 f}{dx^3} = \frac{d^3 g}{dx^3} = -\frac{F_0}{4D'} \text{ for } x = L/2. \quad (7.127)$$

The functions f and g are symmetric around the excitation point $x = L/2$. The functions f and g should also satisfy the eigenvalue Eq.(7.123). The solutions are consequently for $0 \leq x \leq L/2$ equal to

$$\begin{aligned}
 f(x) &= \frac{F_0}{8D'\kappa^3} \left[\frac{\sin(\kappa x)}{\cos(\kappa L/2)} - \frac{\sinh(\kappa x)}{\cosh(\kappa L/2)} \right] \\
 g(x) &= \frac{F_0}{8D'\kappa_x^3} \left[\frac{\sin(\kappa_x x)}{\cos(\kappa_x L/2)} - \frac{\sinh(\kappa_x x)}{\cosh(\kappa_x L/2)} \right].
 \end{aligned} \tag{7.128}$$

As the frequency of the driving force approaches the resonance frequency, the real part of the wave number κ_x tends to zero as given by Eq. (7.121). The expansion of the functions containing κ_x in Taylor series as $\omega \rightarrow \omega_0$ yields

$$\lim_{\omega \rightarrow \omega_0} g(x) = \frac{F_0}{8D'} \left(\frac{xL^2}{4} - \frac{x^3}{3} \right).$$

This expression is equal to the static solution to Eq. (7.123).

Three solutions to the problem are shown in Fig. 7.14. The first figure shows the displacement of the beam for $0 \leq x \leq L/2$ in the low frequency range or for $f = f_0/4$ where f_0 is the resonance frequency of the coupled system or the simple mass-spring-mass system. The displacements of the top and bottom beams are shown in the figure. For comparison the displacement for a single beam which is identical to the top beam is also indicated at the center of the graph. The deflection of the single beam is almost twice the deflection of the entire composite structure. The displacements of the top and bottom beams are almost in phase and of the same magnitude. The bending of the composite beam is approximately the same as the bending of single beam with twice the stiffness as each beam element of the structure.

The displacements of the elements at resonance, $f = f_0$, are also shown in Fig. 7.14. At this frequency $g(x) \gg f(x)$ and the displacements of the plates are almost entirely out of phase. The amplitudes of the beam elements are due to resonance effects much larger than the amplitude for a single beam.

The final result shown in Fig. 7.14 gives the displacement for frequencies well above the resonance frequency i.e., for $f = 4f_0$. The displacement of the top beam is almost identical to the displacement of the single beam exposed to the same force. The excitation of the bottom beam is comparatively small in this frequency range. The resulting displacement is therefore also small.

For any type of double construction for which one element is exposed to some type of force function the response depends on the frequency of the force as compared to the simple resonance frequency of the system. In the low frequency range, the elements move almost entirely in phase with the same amplitudes. At resonance, the response is large and the elements move out of phase. Well above the simple resonance frequency, the element exposed to the external force moves as if completely decoupled from the other structures. The amplitude of the element which is not directly excited is small and decreases as the excitation frequency increases.

Yet another example of interest describes the coupled beams being excited by a pressure p_o instead of a point force as in the previous example. When excited by a pressure the governing equations are

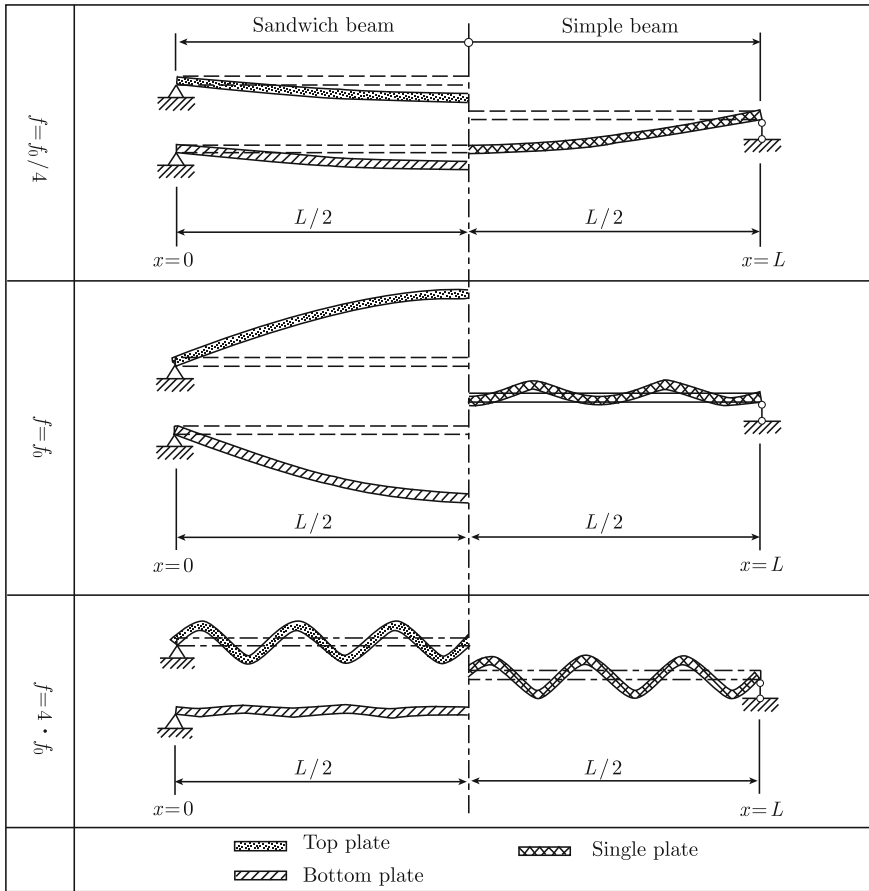


Fig. 7.14 Mode of vibration for a simple sandwich beam construction for $f = f_0/4$, $f = f_0$ and $f = 4f_0$

$$\begin{aligned} \frac{d^4 y_1}{dx^4} - \kappa^4 y_1 + \frac{s}{D'} y_1 &= \frac{s}{D'} y_2 + \frac{p_0}{D'} \\ \frac{d^4 y_2}{dx^4} - \kappa^4 y_2 + \frac{s}{D'} y_2 &= \frac{s}{D'} y_1. \end{aligned}$$

Again the two solutions are written $y_1(x) = f(x) + g(x)$ and $y_2(x) = f(x) - g(x)$. The functions f and g are

$$f(x) = -\frac{p_0}{2D'\kappa^4} + \frac{p_0}{4D'\kappa^4} \left\{ \frac{\cos[\kappa(x - L/2)]}{\cos(\kappa L/2)} + \frac{\cosh[\kappa(x - L/2)]}{\cosh(\kappa L/2)} \right\}$$

$$g(x) = -\frac{p_0}{2D'\kappa_x^4} + \frac{p_0}{4D'\kappa_x^4} \left\{ \frac{\cos[\kappa_x(x - L/2)]}{\cos(\kappa_x L/2)} + \frac{\cosh[\kappa_x(x - L/2)]}{\cosh(\kappa_x L/2)} \right\}$$

For highly damped beams, it can be shown that in the very high frequency region that the velocity level difference between the bottom beam and the top beam is

$$\Delta L_v = 10 \log \left| \frac{\dot{y}_1}{\dot{y}_2} \right|^2 \approx 40 \log(f/f_0),$$

where $f_0 = \frac{1}{2\pi} \sqrt{\frac{2s}{m'}}$. Compare Sect. 8.11.

Problems

7.1 The ends of a homogeneous beam of length L can slide with zero rotation as indicated in Fig. 7.15. No force can be supported at the ends of the beam. Determine the eigenfunctions and natural frequencies for a beam having these boundary conditions. Show that the eigenfunctions are orthogonal.

7.2 The first natural frequency for a clamped beam is 52 Hz. Determine the number of natural frequencies in the octave bands from 63 to 8000 Hz.

7.3 A simply supported beam, length L , total mass m and bending stiffness D' is excited by a point force with the one sided spectral density G_{FF} , white noise excitation. The force is exciting the beam perpendicular to the axis of the beam. Determine the total energy of the beam and the total input power to the beam in a frequency band Δf which includes a large number of natural frequencies of the beam.

7.4 Determine the modal parameters for a homogeneous beam clamped at both ends and excited by a force $F'(x) \cdot \exp(i\omega t)$ in the direction of the axis of the beam and thus exciting L-waves in the structure.

7.5 A homogeneous beam is simply supported and excited by two point forces, F_1 and F_2 as shown in Fig. 7.16. The forces are random, white noise, and uncorrelated. Each force having a power spectral density G_{FF} . Determine the power spectral

Fig. 7.15 Beam with stiff and sliding edge

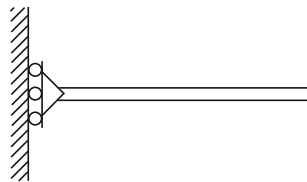
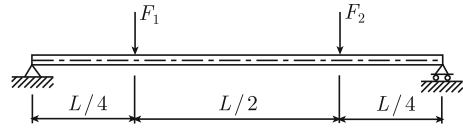


Fig. 7.16 Simply supported beam excited by two point forces



density G_{vv} of the spatial average the velocity squared of the beam. Use the mode summation technique.

7.6 A steel bar, length 5 m, with a cross section shown in Fig. 7.17 and clamped at both ends is vibrating in the vertical plane. Determine the first natural frequency of the beam.

7.7 A simply supported beam, length L , total mass m and bending stiffness D' is at $x = x_1$ excited by a bending moment $M \cdot \exp(i\omega t)$. Determine the response of the beam (Fig. 7.18).

7.8 A simply supported beam, length L , total mass m and bending stiffness D' is excited by a force $F'(x, t) = (F/L) \cdot \sin(\pi x/L) \cdot \exp(i\omega t)$ per unit length of the beam. Use Green's function to determine the response of the beam.

7.9 Use the mode summation technique to solve the previous problem.

7.10 A beam is exposed to white noise excitation. A constraining viscoelastic layer is applied to the beam to reduce its velocity. The layer increases the weight of the beam by 20 % and its stiffness by 40 %. The losses are increased by a factor 10. Determine the reduction of the total energy of the beam due to the alterations. Consider the

Fig. 7.17 Cross section of steel bar

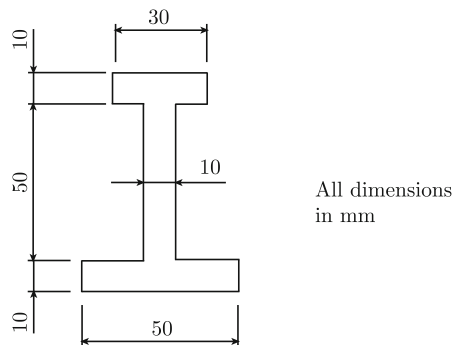


Fig. 7.18 A simply supported beam excited by a bending moment

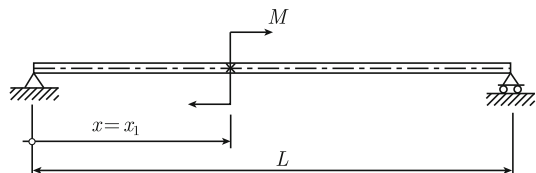
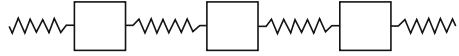


Fig. 7.19 An infinite set of coupled mass-spring systems



effect within a frequency band, which includes a large number of modes. The losses are assumed to be viscous.

7.11 The Fig. 7.19 illustrates an infinite set of mass-spring systems. Each mass is equal to m and each spring constant equal to k . The losses in the springs are neglected. In which frequency range can the motion of the masses be maintained without attenuation? Use Floquet's theorem. Show also that the wavenumber for longitudinal waves can be derived by using an infinite set of mass-spring systems shown in the figure by allowing each mass-spring section to become small.

7.12 One of the masses in the previous example is excited by a force $F \cdot \exp(i\omega t)$ in the direction of the infinite chain. Determine the response of the masses.

7.13 Determine the eigenfunctions and eigenvalues for a homogeneous beam simply supported at one end and free at the other.

7.14 A beam is oriented along the x -axis of a coordinate system. The displacement $w(x, t) = w(x) \cdot \exp(i\omega t)$ of the beam in flexure is governed by the equation

$$D' \frac{d^4 w}{dx^4} - m' \omega^2 w = F'(x).$$

The beam is assumed to satisfy one of the natural boundary conditions or any other boundary condition resulting in orthogonal eigenfunctions. The Green's function $G(x|x_0)$ is the solution to

$$D' \frac{d^4 G}{dx^4} - m' \omega^2 G = \delta(x - x_0),$$

with G satisfying the same boundary conditions as w . Show that the response w of the beam is

$$w(x, t) = e^{i\omega t} \int_0^L F'(\zeta) \cdot G(\zeta|x) d\zeta.$$

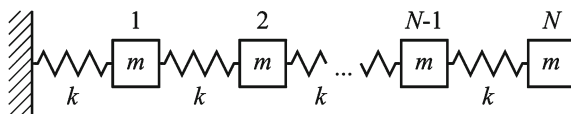
The length of the beam is L .

7.15 A homogeneous and simply supported beam of length L is excited by a force $F_0 \cdot \exp(i\omega t)$ at a point, the distance ξ from one of the supports. Give a general formulation defining the response of the beam by using the matrix method.

7.16 Give approximate expressions for the eigenfunctions listed in Tables 7.2, 7.3 and 7.5 for $n \geq 4$.

7.17 N equal masses are coupled by identical springs as shown in Fig. 7.20. Determine the natural frequencies of the system.

Fig. 7.20 N coupled mass-spring systems



7.18 A homogeneous beam is clamped at both ends. The length of the beam is L , its bending stiffness and mass per unit length are D' and m' . At midpoint the beam is excited by a force $F = F_0 \exp(i\omega t)$ normal to the axis of the beam. Determine the resulting forces and bending moments at each end of the beam.

Chapter 8

Flexural Vibrations of Finite Plates

The displacement of a vibrating beam can be described in a closed form or as an infinite sum over the eigenfunctions for certain boundary conditions. For vibrating plates, it is not possible to formulate closed analytical solutions even for the most simple boundary conditions. Further, the mode summation technique applies only to a very limited number of boundary conditions. One of these cases corresponds to a rectangular plate, which is simply supported along the edges. For this case, the mode summation technique can be used for solving the forced response of the plate. For rectangular plates, other analytical solutions can be formulated if two opposite sides of the plate are simply supported. However, for circular plates eigenfunctions can be described analytically for several different edge conditions. This is discussed at the end of the chapter.

However, the eigenfrequencies for plates with arbitrary boundary conditions can be determined by means of the Rayleigh–Ritz method. The corresponding mode shapes can also be estimated based on the same method.

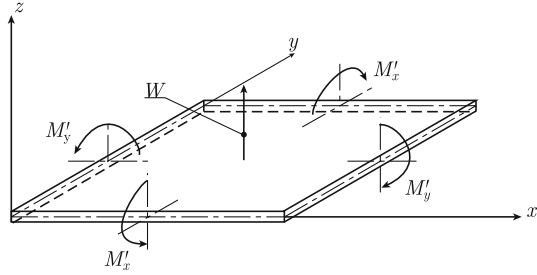
The mounting of a small mass on a plate will influence the vibration pattern of plate. Various methods for estimating the change of natural frequencies due to certain perturbations are introduced. In this chapter, the response or mobility of finite and infinite plates is compared. Energy of plates and energy flows between plates are discussed. Later these results form the basis for various statistical energy methods. Finally the so called floating floor concept is presented. The floating floor is a standard noise reducing measure in many vehicles like ships, trains, and buses.

8.1 Free Vibrations of Simply Supported Plates

For an uniform and rectangular plate oriented in the x - y plane, as shown in Fig. 8.1, the displacement w should satisfy the wave Eq. (3.115) or

$$\frac{\partial^4 w}{\partial x^4} + 2 \frac{\partial^4 w}{\partial x^2 \partial y^2} + \frac{\partial^4 w}{\partial y^4} + \frac{\mu}{D} \frac{\partial^2 w}{\partial t^2} = 0. \quad (8.1)$$

Fig. 8.1 Bending moments along edges and displacement of a rectangular plate



The thickness of the plate is h . It is assumed that the plate is thin as defined in Chap. 4. Indicating that rotation and shear effects within the plate can be neglected. The mass per unit area is $\mu = \rho h$, where ρ is the density. The bending stiffness D in Eq. (8.1) is given by $Eh^3/[12(1 - \nu^2)]$ as defined in Chap. 3. In analogy with the discussion in Sects. 6.1 and 7.1, it is assumed that the solution to the wave Eq. (8.1) is of the form

$$w(x, y, t) = X(x)Y(y)g(t). \quad (8.2)$$

The expression (8.2) in combination with the wave equation yields

$$\frac{1}{X} \frac{d^4 X}{dx^4} + 2 \left(\frac{1}{X} \frac{d^2 X}{dx^2} \right) \left(\frac{1}{Y} \frac{d^2 Y}{dy^2} \right) + \frac{1}{Y} \frac{d^4 Y}{dy^4} = -\frac{1}{g} \frac{\mu}{D} \frac{d^2 g}{dt^2} = 0. \quad (8.3)$$

The functions X and Y are assumed to satisfy the additional conditions

$$\frac{d^2 X}{dx^2} = -k_m^2 X, \quad \frac{d^2 Y}{dy^2} = -k_n^2 Y. \quad (8.4)$$

This is in accordance with the discussions in Chaps. 6 and 7. However, the conditions given in Eq. (8.4) are not necessarily required for finding a solution to Eq. (8.1) as discussed in Sect. 8.3. The fourth derivatives of X and Y are according to Eq. (8.4) equal to

$$\frac{d^4 X}{dx^4} = -k_m^2 \frac{d^2 X}{dx^2} = k_m^4 X, \quad \frac{d^4 Y}{dy^4} = k_n^4 Y. \quad (8.5)$$

These results inserted in Eq. (8.3) give

$$\frac{D}{\mu} \kappa_{mn}^4 g + \frac{d^2 g}{dt^2} = 0, \quad \kappa_{mn}^2 = k_m^2 + k_n^2. \quad (8.6)$$

The solutions to Eq. (8.4) are of the form

$$X = A_1 \sin(k_m x) + B_1 \cos(k_m x), \quad Y = A_2 \sin(k_n y) + B_2 \cos(k_n y).$$

These expressions can satisfy only two simple boundary conditions at any edge. At the boundary $x = 0$ these conditions are

$$(i) X = \frac{d^2 X}{dx^2} = 0 \text{ for } B_1 = 0,$$

$$(ii) \frac{dX}{dx} = \frac{d^3 X}{dx^3} = 0 \text{ for } B_2 = 0.$$

All other combinations like $X = dX/dx = 0$ etc. can only be satisfied if both A_1 and B_1 are equal to zero. The first condition (i) corresponds to a simply supported edge. The second (ii) corresponds to a stiff and sliding edge, which is not exactly a boundary condition easily found in practice. The condition (ii) is illustrated in Fig. 8.2.

For the homogeneous rectangular plate shown in Fig. 8.1, the bending moment per unit length around an edge parallel to the y -axis is M'_y . The moment M'_x is rotating the plate around an edge parallel to the x -axis. According to Eqs. (3.105) and (3.107) these moments are

$$M'_y = -D \left(\frac{\partial^2 w}{\partial x^2} + \nu \frac{\partial^2 w}{\partial y^2} \right), \quad M'_x = -D \left(\frac{\partial^2 w}{\partial y^2} + \nu \frac{\partial^2 w}{\partial x^2} \right). \quad (8.7)$$

For a simply supported plate the boundary conditions are

$$\begin{aligned} w = 0, \quad M'_x = 0 \text{ for } y = 0 \text{ and } y = L_y \\ w = 0, \quad M'_y = 0 \text{ for } x = 0 \text{ and } x = L_x. \end{aligned} \quad (8.8)$$

These conditions are satisfied by

$$X(x)Y(y) = \varphi_{mn}(x, y) = \sin(k_m x) \sin(k_n y), \quad k_m = \frac{m \pi}{L_x}, \quad k_n = \frac{n \pi}{L_y}, \quad (8.9)$$

where m and n are integers. The function $\varphi_{mn}(x, y)$ is consequently an eigenfunction describing the motion of a simply supported rectangular plate. Further, these eigenfunctions are orthogonal or

$$\int_0^{L_x} dx \int_0^{L_y} dy \varphi_{mn}(x, y) \varphi_{rs}(x, y) = \langle \varphi_{mn} | \varphi_{rs} \rangle = \frac{L_x L_y}{4}, \quad (8.10)$$

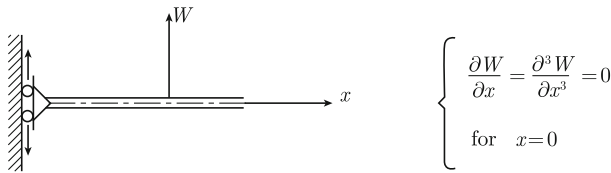


Fig. 8.2 Stiff and sliding edge, rotation, and force equal to zero at edge

if $m = n$ and $r = s$, otherwise zero.

Since the eigenfunctions are orthogonal the displacement of the plate can, following the discussion in Chap. 7, be written as

$$w(x, y, t) = \sum_{m,n} g_{mn}(t) \cdot \varphi_{mn}(x, y). \quad (8.11)$$

The time-dependent function $g_{mn} = g$ must satisfy Eq. (8.6). The same type of problem was discussed in Sect. 7.1—Eqs. (7.4) and (7.11). The general solution to Eq. (8.6) is, assuming the loss factor to be $\eta \ll 1$,

$$\begin{aligned} g_{mn}(t) &= [C_{mn} \cdot \sin(\omega_{mn0}t) + D_{mn} \cdot \cos(\omega_{mn0}t)] \cdot \exp(-\omega_{mn0}\eta t/2) \\ \omega_{mn} &= \kappa_{mn}^2 \sqrt{\frac{D}{\mu}} = \kappa_{mn}^2 \sqrt{\frac{D_0}{\mu}} (1 + i\eta/2) = \omega_{mn0} (1 + i\eta/2). \end{aligned} \quad (8.12)$$

If at $t = 0$ the displacement of the plate is given by $w_0(x, y)$ and the velocity by $v_0(x, y)$ and if for $t > 0$ the plate is vibrating freely—no external force—then the initial conditions for $t = 0$ are

$$w_0 = \sum_{mn} D_{mn} \varphi_{mn}, \quad v_0 = \sum_{mn} \omega_{mn0} \varphi_{mn} [C_{mn} - \eta D_{mn}/2]. \quad (8.13)$$

The parameters D_{mn} and C_{mn} are obtained by multiplying the expressions above by φ_{mn} . The resulting expressions are thereafter integrated over the plate area. Considering the orthogonality of the eigenfunctions—Eq. (8.10)—the result is

$$\begin{aligned} D_{mn} &= \frac{\langle w_0 | \varphi_{mn} \rangle}{\langle \varphi_{mn} | \varphi_{mn} \rangle} = \frac{4 \langle w_0 | \varphi_{mn} \rangle}{L_x L_y}, \\ C_{mn} - \eta D_{mn}/2 &= \frac{\langle v_0 | \varphi_{mn} \rangle}{\omega_{mn0} \langle \varphi_{mn} | \varphi_{mn} \rangle} = \frac{4 \langle v_0 | \varphi_{mn} \rangle}{\omega_{mn0} L_x L_y}. \end{aligned} \quad (8.14)$$

The average of the velocity squared over the surface $S = L_x L_y$ of the plate and the time corresponding to one period is for $\eta \ll 1$

$$\begin{aligned} \langle \bar{v}^2 \rangle &= \frac{1}{T} \int_t^{t+T} dt \frac{1}{S} \iint_S |v|^2 dx dy \\ &= \frac{1}{8} \sum_{mn} \left(|C_{mn}|^2 + |D_{mn}|^2 \right) \omega_{mn0}^2 \cdot \exp(-\omega_{mn0}\eta t). \end{aligned} \quad (8.15)$$

The kinetic energy for mode (m, n) is decaying as $\exp(-\omega_{mn0}\eta t)$.

For no external force the plate can only oscillate at certain eigen- or natural frequencies f_{mn} . The eigenfrequency f_{mn} for mode (m, n) is

Table 8.1 Eigenfrequencies for a 6 mm thick and 1.4 m by 0.8 m simply supported steel plate

Mode number	m	n	$f_{mn}(\text{Hz})$
1	1	1	31.1
2	2	1	54.0
3	3	1	92.3
4	1	2	101.3
5	2	2	124.3
6	4	1	145.8
7	3	2	162.5
8	5	1	214.7
9	4	2	216.1
10	1	3	218.5

$$\begin{aligned}
 f_{mn} &= \frac{\omega_{mn0}}{2\pi} = \frac{\pi}{2} \sqrt{\frac{D_0}{\mu}} \left[\left(\frac{m}{L_x} \right)^2 + \left(\frac{n}{L_y} \right)^2 \right] \\
 &= \frac{\pi h}{2} \sqrt{\frac{E_0}{12(1-\nu^2)\rho}} \left[\left(\frac{m}{L_x} \right)^2 + \left(\frac{n}{L_y} \right)^2 \right]. \quad (8.16)
 \end{aligned}$$

The first few eigenfrequencies and the corresponding mode numbers are in Table 8.1, given for a 6 mm steel plate with the length $L_x = 1.4$ m and the width $L_y = 0.8$ m.

The eigenfrequencies are proportional to h as shown in Eq. (8.16). Showing that a doubling of the plate thickness increases the eigenfrequencies by a factor of 2. A doubling of the length scale, $L_x \rightarrow 2L_x$ and $L_y \rightarrow 2L_y$, decreases a natural frequency by a factor 4.

The number of modes N , which exists for $f_{mn} < f_0$, can be estimated based on the expression Eq. (8.16), which with $f = f_{mn}$ can be rewritten as

$$\frac{\pi}{2} \sqrt{\frac{D_0}{f^2 \mu}} \left[\left(\frac{m}{L_x} \right)^2 + \left(\frac{n}{L_y} \right)^2 \right] = 1.$$

This is the equation for an ellipse with the axes

$$a = L_x \left(\frac{4\mu f^2}{\pi^2 D_0} \right)^{1/4}, \quad b = L_y \left(\frac{4\mu f^2}{\pi^2 D_0} \right)^{1/4}.$$

The equation for the ellipse is thus

$$\left(\frac{m}{a} \right)^2 + \left(\frac{n}{b} \right)^2 = 1.$$

The possible combinations of m and n or rather the possible modes for frequencies less than f are shown in Fig. 8.3. For $n = 0$, m can vary between 0 and the integer of the parameter “ a ” defined above. All solutions are in the first quadrant since the integers m and n are always positive. The total number of modes N , for frequencies less than f , is approximately equal to 1/4 of the area of the ellipse i.e.,

$$N = \iint dm dn = \frac{\pi ab}{4} = \frac{f \cdot L_x L_y}{2} \sqrt{\frac{\mu}{D_0}}. \quad (8.17)$$

The modal density $\mathcal{N}_f = \Delta N / \Delta f$ is from Eq. (8.17) obtained as

$$\mathcal{N}_f = \frac{\Delta N}{\Delta f} = \frac{L_x L_y}{2} \sqrt{\frac{\mu}{D_0}}. \quad (8.18)$$

The average distance Δf in the frequency domain between two eigenfrequencies, i.e., for $\Delta N = 1$, is

$$\Delta f = \frac{2}{L_x L_y} \sqrt{\frac{D_0}{\mu}}. \quad (8.19)$$

In Fig. 8.4, the accumulated number of modes is shown as a function of frequency. The solid line represents the actual number of modes below a certain frequency for a 6 mm steel plate with the dimensions $L_x = 1.4$ m and $L_y = 0.8$ m. The plate is simply supported. Each cross represents a mode. The dashed line is given by the approximate formula Eq. (8.17). The approximate formula tends to overestimate the number of modes. If the thickness of the plate is decreased from 6 to 1 mm the number of modes shown in Fig. 8.4 should be multiplied by a factor 6. A 1 mm plate with the sides 1.4 and 0.8 m could be used in car constructions. The number of modes below 1 kHz is of the order 300 for such a panel. This high number of modes implies that it can be justified to use statistical methods to calculate the energy of this type of structure. As a comparison, the first natural frequency of a 1 m long clamped steel beam is 2628 Hz as shown in Table 6.2.

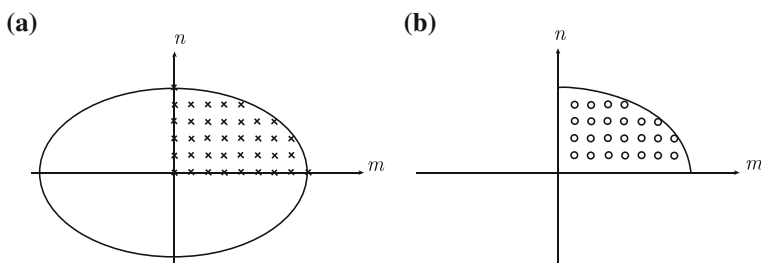
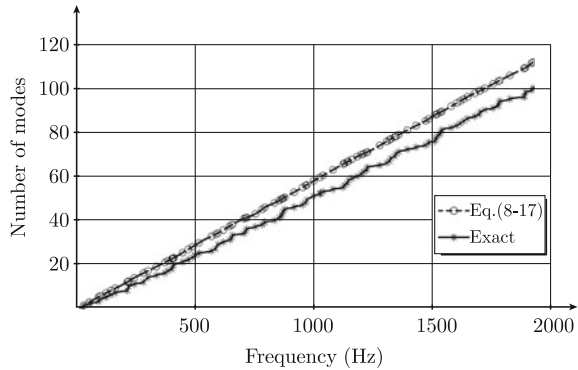


Fig. 8.3 Possible modes for a plate with **a** free edges and **b** simply supported edges

Fig. 8.4 Number of modes for a 6 mm thick simply supported steel plate, $0.8 \times 1.4 \text{ m}^2$



As shown in Ref. [58], the expression Eq.(8.17) gives the upper limit of the number of modes which can exist below a certain frequency. The maximum number is independent of the boundary conditions for the plate. For the particular case shown in Fig. 8.3, the estimate Eq.(8.17) gives a value approximately 10% higher than the actual number of modes for frequencies below 2 kHz. For most applications this is an acceptable error. However the error also depends on the ratio between L_x and L_y . The number of modes given by Eq.(8.17) includes those modes for which either m or n or both are equal to zero. For a simply supported plate m and n are always different from zero. Thus, the actual number of modes is smaller than predicted by the approximate formula Eq.(8.17). For clamped plates the deviation between the actual and estimated number of modes is even larger than for simply supported plates.

By excluding the modes $(m, 0)$ and $(0, n)$ in the summation, the total number of modes is given by

$$N' = N - (L_x + L_y) \left(\frac{f}{2\pi} \right)^{1/2} \left(\frac{\mu}{D_0} \right)^{1/4},$$

where N is defined in Eq.(8.17). The corrected number N' is almost identical to the actual number of modes for a simply supported plate. The modal density based on the corrected number of modes is

$$\mathcal{N}'_f = \frac{\Delta N'}{\Delta f} = \frac{L_x L_y}{2} \sqrt{\frac{\mu}{D_0}} - \frac{L_x + L_y}{\sqrt{8\pi f}} \left(\frac{\mu}{D_0} \right)^{1/4}.$$

For increasing frequencies \mathcal{N}'_f tend to \mathcal{N}_f . For sufficiently high frequencies the modal density for a plate in flexure is approximately independent of boundary conditions—compare Problem 8.16.

In practice it is of great importance to determine the location in the frequency domain of the first few resonances. For higher frequencies only the modal density is of interest if for example the average plate energy or response in a certain frequency band is to be calculated. In order to obtain an acceptable average of energy or power

input, the width of the frequency band must be such that it contains a sufficient number of resonances. The modal density of a structure can be estimated by means of some measurements of mobility functions as discussed in Sect. 8.5.

8.2 Forced Response of a Simply Supported Plate

The forced response of a simply supported isotropic and homogeneous plate can be determined by means of the mode summation technique. This technique has previously been used in conjunction with forced longitudinal vibrations, Sect. 6.3, and forced flexural vibrations of finite beams, Sect. 7.4. The wave equation governing the forced response of a plate is

$$\nabla^2(\nabla^2 w) + \frac{\mu}{D} \frac{\partial^2 w}{\partial t^2} = \frac{f(x, y, t)}{D}. \quad (8.20)$$

For a time dependence, or rather for $f(x, y, t) = p(x, y) \cdot \exp(i\omega t)$ and $w = w(x, y) \cdot \exp(i\omega t)$, the differential equation (8.20) is reduced to

$$\nabla^2(\nabla^2 w) - \kappa^4 w = \frac{p(x, y)}{D}, \quad \kappa^4 = \frac{\mu\omega^2}{D}. \quad (8.21)$$

The force or rather the pressure $p(x, y)$ on the plate and the displacement w of the plate are defined positive in the same direction perpendicular to the plate. The coordinates for the corners of the rectangular plate are $(0, 0)$, $(L_x, 0)$, (L_x, L_y) , and $(0, L_y)$. For a uniform and simply supported plate the eigenfunctions are

$$\varphi_{mn}(x, y) = \sin(k_m x) \sin(k_n y), \quad k_m = \frac{m\pi}{L_x}, \quad k_n = \frac{n\pi}{L_y}. \quad (8.22)$$

These eigenfunctions are orthogonal. Consequently, the displacement can be written as

$$w(x, y) = \sum_{m,n} C_{mn} \cdot \varphi_{mn}(x, y). \quad (8.23)$$

Due to the orthogonality condition, the parameters C_{mn} are obtained from Eq. (8.23) as

$$C_{mn} = \frac{\langle w | \varphi_{mn} \rangle}{\langle \varphi_{mn} | \varphi_{mn} \rangle} = \frac{4 \langle w | \varphi_{mn} \rangle}{L_x L_y}. \quad (8.24)$$

The parameters C_{mn} are obtained by multiplying the wave Eq. (8.21) by φ_{mn} . The result is thereafter integrated over the plate area giving

$$\iint_S dS \varphi_{mn} \nabla^2(\nabla^2 w) - \kappa^4 \langle w | \varphi_{mn} \rangle = \frac{\langle f | \varphi_{mn} \rangle}{D}. \quad (8.25)$$

The procedure is analogous to that presented in Sect. 7.4. The eigenfunctions φ_{mn} and the displacement w satisfy the same boundary conditions. The first expression on the left-hand side of Eq. (8.46) is integrated by parts. Thus

$$\begin{aligned} \iint_s dS \varphi_{mn} \nabla^2 (\nabla^2 w) &= \iint_s dS w \nabla^2 (\nabla^2 \varphi_{mn}) \\ &= (k_m^2 + k_n^2)^2 \iint_s dS w \varphi_{mn} \\ &= \kappa_{mn}^4 C_{mn} \langle \varphi_{mn} | \varphi_{mn} \rangle, \end{aligned} \quad (8.26)$$

where $\kappa_{mn}^4 = (k_m^2 + k_n^2)^2$. The procedure is the same as for the one-dimensional case previously discussed in Sect. 7.4. The wave equation and the expression Eq. (8.25) are, based on the result (8.26), reduced to

$$C_{mn} (\kappa_{mn}^4 - \kappa^4) = \frac{\langle p | \varphi_{mn} \rangle}{D \langle \varphi_{mn} | \varphi_{mn} \rangle}. \quad (8.27)$$

The norm of an eigenfunction defined in Eq. (8.22) is $\langle \varphi_{mn} | \varphi_{mn} \rangle = L_x L_y / 4$. Consequently Eqs. (8.23) and (8.27) give

$$w(x, y) = \sum_{mn} \frac{4 \langle p | \varphi_{mn} \rangle \varphi_{mn}(x, y)}{D L_x L_y (\kappa_{mn}^4 - \kappa^4)}. \quad (8.28)$$

For a point force F exciting the plate at (x_0, y_0) the pressure p is given by $p(x, y) = F \cdot \delta(x - x_0) \cdot \delta(y - y_0)$ and the response by

$$w(x, y) = \sum_{mn} \frac{4 F \varphi_{mn}(x_0, y_0) \varphi_{mn}(x, y)}{D L_x L_y (\kappa_{mn}^4 - \kappa^4)}. \quad (8.29)$$

Equation (8.28) can also be written as

$$\begin{aligned} w(x, y) &= \iint_{S_0} dx_0 dy_0 p(x_0, y_0) G(x, y | x_0, y_0) \\ G(x, y | x_0, y_0) &= \sum_{mn} \frac{4 \varphi_{mn}(x_0, y_0) \varphi_{mn}(x, y)}{D L_x L_y (\kappa_{mn}^4 - \kappa^4)}. \end{aligned} \quad (8.30)$$

This is in accordance with Green's formulation as discussed in Chaps. 6 and 7. The reciprocity condition $G(x, y | x_0, y_0) = G(x_0, y_0 | x, y)$ is satisfied by Eq. (8.30).

Whenever a time dependence $\exp(i\omega t)$ is introduced, then, as discussed in Sect. 2.2, the amplitudes of force and displacement can be interpreted as the Fourier transforms of force and displacement, respectively. Since \hat{v} , the FT of velocity, is

given by $i\omega\hat{w}$ where \hat{w} is the FT of the displacement, Eq. (8.29) gives

$$\hat{v}(x, y) = \sum_{mn} \frac{4i\omega\hat{F}\varphi_{mn}(x_0, y_0)\varphi_{mn}(x, y)}{DL_xL_y(\kappa_{mn}^4 - \kappa^4)} \quad (8.31)$$

Considering that $\kappa_{mn}^4 = \mu\omega_{mn}^2/D_0 = \mu(2\pi f_{mn})^2/D_0$, $\kappa^4 = \mu\omega^2/D$ and $D = D_0(1 + i\eta)$, Eq. (8.31) is also equal to

$$\hat{v}(x, y) = \sum_{mn} \frac{4i\omega\hat{F}\varphi_{mn}(x_0, y_0)\varphi_{mn}(x, y)}{m_p[\omega_{mn}^2(1 + i\eta) - \omega^2]}. \quad (8.32)$$

The mass of the entire plate is $m_p = \mu L_x L_y$.

The one-sided power spectral densities of force and velocity are defined as

$$G_{vv}(\omega) = 2 \lim_{T \rightarrow \infty} \frac{|\hat{v}|^2}{T}, \quad G_{FF}(\omega) = 2 \lim_{T \rightarrow \infty} \frac{|\hat{F}|^2}{T}.$$

The space average of G_{vv} is defined as

$$\langle G_{vv} \rangle = \frac{1}{L_x L_y} \int_0^{L_x} \int_0^{L_y} dx dy G_{vv}.$$

Introducing the definition of the one-sided spectral density and the FT of the velocity the quantity $\langle G_{vv} \rangle$ is, considering the orthogonality of the eigenfunctions, written as

$$\langle G_{vv}(\omega) \rangle = \sum_{mn} \frac{4\omega^2 G_{FF} \varphi_{mn}^2(x_0, y_0)}{m_p^2[(\omega_{mn}^2 - \omega^2)^2 + (\eta\omega_{mn}^2)^2]}. \quad (8.33)$$

For white noise excitation, G_{FF} constant, the time and space average of the velocity squared is

$$\begin{aligned} \langle \bar{v}^2 \rangle &= \frac{1}{2\pi} \int_0^\infty d\omega \langle G_{vv} \rangle = \frac{G_{FF}}{2\pi} \int_0^\infty d\omega \sum_{mn} \frac{4\omega^2 \varphi_{mn}^2(x_0, y_0)}{m_p^2[(\omega_{mn}^2 - \omega^2)^2 + (\eta\omega_{mn}^2)^2]} \\ &= G_{FF} \sum_{mn} \frac{\varphi_{mn}^2(x_0, y_0)}{m_p^2 \omega_{mn} \eta} \end{aligned} \quad (8.34)$$

The integral of Eq. (8.34) is discussed in Sect. 2.7. The time average of the total energy of the plate is for white noise excitation twice its kinetic energy. Thus

$$\bar{E} = m_p \langle \bar{v}^2 \rangle = \sum_{mn} \bar{E}_{mn} = G_{FF} \sum_{mn} \frac{\varphi_{mn}^2(x_0, y_0)}{m_p \omega_{mn} \eta}. \quad (8.35)$$

The one-sided power spectral density of the power input at the point (x_0, y_0) is

$$G_{\Pi} = G_{Fv} = \sum_{mn} \frac{\eta \omega \omega_{mn}^2 G_{FF} \varphi_{mn}^2(x_0, y_0)}{m_p [(\omega_{mn}^2 - \omega^2)^2 + (\eta \omega_{mn}^2)^2]}.$$

Thus $\bar{\Pi}$, the time average of the power input Π to the system, is for white noise excitation

$$\bar{\Pi} = \frac{1}{2\pi} \int_0^\infty d\omega G_{Fv} = \sum_{mn} \bar{\Pi}_{mn} = \sum_{mn} \frac{G_{FF} \varphi_{mn}^2(x_0, y_0)}{m_p}. \quad (8.36)$$

It follows that

$$\bar{\Pi}_{mn} = \eta \omega_{mn} \bar{E}_{mn}. \quad (8.37)$$

The expressions (8.34)–(8.36) were derived assuming a random force exciting the plate at the point (x_0, y_0) . For a plate excited by a number of random forces, the total energy of the plate is quite simply the sum of the energies induced by each source. This is a consequence of the system being linear and all the sources being random and thus uncorrelated. The input power $\bar{\Pi}_{mn}$ to mode (m, n) of a plate excited by N random forces is, following Eq. (8.55), given by

$$\bar{\Pi}_{mn} = \sum_{i=1}^N (G_{FF})_i \frac{\varphi_{mn}^2(x_i, y_i)}{m_p}.$$

The one-sided power spectral density for source i is given by $(G_{FF})_i$. The coordinates for the same source are (x_i, y_i) . Assuming that all sources have the same power spectral density $(G_{FF})_i = G_{FF}/N$, the power input to mode (m, n) is

$$\bar{\Pi}_{mn} = \frac{G_{FF}}{N m_p} \sum_{i=1}^N \varphi_{mn}^2(x_i, y_i).$$

For a large number of forces randomly distributed over the surface of the plate the input power is approximately given by

$$\bar{\Pi}_{mn} = \frac{G_{FF}}{N m_p} \langle \varphi_{mn}^2(x_i, y_i) \rangle_i \cdot N = \frac{G_{FF}}{4 m_p}. \quad (8.38)$$

The space average of $\varphi_{mn}^2(x_i, y_i)$ with respect to the coordinates x_i and y_i as defined by $\langle \varphi_{mn}^2(x_i, y_i) \rangle_i$ is $1/4$.

In a similar way the time average of the total modal energy due to the same type of excitation is

$$\bar{E}_{mn} = \frac{G_{FF}}{4 \eta \omega_{mn} m_p}. \quad (8.39)$$

For the losses being viscous the product $\eta\omega_{mn}$ is constant which in turn leads to \bar{E}_{mn} being constant and thus independent of mode number. The total energy of the plate is equally distributed between the modes, or in other words, there is an equipartition of energy.

The type of excitation leading up to the results (8.38) and (8.39) is often referred to as “rain on the roof” excitation. This is equivalent to the plate being excited by a large number of sources randomly scattered over the surface of the plate. Each source has the same strength or rather the same power spectral density. The sources are uncorrelated and have white noise spectra.

An alternative procedure to formulate a solution to Eq. (8.20) is to introduce modal parameters. As in Eq. (8.11) the solution is assumed to be in the form

$$w(x, y, t) = \sum_{m,n} g_{mn}(t) \cdot \varphi_{mn}(x, y). \quad (8.40)$$

The wave Eq. (8.1) is multiplied by eigenfunctions φ_{mn} and integrated over the area of the plate. After an additional partial integration, compare Eq. (8.26), the result is

$$\kappa_{mn}^4 \langle D\varphi_{mn} | \varphi_{mn} \rangle g_{mn} + \langle \mu\varphi_{mn} | \varphi_{mn} \rangle \frac{d^2 g_{mn}}{dt^2} = \langle f | \varphi_{mn} \rangle.$$

Symbolically this can be written as

$$K_{mn} g_{mn} + M_{mn} \frac{d^2 g_{mn}}{dt^2} = F_{mn}. \quad (8.41)$$

This is again equivalent to the equation of motion for a 1-DOF system. Compare Sect. 7.4. The generalized or modal parameters are

$$\begin{aligned} \text{Modal mass} \quad M_{mn} &= \iint_S dS \mu \varphi_{mn}^2(x, y) \\ \text{Modal stiffness} \quad K_{mn} &= \iint_S dS D \kappa_{mn}^4 \varphi_{mn}^2(x, y) \\ \text{Modal force} \quad F_{mn} &= \iint_S dS \cdot f(x, y, t) \varphi_{mn}^2(x, y) \end{aligned} \quad (8.42)$$

For a homogeneous plate D and μ are constant over the area of the plate. For the force having the time dependence $\exp(i\omega t)$ or rather for $f(x, y, t) = p(x, y) \cdot \exp(i\omega t)$ the modal force is

$$F_{mn} = \langle p | \varphi_{mn} \rangle \cdot \exp(i\omega t).$$

As discussed in Sect. 7.4 the modal parameters are not absolute quantities. The magnitude of a parameter depends on the norm of the eigenfunction. However, the ratio between two parameters is independent of the norm. Thus, the natural frequency for mode (m, n) is $f_{mn} = \omega_{mn}/(2\pi)$ is obtained from

$$\omega_{mn}^2 = \frac{K_{mn}}{M_{mn}} \quad (8.43)$$

For $E = E_0(1 + i\eta)$, the modal loss factor is

$$\eta_{mn} = \frac{\text{Im}(K_{mn})}{\text{Re}(K_{mn})} = \eta. \quad (8.44)$$

If the force per unit area is given the time dependence $\exp(i\omega t)$, $f(x, y, t) = p(x, y) \cdot \exp(i\omega t)$, the solution to Eq. (8.41) is

$$g_{mn}(t) = \frac{F_{mn} \cdot e^{i\omega t}}{K_{mn} - \omega^2 M_{mn}} = \frac{\langle p | \varphi_{mn} \rangle \cdot e^{i\omega t}}{K_{mn} - \omega^2 M_{mn}}. \quad (8.45)$$

The total response is thus

$$\begin{aligned} w(x, y, t) &= \sum_{mn} g_{mn} \varphi_{mn}(x, y) = \sum_{mn} \frac{F_{mn} \varphi_{mn}(x, y) e^{i\omega t}}{K_{mn} - \omega^2 M_{mn}} \\ &= \sum_{mn} \frac{\langle p | \varphi_{mn} \rangle \varphi_{mn}(x, y) e^{i\omega t}}{D(\kappa_{mn}^4 - \kappa^4) \langle \varphi_{mn} | \varphi_{mn} \rangle}. \end{aligned}$$

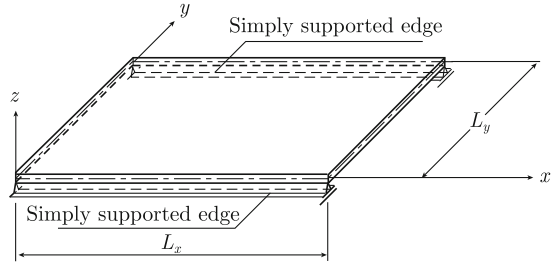
This should be compared to Eq. (8.28).

8.3 Forced Excitation of a Rectangular Plate with Two Opposite Sides Simply Supported

As previously pointed out, problems concerning free and forced vibrations of rectangular plates can be solved if two opposite sides of the plate are simply supported. The differential equation governing flexural waves on a homogeneous plate is given by the expression Eq. (8.20). For a plate excited by a harmonic point force $F \cdot \exp(i\omega t)$ at $\mathbf{r}_1 = (x_1, y_1)$ the forced response is of the form $w(x, y) \cdot \exp(i\omega t)$. It is assumed that a separation of variables can be made. For $w(x, y) = X(x) \cdot Y(y)$ the governing wave equation can be written as

$$\frac{d^4 X}{dx^4} Y + 2 \frac{d^2 X}{dx^2} \cdot \frac{d^2 Y}{dy^2} + X \frac{d^4 Y}{dy^4} - \kappa^4 X Y = \frac{F}{D} \delta(\mathbf{r} - \mathbf{r}_1). \quad (8.46)$$

Fig. 8.5 A rectangular plate simply supported along two opposite sides



The orientation of the coordinate axes is shown in Fig. 8.5. The two-dimensional Dirac function is $\delta(\mathbf{r} - \mathbf{r}_1) = \delta(x - x_1)\delta(y - y_1)$. The Dirac function satisfies

$$\int_{-\infty}^{\infty} \int_{-\infty}^{\infty} dx dy \delta(\mathbf{r} - \mathbf{r}_1) = 1, \quad \int_{-\infty}^{\infty} \int_{-\infty}^{\infty} dx dy f(x, y) \delta(\mathbf{r} - \mathbf{r}_1) = f(x_1, y_1).$$

In cylindrical coordinates and for $r = |\mathbf{r} - \mathbf{r}_1|$ the first integral can be written as

$$\int_0^{\infty} 2\pi r \delta(r) dr = 1.$$

For simply supported edges along the boundaries $y = 0$ and $y = L_y$ the bending moment and the displacement along these parallel edges must be zero. This implies

$$w(x, y) = 0, \quad M'_x = -D \left(\frac{\partial^2 w}{\partial y^2} + \nu \frac{\partial^2 w}{\partial x^2} \right) \text{ for } y = 0 \text{ and } y = L_y.$$

For $w(x, y) = X(x) \cdot Y(y)$ these boundary conditions are equivalent to

$$Y = \frac{d^2 Y}{dy^2} = 0 \text{ for } y = 0 \text{ and } y = L_y \quad (8.47)$$

The condition Eq. (8.47) is satisfied by an infinite set of functions $Y = \varphi_n(y)$ given by

$$\varphi_n(y) = \sin(k_n y), \quad k_n = n\pi / L_y \text{ for } n = 1, 2, 3, \dots \quad (8.48)$$

For each function $\varphi_n(y)$ there must be an associated x -dependent solution $X_n(x)$. The total solution is equal to the sum of all possible solutions or

$$w(x, y) = \sum_n X_n(x) \varphi_n(y) \quad (8.49)$$

Since the functions $\varphi_n(y)$ are orthogonal the function $X_n(x)$ can be expressed as

$$X_n(x) = \frac{\langle w|\varphi_n \rangle}{\langle \varphi_n|\varphi_n \rangle}. \quad (8.50)$$

This result is obtained according to standard procedure by multiplying Eq. (8.49) by $\varphi_n(y)$. The result is thereafter integrated with respect to y from 0 to L_y . The basic Eq. (8.46) is processed in a similar way—multiplied by $\varphi_n(y)$ and integrated over y . Considering that $d^2\varphi_n/dy^2 = -k_n^2\varphi_n$ and $d^4\varphi_n/dy^4 = k_n^4\varphi_n$, the result is

$$\langle \varphi_n|\varphi_n \rangle \left(\frac{d^4 X_n}{dx^4} - 2k_n^2 \frac{d^2 X_n}{dx^2} + k_n^4 X_n - \kappa^4 X_n \right) = \frac{F}{D} \varphi_n(y_1) \delta(x - x_1). \quad (8.51)$$

This is now a standard differential equation. For $x \neq x_1$ the function X_n must satisfy the equation inside the bracket of the expression Eq. (8.51). According to standard procedure, it is assumed that X_n can be written in the form of $A_n \exp(\lambda_n x)$, with λ_n satisfying the equation

$$\lambda_n^4 - 2k_n^2 \lambda_n^2 + k_n^4 - \kappa^4 = 0.$$

The four resulting solutions to this equation are

$$\begin{aligned} \lambda_{n1} &= i\sqrt{\kappa^2 - k_n^2} = i\kappa_1, \\ \lambda_{n2} &= -i\sqrt{\kappa^2 - k_n^2} = -i\kappa_1 \\ \lambda_{n3} &= \sqrt{\kappa^2 + k_n^2} = \kappa_2, \\ \lambda_{n4} &= -\sqrt{\kappa^2 + k_n^2} = -\kappa_2. \end{aligned} \quad (8.52)$$

It should be noted that for $\kappa < k_n$ the solutions λ_{n1} and λ_{n2} are real and κ_1 consequently imaginary. For $\kappa < k_n$, or for frequencies below the so called cut-off frequency, all solutions λ_{ni} are real. The resulting waves are for this case in the form $\exp(i\omega t \pm \lambda_n x)$. For a loss free medium, the waves are non-propagating or evanescent below the cut-off frequency.

The general solution to Eq. (8.51) can be separated into two parts—one, X_{n-} , to the left of the excitation point, and one, X_{n+} , to the right of the same point. The general solutions in the two domains are

$$\begin{aligned} x_1 &\geq x \geq 0 \\ X_{n-} &= A_{1n} \sin(\kappa_1 x) + A_{2n} \cos(\kappa_1 x) + A_{3n} \sinh(\kappa_2 x) + A_{4n} \cosh(\kappa_2 x) \\ L_x &\geq x \geq x_1 \\ X_{n+} &= B_{1n} \sin[\kappa_1(L_x - x)] + B_{2n} \cos[\kappa_1(L_x - x)] \\ &\quad + B_{3n} \sinh[\kappa_2(L_x - x)] + B_{4n} \cosh[\kappa_2(L_x - x)] \end{aligned} \quad (8.53)$$

The boundary conditions for a plate clamped at $x = 0$ and $x = L_x$ are

$$\begin{aligned} X_{n+} &= dX_{n+}/dx = 0 \text{ for } x = L_x \\ X_{n-} &= dX_{n-}/dx = 0 \text{ for } x = 0. \end{aligned} \quad (8.54)$$

At the excitation point continuity of displacement must be satisfied. The bending moments at each side of the excitation points must be equal. This leads to

$$X_{n-} = X_{n+}, \quad dX_{n-}/dx = dX_{n+}/dx, \quad d^2X_{n-}/dx^2 = d^2X_{n+}/dx^2 \text{ for } x = x_1. \quad (8.55)$$

The remaining boundary condition is obtained by integrating Eq. (8.51) across the line $x = x_1$ resulting in

$$\left[\frac{d^3X_{n+}}{dx^3} - \frac{d^3X_{n-}}{dx^3} \right]_{x=x_1} = \frac{2F \cdot \varphi_n(y_1)}{DL_y}. \quad (8.56)$$

It is now straight forward, though somewhat cumbersome, to solve the eight unknown parameters A_{ni} and B_{ni} from the eight boundary conditions Eqs. (8.54)–(8.56). If for example $x_1 = L_x/2$, the result is

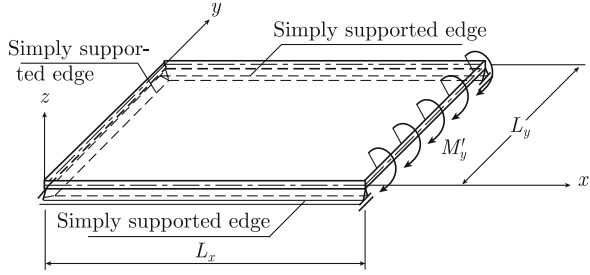
$$\begin{aligned} A_{n1} = B_{n1} &= \frac{F \cdot \varphi_n(y_1) \cdot (\kappa_1 \cdot \sin \alpha + \kappa_2 \sinh \beta)}{2DL_y \kappa_1 \kappa_2 (\kappa_2 \cos \alpha \cdot \sinh \beta + \kappa_1 \sin \alpha \cdot \cosh \beta)} \\ A_{n2} = B_{n2} &= \frac{F \cdot \varphi_n(y_1) \cdot (\sin \alpha - \cosh \beta)}{2DL_y \kappa_2 (\kappa_2 \cos \alpha \cdot \sinh \beta + \kappa_1 \sin \alpha \cdot \cosh \beta)} \\ A_{n3} = B_{n3} &= -\frac{\kappa_1}{\kappa_2} A_{n1} \\ A_{n4} = B_{n4} &= -A_{n2} \\ \alpha &= \kappa_1 L_x/2, \quad \beta = \kappa_2 L_x/2. \end{aligned} \quad (8.57)$$

It should be noted that the parameters κ_1 and κ_2 depend on n as given by Eq. (8.52). The amplitudes have maxima whenever the real part of the common denominator of the amplitudes given in Eq. (8.57) is zero. In addition, the amplitude A_{n1} and B_{n1} have maxima, when the real part of κ_1 is zero. However, this maximum is not equivalent to a resonance, since the response of the plate is proportional to $A_{n1} \sin(\kappa_1 x)$. For κ_1 small, this product tends to $A_{n1} \kappa_1 x$ which is finite even for κ_1 approaching zero despite A_{n1} being very large. The solution $\text{Re}(\kappa_1) = 0$ is consequently not equivalent to a resonance.

The technique described above to determine the response of a plate can be used for any type of source distribution across the plate, as well as for any boundary conditions for two opposite sides, if the two remaining sides of the rectangular plate are simply supported.

Another problem of interest is illustrated in Fig. 8.6. A homogeneous rectangular plate is simply supported along three edges. Along the fourth side the plate is excited by a bending moment $M' \cdot \exp(i\omega t)$ per unit width of the plate, where M' is constant along the edge $x = L_x$. The displacement along the edge is zero. The problem can illustrate the coupling between two plates across a junction, which can only rotate. The model may be extended to describe a set of coupled plates. This more general problem is discussed in Chap. 14, describing the coupling between plates bounded by parallel stiffeners.

Fig. 8.6 A rectangular plate, simply supported along three edges. The remaining side is excited by a bending moment



For the single plate excited by a bending moment as shown in Fig. 8.6 the displacement can be written as defined in Eq. (8.49) or

$$w(x, y, t) = \exp(i\omega t) \sum_n X_n(x) \varphi_n(y).$$

The functions X_n are in the form

$$X_n = C_{1n} \sin(\kappa_1 x) + C_{2n} \cos(\kappa_1 x) + C_{3n} \sinh(\kappa_2 x) + C_{4n} \cosh(\kappa_2 x).$$

The function X_n must satisfy the boundary conditions

$$X_n = 0 \text{ for } x = 0 \text{ and } x = L_x, \quad d^2 X_n / dx^2 = 0 \text{ for } x = 0.$$

Based on these three boundary conditions the parameters C_{2n} , C_{3n} and C_{4n} are eliminated. The basic expression defining the displacement is thus reduced to

$$X_n = C_{1n} [\sin(\kappa_1 x) - \sinh(\kappa_2 x) \cdot \sin(\kappa_1 L_x) / \sinh(\kappa_2 L_x)]. \quad (8.58)$$

The bending moment per unit length along the edge $x = L_x$ is

$$M' = -D \left[\frac{\partial^2 w}{\partial x^2} + \nu \frac{\partial^2 w}{\partial y^2} \right] = -D \sum_n \frac{d^2 X_n}{dx^2} \varphi_n(y). \quad (8.59)$$

The second term inside the bracket is equal to zero since the second derivative with respect to y is proportional to X_n which is zero on the boundary. A combination of the Eqs. (8.58) and (8.59) gives

$$M' = D \sum_n 2C_{1n} \kappa^2 \sin(\kappa_1 L_x) \varphi_n(y). \quad (8.60)$$

The functions $\varphi_n(y)$ are orthogonal. Equation (8.60) is multiplied by $\varphi_n(y)$ and integrated over y from 0 to L_y . Thus, the parameters C_{1n} are obtained as

$$C_{1n} = \frac{2M'}{D\kappa^2 \sin(\kappa_1 L_x) n \pi} \text{ for } n \text{ odd, } C_{1n} = 0 \text{ for } n \text{ even.}$$

The response of the plate due to a bending moment $M' \cdot \exp(i\omega t)$ per unit width of the plate at the edge $x = L_x$ is consequently

$$w(x, y, t) = \sum_{n \text{ odd}} \frac{2M' \cdot \sin(n \pi y / L_y)}{D\kappa^2 \sin(\kappa_1 L_x) n \pi} \left[\sin(\kappa_1 x) - \frac{\sinh(\kappa_2 x) \cdot \sin(\kappa_1 L_x)}{\sinh(\kappa_2 L_x)} \right] e^{i\omega t}. \quad (8.61)$$

8.4 Power and Energy

If a point force excites a plate, which is coupled to other structures by means of conservative joints, a certain part of the power is transmitted to adjoining structures and some dissipated in the plate itself. The input power to the plate should be equal to the sum of the power transmitted and dissipated. This obvious statement can be demonstrated by means of the basic wave equation and the definitions of forces, bending moments, rotations, and deflections along the boundaries.

Thus, consider a set of plates joined together as shown in Fig. 8.7. In this particular case, it is assumed that the common boundaries are parallel and defined by the lines $y = 0$ and $y = L_y$. The plates are simply supported along these lines. At each junction, the mounting is such that the displacement is zero. The plates can rotate freely around the junctions. No power is dissipated due to the rotation of the junctions. A point force $F \cdot \exp(i\omega t)$ excites the plate denoted 2 at $\mathbf{r} = (x_1, y_1)$. The force is driving plate number 2, which in turn excites the plates numbered 1 and 3. The excitation of these plates is caused by bending moments at the junctions. The resulting deflections and bending moments at the junctions, limiting plate number 2, are shown in Fig. 8.8.

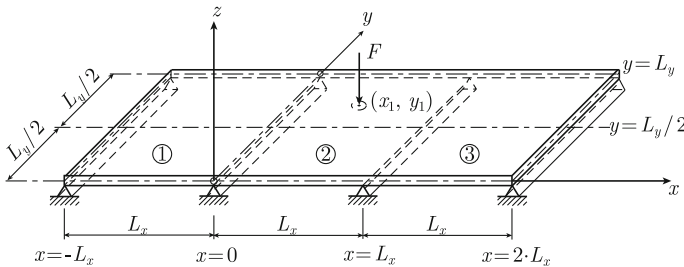


Fig. 8.7 Three coupled plates. Plate 2 is excited by a point force. The plates are simply supported along the lines $y = 0$ and $y = L_y$. The boundaries $x = 0$ and $x = L_x$ are allowed to rotate

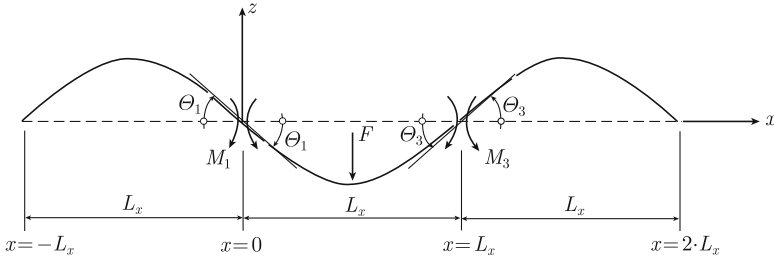


Fig. 8.8 The resulting deflections and bending moments at the junctions of Plate 2

The time average of the power Π_{23} transmitted from plate 2 to plate 3 is

$$\bar{\Pi}_{23} = \frac{1}{2} \text{Re} \int_0^{L_y} dy M'_3 \dot{\Theta}_3^*.$$

The bending moment M'_3 per unit length and rotation Θ_3 or rather $\dot{\Theta}_3$ are

$$\begin{aligned} M'_3 &= -D \left(\frac{\partial^2 w}{\partial x^2} + \nu \frac{\partial^2 w}{\partial y^2} \right)_{x=L_x} = -D \left(\frac{\partial^2 w}{\partial x^2} \right)_{x=L_x}, \\ \dot{\Theta}_3 &= \left(\frac{\partial^2 w}{\partial x \partial t} \right)_{x=L_x} = i\omega \left(\frac{\partial w}{\partial x} \right)_{x=L_x}. \end{aligned} \quad (8.62)$$

The time average of the transmitted power from plate 2 to plate 3 is thus

$$\bar{\Pi}_{23} = \frac{1}{2} \text{Re} \left\{ i\omega D \int_0^{L_y} dy \left[\frac{\partial^2 w}{\partial x^2} \left(\frac{\partial w}{\partial x} \right)^* \right]_{x=L_x} \right\}. \quad (8.63)$$

At the other junction bending moment and rotation are

$$M'_1 = -D \left(\frac{\partial^2 w}{\partial x^2} \right)_{x=0}, \quad \dot{\Theta}_1 = -i\omega \left(\frac{\partial w}{\partial x} \right)_{x=0}. \quad (8.64)$$

The resulting energy flow from plate 2 to plate 1 is consequently

$$\bar{\Pi}_{21} = -\frac{1}{2} \text{Re} \left\{ i\omega D \int_0^{L_y} dy \left[\frac{\partial^2 w}{\partial x^2} \left(\frac{\partial w}{\partial x} \right)^* \right]_{x=0} \right\}. \quad (8.65)$$

In the first case, the energy flow is along the positive direction of the x -axis. In the second, the flow is in the opposite direction. Hence the opposite signs in the Eqs. (8.64) and (8.65).

For harmonic excitation, $F \cdot \exp(i\omega t)$, the basic equation governing the motion of plate 2 can be written as

$$D \left(\frac{\partial^4 w}{\partial x^4} + 2 \frac{\partial^4 w}{\partial x^2 \partial y^2} + \frac{\partial^4 w}{\partial y^4} \right) - \mu \omega^2 w = F \cdot \delta(\mathbf{r} - \mathbf{r}_1). \quad (8.66)$$

The force and displacement are defined positive in the same direction. The time average of the input power to plate 2 depends on the force F and the plate velocity $w(\mathbf{r}_1)$ at the excitation point as

$$\bar{\Pi}_{in} = \frac{1}{2} \text{Re} [F \cdot \dot{w}^*]_{r=r_1} = \frac{1}{2} \text{Re} [-i\omega F \cdot w^*]_{r=r_1}. \quad (8.67)$$

The basic wave Eq. (8.66) is now multiplied by $\dot{w}^* = -i\omega w^*$. The resulting expression is thereafter integrated with respect to x and y over the entire area of plate 2. This gives

$$\begin{aligned} & \int_0^{L_x} \int_0^{L_y} dx dy (-i\omega D) \left(\frac{\partial^4 w}{\partial x^4} w^* + 2 \frac{\partial^4 w}{\partial x^2 \partial y^2} w^* + \frac{\partial^4 w}{\partial y^4} w^* \right) \\ & + i\mu\omega^3 \int_0^{L_x} \int_0^{L_y} dx dy |w|^2 = \int_0^{L_x} \int_0^{L_y} dx dy [-i\omega F w^*(\mathbf{r}) \delta(\mathbf{r} - \mathbf{r}_1)] \end{aligned} \quad (8.68)$$

The second integral on the left hand side is imaginary since the integrand is real. The integral on the right hand side of Eq. (8.68) is quite simply equal to $-i\omega F \cdot w^*(\mathbf{r}_1)$. The real part of this expression is according to Eq. (8.67) identical to two times the time average of the input power $\bar{\Pi}_{in}$ to plate 2. By considering only the real part of Eq. (8.68) the time average of the input power can be written as

$$\bar{\Pi}_{in} = \frac{1}{2} \text{Re} \int_0^{L_x} \int_0^{L_y} dx dy (-i\omega D) \left(\frac{\partial^4 w}{\partial x^4} w^* + 2 \frac{\partial^4 w}{\partial x^2 \partial y^2} w^* + \frac{\partial^4 w}{\partial y^4} w^* \right) = I_1 + I_2. \quad (8.69)$$

The expression Eq. (8.69) is integrated by parts. Starting with the first term inside the bracket, the result is

$$\begin{aligned} I_1 &= \frac{1}{2} \text{Re} \int_0^{L_x} \int_0^{L_y} dx dy (-i\omega D) \left(\frac{\partial^4 w}{\partial x^4} w^* \right) \\ &= \frac{1}{2} \text{Re} \left\{ (-i\omega D) \int_0^{L_x} \int_0^{L_y} dx dy \left| \frac{\partial^2 w}{\partial x^2} \right|^2 \right. \\ &\quad \left. + (-i\omega D) \int_0^{L_y} dy \left[\frac{\partial^3 w}{\partial x^3} w^* - \frac{\partial^2 w}{\partial x^2} \frac{\partial w^*}{\partial x} \right]_0^{L_x} \right\}. \end{aligned}$$

The surface integral of the last part, second line, of the equation is real. However D is complex or equal to $D_0(1 + i\eta)$. The first part of the last integral is zero since $w = w^* = 0$ for $x = 0$ and $x = L_x$. Considering these points

$$I_1 = \frac{1}{2}\eta\omega D \int_0^{L_x} \int_0^{L_y} dx dy \left| \frac{\partial^2 w}{\partial x^2} \right|^2 + \frac{1}{2}\text{Re} \left\{ (i\omega D) \int_0^{L_y} dy \left[\frac{\partial^2 w}{\partial x^2} \frac{\partial w^*}{\partial x} \right]_{x=L_x} - (i\omega D) \int_0^{L_y} dy \left[\frac{\partial^2 w}{\partial x^2} \frac{\partial w^*}{\partial x} \right]_{x=0} \right\}.$$

The last two expressions are according to Eqs. (8.63) and (8.65) equal to the energy flows to plate 3 and plate 1, respectively. Thus

$$I_1 = \frac{1}{2}\eta\omega D_0 \int_0^{L_x} \int_0^{L_y} dx dy \left| \frac{\partial^2 w}{\partial x^2} \right|^2 + \bar{\Pi}_{23} + \bar{\Pi}_{21}. \quad (8.70)$$

The second and third terms of the integral Eq. (8.69) are integrated by parts in a similar way. The results are

$$\begin{aligned} I_2 &= \frac{1}{2}\text{Re} \int_0^{L_x} \int_0^{L_y} dx dy (-i\omega D) \left[2 \frac{\partial^4 w}{\partial x^2 \partial y^2} w^* + \frac{\partial^4 w}{\partial y^4} w^* \right] \\ &= \frac{1}{2}\eta\omega D_0 \int_0^{L_x} \int_0^{L_y} dx dy 2 \left| \frac{\partial^2 w}{\partial x \partial y} \right|^2 + \frac{1}{2}\eta\omega D_0 \int_0^{L_x} \int_0^{L_y} dx dy 2 \left| \frac{\partial^2 w}{\partial y^2} \right|^2. \end{aligned} \quad (8.71)$$

The total result is obtained from Eqs. (8.69) to (8.71) as

$$\bar{\Pi}_{in} = \bar{\Pi}_{21} + \bar{\Pi}_{23} + \frac{1}{2}\eta\omega D_0 \int_0^{L_x} \int_0^{L_y} dx dy \left[\left| \frac{\partial^2 w}{\partial x^2} \right|^2 + 2 \left| \frac{\partial^2 w}{\partial x \partial y} \right|^2 + \left| \frac{\partial^2 w}{\partial y^2} \right|^2 \right].$$

The surface integral is equal to two times the time average of the potential energy \mathcal{U} of a plate with zero displacement along the boundaries. Hence

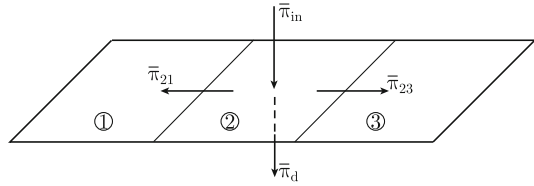
$$\bar{\Pi}_{in} = \bar{\Pi}_{21} + \bar{\Pi}_{23} + 2\eta\omega\bar{\mathcal{U}}.$$

For white noise excitation the time averages of kinetic and potential energies are equal or $\bar{\mathcal{U}} = \bar{\mathcal{T}} = \bar{\mathcal{E}}/2$, where $\bar{\mathcal{E}}$ is the total energy. Thus for white noise excitation of a plate, or in fact any structure, the result concerning the energy balance is

$$\bar{\Pi}_{in} = \bar{\Pi}_{transmitted} + \bar{\Pi}_d, \quad \bar{\Pi}_d = \eta\omega\bar{\mathcal{E}}. \quad (8.72)$$

Thus, the power input to a structure is equal to the sum of power $\bar{\Pi}_d$ dissipated in the structure and the total power transmitted to adjoining structures as illustrated in Fig. 8.9.

Fig. 8.9 Energy flow. Plate I excited by a point force



The total losses in the plate are equal to the sum of the internal dissipation of energy and the flow of energy to adjoining structures. This could be formulated as

$$\bar{\Pi}_{in} = \omega \eta_{tot} \bar{E} = \omega \bar{E} [\eta + \bar{\Pi}_{transmitted} / (\omega \bar{E})].$$

The total loss factor is a function of the internal loss factor, the ratio between the input power to the structure and its total energy. The internal loss factor is in general small, as compared to the losses to other structures. Still, surprisingly enough, the loss factor measured on plate elements, which are parts of a larger construction are fairly consistent. For example, the loss factors measured on bare steel plates on ships are of the order

$$\eta_{tot} = 0.25 \cdot f^{-0.275}$$

The frequency is given by f . These losses can neither be described as viscous, frictional nor as structural. Compare also the discussion of transmission losses in Sect. 5.11. In Chap. 12 the so-called radiation losses are defined.

8.5 Mobility of Plates

The response of a rectangular simply supported plate excited by a point force was derived in Sect. 8.2. The FT of the velocity at a point (x, y) was derived as function of the FT of a point force exciting the plate at (x_0, y_0) and was given by Eq. (8.32) as

$$\hat{v}(x, y) = \sum_{mn} \frac{4i\omega \hat{F} \varphi_{mn}(x_0, y_0) \varphi_{mn}(x, y)}{m_p [\omega_{mn}^2 (1 + i\eta) - \omega^2]}.$$

Consequently the transfer mobility, the ratio between the FT of the velocity at (x, y) and the FT of the force at (x_0, y_0) is

$$Y(x, y|x_0, y_0) = \sum_{mn} \frac{4i\omega \varphi_{mn}(x_0, y_0) \varphi_{mn}(x, y)}{m_p [\omega_{mn}^2 (1 + i\eta) - \omega^2]}. \quad (8.73)$$

The reciprocity relation holds as shown by Eq. (8.73), i.e.,

$$Y(x, y|x_0, y_0) = Y(x_0, y_0|x, y)$$

In other words, the velocity at a point (x, y) due to a force at (x_0, y_0) on the plate is identical to the velocity at the point (x_0, y_0) caused by the same force exciting the plate at the point (x, y) .

The corners of the rectangular plate have the coordinates $(0, 0)$, $(L_x, 0)$, (L_x, L_y) , and $(0, L_y)$. Consequently the eigenfrequencies for the simply supported plate are $\varphi_{mn} = \sin(m \pi x/L_x) \sin(n \pi y/L_y)$. If the force is applied at the center of the plate i.e., at $(L_x/2, L_y/2)$ the point mobility at this point is obtained from Eq. (8.73) as

$$\begin{aligned} Y(L_x/2, L_y/2) &= \sum_{mn} \frac{4i\omega \sin^2(m \pi /2) \sin^2(n \pi /2)}{m_p[\omega_{mn}^2(1 + i\eta) - \omega^2]} \\ &= \sum_{mn} \frac{4i\omega \sin^2(m \pi /2) \sin^2(n \pi /2)}{DL_x L_y (\kappa_{mn}^4 - \kappa^4)}. \end{aligned} \quad (8.74)$$

The equalities $\kappa_{mn}^4 = \mu\omega_{mn}^2/D_0$, $\kappa^4 = \mu\omega^2/D$, and $D = D_0(1 + i\eta)$ have been used to obtain the second part of Eq. (8.74). For m and n being even the sine functions are zero. For m and n being odd the absolute value of the functions is equal to unity. The expression Eq. (8.74) can thus be reduced to

$$Y = \frac{4i\omega}{DL_x L_y} \sum_{mn} \frac{1}{Q_{mn}}, \quad Q_{mn} = \left\{ \left[\frac{(2m+1)\pi}{L_x} \right]^2 + \left[\frac{(2n+1)\pi}{L_y} \right]^2 \right\}^2 - \kappa^4. \quad (8.75)$$

If the dimensions of the plate tend to infinity, the summation in Eq. (8.75) can be carried out as an integration i.e.,

$$\sum_{mn} \frac{1}{Q_{mn}} \rightarrow \int_0^\infty \int_0^\infty \frac{dmdn}{Q_{mn}}.$$

In order to solve this integral the following substitutions are made

$$(2m+1)\pi/L_x = \xi \cos \alpha, \quad (2n+1)\pi/L_y = \xi \sin \alpha.$$

According to standard procedure these substitutions lead to

$$dmdn = \xi d\xi d\alpha L_x L_y / (4\pi).$$

The integers m and n are always positive i.e., $0 \leq \alpha \leq \pi/2$. The function ξ can vary between zero and plus infinity. Based on these assumptions the point mobility for a large or rather infinite plate is

$$Y_\infty = \frac{i\omega}{\pi^2 D} \int_0^\infty \xi d\xi \int_0^{\pi/2} \frac{d\alpha}{\xi^4 - \kappa^4} = \frac{i\omega}{2\pi D} \int_0^\infty \frac{\xi d\xi}{\xi^4 - \kappa^4}.$$

By introducing $z = \xi^2$ the integral is written

$$Y_\infty = \frac{i\omega}{4\pi D} \int_0^\infty \frac{dz}{z^2 - \kappa^4} = \frac{i\omega}{8\pi D} \int_{-\infty}^\infty \frac{dz}{z^2 - \kappa^4}.$$

The integral is solved by means of a contour integration in the complex plane as shown in Fig. 8.10. The integral along the semi-circle approaches zero as the radius of the circle goes to infinity. The integrand has two poles; $z_1 = \kappa_0^2 \sqrt{1 - i\eta} \approx \kappa_0^2 (1 - i\eta/2)$ and $z_2 = -\kappa_0^2 \sqrt{1 - i\eta} \approx -\kappa_0^2 (1 - i\eta/2)$. The pole z_2 is located in the upper half part of the complex plane. The point mobility is given by the contour integral

$$Y_\infty = \frac{i\omega}{8\pi D} \oint \frac{dz}{z^2 - \kappa^4}. \quad (8.76)$$

This integral is identical to Eq. (5.81) which was derived using spatial Fourier transforms. This is a natural consequence of that a Fourier series in the limit turns into a Fourier integral as discussed in Sect. 2.1.

This type of contour integral is solved as indicated in Sect. 5.4, Eq. (5.81). The result is

$$Y_\infty = \frac{i\omega}{8\pi D} \cdot \frac{2\pi i}{2z_2} = \frac{\omega}{8D\kappa_0^2(1 - i\eta/2)} \approx \frac{\omega(1 - i\eta/2)}{8D_0\kappa_0^2} = \frac{1 - i\eta/2}{8\sqrt{\mu D_0}}. \quad (8.77)$$

It has been assumed that $\eta \ll 1$. The point mobility for an infinite plate given by Eq. (8.77) is identical to the expression previously derived in Sects. 5.3 and 5.4.

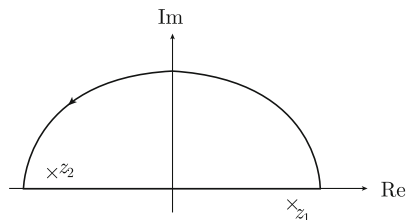
The one-sided spectral density $G_\Pi(\omega)$ of the power input to a structure is a function of the power spectral density of the point force and the point mobility as

$$G_\Pi = G_{FF} \text{Re}Y.$$

This expression was derived in Sect. 7.5, Eq. (7.80). The point mobility for a finite plate is high close to a resonance if the losses are small. The real part of the point mobility at (x_0, y_0) is according to Eq. (8.73) equal to

$$\text{Re}Y = \sum_{mn} \frac{4\omega\omega_{mn}^2\eta\varphi_{mn}^2(x_0, y_0)}{m_p[(\omega_{mn}^2 - \omega^2)^2 + (\eta\omega_{mn}^2)^2]}. \quad (8.78)$$

Fig. 8.10 Poles and integration path for solving Eq. (8.93)



The time average of the power injected is for white noise excitation, i.e., G_{FF} constant, equal to

$$\begin{aligned}
 \bar{\Pi} &= \frac{1}{2\pi} \int_0^\infty G_{\Pi} d\omega = \frac{G_{FF}}{2\pi} \int_0^\infty \text{Re} Y d\omega \\
 &= \sum_{mn} \frac{2G_{FF}\eta\omega_{mn}^2\varphi_{mn}^2(x_0, y_0)}{\pi m_p} \int_0^\infty \frac{\omega d\omega}{[(\omega_{mn}^2 - \omega^2)^2 + (\eta\omega_{mn}^2)^2]} \\
 &= \sum_{mn} \frac{2G_{FF}\eta\omega_{mn}^2\varphi_{mn}^2(x_0, y_0)}{\pi m_p} \cdot J.
 \end{aligned} \tag{8.79}$$

By substituting ω^2 by z and thus $\omega d\omega$ by $dz/2$ the integral in Eq. (8.79) is rewritten as

$$J = \int_{-\infty}^\infty \frac{dz}{2[(\omega_{mn}^2 - z)^2 + (\eta\omega_{mn}^2)^2]} = \oint \frac{dz}{2[(\omega_{mn}^2 - z)^2 + (\eta\omega_{mn}^2)^2]} = \frac{\pi}{2\omega_{mn}^2\eta}. \tag{8.80}$$

For small η the main contribution to the integral J is obtained for $z = \omega_{mn}^2$. The lower integration limit can therefore be extended to $-\infty$. The integral is solved by a contour integration in upper half of the complex plane as shown in Fig. 8.10. The pole in the upper half plane is $z_1 = \omega_{mn}^2(1 + i\eta)$. The power input to the plate is according to Eq. (8.79) equal to

$$\bar{\Pi} = \sum_{mn} G_{FF}\varphi_{mn}^2(x_0, y_0)/m_p.$$

The power input $\bar{\Pi}_{\Delta f}$ within a frequency band defined by f and $f + \Delta f$ is

$$\bar{\Pi}_{\Delta f} = \sum_{m'n'} G_{FF}\varphi_{mn}^2(x_0, y_0)/m_p. \tag{8.81}$$

The summation over m' and n' should only include the modes within the frequency band f to $f + \Delta f$. For a sufficiently large number of modes N within the frequency band, the sum of the square of the eigenvectors is approximately equal to $N/4$. The number of modes N within a frequency band is approximately equal to $\Delta f \cdot \mathcal{N}_f$ where Δf is the width of the frequency band and \mathcal{N}_f the modal density defined in Eq. (8.18). Considering this, the input power $\bar{\Pi}_{\Delta f}$ to the structure within the frequency band Δf is

$$\bar{\Pi}_{\Delta f} = \Delta f \cdot \mathcal{N}_f \cdot G_{FF}/(4m_p) = \Delta f \cdot \frac{G_{FF}}{8\sqrt{\mu D_0}} = G_{FF}\Delta f \text{Re}(Y_\infty), \tag{8.82}$$

where $\mu = \rho h = m_p/(L_x L_y)$. Again it has been demonstrated, that if a plate is excited by white noise, the power input in the high frequency region to the plate can

be calculated as if the plate were infinite. In the high frequency region, the modal density is independent of the boundary conditions of the plate. Thus, in the high frequency region the input power to a plate is almost independent of its boundary conditions. However, the frequency interval considered must include a sufficient number of natural frequencies as discussed in Sect. 6.4.

The modal density of a structure can be estimated by measuring the frequency and space average $\langle \bar{Y} \rangle$ of the point mobility of a plate. If this average is set to approximate the point mobility of an infinite plate then Eq. (8.82) gives

$$\mathcal{N}_f = 4m_p \text{Re}(Y_\infty) \approx 4m_p \text{Re}(\langle \bar{Y} \rangle). \quad (8.83)$$

The number of modes within a frequency band must exceed at least four for Eq. (8.83) to be valid, i.e., $\Delta f \cdot \mathcal{N}_f > 4$. The result is valid for any homogeneous structure. The quality of the estimate depends on how accurately the frequency and space average can be determined.

8.6 The Rayleigh–Ritz Method

As previously discussed it is often of great importance to determine the first few eigenfrequencies for a system. In the high frequency range, the approximate expression Eq. (8.18) giving the modal density can be sufficient for the calculation of energies and input power to a system as discussed in Sect. 8.5.

The Rayleigh method is a very powerful tool for the calculation of the first few natural frequencies for a plate with arbitrary boundary conditions. However the method is not exact. Eigenfrequencies are derived using approximate or trial functions describing the displacement of a structure. For example, the displacement w of a thin plate, assuming harmonic motion, is defined as

$$w(x, y, t) = F(x, y) \cdot \sin \omega t,$$

where $F(x, y)$ is an as yet unknown trial function describing the displacement of the plate. The plate velocity is $\dot{w} = \omega F(x, y) \cdot \cos \omega t$. The maximum kinetic energy is obtained for $\cos \omega t = 1$ when the velocity has a maximum. Thus

$$\mathcal{T}_{\max} = \frac{\omega^2}{2} \iint_S dx dy \mu(x, y) F^2(x, y), \quad (8.84)$$

where μ is the mass per unit area of the plate and S its area. The maximum potential energy is obtained when the displacement is maximum, i.e., for $\sin \omega t = 1$. The maximum potential energy is equal to

$$\begin{aligned} \mathcal{U}_{\max} = \frac{1}{2} \iint_S dx dy D(x, y) & \left[\left(\frac{\partial^2 F}{\partial x^2} \right)^2 + \left(\frac{\partial^2 F}{\partial y^2} \right)^2 \right. \\ & \left. + 2\nu \left(\frac{\partial^2 F}{\partial x^2} \right) \left(\frac{\partial^2 F}{\partial y^2} \right)^2 + 2(1-\nu) \left(\frac{\partial^2 F}{\partial x \partial y} \right)^2 \right]. \end{aligned} \quad (8.85)$$

This expression is obtained from Eq.(3.124). It is assumed that both the bending stiffness D and the mass μ per unit area can vary across the surface of the plate.

For the case where the displacement along the edges is zero, the expression Eq.(8.85) can be somewhat simplified. The surface integral of the ν dependent terms in Eq.(8.85) is equal to zero if $F = 0$ along the boundary. For a rectangular plate, sides L_x and L_y , the surface integral J of the terms which depend on ν can be rearranged and thereafter integrated by parts as

$$\begin{aligned} J &= \iint_S dx dy \left[\left(\frac{\partial^2 F}{\partial x^2} \right) \left(\frac{\partial^2 F}{\partial y^2} \right) - \left(\frac{\partial^2 F}{\partial x \partial y} \right)^2 \right] \\ &= \iint_S dx dy \left[\frac{\partial}{\partial x} \left(\frac{\partial F}{\partial x} \right) \left(\frac{\partial^2 F}{\partial y^2} \right) - \frac{\partial}{\partial y} \left(\frac{\partial F}{\partial x} \right) \left(\frac{\partial^2 F}{\partial x \partial y} \right) \right] \\ &= \int_0^{L_y} dy \left[\frac{\partial F}{\partial x} \frac{\partial^2 F}{\partial y^2} \right]_0^{L_x} - \int_0^{L_x} dx \left[\frac{\partial F}{\partial x} \frac{\partial^2 F}{\partial x \partial y} \right]_0^{L_y}. \end{aligned}$$

For $F(x, y) = 0$ for $x = 0$ and $x = L_x$ it follows that also $\partial F / \partial y$ is equal to zero along the same boundaries. The first integral on the last line above is consequently equal to zero. Further, $F(x, y) = 0$ for $y = 0$ and $y = L_y$. Thus $\partial F / \partial x$ and $\partial^2 F / \partial x \partial y$ are both equal to zero along the edges $y = 0$ and $y = L_y$. The integral J is consequently equal to zero if $F(x, y) = 0$ along the edges of the plate. Thus, if the displacement along the periphery of a plate is zero, the maximum potential energy for harmonic displacement is given by

$$\mathcal{U}_{\max} = \frac{1}{2} \iint_S dx dy D(x, y) \left[\left(\frac{\partial^2 F}{\partial x^2} \right)^2 + \left(\frac{\partial^2 F}{\partial y^2} \right)^2 + 2 \left(\frac{\partial^2 F}{\partial x \partial y} \right)^2 \right]. \quad (8.86)$$

Since for a conservative system \mathcal{T}_{\max} is equal to \mathcal{U}_{\max} , the angular frequency for the general case is, based on the results Eqs.(8.84) and (8.85), obtained as

$$\begin{aligned} \omega^2 = & \frac{\iint_S dx dy D(x, y) \left[\left(\frac{\partial^2 F}{\partial x^2} \right)^2 + \left(\frac{\partial^2 F}{\partial y^2} \right)^2 + 2\nu \left(\frac{\partial^2 F}{\partial x^2} \right) \left(\frac{\partial^2 F}{\partial y^2} \right)^2 + 2(1-\nu) \left(\frac{\partial^2 F}{\partial x \partial y} \right)^2 \right]}{\iint_S dx dy \mu F^2}. \end{aligned} \quad (8.87)$$

The expressions in Eq. (8.87) are integrated over the entire plate area. The technique leading up to Eq. (8.87) is referred to as the Rayleigh method. If the correct expression for the first eigenfunction φ_{11} is set to equal F in Eq. (8.87), the resulting angular frequency is identical to $\omega_{11} = 2\pi f_{11}$, where f_{11} is the exact first eigenfrequency for the system. However, in most cases the eigenfunction is not known. It can be shown that if a function approximating φ_{11} is substituted in Eq. (8.87) the resulting value ω is an approximation to the fundamental angular frequency. The approximation ω obtained from Eq. (8.87) is always equal to or larger than the correct value. If the error for the assumed eigenfunction is of the order ε , the error of the calculated eigenvalue is of the order ε^2 . The assumed trial function F must always satisfy the proper boundary conditions for the plate but not necessarily the governing differential equation of the plate in flexure.

The technique developed by Ritz can be used to calculate the approximate eigenfrequencies for rectangular plates, clamped along all four edges. In order to describe the displacement of a clamped plate, so called beam functions are used. The eigenfunctions φ_m for clamped-clamped beams are given in Table 7.2. The rectangular plate is oriented in the $x - y$ plane of a Cartesian coordinate system. The sides of the plate are along the lines $x = 0$, $y = 0$, $x = L_x$, and $y = L_y$. The trial function F approximating mode (m, n) for a uniform rectangular plate clamped at the edges can, using the eigenfunctions for a clamped beam, be written as

$$F(x, y) = \varphi_m(x)\varphi_n(y). \quad (8.88)$$

This trial function satisfies the boundary conditions for a clamped plate but not the corresponding wave equation for a plate in flexure. In the expressions for $\varphi_m(x)$ and $\varphi_n(y)$ the length L is substituted by L_x and L_y , respectively. The eigenfunctions are orthogonal as discussed in Chap. 7. For each mode an approximate expression for the eigenfrequency is obtained using Eq. (8.87). Numerical results are listed in Ref. [62] and tabulated in Tables 8.2 and 8.3.

The same technique can be used for other boundary conditions. If for example the edges of the plate are free along the sides $x = 0$ and $x = L_x$ and clamped along the sides $y = 0$ and $y = L_y$, the trial function would be $F(x, y) = \varphi_m(x)\varphi_n(y)$ where $\varphi_m(x)$ is obtained from Table 7.3 by setting $L = L_x$ and $\varphi_n(y)$ from Table 7.2 by setting $x = y$ and $L = L_y$. A number of other boundary conditions are also discussed in Ref. [62]. Approximate expressions giving the eigenfrequencies for clamped and free rectangular plates are presented in Eqs. (8.89) and (8.90). The resulting eigen-

Table 8.2 Parameters G_m and H_m in Eq. (8.89), homogeneous rectangular plate, all sides clamped

m	G_m	H_m
$m = 1$	1.506	1.248
$m > 1$	$m + 1/2$	$G_m^2 \left[1 - \frac{2}{\pi G_m} \right]$

G_n and H_n are obtained by replacing m by n in the table above

Table 8.3 Parameters G_m , H_m , and J_m in Eq. (8.90), homogeneous rectangular plate, all sides free

m	G_m	H_m	J_m
0	0	0	0
1	0	0	1.216
2	1.506	1.248	5.017
>2	$m - 1/2$	$G_m \left[1 - \frac{2}{\pi G_m} \right]$	$G_m^2 \left[1 + \frac{6}{\pi G_m} \right]$

G_n , H_n and J_n are obtained by replacing m by n in the table above

frequencies given by the Eqs. (8.89) and (8.90) should, according to Ref. [62], be within 1.05 times of the correct value.

1. Natural frequencies for homogeneous rectangular plate with clamped edges, bending stiffness D_0 , mass per unit area μ and sides L_x and L_y

$$f_{mn} = \frac{\pi}{2} \sqrt{\frac{D_0}{\mu}} \left[\left(\frac{G_m}{L_x} \right)^4 + \left(\frac{G_n}{L_y} \right)^4 + \frac{2H_m H_n}{(L_x L_y)^2} \right]^{1/2}. \quad (8.89)$$

The parameters G_m and H_m are given in Table 8.2.

2. Natural frequencies for homogeneous rectangular plate with free edges, bending stiffness D_0 , mass per unit area μ and sides L_x and L_y

$$f_{mn} = \frac{\pi}{2} \sqrt{\frac{D_0}{\mu}} \left[\left(\frac{G_m}{L_x} \right)^4 + \left(\frac{G_n}{L_y} \right)^4 + \frac{2J_m J_n + 2\nu(H_m H_n - J_m J_n)}{(L_x L_y)^2} \right]^{1/2} \quad (8.90)$$

The parameters G_m , H_m , and J_m are given in Table 8.3.

Predicted and measured eigenfrequencies have been compared for a 4-mm Al plate with the dimensions $L_x = 1.34$ m and $L_y = 0.74$ m. The plate was bolted to a wooden frame. The edges were assumed to be clamped. In practice this boundary condition can never quite be achieved. The wooden box has a certain flexibility and is consequently far from being infinitely stiff. The mode shapes and eigenfrequencies for the plate were determined by means of the modal-analysis technique, see for example Ref. [12]. A comparison between predicted and measured eigenfrequencies is made in Table 8.4.

Except for mode (1,2) the eigenfrequencies predicted according to Eq. (8.25) deviate by less than 5 % from the measured values. Some resulting measured mode shapes are shown in Fig. 8.11.

The method discussed can be used to calculate eigenfrequencies for any combination of simply supported, clamped, and free edges for a rectangular plate. A number of examples are given in Ref. [62].

It can be shown—see Ref. [58]—that if a plate is subjected to constraining conditions, the fundamental tone and every overtone become higher. Conversely, if the

Table 8.4 Eigenfrequencies for a clamped 4 mm thick and 1.34 m by 0.74 m Al plate

Mode		f_{mn} (Hz)	
m	n	Predicted	Measured
1	1	45.3	45.0
2	1	62.2	61.9
3	1	91.8	90.1
1	2	116.2	107.1
2	2	132.2	126.6
4	1	133.4	130.5

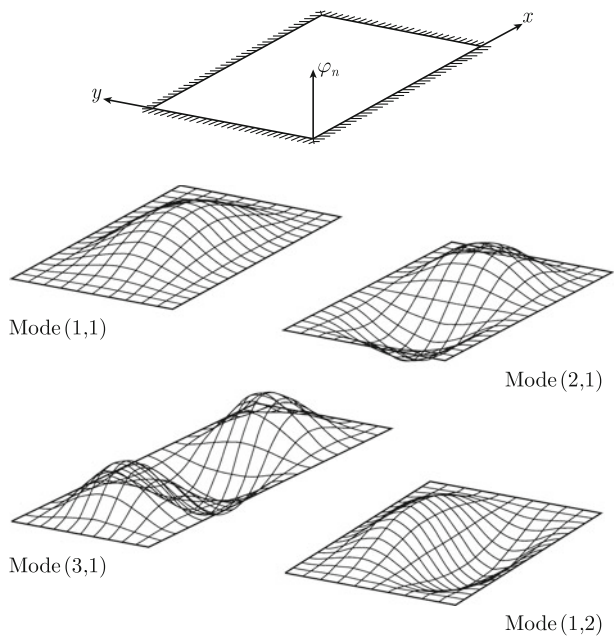


Fig. 8.11 Measured mode shapes for a clamped 4 mm rectangular aluminum plate, length 1.34 m and width 0.74. The first four modes are (1,1), (2,1), (3,1), and (2,1)

constraining condition is removed, the fundamental eigenfrequency and every consecutive eigenfrequency become lower. Therefore, if a plate develops a crack, its eigenfrequencies decrease. This general observation can form the basis for the condition monitoring of plates. The first few eigenfrequencies for various plate structures, which are vital parts of a large construction, are measured at regular time intervals. If the resonance frequencies decrease over time, this indicates that the structure has been damaged or cracks developed.

The Rayleigh method has been further developed by Ritz. According to the Rayleigh–Ritz method the deflection of a plate could be given by several functions

$\Phi_i(x, y)$. Each function must satisfy the boundary conditions for the plate. The trial function F can thus be written as

$$F(x, y) = C_1 \cdot \Phi_1(x, y) + C_2 \cdot \Phi_2(x, y) + \cdots + C_n \cdot \Phi_n(x, y). \quad (8.91)$$

The parameter C_i can be considered as an amplitude for each function Φ_i each approximating the first to the n :th vibrational mode of the plate. The expression Eq. (8.91) inserted in the Eqs. (8.84) and (8.85) results in

$$\mathcal{U}_{\max} = \mathcal{H}_1(C_1, C_2, \dots, C_n), \quad \mathcal{T}_{\max} = \omega^2 \cdot \mathcal{H}_2(C_1, C_2, \dots, C_n). \quad (8.92)$$

If these expressions are somewhat cumbersome to calculate, trial functions are preferably chosen so that the functions $\Phi_i(x, y)$ are orthogonal to eliminate cross products. In the previous case leading up to Eq. (8.87), only one mode was considered at each time. The eigenfrequency was obtained by setting \mathcal{T}_{\max} equal to \mathcal{U}_{\max} . Using the Rayleigh–Ritz method, several trial functions are introduced and the difference $\mathcal{U}_{\max} - \mathcal{T}_{\max}$ is instead minimized with respect to the constants C_1 to C_n . This results in

$$\frac{\partial \mathcal{H}_1}{\partial C_i} - \omega^2 \cdot \frac{\partial \mathcal{H}_2}{\partial C_i} = 0. \quad (8.93)$$

This operation leads to a system of equations of the form

$$\begin{bmatrix} a_{11} - \omega^2 b_{11} & \cdots & a_{1n} - \omega^2 b_{1n} \\ \vdots & \ddots & \vdots \\ a_{n1} - \omega^2 b_{n1} & \cdots & a_{nn} - \omega^2 b_{nn} \end{bmatrix} \begin{Bmatrix} C_1 \\ \vdots \\ C_n \end{Bmatrix} = 0 \quad (8.94)$$

By setting the determinant of the $n \times n$ matrix equal to zero an equation of the n -th order in ω^2 is obtained. The solutions result in the n natural frequencies. The lowest value of ω corresponds to the first mode etc. The predicted eigenfrequencies are always higher or equal to the correct results. Equality holds if the assumed mode shapes or trial functions are identical to the correct ones. The mode shape is also obtained by solving C_i for each natural frequency and substituting the results into Eq. (8.91) which then gives the approximate mode shape corresponding to each natural frequency. The technique plus other variational methods are discussed further in Chap. 9.

8.7 Application of the Rayleigh–Ritz Method

The variational technique or the Rayleigh–Ritz method is preferably illustrated by an example. In many types of constructions stiffened plates are used as supporting elements. Typical examples are ships, aircrafts, trains, and in fact also ordinary

buildings. When this type of stiffened structure is excited by a mechanical force the response very much depends on frequency. In the low frequency range global vibrations dominate. This means that stiffeners and plates to a very large extent move together like some equivalent plate structure. At and above the first eigenfrequency of a subsystem, plate elements between frames and junctions tend to vibrate as more or less separate systems.

One problem is illustrated in Fig. 8.12 showing a stiffened simply supported rectangular plate. The ratio L_x/L_y between the lengths of the sides is set to equal 3 in this example. The Young's modulus, density, Poisson's ratio, and thickness are for the plate denoted E , ρ , ν , and h , respectively. The eigenfrequencies for the unribbed and simply supported plate are

$$f_{mn} = \frac{1}{2\pi} \sqrt{\frac{D_0}{\mu}} \cdot \left[\left(\frac{m\pi}{L_x} \right)^2 + \left(\frac{n\pi}{L_y} \right)^2 \right], \quad D_0 = \frac{E_0 h^3}{12(1-\nu^2)}, \quad \mu = \rho h.$$

For this specific case, $L_x = 3L_y$, the first few natural frequencies are

$$\begin{aligned} f_{11} &= \frac{5\pi}{L_x^2} \sqrt{\frac{D_0}{\mu}}, & f_{21} &= 1.3 \cdot f_{11}, & f_{31} &= 1.8 \cdot f_{11} \\ f_{41} &= 2.5 \cdot f_{11}, & f_{51} &= 3.4 \cdot f_{11}, & f_{12} &= 3.7 \cdot f_{11}. \end{aligned} \quad (8.95)$$

In order to reinforce the plate, a rib is mounted symmetrically across the plate along the line $x = L_x/2$. The total height of the rib is H and its width is b . The material parameters for rib and plate are the same. Obviously the addition of the rib changes the mass and stiffness of the plate element. This in turn changes the vibration pattern as well the eigenfrequencies of the system. If the rib is sufficiently stiff, it can be expected that the boundary conditions for the two plate elements on each side of the stiffener vibrate as if they were simply supported along three edges and clamped along the fourth edge defined by the rib.

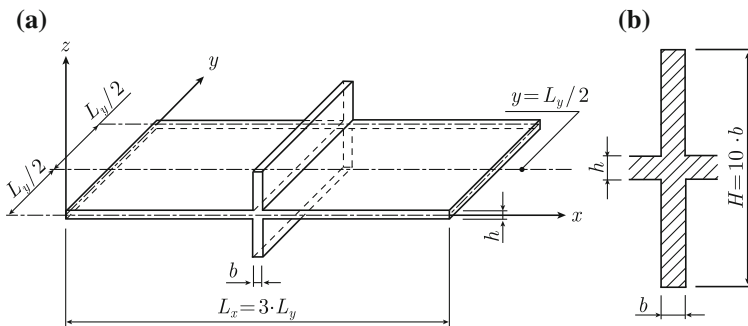


Fig. 8.12 A rectangular and ribbed simply supported plate

For the plate without the rib, the first four eigenfrequencies f_{11} , f_{21} , f_{31} , and f_{41} are given in Eq. (8.95). These frequencies can also be obtained by using a suitable trial function in combination with the Rayleigh–Ritz technique. The trial function $F(x, y)$ is defined as

$$F(x, y) = \sin(k_y y)[C_1 \sin(k_x x) + C_2 \sin(2k_x x) + C_3 \sin(3k_x x) + C_4 \sin(4k_x x)]$$

$$k_x = \pi / L_x, \quad k_y = \pi / L_y = 3k_x. \quad (8.96)$$

The trial function satisfies the simply supported boundary condition along the periphery of the plate. The functions $\sin(k_y y)$, $\sin(k_x x)$, etc., are orthogonal for the plate element. For the plate without the rib, the trial function (8.96) yields the correct eigenfrequencies for the first four modes, namely the modes (1,1), (2,1), (3,1), and (4,1). The parameters C_i are determined as described in Sect. 8.6.

The first few eigenfrequencies for the reinforced plate can be estimated following the Rayleigh–Ritz procedure. Consequently the kinetic and potential energies for the total system, plate and reinforcing beam, must be calculated. For the plate, the maximum potential energy is, according to Eq. (8.86), equal to

$$v_p = \frac{D_0}{2} \iint_S dx dy \left[\left(\frac{\partial^2 F}{\partial x^2} \right)^2 + \left(\frac{\partial^2 F}{\partial y^2} \right)^2 + 2 \left(\frac{\partial^2 F}{\partial x \partial y} \right)^2 \right].$$

Considering the orthogonality of the sine functions, the trial function Eq. (8.96) inserted in the integral expression yields

$$v_p = \frac{100 D_0 L_x L_y k_x^4}{8} [C_1^2 + 1.69 \cdot C_2^2 + 3.24 \cdot C_3^2 + 6.25 \cdot C_4^2]. \quad (8.97)$$

The corresponding expression defining the maximum kinetic energy for the plate is

$$T_p = \frac{\mu \omega^2}{2} \iint_S dx dy F^2 = \frac{\mu \omega^2 L_x L_y}{8} [C_1^2 + C_2^2 + C_3^2 + C_4^2]. \quad (8.98)$$

The stiffener is exposed to both bending and twisting or torsion. The bending stiffness D_s , torsional stiffness T_s , and moment of inertia I_s are as defined in Sects. 3.5 and 3.7, given by

$$D_s = b H^3 E / 12, \quad T_s = G \cdot f(H/b) \cdot H b^3 / 3, \quad I_s = (b H^3 + H b^3) / 12. \quad (8.99)$$

The shear stiffness of the stiffener is G . The function $f(H/b)$ is tabulated in Sect. 3.5. For simplicity it is assumed that $H/b = 10$. This means that $f(H/B) = 0.937$ and $I_s \approx b H^3 / 12$.

The angle $\theta(y)$, defining the rotation of the stiffener, is given by $\partial F / \partial x$ evaluated for $x = x_1 = L_x / 2$. The potential energy, due to bending and rotation, is obtained for stiffener as discussed in Sects. 3.5 and 3.7. Considering the definition of the rotational

angle and the deflection along the line $x = x_1 = L_x/2$, the potential energy for the stiffener is given by

$$\mathcal{U}_s = \frac{D_s}{2} \int_0^{L_y} dy \left[\frac{\partial^2 F(x_1, y)}{\partial y^2} \right]^2 + \frac{T_s}{2} \int_0^{L_y} dy \left[\frac{\partial \theta(y)}{\partial y} \right]^2.$$

The general function $F(x, y)$, Eq. (8.96), defines the deflection of plate and stiffener. This function $F(x, y)$ inserted in the expression for the potential energy for the stiffener results in

$$\begin{aligned} \mathcal{U}_s &= 81 \cdot \frac{D_s k_x^4 L_y}{4} [C_1 - C_3]^2 + 9 \cdot \frac{T_s k_x^4 L_y}{4} [2C_2 - 4C_4]^2 \\ &= 100 \cdot \frac{D_0 k_x^4 L_x L_y}{8} [X(C_1 - C_3)^2 + Y(C_2 - 2C_4)^2]. \end{aligned} \quad (8.100)$$

The parameters X and Y are

$$X = 0.81 \left(\frac{H}{h} \right)^3 \left(\frac{2b}{L_x} \right) (1 - \nu^2), \quad Y = 1.35(1 - \nu) \left(\frac{Hb^3}{h^3 L_x} \right). \quad (8.101)$$

The kinetic energy for the stiffener is

$$\begin{aligned} \mathcal{T}_s &= \frac{\omega^2 b H \rho}{2} \int_0^{L_y} dy [F(x_1, y)]^2 + \frac{\omega^2 I_s \rho}{2} \int_0^{L_y} dy [\theta(y)]^2 \\ &= \frac{\omega^2 b H \rho L_y}{4} (C_1 - C_3)^2 + \frac{\omega^2 I_s \rho k_x^2 L_y}{4} (2C_2 - 4C_4)^2 \\ &= \frac{\mu \omega^2 L_x L_y}{8} [Z(C_1 - C_3)^2 + W(2C_2 - 4C_4)^2]. \end{aligned} \quad (8.102)$$

The parameters Z and W are

$$Z = \frac{2bH}{hL_x}, \quad W = \frac{2k_x^2 b H^3}{3hL_x}. \quad (8.103)$$

For the total kinetic energy to be equal to the potential energy, it follows that $\mathcal{U}_p + \mathcal{U}_s = \mathcal{T}_p + \mathcal{T}_s$. Based on the results Eqs. (8.92) and (8.95) and the expressions defining the energies, i.e., Eqs. (8.97), (8.98), (8.100), and (8.102), this condition can be formulated as

$$\begin{aligned} \left(\frac{f}{f_{11}} \right)^2 &= \frac{\mathcal{H}_1}{\mathcal{H}_2} \\ \mathcal{H}_1 &= C_1^2 + 1.69C_2^2 + 3.24C_3^2 + 6.25C_4^2 + X(C_1 - C_3)^2 + Y(C_2 - 2C_4)^2 \\ \mathcal{H}_2 &= C_1^2 + C_2^2 + C_3^2 + C_4^2 + Z(C_1 - C_3)^2 + W(C_2 - 2C_4)^2. \end{aligned} \quad (8.104)$$

The eigenfrequencies for the entire system are given by f satisfying Eq. (8.104). The ratio $(f/f_{11})^2 = \Omega$ is according to Eq. (8.92) obtained by minimizing the expression $(f/f_{11})^2 = \mathcal{H}_1/\mathcal{H}_2$ in (8.104) with respect to the parameters C_i . This leads to a set of equations given by

$$\frac{\partial \mathcal{H}_1}{\partial C_i} - \Omega \frac{\partial \mathcal{H}_2}{\partial C_i} = 0.$$

The result can be written in matrix form as

$$[W] \begin{Bmatrix} C_1 \\ C_2 \\ C_3 \\ C_4 \end{Bmatrix} = 0$$

where

$$[W] = \begin{bmatrix} 1 + X - \Omega(1 + Z) & 0 & -(X - Z\Omega) & 0 \\ 0 & 1.69 + Y - \Omega(1 + W) & 0 & -2(Y - W\Omega) \\ -(X - Z\Omega) & 0 & 3.24 + X - \Omega(1 + Z) & 0 \\ 0 & -2(Y - W\Omega) & 0 & 6.25 + 4Y - \Omega(1 + 4W) \end{bmatrix} \quad (8.105)$$

Solutions in Ω are obtained by setting the determinant of the 4×4 matrix equal to zero. Due to the symmetry of the matrix, the result is two second degree equations in Ω . The solution giving the lowest value corresponds to the first eigenfrequency etc. The resulting natural frequencies are $f = f_{11}\sqrt{\Omega}$. The result is shown in Fig. 8.13. The eigenfrequencies are calculated as functions of the ratio b/h between the width of the stiffener and the thickness of the plate. The total height H of the beam is as before $10 \cdot b$. The figure shows that with no stiffener the first four eigenfrequencies are f_{11} , $1.3 \cdot f_{11}$, $1.8 \cdot f_{11}$, and $2.5 \cdot f_{11}$ as given in Eq. (8.95) for the undisturbed case. As the stiffness of the rib increases the eigenfrequencies for the first and second modes get closer. The eigenfrequency for the third mode increases rapidly as the stiffness

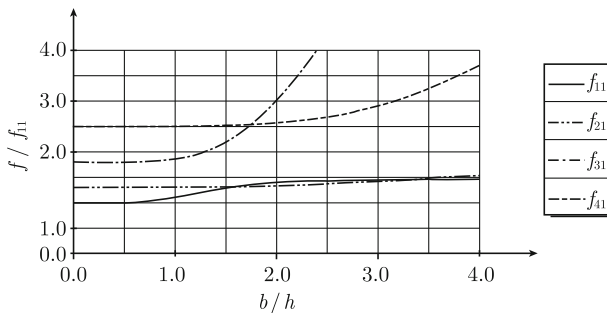


Fig. 8.13 The first four eigenfrequencies for a stiffened plate as function of the stiffness of the rib. The thickness of the beam is b and of the plate h . The total height of the beam is $H = 10b$. The first eigenfrequency of the unribbed plate $b/h = 0$ is f_{11}

of the rib increases. This is obvious since the rib tend to prevent the excitation of this particular mode. As the stiffness of the mode is increased due to the rib so is the eigenfrequency for the mode. The accuracy of the estimates f_{31} and f_{41} is much improved if in Eq. (8.96) additional trial functions like $\sin(5k_x x)$ and $\sin(6k_x x)$ are included. In particular this is the case when the ratio b/h is increased.

The parameters C_i are the solutions to the matrix equation by inserting solutions of Ω . For the first mode the ratio between C_3 and C_1 is obtained from the third line as

$$C_3[3.24 + X - \Omega(1 + Z)] = C_1(X - Z\Omega).$$

For the first mode the amplitude C_1 can be set to equal unity. For the first mode C_2 and C_4 are always equal to zero. For the second mode C_2 is for $C_4 = 1$ obtained from the second line in the matrix and so on. The resulting first two mode shapes along the line $y = L_y/2$ are shown in Figs. 8.14 and 8.15. For the unribbed plate, $b/h = 0$, the displacement along the center line $y = L_y/2$ is given by a simple sine function. The introduction of the rib as given by the curve $b/h = 1$ slightly flattens the mode shape as compared to the undisturbed case. The motion of the entire

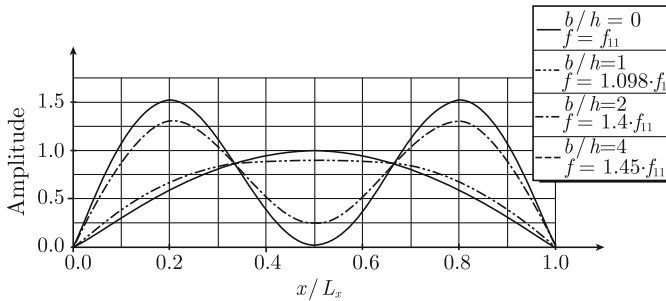


Fig. 8.14 Displacement along the line $y = L_y/2$ for the first vibrational mode for the unribbed plate, $b/h = 0$, and for the plate with a rib of increasing stiffness $b/h = 1, 2$ and 4

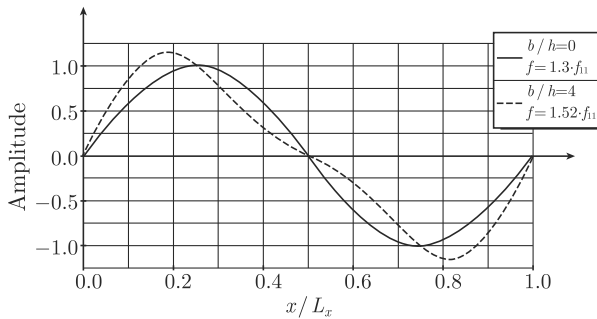


Fig. 8.15 Displacement along the line $y = L_y/2$ for the second vibrational mode for the unribbed plate, $b/h = 0$, and for the plate with a rib for which $b/h = 4$

structure is still dominated by global vibrations. As the stiffness of the rib increases the motion along the rib decreases. The plate sections tend to vibrate as if they were clamped along the rib. For the first mode the displacement is symmetric with respect to the rib. The second mode shown in Fig. 8.15 is asymmetric. Even for the second mode, the rotation at the center of the plate decreases as the stiffness increases. The displacements of the first and second modes have for $x < L_x/2$ similar shapes for $b/h = 4$. The corresponding eigenfrequencies are consequently rather close.

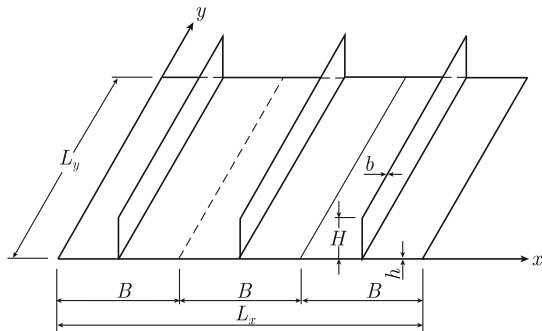
The accuracy of the calculations is improved as the number of trial functions increases. If many modes are considered, the complexity of the calculations could be a limiting factor. A Finite Element Method, FEM, calculation should then be preferred. The FEM procedure is in fact also a variational technique.

The problem discussed does not really represent a typical case of a ribbed panel. In most cases a rib or stiffener is mounted asymmetrically, i.e., the stiffener is mounted on one side of the plate. This means that the neutral axes for rib and plate do not coincide. The implication of this effect is discussed for some stiffened structures in Ref. [25]. In this reference, expressions giving the fundamental mode of stiffened plates are derived. According to this simplified model, the maximum potential energy for a stiffened plate of the type shown in Fig. 8.16 is written as

$$\mathcal{U}_{\max} = \frac{1}{2} \iint_S dx dy \left[D_x \left(\frac{\partial^2 F}{\partial x^2} \right)^2 + D_y \left(\frac{\partial^2 F}{\partial y^2} \right)^2 + 2\sqrt{D_x D_y} \left(\frac{\partial^2 F}{\partial x \partial y} \right)^2 \right].$$

The bending stiffness D_x per unit width of the plate is set to equal the bending stiffness of the plate element in the x direction. Thus, for the geometry shown in the figure, $D_x = Eh^3/[12(1 - \nu^2)]$. The bending stiffness in the y direction is assumed to be determined by the stiffener and part of the plate element. The width of the plate element is B or equal to the distance between two of the equi-distant frames. For the structure in Fig. 8.16 the bending stiffness D_y per unit width of the plate is given by the bending stiffness of the beam element divided by the width of the beam which is B or the distance between two equi-distant frames. Consequently the bending stiffness D_y per unit width is given by

Fig. 8.16 Stiffener mounted to one side of plate only



$$D_y = \frac{E}{B} \left[\frac{bH^3}{12} + q^2(bH + Bh) - qH^2b + \frac{Bh^3}{12(1 - \nu^2)} \right], \quad q \approx \frac{bH^2}{2(bH + Bh)}.$$

The kinetic energy can be calculated as indicated above with respect to the symmetric beam. For the first fundamental mode, the rotation of the beam can be neglected, i.e., the moment of inertia is set to equal zero.

Although the method discussed above is widely used to predict eigenfrequencies of stiffened plates it is obvious that a number of simplifications are made. A more rigorous approach is presented in Ref. [63]. In this case the FEM technique is used to solve the problem. It can be concluded that more complicated problems concerning stiffened plates are most easily solved by means of a FEM calculation. However the variational approach discussed in for example Ref. [64] can be a powerful alternative to a traditional FEM calculation.

8.8 Non-Flat Plates

In the previous, section methods for predicting eigenfrequencies for plates were discussed. The plates were assumed to be completely flat and the boundary conditions were idealized. It was found that the first eigenfrequency for a simply supported plate was approximately increased by a factor 2.25 by clamping the edges of the plate. The boundary conditions for plates which are part of large built-up constructions are neither completely simply supported nor clamped. For many practical applications a proper modelization of the boundary conditions can be difficult or even impossible. Boundary conditions not only depend on geometries of the complete built-up structure but also on joints and couplings supporting each individual element. It has been demonstrated, Ref. [65], that apparently identical and simple objects like beer cans can exhibit very different dynamic properties. These differences are caused by minor irregularities which shift the eigenfrequencies of the objects.

Not only the boundary conditions but also the shape of a structure can be changed during a manufacturing and mounting process. A slight curvature of a structure can be introduced during this process. Plate elements in real constructions like cars, trains, ships, aircrafts, etc., are seldom or never completely flat. Even a slight curvature introduced in a plate can alter its stiffness considerably. This effect has been investigated by Jarvis and is discussed in Ref. [66]. A thin rectangular steel plate with free boundaries is considered. A curvature of the plate is introduced. The Finite Element Method is used to calculate the first few eigenfrequencies for the plate with different curvatures. The plate, made of steel, is 0.8 mm thick, 400 mm long and 200 mm wide. The dimensions are representative for plate elements used in many types of vehicles. The plate structure is shown in Fig. 8.17.

The curvature of the plate is defined by the parameter δ , measured as the center point displacement as shown in Fig. 8.17. The modes (1,0), (2,0), (0,1), and (3,0) for a perfectly flat plate are shown in Fig. 8.18. The modes (m , 0) are along the length of the plate. The torsional modes are not included. The predicted eigenfrequencies are given

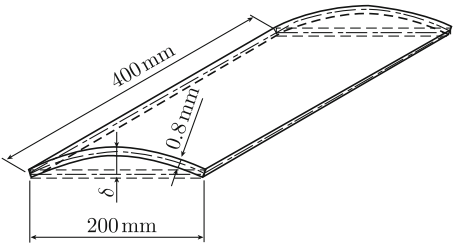


Fig. 8.17 A rectangular plate with a curvature

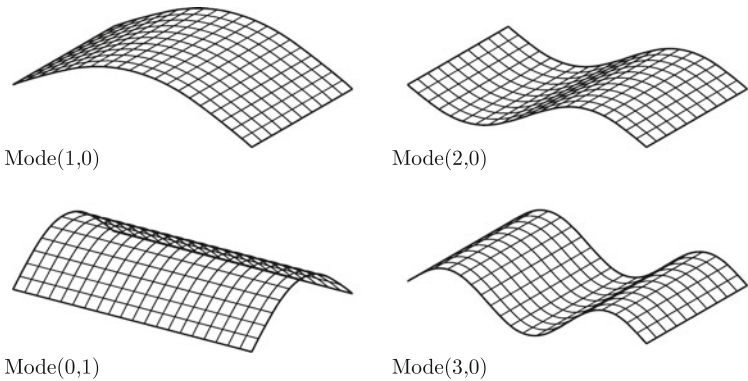


Fig. 8.18 The modes (1,0), (2,0), (0,1), and (3,0) for a perfectly flat plate

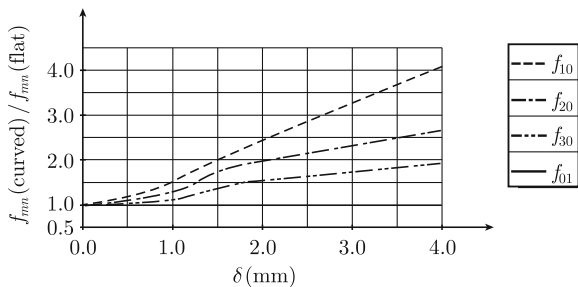
Table 8.5 Eigenfrequencies for an 0.8 mm rectangular steel plate, 200 mm \times 400 mm, with free edges and a curvature δ

Curvature δ (mm)	Eigenfrequency f_{mn} for mode (m, n)			
	f_{10} (Hz)	f_{20} (Hz)	f_{01} (Hz)	f_{30} (Hz)
0	26.5	73.6	108.7	146.6
0.5	30.6	80.2	108.7	152.8
1	40.4	96.6	109.2	167.5
2	65.2	145.1	109.6	223.9
4	107.9	194.2	111.2	282.0

in Table 8.5 for $\delta = 0, 0.5, 1, 2$, and 4 mm. The results are also illustrated in Fig. 8.19 as the ratio between the eigenfrequency for a curved plate and the corresponding eigenfrequency for the flat plate.

The effect of a curvature on some of the eigenfrequencies is quite dramatic. The eigenfrequencies of thin plates are very sensitive to an out-of-plane curvature. The modes $(m, 0)$, orthogonal to the direction of curvature, being the most influenced. It is also concluded in Ref. [66] that thick plates are less sensitive than thin plates to a change of curvature.

Fig. 8.19 The ratio between some eigenfrequencies $(f_{mn})_{\text{curved}}$ for a *curved* plate and the corresponding eigenfrequencies $(f_{mn})_{\text{flat}}$ for a *flat* plate. The ratio is given as function of the curvature δ for the modes (1,0), (2,0), (0,1), and (3,0)



When part of a large construction, thin plates often have a double curvature. It could be claimed that there is no such thing as an absolutely flat thin plate. Certain statistical methods have been developed for the prediction of the response of plates with boundary conditions and dynamic parameters which are not well defined. This is often referred to as fuzziness. The technique to deal with fuzzy structures is discussed in detail in Ref. [68].

8.9 The Effect of an Added Mass or Mass-Spring System on Plate Vibrations

If for example a small object is mounted on a homogeneous plate, the effective mass of the structure is no longer uniformly distributed over the surface. The natural question is then: How does the added mass affect the vibration pattern of the plate? A typical practical problem is the measurement of plate vibrations by means of accelerometers. An accelerometer, a small mass Δm , is mounted on the plate in order to determine the response of the plate. The Rayleigh–Ritz method discussed in Sect. 8.6 could always be used to estimate mode shapes and natural frequencies for the perturbed case, as well as for the plain plate. However, the effect of the added mass on the natural frequencies of the system could also be estimated, by considering the modal stiffness and the modal mass of the system.

Assume that the eigenvectors φ_{mn} and the corresponding eigenfrequencies f_{mn} are known for the unperturbed plate. Let the corners of the rectangular plate have the coordinates $(0, 0)$, $(L_x, 0)$, (L_x, L_y) , and $(0, L_y)$. The modal stiffness K_{mn} and modal mass M_{mn} are obtained from Eq. (8.38) as

$$M_{mn} = \int_0^{L_x} \int_0^{L_y} dx dy \mu(x, y) \varphi_{mn}^2(x, y), \quad K_{mn} = \int_0^{L_x} \int_0^{L_y} dx dy D \kappa_{mn}^4 \varphi_{mn}^2(x, y)$$

The function $\mu(x, y)$ is the mass per unit area of the plate. For a homogeneous plate, density ρ , thickness h , $\mu(x, y) = \rho h$. For the same plate with a point mass Δm attached at the coordinates (x_0, y_0) the mass per unit area of the entire plate is

$$\mu(x, y) = \rho h + \Delta m \cdot \delta(x - x_0)\delta(y - y_0).$$

The modal mass but not the modal stiffness is changed by the added mass. For a simply supported rectangular plate the eigenvectors φ_{mn} are

$$\varphi_{mn}(x, y) = \sin(m \pi x / L_x) \sin(n \pi y / L_y).$$

The total modal mass of the plate plus the point mass is

$$\begin{aligned} M_{mn} &= \int_0^{L_x} \int_0^{L_y} dx dy [\rho h + \Delta m \delta(x - x_0)\delta(y - y_0)] \varphi_{mn}^2(x, y) \\ &= \frac{L_x L_y \rho h}{4} + \Delta m \cdot \varphi_{mn}^2(x_0, y_0) \\ &= \frac{m_p}{4} \left[1 + \frac{4 \Delta m}{m_p} \varphi_{mn}^2(x_0, y_0) \right]. \end{aligned} \quad (8.106)$$

The mass of just the plate is given by m_p . The eigenfrequency f_{mn} for the plate with the added mass is

$$f_{mn} = \frac{1}{2 \pi} \sqrt{\frac{K_{mn}}{M_{mn}}}.$$

The ratio between the natural frequencies f'_{mn} —with the added mass—and f_{mn} without the mass is

$$\frac{f'_{mn}}{f_{mn}} = \frac{1}{\left[1 + \frac{4 \Delta m}{m} \cdot \varphi_{mn}^2(x_0, y_0) \right]^{1/2}}. \quad (8.107)$$

The ratio given in Eq. (8.107) represents the frequency shift due to the mass for mode (m, n) . The addition of a mass decreases the natural frequency of the structure. The wavenumber is a function of the mass of the plate and it is consequently also shifted due to the perturbation. The wavenumber for the perturbed plate is

$$\kappa^4 = \kappa_0^4 \left[1 + \frac{4 \Delta m}{m} \varphi_{mn}^2(x_0, y_0) \right]. \quad (8.108)$$

In this context, κ_0 is the wavenumber for the plate without the small mass.

A small added mass can change the point mobility of a plate considerably. This is a problem encountered when the impedance or mobility of a plate is measured by a force transducer and an accelerometer instead of an impedance head. The problem is illustrated in Fig. 8.20. A force $F = F_0 \cdot \exp(i\omega t)$ is applied to a plate. An accelerometer with the mass Δm is mounted on the opposite side of the plate. The velocity at the point of excitation is v . The resulting force F_r on the plate due to the mass is



Fig. 8.20 Measurement of point mobility

$$F_r = \Delta m \cdot i\omega v \cdot \exp(i\omega t).$$

The plate without the small mass has the point mobility Y_0 . The resulting effective force F_{eff} acting on the plate itself is

$$F_{\text{eff}} = (F_0 - \Delta m \cdot i\omega v) \cdot \exp(i\omega t).$$

The velocity at the excitation point can also be expressed by means of the point mobility Y_0 of the plate as

$$v = Y_0 F_{\text{eff}} = F_0 Y_0 \exp(i\omega t) / (1 + i\omega \Delta m Y_0). \quad (8.109)$$

The measured point mobility is the ratio between the Fourier transform of the external force and the Fourier transform of the resulting velocity or $Y_{\text{measured}} = v/F_0$. Thus, $F_0 = v/Y_{\text{measured}}$. This expression inserted in Eq. (8.109) yields

$$Y_{\text{measured}} = \frac{Y_0}{1 + i\omega \Delta m Y_0}. \quad (8.110)$$

In the low frequency region the measured point mobility is approximately equal to the actual mobility Y_0 of the plate. However as the frequency increases the second term in the denominator tends to increase. At the limit, the measured mobility is equal to $1/(i\omega \Delta m)$ which is the point mobility of the added mass.

If a constant force is acting on a structure the power input to the structure is proportional to the real part of the point mobility at the excitation point. In order to minimize the input power the mobility of the structure should be made as low as possible. For example the mobility of an engine foundation should be small to reduce the power to the foundation and to the supporting structures. In certain cases the mobility of a plate structure can be drastically changed by the addition of a tuned damper to the plate. As an example let the mobility of the added structure be Y_x . The resulting FT of the force on the structure is $F = v/Y_x$ where v is the FT of the velocity of the plate. Following the discussion leading up to Eq. (8.109), that the total mobility, plate plus added structure, is

$$Y_{\text{tot}} = \frac{1}{1/Y_0 + 1/Y_x} = \frac{Y_0 Y_x}{Y_0 + Y_x}.$$

Consider a simple tuned damper or rather a mass-spring system shown in Fig. 1.11b. Let the velocity of the mass and foundation be v_x and v_y , respectively. The equation of motion of the system is $v_x(k - m\omega^2) = kv_y$. The mass is m and the stiffness of the spring $k = k_0(1 + i\delta)$ where δ is the loss factor of the spring. The reacting force on the foundation is $F_y = k(v_y - v_x)/(i\omega)$. Using the first expression the force on the plate is

$$F_y = -\frac{v_y km\omega^2}{i\omega(k - m\omega^2)}.$$

The mobility of the mass-spring is consequently

$$Y_x = \frac{v_y}{F_y} = -\frac{i}{m\omega} \left(1 - \frac{m\omega^2}{k}\right) = -\frac{i}{m\omega} \left[1 - \left(\frac{f}{f_0}\right)^2 (1 - i\delta)\right],$$

where f_0 is the natural frequency of the simple mass-spring system. For $f = f_0$ the imaginary part of Y_x is zero resulting in that the total mobility also is small. For an infinite plate with a point mobility $Y_0 = 1/(8\sqrt{\mu D})$ and an added mass-spring system at the excitation point the real part of the point mobility of plate plus damper is for $f = f_0$

$$\text{Re}Y_{\text{tot}} \approx \frac{\delta}{m\omega}.$$

For a mechanical source running at a constant rpm tuned dampers can effectively reduce the power input to the foundation if the tuned damper is mounted at or close to the coupling point between source and foundation. However for $f \neq f_0$ the effect of the damper is insignificant or even negative. By increasing the losses of the mass-spring system, the device can have a good effect at frequencies slightly off the natural frequency f_0 . The added losses will also increase the total mobility Y_{tot} which will reduce the efficiency of the system at $f = f_0$.

If just a mass m is mounted to the foundation the mobility Y_x is obtained as $Y_x = 1/(im\omega)$. For an infinite plate and an added mass the real part of the total mobility at the point where the mass is mounted is

$$\text{Re}Y_{\text{tot}} \approx \frac{8\sqrt{\mu D_0}}{(8\sqrt{\mu D_0})^2 + (m\omega)^2}.$$

For the added mass to have a significant effect on the input power to the plate it is required that $m\omega \gg 8\sqrt{\mu D}$. Engine foundations and resilient mounting of mechanical sources or engines are discussed in Chap. 10.

8.10 Small Disturbances

The effect on eigenfrequencies caused by a small mass mounted on a plate was discussed in the previous section. Based on elementary perturbation theory the calculation procedure can be formulated in a more general way as described in Ref. [69]. The starting point is a general formulation of an eigenvalue problem defined as

$$Lw = \lambda w. \quad (8.111)$$

L is a linear operator and λ the corresponding eigenvalue. The displacement of the structure is w . For a plate under flexure, time dependence $\exp(i\omega t)$, the differential equation governing the lateral displacement w is

$$\frac{D}{\mu} \nabla^2 (\nabla^2 w) - \omega^2 w = 0.$$

Bending stiffness and mass per unit area are denoted D and μ , respectively. For this particular case the operator L is defined as $(D/\mu) \nabla^2 \nabla^2$. The eigenfunctions and the corresponding eigenvalues which satisfy Eq. (8.111) are φ_m and λ_m , respectively. Thus $L\varphi_m = \lambda_m \varphi_m$. For small disturbances the operator L is almost equal to the operator L^0 for the undisturbed case, or expressed as

$$L = L^0 + Q \quad (8.112)$$

The operator Q is small as compared to L^0 . It is assumed that the eigenvalues λ_m and eigenfunctions corresponding to the disturbed case can be expressed as

$$\lambda_m = \lambda_m^0 + \lambda_m^1 + \dots, \quad \varphi_m = \varphi_m^0 + \sum_n a_{mn} \varphi_n^0. \quad (8.113)$$

For the disturbance to be termed “small” it is required that $|\lambda_m^0| \gg |\lambda_m^1|$ and $|a_{mn}| < 1$. From Eq. (8.113) it follows that φ_m satisfies the same boundary conditions as φ_m^0 . It is convenient to impose the additional conditional that the norm of φ_m is equal to the norm of φ_m^0 . The norm of φ_m is obtained from (8.113) as

$$\begin{aligned} \langle \varphi_m | \varphi_k \rangle &= \int \varphi_m \varphi_k dx = \int dx \left(\varphi_m^0 + \sum_n a_{mn} \varphi_n^0 \right) \left(\varphi_k^0 + \sum_n a_{kn} \varphi_n^0 \right) \\ &= \langle \varphi_m^0 | \varphi_k^0 \rangle + a_{mk} \langle \varphi_k^0 | \varphi_m^0 \rangle + a_{km} \langle \varphi_m^0 | \varphi_k^0 \rangle + \dots \end{aligned}$$

The eigenfunctions φ_m are orthogonal. Thus for $m = k$ it follows that $a_{mm} = 0$, since the norms of the perturbed and unperturbed eigenvectors are set to be equal. The basic eigenvalue problem Eq. (8.111) can, according to the Eqs. (8.112) and (8.113), be written as

$$(\mathbf{L}^0 + \mathbf{Q}) \left(\varphi_m^0 + \sum_{n \neq m} a_{mn} \varphi_n^0 \right) = (\lambda_m^0 + \lambda_m^1) \left(\varphi_m^0 + \sum_{n \neq m} a_{mn} \varphi_n^0 \right).$$

Neglecting second-order terms, i.e., $Q a_{mn} \varphi_n^0$ etc., this result is reduced to

$$\mathbf{L}^0 \varphi_m^0 + \sum_{n \neq m} a_{mn} \mathbf{L}^0 \varphi_n^0 + \mathbf{Q} \varphi_m^0 = \lambda_m^0 \varphi_m^0 + \lambda_m^0 \sum_{n \neq m} a_{mn} \varphi_n^0 + \lambda_m^1 \varphi_m^0. \quad (8.114)$$

According to the definitions, $\mathbf{L}^0 \varphi_n^0 = \lambda_n^0 \varphi_n^0$. Considering this, the expression Eq. (8.114) is reduced to

$$\sum_{n \neq m} a_{mn} \mathbf{L}^0 \varphi_n^0 + \mathbf{Q} \varphi_m^0 = \lambda_m^0 \sum_{n \neq m} a_{mn} \varphi_n^0 + \lambda_m^1 \varphi_m^0. \quad (8.115)$$

This result is multiplied by φ_m^0 and integrated over x . Thus

$$a_{mm} \lambda_m^0 \langle \varphi_m^0 | \varphi_m^0 \rangle + \int dx \varphi_m^0 \mathbf{Q} \varphi_m^0 = a_{mm} \lambda_m^0 \langle \varphi_m^0 | \varphi_m^0 \rangle + \lambda_m^1 \langle \varphi_m^0 | \varphi_m^0 \rangle.$$

However $a_{mm} = 0$, thus λ_m^1 is given as

$$\lambda_m^1 = \frac{\int dx \varphi_m^0 \mathbf{Q} \varphi_m^0}{\langle \varphi_m^0 | \varphi_m^0 \rangle}. \quad (8.116)$$

The parameters a_{mn} are obtained by multiplying Eq. (8.115) by φ_n^0 and integrating the result with respect to x . Hence

$$\begin{aligned} a_{mn} \lambda_n^0 \langle \varphi_n^0 | \varphi_n^0 \rangle + \int dx \varphi_n^0 \mathbf{Q} \varphi_m^0 &= a_{mn} \lambda_m^0 \langle \varphi_n^0 | \varphi_n^0 \rangle \\ a_{mn} &= \frac{\int dx \varphi_n^0 \mathbf{Q} \varphi_m^0}{\langle \varphi_n^0 | \varphi_n^0 \rangle (\lambda_m^0 - \lambda_n^0)} \text{ for } m \neq n. \end{aligned} \quad (8.117)$$

By repeating the procedure and including second-order terms the result is

$$\begin{aligned} \lambda_m &= \lambda_m^0 + \mathbf{Q}_{nm} + \sum_{n \neq m} \frac{\mathbf{Q}_{nm} \mathbf{Q}_{mn}}{\lambda_n^0 - \lambda_m^0} + \dots \\ \varphi_m &= \varphi_m^0 + \sum_{n \neq m} \frac{\varphi_n^0 \mathbf{Q}_{nm}}{\lambda_m^0 - \lambda_n^0} + \sum_{r \neq m} \sum_{n \neq m} \frac{\varphi_r^0 \mathbf{Q}_{nm} \mathbf{Q}_{rn}}{(\lambda_m^0 - \lambda_n^0)(\lambda_m^0 - \lambda_r^0)} + \dots \\ \mathbf{Q}_{nm} &= \int dx \varphi_n^0 \mathbf{Q} \varphi_m^0 / \langle \varphi_n^0 | \varphi_n^0 \rangle. \end{aligned} \quad (8.118)$$

The eigenvalue corresponding to the unperturbed case is

$$\lambda_m^0 = \int dx \varphi_m^0 L^0 \varphi_m^0 / \langle \varphi_m^0 | \varphi_m^0 \rangle. \quad (8.119)$$

For a degenerate case, for which $\lambda_m = \lambda_n$, the product Q_{mn} is also equal to zero. The second-order terms given in Eq. (8.118) are discussed in Problem 8.16.

The procedure outlined above can be used to determine eigenfrequencies etc. for a simply supported plate with a small point mass. The problem was previously discussed in Sect. 8.9. The corners of the rectangular plate have the coordinates $(0, 0)$, $(L_x, 0)$, (L_x, L_y) , and $(0, L_y)$. For a plate in flexure, time dependence $\exp(i\omega t)$, with the mass μ and a small added mass distribution $\Delta\mu$ per unit area, the differential equation for free vibrations is

$$\nabla^2(\nabla^2 w) - \frac{\omega^2(\mu + \Delta\mu)}{D} w = 0.$$

This expression is rewritten as

$$\frac{D}{\mu + \Delta\mu} \nabla^2(\nabla^2 w) - \omega^2 w = 0.$$

For $\Delta\mu \ll \mu$

$$\frac{D}{\mu + \Delta\mu} \approx \frac{D}{\mu} - \frac{D\Delta\mu}{\mu^2}.$$

Considering this, the perturbed differential equation for the plate in flexure is approximated by

$$\frac{D}{\mu} \nabla^2(\nabla^2 w) - \frac{D\Delta\mu}{\mu^2} \nabla^2(\nabla^2 w) - \omega^2 w = 0. \quad (8.120)$$

For a small added mass Δm located at $\mathbf{r}_0 = (x_0, y_0)$ the function $\Delta\mu$ is equal to $\Delta m \cdot \delta(\mathbf{r} - \mathbf{r}_0)$. The operators L and Q and the eigenvalue λ are consequently

$$L^0 = \frac{D}{\mu} \nabla^2 \nabla^2, \quad Q = -\frac{D\Delta\mu}{\mu^2} \nabla^2 \nabla^2, \quad \lambda = \omega^2. \quad (8.121)$$

The orthogonal eigenfunctions for the simply supported and rectangular plate are $\varphi_{mn}^0 = \sin(m\pi x/L_x) \sin(n\pi y/L_y)$ with the norm $\langle \varphi_{mn}^0 | \varphi_{mn}^0 \rangle = L_x L_y / 4$. The eigenvalues are, for $\kappa_{mn}^2 = (m\pi/L_x)^2 + (n\pi/L_y)^2$

$$\lambda_{mn}^0 = \int_0^{L_x} \int_0^{L_y} dx dy \int dx \varphi_{mn}^0 L^0 \varphi_{mn}^0 / \langle \varphi_{mn}^0 | \varphi_{mn}^0 \rangle = \frac{D\kappa_{mn}^4}{\mu}$$

$$\lambda_{mn}^1 = \int_0^{L_x} \int_0^{L_y} dx dy \frac{\varphi_{mn}^0 Q \varphi_{mn}^0}{\langle \varphi_{mn}^0 | \varphi_{mn}^0 \rangle}$$

$$\begin{aligned}
&= - \int_0^{L_x} \int_0^{L_y} dx dy \frac{4\varphi_{mn}^0 D \Delta m \nabla^2 (\nabla^2 \varphi_{mn}^0) \delta(\mathbf{r} - \mathbf{r}_0)}{L_x L_y} \\
&= - \frac{4D\kappa_{mn}^4 \cdot \Delta m [\varphi_{mn}^0(\mathbf{r}_0)]^2}{\mu^2 L_x L_y}.
\end{aligned} \tag{8.122}$$

The approximate eigenvalue for the disturbed case, including only first order terms, is

$$\lambda_{mn} = \lambda_{mn}^0 + \lambda_{mn}^1 = \frac{D}{\mu} \kappa_{mn}^4 \left\{ 1 - \frac{4 \cdot \Delta m [\varphi_{mn}^0(\mathbf{r}_0)]^2}{m_p} \right\}, \tag{8.123}$$

where $m_p = \mu L_x L_y$ is the mass of the unperturbed plate. The ratio between the eigenfrequencies f'_{mn} and f_{mn} for the disturbed and undisturbed case are obtained from Eqs. (8.114) and (8.116) as

$$\frac{f'_{mn}}{f_{mn}} = \left(\frac{\lambda_{mn}}{\lambda_{mn}^0} \right)^{1/2} = \left\{ 1 - \frac{4 \cdot \Delta m [\varphi_{mn}^0(\mathbf{r}_0)]^2}{m_p} \right\}^{1/2}.$$

For small perturbations this result agrees with the result obtained by means of the Rayleigh–Ritz method given in Eq. (8.107). The eigenfunctions corresponding to λ_{mn} are according to the basic definitions (8.121) and (8.123) equal to

$$\begin{aligned}
\varphi_{mn}(\mathbf{r}) &= \varphi_{mn}^0(\mathbf{r}) + \sum_{r \neq m} \sum_{s \neq n} a_{mnrs} \varphi_{rs}(\mathbf{r}) \\
a_{mnrs} &= - \frac{4 \cdot \kappa_{mn}^4 \cdot \Delta m \cdot \varphi_{mn}^0(\mathbf{r}_0) \varphi_{rs}^0(\mathbf{r}_0)}{m_p (\kappa_{mn}^4 - \kappa_{rs}^4)}.
\end{aligned} \tag{8.124}$$

For equality, i.e., $r = m$ and $s = n$, $a_{mnrs} = a_{mnmn} = 0$ as previously specified. The procedure can be repeated to determine second order terms, see Problem 8.12. An alternative method is discussed in Problem 8.13. The Rayleigh–Ritz technique can be used. In the low frequency region the displacement is written as a sum over the first few eigenfunctions or as $w = C_1 \varphi_{11} + C_2 \varphi_{21} + \dots$. The natural frequencies and amplitudes C_i are thereafter solved as discussed in Sect. 8.6.

8.11 Plates Mounted on Resilient Layers

In many applications, plates or beams are mounted on some type of resilient layer or foundation. A typical example is floating floor constructions used in ships, railway cars, buses, and in buildings. The floating floor is used to reduce the transmission of structure borne sound, from the main frame of construction to some type of accommodation space or passenger compartment. The same type of construction can be used to reduce the energy flow, from a machine or other dynamical source

to the main frame of a building. In this case, the engine foundation is mounted on a resilient layer, which in turn is mounted on the supporting structure or on the floor of a building. Two examples of these applications are illustrated in Figs. 8.21 and 8.22. Another application is the testing of “freely suspended” structures by mounting the test object on a resilient layer.

A resilient layer is said to be locally reacting, if a small section of the layer is reacting to pressure, independently of other sections of the layer. This means: the layer is assumed to react as if it consisted of a large number of separate and closely spaced springs. The elastic properties of various types of mineral wool can, as a first approximation, be described in this way.

First consider the simple problem of a plate mounted on a resilient layer, which in turn is mounted on a completely stiff and flat foundation. For a uniform plate, bending stiffness D , mass per unit area μ , mounted on a locally reacting resilient layer, with the spring constant s per unit area perpendicular to the surface of the layer, the equation of motion for a point force excitation is

$$\nabla^2(\nabla^2 w) + \frac{\mu}{D} \frac{\partial^2 w}{\partial t^2} = \frac{F\delta(x - x_1)\delta(y - y_1)}{D} - \frac{sw}{D}. \quad (8.125)$$

The reacting pressure on the plate from the layer is sw where w is the displacement of the structure. For a time dependence $\exp(i\omega t)$ the equation of motion is reduced to

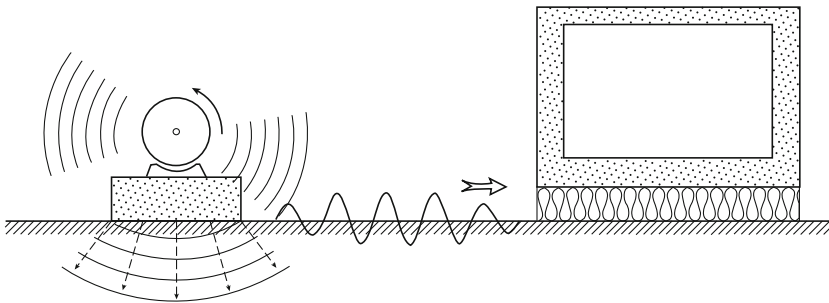


Fig. 8.21 Floating floor. Application 1

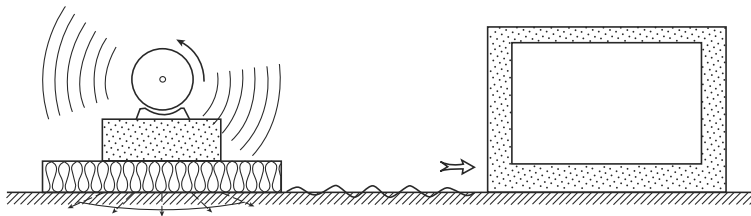


Fig. 8.22 Floating floor. Application 2

$$\nabla^2(\nabla^2 w) - w(\kappa^4 - s/D) = \frac{F\delta(x - x_1)\delta(y - y_1)}{D}, \quad \kappa^4 = \frac{\mu\omega^2}{D}. \quad (8.126)$$

The wave number κ_s for the composite structure i.e., plate plus resilient layer is introduced as

$$\kappa_s = \left(\kappa^4 - \frac{s}{D}\right)^{1/4} = \kappa \left(1 - \frac{s}{\omega^2 \mu}\right)^{1/4}. \quad (8.127)$$

The definition (8.127) inserted in Eq. (8.126) yields

$$\nabla^2(\nabla^2 w) - \kappa_s^4 w = \frac{F\delta(x - x_1)\delta(y - y_1)}{D}. \quad (8.128)$$

This is again the standard wave equation discussed in Sects. 8.2 and 8.3. The solutions previously derived are also solutions to Eq. (8.128) if the wave number κ is replaced by κ_s . For free waves, i.e., for $F = 0$, simple propagating waves can only exist as long as $s < \omega^2 \mu$. The limiting frequency is equal to the first natural frequency of the system, at which every point on the plate is moving in phase in the vertical direction. From Eq. (8.128) it is evident that the plate is moving as if it were freely suspended when $\omega^2 \mu \gg s$. This condition means that $\kappa_s \approx \kappa$. The reaction of the resilient layer on the plate can be neglected in this high frequency range.

The apparent stiffness of the plate mounted on the resilient layer increases as frequency is reduced. The result Eq. (8.127) also confirms the discussion in Sect. 4.10 concerning the wave number for bending waves in a sandwich structure. The laminates of a sandwich construction are mounted on an elastic core. In the high frequency region the laminates are vibrating as if they were isolated from and not connected to the core.

If a structure—for example a deck construction in a ship's cabin—is vibrating excessively, a floating floor in the form of a resilient layer and a plate can be mounted on the deck. The floating construction will reduce the acoustical power radiated by the deck into the cabin and also the structure borne sound transmitted to bulkheads etc. mounted on top of the upper plate. A typical construction is schematically shown in Fig. 8.23. The top plate is excited through the resilient layer by the supporting structure or by the deck. For a locally reacting inter-layer with the spring constant s

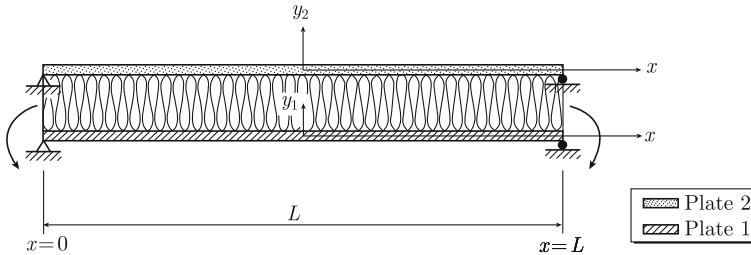


Fig. 8.23 Floating floor

per unit area, the governing equations for the plates are

$$\nabla^2(\nabla^2 w_1) - \kappa_1^4 w_1 = -\frac{s}{D_1}(w_1 - w_2), \quad \nabla^2(\nabla^2 w_2) - \kappa_2^4 w_2 = -\frac{s}{D_2}(w_2 - w_1). \quad (8.129)$$

The displacements for the upper and lower plates are w_1 and w_2 , respectively. The corresponding wavenumbers for the free or isolated plates are κ_1 and κ_2 , i.e.,

$$\kappa_i^4 = \frac{\mu_i \omega^2}{D_i}, \quad i = 1 \text{ or } 2.$$

If a certain displacement w_2 of the main structure is assumed, the resulting displacement w_1 of the top plate can be derived as described in Ref. [74]. The velocity level difference ΔL_v between the bottom and top plates is a measure of the vibration isolation properties of the construction. The velocity level difference is defined as

$$\Delta L_v = 20 \log \left| \frac{\dot{w}_1}{\dot{w}_2} \right| = 20 \log \left| \frac{w_1}{w_2} \right|. \quad (8.130)$$

For a heavily damped top plate the velocity level difference between bottom and top structures can be written as

$$\Delta L_{v1} = C_1 + 40 \log f. \quad (8.131)$$

For lightly damped structures and for $\kappa_1 \ll \kappa_2$ or $\kappa_1 \gg \kappa_2$

$$\Delta L_{v2} = C_2 + 25 \log f. \quad (8.132)$$

For $\kappa_1 \approx \kappa_2$ the corresponding result is

$$\Delta L_{v3} = C_3 + 30 \log f. \quad (8.133)$$

In these expressions, f is the frequency. The constants C_i depend on the material parameters for the top and bottom plates and the inter-layer as well as the dimensions of the floor. The parameters C_i are derived in Ref. [74].

The results can be expressed as a function of the standard material parameters E_i , ρ_i , and ν_i for each plate. The thickness of plate i is h_i . The subscript 1 is used for the upper plate and 2 for the bottom plate. The loss factor for the top plate is η_1 . Based on these parameters, the so called critical frequency f_{ci} for plate i , is defined as

$$f_{ci} = \frac{c^2}{2\pi} \left[\frac{12\rho_i(1-\nu_i^2)}{E_i h_i^2} \right]^{1/2} \approx 6.37 \left[\frac{\rho_i}{E_i h_i^2} \right]^{1/2}. \quad (8.134)$$

The speed of sound in air is $c = 340$ m/s. The vertical stiffness of the inter-layer is characterized by its equivalent E -modulus, denoted E_w and its loss factor δ and

height or thickness H . The dimensions, length and width, of top and bottom plates are equal. The lengths of the sides of the rectangular plates are L_x and L_y . The edges of the top plate are free. Two additional parameters, f_2 and L_{eq} , are introduced as

$$f_2 = \frac{1}{2\pi} \left(\frac{E_w}{\rho_2 H h_2} \right)^{1/2}, \quad L_{eq}^2 = \frac{L_x^2 L_y^2}{L_x^2 + L_y^2}. \quad (8.135)$$

The parameters C_i are given as (Compare Sect. 7.9)

$$\begin{aligned} C_1 &= -40 \log f_2 \\ C_2 &= 10 \log \left[\frac{\pi \delta(f_{c1}^2 - f_{c2}^2)^2 (L_x + L_y)}{2c f_2^2 \cdot f_{c1}^{3/2} \cdot f_{c2}^2} \right], \quad f_{c2} > f_{c1} \\ C_2 &= 10 \log \left[\frac{\pi \delta(f_{c1}^2 - f_{c2}^2)^2 (L_x + L_y)}{3c f_2^2 \cdot f_{c1}^3 \cdot f_{c2}^{1/2}} \right], \quad f_{c2} < f_{c1} \\ C_3 &= 10 \log \left[\frac{8c^2}{f_2^4 (2\pi)^2 f_{c2} L_{eq}^2} \right]. \end{aligned} \quad (8.136)$$

The expressions are only valid as long as $\Delta L_{vi} > 4$ dB. The transmission through the inter-layer to the top plate depends on both resonant and forced transmission as described by ΔL_{v1} and ΔL_{v2} . For including both resonant and forced transmission the velocity level difference is

$$(\Delta L_{v2})_{\text{total}} = 10 \log \left(\frac{1}{10^{-L_{v2}/10} + 10^{-L_{v1}/10}} \right).$$

The material parameters in the Tables 8.6 and 8.7 are, except for steel, very approximate. The velocity level difference between bottom and top plates increases if a parameter C_i is increased i.e., if

- (i) the stiffness of the inter-layer is decreased.
- (ii) the loss factor of the inter-layer is increased.
- (iii) the area of the floor is increased.
- (iv) the weight of the top floor increased.

Table 8.6 Some material parameters for plates

Material	Thickness (mm)	f_c (Hz)	μ (kg/m ²)
Steel	3	4140	23
Steel	6	2070	46
Chipboard	22	1600	22
Concrete	40	440	64

Table 8.7 Some material properties for mineral wool

Density (kg/m ³)	E_w (Pa)	Loss factor δ
50	$0.9 \cdot 10^5$	0.27
100	$1.3 \cdot 10^5$	0.28
150	$2.7 \cdot 10^5$	0.23
200	$4.2 \cdot 10^5$	0.20

In general the total weight of the floor must be kept to a minimum. In particular this is the case for ships and vehicles. In ordinary buildings the weight is probably of less concern. However, if the weight of the top plate is increased by increasing its thickness the radiation factor σ of the plate is also increased. This is of course yet another disadvantage. The acoustic power radiated by the top plate is proportional to $\rho c \langle \bar{v}^2 \rangle \sigma S$, where ρc is the waveimpedance of the fluid, typically air, $\langle \bar{v}^2 \rangle$ is the time and space average of the velocity squared of the plate and S its area.

Comparisons between predicted and measured velocity level differences for two floating floors are shown in Fig. 8.24. Floor A consists of a 6 mm steel deck plus a layer of 60 mm Rockwool (density 100 kg/m³) and 22 mm chipboard panel. For floor B the inter-layer consists of 50 mm Rockwool with a density of 200 kg/m³. The stiffness of the inter-layer for floor B is approximately four times as high as for floor A. The dimensions of the floor are 2.9×3.4 m². The bottom structure is a 6 mm steel plate. The effect of increasing the stiffness of the floor is evident in Fig. 8.24.

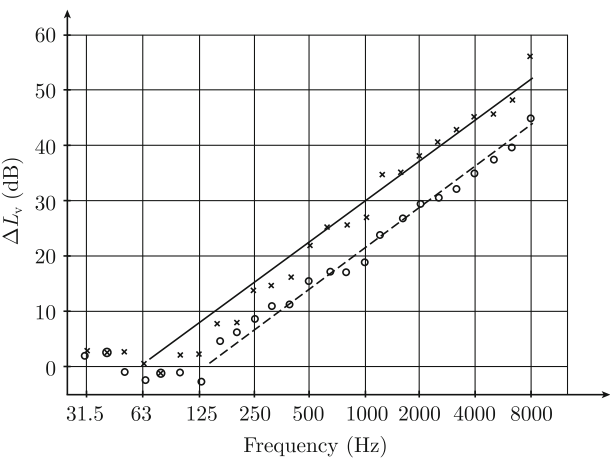


Fig. 8.24 Velocity level difference between the *bottom* and *top* plates of a floating floor. For type A floor, *solid line* is predicted and $\times \times \times$ line measured. For type B floor, *dashed line* is calculated and $o o o$ line measured

It has been argued that the stiffness of the air volume entrapped between the bottom and top plates should be considered. However in Ref. [74] it is concluded that there is no additional stiffness effect due to the enclosed air volume. This hypothesis is confirmed by tests reported in Ref. [75].

8.12 Vibration of Orthotropic Plates

The differential equation governing the bending of thin orthotropic plates is given by Eq. (3.134). If the torsional rigidity B can be approximated by the expression Eq. (3.135) the differential Eq. (3.132) is reduced to

$$D_x \frac{\partial^4 w}{\partial x^4} + 2\sqrt{D_x D_y} \frac{\partial^4 w}{\partial x^2 \partial y^2} + D_y \frac{\partial^4 w}{\partial y^4} + \mu \frac{\partial^2 w}{\partial t^2} = f(x, y, t), \quad (8.137)$$

where $f(x, y, t)$ is the force per unit area exciting the plate. This differential equation can be reduced to standard format by the coordinate transforms

$$x = x_1 \left(\frac{D_x}{D_y} \right)^{1/8}, \quad y = y_1 \left(\frac{D_y}{D_x} \right)^{1/8}, \quad D_{xy} = \sqrt{D_x D_y}. \quad (8.138)$$

Thus

$$\frac{\partial w}{\partial x} = \frac{\partial w}{\partial x_1} \frac{dx_1}{dx} = \left(\frac{D_y}{D_x} \right)^{1/8} \frac{\partial w}{\partial x_1}, \quad \frac{\partial^4 w}{\partial x^4} = \left(\frac{D_y}{D_x} \right)^{1/2} \frac{\partial^4 w}{\partial x_1^4} \text{ etc.}$$

The coordinate transforms plus the differential Eq. (8.137) yield

$$\frac{\partial^4 w}{\partial x_1^4} + 2 \frac{\partial^4 w}{\partial x_1^2 \partial y_1^2} + \frac{\partial^4 w}{\partial y_1^4} + \frac{\mu}{D_{xy}} \frac{\partial^2 w}{\partial t^2} = \frac{f(x, y, t)}{D_{xy}}. \quad (8.139)$$

After the transformation the apparent plate dimensions L_{x1} and L_{y1} are

$$L_{x1} = L_x \left(\frac{D_y}{D_x} \right)^{1/8}, \quad L_{y1} = L_y \left(\frac{D_x}{D_y} \right)^{1/8}. \quad (8.140)$$

By introducing these apparent dimensions in Eq. (8.16) the eigenfrequencies for a simply supported orthotropic plate with the dimensions L_x and L_y are obtained as

$$\begin{aligned} f_{mn} &= \frac{\pi}{2} \left(\frac{D_{xy}}{\mu} \right)^{1/2} \left[\left(\frac{m}{L_{x1}} \right)^2 + \left(\frac{n}{L_{y1}} \right)^2 \right] \\ &= \frac{\pi}{2} \left(\frac{D_x D_y}{\mu^2} \right)^{1/4} \left[\left(\frac{m}{L_x} \right)^2 \left(\frac{D_x}{D_y} \right)^{1/4} + \left(\frac{n}{L_y} \right)^2 \left(\frac{D_y}{D_x} \right)^{1/4} \right]. \end{aligned} \quad (8.141)$$

Eigenfrequencies for rectangular orthotropic plates for other boundary conditions are estimated by means of the Rayleigh–Ritz method described in Sect. 8.6 and by using the transforms defined in Eq. (8.138) or by substituting the real plate dimensions L_x and L_y by L_{x1} and L_{y1} .

8.13 Circular and Homogeneous Plates

In Sect. 8.1 the eigenfunctions for simply supported rectangular plates were derived. For some of the other basic boundary conditions like clamped and free edges the analytical expressions for the eigenfunctions could not be formulated. However it could be proved that if these eigenfunctions did exist they would be orthogonal. For circular panels it is possible to find analytical expressions for the eigenfunctions for clamped, simply supported and free edges. Thus the existence of an analytical solution depends on the geometry of the structure. Another similar case relates to longitudinal vibrations of infinite beams. Exact solutions giving the displacement in the beam can be found for beams with a circular cross section but not for beams with rectangular cross sections. The analytical solution of longitudinal vibrations of cylindrical beams is attributed to Pochhammer and Chree Ref. [15] and is discussed in Chap. 10.

The eigenfunctions for circular plates are derived in the same way as for rectangular plates. First a solution using a separation of variables is assumed. The functions depending on the cylindrical coordinates together with the boundary conditions determine the eigenfunctions and the corresponding eigenvalues. The natural frequencies of the structure are obtained from these eigenvalues. The equation governing the free flexural vibrations of a homogeneous plate is according to Eq. (3.115)

$$\nabla^2(\nabla^2 w) + \frac{\mu}{D} \frac{\partial^2 w}{\partial t^2} = 0, \quad (8.142)$$

where μ is the mass per unit area of the plate, D its bending stiffness, and w its displacement perpendicular to the plate. As in the case with the rectangular plate it is convenient to make a separation of variables, now in cylindrical coordinates, to define the displacement of the plate as

$$w(r, \varphi, t) = u(r, \varphi)g(t), \quad u(r, \varphi) = R(r)\Phi(\varphi). \quad (8.143)$$

Assume that the time dependent function $g(t)$ satisfies the equation

$$\frac{\mu}{D} \frac{d^2 g}{dt^2} = -\kappa^4 g. \quad (8.144)$$

For Eq. (8.142) to be fulfilled $u(r, \varphi)$ should satisfy

$$\nabla^2(\nabla^2 u) - \kappa^4 u = 0. \quad (8.145)$$

This result can, as discussed in Sect. 5.3, be rewritten as

$$(\nabla^2 - \kappa^2)(\nabla^2 + \kappa^2)u = 0. \quad (8.146)$$

Again, as in Sect. 5.3, this equation can be replaced by two second-order differential equations on the form

$$\nabla^2 u_1 - \kappa^2 u_1 = 0, \quad \nabla^2 u_2 + \kappa^2 u_2 = 0. \quad (8.147)$$

The total solution to Eq. (8.146) is now given as the sum of the two solutions or

$$u = u_1 + u_2. \quad (8.148)$$

In cylindrical coordinates the operator ∇^2 is defined as

$$\nabla^2 = \frac{\partial^2}{\partial r^2} + \frac{1}{r} \frac{\partial}{\partial r} + \frac{1}{r^2} \frac{\partial^2}{\partial \varphi^2}.$$

Assuming the angular dependence to be governed by

$$\frac{\partial^2 u}{\partial \varphi^2} = -m^2 u \quad \text{or} \quad \frac{d^2 \Phi}{d\varphi^2} = -m^2 \Phi, \quad (8.149)$$

the Eq. (8.147) can be reduced to

$$\frac{d^2 R_1}{dr^2} + \frac{1}{r} \frac{dR_1}{dr} + \left(\kappa^2 - \frac{m^2}{r^2} \right) R_1 = 0 \quad (8.150)$$

$$\frac{d^2 R_2}{dr^2} + \frac{1}{r} \frac{dR_2}{dr} - \left(\kappa^2 + \frac{m^2}{r^2} \right) R_2 = 0. \quad (8.151)$$

The solution to Eq. (8.149) is

$$\Phi(\varphi) = A_1 \cdot \sin(m\varphi) + A_2 \cdot \cos(m\varphi) = A_0 \cdot \cos(m\varphi + \varphi_m), \quad (8.152)$$

where A_0 , A_1 , A_2 , and φ_m are some parameters determined by the boundary conditions. The general solution to the Bessel Eq. (8.150) is for m a positive integer

$$R_1(r) = B_1 \cdot J_m(\kappa r) + B_2 \cdot Y_m(\kappa r). \quad (8.153)$$

However, the Neumann function $Y_m(\kappa r)$ tends to infinity as r approaches zero. The amplitude of the plate is kept finite by setting the parameter B_2 equal to zero. For each positive integer m there is a solution R_1 and a corresponding solution for Φ . Considering all possible solutions, w_1 is written

$$w_1(r, \varphi, t) = \sum_m C_m \cdot J_m(\kappa r) \cdot \cos(m\varphi + \varphi_m) g_m(t), \quad (8.154)$$

where C_m is some as yet unknown parameter. The function $g(t)$ should satisfy Eq. (8.154). The solution to Eq. (8.151) is

$$R_2(r) = B_3 \cdot J_m(i\kappa r). \quad (8.155)$$

Again the Neumann function is not included. The Bessel function $J_m(iz)$ of imaginary values and the modified Bessel function $I_m(z)$ are related as

$$I_m(z) = J_m(iz)/i^m, \quad (8.156)$$

where $I_m(z) \rightarrow 0$ as $z \rightarrow 0$ for $m > 0$ and $I_0(0) = 0$. Thus the solution w_2 is written

$$w_2(r, \varphi, t) = \sum_m D_m \cdot I_m(\kappa r) \cdot \cos(m\varphi + \varphi_m) \cdot g_m(t), \quad (8.157)$$

where D_m are some constants. The total general solution is

$$w(r, \varphi, t) = w_1 + w_2 = \sum_m [C_m \cdot J_m(\kappa r) + D_m \cdot I_m(\kappa r)] \cdot \cos(m\varphi + \varphi_m) \cdot g_m(t). \quad (8.158)$$

For a circular plate, radius r_0 and clamped along its perimeter, the boundary conditions are

$$w(r_0, \varphi, t) = 0, \quad \left[\frac{\partial w}{\partial r} \right]_{r=r_0} = 0. \quad (8.159)$$

These boundary conditions should be satisfied for any angle φ . Thus from Eq. (8.158)

$$C_m J_m(\kappa r_0) + D_m I_m(\kappa r_0) = 0, \quad C_m J'_m(\kappa r_0) + D_m I'_m(\kappa r_0) = 0. \quad (8.160)$$

The existence of a nontrivial solution yields the characteristic determinant

$$\text{Det} \begin{bmatrix} J_m(\kappa r_0) & I_m(\kappa r_0) \\ J'_m(\kappa r_0) & I'_m(\kappa r_0) \end{bmatrix} = 0. \quad (8.161)$$

Using the recursion relationships

$$\lambda J'_m(\lambda) = m J_m(\lambda) - \lambda J_{m+1}(\lambda), \quad \lambda I'_m(\lambda) = m I_m(\lambda) - \lambda I_{m+1}(\lambda).$$

Equation (8.161) gives

$$J_m(\kappa r_0) I_{m+1}(\kappa r_0) + I_m(\kappa r_0) J_{m+1}(\kappa r_0) = 0. \quad (8.162)$$

For each m there is an infinite number of solutions of κr_0 to this equation. Each solution is identified by $\kappa_{mn} r_0 = \lambda_{mn}$. The corresponding time-dependent solutions to Eq. (8.144) are identified as $g_{mn}(t)$. The solution to Eq. (8.144) is after replacing $g(t)$ by $g_{mn}(t)$ and κ by κ_{mn}

$$g_{mn}(t) = U_{mn} \sin(\omega_{mn} t) + V_{mn} \cos(\omega_{mn} t), \quad \omega_{mn} = \kappa_{mn}^2 \sqrt{\frac{D_0}{\mu}}. \quad (8.163)$$

The parameters U_{mn} and V_{mn} are determined from the initial conditions. The natural frequencies f_{mn} of the clamped panel are

$$f_{mn} = \frac{\omega_{mn}}{2\pi} = \frac{\kappa_{mn}^2}{2\pi} \sqrt{\frac{D_0}{\mu}} = \frac{1}{2\pi} \left(\frac{\lambda_{mn}}{r_0} \right)^2 \sqrt{\frac{D_0}{\mu}}. \quad (8.164)$$

Values of $\lambda_{mn} = \kappa_{mn} r_0$, which are solutions to Eq. (8.162), are listed in Table 8.8. The results are from Ref. [75].

In the limit as $n \rightarrow \infty$ the eigenvalues $\lambda_{mn} \rightarrow \pi(n + m/2)$. The boundary conditions are satisfied for all functions

$$u_{nm}(r, \varphi) = [J_m(\kappa_{mn} r) \cdot I_m(\kappa_{mn} r_0) - J_m(\kappa_{mn} r_0) \cdot I_m(\kappa_{mn} r)] \cos(m\varphi + \varphi_m). \quad (8.165)$$

These are the eigenfunctions describing the flexural vibrations of a clamped circular plate. The quantity $\lambda_{mn} = \kappa_{mn} r_0$ satisfies the eigenvalue Eq. (8.162). The eigenfunctions are orthogonal. Thus

Table 8.8 Values of $\lambda_{mn} = \kappa_{mn} r_0$ for a clamped and circular plate of radius r_0

m	$n = 1$	$n = 2$	$n = 3$	$n = 4$
0	3.196	6.306	9.439	12.575
1	4.611	7.799	10.958	14.109
2	5.906	9.197	12.402	15.579
3	7.144	10.536	13.795	17.005

$$\langle u_{mn} | u_{rs} \rangle = \int_0^{2\pi} d\varphi \int_0^{r_0} r dr \cdot u_{mn}(r, \varphi) u_{rs}(r, \varphi) = \delta_{mr} \delta_{nr} \Lambda_{mn}$$

$$\Lambda_{mn} = \frac{2\pi r_0^2}{\varepsilon_m} \left\{ [J_m(\kappa_{mn} r_0)]^2 + [J'_m(\kappa_{mn} r_0)]^2 \right\}, \quad (8.166)$$

where the Kronecker symbol δ_{mr} is equal to unity for $m = r$, otherwise equal to zero. The norm of the eigenfunction is denoted Λ_{mn} . Finally the so called Neumann constant ε_m is equal to 2 for $m \geq 1$. For $m = 0$, $\varepsilon_m = 1$.

For a circular and simply supported plate the boundary conditions are zero displacement and zero bending moment M'_r per unit length of the circumference. In cylindrical coordinates the bending moment M'_r is given by

$$M'_r = -D \left(\frac{\partial^2 w}{\partial r^2} + \frac{\nu}{r} \frac{\partial w}{\partial r} + \frac{\nu}{r^2} \frac{\partial^2 w}{\partial \varphi^2} \right).$$

At the boundary the displacement w is zero. Consequently also $\partial^2 w / \partial \varphi^2$ is equal to zero. Thus the boundary conditions for a simply supported circular plate are

$$w(r_0, \varphi, t) = 0, \quad M'_r(r_0) = -D \left(\frac{\partial^2 w}{\partial r^2} + \frac{\nu}{r} \frac{\partial w}{\partial r} \right)_{r=r_0} = 0. \quad (8.167)$$

The boundary condition not only depends on the bending stiffness of the plate but also on the Poisson's ratio ν . As in the previous case, the clamped plate, the general solution Eq. (8.158) satisfies the differential equation. In addition the boundary conditions (8.167) should be fulfilled. The Eqs. (8.158) and (8.167) give

$$C_m J_m(\kappa r_0) + D_m I_m(\kappa r_0) = 0$$

$$C_m \left[J''_m(\kappa r_0) + \frac{\nu}{\kappa r_0} J'_m(\kappa r_0) \right] + D_m \left[I''_m(\kappa r_0) + \frac{\nu}{\kappa r_0} I'_m(\kappa r_0) \right] = 0. \quad (8.168)$$

These equations lead to the frequency equation. Using as before the notation $\lambda = \kappa r_0$ and the standard recursion formulas for the derivatives of the Bessel functions, Ref. [43], the frequency equation is reduced to

$$\frac{J_{m+1}(\lambda)}{J_m(\lambda)} + \frac{I_{m+1}(\lambda)}{I_m(\lambda)} = \frac{2\nu}{1-\nu}. \quad (8.169)$$

Thus, the eigenfunctions $u_{mn}(r, \varphi)$ for a circular and simply supported plate are

$$u_{nm}(r, \varphi) = [J_m(\kappa_{mn} r) \cdot I_m(\kappa_{mn} r_0) - J_m(\kappa_{mn} r_0) \cdot I_m(\kappa_{mn} r)] \cos(m\varphi + \varphi_m). \quad (8.170)$$

This is the same general solution as for the clamped plate. However for the simply supported boundary conditions to be satisfied the eigenvalues $\lambda_{mn} = \kappa_{mn}r_0$ must satisfy the characteristic Eq. (8.169).

The eigenfunctions are orthogonal and the norm is given by Eq. (8.166). The eigenvalues are listed in Table 8.9. The natural frequencies are defined in the expression Eq. (8.164). The first natural frequency for a simply supported circular plate is approximately 4/5 of the natural frequency of a simply supported quadratic plate of the same area and of same material. When the boundary conditions for a circular plate are changed from simply supported to clamped the first natural frequency is approximately doubled.

For a circular plate with free edges the boundary conditions at $r = r_0$ are

$$M'_r = -D \left(\frac{\partial^2 w}{\partial r^2} + \frac{\nu}{r} \frac{\partial w}{\partial r} + \frac{\nu}{r^2} \frac{\partial^2 w}{\partial \varphi^2} \right)_{r=r_0} = 0$$

$$T'_r = -D \left[\frac{\partial}{\partial r} (\nabla^2 w) - D(1 - \nu) \frac{1}{r} \frac{\partial}{\partial r} \left(\frac{1}{r} \frac{\partial^2 w}{\partial \varphi^2} \right) \right]_{r=r_0} = 0. \quad (8.171)$$

The resulting eigenfunctions are somewhat more complicated than in the previous two cases. Solutions are given by Leissa in Ref. [76]. However some eigenvalues are given in Table 8.9 from Ref. [76].

For large m and n the eigenvalues $\lambda_{mn} = \kappa_{mn}r_0$ tend to $[m + 2(n - 1)] \pi / 2$. Note that there are no solutions for $m = 0$ and $n = 1$ and $m = n = 1$. In Table 8.9 Poisson's ratio is 0.3 in the Table 8.10 the eigenvalues are computed for $\nu = 0.33$. The natural frequencies for a free plate are obtained from Eq. (8.164) in combination with Table 8.10.

Table 8.9 Values of $\lambda_{mn} = \kappa_{mn}r_0$ for a simply supported circular plate of radius r_0 , $\nu = 0.3$

m	$n = 1$	$n = 2$	$n = 3$	$n = 4$
0	2.231	5.455	8.614	11.762
1	3.734	6.965	10.139	13.298
2	5.065	8.375	11.590	14.773

Table 8.10 Values of $\lambda_{mn} = \kappa_{mn}r_0$ for a circular plate with free edges, radius r_0 and $\nu = 0.33$

m	$n = 1$	$n = 2$	$n = 3$	$n = 4$
0	–	3.014	6.209	9.370
1	–	4.530	7.737	10.909
2	2.292	5.937	9.160	12.410
3	3.497	7.274	10.550	13.860

8.14 Bending of Plates in Tension

In certain cases a structure can be exposed to in-plane tension as well as lateral forces. This in-plane tension influences the vibration pattern of the structure. The natural frequencies of the structure are shifted due to the in-plane tension. For example, the plate elements of a fuselage are subjected to in-plane stress caused by the difference between the inside high pressure and the external low pressure during flight. The dynamic behavior of a fuselage is therefore different on ground as compared to under normal flight conditions.

In Sect. 3.6 the lateral vibration of a string was discussed. It was found that the vibration of the string depends on the tension inside the string itself. The lateral vibration of a plate under tension can be derived in a similar way as the equation governing the vibrating string. Consider the homogeneous plate shown in Fig. 8.25.

The plate is subjected in the x -direction to a tension T'_x per unit width of the plate. The resulting forces on the plate are shown in Fig. 8.26. The forces are shown along a line parallel to the x -axis. The lateral displacement of the plate is w . The lateral forces per unit width of the are T'_{z1} and T'_{z2} .

From Fig. 8.26 the resulting force $\Delta T'_z$ on a plate element of length Δx is

$$\begin{aligned}\Delta T'_z &= T'_{z2} - T'_{z1} = T'_x \left[\frac{\partial w(x + \Delta x)}{\partial x} - \frac{\partial w(x)}{\partial x} \right] \\ &= T'_x \left[\frac{\partial w(x)}{\partial x} + \Delta x \frac{\partial^2 w(x)}{\partial x^2} - \frac{\partial w(x)}{\partial x} \right] = \Delta x T'_x \frac{\partial^2 w(x)}{\partial x^2}. \quad (8.172)\end{aligned}$$

Fig. 8.25 Plate subjected to a strain T'_x per unit width

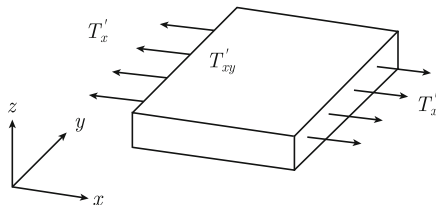
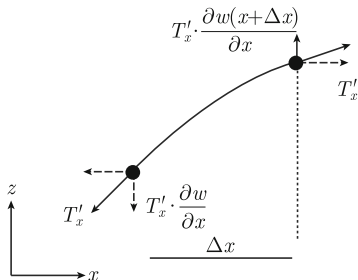


Fig. 8.26 Tension components acting on plate element



This vertical component of the tension is equivalent to a pressure p_T on the plate where

$$p_T = \frac{\Delta T'_z}{\Delta x} = T'_x \frac{\partial^2 w(x)}{\partial x^2}. \quad (8.173)$$

The equation governing the flexural vibration of a homogeneous plate excited by a pressure p is

$$\nabla^2(\nabla^2 w) + \frac{\mu}{D} \frac{\partial^2 w}{\partial t^2} = \frac{p}{D}.$$

By replacing p by p_T the result is

$$\nabla^2(\nabla^2 w) + \frac{\mu}{D} \frac{\partial^2 w}{\partial t^2} = \frac{T'_x}{D} \frac{\partial^2 w}{\partial x^2}. \quad (8.174)$$

If in addition the plate is also subjected to a force $f(x, y, t)$ per unit area the governing equation reads

$$\nabla^2(\nabla^2 w) - \frac{T'_x}{D} \frac{\partial^2 w}{\partial x^2} + \frac{\mu}{D} \frac{\partial^2 w}{\partial t^2} = \frac{f}{D}. \quad (8.175)$$

For a simply supported rectangular plate the eigenfunctions are $\varphi_{mn}(x, y) = \sin(m \pi x/L_x) \sin(n \pi y/L_y)$. For free vibrations of a homogeneous plate of this type the displacement is

$$w(x, y, t) = \sum_{mn} A_{mn} \varphi_{mn}(x, y) \cdot \exp(i\omega_{mn}t).$$

This expression inserted in Eq. (8.174) yields

$$\kappa_{mn}^4 + k_{mn}^2 \frac{T'_x}{D} = \omega_{mn}^2 \frac{\mu}{D}; \quad \kappa_{mn}^2 = \left(\frac{m \pi}{L_x}\right)^2 + \left(\frac{n \pi}{L_y}\right)^2; \quad k_m = \frac{m \pi}{L_x}.$$

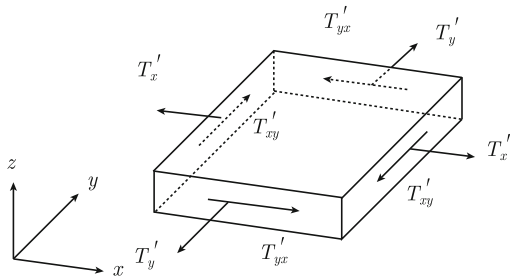
The natural frequencies f_{mn} are consequently

$$f_{mn} = \text{Re} \frac{\omega_{mn}}{2 \pi} = \frac{1}{2 \pi} \sqrt{\frac{D_0}{\mu} \left\{ \left[\left(\frac{m \pi}{L_x}\right)^2 + \left(\frac{n \pi}{L_y}\right)^2 \right]^2 + \frac{T'_x}{D} \left(\frac{m \pi}{L_x}\right)^2 \right\}^{1/2}}. \quad (8.176)$$

With no external tension, $T'_x = 0$, the natural frequencies given by Eq. (8.176) are identical to the previously derived expression Eq. (8.16). Whenever the plate is stretched, i.e., $T'_x > 0$, the natural frequencies of the plate are increased.

The results can be generalized for plates subjected to added tension in other directions. For the general case shown in Fig. 8.27 the equation governing the lateral

Fig. 8.27 Plate subjected to strains



vibration of a plate under tension is

$$\nabla^2(\nabla^2 w) - \frac{T'_x}{D} \frac{\partial^2 w}{\partial x^2} - \frac{T'_y}{D} \frac{\partial^2 w}{\partial y^2} - 2 \frac{T'_{xy}}{D} \frac{\partial^2 w}{\partial x \partial y} + \frac{\mu}{D} \frac{\partial^2 w}{\partial t^2} = \frac{f}{D}. \quad (8.177)$$

If the plate is completely limp, i.e., its bending stiffness is zero, Eq. (8.177) is reduced to

$$T'_x \frac{\partial^2 w}{\partial x^2} + T'_y \frac{\partial^2 w}{\partial y^2} + 2T'_{xy} \frac{\partial^2 w}{\partial x \partial y} - \mu \frac{\partial^2 w}{\partial t^2} = -f. \quad (8.178)$$

This is the equation governing the vibration of a membrane. Compare also Eq. (3.64) which gives the vibration of a string.

Problems

8.1 A quadratic simply supported plate with the area S has its first natural frequency at 20 Hz. Determine the next five natural frequencies. In addition determine the first six natural frequencies if the plate is rectangular, one side twice as long as the other. The plate area and the boundary conditions are the same in both cases.

8.2 A simply supported rectangular plate is loaded by a static point force F at its center. At $t = 0$ the load is removed. Determine the response of the plate for $t > 0$.

8.3 Use the Ritz technique to determine the first natural frequency for a rectangular simply supported plate. The displacement of the plate is assumed to be

$$w(x, y) = A(x^4 - 2x^3 L_x + x L_x^3)(y^4 - 2y^3 L_y + y L_y^3).$$

Compare with exact result for $L_x = 3L_y$.

8.4 The sides of a homogeneous rectangular plate are $L_x = \xi \cdot L$ and $L_y = L/\xi$. The edges of the plate are clamped. Determine $f_{11}(\xi)$, the first natural frequency of the plate as function of ξ , and determine also the ratio $f_{11}(\xi)/f_{11}(1)$. Use the Ritz technique. Assume that the displacement $F(x, y)$ of the first mode is given by

$$F(x, y) = [1 - \cos(2\pi x/L_x)][1 - \cos(2\pi y/L_y)].$$

The corners of the plate are at $(0, 0)$, $(L_x, 0)$, (L_x, L_y) and $(0, L_y)$.

8.5 The first natural frequency of a simply supported rectangular plate is f_{11} . The plate is excited by a pure tone force with the frequency $0.9 \cdot f_{11}$. The loss factor for the plate is 0.01 at this frequency. In order to reduce the velocity level of the plate a visco-elastic layer is mounted to the plate. Due to this, the loss factor is increased to 0.1. At the same time the total mass is increased by 35 % and the bending stiffness by 20 %. Determine the average velocity level of the plate before and after the change. Consider only the first vibrational mode.

8.6 A homogeneous rectangular plate is simply supported. The corners have the coordinates $(0, 0)$, $(L_x, 0)$, (L_x, L_y) , and $(0, L_y)$. The plate is excited by a force $F_1 = F_0 \cdot \exp(i\omega t)$ at $(L_x/4, L_y/2)$ and by a force $F_1 = -F_0 \cdot \exp(i\omega t)$ at $(3L_x/4, L_y/2)$. Determine the time average of the kinetic energy of the plate. The loss factor is η .

8.7 A homogeneous rectangular plate is simply supported. The corners have the coordinates $(0, 0)$, $(L_x, 0)$, (L_x, L_y) , and $(0, L_y)$. The plate is excited by a force function $f(x, y) = F_0 \exp(i\omega t) \cdot xy(L_x - x)(L_y - y)/(L_x L_y)^3$. Determine the response of the plate.

8.8 A thin rectangular homogeneous plate has the total weight M . The plate is simply supported. In order to decrease the first natural frequency of the plate a limp material with the total mass $M/4$ is mounted to the plate. The material covers 1/4 of the plate area and is mounted over the area $L_x/4 < x < 3L_x/4$ and $L_y/4 < y < 3L_y/4$. Determine the reduction of the first natural frequency due to this change. Consider only the first vibrational mode.

8.9 A thin rectangular homogeneous plate is simply supported along two opposite edges. The two other edges are free. Determine the exact expression giving the first natural frequency of the plate.

8.10 A homogeneous rectangular plate is simply supported. The corners have the coordinates $(0, 0)$, $(L_x, 0)$, (L_x, L_y) , and $(0, L_y)$. The plate is supported by two identical springs at $(L_x/4, L_y/2)$ and $(3L_x/4, L_y/2)$. Each spring has the spring constant s . Determine the first natural frequency of the plate as function of material parameters, spring constant s and plate dimensions. Use the Ritz technique. The springs are coupled to a stiff foundation.

8.11 A homogeneous plate is excited by randomly distributed forces with constant power spectral density—white noise. Within a frequency band Δf determine the time and space average of the velocity squared of the plate as function of the plate thickness and loss factor. Assume that the frequency band includes a large number of natural frequencies.

8.12 Determine the eigenvalue to Eq. (8.111) by including second order terms λ_m^2 by using the perturbation theory discussed in Sect. 8.10.

8.13 Determine the eigenfrequencies for a rectangular and simply supported plate with a small mass mounted to the plate. Use perturbation theory, Sect. 8.10, to improve the result Eq. (8.123) by adding another term.

8.14 A floating floor consists of a 50 mm layer of mineral wool (200 kg/m³) and a 4 mm steel plate as top plate. What is the effect in the high frequency region if the thickness of the top plate is reduced to 2 mm and at the same time the density of the mineral wool is reduced to 100 kg/m³. The bottom plate is a 6 mm steel plate. Material properties for mineral wool are given in Table 8.7.

8.15 A rectangular plate—length L_x and width L_y —is orthotropic with the bending stiffness D_x in the x -direction and D_y in the y -direction. All edges are free. Show that the eigenfrequencies can be estimated by the expression

$$f_{mn} = \frac{\pi}{2} \left[\frac{1}{\mu} \right]^{1/2} \left[D_x \left(\frac{G_m}{L_x^4} \right)^4 + D_y \left(\frac{G_n}{L_y^4} \right)^4 + \sqrt{D_x D_y} \cdot \frac{2J_m J_n + 2\nu(H_m H_n - J_m J_n)}{(L_x L_y)^4} \right]^{1/2}$$

where G_m , H_m , and J_m are defined in Sect. 8.6.

8.16 Show that the eigenfrequency f_{mn} for a rectangular plate tends to the same value for increasing frequencies when the edges are clamped or simply supported.

8.17 Consider an eigenvalue problem $Lw = \lambda w$ where L is a linear operator and λ the corresponding eigenvalue and w the displacement of a structure. The operator L is $L = L^0 + Q$. The operator L is almost equal to the operator L^0 for which the orthogonal eigenfunctions φ_n^0 and the corresponding eigenvalues λ_n^0 satisfy $L^0 \varphi_n^0 = \lambda_n^0 \varphi_n^0$. Show that the eigenvalue λ_n satisfying $L \varphi_n = \lambda_n \varphi_n$ can be written as

$$\lambda_m = \lambda_m^0 + Q_{mn} + \sum_n \frac{Q_{nm} Q_{mn}}{\lambda_m - \lambda_n^0} + \sum_n \sum_r \frac{Q_{mn} Q_{nr} Q_{rm}}{(\lambda_m - \lambda_n^0)(\lambda_m - \lambda_r)},$$

where $Q_{ij} = \int dx \varphi_i^0 Q \varphi_j^0 / \langle \varphi_j^0 | \varphi_j^0 \rangle$.

In the summations terms for which $n = m$ and $r = m$ are excluded.

References

1. W.T. Thomson, *Theory of Vibration with Applications*, 3rd edn. (Unwin Hyman, London, 1989)
2. A.H. Nayfeh, D.T. Mook, *Nonlinear Oscillations* (Wiley, New York, 1979)
3. J.C. Snowdon, *Vibration and Shock in Damped Mechanical Systems* (Wiley, New York, 1968)
4. W.F. Ames, *Numerical Methods for Partial Differential Equations*, 3rd edn. (Academic Press, San Diego, 1992)
5. E. Kreyszig, *Advanced Engineering Mathematics*, 7th edn. (Wiley, New York, 1993)
6. J.R. Hassal, K. Zaveri, *Acoustic Noise Measurements* (Brüel & Kjær, Nærum, Denmark, 1988)
7. R.B. Randall, *Frequency Analysis* (Brüel & Kjær, Nærum, Denmark, 1987)
8. J.S. Bendat, A.G. Piersol, *Measurement and Analysis of Random Data* (Wiley, New York, 1968)
9. A. Papoulis, *Signal Analysis* (McGraw-Hill Book Company, New York, 1984)
10. J.D. Robson, *Random Vibration* (Edinburgh University Press, Edinburgh, 1963)
11. D.E. Newland, *Random Vibrations and Spectral Analysis*, 2nd edn. (Longman Group Ltd., Harlow, Essex, UK, 1984)
12. D.J. Ewins, *Modal Testing: Theory and Practice* (Research Studies Press Ltd., Letchworth, UK, 1985)
13. L. Boltzman, Zur. Theorie der Elastische Nachwirkung. *Analene der Physik* 7, 624 (1876)
14. V. Volterra, E. Volterra, *Sur le Distortion des Corps Elastique* (Gauthier-Villars, Paris, 1960)
15. E. Volterra, E.C. Zachmanoglou, *Dynamics of Vibrations* (Charles E. Merrill Books Inc, Columbus, Ohio, 1965)
16. Y.C. Fung, *Foundations of Solid Mechanics* (Prentice Hall Inc, New Jersey, 1965)
17. K. Dovstam, On material damping modelling and modal analysis in structural dynamics, Dr. Tech. thesis, Department of Solid Mechanics, KTH Stockholm, 1998
18. L. Kari, Structure-borne sound properties of vibration isolators, Dr. Tech. thesis, report 98-02, MWL, Department of Vehicle Engineering, KTH Stockholm, Sweden, 1998
19. G.A. Lesieutre, Finite element modelling of frequency dependent material damping using augmenting thermodynamic fields, Ph.D. dissertation, Aerospace Engineering, University of California, Los Angeles, 1989
20. K. Dovstam, Augmented Hooke's law in frequency domain. A three dimensional, material damping formulation. *J. Solids Struct.* **32**(19), 2835-2852 (1995)
21. F. Odquist, *Hållfasthetslära* (Natur och Kultur, Stockholm, Sweden, 1961)
22. S.P. Timoshenko, *Strength of Materials*, 3rd edn. (D. Van Nostrand Company Inc, New York, 1978)
23. P.M. Morse, K.U. Ingard, *Theoretical Acoustics* (McGraw-Hill Book Company, New York, 1968)

24. B. Sundström, *Handbok och formelsamling i hållfasthetslära* (Institutionen Hållfasthetslära, KTH, Stockholm, 1998)
25. R. Szilard, *Theory and Analysis of Plates. Classical and Numerical Methods* (Prentice Hall Inc., Englewood Cliffs, New Jersey, 1974)
26. J. Whitney, *Structural Analysis of Laminated Anisotropic Plates* (Technomic Publishing Company, Lancaster, Basel, 1987)
27. G. Pavic, *Energy Flow Induced by Structural Vibrations of Elastic Bodies* (The American Society of Mechanical Engineers, Winter Annual Meeting, San Fransisco, California, 1989)
28. D. Noiseux, Measurements of power flow in uniform beams and plates. *J. Acoust. Soc. Am.* **47**(1), 238 (1970)
29. *3rd International Congress on Intensity Techniques* (CETIM, Senlis, France, 1990)
30. *4th International Congress on Intensity Techniques* (CETIM, Senlis, France, 1993)
31. L. Cremer, M. Heckl, E. Unger, *Structure-Borne Sound* (Springer, Berlin, 1973)
32. D. Zenkert, *An Introduction to Sandwich Construction* (EMAS Publishing, Warley, West Midlands, UK, 1997)
33. R.M. Jones, *Mechanics of Composite Materials* (Taylor & Francis, Hemisphere Publishing Corporation, USA, 1975)
34. I.H. Marshall, *Composite Structures* (Applied Science Publishers, London, 1981)
35. *Proceedings of the International Conference. Sandwich Constructions.* (1) First Conference. Stockholm, Sweden, 1989. (2) Second Conference. Gainesville, Florida, 1992. (3) Third Conference. Southampton, UK, 1995. (4) Fourth Conference. Stockholm, Sweden, 1998
36. O. Zienkiewics, R. Taylor, *The Finite Element Method, vol. 1: Basic Formulation and Linear Problems, vol. 2: Solid and Fluid Mechanics, Dynamics and Non Linearity* (McGraw-Hill, London, 1991)
37. R. Cook, R. Malkus, M. Plesha, *Concepts and Applications of Finite Element Analysis* (Wiley, New York, 1989)
38. B. Szabo, I. Babushka, *Finite Element Analysis* (Wiley, New York, 1991)
39. A.C. Nilsson, *Description of Structure-Borne Sound Transmission in Ship Structures. New materials* (WEGEMT, 16th Graduate School Genova, Italy, 1992)
40. A.C. Nilsson, Wave propagation in and sound transmission through sandwich plates. *J. Sound Vib.* **138**(1), 73–94 (1990)
41. S. Tavallaey Sander, Wave propagation in sandwich structures, Dr.tech. thesis, TRITA-FKT 2001:01. MWL, KTH 2001
42. A.C. Nilsson, Wave propagation in simple hull-frame structures on ships. *J. Sound Vib.* **44**(3), 393–405 (1976)
43. M. Abramowitz, I. Stegun, *Handbook of Mathematical Functions* (National Bureau of Standards, Washington DC, 1970)
44. Ulf Carlsson, Mechanical mobility: a tool for the analysis of vibrations in mechanical structures, Dr.Tech. thesis, report 93–31, MWL, Department of Vehicle Engineering, KTH, Stockholm, 1993
45. T. Derby, J. Ruzicka, Loss Factor and resonant frequency of visco elastic shear-damped structural composites. *NASA CR-1269, National Aeronautics and Space Administration, Federal Scientific and Technical Information.* Springfield, Virginia
46. SWEDAC Product Catalogue, (Göteborg, Sweden, 1990)
47. A. Nashif, D. Jones, J. Henderson, *Vibration Damping* (Wiley, New York, 1985)
48. L. Beranek, *Noise and Vibration Control* (McGraw-Hill Book Company, New York, 1988)
49. L. Cremer, M. Heckl, *Körperschall* (Springer, Berlin, 1995)
50. L. Feng, A. Nilsson, Characterisation methods and ranking of mechanical joints. *ISMA 25*, Leuven, Belgium, 2000
51. A. Mazelet, Measurement of the reflection and transmission properties of junctions in beams. *Report 97–28*, MWL, Department of Vehicle Engineering, KTH, Stockholm, 1997
52. M. Åbom, Measurement of the scattering-matrix of acoustical two-ports. *Inter-Noise* **90** (1990)
53. H. Bodén, M. Åbom, Influence of errors on the two-microphone method for measuring acoustic properties in ducts. *J. Acoust. Soc. Am.* **72**(2), 541–549 (1986)

54. L. Feng, Vibration reduction through joints in finite systems. *Inter-Noise 98*, Auckland, 1998
55. R. Haettel, Propagation in built-up plate structures. Prediction and measurement. *Report 97–37*. MWL, Department of Vehicle Engineering, KTH, Stockholm, 1997
56. A.C. Nilsson, Reduction of structure-borne sound in simple ship structures. Results of model tests. *J. Sound Vib.* **61**(1), 45–60 (1978)
57. J. Rongong, Reducing transmitted vibration using "smart joint" concepts. *ISMA 25*, Leuven, Belgium, 2000
58. R. Courant, D. Hilbert, *Methods of Mathematical Physics* (Interscience Publishers, New York, 1966)
59. A. Nordborg, Vertical rail vibrations. Noise and structure-borne sound generation, Dr. Tech. thesis 95–35, MWL, Department of Vehicle Engineering, KTH, Stockholm, 1995
60. D. Thompson, Wheel-rail noise generation. Part III: rail vibration. *J. Sound Vib.* **161**(3), 421–446 (1993)
61. R. Hildebrand, *Sound attenuation in railway track (Report 99–15)* (MWL, Department of Vehicle Engineering, KTH, Stockholm, 1999)
62. R.D. Blevins, *Formulas for Natural Frequency and Mode Shape* (Van Nostrand, New York, 1979)
63. M. Petyt, *Introduction to Finite Element Vibration Analysis* (Cambridge University Press, Cambridge, 1990)
64. S. Finnveden, Spectral Finite Element Analysis of stationary vibrations in a beam-plate structure. *Acustica/Acta Acustica* **82**, 478–497 (1996)
65. F. Fahy, *Statistical Energy Analysis, A Wolf in Sheep's Clothing? Inter-Noise-93* (Belgium, Leuven, 1993)
66. B. Jarvis, Simple joint models. *ISMA 25*, Leuven, Belgium, 2000
67. T. Kihlman, *Transmission of structure-borne sound in buildings* (Swedish Institute of Building Research, Stockholm, 1967)
68. R. Ohayon, C. Soize, *Structural Acoustics and Vibration* (Academic Press, New York, 1998)
69. J. Matthews, R.L. Walker, *Mathematical Methods of Physics* (W. A. Benjamin, New York, 1965)
70. G.R. Cowper, The shear coefficient in Timosenko's beam theory. *J. Appl. Mech.* **66**, 335–340 (1966)
71. J.W. Nicholson, J.G. Simmonds, Timoshenko beam theory is not always more accurate than elementary beam theory. *J. Appl. Mech.* **77**, 337–338 (1977)
72. Discussion on the note ref. [71]. *J. Appl. Mech.* 357–360, June 1977
73. R.D. Mindlin, Influence of rotary inertia and shear on flexural motions of isotropic elastic plates. *J. Appl. Mech.* **51**, 31 (1951)
74. A.C. Nilsson, Some acoustical properties of floating floor constructions. *J. Acoust. Soc. Am.* **61**(6), 1533–1539 (1977)
75. H. Jutulstad, *Flytande gulv påfjaerer-lydreduserande konstruksjon for fartyg* (MSc-thesis, NTNU, ELAB, Trondheim, Norway, 1985)
76. A. Leissa, *Vibration of Plates* (Acoustical Society of America, American Institute of Physics, 1993)

Index

A

- Absorption, junction, 203
- Angular frequency
 - complex, 219
- Antiphase motion
 - plate, 125
- Attenuation
 - F-waves (beams), 158
 - L-waves (beams), 153
- Auto correlation function, 36
 - harmonic signal, 37
 - random signal, 36

B

- Beam
 - bending moment, 91
 - bending stiffness, 91
 - Bernoulli-Euler, 89
 - flexural waves, 89
 - I-beam, 146
 - longitudinal waves, 82
 - moment of inertia, 91
 - neutral axis, 90, 174
 - point excited, 264
 - sandwich, 138
 - strain, 75
 - Timoshenko, 121
 - thick, 132
- Bending
 - I-beams, 146
 - sandwich beams, 146
 - thick beam, 121
- Bending of plate
 - boundary conditions, 103
 - isotropic, 99
 - orthotropic, 105

- strain, 100
 - thick, 132
- Bending stiffness
 - apparent, 145
 - beam, 90
 - complex, 122, 159
 - plate, 101
 - plate and layer, 174
 - plate, constrained, 179
 - sandwich, 144
- Bending waves. *See* Flexural waves
- Bernoulli-Euler beam. *See* Euler beam
- Bessel function, 162
- Bessel inequality, 229
- Boundary conditions
 - bending, beam, 252
 - bending, plate, 103
 - closed-, 252
 - L-waves, beam, 218
- Bulk modulus, 73

C

- Characteristic frequency, 8
- Clamped edge, beam
 - F-waves, 158
 - L-waves, 153
- Coherence function, 44
- Completeness relation, 229
- Complex E -modulus, 155
- Complex notation, 25
- Composite structure, 292
- Contour integration, 50
- Convolution integral, 13, 33
- Correction, L-waves, 136
- Correlation function, 36
- Coupling

- F- and L-waves, 182
- L- and T-waves, 123
- Critically damped motion, 7
- Cross correlation function, 37
- Curvature, plate, 338

D

- Damped oscillatory motion, 6
- Damping, added, 153
- Density, 80
- Dirac pulse/function, 11, 33, 223
- Dispersion, thick plate
 - bending, 126
 - longitudinal waves, 126, 134
- Dispersive waves, 92
- Displacement, solids, 75
- Divergence free, 113

E

- Eigenfrequency
 - F-waves, beam, 261
 - F-waves, plate, 303, 327, 328, 356
 - L-waves, beam, 218
 - plate, curvature, 338
- Eigenfunctions
 - F-waves, beam, 260
 - F-waves, plate, 299
 - L-waves, beam, 308
 - norm, 260
 - orthogonal, 215
 - orthonormal, 215
- Eigenvalue
 - F-waves, beam, 260
 - F-waves, plates, 299
 - L-waves, beam, 218
- Elastic interlayer, 198, 199
- E*-modulus. *See* Young's modulus
 - complex, 109
- Energy
 - decay, 28, 222, 304
 - time average, 45
- Energy flow, 56, 107, 319
- Equipartition of energy, 233, 312
- Euler beam, 89
- Euler constant, 163
- Evanescent waves, 92
- Expected value, 36

F

- Flexural waves, beams, 260
 - displacement, 251

- eigenfunctions, 257
- eigenvalue, 256
- energy flow, 94
- group velocity, 92
- intensity, 108
- kinetic energy, 93
- phase velocity, 92
- potential energy, 93
- wavenumber, 92
- wave equation, 92
- Flexural waves, plates, 99
 - eigenfunctions, 292, 297
- Floating floor, 347
- Floquet theorem, 282
- Forced response
 - 1-DOF system, 22
 - F-waves, beams, 261
 - F-waves, plate, 306
 - L-waves beams, 223
 - periodic structure, 285
- Form factor, T-waves, 83
- Fourier series, 23
- Fourier transform
 - spatial, 166
 - temporal, 31
- Free end, beam
 - F-waves, 253
 - L-waves, 218
- Free vibrations
 - 1-DOF system, 4
- Frequency Response Function, 34, 50, 157

G

- Generalized wave equation, 111
- Green's function, 264
 - F-waves, beam, 264
 - F-waves, plate, 309
 - L-waves, beam, 223
- Group velocity, 92, 132

H

- Half band frequency method, 58
- Hankel function, 163
- Harmonic excitation, 25
- Heavily damped system, 7
- Hooke's generalized law, 72
- Hooke's law, 68

I

- Impedance, 118
- Inphase motion, 125

Intensity

- flexural waves, 127
- infinite solids, 69, 114
- longitudinal waves, 82
- thick plates, 131
- transverse waves, 79

Irrotational field, 112

K

Kelvin Voigt model, 76

Kinetic energy

- 1-DOF system, 8
- flexural waves, 92
- in solid, 75
- longitudinal waves, 250
- plate, bending, 105
- random excitation, 47
- time, average, 40
- transverse waves, 79

Kirchhoff plate, 99

Kronecker delta, 215

L

Lamé constant, 73

Locally reacting, 292

Longitudinal waves, 82

- correction, 136
- finite beam, 213
- free vibration, beam, 213
- intensity, 82
- kinetic energy, 85
- phase velocity, 84
- potential energy, 85
- quasi, 84
- wave equation, 81, 111

Losses

- Coulomb/frictional, 2
- hysteretic, 2, 4
- solids, 75
- structural, 3
- viscous, 2

Loss factor

- constrained layer, 179
- complex, spring, 28
- internal, 75
- junctions, 201
- measurements of, 56
- plate, damped, 173
- sandwich plate, 178
- spacer, 175
- structures, 199, 238

-total, 178

M

Mass-spring system, 1

Maximum displacement, 18

Maxwell model, 76

Memory function, 75

Mindlin plate, 123

Mineral wool, 348

Modal density

- F-waves, beam, 260
- F-waves, plate, 306
- L-waves, beam, 220

Modal force, 271, 312

Modal loss factor, 269, 313

Modal mass, 269, 312

Modal stiffness, 269, 312

Mode summation, 228, 268

Modes, plate, 325, 330

Moment of inertia, 86, 87

-beam, 91

-plate, 103

Moment, bending beam, 91

Moment, bending plate, 102

N

Natural frequency, 21, 326

Neumann function, 162

Neutral axis, bending, 140, 174

Non-oscillatory motion, 8

Norm, eigenfunctions, 260

Normal stress

-thick plates, 127

Nyquist diagram, 52

O

Orthogonal eigenfunctions, 215, 260

Orthonormal eigenfunctions, 215

Orthotropic plate, 105

P

Periodic boundary conditions, 217

Periodic force, 19

Periodic structure, 282

Perturbation, 341, 344

Phase angle, 8, 52, 54

-mobility, 54

-response, 20, 52

Phase velocity, 79

-flexural waves, 92, 132

- longitudinal waves, 84
- transverse waves, 84
- Plate
 - added mass, 340
 - bending stiffness, 103
 - boundary condition, 103
 - circular, 354
 - clamped edges, 103, 329
 - eigenfrequency, 304
 - eigenfunctions, 301
 - flexural waves, 99
 - free edges, 329
 - isotropic, 99
 - moment of inertia, 104
 - non-flat, 338
 - orthotropic, 353
 - point excited, 162
 - ribbed, 331
 - sandwich, 138
 - simply-supported, 303
 - stiffened, 335
 - thick, 121
- Point mobility
 - 1-DOF system, 51
 - beam, F-waves, 158, 268
 - beam, L-waves, 156
 - plate, F-waves, 158, 315
- Poissons's ratio, 68, 79
- Potential
 - scalar, 112
 - vector, 112
- Potential energy, 73
 - 1-DOF system, 8
 - bending, plate, 104
 - flexural waves, 92
 - in solid, 67, 114
 - longitudinal waves, 84
 - random excitation, 110
 - time average, 45
 - transverse waves, 81
- Power
 - 1-DOF system, 22
 - time average, 22
- Power spectral density
 - examples, 40
 - one sided, 39
 - two sided, 40
- Pulse excitation, 14
- Q**
 - Quasi-longitudinal waves, 84, 134

- R**
 - Radius of curvature, 89
 - Rain on the roof, 312
 - Random forces, 278
 - Random function, 31
 - ergodic, 31
 - stationary, 31
 - Rayleigh method, 326
 - Rayleigh–Ritz method, 326
 - Rayleigh waves, 135
 - phase velocity, 132
 - wavenumber, 131
 - Reciprocity, 226, 309
 - Reflection
 - coefficient, 185
 - L-waves, 118
 - T-waves, 118
 - Reinforced plate, 146
 - Relaxation function, 75
 - Resilient layer, 251
 - Resonance
 - double construction, 295
 - Response, 1-DOF, 60
 - Reverberation time, 58
 - Rod, 240
 - Rotation, angle of, 85
 - Rotation free field, 112
 - Rubber element, 77, 241

- S**
 - Sandwich plate, 138
 - bending, 139
 - bending stiffness, 145
 - dilatation frequency, 145
 - losses, 179
 - wavenumbers, 141
 - Scalar potential, 112
 - Shape/form function, 87
 - Shear force, plate, 70
 - Shear modulus, 70, 73, 106
 - plexiglas, 77
 - rubber, 77
 - Shear parameters, 73, 178
 - Shear stress
 - bending plate, 127
 - thick plate, 131
 - Simply supported
 - F-waves beam, 260
 - Sliding edge, 303
 - Spacer, 175
 - Spectral density, 38
 - cross, 37

- one-sided, 40
- power, 40
- two-sided, 41
- Spring constant, 1
- Standard linear model, 76
- Static deflection
 - mass-spring system, 1
- Strain, 67
 - bending, beam, 89
 - bending, plate, 99
 - infinite body, 70
 - thin beam, 69
 - thin plate, 69
- Stress, 67
 - bending beam, 101
 - infinite body, 70
 - thin beam, 70
 - thin plate, 69
- String, 87

T

- Timoshenko beam, 122
- Timoshenko constant, 122
- Torsional rigidity, 107
- Torsional waves, 85
- Transfer function. *See* Frequency response function
- Transfer matrix, F-waves, 278
- Transfer matrix, L-waves, 244
 - mass, 246
 - spring, 246
- Transfer mobility
 - beam, 237
 - plate, 316
- Transient vibrations
 - 1-DOF system, 11
- Transmissibility, 244
- Transmission coefficient, 185, 191, 201, 206
- Transmission loss, 199
 - elastic interlayer, 198
 - junctions, 186, 193

- measurements, 202
- rib, 199
- Transverse waves, 79
 - intensity, 82
 - kinetic energy, 81
 - phase velocity, 81
 - potential energy, 81
 - wave equation, 81, 111
- Trial function, 326, 328

V

- Vector potential, 113
- Viscoelastic layers, 179
 - constrained, 179

W

- Wave equation
 - F-waves, beams, 90
 - F-waves, plates, 101, 354
 - L-waves, 82, 111
 - string, 87
 - T-waves, 79, 111
 - torsional waves, 85
- Wavenumber
 - complex, F-waves, 158
 - complex, L-waves, 153
 - error, 127, 134
 - flexural waves, 92, 93
 - longitudinal waves, 82
 - Rayleigh waves, 130
 - thick plate, 131
 - Timoshenko beam, 129
 - transverse waves, 82
- White noise, 47
 - band pass, 43
 - low pass, 43

Y

- Young's modulus, 68, 79